Karlsruher Institut für Technologie

Moleküle als potentielle Datenspeichersysteme: Multikomponentenreaktionen sind der Schlüssel

Molecules as potential data storage systems: Multicomponent reactions are the key

Juli 2018

Andreas C. Boukis, M.Sc. Chem.

Arbeitsgruppe: Professor Dr. Michael A. R. Meier

KIT – Die Forschungsuniversität in der Helmholtz-Gemeinschaft

Die vorliegende Dissertation wurde vom 15. September 2015 bis zum 05. Juni 2018 am Institut für Organische Chemie der Fakultät für Chemie und Biowissenschaften in der Arbeitsgruppe von Professor Dr. Michael A. R. Meier am Karlsruher Institut für Technologie (KIT) – Universitätsbereich (Campus Süd) angefertigt. Die mündliche Prüfung fand am 19. Juli 2017 mit Professor Dr. Frank Breitling als Prüfungsvorsitzendem, Professor Dr. Michael A. R. Meier als Referent, Professor Dr. Joachim Podlech als Korreferent sowie Professor Dr. Peter Roesky und Privatdozent Dr. Detlef Schooß als weitere Prüfer, gemäß der Prüfungsordnung vom 18. August 2008 bzw. dem 10. September 2012 am KIT statt.

Moleküle als potentielle Datenspeichersysteme: Multikomponentenreaktionen sind der Schlüssel

Zur Erlangung des akademischen Grades eines

DOKTORS DER NATURWISSENSCHAFTEN

(Dr. rer. nat.)

Fakultät für Chemie und Biowissenschaften

Karlsruher Institut für Technologie (KIT) - Universitätsbereich

genehmigte

DISSERTATION

von

Andreas Christos Boukis, M.Sc. Chem.

aus

Karlsruhe

Dekan: Professor Dr. Reinhard Fischer

Referent: Professor Dr. Michael A. R. Meier

Korreferent: Professor Dr. Joachim Podlech

Tag der mündlichen Prüfung: 19. Juli 2018

„Meinen Eltern verdanke ich das Leben und meinem Lehrer das gute Leben“

Alexander der Große (356 v. Chr. – 323 v. Chr.)

I. Abstract/Zusammenfassung

Multikomponentenreaktionen sind Eintopfreaktion in denen drei oder mehr Komponenten zu einem Produkt reagieren, welches Teile aller Ausgangskomponenten enthält. Folglich lassen sich hierbei mehrere chemische Bindungen und strukturell komplexere Reaktionsprodukte in nur einem synthetischen Schritt darstellen.

In der vorliegenden Arbeit wurde der Einsatz von Multikomponentenreaktionen im Hinblick auf Datenspeichersysteme untersucht. In einem ersten Ansatz wurde die Ugi-Vierkomponenten-Reaktion von perfluorierten Säuren genutzt, um eine exemplarische Datenbank, bestehend aus 130 kommerziell erhältlichen Komponenten, zu erstellen. Betrachtet man alle möglichen Permutationen, so kann dieser Ansatz bis zu 500.000 Moleküle generieren, die jeweils in einem einzigen Schritt synthetisiert werden. 500.000 Permutationen entsprechen *ca.* 18 Bits pro Molekül. Die hier erstmals beschriebenen perfluorierten Ugi-Reaktionsprodukte wurden in Kombination mit Advanced Encryption Standard Kryptographie und molekularer Steganographie als molekulare Schlüssel eingesetzt. Diese molekularen Schlüssel dienen als Passwörter für verschlüsselte Daten und wurden auf versteckten und nicht-digitalen Kanälen übertragen, z.B. adsorbiert auf einem festen Trägermaterial oder aufgelöst in einer Flüssigkeit. Die Rückgewinnung und Aufreinigung der molekularen Schlüssel wurde durch die perfluorierten Seitenketten erleichtert. Mittels hochauflösender Tandem-Massenspektrometrie wurde anschließend die molekulare Struktur eindeutig aufklärt und somit der versteckte Schlüssel zur Entschlüsselung geheimer Nachrichten bestimmt. Zum einfacheren Auslesen der Massespektren wurde ein eigens programmiertes Computerskript benutzt. Die Verschlüsselung und Entschlüsselung von Nachrichten oder Daten wurde mit einem unabhängigen Programm durchgeführt.

In einem weiteren Ansatz wurde die Biginelli-Reaktion mit der Passerini-Reaktion in einem sequentiellen Multikomponenten-Reaktionssystem verknüpft. Nach der Bewertung der möglichen Linker-Moleküle und der Etablierung eines geeigneten Lösungsmittelsystems wurden diverse Dihydropyrimidon-α-acyloxycarboxamid-Strukturen in guten bis ausgezeichneten Ausbeuten dargestellt. In einem ersten Reaktionsschritt wurden dazu unterschiedliche Biginelli-Säuren synthetisiert und

daraufhin in einer Passerini-Reaktion eingesetzt. Durch die Variation der Komponenten wurde eine Bibliothek strukturell vielseitiger Moleküle synthetisiert. Darüber hinaus wurde erstmalig eine Biginelli-Passerini-Eintopf-Tandem-Reaktion demonstriert, wobei fünf Komponenten in einem Schritt im selben Reaktionsprodukt vereint werden.

In einem dritten Ansatz wurden sequenzdefinierte und informationscodierende Makromoleküle, welche potentiell als Datenspeichermaterialien geeignet sind, dargestellt. Für diese Untersuchung wurde die zuvor erarbeitete Kombination der Passerini- und Biginelli-Reaktion angewandt, um unterschiedliche bifunktionelle Monomere zu synthetisieren. Das Datenspeichersystem basiert auf der Variation von sechs Komponenten pro Wiederholeinheit, wobei aus einer eigens erstellten Datenbank von über 100 unterschiedlichen Komponenten gewählt werden kann. Diese strukturelle Diversität ermöglicht eine Datenspeicherdichte von *ca.* 24 Bits pro Wiederholeinheit. Die molekulare Information wurde mittels Tandem-Massenspektrometrie ausgelesen, wobei drei wesentliche Fragmentationsmuster identifiziert wurden.

Schlagwörter: Sequenzdefinierte Makromoleküle, Multikomponentenreaktionen, Biginelli-Reaktion, Passerini-Reaktion, Ugi-Reaktion, molekulare Datenspeicher, digitale Polymere, molekulare Kryptographie.

II. Abstract

Multicomponent reactions are one-pot reactions wherein three or more components react to a product containing parts of all precursors. Thus, several new chemical bonds and structurally more complex reaction products are obtained in a single synthetic step.

In the present thesis, the utilization of multicomponent reactions for data storage devices was investigated. In a first approach, the Ugi four-component reaction of perfluorinated acids was utilized to establish an exemplary database consisting of 130 commercially available components. Considering all permutations, this combinatorial approach can in principle provide 500,000 molecules, in only one synthetic step per molecule. The 500,000 permutations translate into approximately 18 bits per molecule. The herein firstly described perfluorinated Ugi compounds were employed as molecular keys by combining Advanced Encryption Standard cryptography with molecular steganography. Molecular keys serve as passwords for encrypted data and were transferred *via* concealed nondigital channels, *e.g.* by adsorption onto solid supports or by dissolution in liquids. Re-isolation and purification from these disguises was simplified by the perfluorinated sidechains of the molecular keys. Analysis *via* high resolution tandem mass spectrometry enabled the determination of the molecular structure and thus the identity the hidden key, for decryption of encoded messages. For straight-forward readout of the mass spectra a custom programed computer script was employed. The encoding and decoding of messages or data was performed by an independent software.

In another set of experiments, the Biginelli reaction was combined with the Passerini reaction in a sequential multicomponent reaction approach. After evaluation of all possible linker components and a suitable solvent system, several dihydropyrimidone–α-acyloxycarboxamide compounds were obtained in good to excellent yields. In a first reaction step, different Biginelli-acids were synthesized and subsequently employed in a Passerini reaction. By variation of the components in both multicomponent reactions, a library of structurally diverse compounds was synthesized. In addition, a one-pot Biginelli-Passerini tandem reaction was demonstrated, herein five components were incorporated in a single reaction step in one product.

In a third approach, sequence-defined and information-coding macromolecules, suitable for data storage materials, were synthesized. For this investigation, the previously established combination of the Passerini reaction with the Biginelli reaction was applied for the synthesis of bifunctional monomers. The data storage system is based on the variation of six different components per repeating unit, choosing from a herein comprised database of more than 100 components. This structural variety offers an information density of *ca.* 24 bits per repeating unit. The structural information was read out *via* tandem mass spectrometry, wherein three predominant fragmentation processes were identified.

Keywords: Sequence-defined macromolecules, multicomponent reactions, Biginelli reaction, Passerini reaction, Ugi reaction, molecular data storage, digital polymers, molecular cryptography.

III. Table of contents

IV. Declaration/Schriftliche Erklärung

Hiermit bestätige ich, gemäß § 5 Absatz b der Promotionsordnung vom 18. August 2008, dass

- die vorliegende Dissertation selbständig durch den Verfasser und ohne Verwendung anderer als der angegebenen Quellen und Hilfsmittel angefertigt wurde,

- diese Arbeit in gleicher oder ähnlicher Form noch keiner Prüfungskommission vorgelegt wurde,

- dass ich mich derzeit in keinem laufenden Promotionsverfahren befinde und auch keine vorausgegangenen Promotionsversuche unternommen habe,

- die benutzten Quellen wörtlich oder inhaltlich als solche kenntlich gemacht wurden

- und die Satzung des KIT zur Sicherung guter wissenschaftlicher Praxis beachtet wurde.

Karlsruhe, 05. Juni 2018

_____

Andreas C. Boukis

V. Danksagung

Vertrauen und Harmonie ist die Basis jeder erfolgreichen Zusammenarbeit. Es ist mir deshalb ein besonderes Vergnügen, mich an dieser Stelle gebührend zu bedanken bei

- Professor Dr. Michael A. R. Meier für die sehr interessante Formulierung des Themas. Er eröffnete mir die Möglichkeit diese Arbeit in seinem Arbeitskreis anzufertigen und dabei eigenständige Forschung zu betreiben, wodurch ich meine Fähigkeiten in vielerlei Hinsicht gesteigert habe. Mit seinem regen Interesse an dieser Arbeit motivierte er mich dabei meine Forschung zügig voranzutreiben und die Promotion erfolgreich abzuschließen.
- Professor Dr. Podlech und seiner Arbeitsgruppe für die freundliche Bereitstellung und Nutzung eines gemeinsamen Arbeitsplatzes.
- Dem Verband der Chemischen Industrie für finanzielle Unterstützung mittels des Fonds der chemischen Industrie Stipendiums (Nummer 197171).
- Der Deutschen Forschungsgemeinschaft (DFG) für die finanzielle Unterstützung im Rahmen des Sonderforschungsbereichs 1176, Projekt A3.
- Den Mitgliedern des Arbeitskreises Meier für die freundliche Atmosphäre, das nützliche Feedback in den Gruppenseminaren und die vielen wissenschaftlichen Diskussionen.
- Den Kooperationspartnern für die wissenschaftlichen Diskussionen und die Beiträge zu den gemeinsamen Publikationen.
- Dem Institut für Organische Chemie, der Analytik Abteilung, sowie allen anderen festangestellten Mitarbeitern.
- Meinen betreuten Studenten/Auszubildenden für die synthetische Unterstützung: Baptiste Monney (2016), Felix Mack (2016), Mareen Stahlberger (2016), Maximiliane Frölich (2017), Elisabeth Horner (2017), Carolin Albrecht (2017).
- Meiner Familie und meinen Freunden für ihre permanente Unterstützung und das Korrekturlesen dieser Arbeit.

VI. Preface

This thesis comprises the results of the author's research performed in the group of Professor Dr. Michael A. R. Meier in the time from September 2015 until June 2018.

Chemical structures in schemes or figures were highlighted by colors to improve comprehensibility. Different colors in chemical reaction schemes illustrate the position of atoms and chemical moieties of the precursor substances in the reaction product (based on the respective generally accepted reaction mechanisms). Newly formed chemical bonds are colored in black. Whenever asymmetric carbon atoms do not include precise stereo chemical information, the compounds can be regarded as the racemic mixture (both enantiomers in equal amounts).

Self-written text passages and/or self-made figures and schemes within this thesis were adapted from previous publications by the author and are cited in the beginning of the corresponding chapter. All publications where Andreas Boukis is listed as first author were written by himself.

The electronic version of this document contains hyperlinks, which are marked in **BOLD**. Chemical substances were referred to by their trivial name/trade mark, IUPAC nomenclature or abbreviated by consecutive numbers in bold. Atom positions for structural elucidations are abbreviated with italic numbers.

Andreas C. Boukis Karlsruhe, 5th June 2018

1 Initial situation & problem analysis

Information is a major driving force for human evolution. Therefore, humans try to memorize, store and access increasing amounts of information in as little time and space as possible. Generally, the term information is directly linked to data. When data is processed, organized, structured and interpreted in a certain context it becomes information. A wise quote stated “An ounce of information is worth a pound of data. An ounce of knowledge is worth a pound of information. An ounce of understanding is worth a pound of knowledge”[1] (1 pound = 16 ounces).

When humans in the prehistoric age realized the significance of data storage, they started to preserve their observations through cave paintings and stone engravings. Starting from rocks, wood, bones, clay tablets, papyri, metal tablets, paper and punched cards, humanity moved on to magnetic tapes, celluloid films, gramophone records, floppy disk, and many more. A major breakthrough was witnessed in 1928, when Fritz Pfleumer invented the magnetic tape, enabling the concentration of data into compact space.[2] In 1958, Jack Kilby introduced the first integrated circuit, a computer chip made out of the semiconductor germanium.[3] Only a few months later Robert Noyce created a more efficient silicon-based chip.[4] The evolving computer technology made increasingly capacious and efficient data storage devices possible. Modern methods of data storage are *e.g.* optical discs, such as CDs, DVDs, and Blu-ray discs or hard drives and flash drives.

Today, the total digital data amounts to approximately 4.4 zettabytes (= 4.4×10^9 TB = 3.52×10^{22} bits) globally and is expected to reach 3×10^{24} bits, at a presumed consistent exponential rate of growth, by 2040.[5] However, data storage on magnetic tapes which are currently employed to maintain large-scale permanent archives begin to deteriorate within 20 – 30 years. To meet the demand for data storage devices, *ca.* 10^9 kg silicon wafers would be necessary, however, the estimated supply only accounts to *ca.* 10^7–10^8 kg.[4] Silicon has limited data storage ability[6] and comes along with other concerns, such as human health hazards[7] and environmental pollution. For instance, a typical chip manufacturing site produces around 2 million chips per month and consumes about 75 million liters of water, while the production of a single 32 MB chip weighing *ca.* two grams requires about 1600 g of secondary fossil fuel and 700 g

of nitrogen gas are consumed.[4] In addition the production for one square centimeter of a silicon wafer consumes about 1.5 kWh of energy (5.4 MJ).[4,8]

To face future problems of data storage, scientist currently discuss the utilization of DNA as means of data storage.[9] Claiming that the entire current global data of (3.52×10^{22} bits) could be packed in a 0.00352 m^3 box (less than three 1.5 liter bottles) and yet around 1 kg of DNA would be sufficient to address the worlds storage requirement in 2040 (3×10^{24} bits).[4] In contrast to the binary system (2^n, encoding data in “1” or “0”), DNA is capable of encoding in a quaternary system (4^n, encoding with the four nucleobases). The synthetic and analytic technologies associated with DNA are already well established and developed.[10] Nevertheless, data storage applications of DNA have inherent disadvantages, such as limited long term stability,[11,12] the current inability to synthesize long DNA homopolymers,[13] various sequencing errors,[14,15] nucleobase mutations,[16,17] *etc.* It should also be considered that DNA is the information storage of life, which can lead to the problem that data encoded in DNA might accidentally (or even on purpose) encode virus sequences acting as pathogens to living organisms (a computer virus has already been encoded in DNA).[13]

In order to introduce additional concepts for data storage devices, non-natural sequence-defined macromolecules are discussed. These sequence-defined macromolecules were described to be one of the biggest goals in polymer science and are thus challenging to synthesize.[18] However, non-natural systems enable the use of different chemistry protocols,[19] offering new perspectives and opportunities for synthetic and analytic methods, and might therefore overcome the limitations of DNA-based data storage systems.[20]

2 Theory

2.1 Multicomponent reactions

Parts of this chapter and following subchapters were adapted from previous passages written by the author.[21–24]

In a multicomponent reaction (referred to as MCR), three or more components react to a product containing parts of all precursors in a one-pot reaction. MCRs have steadily gained importance in synthetic organic chemistry and recently also in polymer science.[24] Because of the capability to form several chemical bonds and thus complex products in a single operation, MCRs are highly convergent, modular and versatile synthetic tools. MRCs also offer many other advantages, such as operational simplicity,[25] facile automation,[26,27] reduction in the number of work-up steps and hence minimized waste production (**Scheme 1**).[28] One-pot reactions in general shorten the time required for a synthetic procedure and can provide higher overall yields compared to multiple-step syntheses.[29] Due to a reduction in the use of material, energy and manpower, one-pot MCRs render chemical transformations as more sustainable processes.[30–34]

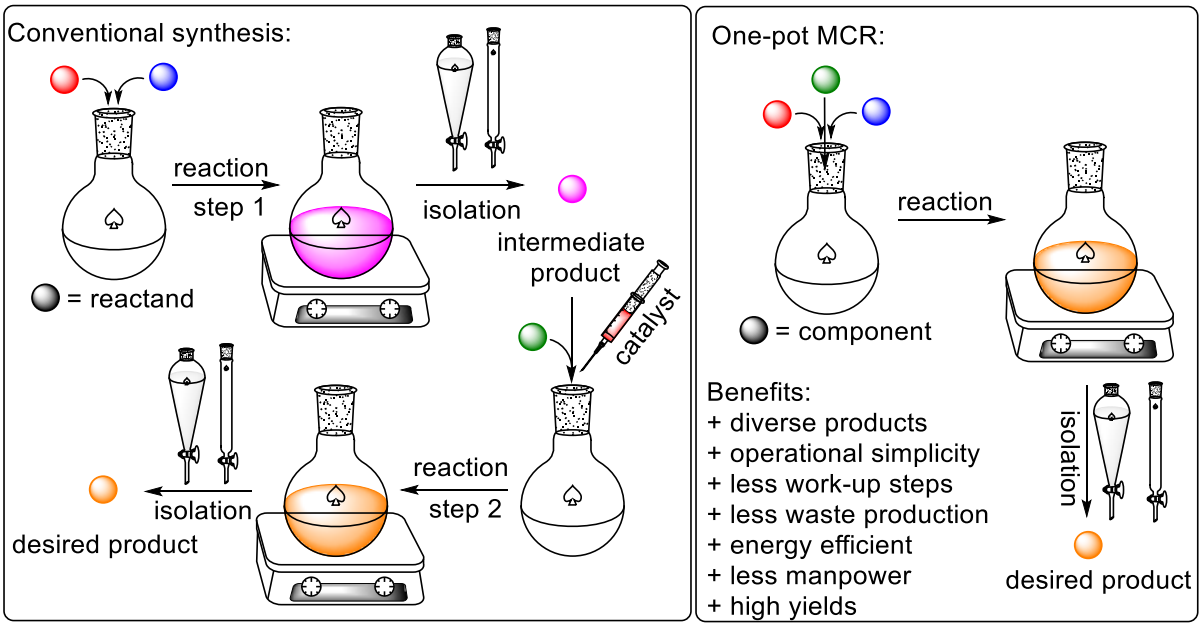

Scheme 1. Conventional synthesis in comparison to one-pot MCRs.[21]

By minimizing the number of synthetic operations, while maximizing the buildup of structural and functional complexity, these highly step- and atom economical reactions[35] are particularly appealing in the context of target-oriented synthesis.[36,37]

In 2000, Dömling and Ugi introduced a classification system categorizing three types of MCRs based on the respective reaction mechanisms (see **Table 1**).[38]

Table 1. Three basic types of MCRs.[38]

MRC type	Mechanistic aspects	Exemplary reaction scheme
I	Mobile equilibrium	A + B ⇌ C ⇌ ... ⇌ O ⇌ P
II	Irreversible in the last step	A + B ⇌ C ⇌ ... ⇌ O → P
III	Irreversible elementary reactions	A + B → C → ... → O → P

According to this classification, MCRs exclusively consisting of equilibrium reaction pathways are referred to as Type I. MCRs of type II include an irreversible last reaction step and are thus more favorable than type I reactions. The irreversible last step shifts the previous equilibria and can therefore achieve higher yields of the desired reaction product P. In many cases, Type II reactions include a strong chemical driving force in the last step such as: an exothermic reaction, for instance an oxidation (*i.e.* isocyanide carbon atoms from C^{II} to C^{III}), the condensation of small and stable molecules (*i.e.* water in the Biginelli reaction), an irreversible ring-closing reaction or the formation of an aromatic system. Type III MCRs consist of irreversible elementary reactions and can be found in biochemical (enzymatic) reaction systems. However, the MCR classification system is only valid for ideal model reactions and many MCRs cannot be categorized in this fashion.[39]

A selection of important and well-known examples for MCRs is presented in **Scheme 2** (in chronologic order), including the Strecker amino acid synthesis (1850, **Scheme 2 a**), the Hantzsch dihydropyridine synthesis (1882, **Scheme 2 b**), the Biginelli dihydropyrimidone synthesis (1891, **Scheme 2 c**), the Mannich reaction (1912, **Scheme 2 d**), the Passerini three-component reaction (1921, **Scheme 2 d**), and the Ugi four-component reaction (1959, **Scheme 2 e**).

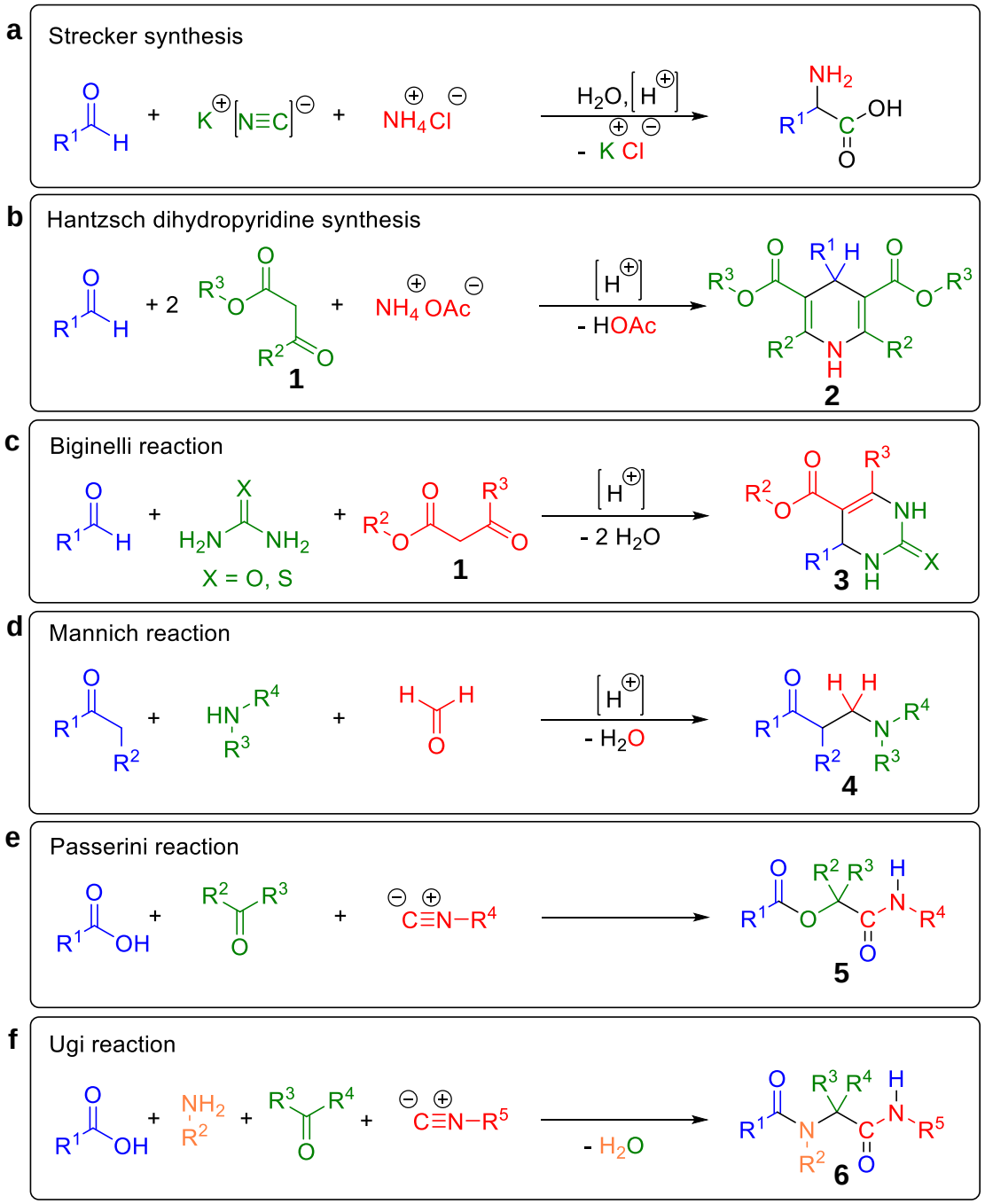

Scheme 2. Selected examples for multi component reactions. **a**, Strecker synthesis.[40] **b**, Hantzsch pyridine synthesis.[40–42] **c**, Biginelli reaction.[43] **d**, Mannich reaction.[40,42,44] **e**, Passerini reaction.[45–47] **f**, Ugi reaction.[48]

The Strecker synthesis (**Scheme 2 a**) was discovered in 1850 and describes the reaction between an aldehyde, a cyanide and a nitrogen source, such as ammonium chloride (or primary/secondary amines). The Strecker reaction is considered a milestone in the field of MCRs and was furthermore the first method for the direct synthesis of α-amino acids.[49,50] Although the classical Strecker synthesis results in a racemic product mixture, many asymmetric methods in which enantioinduction is achieved *e.g.* utilizing chiral auxiliaries[51–53] or chiral catalysts[54] have been described.

In the Hantzsch dihydropyridine synthesis (**Scheme 2 b**), an aldehyde (aliphatic or aromatic) reacts with two equivalents of an acetoacetate (β-keto ester) **1** and a nitrogen donor (ammonia or primary aliphatic amines).[55] The initially formed reaction product is a 1,4-dihydropyridine (DHP) **2**, which can subsequently be oxidized to the corresponding aromatic pyridine derivate.[41,56] Some DHP compounds display pharmacologic activities and can be applied, for instance, as calcium channel blockers (*e.g.* nifedipine, amlodipine or nimodipine).[57,58] The Biginelli reaction (illustrated in **Scheme 2 c**) involves the reaction between an aldehyde (preferably aromatic), a urea and an acetoacetate **1** under acidic conditions. The heterocyclic reaction product is a so-called 3,4-dihydropyrimidin-2(1*H*)-one (DHMP) **3**. DHMPs **3** were also utilized in medicinal chemistry.[59] In the Mannich reaction (**Scheme 2 d**), an acidic proton in α-position to a carbonyl functional group (acting as a carbon nucleophile) is amino alkylated in the presence of formaldehyde and amines (or ammonia).[60] The β-amino carbonyl products **4** of the Mannich reaction (also called Mannich-Bases) can be synthesized with high optical purity *via* different asymmetric methods *e.g.* proline organo-catalysis.[61–63] The Passerini three-component reaction (**Scheme 2 e**) is an example for an isocyanide-based MCR. The Passerini reaction is formally an addition reaction between a carboxylic acid, a carbonyl component and an isocyanide forming an α-acyloxycarboxamide **5** in 100% atom economy.[35] Nowadays, the Passerini reaction has been successfully introduced to numerous fields of chemistry including combinatorial chemistry for drug discovery,[64] natural product synthesis[65] and polymer science.[24] In the field of isocyanide-based MCRs, the Ugi four-component reaction (Ugi-4CR) (**Scheme 2 f**) is another well-known example. Herein, the reaction of four components (carboxylic acid, amine, carbonyl compound and isocyanide) leads to the formation of a *bis*-amide product **6** *via* previous imine condensation of the aldehyde and the amine.[38] As for many other MCRs, the Ugi reaction has also been applied in the fields of combinatorial chemistry and polymer science.[66,67]

Polymer material properties highly depend on their functionality, topology and macromolecular architecture. Hence, polymer- and soft-matter science require a variety of functionalized polymers specifically designed for novel applications. Macro- and microscopic functionality can be introduced *e.g.* by the precise installation of functional groups within a polymer chain or in the side groups. In this context, MCRs offer many attractive features and evolved to versatile tools, which have been appreciated in polymer science.[68] On the one hand, many MCR benefit from one-pot

procedures, but on the other hand a great advantage for polymer chemistry is the high diversity of functionality, which can be introduced by variation of the components, allowing macromolecular engineering. In the present thesis, three MCRs were utilized for the synthesis of novel compounds and sequence-defined macromolecules and will therefore be discussed more into detail in the following chapters (chapter **2.1.1** for Biginelli; **2.1.2** for Passerini and **2.1.3** for Ugi).

2.1.1 The Biginelli reaction

In 1893, Pietro Biginelli observed the formation of a precipitate in the reaction between benzaldehyde, ethyl acetoacetate and urea in the presence of catalytic amounts of hydrochloric acid in absolute ethanol. Elemental analysis of this precipitate evidenced the incorporation of all starting precursors under the elimination of two equivalents water.[69] Biginelli initially proposed the formation of ternary adducts with acyclic (open chain) structures and hence did not recognize the novelty of his discovery. However, after further investigations, Biginelli evidenced the formation of a heterocyclic compound, a so-called 3,4-dihydropyrimidin-2(1*H*)-one (DHMP) **3**.[59]

The Biginelli reaction is a three-component reaction involving a series of reversible reaction steps followed by the irreversible elimination of water. In **Scheme 3**, a proposed mechanism of the Biginelli reaction with respect to the generally accepted mechanism of Kappe *et al.* is illustrated.[70] In the first reaction step, the aldehyde is activated by a Lewis- or a Brønsted acid (H^+). Subsequently, urea can react as a nucleophile and attacks the activated carbonyl with the lone pair of the nitrogen atom to form a hemiaminal species **7**. Hemiaminals **7** are unstable in acidic conditions and can eliminate water to form a reactive *N*-acyliminium cation **8**. In the next step, the *N*-acyliminium ion **8** reacts with the nucleophilic α-carbon atom of the acetoacetate component **1** (*i.e.* after keto-enol tautomerization) resulting in an open chain ureide **9**. Subsequent ring closure forms a six-membered ring. After two proton transfer reactions (referred to as P.T.), the cyclic hexahydropyrimidine intermediate **10** is obtained. The irreversible elimination of a second equivalent of water results in the formation of the thermodynamically favored DHMP product **3**.

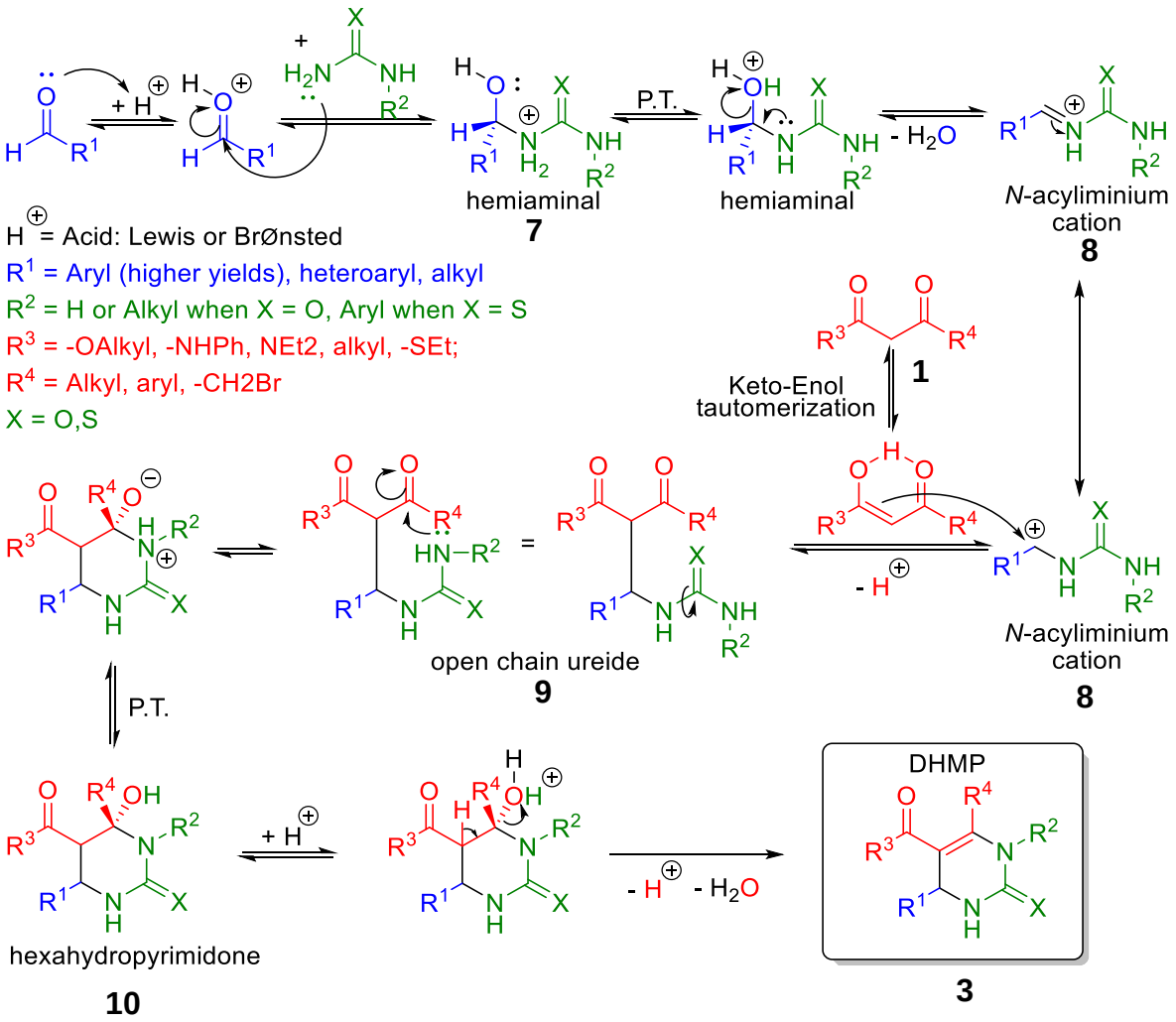

Scheme 3. Proposed mechanism of the Biginelli reaction.[70] Acid-catalyzed condensation of urea with the aldehyde affording an hemiaminal **7**, which dehydrates to an *N*-acyliminium ion **8**. Subsequently, the enol form of the β-keto ester **1** attacks the *N*-acyliminium ion **8** to generate an open chain ureide **9**, which readily cyclizes to a hexahydropyrimidine derivative **10** and dehydrates to the DHMP product **3**.[23,42]

The accepted mechanism illustrated in **Scheme 3** was supported by spectroscopic data. However, alternative mechanisms are discussed.[71,72] For instance, the so-called enamine mechanism starts with an enamine formation between urea and the β-ketoester. Subsequently, the enamine reacts with the aldehyde.[73] A third alternative reaction mechanism begins with a Knoevenagel type reaction between the aldehyde and the β-ketoester followed by the reaction with urea.[74]

The scope of accessible DHMP structures was enriched in 1989 by Atwal *et al*.[75] In the so-called Atwal modification unsaturated keto esters are reacted with substituted (in this case protected) urea derivatives to yield protected DHMPs, presumably *via* a Michael addition. The protected DHMPs can subsequently be alkylated/acylated in a regiospecific manner by various electrophiles.[76] After deprotection of the products, functionalized DHMPs are obtained, which would not have been accessible by the

conventional Biginelli reaction. However, the additional reaction steps depart from the one-pot reaction convenience.[43] The manifold chemistry of the Biginelli reaction found numerous applications including combinatorial and medicinal chemistry, which will be discussed hereafter.

2.1.1.1 The Biginelli reaction in combinatorial and medicinal chemistry

In the context of medicinal chemistry, DHMPs can mimic the pharmacologic properties of the Nifedipine type Hantzsch dihydropyridine (DHP) drugs (*i.e.* active calcium channel modulators, displayed in **Figure 1**). The pharmacological scope of DHMPs includes calcium channel modulation for the treatment of cardiovascular diseases (*e.g.* hypertension),[58] cardiac arrhythmias[76,77] or angina (see **Figure 1**, SQ 32926 and SQ 32547).[57,58,78–81] Furthermore, DHMPs (*e.g.* SNAP 6201), can function as α_{1a} adrenoceptor-selective antagonists for the treatment of benign prostatic hyperplasia (progressive enlargement of the prostate effecting *ca.* 70% of males older than 70 years, resulting in a number of disruptive symptoms).[82]

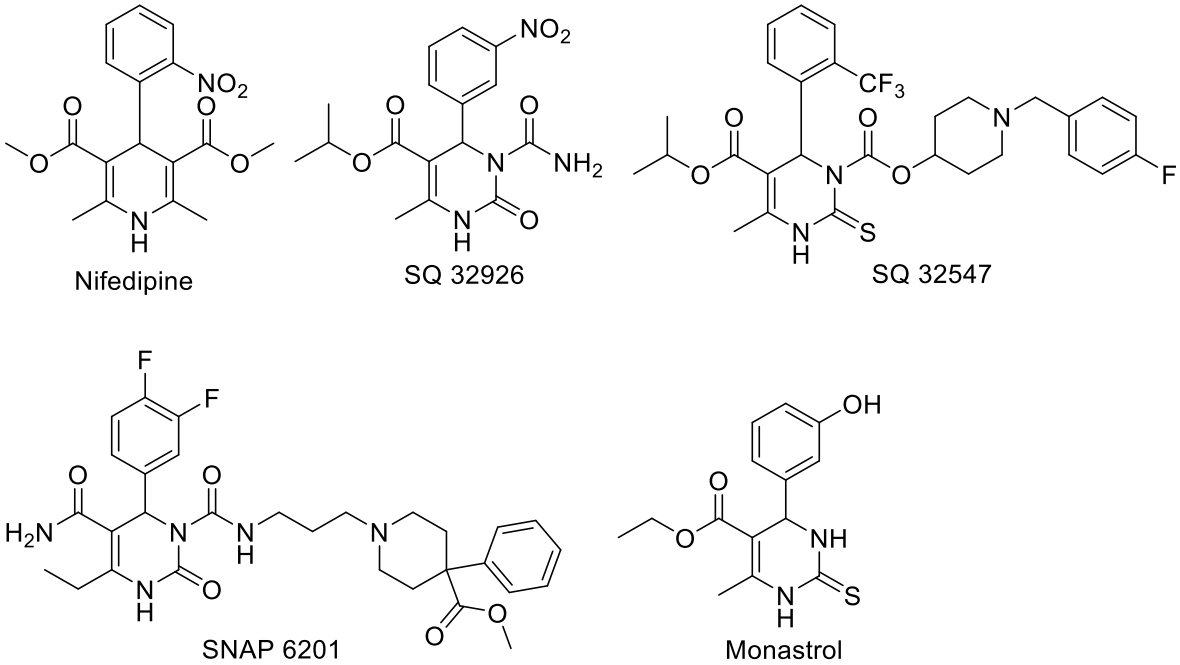

Figure 1. Structures of selected pharmacological active DHP (Nifedipine) and DHMP compounds.

Other drug applications include cancer therapy (*e.g.* Monastrol),[76,83] treatment of trachoma viruses,[84] anti-HIV alkaloids (*e.g.* Batzelladine B,)[85,86] antibacterial activity

and fungicidal activity (*e.g.* 2-thioxo DHMPs against *Aspergillus niger* and *Aspergillus ochraceus*).[76] The modular nature of the Biginelli reaction also suggests an application in combinatorial chemistry. In 1995, Wipf *et al.* developed a solid phase protocol for the Biginelli reaction based on a urea derivate linked to a Wang resin and demonstrated the synthesis of ten DHMPs in high yields.[87] A automated, solution-based and microwave-assisted, combinatorial system was established by Kappe *et al.* and generated an automatically produced library of 48 DHMPs.[27] Other combinatorial methods for the preparation of different DHMPs utilized polymer-supported catalysts.[88] A review including further examples and detailed descriptions of the Biginelli reaction in combinatorial chemistry can be found in literature.[89]

2.1.1.2 The Biginelli reaction in polymer science

The Biginelli reaction proved to be a versatile and efficient reaction for the preparation of small molecules but was further employed in polymer chemistry. In 2013, Tao *et al.* utilized the Biginelli reaction for polymer conjugation of two methoxy poly(ethylene glycol) (mPEG) chains of different chain lengths equipped with suitable end groups (aldehyde **11** and β-acetamide **12**). The addition of urea promoted the coupling step (see **Scheme 4 a**).[90] Hence, the Biginelli reaction evolved as a multicomponent reaction tool for the preparation of block copolymers. Block copolymers represent a class of interesting materials, because different physical and/or chemical properties can be combined in the same polymer (for applications as surfactants or thermoplastic elastomers, *etc.*).[91] In other experiments, the Biginelli reaction was employed for polymer side group modification (a post-polymerization modification), wherein a polymethacrylate backbone bearing acetoacetate side chains was reacted with urea and benzaldehyde.[92] Some of the DHMP sidechain polymers were utilized as water-soluble adhesives.[93] Moreover, the Biginelli reaction was combined with a reversible addition–fragmentation chain transfer polymerization (RAFT) of an acetoacetate functionalized methacrylate **13** in a one-pot reaction with urea and benzaldehyde (illustrated in **Scheme 4 b**).[94]

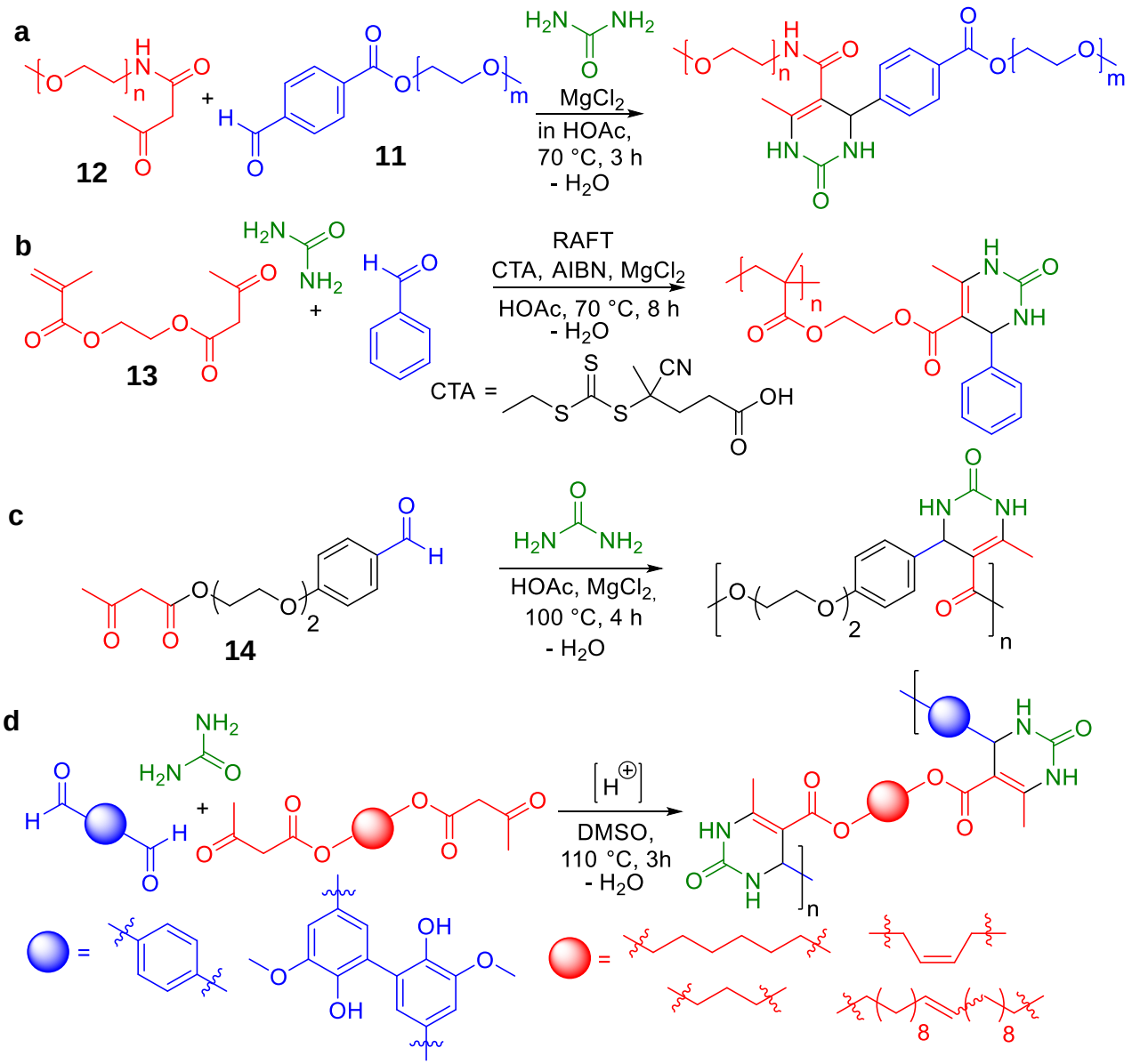

Scheme 4. Selected examples of the Biginelli reaction in polymer chemistry. **a**, polymer conjugation, two mPEG chains with suitable end groups (**11** and **12**) coupled *via* the Biginelli reaction. **b**, one-pot combination of the Biginelli reaction with RAFT polymerization.[90] **c**, Biginelli polycondensation of a AB-type monomer.[95] **d**, Biginelli polycondensation of renewable AA- and BB-type monomers.[22]

Under optimized conditions, the Biginelli reaction proved to be very efficient, hence suggesting the application of the Biginelli reaction as a step-growth multicomponent polymerization method. In 2015, AB type monomers, displaying an acetoacetate and aldehyde functional group **14**, were polymerized in the presence of urea *via* a Biginelli polycondensation (**Scheme 4 c**).[95] In another study, the Biginelli polycondensation was utilized to polymerize AA- and BB-type monomers (dialdehydes and diacetoacetates) derived from renewable resources. The respective polymers (polyDHMPs), with molar masses of up to 20 kDa, showed interesting thermal properties such as high glass transition temperatures (T_g up to 203°C) and high thermal stability.[22] This concept was further extended by investigating different AA- and

BB-type monomers (eight diacetoacetates, four dialdehydes and two urea derivates) in a combinatorial high throughput screening approach for different glass transition temperatures.[96] If thiourea is applied in Biginelli reactions, the respective dihydropyrimidin-2(1*H*)-thiones can be functionalized at the sulfur atom *e.g. via* alkylation. This concept was also utilized as a post-polymerization modification method for poly(dihydropyrimidin-2(1*H*)-thiones).[97] Acetoacetates and aldehydes can also participate in other chemical transformations such as the Hantzsch reaction (see **Scheme 2 b**), which enabled the preparation of copolycondensates *via* simultaneous Hantzsch and Biginelli polymerization.[98] In conclusion, the Biginelli reaction was developed as a versatile tool for polymer science and enabled the synthesis of interesting and functional materials.

2.1.2 The Passerini reaction

The Passerini reaction (discovered in 1891 by Mario Passerini) is an isocyanide-based three-component reaction involving a carboxylic acid, a carbonyl compound and an isocyanide.[99] In most cases, the Passerini reaction is very efficient if performed in aprotic polar solvents like dichloromethane. The proposed mechanism of the Passerini reaction is illustrated in **Scheme 5**. In the first step, a six-membered cyclic hydrogen bonded adduct **15** is formed between the carboxylic acid and the carbonyl component (now two out of three reacting components are in the same place at the same time). Subsequently, the isocyanide reacts with the loosely bound H-bonded adduct **15**, in a so-called α-addition. Remarkably, in the α-addition the isocyanide displays nucleophilic and electrophilic reactivity simultaneously. The consequently formed intermediate **16** (proposed as seven-membered ring) has not been isolated and characterized yet, because **16** immediately undergoes an irreversible rearrangement reaction, affording the final Passerini α-acyloxycarboxamide adduct **5**.[72,100] The above presented and commonly accepted mechanism was supported by kinetic experiments.[101,102] An alternative mechanism proposes the protonation of the isocyanide in the first step and confirms the observation that Passerini reactions are accelerated in the presence of inorganic mineral acids.[103]

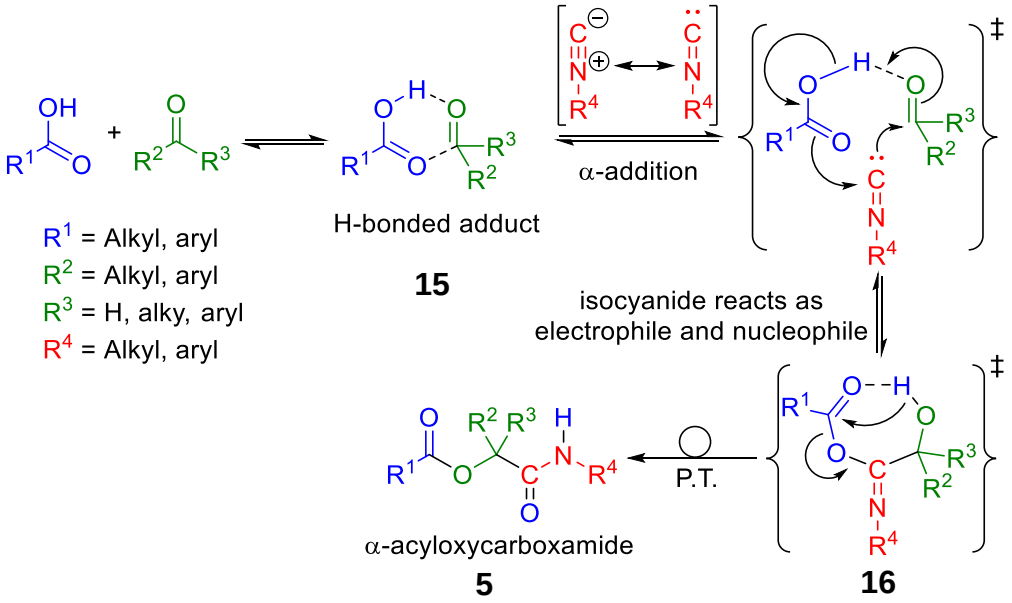

Scheme 5. Proposed mechanism of the Passerini reaction. First, the carboxylic acid and the carbonyl compound form a hydrogen bonded adduct **15**. Subsequently the isocyanide attacks the H-bonded adduct **15** in in a concerted fashion (so-called α-addition). The respectively formed seven-membered transition state **16** undergoes a rearrangement to the final α-acyloxycarboxamide Passerini product **5**.

In addition, Passerini and Ugi reactions can be accelerated in the presence of water and upon the addition of salts.[104] However, quantum mechanical calculations suggest a mechanism, in which a second carboxylic acid molecule functions as an organo-catalyst.[105,106] The Passerini reaction is classically leading to racemic product mixtures, however asymmetric methods were investigated for instance by utilizing chiral components (isocyanides,[107] carboxylic acids,[108] aldehydes[109,110]) or Lewis acids with chiral ligands, achieving up to 98% enantiomeric excess (*ee*).[111,112]

2.1.2.1 The Passerini reaction in combinatorial and medicinal chemistry

The modular nature of the Passerini reaction provides combinatorial access to a large variety of reaction products, of which some have found their application as drugs, *e.g.* Passerini depsipeptides.[113,114] Bicalutamide is the pharmacologically active substance in Casodex® and can be synthesized *via* a Passerini reaction with water as acid component (see **Scheme 6**). Casodex® is a nonsteroidal selective antiandrogen for the treatment of prostate cancer by inhibition of the androgen receptor.[115] The Passerini reaction was also employed for the synthesis of a molecule targeting the HI virus *via* inhibition of the enzyme HIV-1 protease (displayed in **Scheme 6 b**).[116,117]

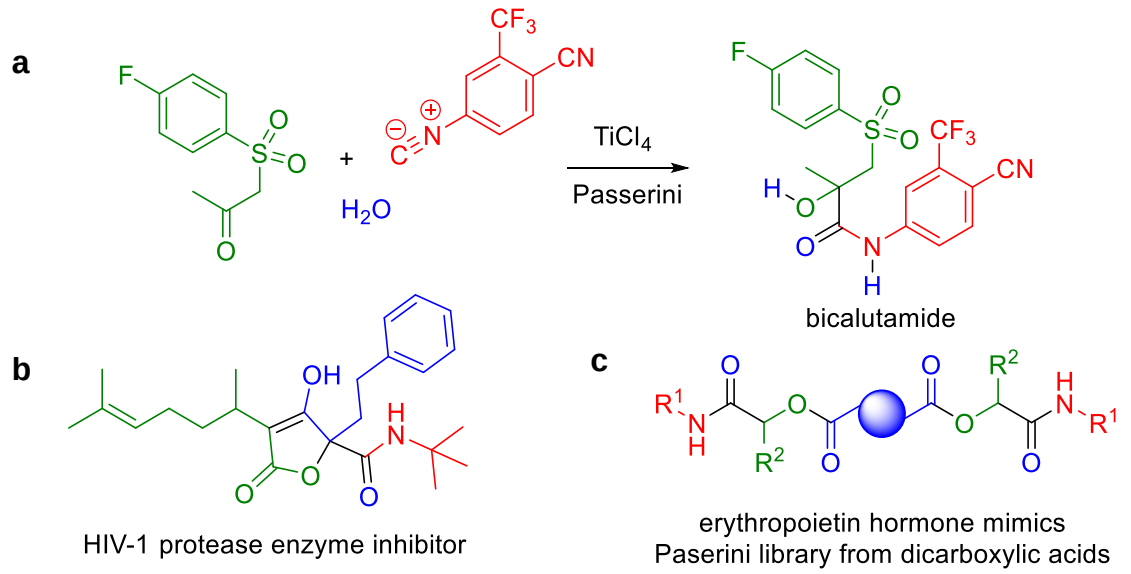

Scheme 6. Selected examples of the Passerini reaction in medicinal chemistry.[118] **a**, synthesis of Bicalutamid *via* a Passerini reaction.[118] **b**, HIV-1 protease inhibitor.[116,117] **c**, general structure for a library of Passerini molecules screened as EPO hormone mimics.[119]

For targeting neuromuscular and neurodegenerative diseases *via* calpain inhibition, a large library (containing hundreds of compounds) based on the Passerini reaction was synthesized and tested. *In vivo* experiments revealed that several compounds exhibited potent activity and sufficient metabolic stability in mice, with no prominent adverse effects.[120] In another combinatorial approach, three libraries of 88 compounds each were prepared utilizing the Passerini reaction of dicarboxylic acids (**Scheme 6 b**) and Ugi reactions of dicarboxylic acids or diamines in order to screen for compounds mimicking the hormone erythropoietin (EPO).[119] In a screening approach of the crude reaction mixtures, several promising compounds were identified. Reviews including further examples of the Passerini reaction in medicinal and combinatorial chemistry are present in literature.[115,118,121,122]

2.1.2.2 The Passerini reaction in polymer science

An early example of the Passerini reaction applied in polymer science was reported by Meier *et al.* in 2011.[123] For instance, the Passerini reaction was employed to synthesize several α,ω-diene monomers (**Scheme 7 a**) derived from undec-10-enoic acid (obtained from ricinoleic acid, a renewable fatty acid from castor oil). These monomers were subsequently utilized in an acyclic diene metathesis polymerization (ADMET) to obtain the corresponding polymers. Additionally, the Passerini reaction

can be used as a multi component-step-growth polycondensation of dicarboxylic acids, dialdehydes and isocyanides (AA- and BB-type monomers, see **Scheme 7 c**).[68,123] Besides AA- and BB-type monomers, AB-type monomers were also employed in the Passerini polyaddition. Therefore, a bifunctional monomer equipped with a carboxylic acid and an aldehyde functional group (prepared *via* thiol-ene addition of undec-10-enal and 3-mercaptopropionic acid) was polymerized upon the addition of an isocyanide.[46]

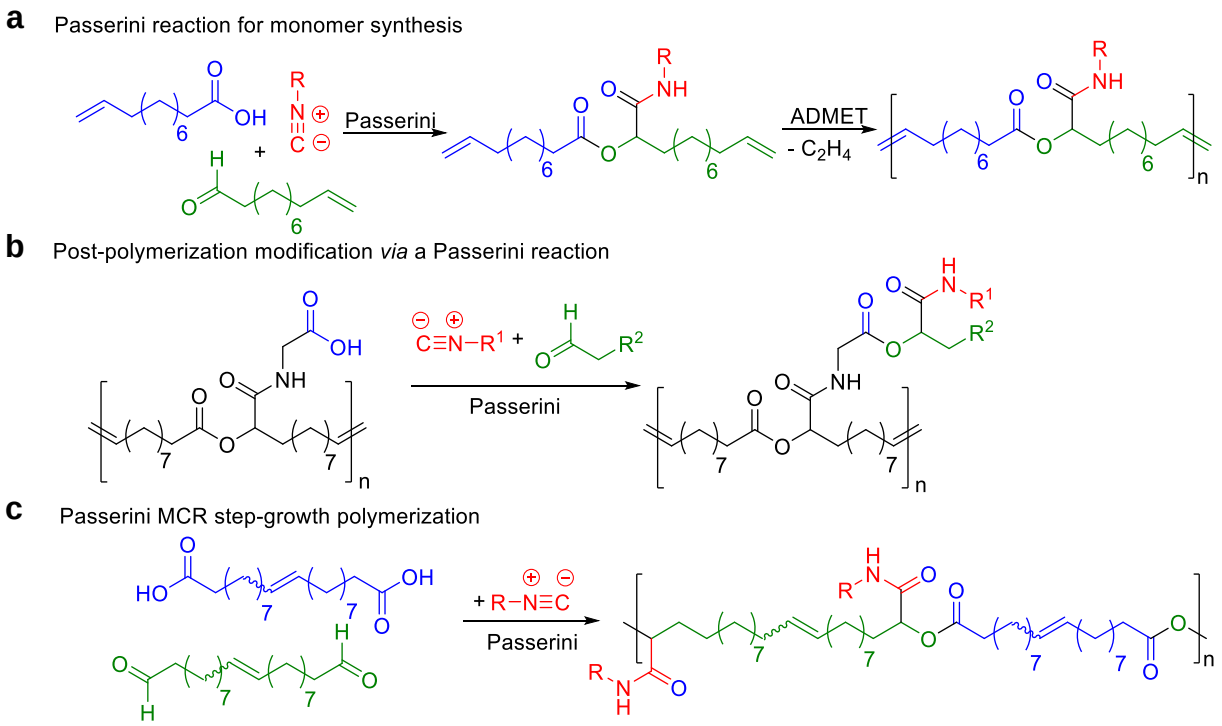

Scheme 7. Early examples of the Passerini reaction in polymer synthesis. **a**, for monomer synthesis. **b**, as post-polymerization modification tool. **c**, Passerini step-growth polymerization employing diacids, dialdehydes and isocyanides.[68,123]

The Passerini step-growth polymerization of sequence-defined macromonomers was reported by Li *et al*.[124] The Passerini reaction also allowed post-polymerization modification reactions (**Scheme 7 b**) on polymers equipped with carboxylic acid side chains (*via* the reaction with isocyanides and aldehydes).[123] Meier and coworkers further utilized the Passerini and Ugi reaction for the synthesis of α,ω-diene monomers employing 2-(2,2-dimethoxyethyl)phenyl isocyanide (a so-called convertible isocyanide), which can be converted into an indole-substituted active amide, thus enabling post-polymerization modifications. The active indole amides were reacted with different nucleophiles to obtain *e.g.* carboxylic acids (by hydrolysis in tetrahydrofuran/water 10:1), esters (by alcoholysis in tetrahydrofuran/methanol 8:5), secondary and tertiary amides (by aminolysis in xylene *via* triazabicyclodecene (TBD)

catalysis), and thioesters (by reaction with thiols) as polymer side groups.[125] Another example of monomer synthesis *via* the Passerini reaction utilizing a convertible isocyanide (*N*-acylindole) was reported by Gianneschi *et al.*[126] The resulting α-hydroxy carboxylic acid monomers were converted to side chain-functionalized hemilactides and subsequently copolymerized with dilactide to poly(α-hydroxy acid)-copolymers.[126] Meier, Hoogenboom, *et al.* postmodified poly(2-oxazoline)s by Passerini and Ugi reactions in order to tune the lower critical solution temperature (LCST) of the resulting polymers in water.[127] The Passerini reaction also enabled the synthesis of star-shaped block copolymers with various side chains and arm lengths[128] and the preparation of dendrimers.[129] Amphiphilic copolymers for potential applications in the biomedical field were synthesized by Passerini polymerization in the group of Xie.[130] Li *et al.* described the synthesis of poly(ε-caprolactone)s *via* Passerini multicomponent polymerization of 6-oxohexanoic acid with five different isocyanides yielding water-soluble polymers, bearing oligo ethylene glycol side chains.[131] Polyacrylates, incorporating a limonene derived sidechain, originating from a limonene-based aldehyde (by catalytic oxidation), were prepared by a Passerini reaction of the limonene aldehyde with acrylic acid and subsequent free radical polymerization of the Passerini acrylate monomers.[132] Another monomer-based approach utilized styrene monomers, produced by the reaction of 3-vinylbenzaldehyde with different isocyanides and carboxylic acids resulting in a series of 15 different (meth)acrylic- and styrene monomers which were subsequently polymerized *via* RAFT.[133] Comprehensive reviews of the Passerini reaction in polymer science can be found in literature.[24,25]

2.1.3 The Ugi reaction

The Ugi reaction (discovered 1959 by Ivar Ugi) is another isocyanide-based MCR and utilizes, in comparison to the Passerini reaction, an amine as fourth component.[134,135] In the Ugi four-component reaction (see **Scheme 8**) a carbonyl component reacts with an amine and initially forms an imine **17**. The imine (Schiff base) **17** is activated *via* protonation from the carboxylic acid and then reacts with the isocyanide in an α-addition to from an acylated isoamide **18**. The intermediate **18** undergoes an irreversible Mumm rearrangement[136] to from the thermodynamically favored *bis*-amide

Ugi product **6** displaying four defined side chains, introduced by the four starting components. The variation of the precursor components creates molecular diversity with minimal synthetic effort.[137] Compared to Passerini products, the Ugi products display two amide bonds instead of one ester and one amide bond. Hence, the Ugi products are chemically and thermally more stable against hydrolysis than Passerini products (due to the amide resonance stabilization). Since the Ugi reaction is assumed to proceed *via* an ionic mechanism, the utilization of polar protic solvents, such as methanol, is favorable in terms of reaction efficiency and yields.

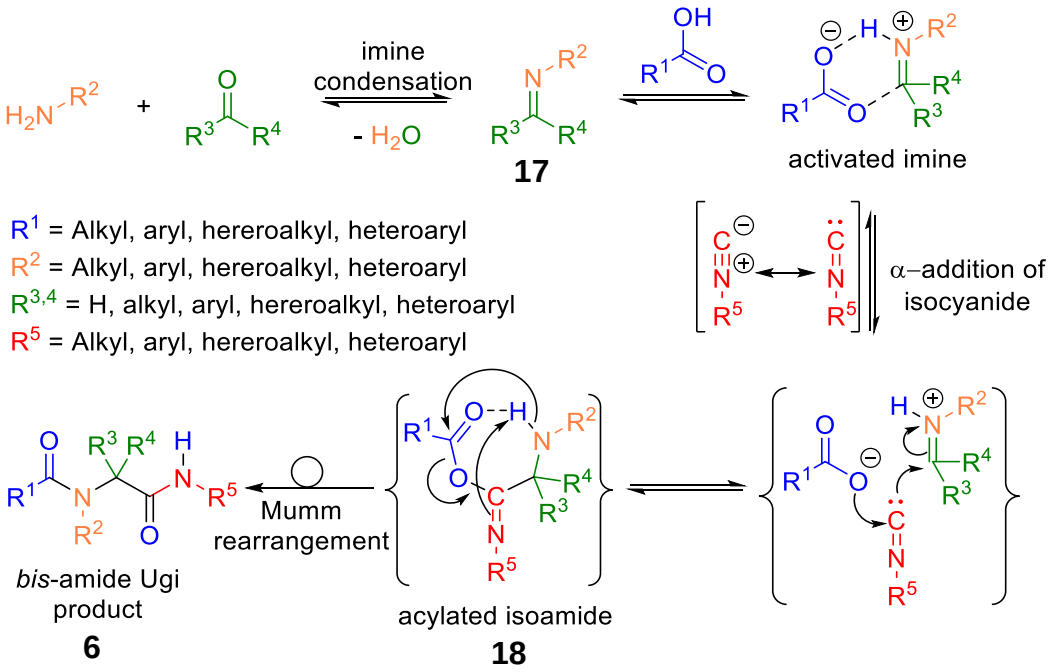

Scheme 8. Proposed mechanism of the Ugi reaction. Amine and aldehyde from an imine **17**, which is subsequently protonated. The subsequent α-addition of the isocyanide results in the formation of **18**. Mumm rearrangement of **18** results in the irreversible formation of the Ugi *bis*-amide product **6**.

The addition of Lewis acids can promote the Ugi reaction *via* activation of the imine.[138] Experimental evidence for the generally accepted mechanism presented in **Scheme 8** was observed by *in situ* ESI-MS/MS experiments of Ugi reactions in methanol.[139,140] Furthermore, the acylated isoamide intermediate **18** could be isolated.[141] However, alternative mechanisms are described in literature. For instance, the α-addition is discussed to proceed in a stepwise manner instead of proceeding in a concerted fashion, thus allowing two plausible pathways (see **Scheme 9**): *i*. first the protonated imine reacts with the isocyanide to a nitrilium ion, followed by subsequent addition of the carboxylic acid; *ii*. the carboxylic acid reacts with the activated imine first to a hemiaminal, followed by insertion of the isocyanide. Density functional theory (DFT) quantum mechanical modelling suggested a protic mechanism in methanol, wherein methanol also promotes the Mumm rearrangement. In toluene, a non-ionic mechanism

is proposed.[142] Furthermore, a second carboxylic acid molecule was proposed to catalyze the rearrangement reaction, similar postulations were previously mentioned for the Passerini reaction.[105,106] The aforementioned pathway *ii*. *via* the hemiaminal, was calculated to be favored for toluene as solvent.[142] Investigations on stereoselective Ugi reactions indicated that the reaction of the iminium ion with the carboxylic acid is probably the stereo directive step.[107]

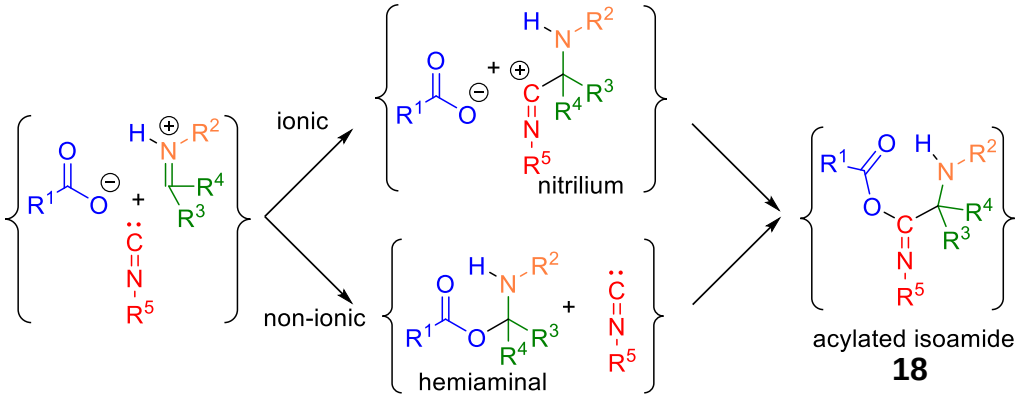

Scheme 9. Stepwise α-addition proceeding *via* an ionic or non-ionic mechanism.

The utilization of chiral isocyanides, carboxylic acids or carbonyl components did not significantly induce enantio- or stereoselectivity. However, chiral glycosylamines enable stereoselective Ugi reactions, allowing the synthesis of non-natural (R)-α-amino acids.[113,143] Chiral ferrocenylalkylamines could also be employed for stereoselective Ugi reactions.[144] Later improvements of this procedure enabled reisolation of the chiral auxiliary after mild hydrolysis[145] and heterogenization on a solid support.[146] Considering the amine-component, primary and secondary amines, hydroxylamines and hydrazine derivatives can be employed.[135] Besides the classical four components, a variety of subsidiary components can be employed for Ugi reactions (see **Scheme 10**). In this context water, cyanates, thiocyanates, or hydrogensulfides can react in Ugi type reactions (as substitute for the carboxylic acid), enabling the preparation of versatile product scaffolds.[135,147] In the so-called Ugi five-component reaction (**Scheme 10 b**) carbamates can be obtained while the acidic component is formed *in situ* by applying carbon dioxide pressure to an alcohol.[148] This reaction was reported to be most effective for low molar mass alcohols (*e.g.* methanol, ethanol, trifluoromethanol, allyl alcohol). If higher alcohols were employed, yields decreased.[149] The scope of the Ugi five-component reaction was extended to the use of carbonyl sulfide (COS) yielding carbamate-thioamides and carbon disulfide (CS_2) resulting in α-aminothioamides.[149] The utilization of isocyanic acid derivatives leads to the formation of hydantoin analogues (**Scheme 10 c**).[150] In the so-called Ugi-Smiles

reaction (**Scheme 10 d**), phenols substituted with electron withdrawing groups (increasing the acidity, *e.g. o*-nitrophenols) can participate as carboxylic acid substitutes.[151] Furthermore, the Ugi-Smiles reaction was described with pyridine and quinoline derivatives.[152] In the Ugi-Smiles reaction mechanism, the last step is a Smiles-rearrangement instead of a Mumm-rearrangement.

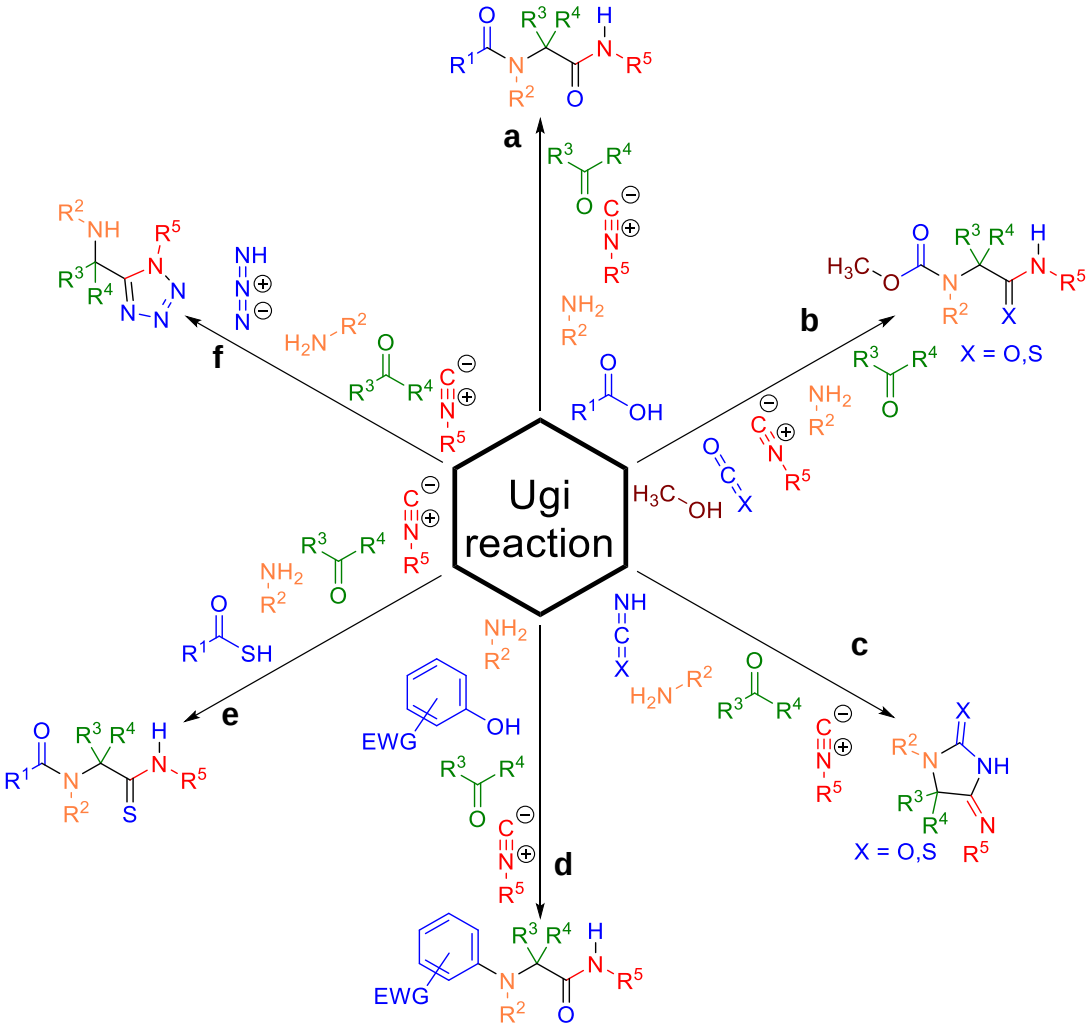

Scheme 10. Variations of the Ugi reaction. **a**, conventional Ugi reaction. **b**, Ugi five-component reaction employing carbon dioxide or carbonyl sulfide. **c**, Ugi reaction of isocyanic acid derivatives resulting in hydantoins. **d**, Ugi-Simles reaction of substituted phenols. EWG = electron withdrawing group **e**, Ugi reaction of thiocarboxylic acids. **f**, Ugi reaction of hydrazoic acid resulting in tetrazoles.

The Smiles-rearrangement (discovered in 1931) was initially described as a rearrangement reaction of hydroxy sulphones to the corresponding sulphinic acids.[153] If thiocarboxylic acids (**Scheme 10 e**) are employed, thioamides can be obtained. The reaction of hydrazoic acids (reacting in analogy to carboxylic acids) with isocyanides, carbonyl components and amines leads to the formation of 1,5-substituted tetrazoles (**Scheme 10 f**).[154]

2.1.3.1 The Ugi reaction in combinatorial and medicinal chemistry

Similar to many other multicomponent reactions, also the Ugi reaction was applied as a versatile tool for combinatorial and medicinal chemistry. For instance, pyridine-4-carboxy and pyrazine carboxy pharmacophores (also present in the antibiotics isoniazid and pyrazinamide, **Figure 2**) were employed in the Ugi reaction as carboxylic acid components. Two libraries of 192 compounds each were produced, and the crude materials were tested directly against *M. tuberculosis* after evaporation of the solvents. Compounds with more than 90% inhibition efficiency were resynthesized, purified and evaluated again with respect to their minimum inhibitory activity (MIC) and cytotoxicity (IC50) against *M. tuberculosis*.[155] The two best candidates of the screening are presented in **Figure 2 a**.

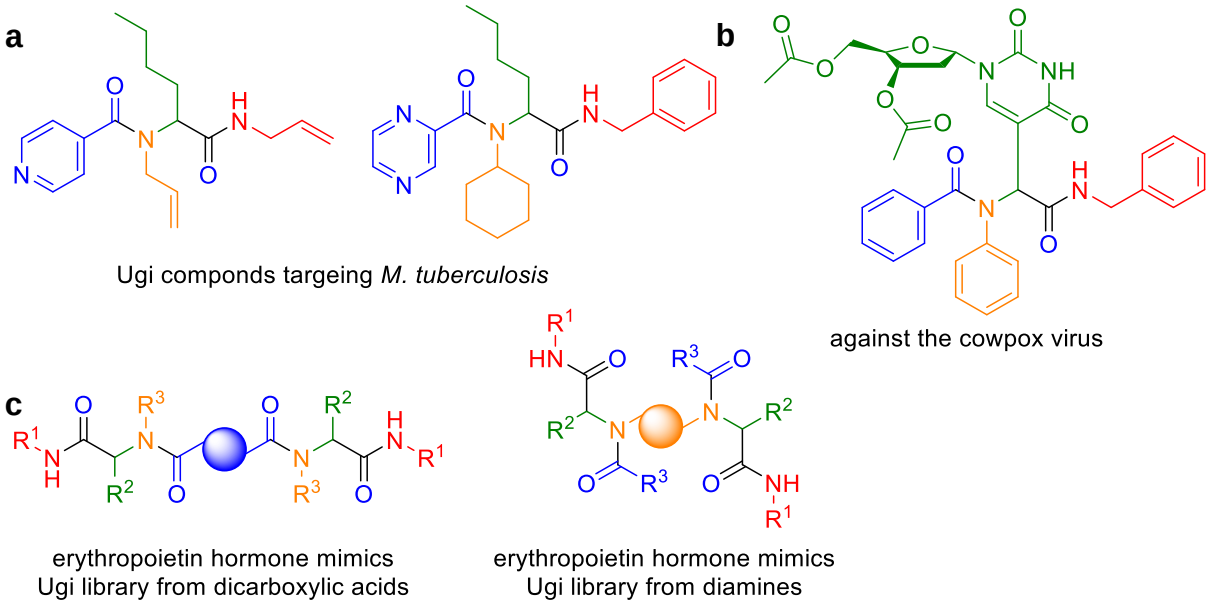

Figure 2. Selected examples of the Ugi reaction in medicinal chemistry.[118] **a**, most potent Ugi antituberculotic compounds (MIC = 3.13 µg·mL^{-1} for both, IC_{50} = 31.1 µg·mL^{-1} for left compound and 27.9 µg·mL^{-1} for the right compound).[155] **b**, Ugi compound targeting the cowpox virus and *Leishmania* parasites.[156] **c**, Ugi compounds derived from dicarboxylic acids or diamines mimicking the EPO hormone.[119]

In another Ugi approach, 5-formyl-20-deoxyuridine was employed as aldehyde component, resulting in a library of 25 different 20-deoxyuridine Ugi compounds, which were tested as antiviral agents (against cowpox) and against protozoa parasites of the *Leishmania* type.[156] A promising compound discovered in this screening is shown in **Figure 2 b**. Furthermore, quinoline containing Ugi compounds were evaluated as anti-malarial drugs.[157] Dömling *et al.* synthesized two libraries comprising 88 Ugi compounds each, utilizing bifunctional components (dicarboxylic acids or diamines,

see **Figure 2 c**).[119] This approach was previously described for the Passerini reaction in chapter **2.1.2.1**. Reviews describing the Ugi reaction in medicinal and combinatorial chemistry can be found in literature.[115,118,121,122]

2.1.3.2 The Ugi reaction in polymer science

The Ugi reaction allows the precise installment of four different side chains, which was not only appreciated in combinatorial chemistry, but also in synthetic polymer chemistry. Due to the modular nature of the Ugi reaction, the properties of monomers and the respective polymers can be tuned. Similar to the Passerini reaction, the Ugi reaction was utilized to prepare α,ω-diene monomers for ADMET polymerization, resulting in highly functionalized polyamides.[48] In addition, the Ugi reaction was utilized to prepare functionalized acrylamide monomers, each displaying three different side chains.[158] Performing the Ugi reaction with acrylic acid (and different carbonyl components, amines and isocyanides) resulted in 14 different monomers, which were successfully polymerized *via* free radical polymerization.[47] Tao *et al.* employed the Ugi reaction under mild conditions for the synthesis of middle-functional block copolymers.[67] Similar to other multicomponent reactions, the Ugi reaction was also employed as step-growth polymerization method (in this case the polymerization is described as a polycondensation due to the imine formation). Meier *et al.* optimized the Ugi polymerization conditions and evaluated different combinations of bifunctional and monofunctional components (the Ugi polymerization offers six possible combinations of AA- and BB-type monomers *e.g.* diisocyanide + dialdehyde, diamine + diisocyanide, *etc.*).[66] Despite the fact that Ugi reactions usually provide the best results in methanol, a mixture of tetrahydrofuran/methanol was necessary to prevent precipitation of the growing oligomers during the polymerization. Luxenhofer *et al.* investigated Ugi polymerization with respect to the six above-mentioned combinations of components for polymers with aromatic moieties, utilizing *N*-methyl-2-pyrrolidone (NMP) as polar aprotic solvent (**Scheme 11 a**).[159] Besides a classical Ugi four-component polycondensation, a Ugi five-component polycondensation enabling the incorporation of carbon dioxide into the respective polymers was reported (see **Scheme 11 c**).[160] The resulting polymers could subsequently be converted into the corresponding poly(hydantoin)s upon treatment with a potassium hydroxide

solution, resulting in a decrease of the glass transition temperature (from 37 to 0 °C in one example).[160] The direct polymerization of levulinic acid (which otherwise needs to be modified prior to polymerization) was reported by Becer *et al.* utilizing the Ugi polycondensation (**Scheme 11 b**).

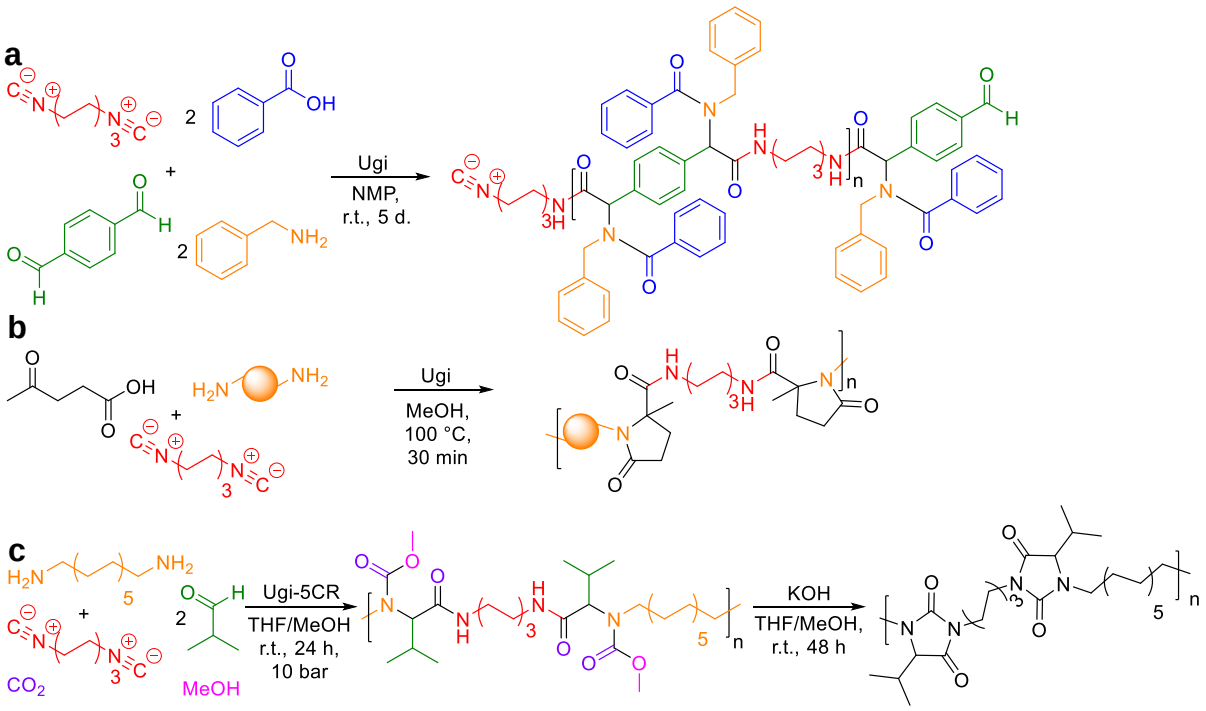

Scheme 11. Selected examples of the Ugi reaction in polymer chemistry.[24] **a**, Ugi polymerization of aromatic monomers.[159] **b**, direct Ugi polycondensation of levulinic acid.[161] **c**, Ugi five-component polycondensation with CO_2 and post-polymerization modification to obtain polyhydantoins.[160]

Levulinic acid can be obtained from renewable resources and displays two functional groups participating in Ugi reactions (carboxylic acid and ketone), hence reacting as an AB-type monomer in the Ugi polymerization.[161] Another type of AB-type monomers in the Ugi reaction was exploited by utilizing natural amino acids resulting in polypeptoid structures. In this investigation it was found, that the reaction of α-amino acids, such as glycine or alanine, leads to the formation of six-membered rings. Nevertheless, lysine (containing an ε-amino group), enabled direct polymerization (after α-amino protection with *tert*-butyloxycarbonyl (BOC)). After the polymerization, the BOC protecting groups were cleaved.[162] As for the Passerini reaction, also several Ugi approaches were applied for dendrimer synthesis.[163,164] Comprehensive reviews on the Ugi reaction in polymer science have already been published.[24,25]

2.2 Tandem multicomponent reactions

Tandem reactions (or cascade[37] and domino reactions[165]) are chemical transformations involving at least two independent reactions with different functional groups participating in either one of the reactions (*via* distinct or orthogonal chemical reactivities).[166–169] Remarkably, in literature the term tandem reaction is not entirely used in consistence with the initial definition by Tieze *et al*.[165] In literature, only a few examples of multicomponent tandem reactions are described.[28,170] For instance, Portlock *et al.* described a Petasis-Ugi tandem reaction, forming products with six different side chains.[171,172] The group of Al-Tel *et al.* combined Passerini or Ugi reactions with the Groebke-Blackburn reaction in a sequential one-pot procedure.[173] Up to eight components were reacted by the combination of three multicomponent reactions by Orru *et al*.[174] In 2010, Westermann *et al.* combined the Ugi reaction and the Ugi-Smiles reaction.[175] Wipf *et al.* synthesized a library of twelve Biginelli compounds and subsequently reacted them with suitable Ugi components under reflux in methanol to yield 30 different DHMP amides in 5 – 51% yield.[176] The Biginelli reaction has been applied in a multicomponent step-growth polymerization combined with the Hantzsch reaction resulting in copolycondensates.[98] Furthermore, the Ugi reaction was combined with the Biginelli reaction by Brodsky *et al.*[177]

2.3 Perfluoroalkyls and fluorous solid phase extraction (F-SPE)

Perfluorocarbon alkyl chains exhibit remarkably different properties if comparison to the respective alkane equivalents. The special nature of these perfluoroalkyl chains originates from the numerous C-F-bonds. Generally, the C-F-bond is the most stable carbon-heteroatom single bond in organic chemistry[178] (C-F-bond energy: 489 kJ·mol^{-1}, C-H-bond energy: 413 kJ·mol^{-1}).[179] C-F bonds are dominated by the high electronegativity of fluorine, the slightly larger Van-der-Waals radius, the smaller polarizability and a higher ionization potential of fluorine compared to hydrogen. Furthermore, hydrocarbon chains are likely to form “zick-zack” structures, while in contrast, perfluoroalkyl chains are less flexible and tend to adapt helical conformations.[180] Hence, perfluoroalkyl chains occupy more space than equivalent alkanes (*e.g.* the volume required for a CF_2-group is approximately 38 Å^3, whereas the

volume of the CH_2 group is *ca.* 27 Å^3).[181] Due to the low polarizability of fluorine, the Van-der-Waals interactions between fluorinated chains are comparably weak. Consequently, fluorocarbons are characterized by low dielectric constants, high vapour pressure and compressibility, low surface tension, high gas solubility and high surface activity in aqueous solutions. Perfluorinated substrates do not favour intermolecular interactions *via* Van-der-Waals forces[181] and thus display very weak interactions with other molecules. In multi-phasic systems, nonfluorinated solvents preferably interact with themselves instead of the perfluorinated molecule (hydrophobic effect, in this case entropy is balanced or overcome by enthalpy). Thus, fluorocarbons exhibit the interesting property of being both hydrophobic and lipophobic, which leads to the formation of triphasic systems. The unique properties of perfluorinated substrates were also utilized in the so-called fluorous solid phase extraction method (F-SPE, see **Scheme 12**).

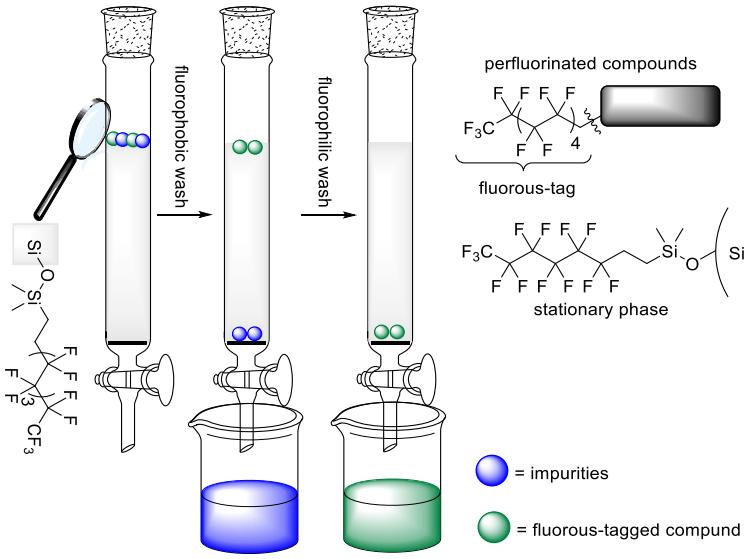

Scheme 12. F-SPE employing fluorous silica gel *e.g.* Fluoro*Flash*® (-$SiMe_2(CH_2)_2C_8F_{17}$) for the purification of F-tagged compounds.[182]

F-SPE enables the separation of perfluorinated substances based on the concept of fluorophilicity (*vice versa* meaning hydro- and lipophobicity). Fluorophilicity is defined as the partition coefficient (ln P) of a substance between equal volumes of perfluoromethylcyclohexane ($CF_3C_6F_{11}$) and toluene.[183] F-SPE chromatography separation protocols were categorised into standard F-SPE and reverse F-SPE. The standard F-SPE employs silica gel equipped with perfluorinated alkyl chains as stationary phase and non-fluorinated solvents as mobile phase. On the contrary, the reverse F-SPE technique utilizes unmodified silica gel as stationary phase and the fluorous components are eluted with a perfluorinated eluent (*e.g.* perfluorohexane or perfluorobutyl-methyl ether sometimes blended with ethyl acetate).[184] In the present

thesis, standard F-SPE was utilized for the purification of perfluoroalkyl-substituted Ugi compounds and is therefore explained in more detail. The fluorous silica gel for standard F-SPE is commercially available under several trade names *e.g.* Fluoro*Flash*® or Silia*Bond*® (synthesized from silica gel and dimethyl[2-(perfluorohexyl)ethyl]silyl chloride).[185] In standard F-SPE, a mixture containing fluorous and a non-fluorous components is separated by first eluting organic non-fluorous compounds with fluorophobic eluents. Fluorophobic eluents are, *e.g.* mixtures of organic solvents and small amounts of water to reduce the fluorophilicity. Prominent examples are methanol/water (4:1), acetonitrile/water (3:2) or pure dimethyl sulfoxide (utilized in case a of water sensitive components). This first elution step is called the "fluorophobic pass" (illustrated in **Scheme 12**) and elutes the organic non-fluorous fraction. In a following step, the "fluorophilic pass", the perfluorinated compounds, so-called fluorous-tagged molecules (F-tag), can be obtained by eluting with a fluorophilic solvent (*e.g.* pure methanol, acetonitrile or tetrahydrofuran), resulting in a fluorous fraction. In general, the F-SPE procedure is robust, straight-forward, offers operational simplicity, is time efficient and can be implemented in automated systems without great effort.[186]

2.4 Sequence-defined macromolecules

Parts of this chapter and following subchapters were adapted from previous passages written by the author.[19,21,24]

Sequence-defined macromolecules are uniform[187] (monodisperse) compounds, consisting of different monomers, arranged in exactly defined positions. In nature, highly precise sequence-defined macromolecular structures *e.g.* DNA, proteins, enzymes, *etc.* are essential for life.[188] Hence, non-natural synthetic sequence-defined macromolecules are inspired by nature and gained significant scientific interest recently, since the properties of polymeric substances directly correlate to their molecular structure, composition and molar mass.[19] Precise control allows to achieve and adjust new features and functions of synthetic macromolecular architectures, facing the increasing demand for tailored materials in polymer science and engineering.[189] Sequence-defined macromolecules can potentially exhibit manifold

properties, *e.g.* self-assembly,[190–192] catalytic activity,[193] molecular recognition or self-replication,[194] offering numerous possible applications, for instance in data storage,[20,195] cell signaling,[196] biocatalysis,[197] and life sciences.[198] Hitherto, the synthesis of artificial sequence-defined macromolecules is considered one of the major challenges in polymer chemistry.[18] An extensive review on sequence-defined macromolecules can be found in literature, wherein different synthetic approaches (*e.g.* liquid phase, solid-phase, fluorous-phase and polymer-tethered synthesis), also including conjugated macromolecules, are discussed.[19] Selected examples are also presented here.

Du Prez *et al.* reported a solid support approach towards sequence-defined oligomers based on iterative and thiolactone chemistry (**Scheme 13**).[199] Two thiolactone building blocks and a second isocyanato thiolactone building block were synthesized. A 2-chlorotrityl chloride resin (solid support) was functionalized with a thiolactone moiety in a coupling efficiency of 53%.

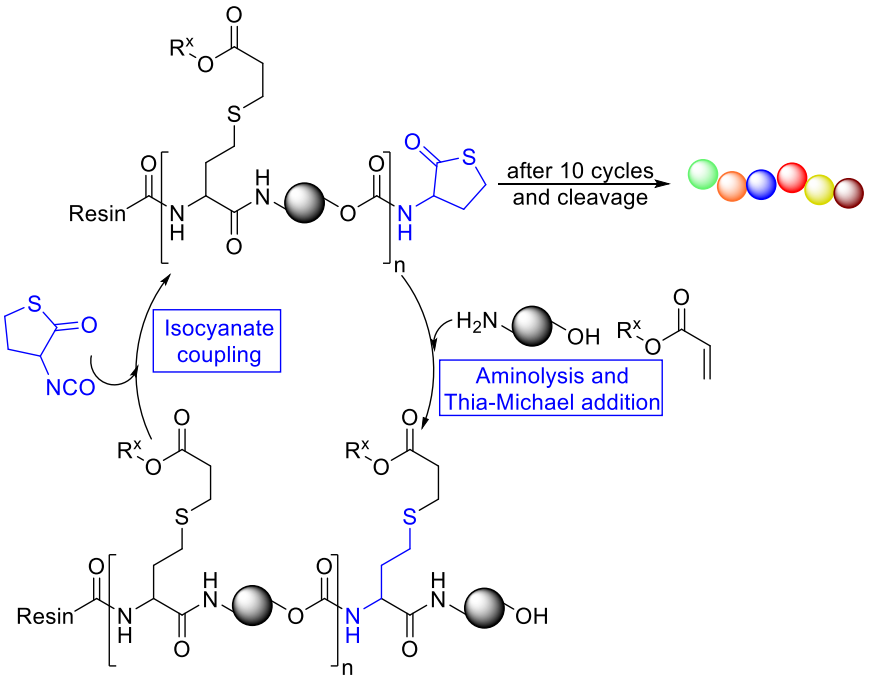

Scheme 13. Macromolecules prepared *via* thiolactone chemistry. Aminolytic ring-opening of the thiolactone releases a thiol, which is subsequently reacted in a thia-Michael addition with an acrylate. Chain-extension was achieved by reacting the hydroxyl group with the isocyanato group of the thiolactone building block.[199]

The iterative synthetic cycles employ ring-opening of the immobilized thiolactone using an amino alcohol (*e.g.* ethanolamine or 4-amino-1-butanol) in the first step, releasing a thiol group. The thiol functionality is then reacted *in situ* with an acrylamide or an acrylate in a thia-Michael addition. In the second step, chain extension is achieved *via*

the reaction of the hydroxyl group (introduced by the amino alcohol) with the isocyanato group of the thiolactone building block. The current strategy enabled the synthesis of several sequence-defined decamers, which were prepared by hand manually and by automated processes. Compared to the manual approach, the decamers from the synthesizer contained small impurities, for instance nonamers or degraded decamers (missing the thiolactone unit). The macromolecules were characterized by NMR spectroscopy, LC-ESI-MS and HRMS.

Barner-Kowollik *et al.* investigated a bidirectional, photochemical approach towards sequence-defined macromolecules.[200] A first monomer, equipped with a *ortho*-methyl benzaldehyde (photoenol) and a sorbyl ester group as well as a second monomer, equipped with a phenacyl sulfide group and a protected maleimide group, were prepared in yields of 59% and 54%, respectively (see **Scheme 14 c**).

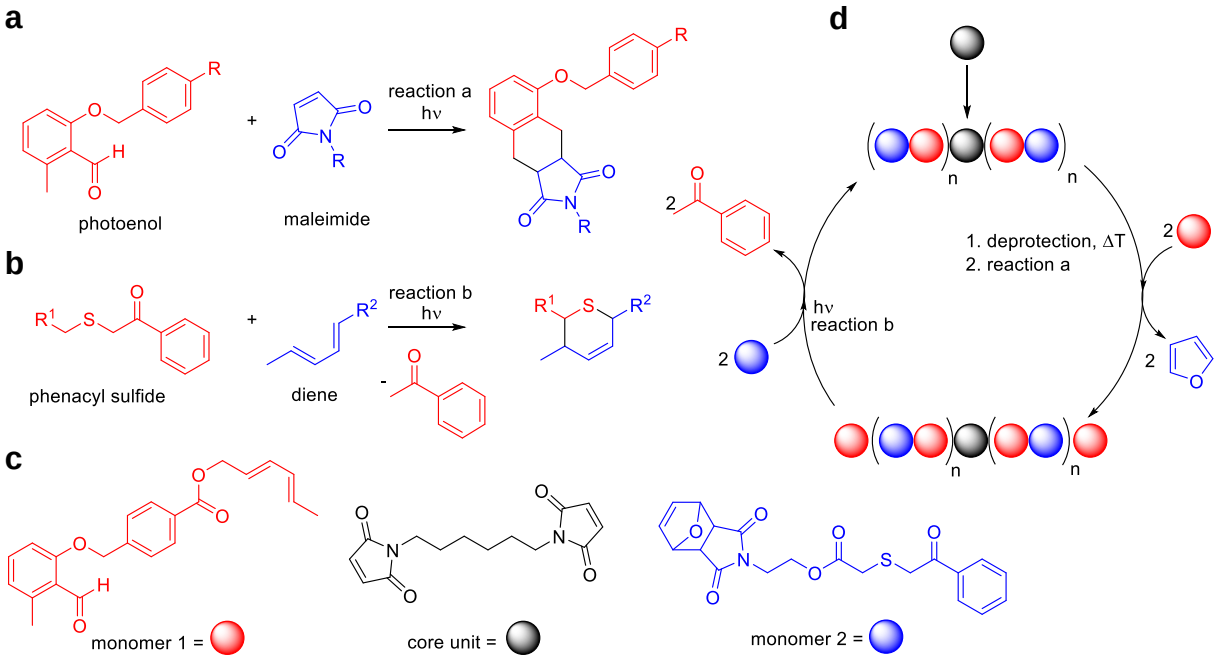

Scheme 14. a & **b**, Photochemical reactions utilized by Barner-Kowollik *et al.* for the synthesis of sequence-defined macromolecules.[200] **c**, monomer structures. **d**, bidirectional growth synthetic strategy utilizing reactions **a** and **b**.

A symmetric core unit equipped with two terminal maleimides was reacted with the photoenol-sorbyl ester monomer (see **Scheme 14 a**). The terminal sorbyl ester was subsequently reacted with a photochemically activated phenacyl sulfide (second monomer) (see **Scheme 14 b**). The phenacyl sulfide monomers were further equipped with a furan-protected maleimide. The furan protective group was removed in a retro-Diels-Alder reaction, resulting in a terminal maleimide group for further synthetic cycles (see **Scheme 14 d**). A sequence-defined decamer was obtained in seven steps in an

overall yield of 1% and analyzed *via* SEC and MALDI-ToF-MS. The structural variation using the afore described photochemical approach was demonstrated by the same group utilizing of a set of different monomers.[201] The resulting sequence-defined macromolecules were characterized by NMR spectroscopy, UV/Vis spectroscopy, ESI-MS, SEC and sequenced by MALDI-ToF-ToF-MS.

An example for sequence-defined macromolecules purified *via* fluorous separation was demonstrated by Anderson *et al*.[202] In this work, hydroxyproline monomers coupled to a F-tag were utilizing in an iterative approach (see **Scheme 15**). A variety of different hydroxyproline blocks were employed in consecutive carbonyldiimidazole-mediated carbamate formation reactions.

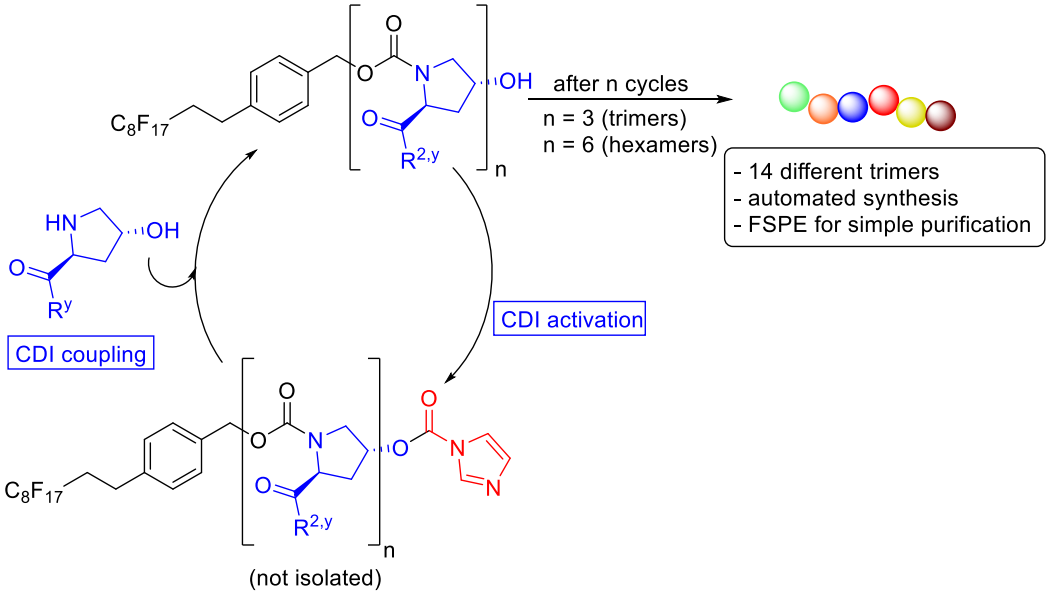

Scheme 15. Fluorous supported synthesis of sequence-defined hydroxyproline macromolecules by Anderson *et al*.[202] CDI: Carbonyldiimidazole.

Using an automated system and FSPE technique, 14 sequence-defined oligomers with three repeating units each were obtained in yields between 14% and 97% and purities between 73% and 100% (determined *via* HPLC). The oligomers were characterized by LC-MS and NMR spectroscopy. Moreover, four sequence-defined macromolecules with six repeating units were synthesized (91% purity is reported for one representative example) and characterized *via* LC-MS.[202]

2.4.1 Sequence-defined macromolecules *via* multicomponent reactions

This chapter mainly focuses on sequence-defined macromolecules synthesized *via* multicomponent reactions. Multicomponent reactions (MCRs) already proved to be very suitable reactions for the preparation of sequence-defined macromolecules and contributed to a great extent in this field. MCRs offer the great advantage of introducing different defined side chains into a macromolecule by variation of one reacting component. The other reacting components allow chain growth utilizing so-called iterative approaches, wherein each monomer unit is installed after another, in a stepwise fashion (see **Scheme 16 a** for a three-component reaction, utilizing the functional groups A+B+C).

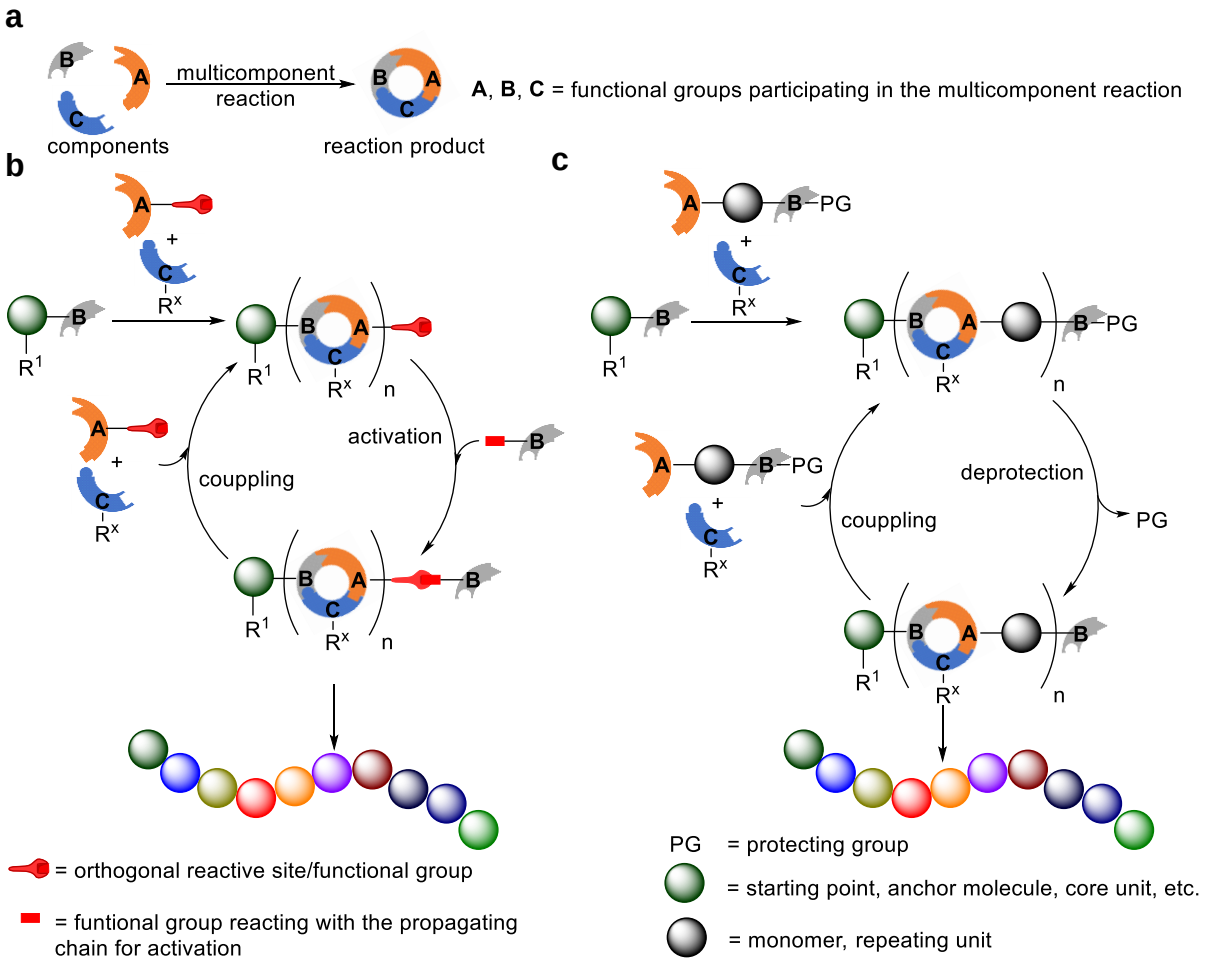

Scheme 16. Iterative step-growth polymerizations *via* multicomponent strategies for the synthesis of sequence-defined macromolecules. **a**, general reaction scheme of the multicomponent reaction A+B+C. **b**, activation-based approach where the growing chain is reacted with a bifunctional substrate displaying an orthogonal reactive site and functional group B. Sequence-definition is achieved by introducing different side chains R^x, through variation of the component with functional group C. **c**, protective group-based approach. In order to propagate the growing chain, the protective group needs to be removed to release functional group B.

For instance, bifunctional monomers equipped with the reactive functional groups A or B can be reacted with a third component bearing functional group C (utilizing A and B for chain growth, while C introduces different side chains). By variation of components (different R^x), sequence definition is achieved, while the degree of polymerization/molar mass depends on the number of iterative reaction steps/cycles. Iterative approaches require the implementation of orthogonal reactions *via e.g.* an activation step (**Scheme 16 b**) or a protective group strategy (**Scheme 16 c**). If a synthesis employing more than three components is utilized, additional side chains can be introduced within the same reaction step and architectures of higher complexity can be generated. In iterative step growth approaches, high yields for the individual reaction step are an important benchmark for efficient chain growth, scalability and applicability of the overall strategy. Thus, suggesting the use of optimized reaction conditions and selective MCRs *e.g.* the Passerini reaction along with robust purification protocols.

In 2014, Meier *et al.* introduced an iterative activation-based approach towards the synthesis of sequence-defined macromolecules based on iterative Passerini and subsequent thiol–ene additions (**Scheme 17 a**).[45] For the Passerini reactions, undec-10-enal was utilized as aldehyde component, which carries a terminal double bond enabling orthogonal thiol-ene reactions. Variation of the isocyanide component introduced several defined side chains. After each Passerini step, the terminal double bond of the unsaturated aldehyde side chain was reacted in a thiol-ene addition with 3-mercaptopropionic acid, for the introduction of another carboxylic acid to the growing chain. After the next Passerini reaction with undec-10-enal and another isocyanide component, the iteration of one cycle is completed. Stearic acid was chosen as starting acid. After seven steps and purification *via* column chromatography (after Passerini steps) or recrystallization (after thiol–ene additions), a sequence-defined tetramer (four different side chains) was obtained in an overall yield of 26% (120 mg, see **Scheme 17 c**).[45] An alternative approach in terms of purification was conducted utilizing a soluble poly(ethylene glycol) support equipped with a carboxylic acid functional group as starting component. This polymer support enabled simple precipitation of the crude reaction mixtures into a solvent with poor solubility for the polymer-tethered macromolecules (*e.g.* cold diethyl ether) for purification (more time efficient than column chromatography). This strategy introduced five sequence-defined repeating units, in 34% overall yield after nine reaction steps.[45]

In another work, an iterative strategy utilizing the Ugi reaction was exploited (**Scheme 17 b**).[203] Due to the application of an amine as fourth component, the Ugi reaction enabled the installation of a second side chain to the growing macromolecule within the same reaction step. Hence, in every repeating unit, a so-called dual side chain control was achieved.

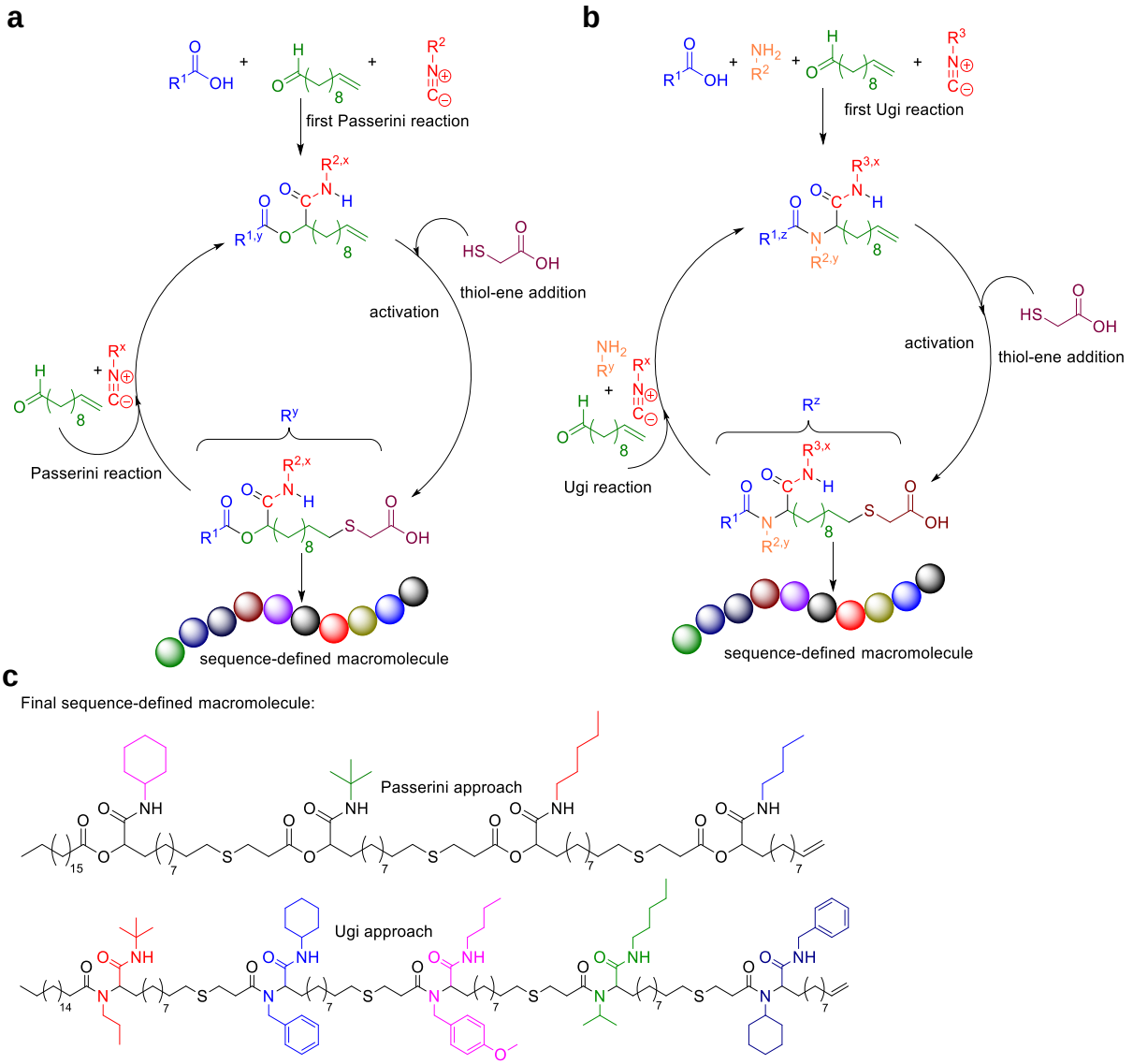

Scheme 17. Activation-based approaches towards sequence-defined macromolecules *via* multicomponent strategies. **a**, by iterative Passerini and thiol-ene reactions.[45] **b**, by iterative Ugi and thiol-ene reactions.[203] **c**, structures of the respective macromolecules.

The first Ugi reaction was conducted with stearic acid as starting point, *tert*-butyl isocyanide and undec-10-enal (again enabling subsequent thiol-ene reactions on the terminal double bond) in combination with varying amine components. After each Ugi step, the terminal double bond of the unsaturated side chain was reacted with 3-mercaptopropionic acid in a thiol–ene addition to introduce another carboxylic acid moiety. A sequence-defined tetramer with four sequence-defined side chains (derived

from the varying amine components) was synthesized in an overall yield of 15% (purification was analogous to the Passerini approach). In a similar approach, both the amine and the isocyanide components were varied in each Ugi step (**Scheme 17 b**), resulting in a sequence-defined pentamer equipped with ten defined side chains in an overall yield of 15% (**Scheme 17 c**).[203] The aforementioned deprotection-based approach (**Scheme 16 c**) was explored *via* combining iterative Passerini- and benzyl ester deprotection reactions.[204] For this approach, a monoprotected, linear AB-type monomer comprising on the one terminus a benzyl-protected carboxylic acid and on the other terminus an isocyanide functional group was employed. The AB-type monomer was synthesized in three steps starting from commercially available 11-aminoundecanoic acid in an overall yield of 63%. The isocyanide-benzyl ester monomer was employed in Passerini reactions with varying aldehyde components in each iterative cycle, introducing sequence-defined side chains into the growing macromolecule (**Scheme 18 a**). The respective Passerini reaction products (equipped with a terminal benzyl ester) were subsequently deprotected by hydrogenolysis with hydrogen gas and a heterogeneous palladium catalyst immobilized on activated charcoal to obtain a terminal free carboxylic acid (enabling further Passerini reactions). The products after each Passerini step were purified *via* column chromatography on silica gel, while the hydrogenolysis products were simply isolated by filtering off the heterogeneous catalyst. A sequence-defined macromolecule with ten different side chains (decamer, structure in **Scheme 18 b**), synthesized in 19 steps was obtained in an overall yield of 44%. In the Passerini step, an unsaturated aliphatic side chain was introduced *via* the aldehyde component for a subsequent self-metathesis reaction, resulting in a sequence-defined symmetric icosamer.[204]

In 2017, Meier and Du Prez *et al.* combined the activation-based Passerini/thiol-ene approach with the thiolactone strategy described previously. In this approach, a thiolactone-carboxylic acid monomer was employed as starting material for iterative Passerini/thiol-ene reactions, resulting in a set of four different sequence-defined trimers. The thiolactone terminated trimers were subsequently subjected to an aminolytic ring opening reaction and reacted *in situ* with an acrylate-isocyanide monomer, to from four different sequence-defined pentamers.

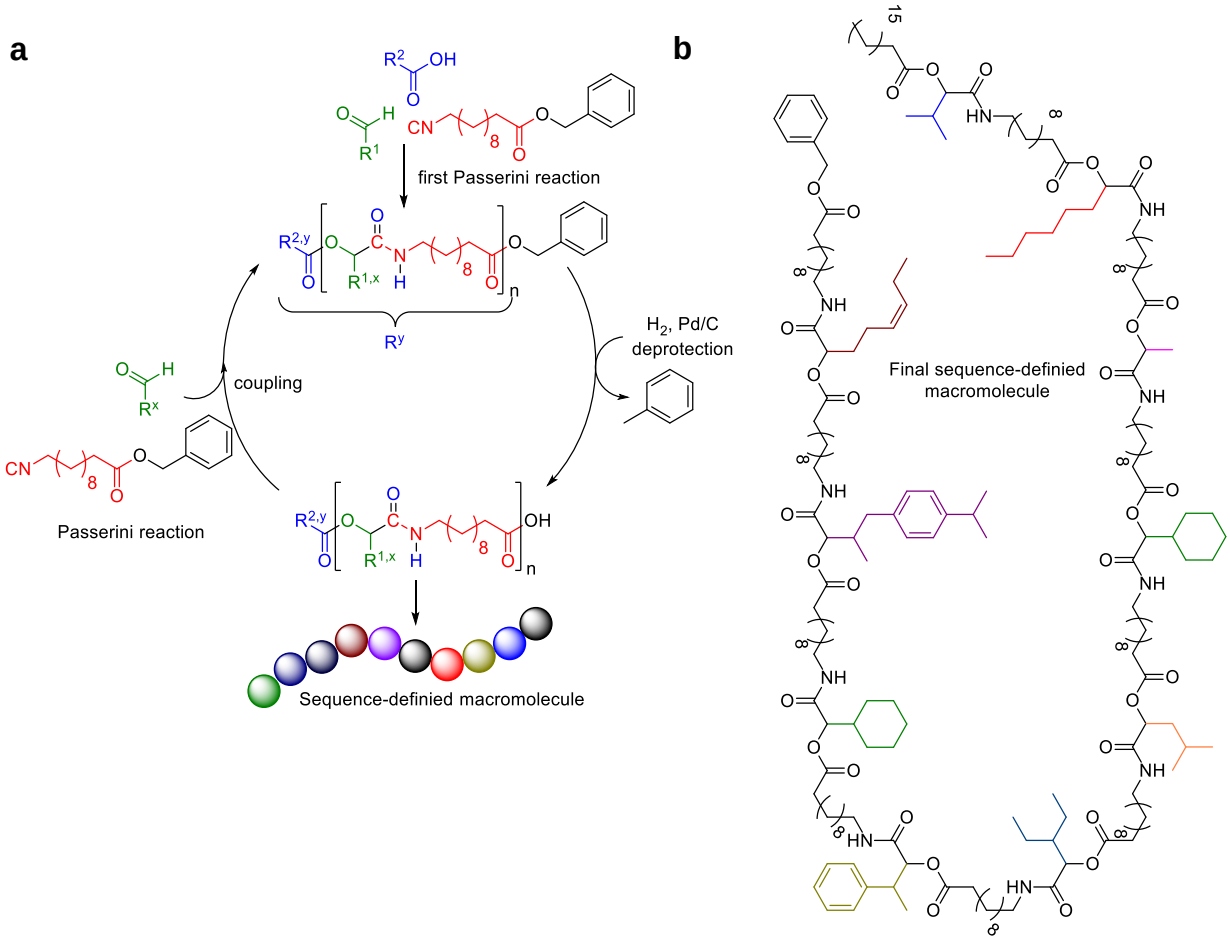

Scheme 18. Protecting group- and monomer-based approach towards sequence-defined macromolecules *via* multicomponent strategies. **a**, iterative Passerini and hydrogenolytic benzyl ester deprotection reactions. **b**, structure of the respective macromolecule (decamer).[204]

These isocyanide-acrylate terminated pentamers acted as a modular building blocks for the previously described Passerini/thiol-ene system, resulting in a macromolecule displaying 15 sequence-defined side chains.[205] Besides the activation or protecting group approaches described in **Scheme 16**, other orthogonal strategies can be employed for the synthesis of macromolecules. A selective Passerini approach utilizing 4-formylbenzoic acid and 4-isocyanobenzoic acid with aliphatic isocyanides and aldehydes was reported in 2017. The concept is based on a kinetic “chemoselectivity” claiming that aliphatic aldehyde and isocyanide groups react faster than aromatic analogs in Passerini reactions.[206] In 2018, Becer *et al.* investigated the Ugi reaction for sequence-defined peptide–peptoid hybrid structures synthesized on a solid support. Amongst other methods, the resulting macromolecules were analyzed *via* high resolution mass spectrometry and fragmented *via* tandem-MS.[207]

2.5 Data storage and encryption methods in combination with chemistry

Parts of this chapter and following subchapters were adapted from previous passages written by the author.[24,208,209]

2.5.1 Data storage devices utilizing molecular architectures

In nature, deoxyribonucleic acid (DNA), proteins, special oligosaccharides and other sequence-defined macromolecules fulfill many different purposes essential for life. DNA carries the genetic code, encoded in form of nucleobases, and can be considered as a biological information storage system. Every form of life known has a similar set of four nucleobases (adenine, cytosine, guanine and thymine for DNA or uracil instead of thymine for RNA) combined into macromolecular strands. The distinct sequence of nucleobases acts as the information storage (**Figure 3 b**). In contrast to nature, today's information technology utilizes the binary system (originating from switches, whereby 1 triggers *on* and 0 *off*). Common (and historical) employed electronic information storage systems such as *e.g.* hard drives or optical storage media, utilize the binary system to store information in sequences of 0 or 1 (**Figure 3 a**). In general aspects, data storage systems (natural and electronic) share common characteristics, for instance, systematic repeating units (1 and 0, or the four nucleobases) are combined to longer sequences in order to store information. For a comparison of different data storage systems, the total number of permutations is an important benchmark, taking the following considerations into account: a sequence of eight binary digits = 1 byte = 8 bits = 2^8 = 256 permutations; storing 256 permutations in a DNA molecule (coding with four nucleobases in a quaternary system 4^n) would theoretically require a sequence of only four nucleobases (4^4 = 256). However, the so-called Shannon information capacity[210] of one nucleotide is lower than two bits and equals approximately 1.83 bits, due to the fact that not all possible combinations of nucleotides can be realized (*e.g.* long DNA homopolymers such as poly(adenine) or DNA macromolecules containing a high content of repetitive guanine or cytosine units are currently challenging to synthesize and analyze).[13] Sequence-defined macromolecules are attractive candidates for information storage and were

investigated utilizing DNA.[5,10,13] In 2017, Erlich *et al.* reported a so-called DNA fountain data storage architecture encoding 2.1 MB (featuring 72,000 oligo-nucleotides, 32 byte each, coding 1.57 bits per nucleotide). DNA storage systems highly benefit for the well-established amplification methods, such as the polymerase chain reaction (PCR),[211,212] as well as from highly developed analytical readout methods.[213–215] The human genome in comparison consists of approximately three billion base pairs, equaling six billion bits (assuming two bits per nucleotide) leading to a storage capacity of 715 MB (which is surprisingly low).[216] This value does of cause not represent the complexity of human life in any means (a tomato genome for instance features 900 billion base pairs which equal approximately 1.07 GB).[217] Even though DNA features many advantages for data storage, there are also certain drawbacks as for example long term stability, because DNA can degrade in the presences of nucleophiles, electrophiles, water, metal ions, *etc.*[11,12] Another jet theoretical problem concerns the choice of the DNA (the information storage of life): the data encoded in DNA can accidentally (or even on purpose) encode virus sequences, which might not only affect computer systems[13] but also be pathogenic to living organisms. Non-natural sequence-defined macromolecules enable the use of different chemistry protocols offering new perspectives and opportunities for synthetic and analytic methods, thus overcoming the limitations of DNA-based data storage systems. In literature, non-natural information-coding macromolecules employing either two varying components (**Figure 3 c**, coding in a binary system, providing one bit per repeating unit)[218–222] or four varying monomers[201] (two bits per repeating unit) were described (**Figure 3 d**). In 2017, Lutz *et al.* demonstrated the synthesis and readout of a macromolecule encoding 64 bits in total. The read out was performed *via* mass spectrometry and simplified by so-called inter-byte fragmentation mediated by exactly positioned mass tags.[218] In another approach, the same group prepared digital macromolecules *via* orthogonal iterative pathways based on successive phosphoramidite and radical-radical coupling steps. In this fashion digital poly(alkoxyamine phosphodiesters) were obtained, coding 16 bits in total. The readout for data-extraction was simplified by favoring the formation of MS/MS fragments containing two bits instead of one.[223] Additional approaches also employed non-natural sequence-defined macromolecules,[201,218–222,224–226] polymeric materials[227] or molecular memory and processing devices[228] as potential data storage devices. The Passerini reaction is a versatile tool in polymer chemistry[24] (see chapter **2.1.2.2**) and

was also utilized for the synthesis of sequence-defined macromolecules (see chapter **2.4**). In the Passerini approach described in **Scheme 18**, one varying component per repeating unit was introduced, while choosing from ten different aldehyde components. Formally, the respective repeating units encode three bits, however, the macromolecules were not sequenced/read out or regarded in the context of data storage at that time.[204]

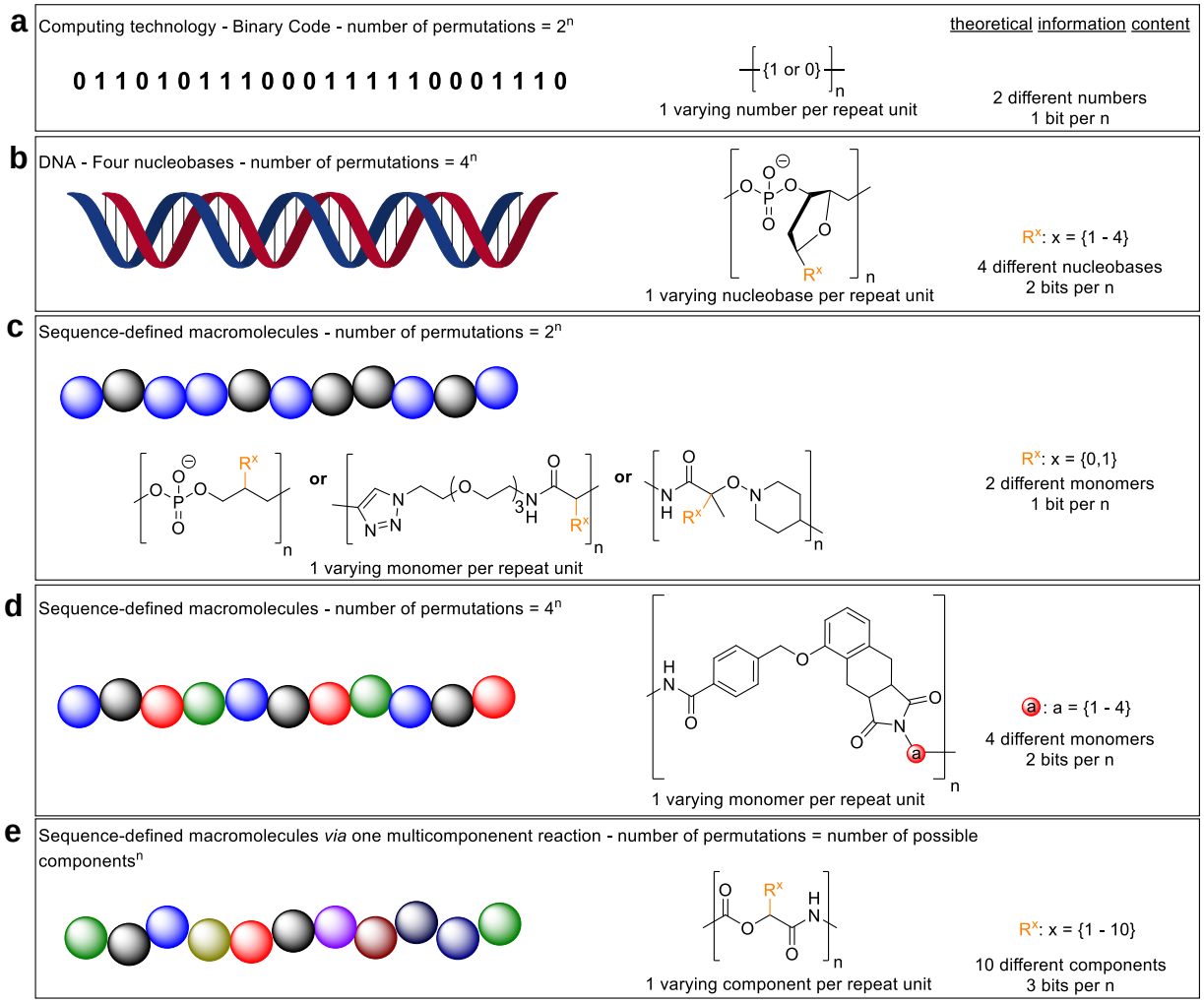

Figure 3. Comparison of selected macromolecules and the theoretical information content per repeating unit. **a**, the binary system. **b**, DNA/RNA coding within sequences of four different nucleobases, each nucleobase theoretically encodes two bits. **c**, non-natural macromolecules[222] with one varying component per repeating unit: left,[218,219] middle,[220] and right.[221] **d**, non-natural macromolecules utilizing four monomers.[201] **e**, sequence-defined macromolecules synthesized *via* the Passerini reaction utilizing ten varying components, each repeating unit formally encodes three bits, however, the sequences were not read out.[204] The theoretical bits per repeating unit were calculated by: Log(Number of possible permutations)/Log(2). The theoretical storage capacity of a macromolecule is calculated as follows: bits per repeating unit × total number of repeating units.

The Ugi approach described in **Scheme 17** led to sequence-defined macromolecules with two varying components per repeating unit, while choosing from five different isocyanides and five different amine components (in total ten components, thus also

encoding three bits per repeating unit, however the macromolecules were not read out or considered for data storage at that time).[229]

2.5.2 Secret communication *via* molecules

In today's digital world, data security, in all facets ranging from every day applications, professional environments to espionage, is of great importance. Even though the goal of ultimate security is unreachable, constant progress and advances in the fields of cryptography and steganography, evolving with the possibilities and demands of new technologies on the one hand and the steadily increasing capabilities of adversaries trying to hack data on the other hand, is required. The term cryptography is a composition of *κρυπτός* (Greek) [*kryptós*], meaning "hidden, secret" and *γράφειν* [*graphein*] "writing". Today, cryptography is referred to as the science and art of secure coding and decoding of information. A main purpose of cryptography is encryption, *i.e.* to convert messages or data in readable form into unintelligible ciphertexts that can only be decrypted by a person possessing the dedicated decryption key (see **Scheme 19**). Cryptography can be dated back to ancient Egypt (3000 BC), where standard hieroglyphs where simply replaced by a different and unusual hieroglyphic writing system, which only selected persons could read, thus concealing the information.[230] The ancient Greeks used ciphers for coding messages and the Spartan military utilized a first encryption/decryption device: the Scytale.[231]

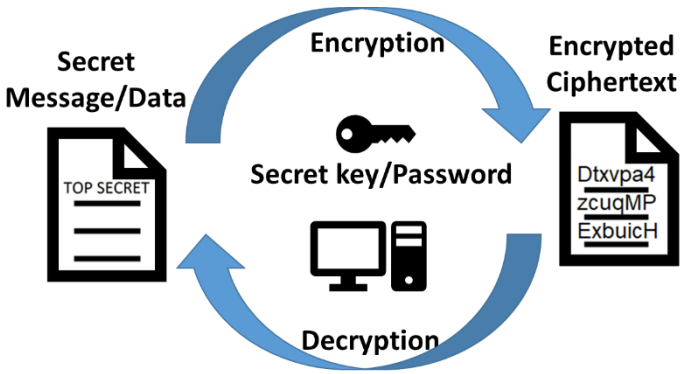

Scheme 19. Schematic representation of symmetric cryptography.

The term steganography originates from στεγανός [*steganos*], meaning "covered, concealed, or protected" and γράφειν "writing" (see also above). Steganography, in contrast to cryptography, hides the fact that a message is being transmitted: only the sender and the receiver know that the message even exists. A major drawback of

steganography is that whenever an adversary reveals the fact that steganography has been used and knows how to apply the decoding, he is able to obtain the secret information.[232,233] Considering cryptography, several state-of-the-art symmetric encryption schemes, such as the Advanced Encryption Standard (AES, also known as Rijndael),[234] Serpent, or Blowfish can protect data reliably (practicably “unbreakable”), but require a secret key (password) for their operation. Practicably “unbreakable”, means that the encoded data cannot be accessed, due to today’s physical limitations in computing power (if the password is long enough, consisting of random characters and remains a secret). An even higher degree of safety is provided by the so-called One-time pad (OTP), which is mathematically perfectly secure, and thus also secure against hypothetical quantum computers.[235] If used correctly, the OTP crypto system cannot be breached, even if the adversary has unlimited computing power and an unlimited amount of time. In practice, the OTP encrypts every letter/sign of the initial document with an individual substitution code,[236] leading to a key document with the same length/number of characters as the secret message. For long messages or large files, this generates long keys requiring electronic storage. If the correct key is applied, the original message can be decoded, but if not, every other possible combination of characters (including any other text with a completely different meaning, but of the same length as the initial code) can be generated, rendering the OTP a perfectly secure algorithm. This can be illustrated by the following example: the text “Let’s meet at 5” has 15 characters. The correct key will generate the correct information, but within the space of false keys any other text with 15 characters *i.e.* “Let’s meet at 1” or also “Hi how are you?” can be obtained. A major weak spot of cryptographic systems is the key itself, *i.e.* the storage of the key in an electronic document as well as the transportation/distribution of the key. The secret key (*i.e.* the password) must be known by both the encryptor and the decryptor and be chosen uniformly at random. An adversary trying to decrypt the hidden information can steal the key, copy the key, or even restore information from an allegedly erased or even destroyed digital storage. Thus, the password/key is one of the most vulnerable parts in modern encryption systems, leaving room for improvements. Secret encryption keys are typically short (*e.g.* 128 bits), but it is not *a priori* clear how encryptor and decryptor exchange/receive common secret keys. The methods utilized to distribute secret keys today involve asymmetric cryptography *e.g.* the Diffie-Hellman key exchange scheme, or key transport based on the Rivest–Shamir–Adleman cryptosystem (RSA).[237] Asymmetric

cryptography is considerably less efficient than symmetric cryptography. Furthermore, state-of-the-art asymmetric encryption schemes require specific algebraic structures, and are thus potentially more prone to attacks *via* structured cryptanalysis.[237] For a higher degree of data security, decryption keys can be concealed by steganography and be hidden *i.e. via* chemicals.[232,238,239] The general idea to employ chemicals for secret communication dates back to the first uses of secret inks.[240] Nowadays, more sophisticated methods for chemical secret communication systems are discussed, *e.g.* fluorescent materials[241–247] or multi-analyte fluorescent molecular sensors.[238,248–250] In 2015, Margulies *et al.* presented an inspiring system based on two fluorescent molecules (one example is displayed in **Figure 4**) that can act as a sensor to "chemical input" (*i.e.* addition of different chemicals at different concentrations).[238] The authors demonstrated that messages can be encrypted by sequentially adding various chemicals to the fluorescent molecules, thereby analyzing characteristic emission patterns recorded between 500 to 700 nm. The chemicals modulated the emission pattern by interactions with certain functionalities in the *cis*-amino proline molecule displayed in **Figure 4** *e.g.* the three spectrally overlapping fluorophores: nile blue (**Figure 4 a**), sulforhodamine B (**Figure 4 e**) and fluorescein (**Figure 4 g**), serving as fluorescence resonance energy transfer (FRET) donor/acceptor system.

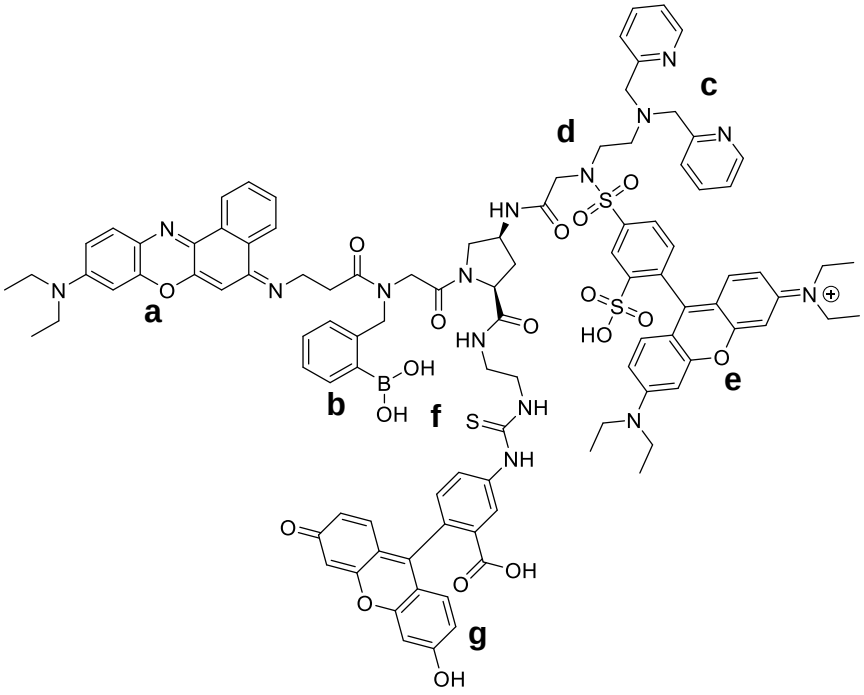

Figure 4. Molecular *cis*-amino proline scaffold sensor. **a**, solvatochromic nile blue; **b**, boronic acid; **c**, dipicolylamine; **d**, sulfonamide; **e**, sulforhodamine B; **f**, thiourea and **g**, pH-sensitive fluorescein.

The fluorescein emission is highly pH dependent,[251] whereas deprotonation of the fluorescein moiety can enable the phenolic ligand to coordinate metal ions.[252]

Solvatochromic sulforhodamine B can interact with DNA and non-polar analytes.[253] In addition, the sensor molecule includes various other chemical recognition elements *e.g.* boronic acid (**Figure 4 b**) and dipicolylamine (**Figure 4 c**) groups. The boronic acid provides an affinity *e.g.* towards saccharides[254] and dipicolylamine to metal ions,[255] respectively. Moreover, dipicolylamine‑metal ion complexes are known to interact with phosphate anions.[256] The thiourea (**Figure 4 f**) and sulfonamide functionalities (**Figure 4 g**) can additionally serve as metal ion-recognition sites,[257–259] but also as anion and hydrogen-bonding motifs.[260–262] Additional chemical recognition sites in the sensor molecule could be formed after binding of certain analytes and supplementary interactions may include hydrogen bonding (*e.g.* of the amides or carboxylic acid functional groups) and hydrophobic interactions (*π*-stacking of aromatic system). The general idea to utilize fluorescent compounds or materials for data encryption has also been investigated by others.[241–247] In addition, DNA was utilized for secure communication.[263–267] Molecular logic gates,[268–273] molecular computing systems[274–276] and systems for authorizing password entries[277–286] also contributed to the filed. Other investigations employed NMR chemical shifts,[287] microorganism colonies,[288] antibodies,[289] 3D photonic crystals[290] and molecular tags.[291]

2.6 Mass spectrometry and ESI-MS

The history of mass spectrometry dates to the late 19th century when Thomson first described the e/m_e determination *via* a cathode ray experiment.[292] For his contributions to the nature of the electron by "*theoretical and experimental investigations on the conduction of electricity by gases*", he was awarded the Noble Prize in physics in 1906.[293] The first mass spectrometers developed in the early 20th century were utilized to measure the mass of atoms and prove the existence of isotopes.[294] In 1918, Dempster invented the first electron impact source,[295] in 1946 Stephens introduced the time-of-flight analyzer (TOF),[296] while in 1953 Paul first utilized a quadrupole mass filter and quadrupole ion trap.[297] Later, in 1978, Yost and Enke described triple-quadropol mass analyzers and selected ion fragmentation[298] and in 1981 Barber developed fast atom bombardment ionization (FAB).[299,300] In the 1980s, mass spectrometry was well established for the analysis of small organic compounds. However, most methods known in the early times of mass spectrometry

did not allow the analysis of larger macromolecules such as proteins, carbohydrates, oligonucleotides or polymers, mainly due to the ionization methods (requiring gas-phase collisions between the analyte and charged species). The challenge of transferring larger particles into the gas-phase without decomposition or fragmentation was encountered in 1988/89 by electrospray ionization (ESI), developed by Fenn,[301] and matrix-assisted laser desorption/ionization (MALDI), developed by Tanaka,[302] almost simultaneously. Both methods were honored with the Nobel prize in chemistry 2002 "*for their development of soft desorption ionisation methods for mass spectrometric analyses of biological macromolecules*". Today, mass spectrometry is amongst the most sensitive and most developed analytical methods. In this thesis, ESI-MS and ESI-MS/MS experiments were of particular interest and therefore ESI-MS be described more into detail. The experimental setup of the utilized Thermo Scientific™ Q Exactive Plus™ orbitrap mass spectrometer is illustrated in **Figure 5**.

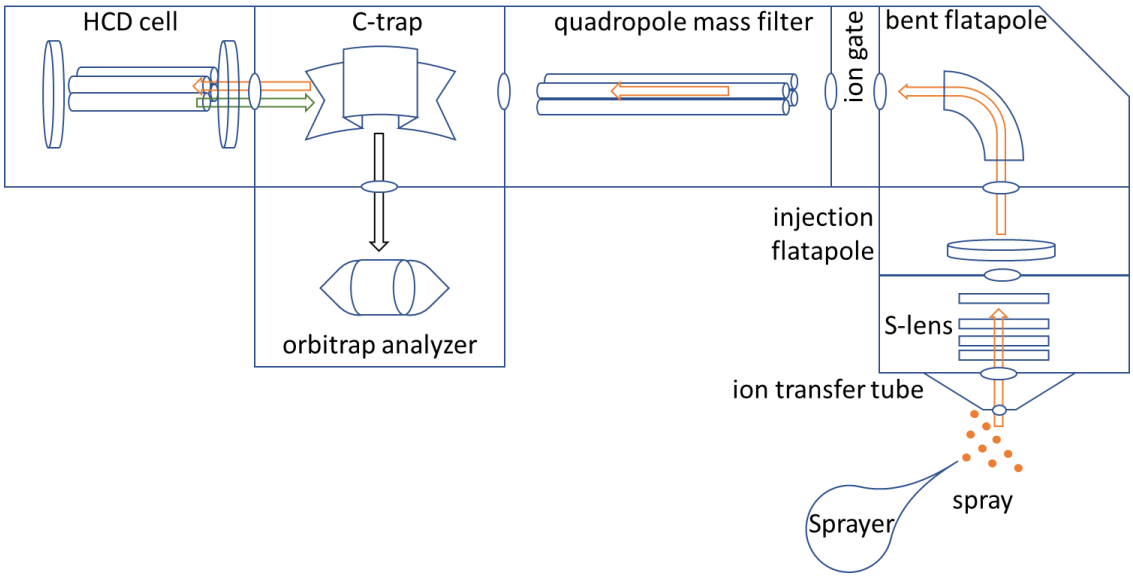

Figure 5. Schematic representation of a Thermo Fisher Q-Exactive ESI-MS mass spectrometer.

First, the sprayer (heated electrospray ionization probe) produces the ions (ionization mechanism will be discussed later). The ions enter the heated ion transfer capillary trough the sweep cone and subsequently enter the S-lens, where the ions are captured, focused into an ion beam and transmitted for increased sensitivity, utilizing a variety of electromagnetic lenses arranged in different distances. The injection flatapole again focuses the ion beam and partly separates neutrals from ions, thus acting as a kind of pre-filter. The bent flatapole enables active beam guiding in order to prevent neutral species from entering the quadrupole and hence enhances operational robustness. The quadrupole mass filter allows precursor selection

(isolation widths down to 0.4 amu) and parallel data acquisition, improving sensitivity and selectivity. The higher-energy collisional dissociation (HCD) cell is an ion-routing multipole, enabling HCD fragmentation experiments at adjustable preselected collision energies through collisions of the precursor ions with neutral inert gases such as nitrogen, further facilitating parallel analysis through accumulation and routing of ions.[303] Despite the name higher-energy, the collision energies are comparably mild in range of 10 – 50 eV. The C-trap focuses the ions, stabilizes their movement (sometimes also referred to cooling down the ion speed) and injects them into the orbitrap mass analyzer. The ultra-high-field orbitrap mass analyzer offers a resolution of up to 450 k (at *m/z* = 200) and scan speeds of up to 12 Hz for high data quality. In the orbitrap, the ions are captured in an orbital motion circulating around the analyzer geometry (parallel outer electrode and spindle like inner electrode) in an axial fashion. The frequency of rotations (frequency of radial oscillations *i.e.* distance of the ions to the middle spindle electrode, frequency of axial oscillation *i.e.* velocity of the ions moving axially along the spindle electrode and frequency of rotation) are related to the *m/z via* a Fourier transformation (FTMS) of the image current generated by the axial oscillation of the ions.[304,305]

For ionization, the analyte solution is distorted into a Taylor cone that emits a fine spray (usually assisted by a coaxial gas flow) producing droplet radii in the micrometer range (see **Figure 6 a**). The fine dust of highly charged micro aerosol droplets evaporates rapidly in the present conditions of high temperatures and externally applied gas flow. In positive mode, the droplets are positively charged mainly due to the presence of excess cations that, for instance, include H^+ (originating from acidic media and/or generated at the metal to solution interface inside the capillary *via* reactions, such as *e.g.* $2\ H_2O \rightarrow 4\ H^+ + 4\ e^- + O_2$), Na^+, K^+, NH_4^+, *etc.* The charge density of the micro droplets steadily increases due to shrinking of their volume until the Coulombic repulsion is balanced by surface tension (so-called Rayleigh limit). Disruptions of this equilibrium state cause spontaneous droplet fission. Repetitive cycles of droplet evaporation and fission ultimately lead to the generation of nano-sized droplets enabling final analyte ionization. The exact electrospray ionization mechanism, *i.e.* ions escaping the micro droplets into the gas-phase, is not fully understood yet, but plausible explanations can be found in literature.[306–315] Three plausible mechanisms are presented in **Figure 6 b – d**. Low molar mass analytes are considered to follow the so-called ion evaporation model (IEM) where the cationic charge typically results from

protonation in solution. Molecular dynamic simulations suggested that the electric field emanating from a Rayleigh-charged ESI nanodroplet is sufficiently high to induce ejection of small solvated ions from the droplet surface. During the ejection process, the cations remain shortly connected to the droplet by a bridge of solvent molecules (**Figure 6 b** middle). The primary IEM product is assumed to be a tiny gas-phase atom cluster, consisting of the analyte cation and a few residual solvent molecules, which are subsequently removed *via* collisions with other species *e.g.* background gas (**Figure 6 e**).

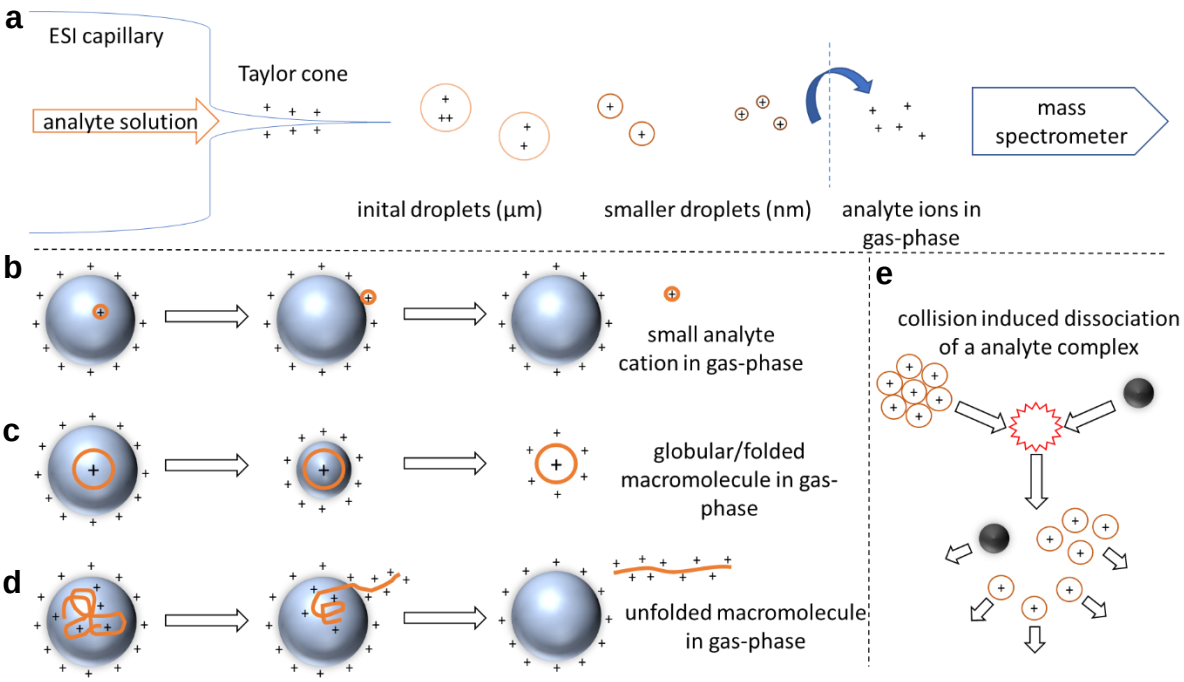

Figure 6. Proposed ESI ionization mechanisms. **a**, schematic illustration of the electrospray process of droplet formation, the blue bended arrow illustrates the generation of ions in the gas-phase. **b**, small analyte ion ejection from a charged nanodroplet into the gas-phase (IEM). **c**, release of a globular macromolecule ion (*i.e.* protein) into the gas-phase through evaporation of all solvent molecules (CRM). **d**, ejection of an unfolded macromolecule into the gas-phase (CEM). **e**, collision-induced dissociation of a gaseous multianalyte/analyte solvent complex.

Larger, globular species *e.g.* folded proteins can ionize *via* the so-called charged residue model (CRM). In CRM, the surrounding solvent molecules of Rayleigh-charged ESI nanodroplets, containing globular analyte cations, evaporate completely. Hereby, the positive charge of the nanodroplet is transferred to the analyte. Experimental evidence for CRM originates from the observation that ESI of globular proteins produces cations with compositions close to $[M + n\ H]^{n+}$, where n is the Rayleigh charge of the corresponding nanodroplets.[309,311,316,317] The folding behavior of macromolecular species in solution is determined by intra molecular interactions *vs.* intermolecular interactions of the macromolecules with solvent molecules. The latter effect depends on several factors such as polarity, pH, hydrogen bonding capabilities

and other intermolecular interactions leading to folded globular macromolecular species or unfolded macromolecular species. The ionization of unfolded, disordered macromolecular conformations is proposed to follow the so-called chain ejection model (CEM) from Rayleigh-charged nanodroplets (see **Figure 6 d**). The following considerations were suggested by molecular dynamic simulations.[318,319] The unfolded macromolecule firstly migrates to the droplet surface. Subsequently, a chain terminus exits the nanodroplet and is expelled into the vapor phase (**Figure 6 d** middle), followed up by sequential ejection of the remaining macromolecular segments, resulting in complete ionization.[306]

3 Goals/Aims

The main objective of this investigation was the conceptional and practical application of multicomponent reactions as tools for the preparation of potential molecular data storage devices. This thesis has three main foci:

- Investigation of perfluoro-tagged Ugi compounds, evaluation of their storage capacity, analysis *via* tandem-MS and application as molecular cryptography keys.
- Method development for the combination of the Biginelli and the Passerini reaction and subsequent synthesis of compounds incorporating up to five varying components.
- Synthesis of bifunctional AB-type monomers *via* sequential Biginelli and Passerini reactions and the establishment of a chemical test system for the application of these monomers. Subsequently, the monomers were employed for the synthesis of sequence-defined, data encoding macromolecules *via* an iterative step-growth polymerization. High resolution tandem mass spectrometric analysis of the macromolecules in order to determine their chemical structure and thus read out the information.

The chapters in the following results and discussion part were ordered according to increasing synthetic complexity: moving from one multicomponent reaction to the combination of two multicomponent reactions and finally to sequence-defined macromolecules.

4 Results and discussion

4.1 Molecular cryptography: Multicomponent reactions are the key

Parts of this chapter and following subchapters were adapted from previous passages written by the author.[208]

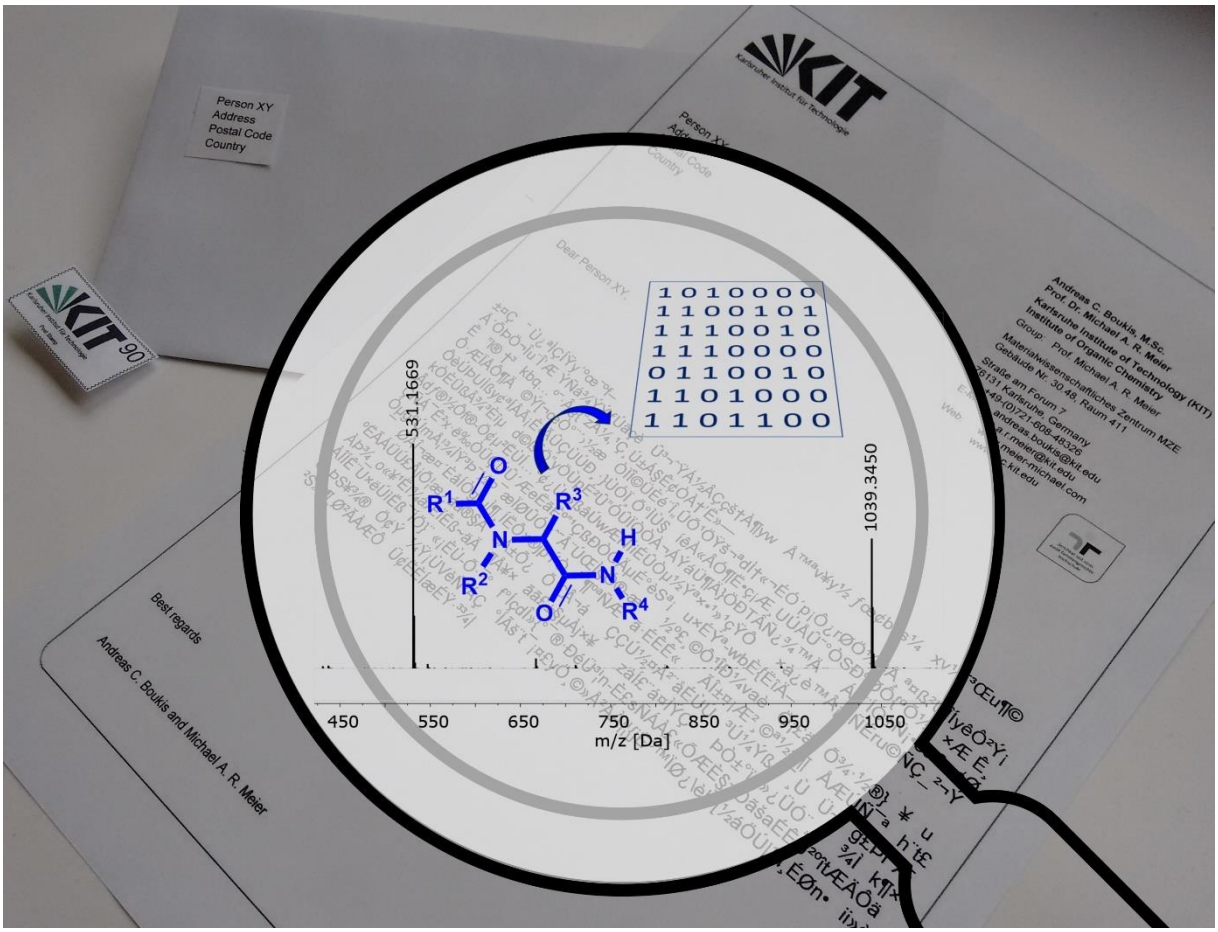

Figure 7. Graphical abstract for the investigation presented in chapter **4.1**.[208]

As previously described in chapter **2.5.2**, hiding of secret cryptography keys/passwords by steganography *i.e. via* chemicals leads to a higher degree of security.[232,238,239] Chemical compounds utilized as cryptographic keys are referred to as molecular keys, respectively. Although the number of chemical compounds known today is tremendously large and steadily growing, the application of a chemical compound as molecular key is limited considering the following requirements: for the chemical design of molecular keys a systematic synthetic protocol should be employed, providing compounds with high structural complexity. Furthermore, simple,

robust and reproducible procedures should be applied. The molecular keys should be chemically and thermally insensitive and designed for simple isolation, purification and analysis. Multicomponent reactions (MCR) represent highly suitable synthetic tools to provide molecular keys, fulfilling these criteria. The Ugi reaction was especially appealing, since four components are combined to a single reaction product in a one-pot reaction (offering all advantages presented in chapter **2.1**).[100] The respective Ugi products display four individually defined side chains (R^{1-4}, introduced by the four starting components), which can be easily varied in order to create molecular diversity with minimal synthetic effort (previously utilized for combinatorial approaches, see chapter **2.1.3.1**).[48,137,320]

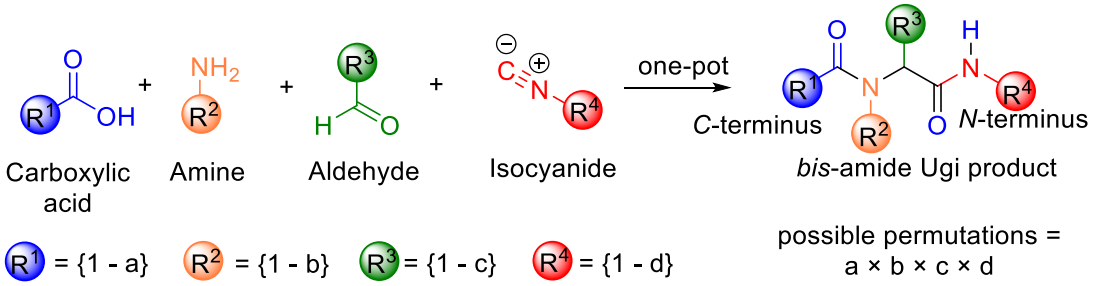

Scheme 20. General reaction scheme of the Ugi reaction and the scope of possible Ugi compounds considering all permutations. The number of all permutations is calculated as follows: number of possible carboxylic acid components (a) × number of possible amines (b) × number of possible aldehydes (c) × number of possible isocyanides (d).

A hypothetical library consisting of the Ugi compounds derived from ten varying carboxylic acids, ten aldehydes, ten isocyanides and ten amines would comprise 10 × 10 × 10 × 10 = 10,000 different compounds in all permutations. The 10,000 permutations equal approximately 13 bits (calculation: $\text{Log}(10^4)/\text{Log}(2)=13.29$). However, in order to convert the chemical information (combination of starting components introducing different side chains to the respective Ugi compounds) into processable alphanumerical codes, a procedure was required. The assignment of chemical information (*i.e.* reacting components of the Ugi reaction introducing the side chains of the respective molecular keys) to alphanumerical codes (*i.e.* systematic combinations of letters, numbers and special characters) is performed with a table, called the list of components. In the list of components, every functional group participating in the Ugi reaction is assigned to a letter (*e.g.* aldehydes → letter A; isocyanides → letter B, *etc.*). The different side chains within the same category of functional groups are counted with arbitrary numbers *e.g.* benzaldehyde → A(001), butyraldehyde → A(003), …; *tert*-butyl isocyanide → B(001), …). This assignment system, comprised in the list of components, is highly flexible and the alphanumerical

assignment can be exchanged or adjusted if necessary, which is highly beneficial in the field of secret communication. An exemplary short list of components can be found in **Table 2**. The full list is provided as supplementary information in the corresponding publication[208] and also provided in the digital from with the submitted thesis.

Table 2. Selected entries from an exemplary list of components

Name	Structure	Formula	Alphanumerical code	Monoisotopic mass [Da]
Perfluoropentanoic acid	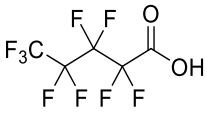	$C_5H_1F_9O_2$	A(001)	263.98328
Perfluorononanoic acid	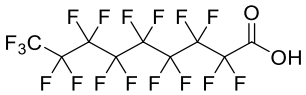	$C_9H_1F_{17}O_2$	A(005)	463.97051
Isopropyl isocyanide		$C_4H_7N_1$	B(001)	83.07350
Pentylamine	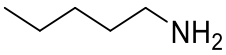	$C_5H_{13}N_1$	C(007)	87.10480
Benzaldehyde	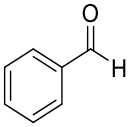	$C_7H_6O_1$	D(007)	106.04186

Additional information, such as *e.g.* a SMILES code for visualizing the molecular structures, or a chemical supplier can be added. The full list of components can be found as supplementary information along with the previously published work[208] and is also included in the electronic version of this thesis.

For exploring the synthetic potential of the Ugi reaction, an evaluation based on previously reported literature was performed in order to identify suitable components for the list of components. Regarding possible side reactions (and modifications of the Ugi reaction discussed in chapter **2.1.3**), a set of limitations considering the reacting components was established. In this context, aldehydes were chosen as carbonyl species exclusively, because of the higher carbonyl activity and better reactivity in Ugi reactions compared to ketones. Nevertheless, the scope of carbonyl components reported for Ugi reactions potentially allows to utilize many more components than the aldehydes selected for this investigation. Generally, the reacting components need to fulfill further requirements which are illustrated in **Figure 8**. The components should

display only one functional group participating in the Ugi reaction (*e.g.* a carboxylic acid and an aldehyde functional group should not be combined in the same component, otherwise polymerization might occur, see **2.1.3.2**). The components should also not contain moieties which are highly redox sensible, photosensitive, hydrolyzed or decomposed under the conditions of the Ugi reaction or in the presence of protic solvents like methanol or water. Functional groups prone to cause side reactions with the other substances/solvents involved in the Ugi reaction were also avoided. Furthermore, electron-poor phenols (*i.e.* nitro-substituted) were avoided due to the potential Ugi-Smiles reaction (acidic phenol reacts as an acid component).[151]

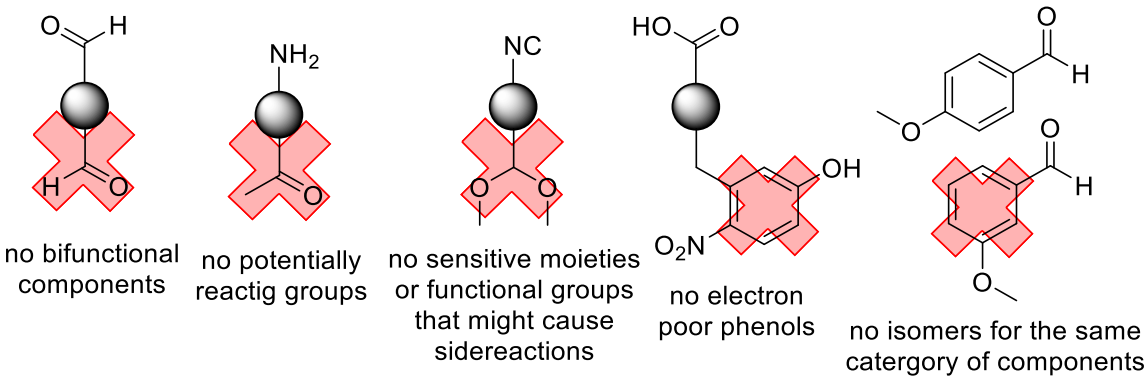

Figure 8. Limitations that should be considered when setting up a list of components.[208]

As the analytical method of choice, high-resolution mass spectrometry (see chapter **2.2**) in combination with tandem-MS fragmentation experiments was selected and thus, the components in the same category of functional groups should not include isomers (same monoisotopic mass).[321] In principle, isotope labeled components can be beneficial for MS experiments, but were also excluded from the list of components. Considering the literature survey and the requirements stated above, an exemplary list of components, including ten perfluorinated carboxylic acids, 50 aldehydes, 50 amines and 20 isocyanides, was compiled. All components chosen for this list are commercially available and selected in order to react selectively to the desired Ugi products. These 130 components can potentially be combined to 10 × 50 × 50 × 20 = 500,000 different molecular keys. This virtual library of 500,000 permutations formally corresponds to an information density of approximately 18 bits per molecule (Log(500,000)/Log(2)=18.93). The possible number of components for the list of components are theoretically only limited by the availability of components suitable for the Ugi reaction and can therefore easily be extended beyond the set of commercially available compounds.

4.1.1 Ugi reactions of perfluorinated acids

Considering the molecular design, the molecular keys were equipped with a perfluorinated side chain (also called F-Tag), enabling a highly simplified purification *via* Fluorous Solid Phase Extraction (F-SPE, see chapter **2.3**).[186,322] F-SPE retains perfluoro-tagged molecules selectively and can hence separate the molecular keys from contaminations and/or matrix materials. The F-tags were introduced *via* the utilization of perfluorinated acid components in the Ugi reaction. For performing the Ugi reactions of perfluorinated acids, methanol was chosen as solvent because Ugi reactions are reported to proceed efficiently in methanol and moreover because methanol is readily dissolving perfluorinated acids (methanol is also utilized for collecting the fluorous fractions in F-SPE). A reaction optimization of the Ugi reaction presented in **Scheme 21** revealed that it is efficient to perform the imine condensation prior to the addition of the other components. For the imine condensation, equistoichiometric amounts of aldehyde and amine were stirred for one hour over sodium sulfate (in order to remove the water formed during the condensation process).

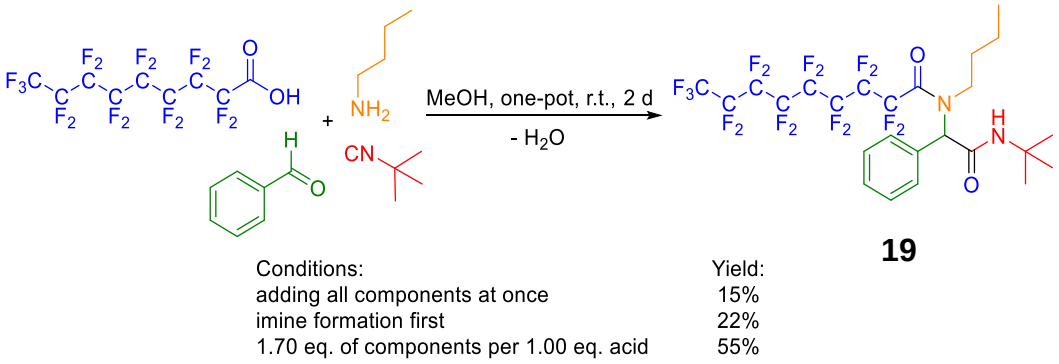

Scheme 21. Optimization of the Ugi reaction of perfluorononanoic acid, benzaldehyde, *tert*-butyl isocyanide and butylamine resulting in compound **19**.

Subsequently, the perfluoro acid dissolved in a minimal amount of methanol, was added to the imine and the resulting mixture was stirred for 2 min. The isocyanide was added last into the stirring reaction mixture. The reaction progress was followed by TLC. Further optimization revealed that an excess of components provides higher yields (best results were achieved employing 1.70 eq. of aldehyde, amine and isocyanide with respect to 1.00 eq. of perfluoro acid). The purity of the isolated material after chromatography was confirmed by GC-MS (**Figure 9 a**).

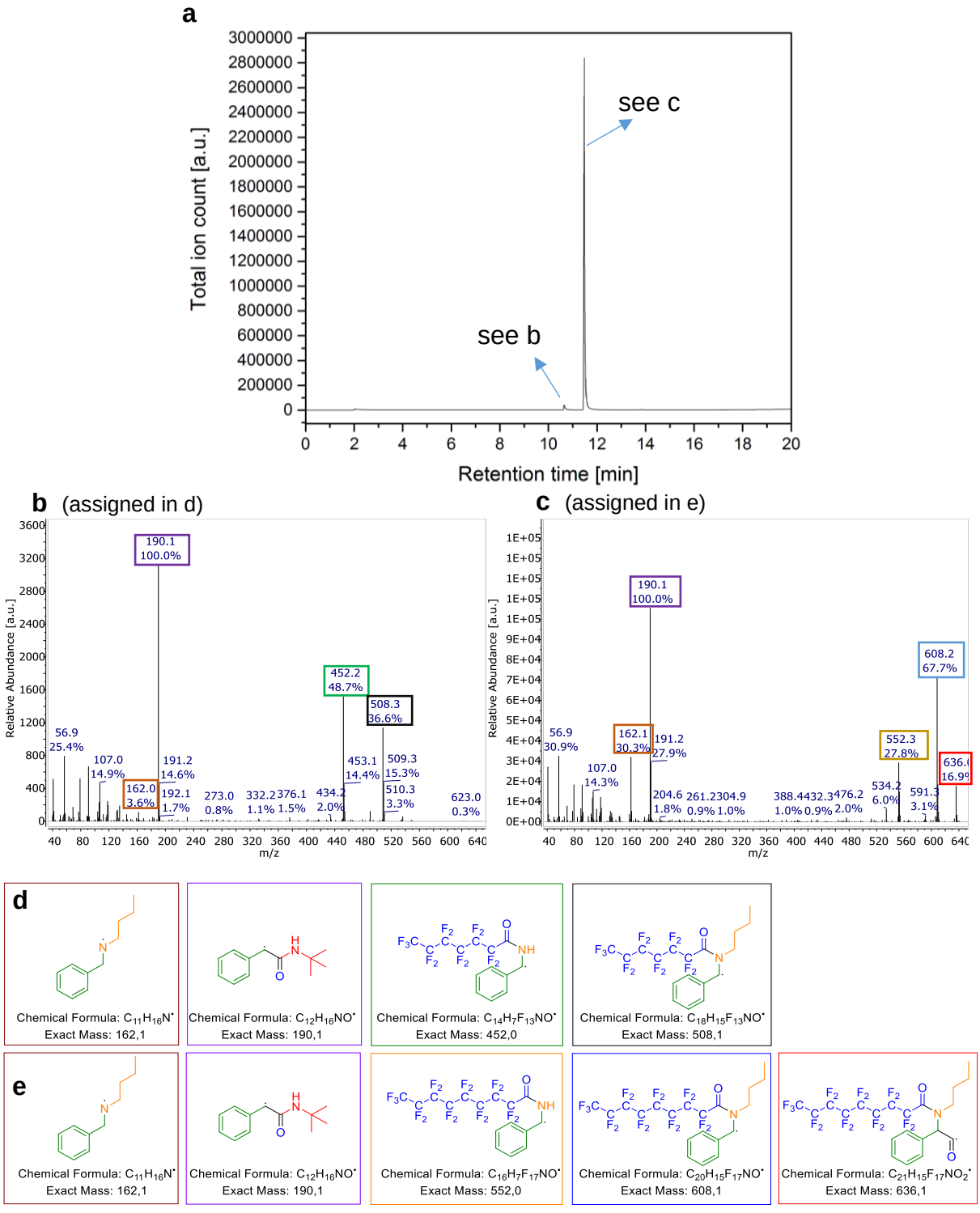

Figure 9. a, GC-MS, chromatogram of a representative molecular key (compound **19**). The respective MS data of the intense signal at 11.5 min retention time (99%) are displayed in **c**. The MS data of the weak signal at 10.6 min retention time (1%) are displayed in **b**. **b**, MS spectrum of the weak signal (1%) at 10.6 min retention time, the *m/z* species are assigned in **d**. **c**, MS spectrum of the intense signal (99%) at 11.5 min retention time, the *m/z* species are assigned **e**. **d**, fragment assignment of the weak signal at 10.6 min indicates the presence of a Ugi compound with a shorter perfluorinated side chain. This impurity (originating from a shorter perfluorinated acid) was already present in the starting material and did not interfere with other analytical methods and the readout. **e**, fragment assignment of the intense signal at 11.5 min.[208]

The intense signal at 11.5 minutes retention time corresponds to the desired Ugi compound **19**, the relative integral is 99%. The small impurity (1%) at 10.6 minutes retention time originates from a species with a shorter perfluorinated sidechain ($5 \times CF_2$ instead of $7 \times CF_2$). This impurity was formed because a shorter perfluorinated acid component was present in the precursor material (ordered and used as received). The respective MS data and the assignment of the *m/z* species is presented in **Figure 9 b - e**. However, since the amount of impurity is small, no interference with other analytical methods or the tandem-MS readout was observed. The chemical identity of the reaction product was confirmed *via* 1D and 2D NMR spectroscopy.

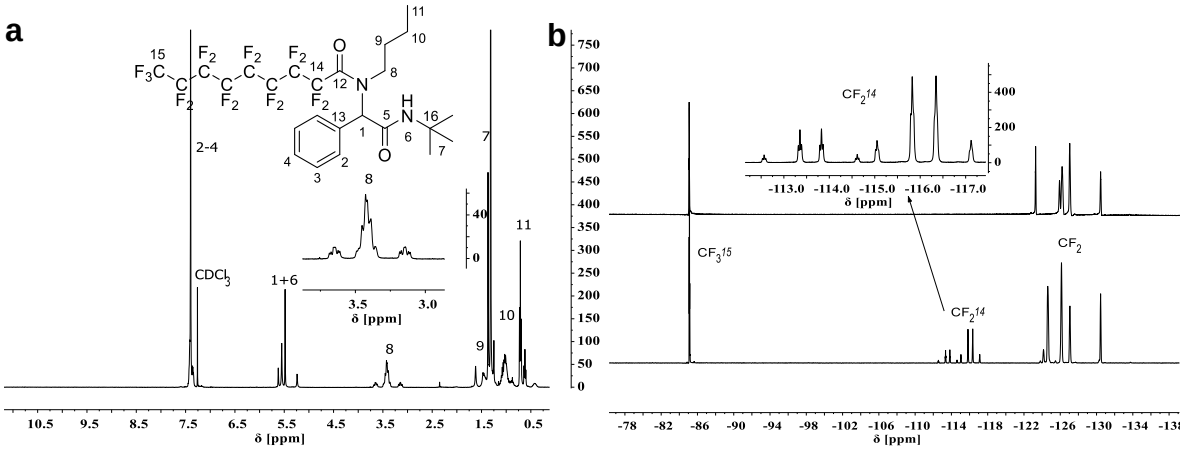

Figure 10. Representative NMR analysis of **19**. **a**, ^{1}H-NMR, the respective signal assignment was performed with respect to additional information obtained from 2D NMR experiments. **b**, ^{19}F-NMR stack of the precursor perfluorononanoic acid (top) and the Ugi compound (bottom). The expansion magnifies the two AB signals of the CF_2*14* group (two species caused by restricted rotation) next to the newly formed amide bond.[208]

The ^{1}H- and ^{19}F-NMR spectra showed an interesting signal splitting, probably due to restricted rotation (analogous to peptides). The restricted rotation theory was further supported by nuclear Overhauser enhancement and exchange spectroscopy (NOESY), indicating chemical exchange of the rotamers in solution.[208] In the ^{1}H-NMR spectrum (**Figure 10 a**), split signals can be observed for the protons on the CH*1* and NH*6* positions resulting in a split signal between 5 – 6 ppm, with a relative integral of two, that does not couple to other protons, as indicated in the correlated spectroscopy experiment (COSY, **Figure 11 b**). Regarding the stacked ^{19}F-NMR spectra (**Figure 10 b**) of the molecular key (bottom) compared to the ^{19}F-NMR spectrum of the precursor perfluorononanoic acid (top), the molecular key displays two new AB signals (magnified in the expansion view). The AB signals originate from the CF_2*14* group next to the newly formed amide bond. The ^{13}C-NMR (**Figure 11 b**, bottom) signal for the quaternary C*12* is weak in intensity compared to the C*5*, probably due to $^{3}J_{(C\text{-}F)}$ coupling

with the vicinal CF_2[14]. The ^{13}CF signals of the perfluorinated chain are also weak in intensity and barely visible, due to the numerous C-F couplings. The distortionless enhancement by polarization transfer experiments (DEPT90 and DEPT135, see **Figure 11 b**) confirm the proposed signal assignment. The heteronuclear single quantum coherence spectroscopy experiment (HSQC) displays all carbon bonded protons *via* $^1J_{(C\text{-}H)}$ correlations (**Figure 11 c**). The heteronuclear multiple bond correlation spectrum (HMBC, **Figure 11 d**) displays correlations between carbons and protons that are separated by two, three and sometimes even four bonds (*i.e.* in conjugated systems). The HSQC and HMBC experiments were both utilized in order to elucidate and confirm the molecular structure.

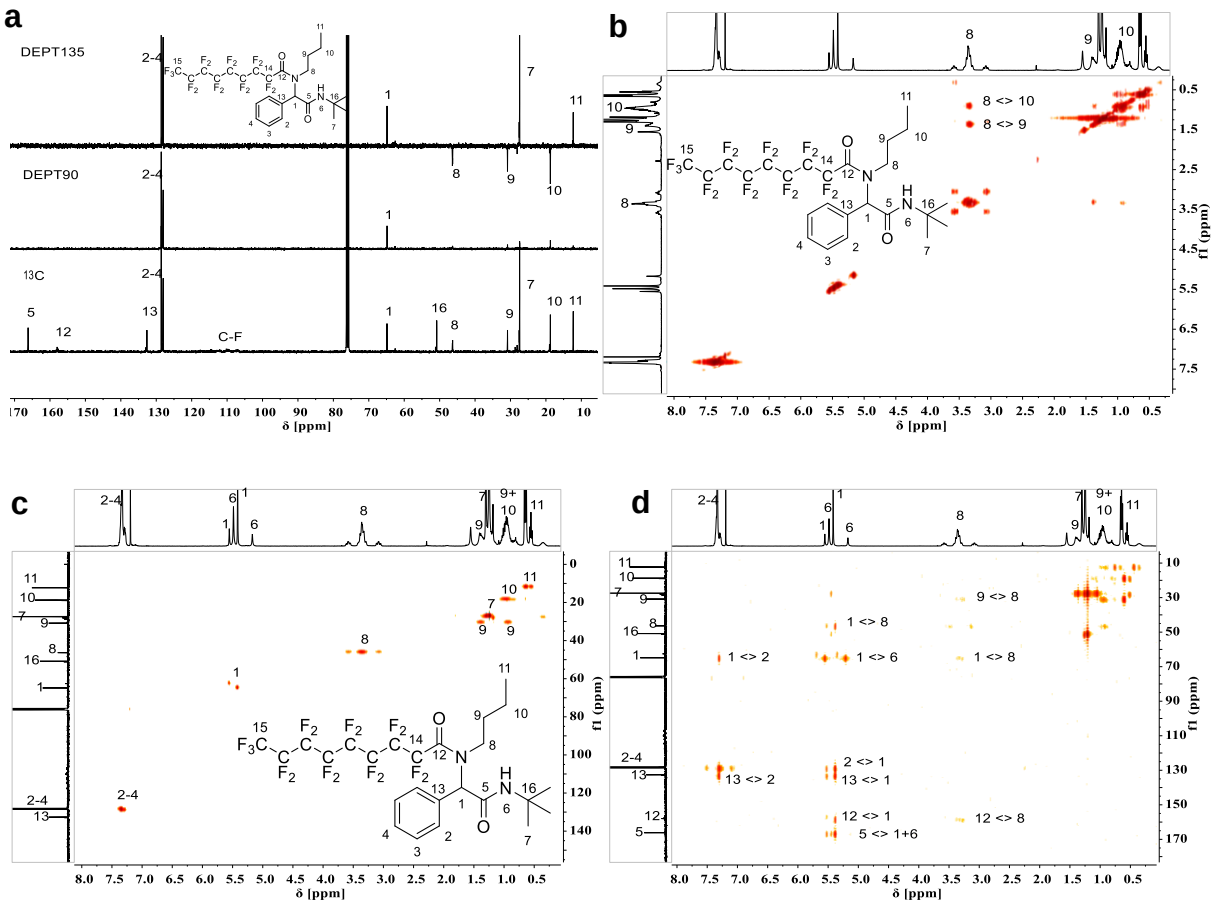

Figure 11. Representative NMR analysis of **19**. **a**, Top: DEPT135 experiment: CH and CH_3 positive, CH_2 negative. Middle: DEPT90 experiment CH positive. Bottom: ^{13}C-NMR. **b**, COSY experiment. **c**, HSQC experiment confirming the structure. **d**, HMBC experiment confirming the signal assignment for the carbon and proton signals.[208]

Subsequent to the identification of the reaction product **19** and understanding of the split NMR signals, the scope of possible components was investigated. As proof of principle, a sub-library of different molecular keys was synthesized. In this investigation, the reacting components, chosen from the list of components, were on one hand selected randomly an on the other hand systematically. The systematic

variation of the different reacting components is illustrated in **Figure 12**. The axes in **Figure 12** represent three varying components and thus the side chains of the Ugi compounds. The variation is presented in a 3D plot (amines in yellow, isocyanides in red and aldehydes in green) for one of the applied perfluorinated acids (here perfluorononanoic acid). Each point in the 3D plot represents a synthesized Ugi compound. Two systematic component variations are represented in the expansions (**Figure 12 c**, **d**).

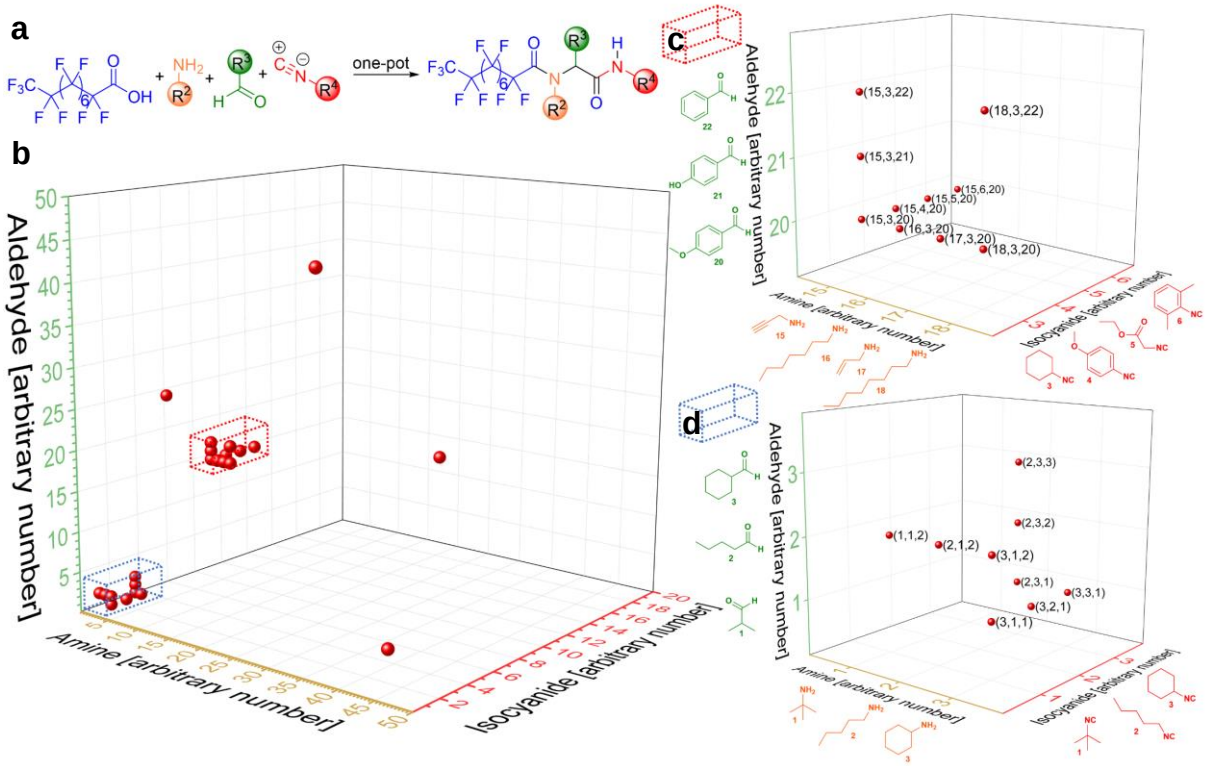

Figure 12. Molecular keys synthesized with perfluorononanoic acid. **a**, schematic representation of the general reaction equation. **b**, 3D plot of a subset of compounds. The three axes represent the different functional groups. The numbers on the axes assign the different components and side chains, respectively. **c** and **d**, expansions of the two systematic component variations, enlarged views of the red and blue box in **b**.[208]

The variation of perfluorinated acids was examined for the shortest and longest member of the list of components and is summarized in **Table 3**. Comparison of the results obtained indicated a clear trend towards higher yields for shorter perfluorinated acid components, probably due to better solubility of the shorter perfluorinated acids in methanol. In the case of long perfluorinated acid components (**Table 3** entry 3), tetrahydrofuran was added after 30 minutes reaction time because a precipitate was formed during the reaction, in order to re-homogenize the reaction mixture.

Table 3. Ugi reaction with perfluorinated acids of different chain length

#	Ugi compound	Yield [%]	**№**
1	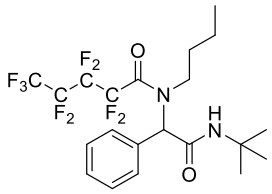	85	**20**
2	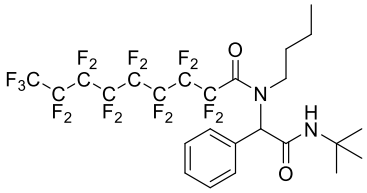	55	**19**
3	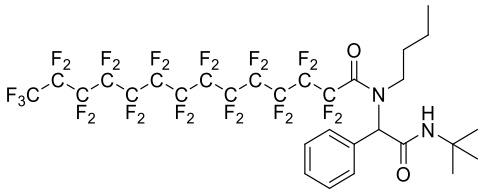	18[a]	**21**

Conditions: Reaction in methanol at r.t. for 3 d, 1.70 eq. of aldehyde, amine and isocyanide with respect to 1.00 eq. of acid.[a] During the reaction a precipitate was formed; in order to homogenize the reaction mixture, tetrahydrofuran was added.

The herein investigated variation of components resulted in a library comprising 28 Ugi compounds, the results are summarized in **Table 4**. The respective molecular keys were analyzed *via* 1D and 2D NMR spectroscopy, high resolution mass spectrometry (HRMS) and infrared spectroscopy to confirm their chemical identity (the respective experimental procedures and analytical data can be found in chapter **6.2**). The yields reported in **Table 4** varied from 85 – 3 %. This discrepancy is correlated to the individual combination of components, a well-known phenomenon of Ugi reactions.[323–325] However, the poor yields for the compounds **22**, **36** and **38** were also caused by unexpected complications which occurred during purification: these compounds were very challenging to visualize on TLC. In this context several staining reagents (Seebach, permanganate, iodine, vanillin reagent, etc.) were tested. However, the spots on the TLC plates were only barely visible and disappeared very fast. Hence, the identification of product containing fractions was complicated. Therefore, the overall product recovery after purification was probably incomplete.

Table 4. Molecular keys.

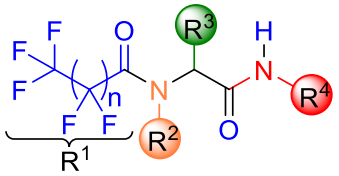

#	R^1	R^2	R^3	R^4	Yield [%]	№
1	C_8F_{17}	C_4H_9	Ph	^{t}Bu	55	**19**
2	C_4F_9	C_4H_9	Ph	^{t}Bu	85	**20**
3	$C_{13}F_{27}$	C_4H_9	Ph	^{t}Bu	18	**21**
4	C_4F_9	C_4H_9	C_4H_9	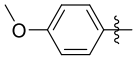	6	**22**
5	C_8F_{17}	C_4H_9	C_6H_{13}	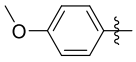	19	**23**
6	C_4F_9	C_4H_9	Ph	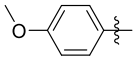	68	**24**
7	C_8F_{17}		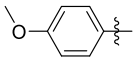	^{c}Hex	56	**25**
8	C_8F_{17}		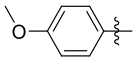	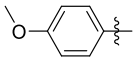	65	**26**
9	C_8F_{17}		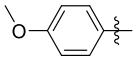		40	**27**
10	C_8F_{17}		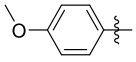	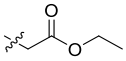	23	**28**
11	C_8F_{17}		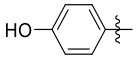	^{c}Hex	34	**29**
12	C_8F_{17}		Ph	^{c}Hex	15	**30**
13	C_8F_{17}	C_5H_{11}		^{c}Hex	25	**31**
14	C_8F_{17}	C_5H_{11}	C_4H_9	^{c}Hex	31	**32**
15	C_8F_{17}	C_5H_{11}	^{c}Hex	^{c}Hex	36	**33**
16	C_8F_{17}	C_5H_{11}	C_4H_9	^{t}Bu	16	**34**
17	C_8F_{17}	C_5H_{11}	Ph	^{c}Hex	42	**35**
18	C_8F_{17}	^{c}Hex	C_4H_9	^{t}Bu	7	**36**
19	C_8F_{17}	^{c}Hex		^{t}Bu	19	**37**
20	C_8F_{17}	^{c}Hex		C_5H_{11}	3	**38**
21	C_8F_{17}	^{c}Hex		^{c}Hex	11	**39**
22	C_8F_{17}	^{c}Hex	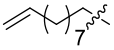	Bn	19	**40**
23	C_8F_{17}		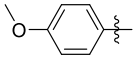	^{c}Hex	69	**41**
24	C_8F_{17}	C_8H_{17}	Ph	^{c}Hex	14	**42**
25	C_8F_{17}	C_7H_{15}	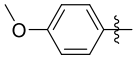	^{c}Hex	25	**43**
26	C_8F_{17}	^{t}Bu	C_4H_9	^{t}Bu	17	**44**
27	C_8F_{17}	Bn	$C_{11}H_{23}$	C_5H_{11}	18	**45**
28	C_8F_{17}		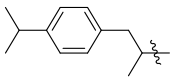	^{t}Bu	17	**46**

The variation of components demonstrated the applicability of perfluorinated acids in the Ugi reaction. Furthermore, the combination of the Ugi reaction with the list of components allowed to encode information into the Ugi compounds. However, a method was required to read out the information encoded *via* the side groups of the respective molecular keys.

4.1.2 Tandem-MS analysis of the molecular keys

Analytical chemistry offers a many different methods for the identification of organic molecules and thus for the readout of Ugi-type molecular keys. The molecular structure of the Ugi compounds is unambiguously solved when the four sidechains (R^{1-4}) originating from the starting components: perfluorinated acid (blue, R^1), amine (orange, R^2), aldehyde (green, R^3), and isocyanide (red, R^4) are determined. In mathematical terms, a four-dimensional problem needs to be solved using four different conditions/parameters (similar to solving matrices in linear algebra). The four parameters can be for instance obtained *via* four different molar masses from high resolution mass spectrometry fragmentation experiments *e.g.* the monoisotopic mass of the intact molecule and the masses of three fragments (obtained *via* collision experiments). Tandem-MS is a well-established and developed technique and has many unique advantages *e.g.*, the detection limits are very small and thus only minimal amounts of substance are required. Moreover, tandem-MS can be applied universally, and minimal sample preparation is required. The herein employed ESI-MS/MS experimental setup was previously discussed in chapter **2.6**. Exemplary ESI-MS spectra are presented in **Figure 13**. ESI-MS provides the monoisotopic mass (full scan mode 200 – 2000 *m/z*). The predominant signals arise from the intact analyte molecule + sodium: $[M + Na]^+$ and two analyte molecules + sodium: $[2\ M + Na]^+$. The sodium was introduced on purpose by utilizing a doped solvent mixture during the ESI sample preparation.

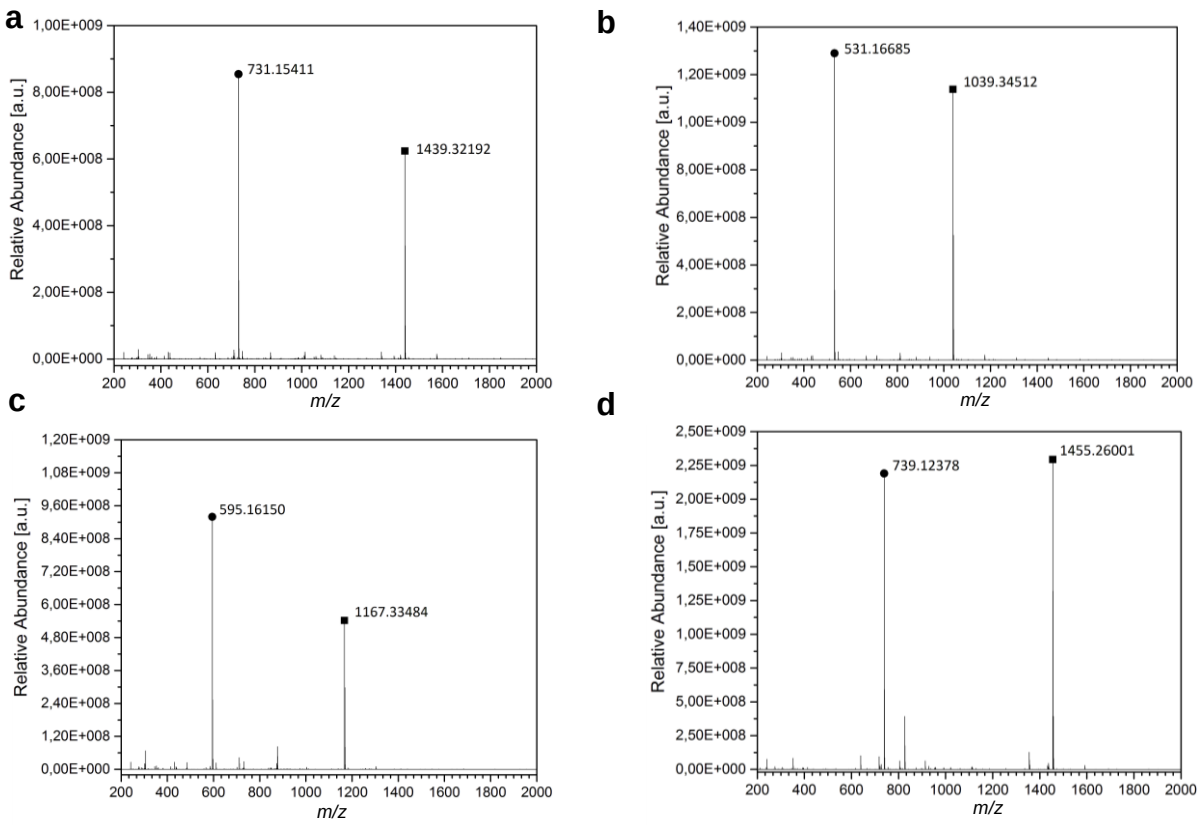

Entry	Label	Resolution	*m/z*(exp)	*m/z*(theo)	Δ*m/z*	Formula	Structure
1 in **a**	●	77000	731.1541	731.1537	0.0004	$C_{25}H_{25}O_2N_2F_{17}Na_1$	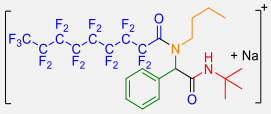
2 in **a**	■	56000	1439.3219	1439.3181	0.0038	$C_{50}H_{50}O_4N_4F_{34}Na_1$	$[2\ M + Na]^+$
3 in **b**	●	90000	531.1669	531.1665	0.0004	$C_{21}H_{25}O_2N_2F_9Na_1$	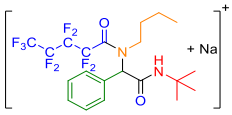
4 in **b**	■	66000	1039.3451	1039.3437	0.0014	$C_{42}H_{50}O_4N_4F_{18}Na_1$	$[2\ M + Na]^+$
5 in **c**	●	93000	595.1615	595.1619	0.0004	$C_{25}H_{25}O_3N_2F_9Na_1$	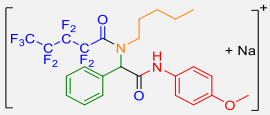
6 in **c**	■	66000	1167.3384	1167.3341	0.0043	$C_{50}H_{50}O_6N_4F_{18}Na_1$	$[2\ M + Na]^+$
7 in **d**	●	83000	739.1238	739.1229	0.0009	$C_{42}H_{50}O_4N_4F_{18}Na_1$	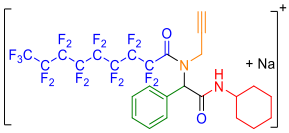
8 in **d**	■	59000	1455.2600	1455.2561	0.0039	$C_{52}H_{42}O_4N_4F_{34}Na_1$	$[2\ M + Na]^+$

Figure 13. ESI-MS of four molecular keys (**a**-**d**). **Table (bottom)**: assignment of the respective *m/z* species presented above. The resolution was obtained by the Xcalibur software from Thermo Fisher.[208]

The next step towards the readout of a molecular key is to isolate the intact molecule ($[M + Na]^+$ *m/z*) and fragment *via* collisions employing ESI-MS/MS. For this purpose, mild conditions (low fragmentation energy) were first used. Subsequently, the energy was gradually increased to higher fragmentation energy levels (see **Figure 14 a**). For the first evaluation, a spectrum with many fragment peaks occurring in a wide range of molar masses (high information density) was chosen and regarded in detail, *i.e.* the

30 eV spectrum (**Figure 14 b**). The 30 eV spectrum provides a high information density, because many fragments and the unfragmented molecule at 595 *m/z* can be observed). The heavier/larger fragment species were observed at small fragmentation energies (less fragmentation of fragments). In case of **Figure 14** it is possible to observe numerous fragments and hence extract the information required for structure elucidation from one single tandem-MS spectrum.

However, for other Ugi compounds, two tandem-MS spectra at different fragmentation energies are necessary to observe the relevant fragments utilized for readout. In **Figure 15**, two tandem-MS spectra of the same species (731 *m/z*) recorded at 35 eV (**Figure 15 a**) and at 50 eV (**Figure 15 b**) are displayed. Herein, the heavier fragments ❖ and ∗ can only be observed in the 35 eV energy spectrum (**Figure 15 a**, expansion). The lighter fragments ● and ◄ can exclusively be observed in the 50 eV spectrum (**Figure 15 b**).

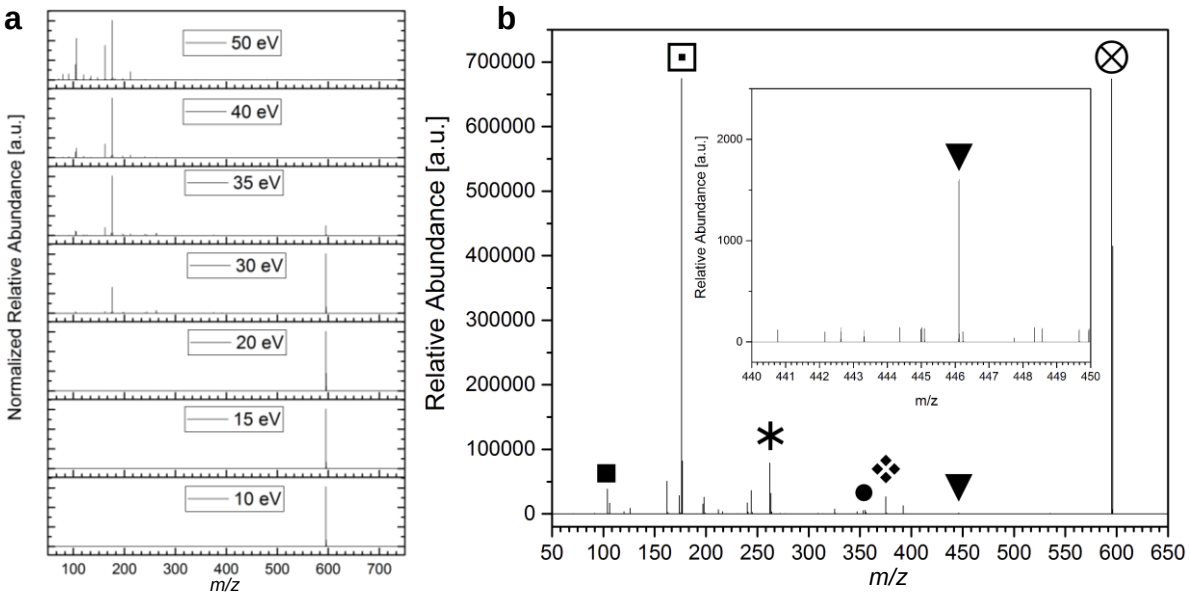

Entry	Label	Resolution	*m/z*(exp)	*m/z*(theo)	Δ*m/z*	Formula	Structure
1	⊗	89000	595.1612	595.1619	0.0007	$C_{25}H_{25}O_3N_2F_9Na_1$	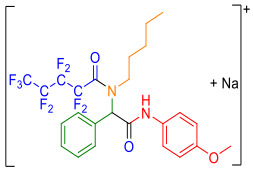
2	▼	97000	446.1137	446.1142	0.0009	$C_{17}H_{18}O_1N_1F_9Na_1$	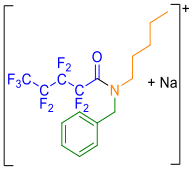
3	❖	112000	375.0274	375.0282	0.0008	$C_{12}H_7O_1N_1F_9Na_1$	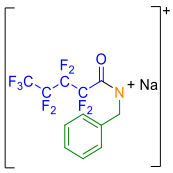
4	●	125000	325.1911	325.1916	0.0005	$C_{20}H_{25}O_2N_2$	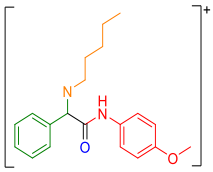
5	∗	135000	262.0839	262.0840	0.0001	$C_{15}H_{13}O_2N_1Na_1$	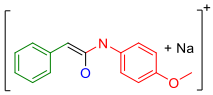
6	⊡	162000	176.1435	176.1439	0.0004	$C_{12}H_{18}N_1$	
7	■	202000	104.0499	104.0500	0.0001	$C_7H_6N_1$	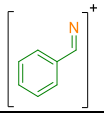

Figure 14. a, Fragmentation energy screening, stacked tandem-MS spectra of a single charged species at 595 *m/z* (⊗) in positive mode with different higher-energy collision dissociation (HCD) energy levels in the range from 50 – 750 *m/z*. **b**, Tandem-MS of a single charged species at 595 *m/z* (⊗). Recoded in positive mode with an HCD energy of 30 eV in the range from 50 – 650 *m/z*. The expansion visualizes the fragment ion (▼). **Table (bottom)**: peak assignment of the ESI-MS/MS spectrum presented in **b**.[208]

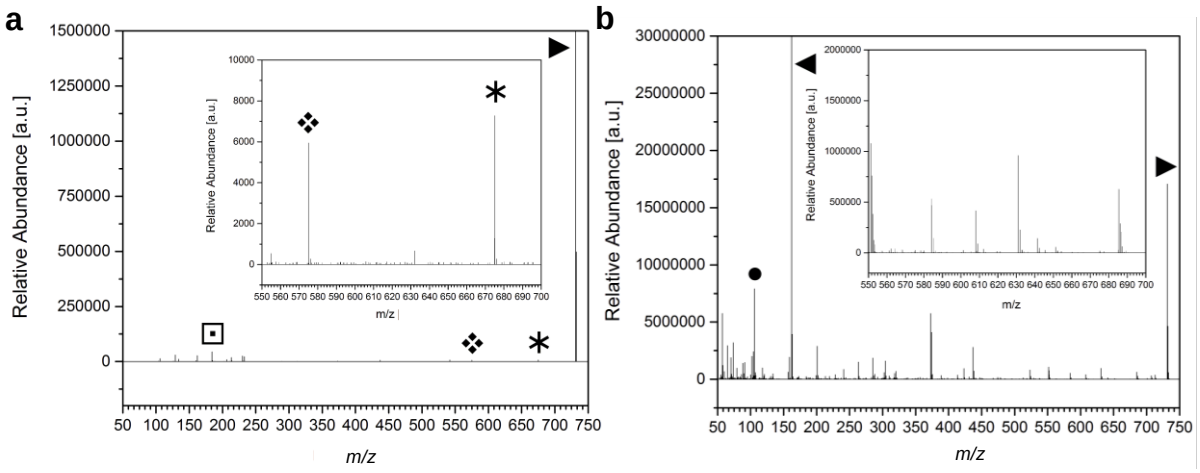

Entry	Label	Resolution	*m/z*(exp)	*m/z*(theo)	Δ*m/z*	Formula	Structure
1	▶	82000	731.1534	731.1542	0.0008	$C_{25}H_{25}O_2N_2F_{17}Na_1$	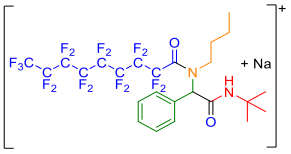
a: 35 eV top							
2 in **a**	✳	82000	675.0910	675.0916	0.0006	$C_{21}H_{17}O_2N_2F_{17}Na_1$	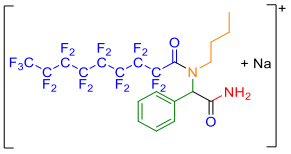
3 in **a**	❖	93000	575.0148	575.0154	0.0006	$C_{16}H_7O_1N_1F_{17}Na_1$	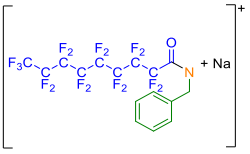
4 in **a**	⊡	157000	184.1098	184.1102	0.0004	$C_{11}H_{15}N_1Na_1$	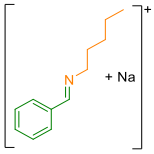
b: 50 eV bottom							
5 in **b**	◀	169000	162.1278	162.1283	0.0005	$C_{11}H_{16}N_1$	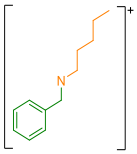
6 in **b**	●	208000	106.0660	106.0657	0.0003	$C_7H_8N_1$	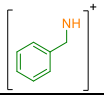

Figure 15. a, Tandem-MS of a single charged species at 731 *m/z* (▶). Recoded in positive mode with an HCD energy of 35 eV. **b**, with an HCD energy of 50 eV. The expansions visualize the range from 550 – 700 *m/z*. The heavier fragments (❖and✳) are exclusively observed in the lower energy spectrum (**a**) and the smaller fragments (●and◀) exclusively in the higher energy spectrum (**b**). **Table (bottom):** peak assignment of the ESI-MS/MS spectra in **a** and **b**.[208]

After evaluating the data of numerous spectra, the most probable fragments were identified (see **Figure 16**) and applied for the subsequent readout of molecular keys. Interestingly, similar fragmentation patterns were observed in FAB-MS and in GC-MS (see **Figure 9**) for several compounds.

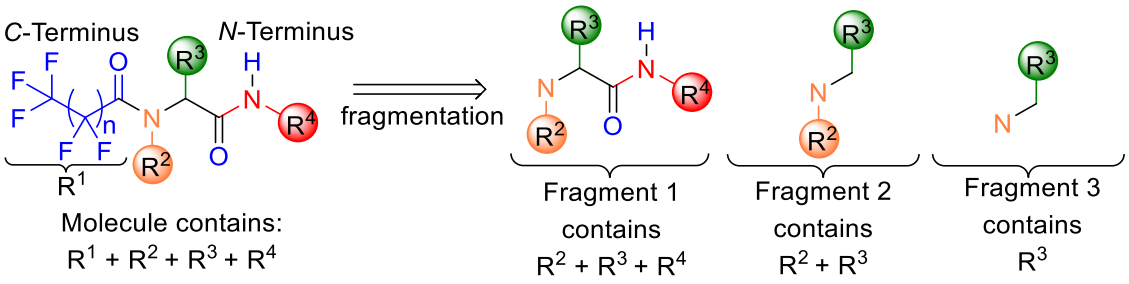

Figure 16. Four sidechains require four parameters. The parameters are determined *via* four masses. The mass of the intact molecule and the three fragments were utilized for readout of molecular keys.[208]

4.1.2.1 Differentiation of isomers

Tandem-MS fragment analysis is also capable of distinguishing between isomers of molecular keys (molecules with the same mass but different structures). In **Figure 17**, two isomeric molecular keys are displayed. These isomers cannot be distinguished by regarding the molar mass of the intact molecule (►) nor the isomer fragments. It is necessary to evaluate the lighter fragments (● and ■), which are unambiguously different. The respective ESI-MS/MS spectra are displayed in **Figure 17 b** (isomer 2) and **Figure 17 c + d** (isomer 1). Unique fragmentation patterns allow differentiation of isomeric molecular keys, if the list of components is known and does not include isomers for the same component (as stated in the criteria for the list of components, see **Figure 8**).

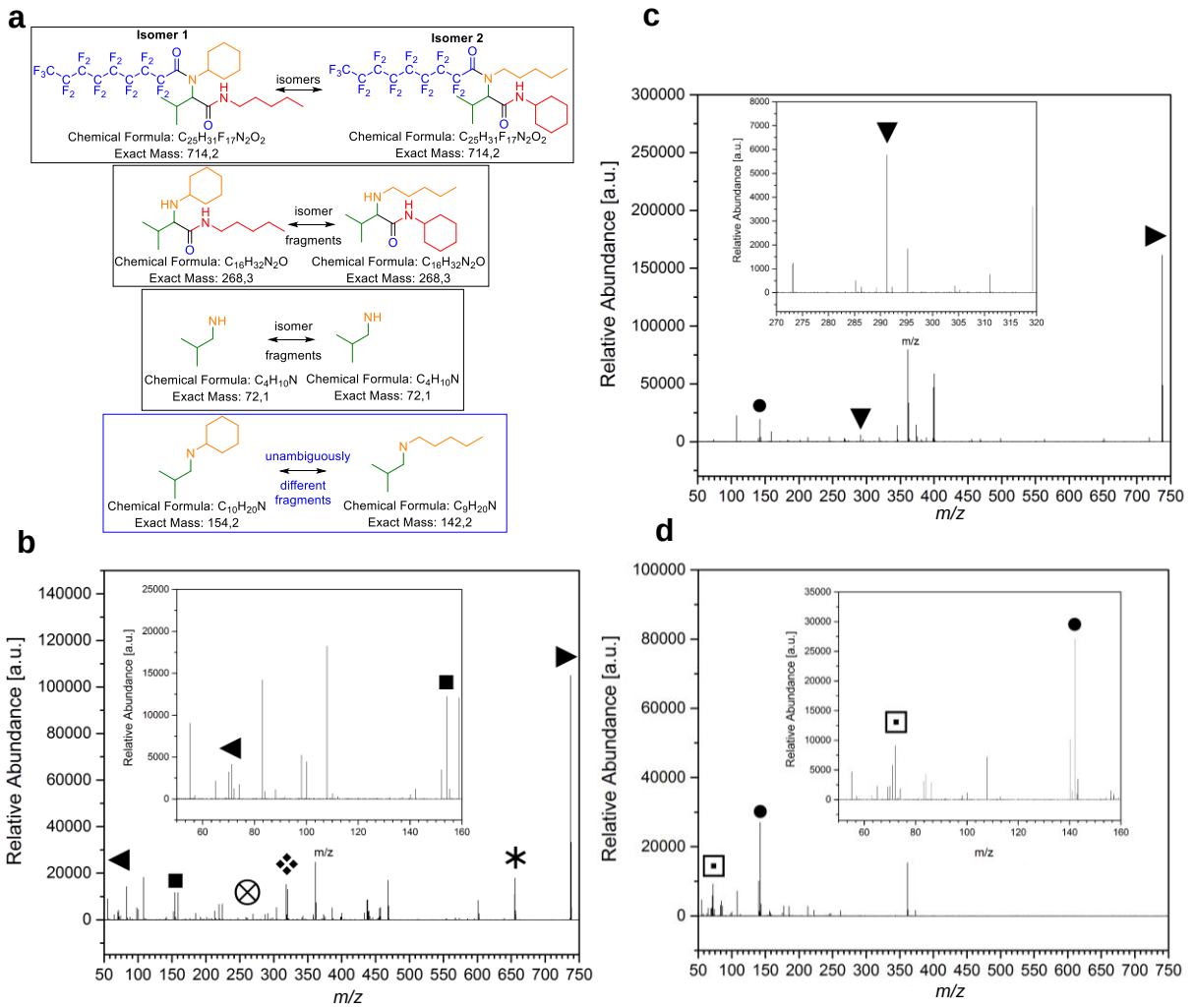

Figure 17. Differentiation of isomers *via* ESI-MS/MS. **a**, two isomeric molecular keys and their respective fragments. **b**, ESI-MS/MS of a single charged species at 737 *m/z* (►) (Isomer 1). **c** and **d**, ESI-MS/MS of a single charged species at 737 *m/z* (►) (Isomer 2). HCD energy = 25 eV (**c**) and 50 eV (**d**). The larger fragment (▼) is observed in the 25 eV spectrum (**c**) and the smaller fragments (⊡and●) in the 50 eV spectrum (**d**). **Table 5** (below), includes fragment assignment.

Table 5. Fragment assignment for the *m/z* species in Figure 17 b – c.

Entry	Label	Resolution	*m/z*(exp)	*m/z*(theo)	Δ*m/z*	Formula	Structure
1 in **c**	▶	75000	737.2000	737.2011	0.0011	$C_{25}H_{31}O_2N_2F_{17}Na_1$	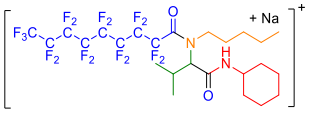
2 in **c**	▼	124000	291.2405	291.2412	0.0007	$C_{16}H_{32}O_1N_2Na_1$	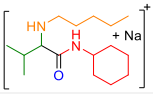
3 in **c**	●	172000	142.1591	142.1596	0.0005	$C_9H_{20}N_1$	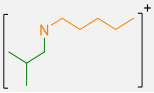
4 in **d**	⊡	252000	72.0815	72.0813	0.0002	$C_4H_{10}N_1$	
5 in **b**	▶	78000	737.2000	737.2011	0.0011	$C_{25}H_{31}O_2N_2F_{17}Na_1$	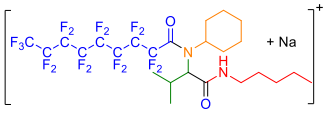
6 in **b**	✳	86000	655.1220	655.1229	0.0009	$C_{19}H_{21}O_2N_2F_{17}Na_1$	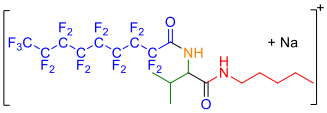
7 in **b**	❖	117000	318.2402	318.2401	0.0001	$C_{18}H_{33}O_2N_1Na_1$	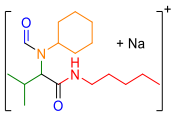
8 in **b**	⊗	137000	269.2588	269.2593	0.0005	$C_{16}H_{32}O_1N_2$	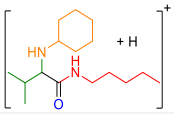
9 in **b**	■	177000	154.1592	154.1596	0.0004	$C_{10}H_{20}N_1$	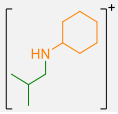
10 in **b**	◀	247000	72.0815	72.0813	0.0002	$C_7H_8N_1$	

Regarding the fragmentation spectra of the above mentioned examples, some of the masses employed for readout out are comparably weak in intensity, complicating the analysis. In order to simplify the analysis a custom made computer script, providing the masses of the expected fragments, was employed. The function and application of this so-called analysis script is described later, in chapter **4.1.2.3**.

4.1.2.2 Influence of stereochemistry

In the course of the Ugi reaction, a new chiral center is formed which was not controlled in the present protocol. Hence, if racemic mixtures of precursor components are utilized, diastereomeric product mixtures will result after the Ugi reaction. In order to

study if diastereoisomers have an influence on either the separation protocol or the ESI-MS/MS fragmentation behavior, a model compound mixture consisting of four diastereoisomers (see **Figure 18**) was synthesized, purified *via* F-SPE and fragmented *via* ESI-MS/MS.

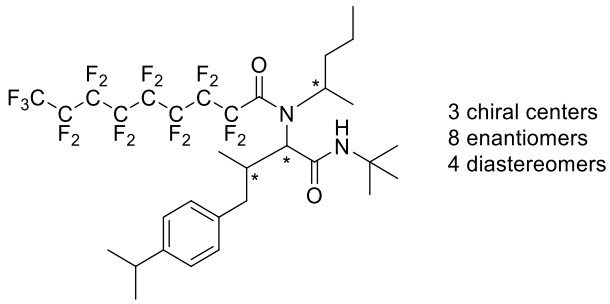

Figure 18. Model compound for investigating the influence of stereochemistry on the ESI-MS/MS readout. The molecular key presented above was synthesized from racemic mixtures of precursor components. The reaction Ugi reaction will thus form a mixture of four different diastereoisomers.

The F-SPE separation protocol retains perfluorinated compounds selectively and is therefore unselective towards the separation of diastereoisomers. This characteristic of F-SPE was utilized in the field of so-called fluorous mixture synthesis (FMS).[326] FMS separation was applied for the synthesis of diastereomer mixtures, wherein F-tagged diastereomers were synthesized stepwise and separated from non-fluorinated contaminations *via* F-SPE.[327] If a diastereomeric mixture is subjected to tandem-MS experiments, it can be assumed that the required fragments for the readout will still be observed. Even if theoretically different fragmentation pathways may occur, the favored fragments presented in the manuscript will still be observed, at least for some of the pathways (perhaps with a lower probability, but still detectable). The observed *m/z* of the fragments is independent from the stereochemical information. The fragmentation behavior of diastereoisomers in tandem-MS methods was previously studied, confirming that the fragmentation leads to a different intensity distribution pattern but all relevant fragments were observed.[328,329] In **Figure 19** the fragmentation of the diastereomeric product mixture is illustrated, indicating that diastereomeric mixtures of molecular keys can be read out in the same manner as described before. In conclusion, diastereomeric mixtures of molecular keys can be synthesized, purified and read out respectively, employing the herein established protocols.

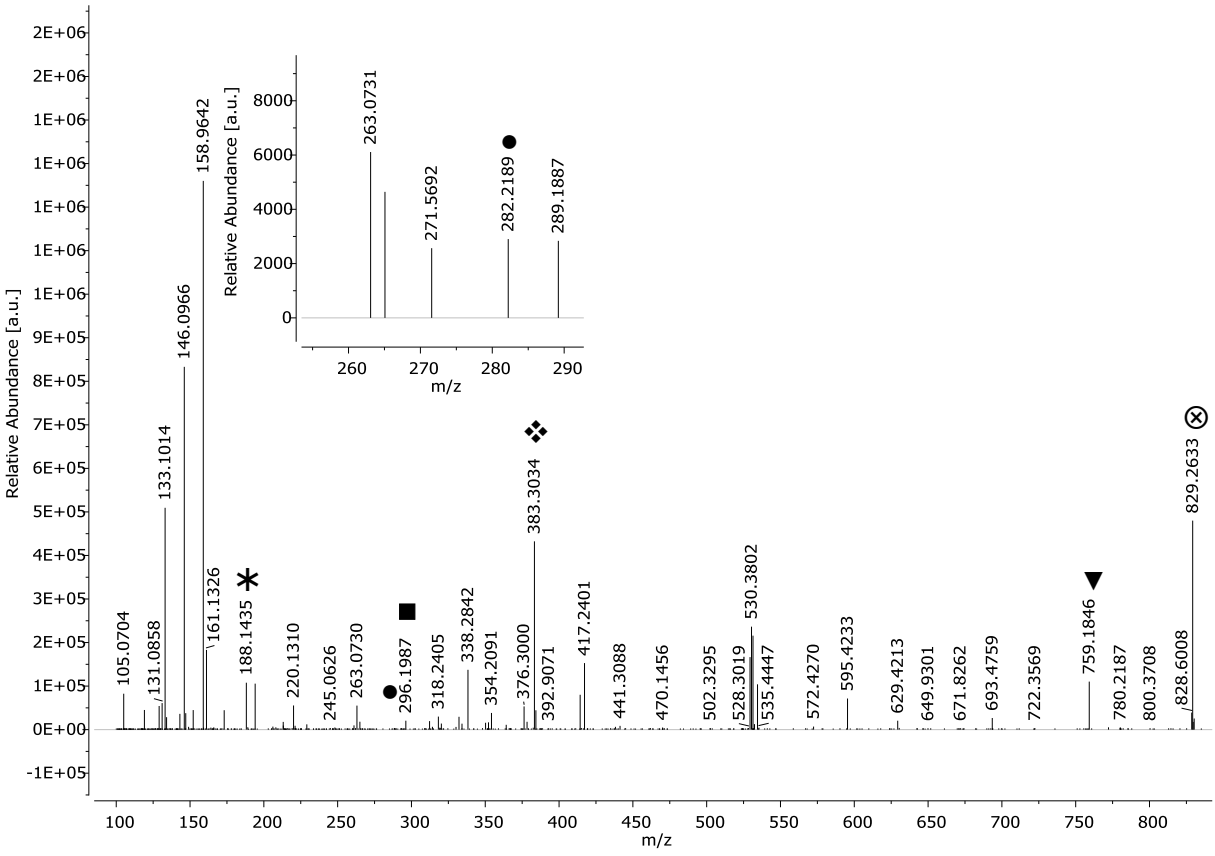

Entry	Label	Resolution	*m/z*(exp)	*m/z*(theo)	Δ*m/z*	Formula	Structure
1	⊗	73800	829.2633	829.2638	0.0005	$C_{32}H_{39}O_2N_2F_{17}Na_1$	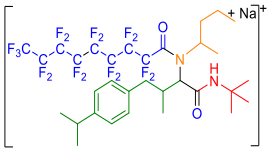
2	▼	71000	759.1846	759.1850	0.0004	$C_{27}H_{29}O_2N_2F_{17}Na_1$	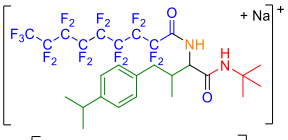
3	❖	106000	383.3034	383.3033	0.0001	$C_{23}H_{40}O_1N_2Na_1$	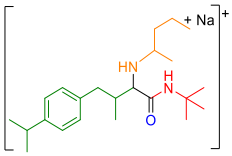
4	■	122000	296.1987	296.1985	0.0002	$C_{18}H_{27}O_1N_1Na_1$	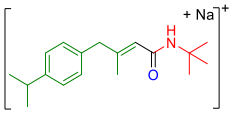
5	●	124000	282.2189	282.2192	0.0003	$C_{18}H_{29}N_1Na_1$	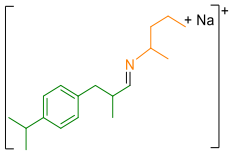
6	∗	165000	188.1435	188.1434	0.0001	$C_{13}H_{18}N_1$	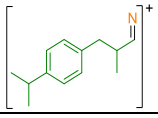

Figure 19. Top: Fragmentation of a molecular key diastereomeric mixture. ESI-MS/MS of a single charged species at *m/z* = 829 (⊗). HCD energy = 35 eV. **Table (bottom):** fragment assignment of the spectrum above.[208]

4.1.2.3 Computer assisted readout for tandem-MS spectra

The analysis of tandem-MS spectra at different energies turned out to be time consuming. At this point a computer script becomes a very useful tool for providing pre-calculated masses of the most probable fragments after the input of the monoisotopic mass of the respective molecular key. The script was conceptionally designed by the author and discussed with Kevin Reiter (cooperation partner). The computer programming and refinement was subsequently performed by Kevin Reiter. The script operates as follows: the database of components is the basis for the alphanumerical coding (*e.g.* aldehydes → letter A; benzaldehyde → A(003), *etc.*), the chemical formula, the corresponding exact masses and SMILES codes for visualizing the molecule; *e.g.* A(003) | benzaldehyde | $C_7H_6O_1$ | 106.04186 g·mol^{-1} | SMILES: [H]C(C1=CC=CC=C1)=O. The script is capable of calculating the molar masses of all possible Ugi compounds with respect to the reaction equation, by adding the molar masses of all components and subtracting the molar mass of water *i.e.* M(Ugi product) = M(carboxylic acid) + M(aldehyde) + M(isocyanide) - M(water). This calculation is performed for all 500,000 permutation and stored in a separate list.

The script uses the input of the monoisotopic mass and then searches for all possible permutations of component combinations within a certain mass range (reduction of possibilities is illustrated in **Figure 20**). The monoisotopic mass $[M + Na]^+$ is entered with four decimals *e.g.* 567.5678 and an appropriate ΔM threshold *e.g*. ΔM = 0.02 Da. The resulting possibilities are again listed by the script and the masses of probable fragments are directly displayed (the fragment masses are calculated with respect to the general fragment structures displayed in **Figure 16**). For small ΔM thresholds the remaining possibilities are reduced several orders of magnitude, *e.g*. if ΔM = 0.001 Da, the initial 500,000 permutations are reduced to a maximum of around 60 possibilities. This reduction can be visualized by comparing the height of a human to the height of Mount Everest. After entering fragments to the script, the resulting possibilities are further reduced and refined until the structure is determined. The fragment masses are entered with two decimals (*e.g.* 123.45). If accidentally a wrong digit was entered, the REDO command will return to the initial selection of possibilities after entering the $[M + Na]^+$ mass.

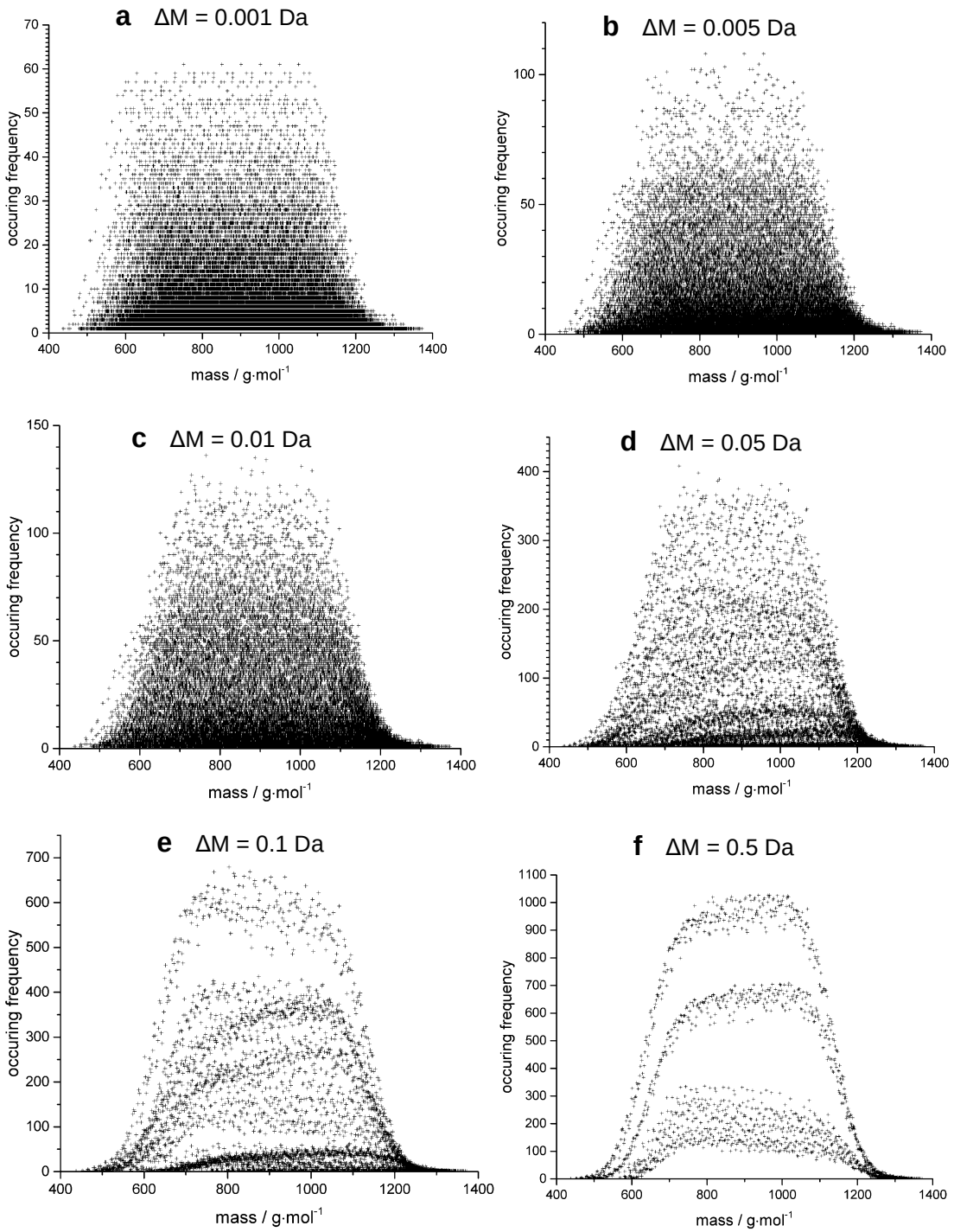

Figure 20. Database evaluation of the list of components, regarding the occurring masses within certain thresholds: **a**, ΔM = 0.001 Da. **b**, ΔM = 0.005 Da. **c**, ΔM = 0.01 Da. **d**, ΔM = 0.05 Da. **e**, ΔM = 0.1 Da. **f**, ΔM = 0.5 Da. This analysis was provided by a cooperation partner: Kevin Reiter.[208]

After entering enough fragments (in most cases two fragments are sufficient information; in case of isomers, three fragments are required), the distinct molecular structure is obtained, and the script generates the alphanumerical code of the molecular key *e.g.* A(005)-B(002)-C(004)-D(007). The script also offers the possibility to display more detailed information about the molecular key *via* the PRINT command. After selecting the print command, a SMILES code for the target molecule and all

precursor components (on basis of the list of components) is displayed. The SMILES code of the Ugi compounds are generated employing a generalized SMILES code for Ugi *bis*-amides with four different variables for the four sidechains (introduced by the four components). *$acid$*N(*$amine$*)C(*$aldehyde$*)C(N*$isocyanide$*)=O.

The variables (between the *$* signs) were then substituted by the corresponding SMILES coded associated with the sidechains obtained from the list of components. The SMILES code of the Ugi products generated by the script can be copied *e.g.* to ChemDraw® (insert with Alt+Crtl+P) for visualization of the respective molecular structure. The evaluation and assignment of ESI/MS/MS fragments can clearly determine the structure of the molecular keys. In principle, further analytical methods could be introduced for the readout (*i.e.* quantitative ^{19}F-NMR spectroscopy for R^1 in combination with three masses from tandem-MS). The analysis script can be downloaded from the supplementary information of reference[208] and is also included in the electronic version of this thesis (on the CD). In addition, the electronic version includes the tandem-MS spectra of three molecular keys for testing the analysis script.

4.1.3 Cryptography integration of the molecular keys

As described previously, the 500,000 permutations equal approximately 18 bits. In order to provide a possible application for the molecular keys and their respective data storage capacity, a cryptography integration is suggested herein. The cryptographic system is based on a secret communication channel employing molecular keys, which can be easily hidden in various media, transferred nondigitally, isolated *via* F-tags and unambiguously read out *via* ESI-MS/MS. Considering cryptography, the well-established Advanced Encryption Standard (AES) algorithm was combined with an effective hiding and transportation of the encryption key. The herein presented molecular keys based on Ugi compounds provide a robust steganographic channel that can be used to transport *i.e.* cryptographic keys. An AES key with 100 bits or more can be considered as physically unbreachable (due to limited computing power), hence the AES key should be encoded on six to seven molecular keys (6 × 18 bits = 108 bits). An exemplary way of key transmission is illustrated in **Figure 21**. The sender and recipient first meet to exchange details on how to secretly communicate in the future

(**Figure 21 a**). They need to agree on how the molecular key will be transferred (*e.g.* adsorbed on paper, dissolved in a perfume, *etc.*), whether the AES decryption key will be fragmented onto several molecular keys, and if so, how many individual molecular keys will be used. Additionally, the list of components, is exchanged and the analytical methods are preselected (tandem-MS). These initially communicated details should remain secret, however, if an adversary reveals one or some of the discussed details, the adversary is still not able to decrypt the message without knowing the other information, the list of components and most importantly the molecular keys.

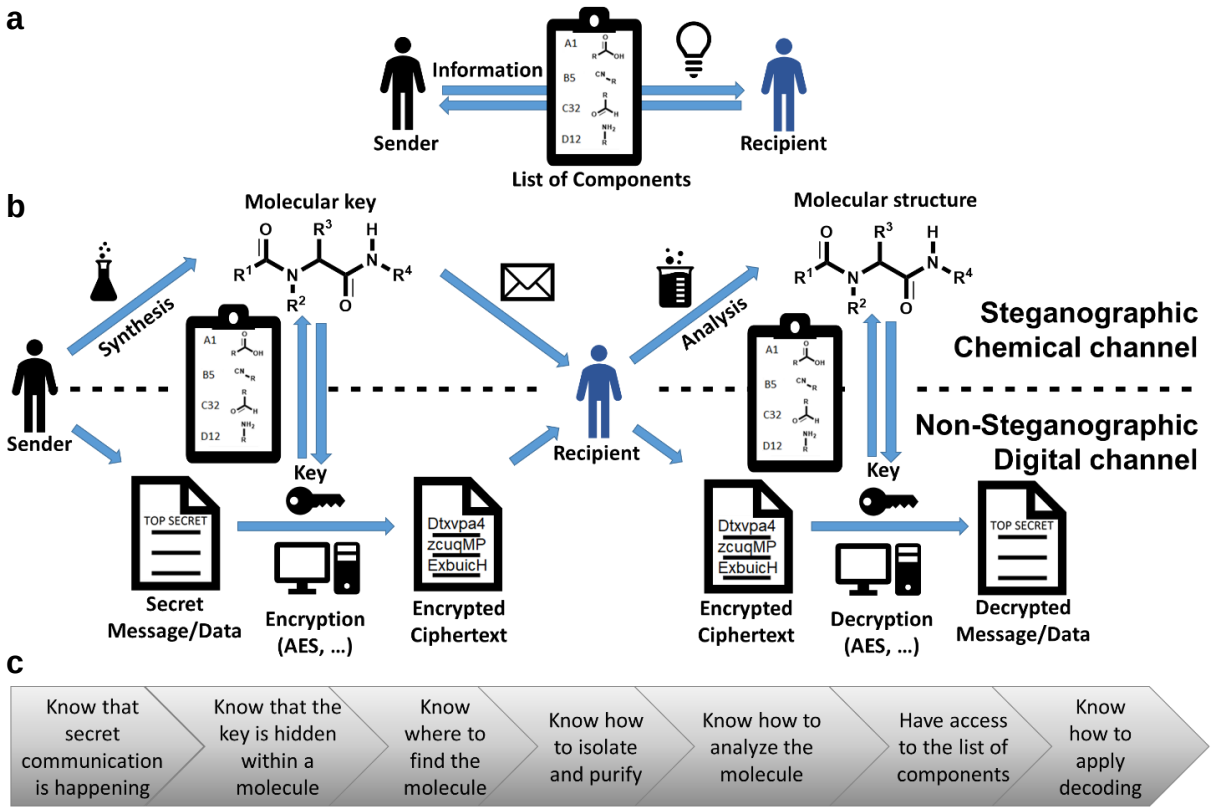

Figure 21. Cryptography integration of molecular keys. **a**, sender and recipient exchange the list of components and discuss details about their secret communication. **b**, from left to right: the sender synthesizes one or several molecular keys and determines the alphanumeric code associated with the chemical structures according to the list of components. The alphanumeric code *e.g.* A(005)-B(013)-C(007)-D(027) is serving as encryption key/password. The molecular key is concealed and transferred to the recipient *via* a steganographic channel. The recipient isolates the key and elucidates the molecular structure for decryption. **c**, hierarchical levels of security and knowledge an adversary needs for decryption.[208]

The molecular keys can hardly be recognized, because *i*. an adversary does not know that a key is hidden in a molecule; *ii*. only the recipient knows where the molecular keys are located/stored (*i.e*. adsorbed on paper, dissolved in perfume, *etc.*, see below) and in which order they should be readout; *iii*. an adversary needs information on how to extract and analyze the molecule, convert the chemical structure into digital information and apply the necessary decryption. *iv*. Since the keys are transferred

physically, an attacker cannot rely on computing power alone. Molecular keys can be hidden and transferred in many creative ways. Since the molecular keys are fluoro-tagged compounds, they can be isolated from various types of surrounding media. The main requirement to the surrounding environment or the matrix material is the absence of any perfluorinated alkyl chains. Furthermore, the extraction of the molecular key should be possible with reasonable effort.

The following extraction examples were performed with the molecular key **19**. As a first transportation example adsorption onto paper was chosen (see **Figure 22**). Therefore, 4.0 mg of the molecular key were dissolved in 0.5 mL methanol and subsequently transferred dropwise onto the top right corner of an envelope. Intermediately, the drops were quickly evaporated by gently blow-drying with a heat gun. For further protection and disguising, a stamp was placed above the covered area (see **Figure 23**).

Figure 22. Transportation and extraction of a molecular key. The molecular key is dissolved and placed in the top right corner of the envelope and covered with a stamp. After the letter reached its destination, the molecular key is extracted and purified *via* F-SPE prior to analysis.[208]

For later extraction, the part of the paper doped with the molecular key (here the area around the stamp) was cut into pieces and extracted in an ultrasonic bath with 15 mL methanol for 15 minutes three times and subsequently three times with 10 mL dichloromethane. The extracts were combined, concentrated under reduced pressure

and purified *via* F-SPE. In this protocol 3.5 mg (90%) of the molecular key were recovered. In another experiment, hiding of molecular keys in solution was demonstrated. Therefore, a molecular key was dissolved in a commercial perfume. 4.0 mg of the molecular key were dissolved in 0.5 mL ethanol and transferred into the same amount of a commercial perfume (see **Figure 23 l** - **o**). The resulting solution is more diluted than the initial perfume, but the dilution cannot be easily recognized by a change of appearance or smell. The molecular key proved to remain in solution throughout the investigated time of more than 14 days. It can be assumed, that the molecular key will not precipitate or phase-separate, because a diluted system is used. For the extraction of the molecular key, the perfume solution was evaporated under reduced pressure and subjected to F-SPE. In this protocol, 3.7 mg (93%) of the molecular key were recovered. Another example was demonstrated by adsorption onto instant coffee powder, tea or sugar (see **Figure 23 f** - **h**): 4.0 mg of the molecular key were dissolved in 0.5 mL dichloromethane and added dropwise onto 1 g of the substrate powder, each drop was placed onto a different spot and allowed to evaporate separately. For the extraction, the powder was ground with a mortar and stirred three times in 5 mL dichloromethane for 3 minutes. The combined extracts were filtered over celite®. The filtrate was washed with 10 mL water, twice. The combined aqueous phases were reextracted with 5 mL dichloromethane, twice. The combined organic phases were washed with 5 mL brine, dried over sodium sulfate, evaporated under reduced pressure and purified *via* F-SPE. Extraction yields: from instant coffee powder 3.4 mg (85%), from green tea 3.6 mg (90%), from sugar 3.4 mg (87%), of the molecular key were recovered. For the extraction from sugar, no further purification *via* F-SPE was necessary, because sugar is a fully water-soluble substrate and was removed during the washing procedure. In order to demonstrate a challenging extraction example for the herein presented F-tagged molecular keys from complex biological media, pig blood was chosen as carrier substrate. Extraction from biological media would be far more challenging for cryptographic keys encoded in DNA or other biomolecules. 5.0 mg of the molecular key were dissolved in 0.5 mL ethanol and concentrated under reduced pressure until a transparent film of the molecular key with a minimized amount of ethanol was obtained. 5 mL of pig blood were added into the vial and gently stirred for 5 min. For stability reasons, the blood should be stored and transported under cooling. For later extraction, the blood sample was diluted with 10 mL water and extracted with 20 mL dichloromethane three times. After the second

extraction, an emulsion was formed, hence the second and third organic extracts were combined and treated separately. The organic extracts were washed separately with 10 mL water, twice. The organic phases were dried over sodium sulfate. The emulsion broke upon drying and a clear solution was obtained. This solution was evaporated under reduced pressure and purified *via* F-SPE. In this protocol, 4.5 mg (91%) of the molecular key were recovered.

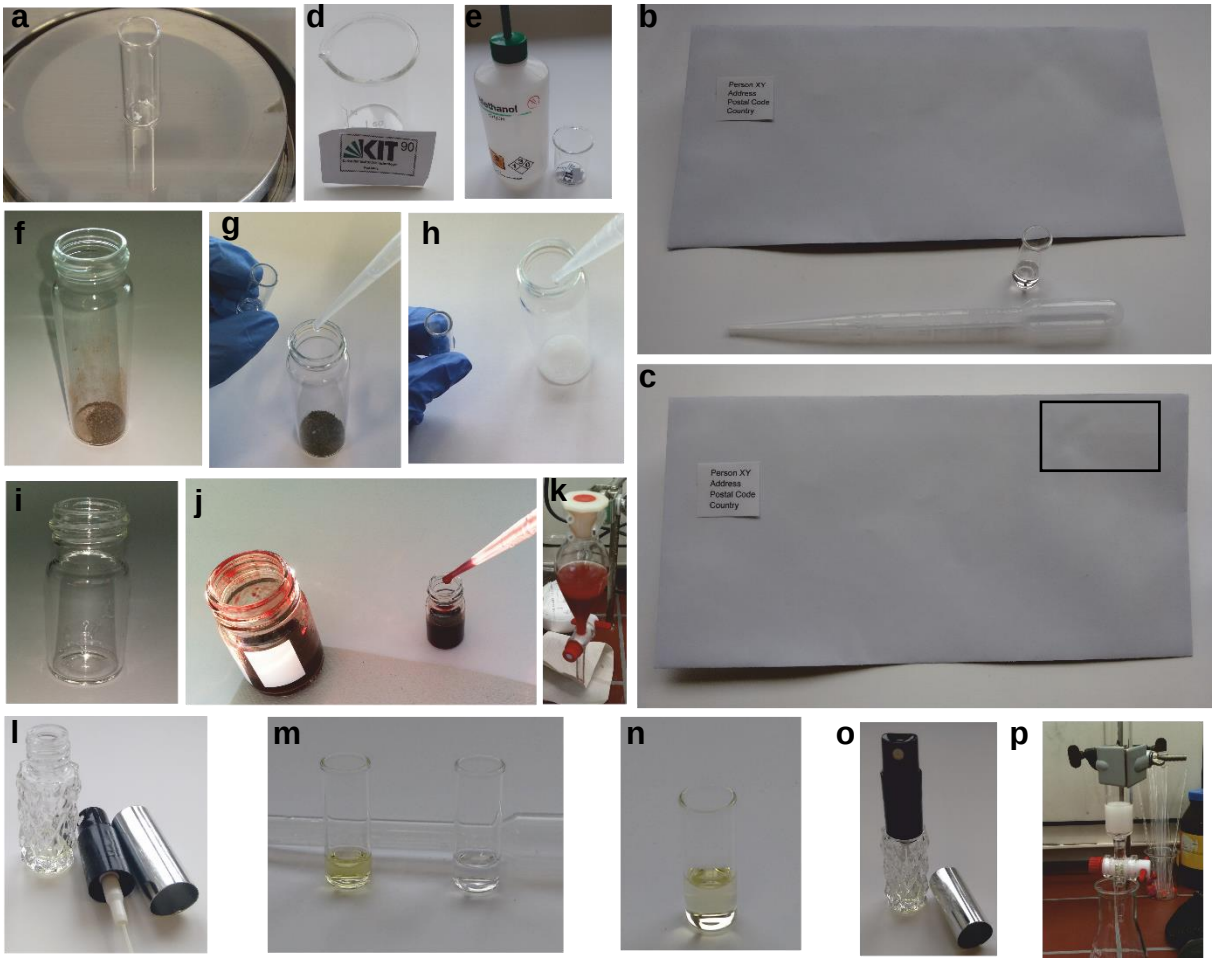

Figure 23. Hiding of molecular keys. **a**, 4.0 mg of powdered molecular key on a scale. **b**, envelope before application. **c**, envelope after adsorption of the molecular key (the black box indicates the treated area, the adsorbed molecular key was not visible with bare eyes). **d**, envelope containing the molecular key cut in pieces **e**, before the extraction with methanol. **f**, molecular key adsorbed onto instant coffee powder. **g**, molecular key adsorbed on green tea. **h**, adsorption onto sugar. **i**, in this vial the molecular key was previously dissolved in ethanol. The solvent was evaporated until a transparent film was obtained, before mixing with blood. **j**, mixing with pig blood. **k**, re-extraction of the molecular key from blood. **l**, empty perfume bottle. **m**, the left vial (yellow liquid) contains the original perfume, right vial (colorless liquid) contains the molecular key dissolved in methanol. **n**, resulting solution after mixing the perfume with the dissolved molecular key. **o**, transferred into the perfume bottle. Although the mixture is now more diluted, it cannot be easily distinguished from the original perfume with bare eyes or by the smell. **p**, typical F-SPE column for the purification of molecular keys.[208]

In principle, for MS analysis, even smaller amounts of substance are sufficient for the readout. However, the herein employed masses of several milligrams were sufficient to further conduct TLC, GC-MS and ^{1}H-NMR experiments for purity determination.

After the molecular key is isolated and purified, (tandem-)MS-spectra are measured and employed to readout the molecular keys. The alphanumerical codes can be employed directly as AES encryption keys *e.g.* A(005)-B(002)-C(004)-D(007) is the password for encrypting secret data. If several molecular keys were utilized, they are entered one after the other.

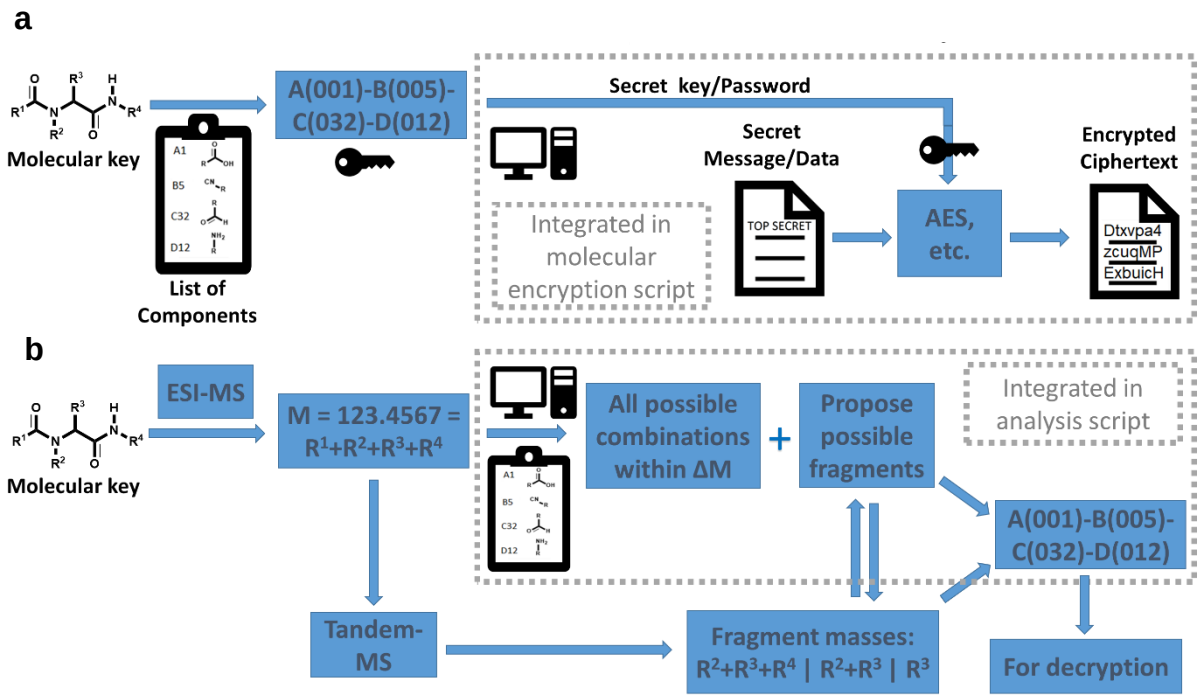

Figure 24. a, Schematic illustration of molecular encryption encryption/decryption process which is conducted by an independent symmetric encryption scheme *e.g.* the molecular encryption script. **b**, Schematic illustration of the analysis script. The alphanumerical codes obtained from the list of components serve as AES keys (passwords).[208]

Inspired by the idea to incorporate even more varying components into one molecule, in order to achieve higher storage capacities, the combination of two multicomponent reaction was investigated (presented in the following chapter **4.2**).

4.2 Combining the Biginelli and Passerini reaction

Parts of this chapter and following subchapters were adapted from previous passages written by the author.[23]

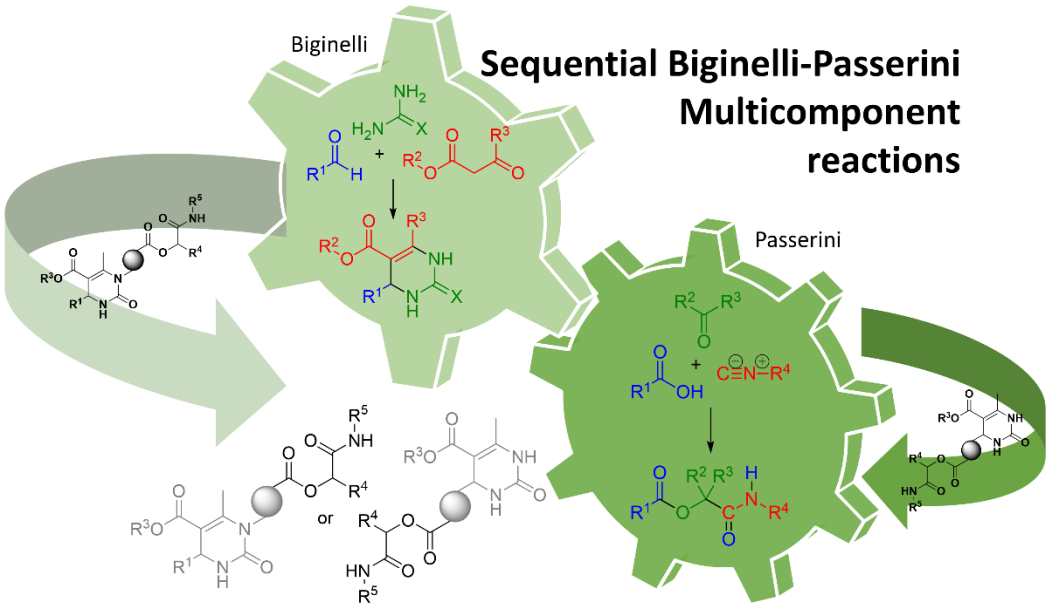

Figure 25. Graphical abstract for the investigation presented in chapter **4.2**.[23]

Multicomponent tandem reactions (previously described in chapter **2.2**.) are powerful synthetic tools in order to introduce multiple varying components into a distinct reaction product with minimal synthetic effort. In this context, the Biginelli reaction was combined in a sequential tandem approach with the Passerini reaction for the first time. In addition, both reactions were combined in a one-pot tandem procedure employing five different components at once.

For the herein described Biginelli-Passerini sequential tandem reactions, the Biginelli reaction was performed first, in order to avoid undesired transesterification reactions (of the ester groups in the Passerini products) due to the acidic conditions of the Biginelli reaction.[174] A challenge, which had to be faced while combining both reactions, was the choice of solvent and the selection of bifunctional components, which can interlink the Biginelli and the Passerini reaction. In the earlier-reported Biginelli-Ugi tandem reaction of Wipf *et al.*,[176] methanol could be used. However, as previously mentioned in chapter **2.1.2**, the solvent of choice for the Passerini reaction is dichloromethane. The DHMP Biginelli products employed herein, however, were in

most cases insufficiently soluble in dichloromethane. A screening of several solvents and solvent mixtures finally identified a mixture consisting of dichloromethane with a small amount of dimethyl sulfoxide (polar but aprotic) to successfully promote the combination of both chemistries. The possible bifunctional components for the Biginelli-Passerini combination are represented in **Figure 26**.

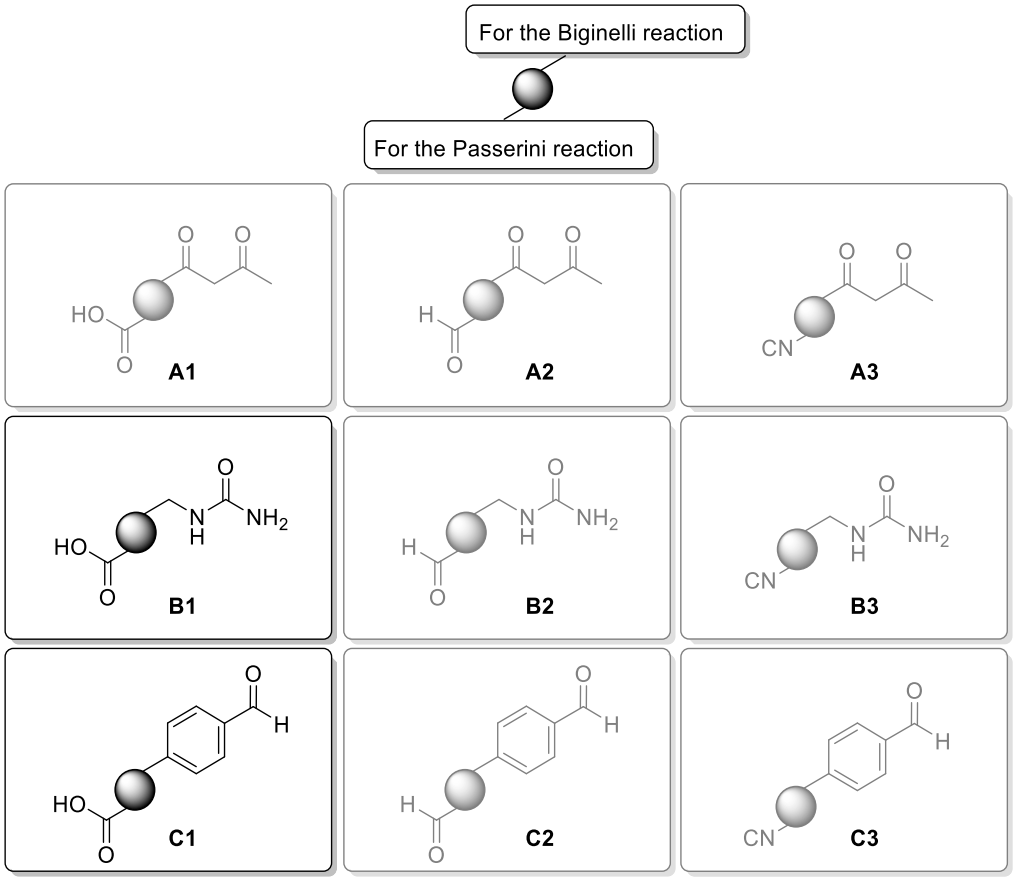

Figure 26. Bifunctional components evaluated for combining the Biginelli and Passerini reaction.[23] Linkers of the B1- and C1-type were employed in this investigation.

Evaluation of the combinations considering pervious reports from literature allowed a pre-selection of bifunctional linker molecules; **A3**, **B3** and **C3** display an isocyanide functionality, which could hydrolyze under the acidic conditions for the Biginelli reaction.[330] Components **A2**, **B2** and **C2** carry an aldehyde functional group for the Passerini reaction, but aldehydes can also react in the Biginelli reaction. Hence, **A2**, **B2**, **C2** as well as **A3**, **B3**, **C3** were excluded from this investigation. The remaining possible components **A1**, **B1** and **C1** seemed most promising for combining the Biginelli and Passerini reaction. The components featuring **A1**, **B1** and **C1** structures tested in synthetic experiments were: **C1**: 4-formylbenzoic acid; **B1**: *N*-carbamoylglycine, **A1**: benzyl acetoacetate (for the Biginelli reaction and subsequent hydrogenolytic deprotection to the corresponding acid).

In the first sequential step, the Biginelli reactions were performed in dimethyl sulfoxide at 110 °C in order to remove the water formed in course of the condensation reaction. The aldehyde was employed as limiting component, the urea and acetoacetate component were employed in 1.20 eq. excess with respect to the aldehyde. 4-Methylbenzenesulfonic acid (*p*-TSA) was added as catalyst. After a straight-forward washing procedure (described in **6.2.2**), the desired Biginelli acids **47** – **52** were obtained in 63 – 92% yields (see **Table 6**). Compared to literature known procedures, the herein established Biginelli protocol is simple, utilizes *p*-TSA as a cheap catalyst, provides high yields and can be used for the preparation of various Biginelli acids, employing different bifunctional linkers. Aliphatic aldehydes were not reactive under the present conditions, even after longer reaction periods of up to six days.

Table 6. Biginelli reactions for the preparation of Biginelli acids.

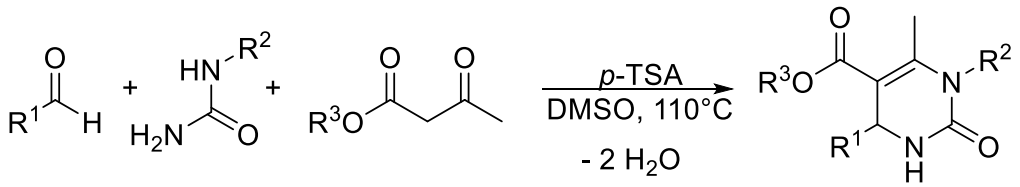

#	R^1	R^2	R^3	Yield [%]	Product **№**
1	Ph	H	Bn	91	**47**
2[a]	Ph	H	CO_2H	93	**48**
3	Ph	CH_2CO_2H	Et	63	**49**
4	Ph	CH_2CO_2H	Bn	77	**50**
5	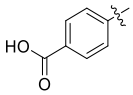	H	Et	90	**51**
6	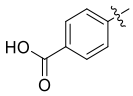	H	Bn	91	**52**

Conditions: 0.10 eq. *p*-TSA, 110 °C, 8 - 48 h in dimethyl sulfoxide. [a] Obtained *via* hydrogenolytic deprotection of product **47** (Entry #1). Conditions: H_2 (balloon), 10 wt.% Pd/C, solvent mixture of acetic acid/ethanol (1:3), 50 °C, 15 h.

For the subsequent Passerini reactions, the Biginelli acids were dissolved in the previously described mixture of dichloromethane with dimethyl sulfoxide as co-solvent. The aldehyde and isocyanide component were added in 1.5 fold excess with respect to the Biginelli acid. After three days reaction time at room temperature and subsequent purification *via* column chromatography, the Biginelli-Passerini products **53** – **61** were obtained in 22 – 99% yields. The results are summarized in **Table 7**.

Table 7. Passerini reactions utilizing Biginelli acids.

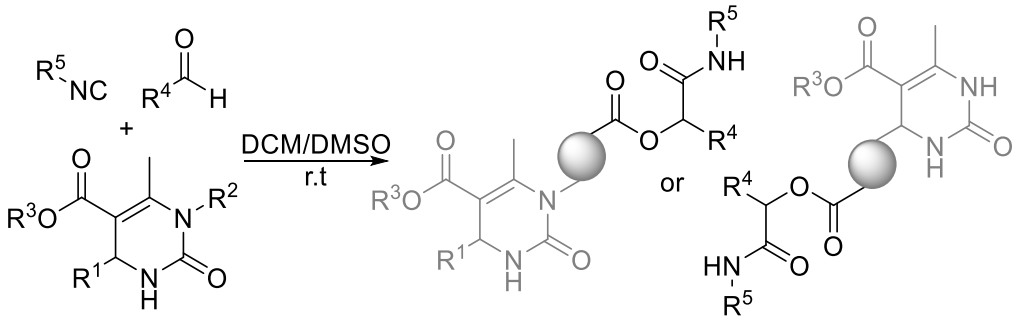

#	Biginelli acid №	R^1	R^2	R^3	R^4	R^5	Yield [%]	Product №
1	**51**	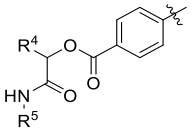	H	Et	C_6H_{13}	^{t}Bu	67	**53**
2	**52**	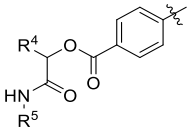	H	Bn	C_6H_{13}	^{t}Bu	22	**54**
3	**51**	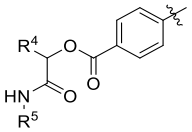	H	Et	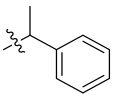	^{c}Hex	98	**55**
4	**49**	Ph	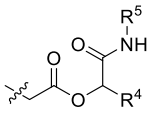	Et	^{i}Pr	^{t}Bu	76	**56**
5	**49**	Ph	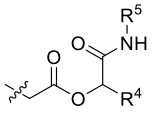	Et	$C_{10}H_{19}$	^{t}Bu	99	**57**
6	**49**	Ph	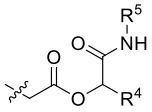	Et	C_7H_{15}	Bn	76	**58**
7	**49**	Ph	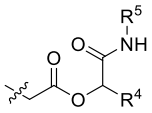	Et	C_7H_{15}	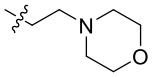	39	**59**
8	**49**	Ph	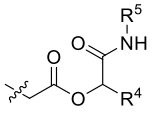	Et		C_5H_{11}	78	**60**
9[a]	not isolated	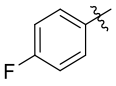	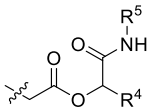	Et	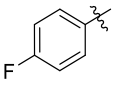	C_5H_{11}	41	**61**

Conditions: room temperature, 3 d reaction time in dichloromethane/dimethyl sulfoxide. [a] one-pot multicomponent tandem procedure, the Biginelli acid was not isolated.

Regarding the yields reported in **Table 7**, the products for entry #3 and #5 were obtained in quantitative yields. The lower yield for compound **59** (39%) is presumably due to the presence of the tertiary amine structure of the morpholinoethyl sidechain. On the one hand, this tertiary amine can act as a base and disrupt the Passerini reaction by deprotonating the acid component, and on the other hand substrate **59** required a different and more complex purification. During the synthesis of compound **54**, the reaction mixture was not completely homogenous, which is assumed to be responsible for the lower yield of 22%. For the other reactions presented in **Table 7**, the Passerini protocol proved to be robust and very effective, providing very good to quantitative yields. Considering the column chromatographic purification on silica gel, substrates employing a linker molecule of type **B1** (ureido-carboxylic acids, **Figure 26**) could be separated better than molecules employing linkers of type **C1** (aromatic aldehyde-carboxylic acids). The **C1** type molecules displayed a strong tailing effect, which is most probably correlated to the additional NH (polar and hydrogen bond donor) causing stronger interference with the polar stationary phase.[331]

In **Figure 27**, a representative ^{1}H-NMR spectra comparison between the Biginelli acid **51** (**Figure 27 a**) and the Biginelli-Passerini product **53** (**Figure 27 b**) is displayed. The CO_2**H** proton at 12.9 ppm is not observed after the Passerini reaction, while all other DHMP signals, *i.e.* the N**H**CH at 9.2 ppm, the C**H**NH at 5.2 ppm or the CC**H**$_3$ at 2.3 ppm, are still observable and did not shift significantly. Furthermore, in **Figure 27 b** the characteristic signals for the NHC**H** at 4.9 ppm, the C(C**H**$_3$)$_3$ at 1.2 ppm and the terminal CH_2C**H**$_3$ methyl group at 0.8 ppm strongly indicate the formation of the Biginelli-Passerini product.

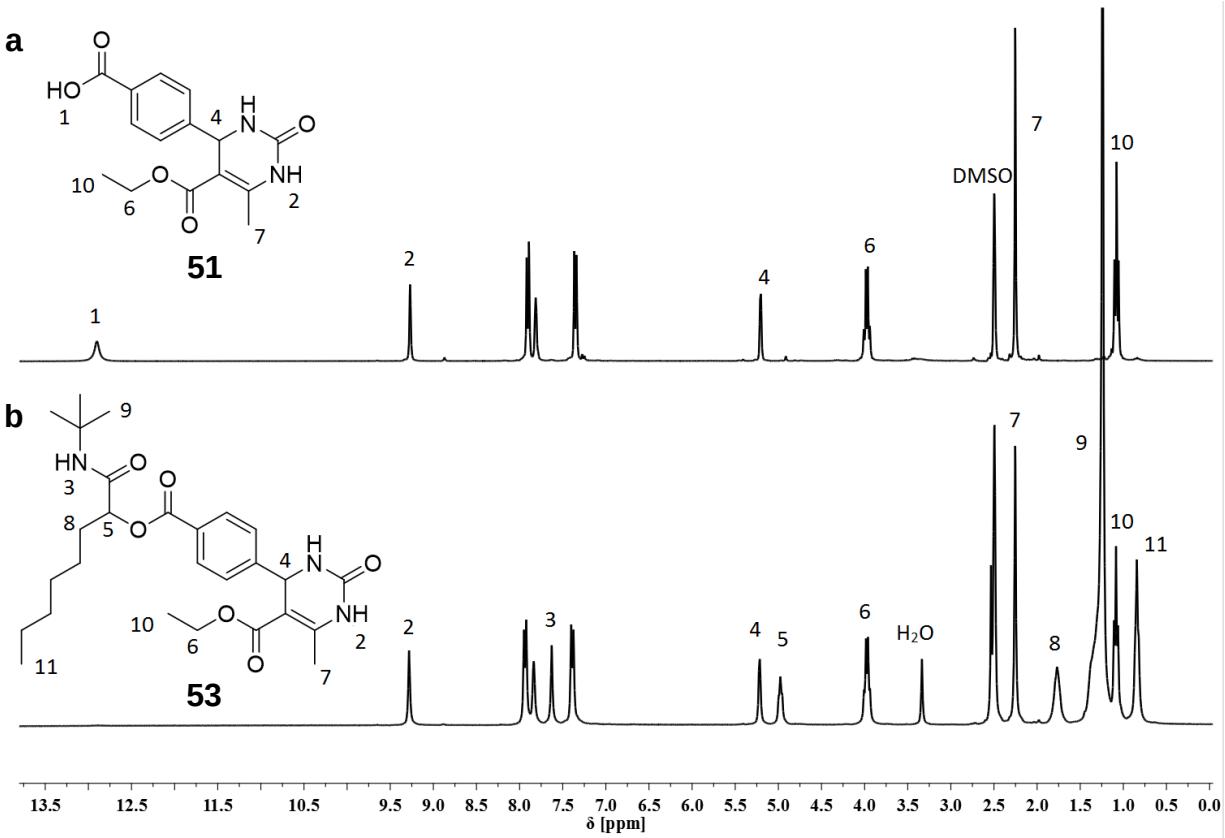

Figure 27. Stacked ^{1}H-NMR spectra and the respective signal assignment. **a**, Biginelli acid **51**. **b**, Biginelli-Passerini product **53**.[23]

Besides the sequential Biginelli-Passerini reactions, both reactions were conducted in a one-pot tandem reaction (see **Scheme 22**). Therefore, the Biginelli reaction was performed with a three-fold excess of the aldehyde component in a minimal amount of dimethyl sulfoxide. After completion of the Biginelli reaction, the crude reaction mixture was cooled to room temperature and diluted with dichloromethane. Subsequently, the isocyanide component was added to the mixture and enabling the Passerini reaction with the exceeding aldehyde.

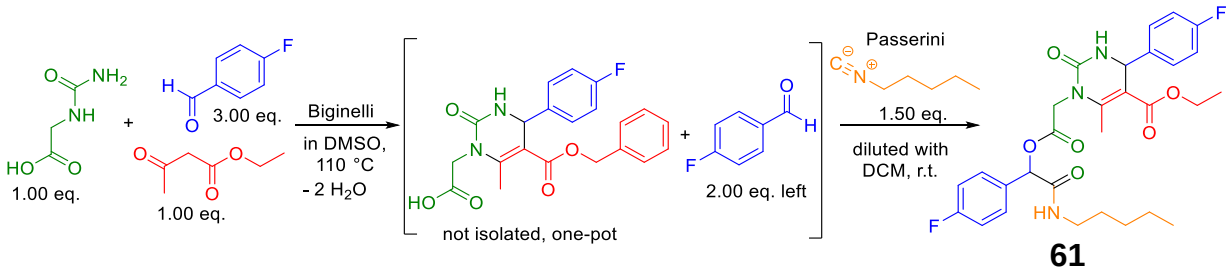

Scheme 22. Biginelli-Passerini one-pot tandem reaction.

The resulting one-pot tandem product **61** was obtained in 41% yield after column chromatographic purification without intermediate workup of the Biginelli acid (**Table 7**, entry #9). However, the structural diversity in the one-pot tandem procedure is more limited if compared to the previously described two-step approach (including isolation

of Biginelli acid) because in the one-pot procedure the same aldehyde component is participating in both multicomponent reactions. Compared to previously described combinations of multicomponent reactions (see chapter **2.2**), the herein described sequential strategy combined the Biginelli and Passerini reaction while utilizing several bifunctional linker components. Interestingly, the ^{1}H- and ^{13}C-NMR spectra of the Biginelli-Passerini tandem products displayed split signals which are illustrated for compound **55** in **Figure 28**.

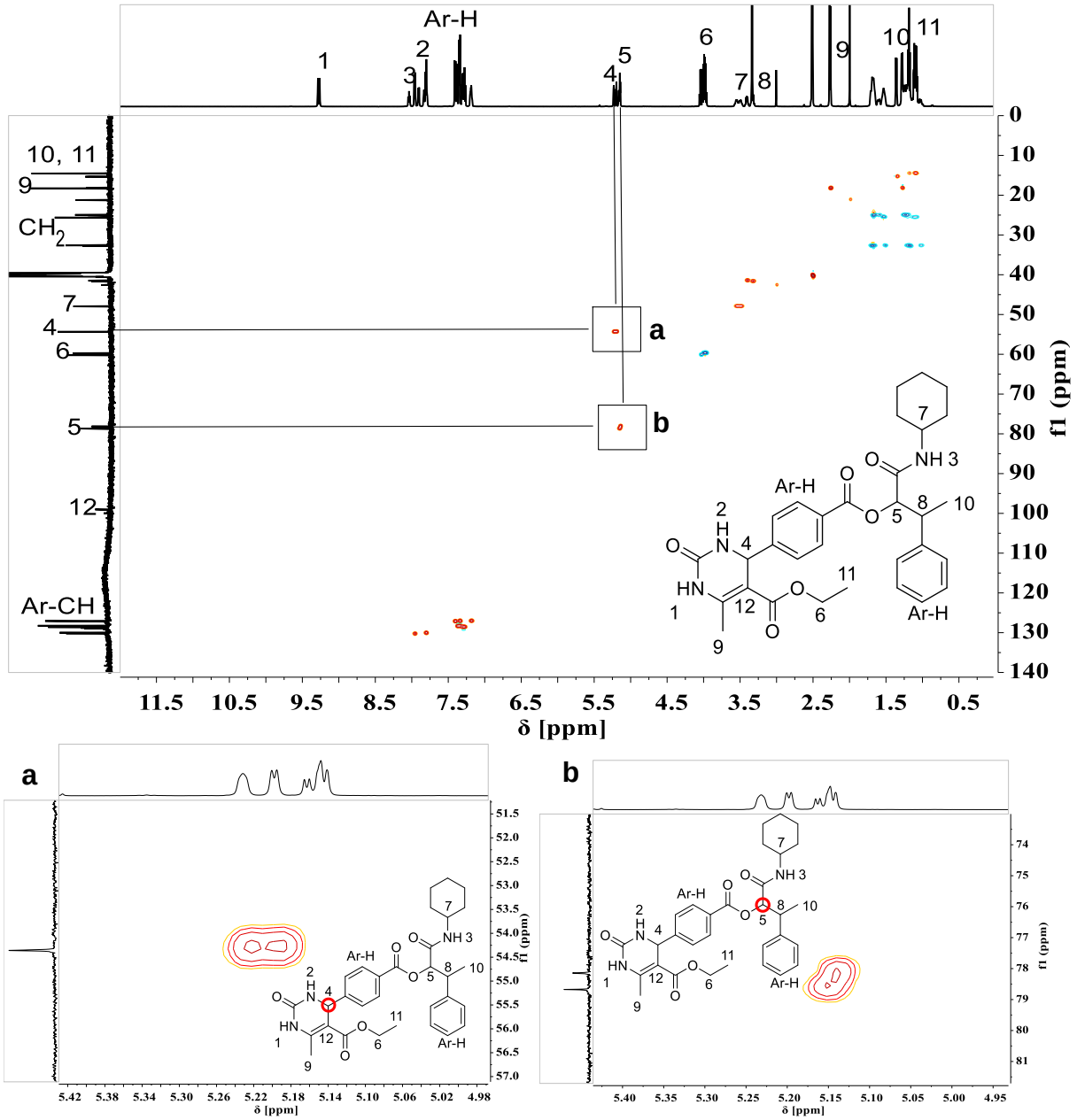

Figure 28. Phase sensitive HSQC spectrum of Biginelli-Passerini compound **55**, expansions and signal assignment for two asymmetric carbon atoms. **a**, diastereomeric signal splitting in ^{1}H-NMR spectrum exclusively. **b**, diastereomeric splitting in both ^{1}H- and ^{13}C-NMR spectra.[23]

Most of the split signals were located either next to chiral centers in the molecule or in the six membered DHMP core. In order to identify the cause of this peak splitting, high

temperature NMR experiments at 40 °C, 60 °C and 80 °C were conducted. Even at higher temperatures the peak splitting was still observed, evidencing that the splitting was not caused by rotational barriers (as described for the perfluorinated Ugi compounds in chapter **4.1.1**) or conformational effects. The signal splitting was not observed for the Biginelli acids, hence a diastereomeric effect was assumed. The Biginelli and Passerini reaction both from a new chiral center, which was not controlled in the present protocols, leading to racemic product mixtures in every multicomponent reaction step. Thus, after the Passerini reactions, four different stereoisomers (RR, RS, SR, SS) are obtained. The homo (RR, SS) and hetero pairs (RS, SR) are diastereomers with slightly different physical properties (causing different chemical shifts in the NMR spectra). However, the diastereoisomers could not be separated by chromatography or crystallization (nor by slow vapor diffusion crystallization). In order to separate the diastereoisomers chiral chromatography could be tested.

In conclusion, the Biginelli reaction was successfully combined with the Passerini reaction for the synthesis of highly functionalized DHMP heterocyclic products. Different Biginelli acids were prepared by variation of the components and the bifunctional linker. The Biginelli acids were employed in a Passerini reaction utilizing a dichloromethane/dimethyl sulfoxide solvent mixture. Furthermore, a one-pot Biginelli-Passerini reaction without intermediate workup was demonstrated. All compounds of this investigation were carefully characterized *via* NMR (1D and 2D) spectroscopy, IR spectroscopy and HRMS (see chapter **6.2.2**). The herein presented strategy was further developed for the preparation of sequence-defined macromolecules, which will be described in the following chapter **4.2**.

4.3 Macromolecules derived from two multicomponent reactions

Parts of this chapter and following subchapters were adapted from previous passages written by the author.[209]

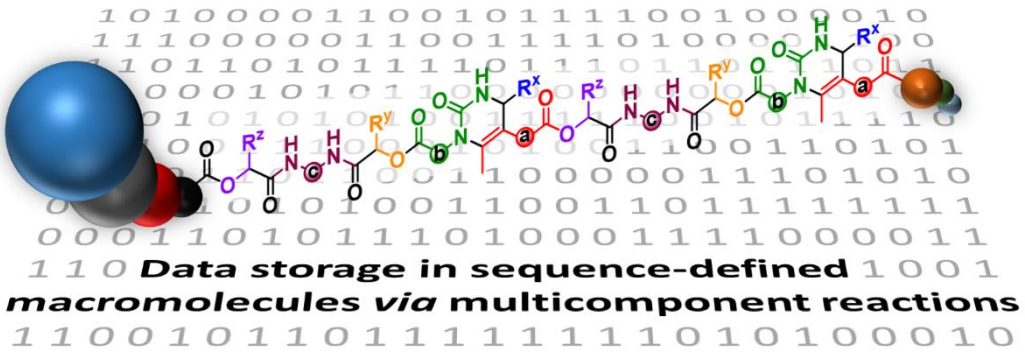

Figure 29. Graphical abstract for the investigation presented in chapter **4.3**.[209]

Sequence-defined macromolecules represent highly ordered structures and were already discussed in the context of data storage in chapter **2.5.1**. In chapter **4.1**, it was demonstrated that multicomponent reactions can be employed to build up a large variety of molecular structures which can be translated into computer processable codes. In the Ugi approach described previously, a virtual library comprising 500,000 permutations translated into approximately 18 bits of storage capacity (for one individual Ugi compound). In addition, a system that allows to utilize even more varying components *via* the combination of the Biginelli reaction and the Passerini reaction was investigated and described in chapter **4.2**. In the present chapter, the Biginelli and Passerini reaction were employed to synthesize bifunctional monomers which can be subsequently combined to information-coding macromolecules suitable for data storage materials.

4.3.1 Monomer design and a qualitative reactivity test system

The bifunctional monomers were designed in order to react in iterative Passerini and hydrogenolytic deprotection steps, inspired by the strategy described in chapter **2.4**, which was reported previously by Meier *et al.*[204] The most generalized structure of the selected design is presented in **Figure 30 a**; one terminus of the molecule is equipped

with an isocyanide for Passerini reactions, the other terminus bears a benzyl ester for subsequent hydrogenolytic deprotection. This bifunctional combination was chosen for practical reasons *i.e.* according to the relative stability of the functional groups participating in the Passerini reaction against degradation. The degradation stability of the functional groups was qualitatively sorted as follows: carboxylic acid > isocyanide > aldehyde (isocyanides hydrolyze under acidic conditions[330] and aldehydes oxidize to the corresponding carboxylic acids). The growing chain is considered the most valuable substrate of the whole strategy and furthermore the terminal end group (allowing chain growth) was regarded as the most critical position. Hence, the terminal end group allowing iterative growth *via* Passerini reactions was equipped with the most stable functional group, the carboxylic acids (obtained after hydrogenolytic deprotection of the corresponding benzyl esters, see **Figure 30 a**).

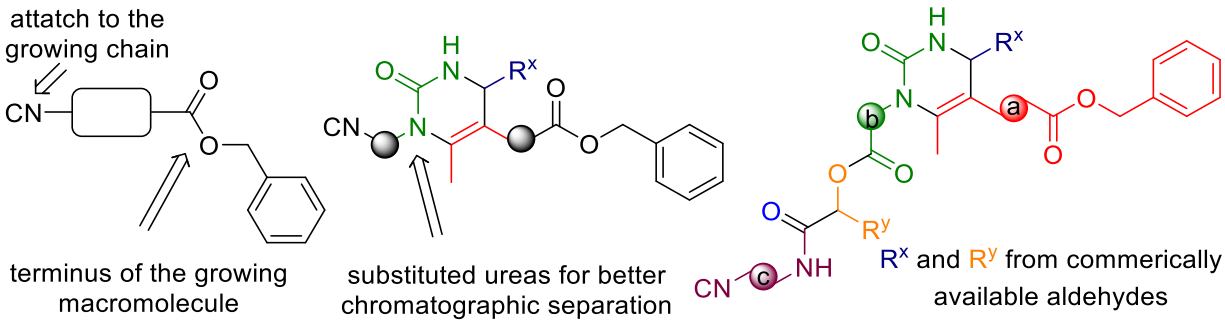

Figure 30. Monomer design chosen for the present investigation.

Considering the results from chapter **4.2**, substituted urea components were employed in the Biginelli reactions because chromatographic separation on silica gel is simplified if the additional NH (polar and hydrogen bond-donor resulting in challenging separation) is blocked *via* substitution with *e.g.* an alkyl chain. The resulting DHMP structures were therefore integrated as shown in **Figure 30 b** into the monomers. For testing the stability of the internal double bond of the DHMP core unit in hydrogenolysis reactions, a stability experiment was performed. In this experiment, the DHMP containing Biginelli-Passerini substrate **56** was dissolved in ethyl acetate and 20 wt.% of palladium on activated charcoal were added. The mixture was stirred at 40 °C for three days in an autoclave system applying 20 bar of H_2 gas. TLC indicated no conversion. After filtration over celite® and evaporation of the solvent the residue was analyzed *via* ^{1}H- and ^{13}C-NMR, confirming the initial structure. Furthermore, high-resolution mass spectrometry confirmed the molecular mass of the precursor, evidencing that the DHMP core is stable against hydrogenolysis under the present conditions. The final monomer design is presented in **Figure 30 c**; the aldehyde

components introducing R^x and R^y were commercially available, the other (bifunctional) components were either commercial or synthesized herein. Regarding the monomers structure, five different components are combined in the same monomer, enabling to leverage the high structural variety of two multicomponent reactions. Thus, for a theoretical data storage system the information is encoded *via* the variation of six different components per repeating unit (five per monomer); choosing from a list of components. In analogy to the previous considerations of chapter **4.2**, bifunctional components are required in order to link the Passerini and Biginelli reaction (illustrated in **Figure 26**). Since not many of the required bifunctional components were commercially available, a set of bifunctional components was synthesized. The synthetic strategies for the bifunctional components starting from commercially available chemicals, are summarized in **Figure 31**.

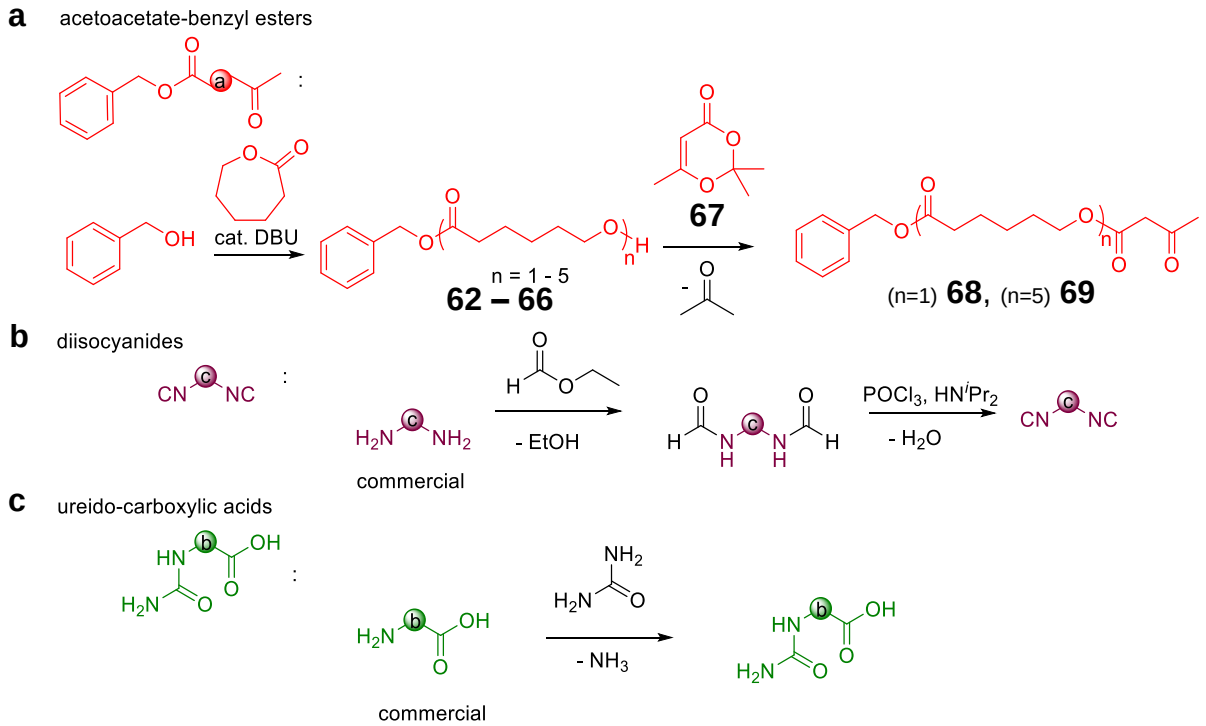

Figure 31. Synthesis of bifunctional components **a**, synthesis of acetoacetate-benzyl esters (AB-type) in two reaction steps *via* a ring opening oligomerization of ε-caprolactone, chromatographic separation of the oligomers and subsequent acetoacetylation with diketene acetone adduct **67**. **b**, synthesis of diisocyanides (AA-type) in two reaction steps starting from diamines which are firstly reacted to diformamides and subsequent dehydration with phosphorus oxychloride in triethylamine. **c**, synthesis of ureido-carboxylic acids in one step (AB type) *via* transamidation of amino acids with urea.[209]

The acetoacetate-benzyl esters were prepared in a two-step procedure (**Figure 31 a**). First, ε-caprolactone was ring-opened by dropwise addition into an excess of benzyl alcohol with the non-nucleophilic base diazabicycloundecene (DBU) as catalyst. The product mixture contained discrete oligomers (**62** – **66**), which were separated by column chromatography. The respective ^{1}H-NMR spectra are stacked in **Figure 32**.

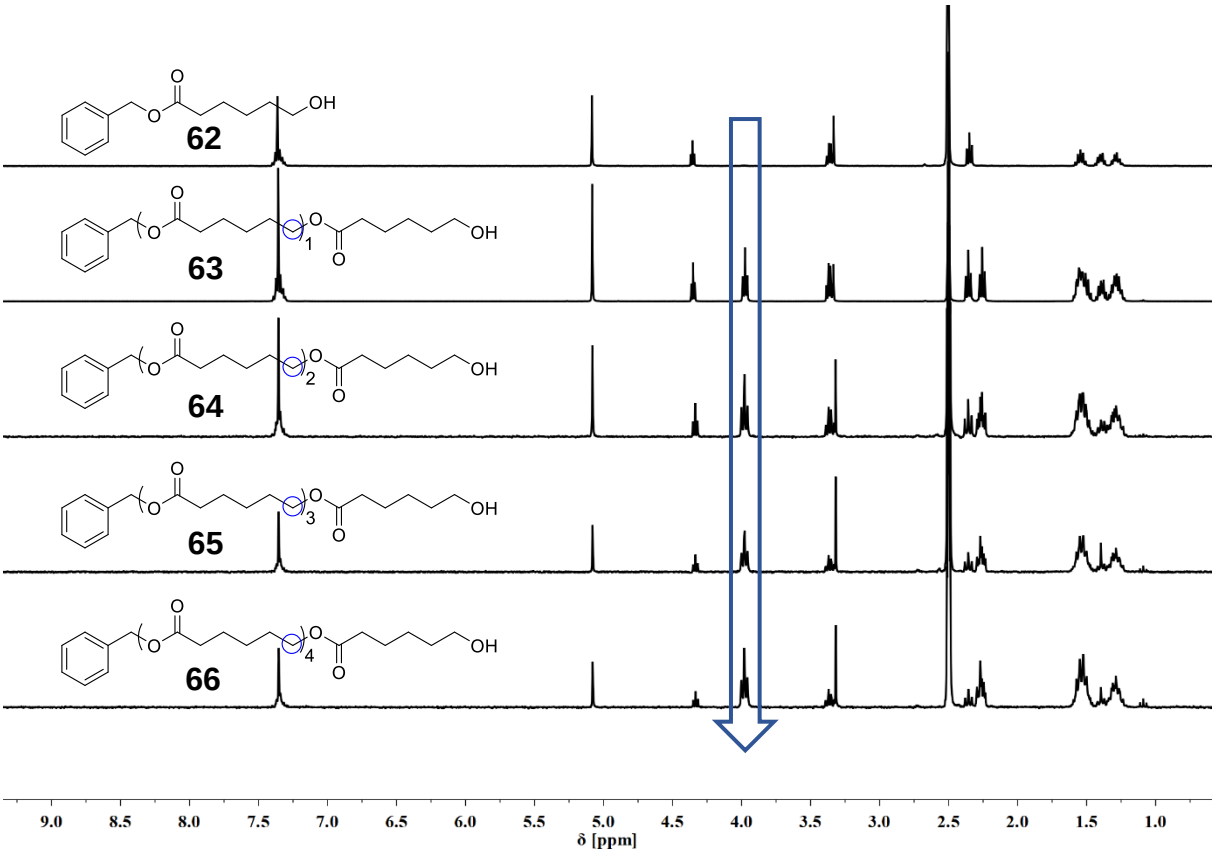

Figure 32. ^{1}H-NMR spectra stack of the oligo alcohol-benzyl esters (monomer – pentamer), measured in DMSO-d_6. The blue arrow illustrates the increasing number of the methylene group next to the oxygen atom of the ester marked with the blue cycle.

The (oligo) alcohol-benzyl esters **62** and **66** were reacted in an acetoacetylation reaction with diketene acetone adduct **67**, to obtain acetoacetate-benzyl esters **68** and **69**, respectively. The diisocyanides were synthesized according to a modified procedure reported earlier, starting from diamines (**Figure 31 b**).[66] The diamines were converted into the corresponding diformamides upon reaction with ethylformate or trimethyl orthoformate. The diformamides were dehydrated by phosphorous oxychloride in the presence of diisopropylamine. After purification *via* column chromatography, typical yields of 40 – 80% were achieved.

In the stacked ^{1}H-NMR spectra of the formamide precursor and the isocyanide product (see **Figure 33**), the disappearance of the formamide signals, and a shift of the methylene protons next to the functional groups (green *vs.* blue box) was clearly observed.

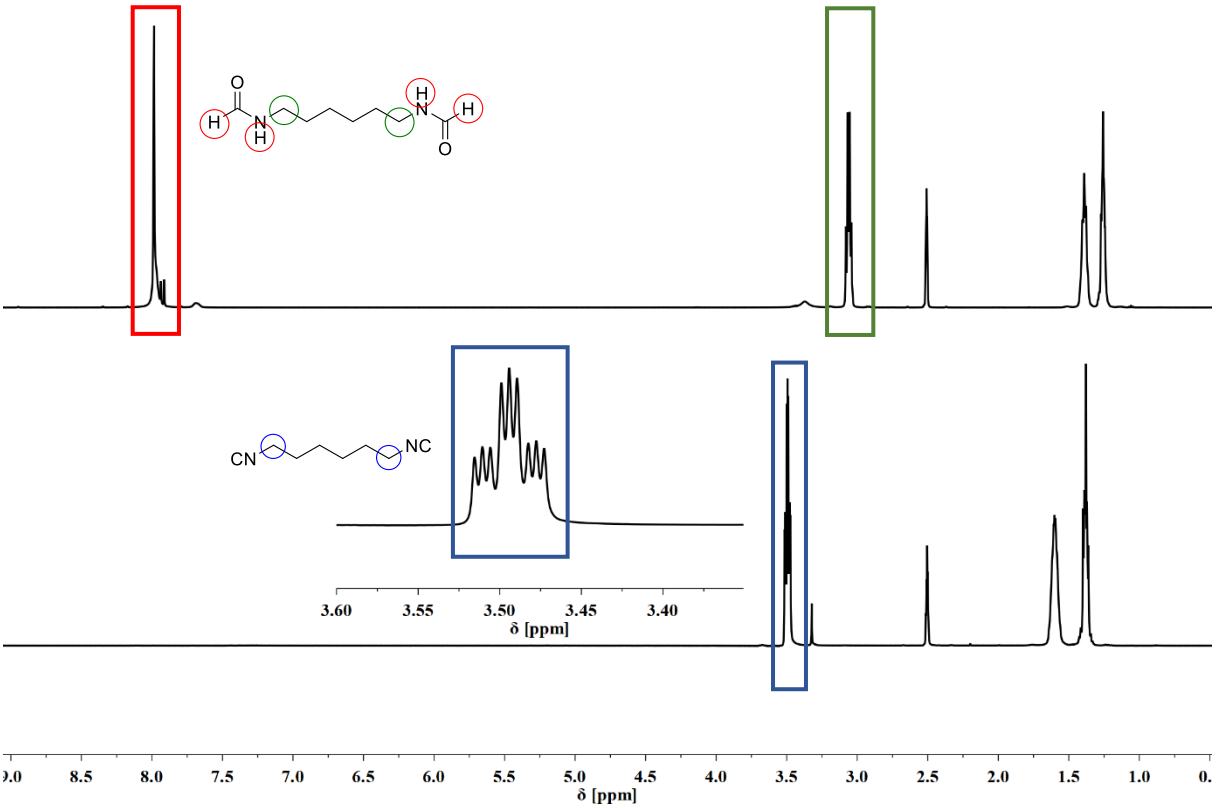

Figure 33. ^{1}H-NMR stack of hexane-1,6-diformamide (top) and hexane-1,6-diisocyanide (bottom) measured in DMSO-d_6. The expansion visualizes the signal of the methylene group next to the isocyanide functional group (triplet of triplets). The formamide signals in the red box are not observed for the isocyanide product.

Ureido-carboxylic acids were prepared by a straight-forward transamination reaction of amino acids with urea at 120 °C in dimethyl sulfoxide and slow addition of hydrochloric acid obtaining typical yields of 70 – 90% after washing or recrystallization (**Figure 31 c**). The synthetic procedures along with characterization for all bifunctional components prepared for this investigation can be found in chapter **6.2.3**.

With the herein utilized protocols, a library of different components can be prepared. In analogy to the Ugi approach described in chapter **4.1**, a list of components was established considering limitations reported in literature for choosing the components (see **Table 8**). Again, the later read out of the sequences is conducted by tandem-MS and hence no isomers should be chosen for the same category of components. In addition to the previous considerations from **Figure 8**, no hydrogenolysis-sensitive side chains should be present (except for the acetoacetate-benzyl ester, where later deprotection is desired).

Table 8. Selected entries from an exemplary list of components

Structure	Formula	Alphanumerical code	Monoisotopic mass [Da]
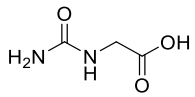	$C_3H_6N_2O_3$	A(001)	118.03784
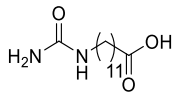	$C_{13}H_{26}N_2O_3$	A(011)	258.19434
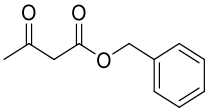	$C_{11}H_{12}O_3$	B(001)	192.07864
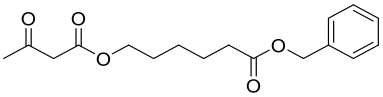	$C_{17}H_{22}O_5$	B(002)	306.14672
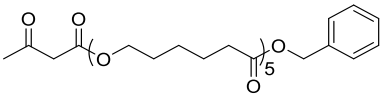	$C_{37}H_{58}O_{11}$	B(006)	678.39791
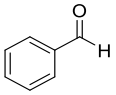	$C_7H_6O_1$	C(001)	106.04186
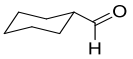	$C_7H_{12}O_1$	D(009)	112.08882
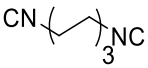	$C_8H_{12}N_2$	E(005)	136.10005
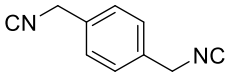	$C_{10}H_8N_2$	E(012)	156.06875

A: ureido-carboxylic acids. B: acetoacetate-benzyl esters. C: aldehydes for Biginelli reactions. D: aldehydes for Passerini reactions. E: diisocyanides. The full list of components can be found as supplementary information along with the previously published work and included in the electronic version of this thesis.[209]

The herein compiled list of components comprised 116 varying components; eleven ureido–carboxylic acids, 18 aldehydes for the Biginelli reaction (aromatic aldehydes only), six acetoacetate–benzyl esters, 29 diamines and 26 aldehydes for the Passerini reaction (the 26 aldehydes can be employed for monomer synthesis and iterative Passerini coupling reactions). The variation of ureido-carboxylic acids was demonstrated for the longest spacers (b = $C_{10}H_{20}$, **Table 9** entry #1 – #4, **70** – **73**) an intermediate length (b = C_5H_{10}, **Table 9** entry #5, **74**) and shortest spacer (b = CH_2, **Table 9** entry #6 – #14, (**50**, **75** – **80**) included in the list of components. Hence, it can be assumed that the present strategy is also applicable for all intermediate spacer lengths (b = C_2H_4 – C_9H_{18}). The respective variation generates a number of 11 different urea components. Following the same argumentation, the variation of acetoacetate-benzyl ester components (red) was demonstrated for the shortest spacer (benzyl acetoacetate, commercially available) an intermediate spacer (a = $(CH_2)_5O(C{=}O)CH_2$,

68) and the longest spacer (a = $[(CH_2)_5O(C=O)CH_2]_5$, **69**). The variation of diisocyanides was demonstrated for cycloaliphatic (**Table 9** entry #9, **83**), aromatic (**Table 9** entry #10, **84**), and aliphatic spacers (all other entries in **Table 9**). The aldehydes, either for Biginelli or Passerini reactions, included in the list of components are commercially available and were selected in order to react effectively and selectively, considering previously reported experiments from literature[23,27,89,332] and the results from chapter **4.2**. For the aromatic aldehydes of the Biginelli reaction (blue, R^x), six different components were demonstrated and nine for the Passerini reaction (orange, R^y). These experiments indicate that the components can be varied according to the list of components and that the anticipated structural diversity of the monomers-NC (**83** – **96**), which translates into data storage density, can be achieved. The permutations are calculated by multiplication of the different component sub libraries: 11 × 18 × 6 × 29 × 26 × 26 = 23,289,552 permutations. The respective information content for one repeating unit can be calculated by the number of possible permutations: Log(number of possible permutations)/Log(2), hence approximately 24 bits (Log(23,289,552)/Log(2)=24.47) can be encoded per repeating unit. If multiple repeating units are combined into longer sequences, the storage capacity of the respective macromolecule is calculated by: bits per repeating unit × number of repeating units. In is noteworthy, that the single step Ugi approach described in chapter **4.1** resulted in a higher storage capacity per reaction step, since a repeating unit structure was not necessary.[208] However, if compared to the iterative approaches of the sequence defined macromolecules discussed herein, the overall storage capacity of the macromolecules can be much larger and mainly depends on the length of the sequence (see **Figure 34**).

The synthesis of the monomers-NC (**Scheme 23 a**) starts with a Biginelli reaction involving an ureido-carboxylic acid (green, spacer b), an aromatic aldehyde (blue, R^x) and an acetoacetate-benzyl ester (red, spacer a) yielding a so-called Biginelli acid. The Biginelli reactions were performed in dimethyl sulfoxide with a high concentration of the reactants at 110 °C overnight employing an 1.20 equivalent excess of ureido-carboxylic acid and acetoacetate-benzyl ester with respect to the aldehyde component under acidic conditions (10 mol.-% *p*-TSA as catalyst) obtaining typical yields of 50 – 80% (according to the methods established in chapter **4.2**). The Biginelli acids were subsequently employed in a Passerini reaction with an aldehyde (orange, R^y) and a diisocyanide (dark purple, spacer c) to from the monomer-NC.

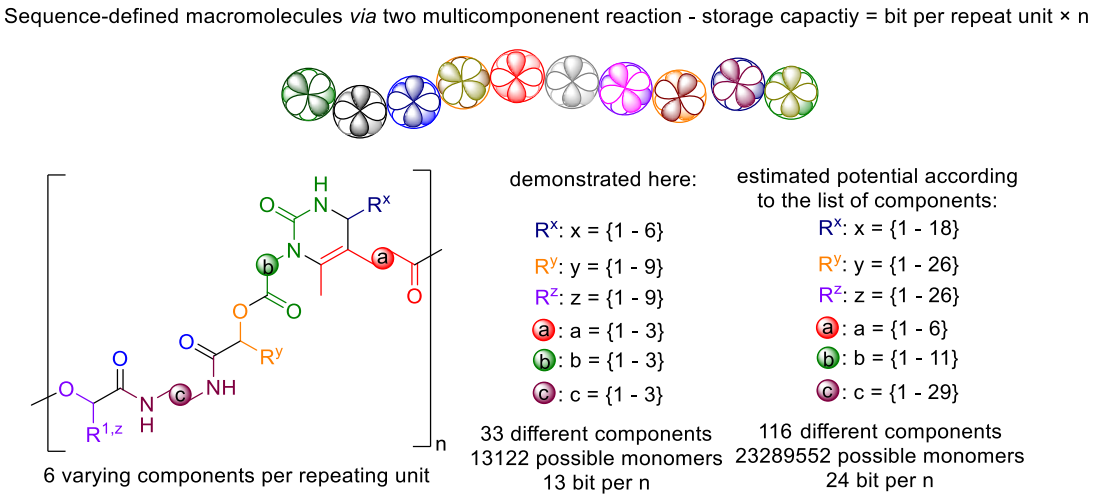

Figure 34. Theoretical information content per repeating unit of the herein described approach utilizing two multicomponent reactions – the variation of all components can potentially provide 24 bits per repeating unit. Bits per repeating unit were calculated as follows: Log(number of possible permutations)/Log(2). The storage capacity of a macromolecule is calculated by: bit per repeating unit × number of repeating units.[209]

The monomer-NC syntheses were performed in a solvent mixture of dichloromethane and a few droplets of dimethyl sulfoxide (required in order to solubilize the Biginelli acids) at room temperature, while employing 5.00 equivalents of diisocyanide and 2.00 equivalents of aldehyde, obtaining typical yields of 50 – 90% (the exceeding diisocyanide could be recovered *via* column chromatographic purification). In **Figure 35** representative stacked ^{1}H-NMR spectra of the Biginelli acid **77**, hexane-1,6-diisocyanide and the monomer-NC product **93** are displayed. Many of the precursor signals can also be found (slightly shifted) in the product spectra (see colored boxes in **Figure 35**).

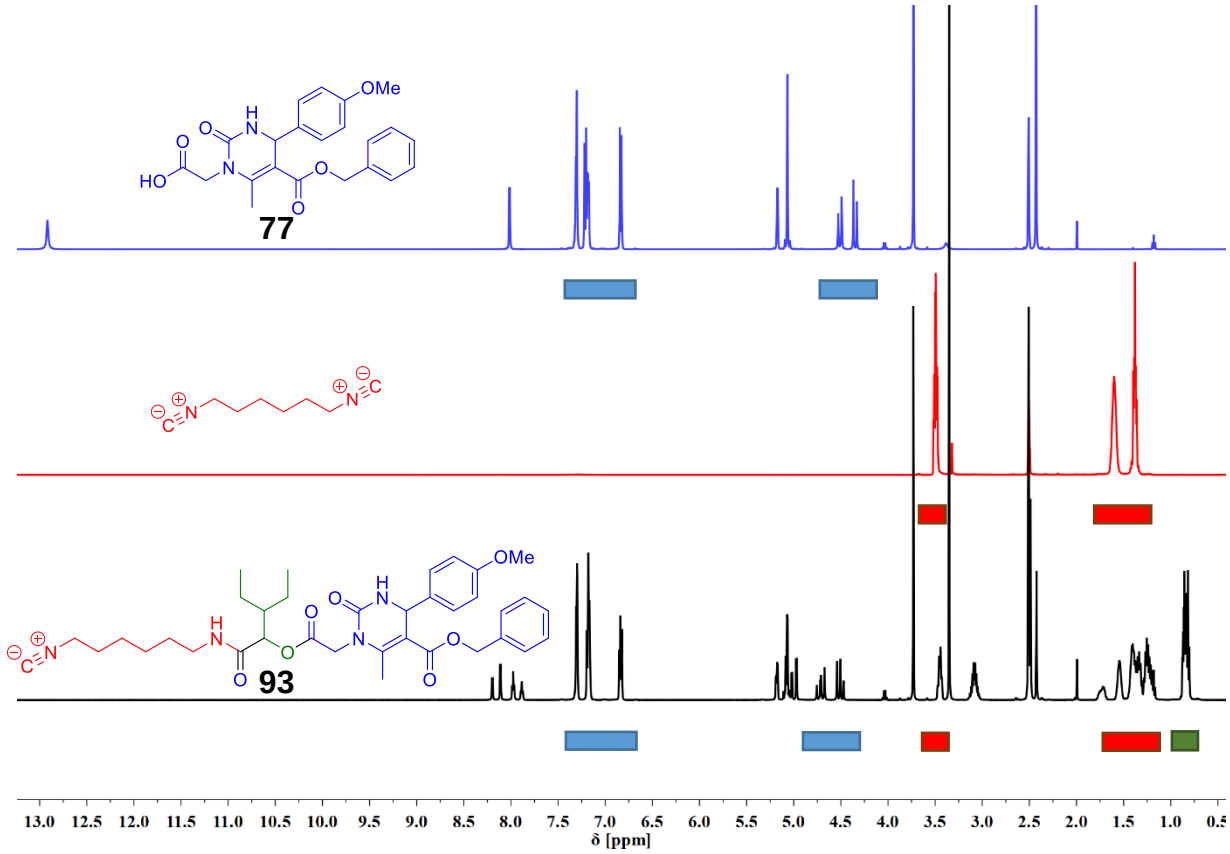

Figure 35. ^{1}H-NMR spectra stack of Biginelli acid **77** (top), hexane-1,6-diisocyanide (middle) and the resulting monomer-NC **93** (bottom). The colored boxes illustrate the origin of the product signals.

The disappearance of the acid signal at 13.0 ppm in the blue spectrum of the Biginelli acid and the incorporation of the aromatic region 7.5 – 6.5 ppm and the aliphatic region 1.5 – 1.0 ppm indicates the formation of the desired Passerini product. For demonstrating the variability of the approach described herein, a subset of 14 different monomers (monomer-NC) was synthesized and evaluated in a test reaction system (see **Scheme 23 b**). This qualitative monomer-NC test system (**Scheme 23 b**), consists of a first Passerini step employing 1.50 equivalents of stearic acid and 2.00 equivalents of octanal to prove the reactivity of the isocyanide end group in Passerini reactions. In a subsequent deprotection step, the reactivity of the benzyl ester towards hydrogenolysis was tested. Except for entry #7 in **Table 9**, all monomers passed the test system. The test system experiments for entry #7 in **Table 9** illustrate that the Passerini step C was successful, however the hydrogenolytic deprotection D failed. Hence, monomer-NC **91** should only be used in order to terminate a macromolecule because further iterations would require a free carboxylic acid functionality.

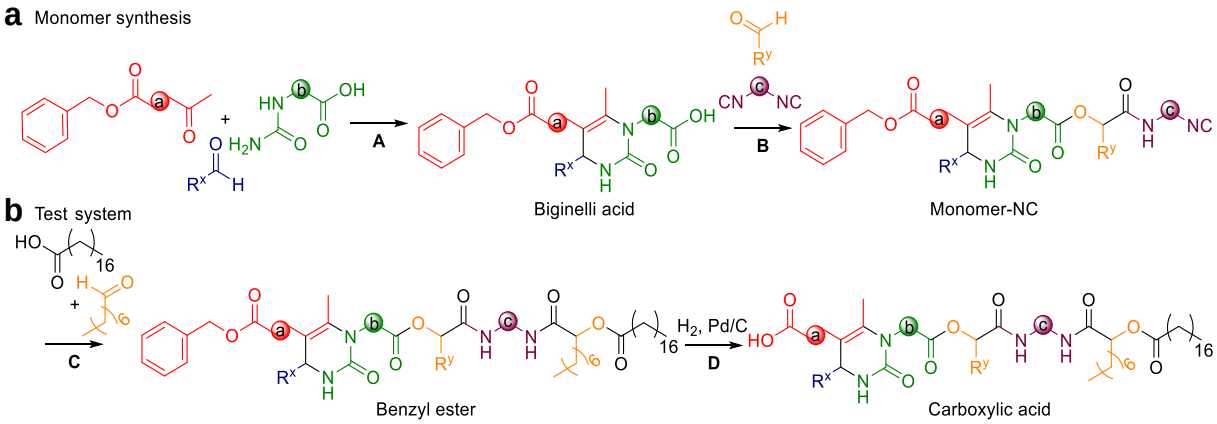

Scheme 23. a, synthesis of monomers-NC. A: Biginelli reaction; B: Passerini reaction. **b**, test system. C: Passerini reaction; D: hydrogenolytic deprotection. The results are summarized in the table below.[209]

Table 9. Monomers for sequence-defined information-coding macromolecules, chosen to achieve large structural variety, and their performance in a Passerini/deprotection test system.

#	R^x	a	b	Yield **A** [%] (**№**)	R^y	c	Yield **B** [%] (**№**)	Yield **C** [%] (**№**)	Yield **D** [%] (**№**)
1	Ph	CH_2	$C_{10}H_{20}$	45 (**70**)	C_7H_{15}	C_6H_{12}	97 (**85**)	77 (**108**)	99 (**123**)
2	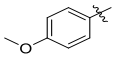	CH_2	$C_{10}H_{20}$	39 (**71**)		C_6H_{12}	83 (**86**)	96 (**109**)	99 (**124**)
3		CH_2	$C_{10}H_{20}$	45 (**72**)		C_6H_{12}	65 (**87**)	94 (**110**)	98 (**125**)
4	Ph	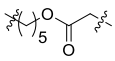	$C_{10}H_{20}$	67 (**73**)	C_6H_{13}	C_6H_{12}	81 (**88**)	78 (**111**)	97 (**126**)
5	Ph	CH_2	C_5H_{10}	55 (**74**)	C_4H_9	C_6H_{12}	84 (**89**)	81 (**112**)	99 (**127**)
6	Ph	CH_2	CH_2	78 (**50**)	CH_3	C_6H_{12}	59 (**90**)	80 (**113**)	99 (**128**)
7		CH_2	CH_2	62 (**75**)	$C_{11}H_{23}$	C_6H_{12}	50 (**91**)	75 (**114**)	0[a]
8		CH_2	CH_2	61 (**76**)	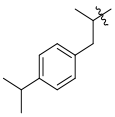	C_6H_{12}	51 (**92**)	42 (**115**)	92 (**129**)
9	Ph	CH_2	CH_2	78 (**50**)	C_7H_{15}		59 (**83**)	78 (**116**)	94 (**130**)
10	Ph	CH_2	CH_2	78 (**50**)	C_7H_{15}	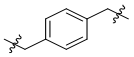	76 (**84**)	98 (**117**)	96 (**131**)
11	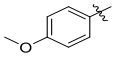	CH_2	CH_2	45 (**77**)		C_6H_{12}	42 (**93**)	95 (**118**)	99 (**132**)
12		CH_2	CH_2	63 (**78**)	C_7H_{15}	C_6H_{12}	69 (**94**)	75 (**119**)	99 (**133**)
13	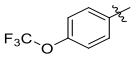	CH_2	CH_2	68 (**79**)	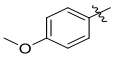	C_6H_{12}	43 (**95**)	71 (**120**)	98 (**134**)
14	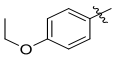	CH_2	CH_2	58 (**80**)	C_7H_{15}	C_6H_{12}	61 (**96**)	52 (**121**)	93 (**135**)

[a] Hydrogenation did not occur, even in an autoclave system at 40 bar H_2 gas pressure at 40 °C or under homogenous conditions utilizing Wilkinson's catalyst, no significant conversion was observed.

In **Figure 36**, two representative IR spectra (recorded in transmittance), of monomer-NC **84** and benzyl ester **117** are stacked. In the IR spectra, the isocyanide vibration band at ~2100 cm^{-1} clearly disappeared after reacting the monomers-NC in the first Passerini step of the test system. In addition, the C-H vibration region around 2900 cm^{-1} increased in intensity, due to the introduction of two aliphatic chains.

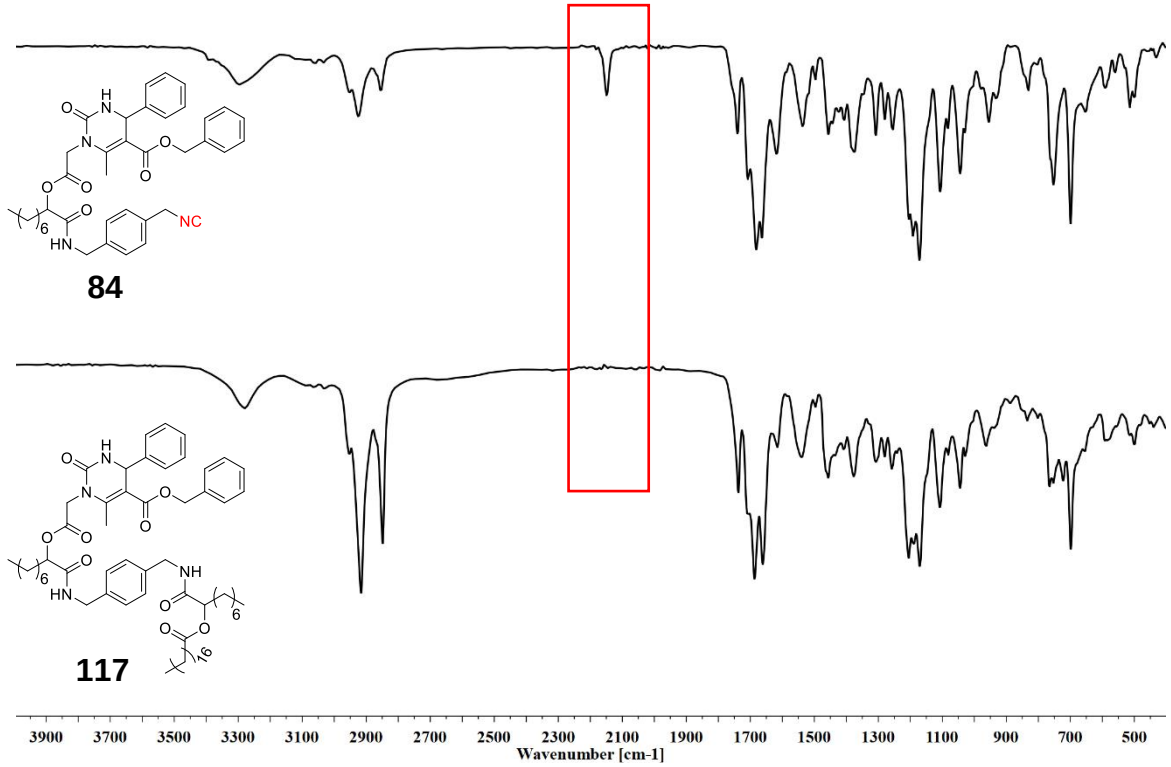

Figure 36. IR stack of monomer-NC **84** and benzyl ester **117**. The isocyanide vibration band (red box) clearly disappeared.

In addition to the monomers described in **Table 9**, a stereochemically different monomer-NC **97** (obtained from Biginelli acid **52**) was synthesized and subjected to the test system (see **Scheme 24**). In order to solubilize the Biginelli acid **52**, more dimethyl sulfoxide was required, leading to longer reaction times and a decrease in reaction efficiency. In the test system, compound **97** passed the Passerini step but was not converted under the hydrogenolytic conditions utilized herein.

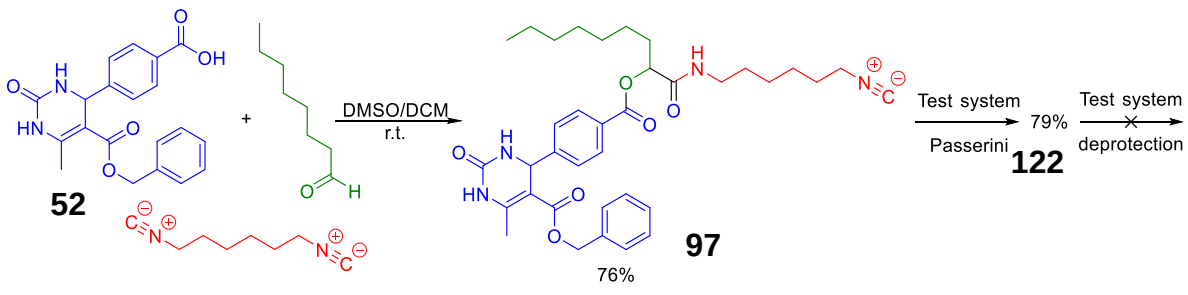

Scheme 24. Synthesis and evaluation of a stereochemically different monomer-NC **97**. Monomer-NC reacted in the Passerini step of the test system but not in the hydrogenolytic deprotection step.

Furthermore, the hydrogenation was tested in an autoclave system applying 40 bar of hydrogen gas, palladium on activated charcoal as catalyst while stirring at 40 °C for three days and under homogeneous conditions employing Wilkinson's catalyst. However, no significant conversion could be achieved. In conclusion, testing new monomers for reactivity in both critical steps (see **Scheme 23**, steps **C** and **D**) before their utilization for iterative chain growth is feasible and should be performed prior to building up of larger macromolecules.

4.3.2 Synthesis and analysis of information-coding macromolecules

The herein employed iterative reaction strategy is based on a protective group approach and illustrated in **Scheme 25**. The monomers-NC can be polymerized by consecutive Passerini reactions, upon addition of an aldehyde (purple, R^z) and a carboxylic acid (black, R^1 for the first reaction sequence), utilizing a modified procedure reported earlier.[204]

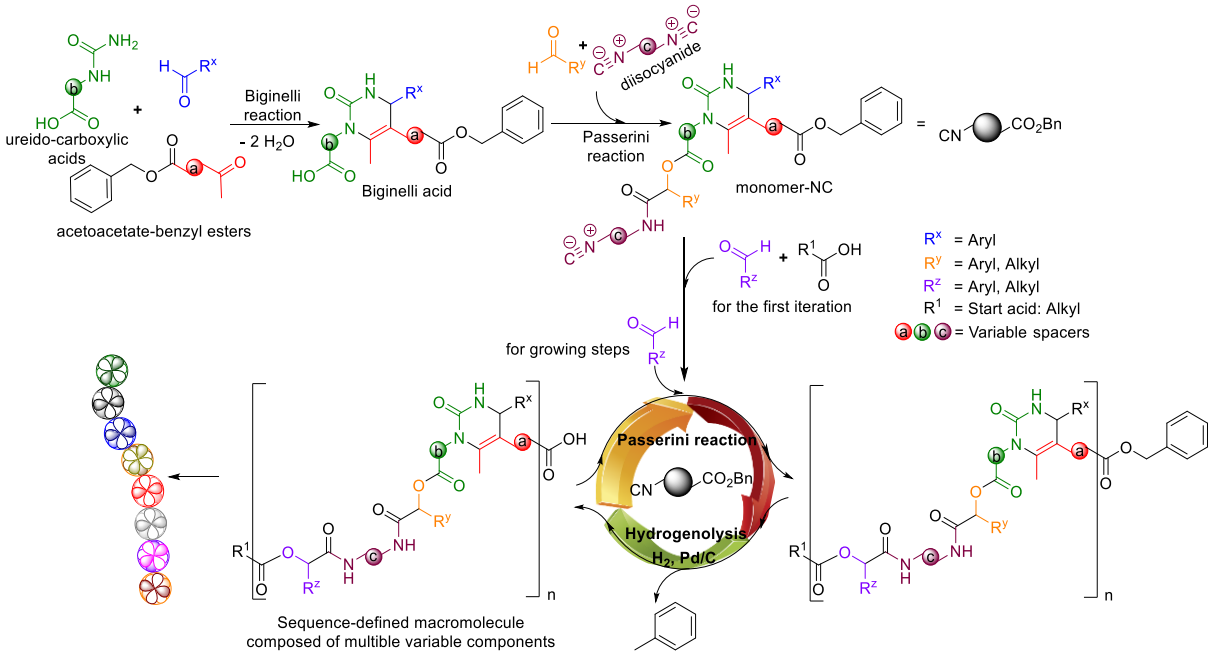

Scheme 25. Synthesis of sequence-defined macromolecules *via* the Biginelli and the Passerini multicomponent reactions. In the Biginelli reaction, an ureido-carboxylic acid (spacer b), an aromatic aldehyde (with sidechain R^x) and an acetoacetate-benzyl ester (with spacer a) are reacted to yield a Biginelli acid, which subsequently reacts with an aldehyde (sidechain R^y) and a diisocyanide (spacer c) to from an isocyanide monomer (monomer-NC). The monomers-NC are polymerized iteratively by consecutive Passerini reactions, adding an aldehyde (sidechain R^z) and a carboxylic acid. After hydrogenolytic benzyl deprotection, the growing macromolecule bears a free terminal carboxylic acid, allowing the addition of the next monomer-NC in a further Passerini step.[209]

In a first test reaction, compound **98** was reacted with Biginelli acid **49** in a Passerini reaction (**Scheme 26**). The desired product **99** was isolated in 73% yield, and utilized in a subsequent hydrogenolytic deprotection, obtaining the corresponding carboxylic acid **100** in 97% yield. However, the compounds **99** and **100** did not feature a clear repeating unit structure (*i.e.* one DHMP core is in a different orientation than the other, as illustrated in **Scheme 25**) and were therefore not employed for further iterative cycles but regarded as a proof of principle.

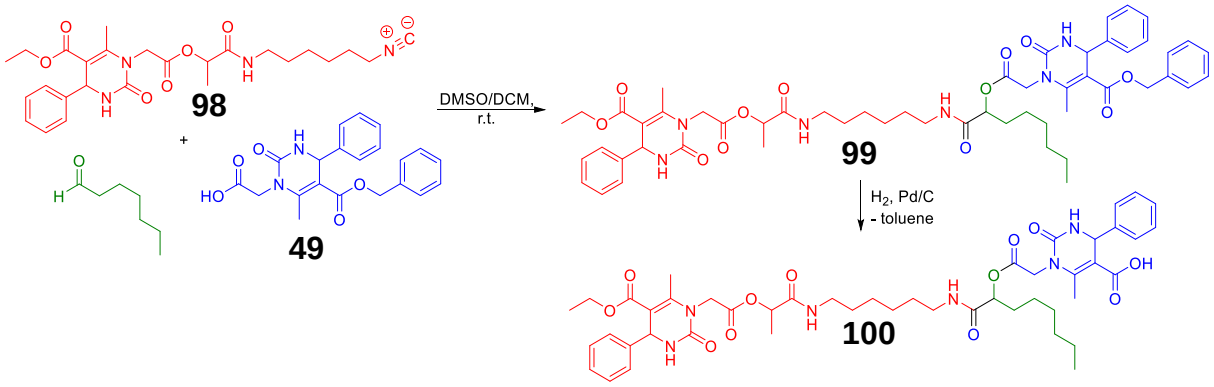

Scheme 26. First test reaction resulting in an asymmetric reaction product.

For the subsequent syntheses, an aliphatic diacid (sebacic acid) was chosen as starting component to achieve bidirectional growth (see **Figure 37 b**). Nevertheless, instead of bifunctional components, mono- or multifunctional core units can potentially be applied, resulting in different macromolecular architectures. The reasons for choosing a bidirectional growth leading to symmetric macromolecules was: *i*. regarding SEC analysis: The differences in molar mass between each iterative cycle is greater than for unidirectional approaches and hence the shift in retention times in SEC analysis is greater; *ii*. regarding purification: Chromatographic separation of *e.g.* tetramers from dimers proved to be more efficient, than separation of tetramers from trimers; *iii*. the tandem-MS readout benefits from symmetry (due to the presence of both symmetric and asymmetric fragments *vs.* asymmetric fragments exclusively for non-symmetric macromolecules). The iterative Passerini polymerizations were conducted in dichloromethane at room temperature employing 1.50 equivalents of monomer-NC and 2.00 equivalents of aldehyde per carboxylic acid group. The reaction progress was monitored *via* size-exclusion chromatography (see **Figure 37 a**, for the reaction monitoring of the reaction between monomer-NC **90**, sebacic acid and heptanal obtaining the symmetric dimer **101**). The reaction mixture was purified by column chromatography on silica gel, obtaining typical yields of 70 – 95%. The exceeding monomer-NC could be partly recovered.

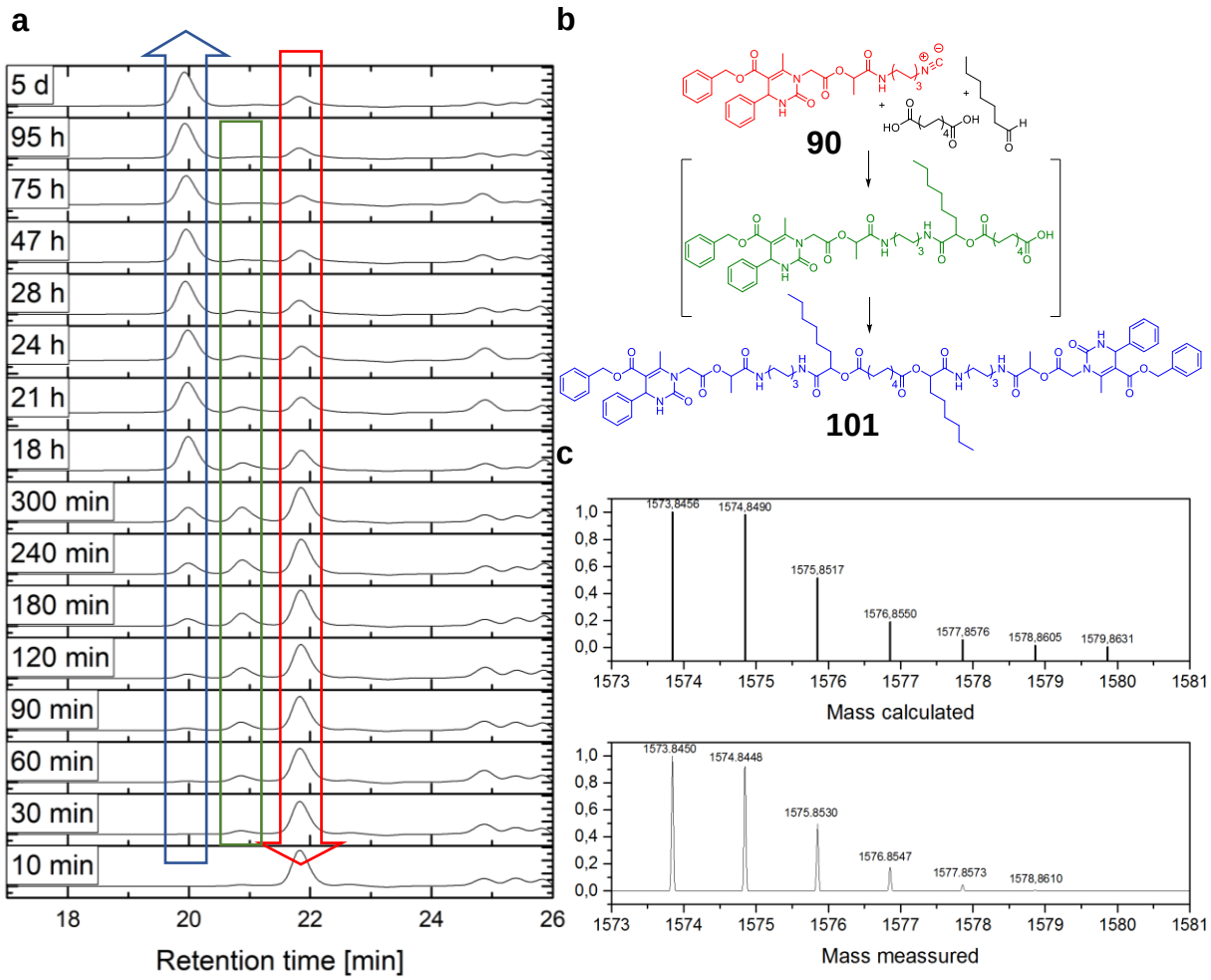

Figure 37. a, SEC reaction monitoring of the Passerini reaction presented in **b**, the monomer-NC **90** is marked by the arrow in red, the intermediately formed monofunctionalized product is marked with the green box and the desired difunctionalized macromolecule **101** is marked with the blue arrow. **b**, reaction equation for the synthesis of a sequence-defined symmetric dimer. **c**, HRMS analysis of the isotope pattern of **101**.[209]

After hydrogenolytic benzyl deprotection, the growing macromolecule is equipped with a terminal free carboxylic acid functional group, allowing the addition of the next monomer-NC in a subsequent Passerini reaction. The hydrogenolytic benzyl ester deprotection reactions were performed *via* heterogenous catalysis utilizing hydrogen gas and palladium on activated charcoal as catalyst. After simple filtration of the heterogenous catalyst and drying in high vacuum, the carboxylic acid terminated macromolecules were obtained in quantitative yields. Noteworthy, the herein selected monomer design is fully compatible with the previously reported iterative Passerini polymerization for sequence-defined macromolecules, potentially allowing the incorporation of chemically different monomers.[333,334] However, in comparison to the previously described approach (illustrated in **Scheme 18**), synthesis of the individual monomers-NC is required, thus enabling to encode more information per repeating

unit, albeit requiring additional synthesis and purification steps. A summary of all macromolecules synthesized for this investigation can be found in **Figure 38**.

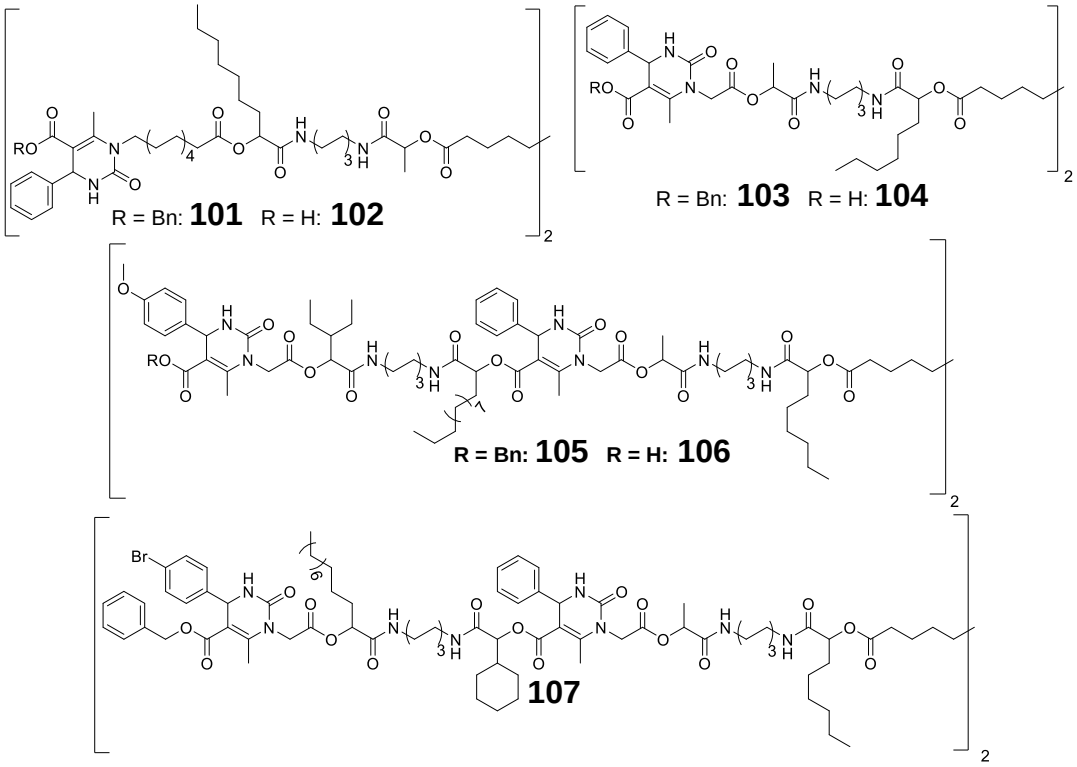

Figure 38. Structures of the macromolecules synthesized for the present investigation.

The macromolecules prepared herein were analyzed *via* size-exclusion chromatography (see **Figure 39**), indicating uniform species and high purity. The structural identity of the macromolecules was investigated *via* 1D and 2D nuclear magnetic resonance spectroscopy and further confirmed by high resolution mass spectrometry (including analysis of the isotope pattern, see **Figure 37 c**) and ESI-MS/MS collision experiments (see chapter **4.3.3**).

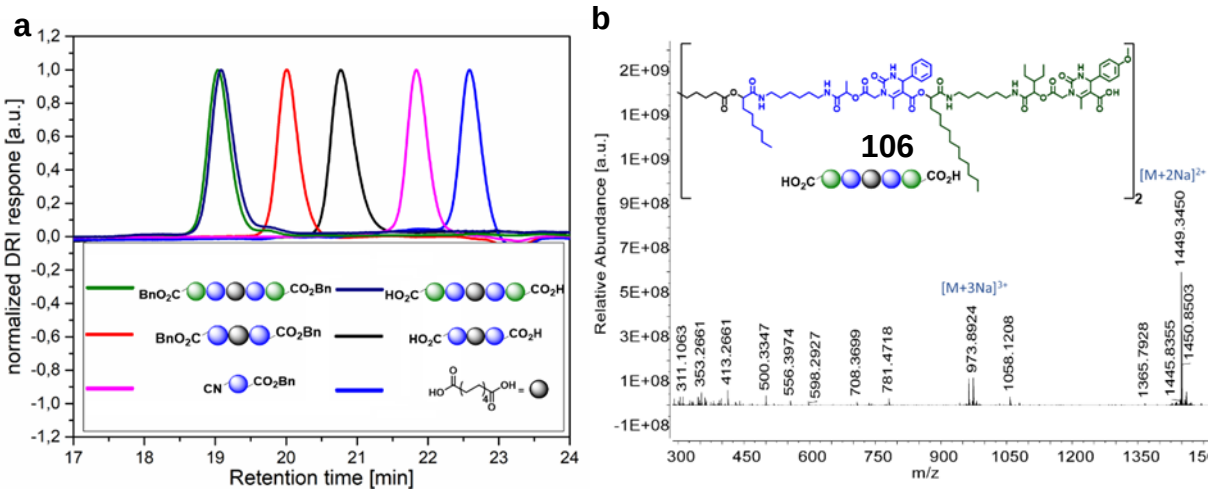

Figure 39. a, Size-exclusion chromatography traces and schematic representation of the iterative growth of the sequence-defined macromolecule **106**. **b**, ESI-MS of **106** recorded in positive mode. The signal at *m/z* = 1449 corresponds to the double charged *bis*-sodium adduct, the signal at *m/z* = 973 corresponds to the triple charged *tris*-sodium adduct.[209]

The symmetric and narrow peak shape of the size-exclusion elugrams (**Figure 39 a**) indicates the high purity of the obtained substances. The shoulders for the blue and green curve towards shorter retention times account for an amount of approximately 1% monofunctionalized chains (trimers), which could not be fully separated *via* column chromatography. However, the monofunctionalized chains did not interfere with the later readout. NMR analysis of the macromolecules (see **Figure 40**) was complicated due the aforementioned diastereomers (see **Figure 28**). Signal splitting caused by the presence of diastereomers was observed for monomers and the respective polymers displaying a short ureido-carboxylic acid spacer (*i.e.* a = CH_2), possibly due to the shorter distance of the chiral centers and the more fixed geometry of the substrates. Compounds derived from longer spacers (a = C_5H_{10} or $C_{10}H_{20}$) did not display split signals. However, careful analysis of 2D NMR spectra (*i.e.* multiplicity edited HSQC in **Figure 40 a** and **b**, or *via* HMBC **Figure 40 c**) and comparison with the spectra of the precursor compounds, clearly identified the reaction products.

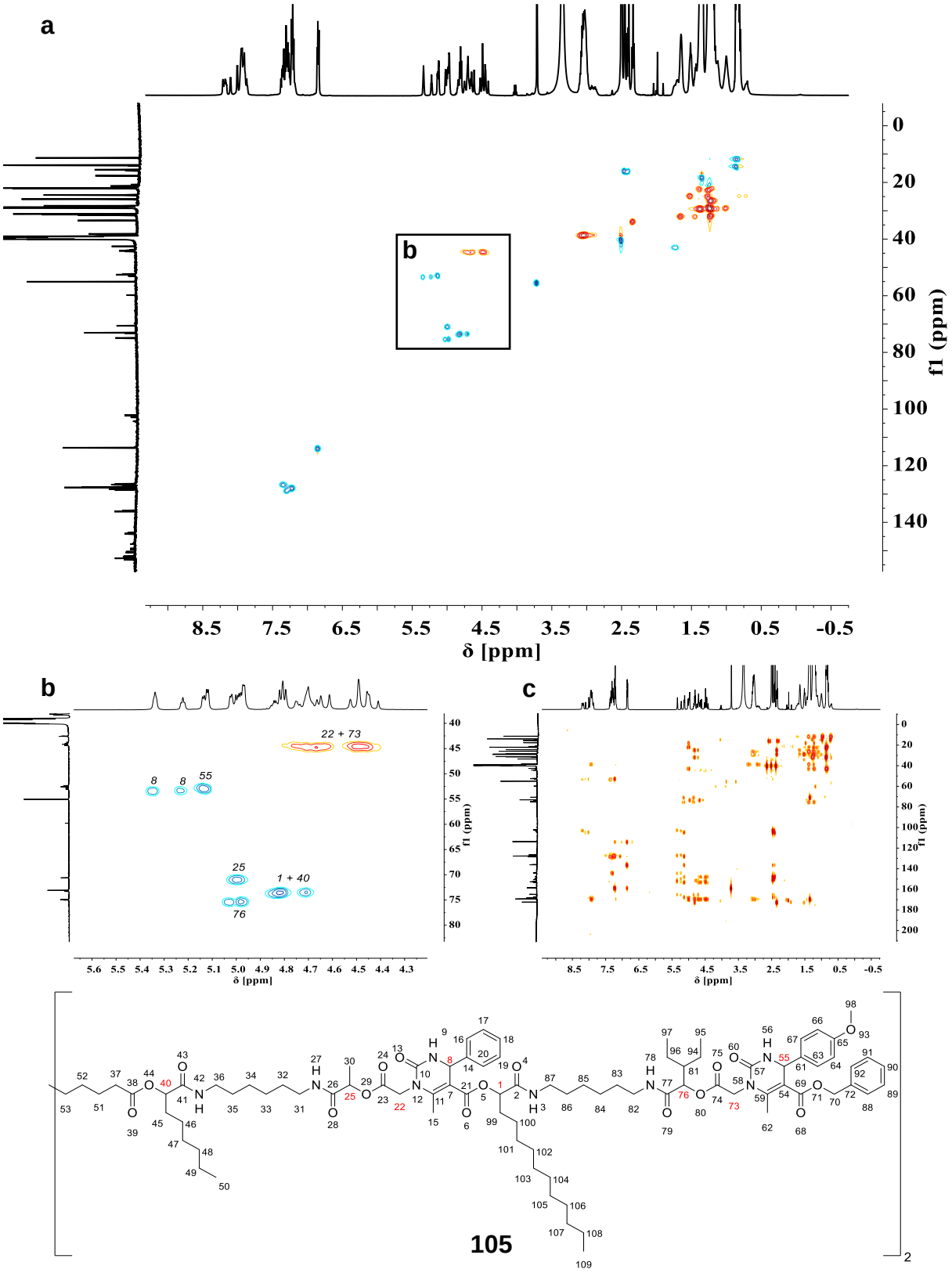

Figure 40. NMR analysis of macromolecule **105** displaying additional diastereomeric signal splitting. **a**, multiplicity edited HSQC. **b**, Expansion of the box in **a** visualizing the CH region. For position *8* and *76* split signals are observed in the proton spectrum. Signal *76* further overlaps with *25*. Positions *1* and *40* or *22* and *73* are too close to each other to be clearly distinguished. **c**, HMBC, employed to further confirm the signal assignment.

4.3.3 Readout *via* distinct fragmentation pathways

In the perspective of data storage materials, it is essential to read out the previously stored information. In the present investigation, several symmetric sequence-defined dimers (**101**, **102**, **103** and **104**) were synthesized and sequenced *via* ESI-MS/MS. The ESI-MS samples were prepared in solvent mixtures doped with sodium trifluoroacetate in order to predominantly observe the sodium adducts in positive mode. The ESI-MS/MS collision experiments were conducted at different fragmentation energies ranging from 10 – 50 eV. ESI-MS/MS analysis of the macromolecules revealed that the complex macromolecular structures are predominantly fragmenting in distinct and repetitive positions along the backbone chain of the macromolecule, such as the ester or amide bonds. This systematic fragmentation allows full sequencing of the structures (considering a limited subset of possible components as proposed in the list of components). After evaluating of the fragmentation patterns of several sequence-defined dimers, three dominant fragmentation patterns were identified: decarboxylation, Mc Lafferty rearrangements and isocyanide formation (see **Figure 41**). Subsequently, different symmetric tetramers (**107**, **105** and **106**) were sequenced accordingly, employing the afore identified fragmentation patterns to predict the fragment masses.

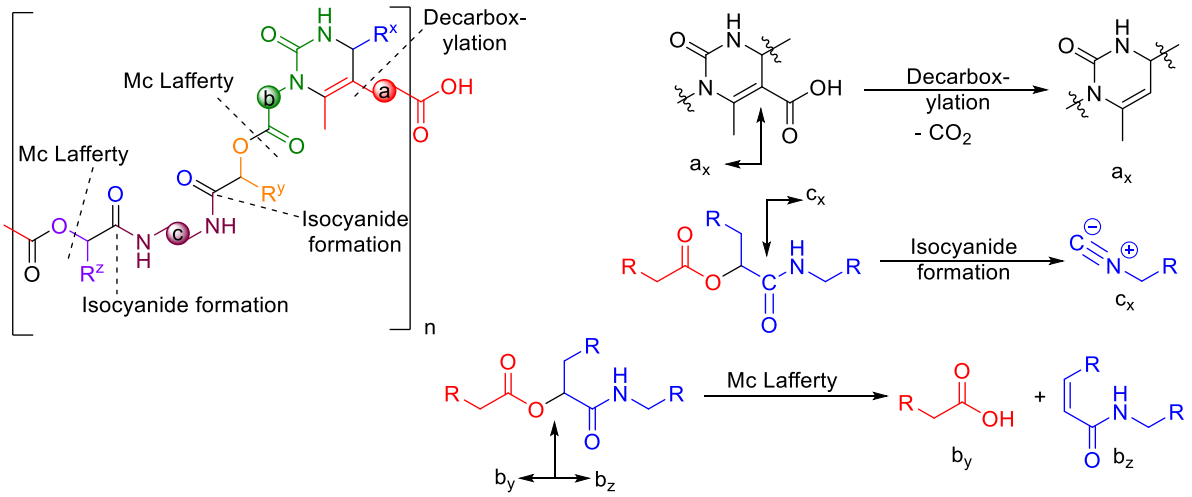

Figure 41. Fragmentation pathways occurring along the chain, utilized to sequence the structures.

In order to reconstruct the molecular structure form the MS readout, the monoisotopic mass of the intact molecule is considered first. As previously described in **Figure 20**, preselection of the monoisotopic mass already significantly reduces the remaining possibilities according to the list of components. Fragmentation of the macromolecules

at different fragmentation energies and comparison of the fragmentation spectra with the above described and predominant fragmentation patterns successively narrows the remaining possibilities until the molecular structure is solved and thus the sequence re-established.

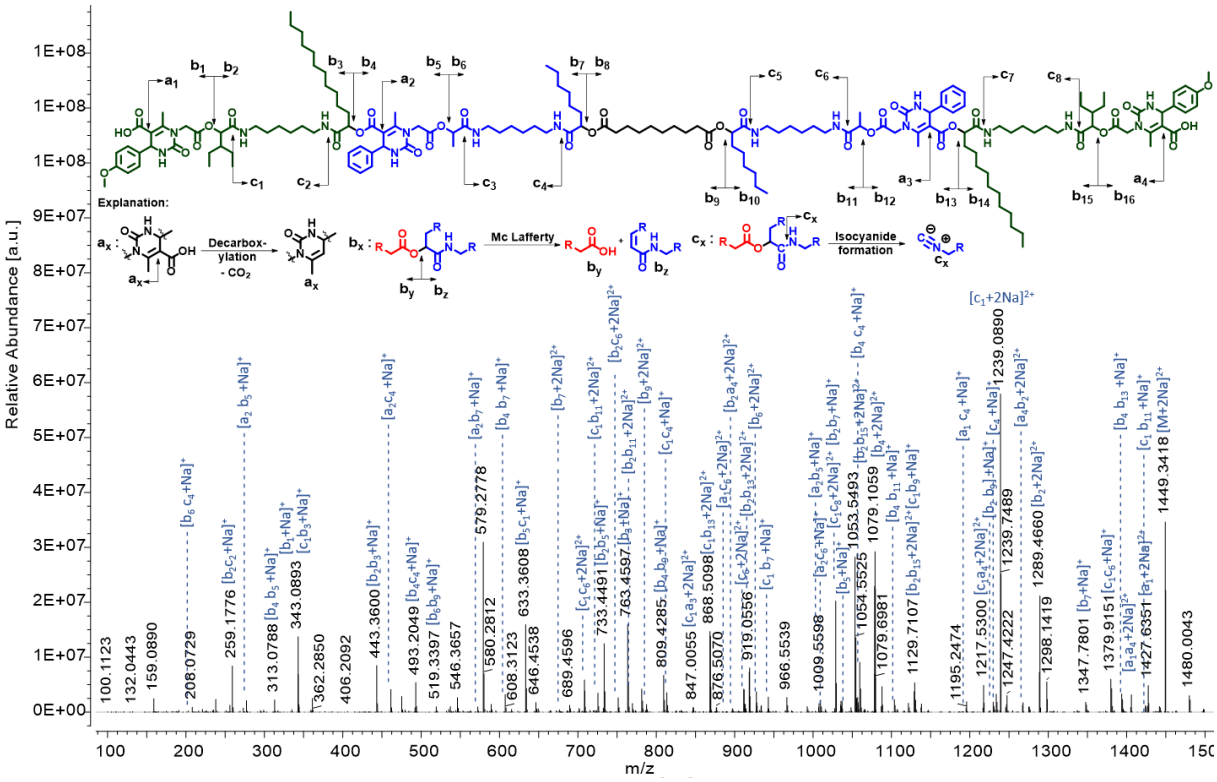

Figure 42. ESI-MS/MS fragmentation of a double charged species at *m/z* = 1449 (**106**) recorded in positive mode at higher-energy collision dissociation of 30 eV. Fragmentation processes are denoted as follows: a_x: decarboxylation at position x; b_x: Mc Lafferty rearrangement of the ester bonds forming a carboxylic acid (b_y) and an enamide (b_z); c_x: Amide bond fragmentation forming an isocyanide. The fragments are labeled accordingly: $[a_xc_y+2Na]^{2+}$ → a doubly charged *bis*-sodium adduct formed by decarboxylation on position x and isocyanide formation on position y.[209] A comprehensive description of each fragment can be found in supplementary information of the open access publication[209] and in the electronic version of this thesis.

Utilizing the above-mentioned fragmentation patterns in combination with the list of components, the position of each component within the macromolecule can be determined (see **Figure 43**) by the analysis of overlapping fragments (in analogy to protein[335,336] or DNA sequencing *via* tandem-MS).[337]

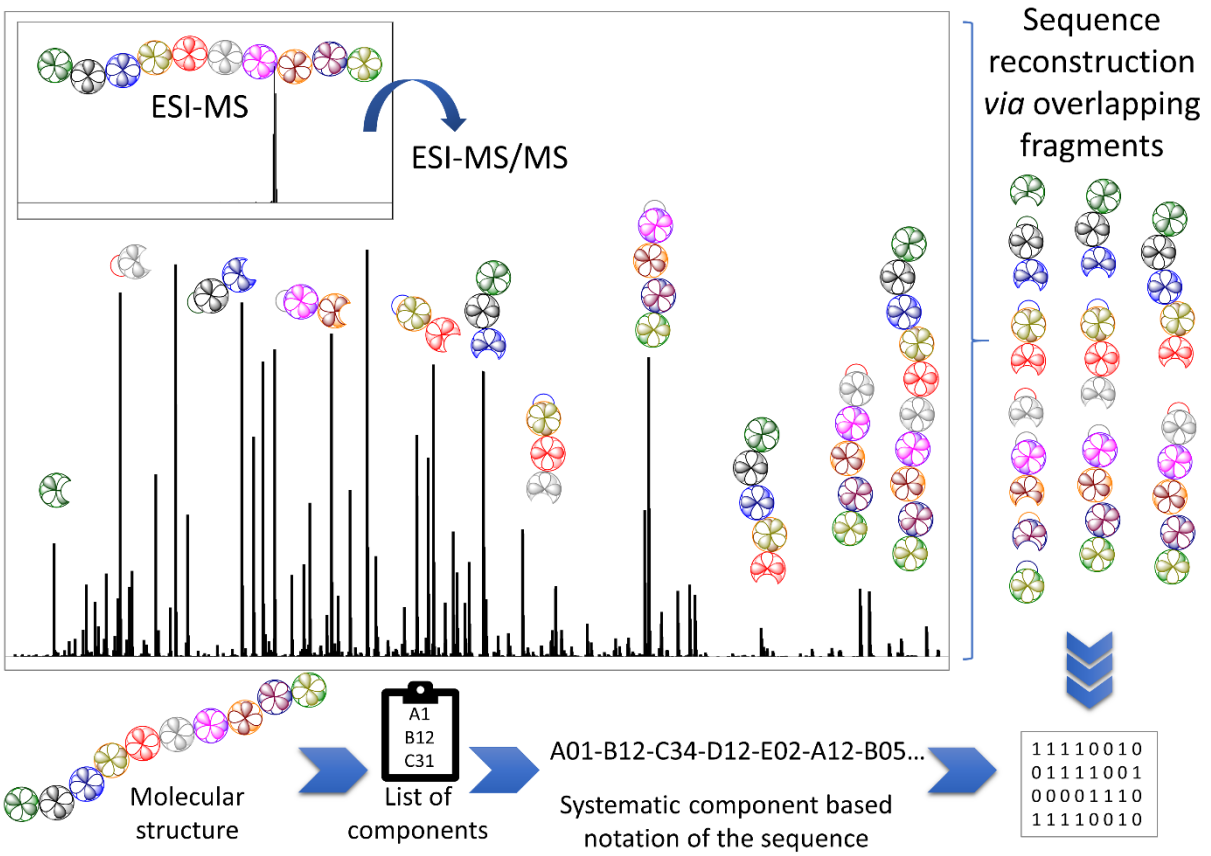

Figure 43. Conceptional reconstruction of the molecular structure *via* the analysis of overlapping fragments. After considering the mass of the intact molecule (determined *via* ESI/MS) and a multitude of fragments (*via* ESI-MS/MS) the molecular structure can be determined precisely. The sequence is subsequently transferred into a systematic component-based notation utilizing the list of components and can be further processed into binary codes.[209]

The investigated symmetric tetramers formally encoded 97 bits each (4 × 24.47 = 97.89), generated by the list of components. Translation of this component-based alphabet back into binary numerical system can be achieved through conversion of the positional notation. If longer sequences are synthesized and/or more compounds are included in the list of components, the storage capacity of the macromolecules can potentially be much higher. However, the herein presented strategy is currently limited in the length of sequences for two reasons: *i*. chromatographic separation on silica gel becomes challenging due to the increasing amount of polar dihydropyrimidone rings and *ii*. the readout of longer sequences generates a large number of fragments. This information needs to be processed and analyzed and would require a computer assisted system (as presented in **4.1.2.3**). However, both limitations could be overcome with further development.

5 Conclusions and outlook

The main objective of this thesis was the application of multicomponent reactions in novel data storage systems. Herein, the Ugi reaction of perfluorinated acids in combination with a list of components (comprising 130 commercially available components for evaluating the possible permutations and further assigning chemical information to alphanumeric codes for computer processing) was introduced. The structural variety resulted in 500,000 permutations and hence 18 bits information density within one Ugi compound (so-called molecular key). The herein investigated molecular key strategy allows secure steganographic key distribution in combination with a flexible and adaptable data safety protocol. The molecular keys were synthesized in a straight-forward, one-pot reaction procedure. The molecular structures were analyzed by a combination of tandem-MS fragmentation and computer assisted readout. Readout of the molecular keys was simplified by a custom programed computer script, provided by a cooperation partner. The respective molecular structures served as decryption keys (passwords) for AES encrypted messages or data files. In principle, the herein presented keys could also be used for other applications, *e.g.* as identification or anti-counterfeit tags (for the identification of trademark products). The encryption/decryption was performed by a second computer script (based on AES). In future research, the synthesis of molecular keys (probably also purification and analysis) could be performed by a robotic system. The investigation of molecular keys with even higher data storage capacities will be of great interest in order to overcome current limitations of the system. Furthermore, it will be important to refine the list of components by synthesizing and testing many permutations by systematic component variations, identify unexpected complications and remove components that caused problems. In this refining, additional components (non-commercial) can be added to the list of components in order to increase the storage capacity of the individual compounds.

Inspired by the idea to utilize even more varying components, the Biginelli reaction was successfully combined with the Passerini reaction to obtain highly functionalized heterocyclic products. For this purpose, different Biginelli acids were prepared by variation of the components and the bifunctional linker. The Biginelli acids were subsequently reacted with different aldehydes and isocyanides in a Passerini reaction.

The combination of both reactions was enabled by a dichloromethane/dimethyl sulfoxide solvent mixture. The respective Biginelli-Passerini reaction products enabled the variation of five components and were obtained in good to excellent yields. Furthermore, a one-pot Biginelli-Passerini tandem reaction without intermediate workup was demonstrated. In future experimental work it will be interesting to evaluate the Biginelli-Passerini compounds towards their pharmacological properties.

In order to leverage the Biginelli-Passerini system, a monomer-based strategy towards sequence-defined macromolecules was established. First, several bifunctional components were prepared and a list of components (for generating the permutations and assigning sidechains to alphanumeric codes) was compiled. Secondly, the bifunctional components were employed in consecutive Biginelli and Passerini reactions for the synthesis of highly functionalized isocyanide-benzyl ester monomers. Thirdly, these monomers were evaluated in a qualitative test system consisting of a Passerini reaction in the first step and a hydrogenolytic benzyl ester deprotection in the second step. Finally, the monomers were polymerized *via* iterative Passerini and benzyl deprotection reactions, resulting in symmetric sequence-defined macromolecules, formally encoding 24 bits per repeating unit (generated through the variation of six components per repeating unit). The macromolecules were sequenced by tandem-MS. Sequencing was enabled *via* the identification of three predominant fragmentation processes occurring along the chain.

The herein presented concepts demonstrate several key advantages contributing to the rapid development of molecular data storage materials: *i.* the number of varying monomers/components can be much higher than for biomacromolecules such as DNA/RNA offering the key benefit of achieving high data storage density within few synthetic steps.; *ii.* DNA/RNA and other biomacromolecules can potentially be pathogenic by coincidentally containing biologically relevant sequences (for instance of viruses in the biological sense). *iii.* different chemical methodologies can be employed or even combined for the preparation of sequence-defined macromolecules.[205,334] Generally, synthetic and non-natural molecules can be designed to be chemically more stable than DNA analogs (for instance, the herein described macromolecules do not contain phosphate esters, which are prone to hydrolysis). However, the long term stability of the herein presented macromolecules should be evaluated under different conditions in future experiments. The combination

of all benefits can promote sequence-defined macromolecules to serve for special applications such as data storage materials, cryptographic keys or anti-counterfeit tags.[242,338] Since the macromolecules in the present investigation are symmetric structures, not every permutation of a corresponding bit sting can be encoded. In future work, it will thus be interesting to synthesize non-symmetric macromolecules in order to also encode non-symmetric bit strings of data. In addition, the Shannon information capacity[210] for the present multicomponent system should be evaluated (as already performed for DNA),[13] in order to prove how many permutations can be practically realized (*i.e.* how many permutations can be synthesized and read-out). Nevertheless, automated synthesis of long sequences and automated analysis (combined with a suitable software) will be crucial for potential applications.

6 Experimental part

The experimental design and logic of all experiments was kept minimalistic in order to be simple, comprehensible and reproducible. Synthetic strategies were planned in convergent routes and compared with each other to achieve high reaction efficiency. Procedures of increasing synthetic complexity were only applied if simpler approaches did not provide satisfying results. Many synthetic procedures included herein were successfully reproduced in undergraduate organic chemistry laboratory courses, by supervised bachelor or "*Vertiefer*" students (specialization subject) or apprentices (chemical laboratory technicians).

All synthesized and subsequently utilized substances were characterized *via* complementary methods (^{1}H-, ^{13}C-NMR spectroscopy, IR spectroscopy, HRMS). Structural characterization and elucidation was carried out *via* 2D NMR methods, enabling assignment of ^{1}H-NMR and ^{13}C-NMR signals. Displayed NMR spectra, tandem-MS fragmentation spectra, *etc.* are not included in the printed version of this thesis but can be found in the electronic version (stored on the CD) and in the supplementary information of the respective peer-reviewed publications (open access). References to the respective publications are provided at the beginning of the corresponding chapters in the experimental part.

6.1 Methods section

6.1.1 Chemical reagents and solvents

All technical solvents were used, if not explicitly described without further purification. Ethyl acetate, hexanes, tetrahydrofuran, dichloromethane and acetone were pre-distilled. If necessary, solvents were additionally dried *via* standard procedures. All commercially available chemicals were used, unless otherwise stated, without further purification and purchased from SIGMA ALDRICH. Aldehydes were tested for oxidative contaminations (carboxylic acids) before use *via* TLC and ^{1}H-NMR. If carboxylic acids were present, the aldehyde was purified *via* distillation (for low boiling

liquids), column chromatography (for high boiling liquids) or recrystallization (for solids) before use. The substances described in chapter **6.2** were synthesized by the author himself or students/apprentices under supervision of the author. Flash column chromatography[339] was performed utilizing Merck SiO_2 60 (230 − 400 mesh).

6.1.2 Thin-layer chromatography

For thin-layer chromatography (TLC) analysis precoated aluminum foils with fluorescence indicator from MERCK (TLC Silica gel 60, F_{254}, layer thickness: 0.25 mm) were employed as stationary phase. The analyte substances were spotted onto the TLC plates with a thin capillary, subsequently the plates were set into a TLC chamber filled and presaturated with eluent solvent mixture, the solvent ratios were reported in (volume:volume). The spots were firstly visualized by fluorescence quenching under UV-light (λ = 254 and 365 nm), fluorescence (λ = 365 nm) and afterwards by staining with Seebach reagent solution. Preparation of Seebach reagent: 6.25 g ammonium heptamolybdate tetrahydrate $(NH_4)_6Mo_7O_{24}\cdot 4H_2O$) and 2.50 g cerium(IV) sulfate tetrahydrate $(Ce(SO_4)_2\cdot 4H_2O)$, were stirred in 225 mL water and 25.0 mL concentrated sulfuric acid were added slowly while stirring and cooling. In some cases, staining with potassium permanganate was more efficient. Preparation of permanganate staining reagent: solution of 3.00 g potassium permanganate ($KMnO_4$), 20.0 g potassium carbonate (K_2CO_3) and 5.00 mL of a 5 wt.% sodium hydroxide (NaOH)-solution in 300 mL water. For some of the perfluorinated Ugi compounds a vanillin staining reagent was the best choice. Preparation of vanillin staining reagent: 15 g of vanillin were dissolved in 250 mL ethanol, subsequently 2.5 mL of concentrated sulfuric acid were slowly added while stirring and cooling.

6.1.3 Nuclear magnetic resonance spectroscopy

^{1}H- and ^{13}C-nuclear magnetic resonance (NMR) spectra were recorded on BRUKER Avance DPX spectrometers (Billerica, MA) with a 5-mm dual proton/carbon probe (operating at 300 MHz or 400 MHz for ^{1}H-NMR spectra and 75.5 MHz for ^{13}C-NMR

spectra) or on a Bruker Avance III with a 5 mm z-gradient cryogenically cooled probe head operating at 600 MHz for ^{1}H- and 75.5 MHz for ^{13}C-NMR) or on a 500 MHz WB Bruker Avance I spectrometer with a proton frequency of 499.97 MHz. ^{13}C-NMR spectra were measured at a frequency of 125.72 MHz on an 8 mm TXI probehead with actively shielded z-gradients (at Θ =0°) and on a 4 mm triple HCX MAS probehead (at *ca.* Θ = 65°) at 298 K, regulated with a Bruker VTU-3000. Unless otherwise stated, all spectra were measured at ambient temperature. The chemical shift for ^{1}H-NMR spectra was reported in parts per million (ppm) referenced to to TMS (0 ppm) or to characteristic solvent signals of partly deuterated solvents *e.g.* $CDCl_3$ at 7.26 ppm or the centroid peak of the DMSO-d^6 quintet at 2.50 ppm. ^{13}C-NMR spectra were reported in ppm relative to characteristic signals of partly deuterated solvents, *e.g.* the centroid peak of the $CDCl_3$ triplet at 77.00 ppm or the DMSO-d_6 septet at 39.52 ppm. All ^{13}C-NMR spectra are decoupled from ^{1}H signals. The signals were listed from low field (large ppm) to high filed (small ppm) with the following notation: NMR-active nucleus (frequency [MHz], deuterated solvent): δ [ppm] = chemical shift (spin multiplicity, scalar coupling constant J [Hz], integral/number of nuclei, assignment$^{Atom\ position}$). The spin multiplicity and corresponding signal patterns were abbreviated as follows: s = singlet, d = doublet, t = triplet, q = quartet, quint. = quintet, m = multiplet, br s = brought singlet. Coupling constants *J* were noted in Hz. Furthermore, 2D NMR methods *e.g.* heteronuclear multiple quantum coherence (HMQC) or heteronuclear single quantum coherence (HSQC), heteronuclear multiple bond correlation (HMBC) and correlated spectroscopy (COSY) or nuclear Overhauser enhancement spectroscopy (NOESY) were carried out, if necessary, for signal assignment and structure elucidation.

6.1.4 Fourier transform infrared spectroscopy

Infrared spectra (IR) were recorded on a BRUKER Alpha-p instrument in a range from 3997 to 374 cm^{-1} applying ATR-technology. The signal shape and intensity was reported relative to the most intense signal in the spectrum and abbreviated in the following pattern: br = brought, vs = very strong, s = strong, m = medium, w = weak, vw = very weak. The signals were noted from large to smaller wavenumbers with the following notation: IR (type of measurement) ν [cm^{-1}] = wave number (signal intensity, proposed molecular oscillation assignment).

6.1.5 Fast-atom-bombardment and electron ionization

Fast-atom-bombardment (FAB) and electron ionization (EI) mass spectra were recorded utilizing a Finnigan MAT 95 mass spectrometer. The signal of the molecule singly charged cation was referred to as $[M]^+$, the protonated singly charged cation of the molecule was referred to as $[(M+H)]^+$. Molecule fragmentations observed in FAB or EI measurements were illustrated in a figure below the text and were formally denoted as homolytic bond cleavage to allow a simple illustration of the observed *m/z* species, but a radical mechanism (or formation) was not proven.

6.1.6 Electrospray ionization – mass spectrometry

Electrospray ionization – mass spectra (ESI-MS and ESI-MS/MS) were recorded on a Q Exactive (Orbitrap) mass spectrometer (Thermo Fisher Scientific, San Jose, CA, USA) equipped with a HESI II probe. Calibration was carried out in the *m/z* range 74-1.822 using premixed calibration solutions (Thermo Fisher Scientific). A constant spray voltage of 4.7 kV and a dimensionless sheath gas of 5 were employed. The S-lens RF level was set to 62.0, while the capillary temperature was set to 250 °C. All samples were dissolved at a concentration range of 0.05 – 0.01 $mg \cdot mL^{-1}$ in a mixture of THF and MeOH (3:2) doped with 100 µmol sodium trifluoroacetate and injected with a flow of 5 $\mu L \cdot min^{-1}$.

6.1.7 Size-exclusion chromatography – mass spectrometry

Size-exclusion chromatography – Mass spectrometry (SEC-ESI-MS) was performed by coupling the above-mentioned Q Exactive (Orbitrap) mass spectrometer to an UltiMate 3000 UHPLC System (Dionex, Sunnyvale, CA, USA) consisting of a pump (LPG 3400SD), autosampler (WPS 3000TSL), and a thermostated column department (TCC 3000SD). Separation was performed on two mixed bed size-exclusion chromatography columns (Polymer Laboratories, Mesopore 250 × 4.6 mm, particle diameter 3 µm) with precolumn (Mesopore 50 × 4.6 mm) operating at 30 °C. THF at a

flow rate of 0.30 mL·min^{-1} was used as eluent. The mass spectrometer was coupled to the column in parallel to a RI-detector (RefractoMax520, ERC, Japan). In this setup 0.27 mL·min^{-1} of the eluent were directed through the RI-detector and 30 µL·min^{-1} infused into the electrospray source after postcolumn addition of a 100 µM solution of sodium iodide in methanol at 20 µL·min^{-1} by a micro-flow HPLC syringe pump (Teledyne ISCO, Model 100DM). A 20 µL aliquot of a analyte solution with a concentration of 1 mg·mL^{-1} was injected onto the HPLC system.

6.1.8 Size-exclusion chromatography

Size-exclusion chromatography (SEC) was conducted on a Varian 390-LC system equipped with a LC-290 pump (Varian), a refractive index detector (24 °C), a PL AS RT GPC-autosampler (Polymer laboratories) and a Varian Pro Star column oven Model 510, operating at 40 °C. For separation two SDV 5 µm linear S columns (8 × 300 mm) and a guard column (8 × 50 mm) were used. Detection was performed by a differential refractive index detector operating in THF (flow rate 1.0 mL·min^{-1}). For calibration linear poly(methyl methacrylate) standards (Agilent) ranging from 875 Da to 1677 kDa were used. Samples were prepared in a concentration of 1 mg·mL^{-1} in THF.

Determinations of molecular weights of polymers insoluble in tetrahydrofuran were performed on a Tosoh EcoSEC HLC-8320 SEC system with hexafluoro isopropanol (HFIP) containing 0.1 wt.% potassium trifluoroacetate as the solvent. The solvent flow was 0.40 mL·min^{-1} at 30 °C. The analysis was performed on a three column system: PSS PFG Micro precolumn (3.0 × 0.46 cm, 10,000 Å), PSS PFG Micro (25.0 × 0.46 cm, 1000 Å) and PSS PFG Micro (25.0 × 0.46 cm, 100 Å). The system was calibrated with linear poly(methyl methacrylate) standards (Polymer Standard Service, Mp 102 – 981 000 Da). For sample preparation a mass of approximately 2 mg was stirred in 1 mL of solvent until a solution was obtained.

6.1.9 Differential scanning calorimetry

Differential scanning calorimetry (DSC) experiments were carried out with a METTLER TOLEDO DSC star^{e} system DSC821e calorimeter measuring in nitrogen atmosphere,

employing a sample mass of approximately 5 mg. The melting temperature, T_m, is recorded as the minimum (endothermic transitions are represented downwards) of the endothermic melting peak with the following method. The glass transition temperature T_g is reported as the curves inflection point (first derivative equals zero) using the following method: heating from 25 °C to 240 °C at 15 °C·min^{-1}, cooling from 240 °C to 0 °C at 15 °C·min^{-1} and heating from 0 °C to 260 °C at 15 °C·min^{-1}. All values were recorded on the second heating cycle to ensure equal thermal history for all samples.

6.1.10 Gas chromatography – mass spectrometry

Gas Chromatography – Mass Spectrometry (GC-MS) (electron impact (EI)) analyses were conducted using a Varian 431-GC instrument with a capillary column FactorFour™ VF-5ms (30 m × 0.25 mm × 0.25 µm) and a Varian 210-MS ion trap mass detector. Scans were performed from 40 to 650 *m/z* at rate of 1 scan per second. The oven temperature program applied during the analysis was: initial temperature 95 °C, hold for 1 min, ramp at 15 °C·min^{-1} to 200 °C, hold for 2 min, ramp at 15 °C·min^{-1} to 300 °C, hold for 5 min. The injector transfer line temperature was set to 250 °C. Measurements were performed in the split-split mode (split ratio 50:1) using helium as carrier gas (flow rate 1.0 mL·min^{-1}).

6.1.11 Microwave reactor

Microwave-assisted syntheses were performed in a CEM EXPLORER 12 HYBRID microwave reactor using a dynamic program at 150 W. The reaction mixture was pre-stirred with a magnetic stir bar for 30 s at medium speed in 10 mL or 35 mL glass vessels sealed with a PTFE rubber band.

6.2 Synthetic procedures

6.2.1 Synthetic procedures for chapter 4.1

Additional data such as displayed NMR spectra and tandem-MS mass spectra can be found in the supplementary information of the previous publication and are included in the electronic version of this thesis on the CD.[208]

6.2.1.1 Ugi reactions of perfluorinated acids

6.2.1.1.1 *Ugi reaction of perfluorononanoic acid, benzaldehyde, tert-butylisocyanide and butylamine 19*

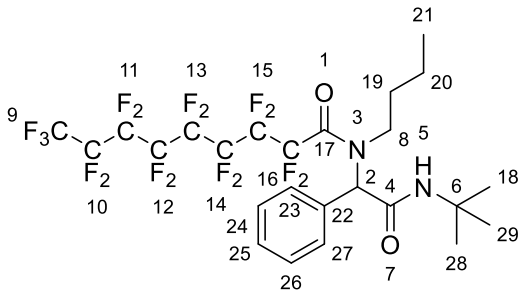

In a 25 mL round bottom flask benzaldehyde (50.0 µL, 52.0 mg, 490 µmol, 1.30 eq.) was dissolved in 1.5 mL methanol, subsequently butylamine (48.5 µL, 35.9 mg, 490 µmol, 1.30 eq.) was added and the resulting mixture was stirred for 60 min over sodium sulfate. Afterwards, the mixture was filtrated. The solid was washed with 10 mL methanol three times. Subsequently, the filtrate was concentrated under reduced pressure. Perfluorononanoic acid (175 mg, 377 µmol, 1.00 eq.) dissolved in 1 mL methanol was added to the imine at room temperature and the resulting mixture was stirred for 2 min. Subsequently, *tert*-butylisocyanide (51.2 µL, 37.6 mg, 453 µmol, 1.20 eq.) was added to the stirring mixture. The reaction was stirred for 18 h at room temperature. The crude reaction mixture was dried under reduced pressure and purified *via* column chromatography employing Fluoro*Flash*® silica gel. The fluorous fraction was concentrated and the residue was adsorbed onto celite® and purified *via* column chromatography employing silica gel and eluting with a gradual solvent mixture

of ethyl acetate and *c*-hexane (0:1 → 1:1) to yield the Ugi product **19** as a pale highly viscous oil (59.4 mg, 83.7 µmol, 22.2%).

R_f = 0.50 in *c*-hexane/ethyl acetate (6:1). Visualized *via* fluorescent quench and Seebach staining solution.

IR (ATR): ν [cm^{-1}] = 3320.6 (w, ν(N-H)), 2968.3 (w, ν(C-H)), 1675.7 (m, ν(C=O)), 1654.1 (m, ν(C=O)), 1553.5 (m), 1477.9 (vw), 1453.2 (w), 1429.2 (w), 1369.4 (w), 1330.5 (w), 1234.3 (m), 1202.1 (vs), 1148.3 (vs), 1111.3 (m), 987.4 (w), 968.1 (vw), 928.5 (w), 806.6 (vw), 772.64 (vw), 736.7 (w), 697.8 (w), 655.0 (m), 631.3 (m), 611.6 (w), 564.8 (w), 519.9 (s), 496.1 (w), 439.3 (vw).

^{1}H-NMR (400 MHz, $CDCl_3$): δ [ppm] = 7.64 – 7.31 (m, 5 H, CH_{Ar}[23-27]), 5.74 – 5.36 (m, 2 H, NH[5] + CH[2]), 3.78 – 3.00 (m, 2 H, CH_2[8]), 1.47 – 1.18 (m, 9 H, CH_3[18,28,29]), 1.14 – 0.96 (m, 4 H, CH_2[19,20]), 0.67 (t, J = 7.2 Hz, 3 H, CH_3[21]).

^{13}C-NMR (101 MHz, $CDCl_3$): δ [ppm] = 166.17 (s, CONR[4]), 157.98 (s, CONR[17]), 132.94 (s, C_{Ar}[22]), 132.64 (s, CH_{Ar}), 128.59 (s, CH_{Ar}), 128.11 (s, CH_{Ar}), 128.05 (s, CH_{Ar}), 64.86 (s, CH[2]), 51.17 (s, C[6]),47.15 (s, CH_2[8]), 30.85 (s, CH_2[20 or 19]), 27.86 (s, CH_3[18, 28, 29]), 27.48 (s, CH_3[18, 28, 29]), 18.87 (s, CH_2[20 or 19]), 12.28 (s, CH_3[21]).

^{19}F-NMR (376 MHz, $CDCl_3$): δ [ppm] = -85.11 (t, J = 10.3 Hz, 3 F, CF_3[9]), AB-signal (δ_A = -113.09, δ_B = -114.08, J_{AB} = 297.4 Hz, A and B are split into t, J = 13.1 Hz, CF_2[16a]), AB-signal (δ_A = -115.56, δ_B = -116.60, J_{AB} = 291.8 Hz, CF_2[16b], additional coupling not resolved, signals broadened), -124.62 (s, CF_2), -126.11 (s, CF_2), -127.05 (s, CF_2), -130.44 (s, CF_2[10]). Total integral of CF_2 region normalized with respect to the CF_3[9] group = 14.

FAB – MS [*m/z*] (relative intensity): 709.2 (35%) $[M + H]^+$, 637.1 (40%) [Fragment A – H]$^+$, 608.1 (55%) [Fragment A – CO]$^+$, 552.1 (20%) [Fragment A – CO – C_5H_9]$^+$, 191.1 (12%), [Fragment B + H]$^+$.

HRMS – FAB [*m/z*]: $[M + H]^+$ calculated for $^{12}C_{25}{}^{1}H_{26}{}^{16}O_2{}^{14}N_2{}^{19}F_{17}$, 709.1717; found, 709.1715; Δ = 0.19 mmu.

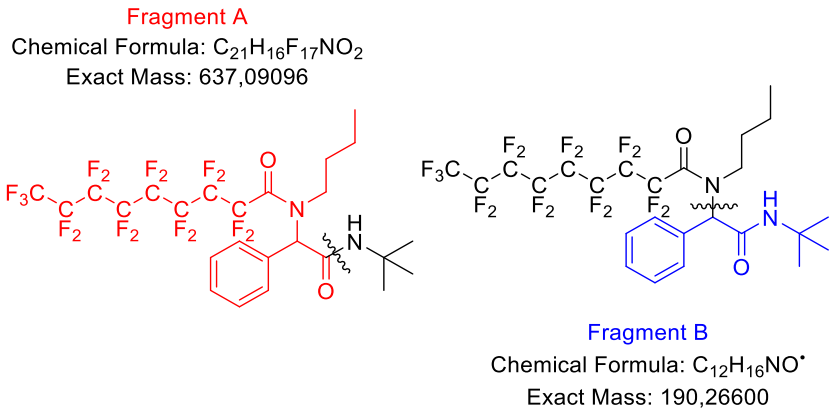

6.2.1.1.2 *Ugi reaction of perfluoropentanoic acid benzaldehyde, tert-butylisocyanide and butylamine 20*

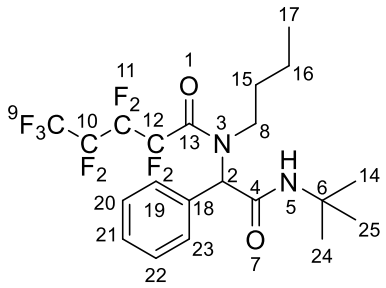

In a 25 mL round bottom flask benzaldehyde (115 µL, 119 mg, 1.12 mmol, 1.70 eq.) was dissolved in 1.5 mL methanol, subsequently butylamine (114 µL, 82.4 mg, 1.12 mmol, 1.70 eq.) was added and the resulting mixture was stirred for 60 min over sodium sulfate. Afterwards, the mixture was filtrated and the solid was washed with 10 mL methanol three times. Subsequently, the filtrate was concentrated under reduced pressure. Perfluoropentanoic acid (175 mg, 663 µmol, 1.00 eq.) dissolved in 1 mL methanol was added to the imine at room temperature and the resulting mixture was stirred for 2 min. Subsequently, *tert*-butylisocyanide (127 µL, 93.7 mg, 1.12 mmol, 1.70 eq.) was added to the stirring mixture. The reaction was stirred for 3 d at room temperature. The crude reaction mixture was dried under reduced pressure and purified *via* column chromatography employing Fluoro*Flash*® silica gel. The fluorous fraction was tested for purity *via* TLC and concentrated under reduced pressure. The remaining perfluoro acid was removed with a short silica gel filter column, eluting with *c*-hexane/ethyl acetate (3:1) to yield the Ugi product **20** as a yellow powder (259 mg, 562 µmol, 85.1%).

R_f = 0.50 in *c*-hexane/ethyl acetate (5:1). Visualized *via* fluorescent quench and Seebach staining solution.

IR (ATR): ν [cm^{-1}] = 3317.9 (w, ν(N-H)), 2963.9 (w, ν(C-H)), 1679.7 (m, ν(C=O)), 1654.9 (s, ν(C=O)), 1556.6 (m), 1475.8 (w), 1454.4 (w), 1429.8 (m), 1355.4 (w), 1305.9 (w), 1233.5 (s), 1214.1 (s), 1187.4 (s), 1137.4 (s), 1125.2 (w), 1110.5 (w), 1029.5 (w), 959.2 (w), 869.7 (w), 855.6 (w), 805.5 (w), 787.1 (w), 764.8 (w), 748.8 (w), 728.1 (w), 699.2 (w), 648.3 (m), 634.3 (s), 610.4 (w), 522.6 (s), 498.2 (w), 435.9 (w).

^{1}H-NMR (400 MHz, CD_3OD): δ [ppm] = 7.67 – 7.06 (m, 5 H, CH_{Ar}[19-23]), 6.09 – 5.59 (m, 2 H, CH[2] + NH[5]), 3.72 – 2.94 (m, 2 H, CH_2[8]), 1.33 (d, J = 15.2 Hz, 9 H, CH_3[14,24,25]), 1.03 – 0.76 (m, 4 H, CH_2[15 + 16]), 0.68 – 0.55 (m, 3 H, CH_3[17]).

^{13}C-NMR (126 MHz, CD_3OD): δ [ppm] = 168.75 (s, CONR[4]), 158.04 (s, CONR[13]), 134.19 (s, C_{Ar}[18]), 130.23 (s, CH_{Ar}), 129.58 (s, CH_{Ar}), 128.87 (s, CH_{Ar}), 128.75 (s, CH_{Ar}), 128.58 (s, CH_{Ar}), 64.24 (s, CH[2]), 50.96 (s, C[6]), 45.82 (s, CH_2[8]), 32.09 (s, CH_2[15 or 16]), 28.96 (s, CH_3[14, 24, 25]), 27.28 (s, CH_3[14, 24, 25]), 19.45 (s, CH_2[15 or 16]), 12.25 (s, CH_3[17]).

^{19}F-NMR (376 MHz, CD_3OD): δ [ppm] = -82.77 (dt, J = 23.6, 11.7 Hz, 3 F, CF_3[9]), AB-signal (δ_A = -110.63, δ_B = -111.89, J_{AB} = 240.9 Hz, A and B are split into t, J = 14.0 Hz, CF_2[12a]), AB-signal (δ_A = -112.48, δ_B = -113.57, J_{AB} = 235.3 Hz, A and B are split into t, J = 14.4 Hz, CF_2[12b]), -122.01 – -122.31 (m, CF_2), -124.75 (s, CF_2), -125.33 (s, CF_2), -125.44 (s, CF_2[10]). Total integral of CF_2 region normalized with respect to the CF_3[9] group = 6.

ESI-MS [*m/z*]: $[M + Na]^+$ calculated for $^{12}C_{21}{}^{1}H_{25}{}^{16}O_2{}^{14}N_2{}^{19}F_9{}^{23}Na_1$, 531.1665; found, 531.1669, Δ = 0.42 mmu.

ESI-MS [*m/z*]: $[2 M + Na]^+$ calculated for $^{12}C_{42}{}^{1}H_{50}{}^{16}O_4{}^{14}N_4{}^{19}F_{18}{}^{23}Na_2$, 1039.3437; found, 1039.3450, Δ = 1.29 mmu.

6.2.1.1.3 *Ugi reaction of perfluorotetradecanoic acid, benzaldehyde, tert-butylisocyanide and butylamine 21*

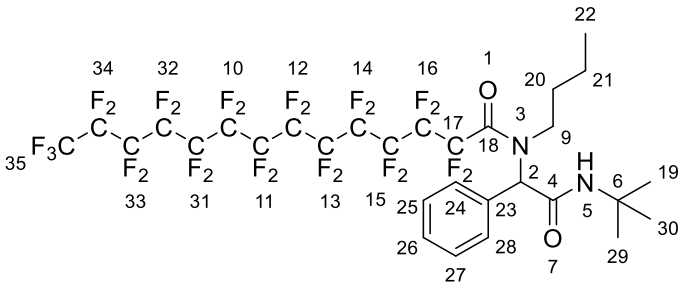

In a 25 mL round bottom flask benzaldehyde (97.2 µL, 101 mg, 952 µmol, 1.70 eq.) was dissolved in 1.5 mL methanol, subsequently butylamine (94.1 µL, 69.6 mg, 952 µmol, 1.70 eq.) was added and the resulting mixture was stirred for 60 min over sodium sulfate. Perfluorotetradecanoic acid (400 mg, 560 µmol, 1.00 eq.) dissolved in 1 mL methanol was added at room temperature and the resulting mixture was stirred for 2 min. Subsequently, *tert*-butylisocyanide (108 µL, 79.2 mg, 952 µmol, 1.70 eq.) was added to the stirring mixture. After 4 h a precipitate was formed, and 2 mL tetrahydrofuran were added to homogenize the reaction mixture. The resulting solution was stirred for 5 d at room temperature. The crude reaction mixture was dried under reduced pressure. The residue was adsorbed onto celite® and purified *via* column chromatography employing silica gel and eluting with a gradual solvent mixture of ethyl acetate and *c*-hexane (1:10 → 1:3) to yield the Ugi product **21** as a yellow solid (98.7 mg, 103 mmol, 18.4%).

R_f = 0.50 in *c*-hexane/ethyl acetate (5:1). Visualized *via* fluorescent quench and Seebach staining solution.

IR (ATR): ν [cm^{-1}] = 3321.1 (w, ν(N-H)), 2968.1 (w, ν(C-H)), 1679.5 (s, ν(C=O)), 1654.5 (s, ν(C=O)), 1553.7 (m), 1452.7 (w), 1429.0 (w), 1363.3 (w), 1021.7 (vs), 1149.1 (vs), 1113.3 (s), 1095.2 (m), 1042.1 (m), 987.1 (w), 968.3 (w), 938.3 (w), 873.6 (w), 827.5 (m), 761.6 (m), 729.6 (m), 699.6 (m), 645.8 (s), 549.9 (s), 524.9 (s), 436.8 (w).

^{1}H-NMR (400 MHz, $CDCl_3$): δ [ppm] = 7.79 – 7.25 (m, 5 H, CH_{Ar}^{24-28}), 5.83 – 5.10 (m, 2 H, NH^5 + CH^2), 3.79 – 3.16 (m, 2 H, CH_2^9), 1.43 (s, 1 H, CH_2^{20a}), 1.40 – 1.22 (m, 9 H, $CH_3^{19,29,30}$), 1.16 – 0.82 (m, 3 H, CH_2^{20b} + CH_2^{21}), 0.77 – 0.56 (m, 3 H, CH_3^{22}).

^{13}C-NMR (101 MHz, $CDCl_3$): δ [ppm] = 166.16 (s, $CONR^4$), 159.78 (s, $CONR^{18}$), 132.56 (s, C_{Ar}^{23}), 129.43 (s, CH_{Ar}), 128.58 (s, CH_{Ar}), 127.55 (s, CH_{Ar}), 64.79 (s, CH^{2a}), 62.05

(s, CH^{2b}), 50.81 (s, C^{6}), 46.33 (s, CH_2^{9}), 30.81 (s, $CH_2^{20\ or\ 21}$), 27.38 (s, $CH_3^{18,\ 29,\ 30}$), 18.72 (s, $CH_2^{20\ or\ 21}$), 12.28 (s, CH_3^{22}).

^{19}F-NMR (376 MHz, $CDCl_3$): δ [ppm] = -80.78 (t, J = 9.7 Hz, 3 F, CF_3^{35}), AB-signal (δ_A = -108.81, δ_B = -109.78, J_{AB} = 237.2 Hz, A and B are split into t, J = 13.1 Hz, CF_2^{17a}), AB-signal (δ_A = -111.27, δ_B = -112.34, J_{AB} = 233.4 Hz, CF_2^{17b}, additional coupling not resolved, signals broadened), -120.31 (s, CF_2), -121.76 (s, CF_2), -122.77(s, CF_2), -126.18 (s, CF_2^{34}). Total integral of CF_2 region normalized with respect to the CF_3^{35} group = 24.

FAB – MS [*m/z*] (relative intensity): 959.1 (25%) $[M + H]^+$, 886.0 (27%) [Fragment A]$^+$, 858.0 (43%) [Fragment B]$^+$, 802.0 [Fragment B – C_4H_9]$^+$.

HRMS – FAB [*m/z*]: $[M + H]^+$ calculated for $^{12}C_{30}{}^{1}H_{26}{}^{16}O_2{}^{14}N_2{}^{19}F_{27}$, 959.1558; found, 959.1557; Δ = 0.09 mmu.

Chemical Formula: $C_{26}H_{15}F_{27}NO_2^{\bullet}$
Exact Mass: 886,06717
Fragment A

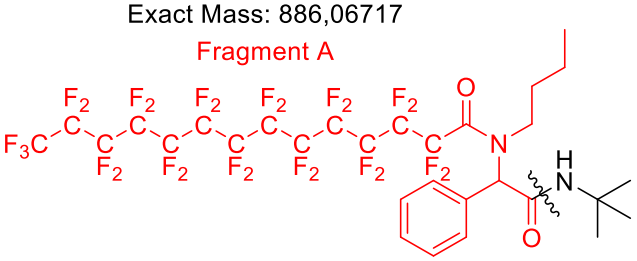

Chemical Formula: $C_{25}H_{15}F_{27}NO^{\bullet}$
Exact Mass: 858,07225
Fragment B

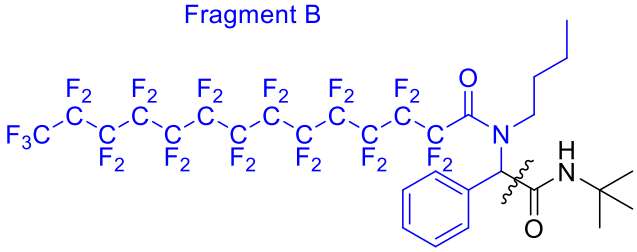

6.2.1.1.4 *Ugi reaction of perfluoropentanoic acid valeraldehyde, 4-methoxyphenylisocyanide and butylamine 22*

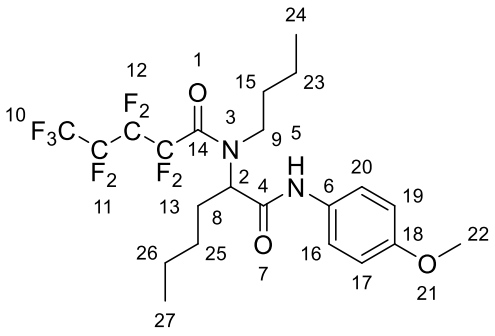

In a 25 mL round bottom flask valeraldehyde (83.2 mg, 966 µmol, 1.70 eq.) was dissolved in 1.5 mL methanol, subsequently butylamine (108 µL, 70.6 mg, 966 µmol, 1.70 eq.) was added and the resulting mixture was stirred for 60 min over sodium sulfate. Afterwards, the mixture was filtrated and the solid was washed with 10 mL methanol three times. Subsequently, the filtrate was concentrated under reduced pressure. Perfluoropentanoic acid (150 mg, 568 µmol, 1.00 eq.) dissolved in 1 mL methanol was added to the imine at room temperature and the resulting mixture was stirred for 2 min. Subsequently, *4*-methoxyphenylisocyanide (108 µL, 129 mg, 966 µmol, 1.70 eq.) was added to the stirring mixture. The reaction was stirred for 3 d at room temperature. The crude reaction mixture was dried under reduced pressure and purified *via* column chromatography employing Fluoro*Flash*® silica gel. The fluorous fraction was tested for purity *via* TLC and concentrated under reduced pressure. The remaining perfluoro acid was removed with a short silica gel filter column, eluting with *c*-hexane/ethyl acetate (3:1) to yield the Ugi product **22** as a yellow powder (18.4 mg, 34.1 µmol, 6.01%).

R_f = 0.48 in *c*-hexane/ethyl acetate (5:1). Visualized *via* fluorescent quench and Seebach staining solution.

IR (ATR): ν [cm^{-1}] = 2957.5 (m, ν(C-H)), 2929.3 (s, ν(C-H)), 2858.8 (m,), 1795.3 (m), 1718.9 (s, ν(C=O)), 1606.3 (vs, ν(C=O)), 1506.0 (m), 1464.9 (m), 1351.9 (m), 1292.8 (vs), 1234.4 (vs), 1136.6 (s), 1099.4 (s), 1036.6 (s), 894.2 (m), 835.9 (s), 793.9 (m), 742.8 (m), 725.7 (m), 691.5 (m), 575.6 (w), 527.3 (w), 435.6 (w).

^{1}H-NMR (400 MHz, CD_3OD): δ [ppm] = 7.47 – 7.35 (m, 2 H, $CH_{Ar}^{16,20}$), 6.94 – 6.80 (m, 2 H, $CH_{Ar}^{17,19}$), 4.75 (t, *J* = 7.6 Hz, 1 H, CH^{2}), 3.76 (s, 3 H, OCH_3^{22}), 3.67 – 3.47 (m, 2

H, CH_2[9]), 2.15 – 2.00 (m, 1 H, CH_2[8a]), 1.94 – 1.76 (m, 1 H, CH_2[8b]), 1.72 – 1.57 (m, 2 H, CH_2), 1.45 – 1.22 (m, 6 H, CH_2), 1.02 – 0.81 (m, 6 H, CH_3[24,27]).

^{13}C-NMR (126 MHz, CD_3OD): *δ* [ppm] = 169.96 (s, CONR[4]), 169.44 (s, CONR[14]), 158.29 (s, C_{Ar}[18]), 132.15 (s, C_{Ar}[6]), 123.58 (s, CH_{Ar}[16,20]), 115.01 (s, CH_{Ar}[17,19]), 62.45 (s, CH[2]), 55.84 (s, OCH_3[22]), 47.15 (s, CH_2[9]), 33.77 (s, CH_2), 29.74 (s, CH_2[8]), 29.56 (s, CH_2), 23.51 (s, CH_2), 21.06 (s, CH_2), 14.25 (s, CH_3[24 or 27]), 13.91 (s, CH_3[24 or 27]).

^{19}F-NMR (376 MHz, CD_3OD): δ [ppm] = -88.25 (t, *J* = 10.5 Hz, 3 F CF_3[10]), -123.93 (s, CF_2[13]), -125.69 – -127.15 (m, CF_2), -133.18 (s, CF_2), -133.32 (s, CF_2), -134.92 (s, CF_2[11]). Total integral of CF_2 region normalized with respect to the CF_3[10] group = 6.

FAB – MS [*m/z*] (relative intensity): 538.3 (28%) $[M + H]^+$, 523.3 (34%) $[M – CH_3]^+$, 220.2 (28%) [Fragment A]$^+$, 122.1 (53%) [Fragment B]$^+$.

HRMS – FAB [*m/z*]: $[M]^+$ calculated for $^{12}C_{22}{}^{1}H_{27}{}^{16}O_3{}^{14}N_2{}^{19}F_9$, 538.1872; found, 538.1870; Δ = 0.26 mmu.

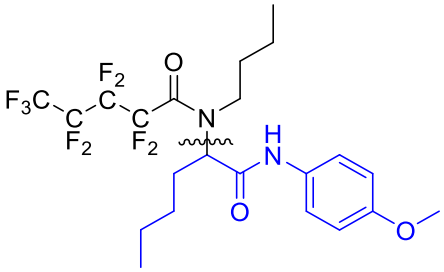

Chemical Formula: $C_{13}H_{18}NO_2^{\bullet}$
Exact Mass: 220,13375
Fragment A

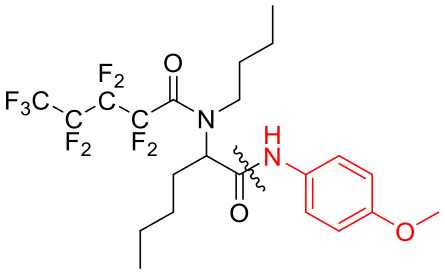

Chemical Formula: $C_7H_8NO^{2\bullet}$
Exact Mass: 122,06059
Fragment B

6.2.1.1.5 *Ugi reaction of perfluorononanoic acid, heptanal, 4-methoxyphenylisocyanide and butylamine 23*

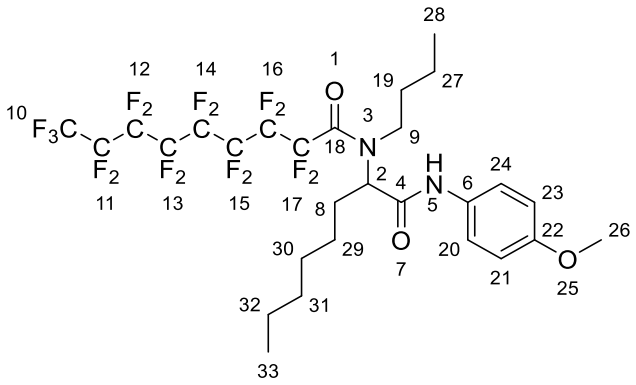

In a 25 mL round bottom flask heptanal (71.0 µL, 56.0 mg, 490 µmol, 1.30 eq.) was dissolved in 1.5 mL methanol, subsequently butylamine (48.5 µL, 35.9 mg, 490 µmol, 1.30 eq.) was added and the resulting mixture was stirred for 60 min over sodium sulfate. Afterwards, the mixture was filtrated and the solid was washed with 10 mL methanol three times. Subsequently, the filtrate was concentrated under reduced pressure. Perfluorononanoic acid (175 mg, 377 µmol, 1.00 eq.) dissolved in 1 mL methanol was added to the imine at room temperature and the resulting mixture was stirred for 2 min. Subsequently, 4-methoxypehnylisocyanide (50.4 µL, 60.3 mg, 453 µmol, 1.20 eq.) was added to the stirring mixture. The reaction was stirred for 3 d at room temperature. The crude reaction mixture was dried under reduced pressure and purified *via* column chromatography employing Fluoro*Flash*® silica gel. The fluorous fraction was tested for purity *via* TLC and concentrated under reduced pressure. The remaining perfluoro acid was removed with a short silica gel filter column, eluting with *c*-hexane/ethyl acetate (3:1) to yield the Ugi product **23** as a highly viscous yellow oil (53.9 mg, 70.3 µmol, 18.6%).

R_f = 0.45 in *c*-hexane/ethyl acetate (6:1). Visualized *via* fluorescent quench and Seebach staining solution.

IR (ATR): ν [cm^{-1}] = 3320.9 (br, ν(N-H)), 2959.5 (m, ν(C-H)), 2932.7 (w, ν(C-H)), 2861.1 (w, ν(C-H)), 1794.9 (w, ν(C=O)), 1665.5 (s), 1605.3 (w), 1511.7 (m), 1466.2 (s), 1414.5 (m), 1298.9 (m), 1236.4 (vs), 1205.4 (vs), 1147.3 (vs), 1037.6 (s), 936.0 (w), 829.4 (m), 722.4 (m), 703.9 (m), 659.9 (m), 559.0 (m), 528.0 (m).

^{1}H-NMR (400 MHz, $CDCl_3$): δ [ppm] = 8.25 (s, 1 H, NH^5), 7.53 – 7.27 (m, 2 H, $CH_{Ar}^{20,24}$), 7.13 – 6.68 (m, 2 H, $CH_{Ar}^{21,23}$), 4.69 (t, J = 7.5 Hz, 1 H, CH^2), 3.79 (s, 3 H, OCH_3^{26}),

3.63 – 3.28 (m, 2 H, CH_2^{9}), 2.42 – 1.68 (m, 2 H, CH_2^{8}), 1.64 – 1.42 (m, 2 H, CH_2^{19}), 1.39 – 1.19 (m, 10 H, CH_2), 1.02 – 0.77 (m, 6 H, $CH_3^{28\,+\,33}$).

^{13}C-NMR (126 MHz, $CDCl_3$): δ [ppm] = 167.73 (s, $CONR^{4}$), 160.32 (s, $CONR^{18}$), 156.77 (s, C_{Ar}^{22}), 130.74 (s, C_{Ar}^{6}), 121.79 (s, $CH_{Ar}^{20,24}$), 114.33 (s, $CH_{Ar}^{21,23}$), 62.04 (s, CH^{2}), 55.62 (s, OCH_3^{26}), 45.61 (s, CH_2^{9}), 31.69 (s, CH_2), 29.09 (s, CH_2), 27.84 (s, CH_2^{8}), 26.13 (s, CH_2), 22.64 (s, CH_2), 20.12 (s, CH_2), 14.11(s, $CH_3^{33\ or\ 28}$), 13.58 (s, $CH_3^{33\ or\ 28}$).

^{19}F-NMR (376 MHz, $CDCl_3$): δ [ppm] = -85.08 (t, J = 9.9 Hz, 3 F, CF_3^{10}), -112.11 – -113.63 (m, CF_2^{17a}), AB-signal (δ_A = -115.34, δ_B = -115.68, J_{AB} = 331.3 Hz, A and B are split into t, J = 12.8 Hz, CF_2^{17b}), -124.74 (s, CF_2), -126.11 (s, CF_2), -127.03 (s, CF_2), -130.42 (s, CF_2^{11}). Total integral of CF_2 region normalized with respect to the CF_3^{10} group = 14.

FAB – MS [*m/z*] (relative intensity): 766.3 (50%) $[M]^+$, 617.2 (85%) [Fragment A + H]$^+$.

HRMS – FAB [*m/z*]: $[M]^+$ calculated for $^{12}C_{28}{}^{1}H_{31}{}^{16}O_3{}^{14}N_2{}^{19}F_{17}$, 766.2058; found, 766.2058; Δ = 0.04 mmu.

Chemical Formula: $C_{20}H_{23}F_{17}NO^{\bullet}$
Exact Mass: 616,15082
Fragment A

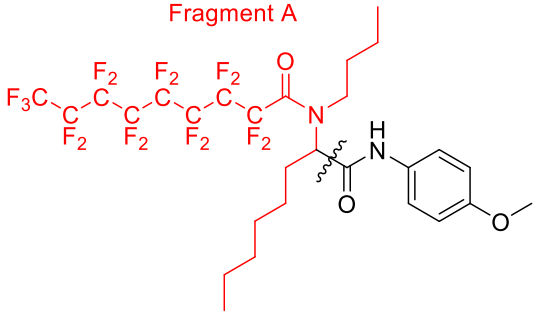

6.2.1.1.6 *Ugi reaction of perfluoropentanoic acid benzaldehyde, 4-methoxyphenylisocyanide and pentylamine 24*

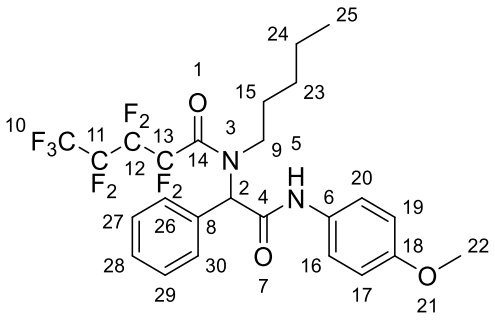

In a 25 mL round bottom flask benzaldehyde (115 µL, 119 mg, 1.12 mmol, 1.70 eq.) was dissolved in 1.5 mL methanol, subsequently butylamine (114 µL, 82.4 mg, 1.12 mmol, 1.70 eq.) was added and the resulting mixture was stirred for 60 min over sodium sulfate. Afterwards, the mixture was filtrated and the solid was washed with 10 mL methanol three times. Subsequently, the filtrate was concentrated under reduced pressure. Perfluoropentanoic acid (175 mg, 663 µmol, 1.00 eq.) dissolved in 2 mL methanol was added to the imine at room temperature and the resulting mixture was stirred for 2 min. Subsequently, *tert*-butylisocyanide (127 µL, 93.7 mg, 1.12 mmol, 1.70 eq.) was added to the stirring mixture. The reaction was stirred for 4 d at room temperature. The crude reaction mixture was dried under reduced pressure and purified *via* column chromatography employing fluoro flash silica gel. The fluorous fraction was tested for purity *via* TLC and concentrated under reduced pressure. The remaining perfluoro acid was removed with a short silica gel filter column, eluting with *c*-hexane/ethyl acetate (3:1) to yield the Ugi product **24** as a colorless powder (258 mg, 451 µmol, 68.1%).

R_f = 0.29 in *c*-hexane/ethyl acetate (4:1). Visualized *via* fluorescent quench and Seebach staining solution.

IR (ATR): ν [cm^{-1}] = 3307.9 (br, ν(N-H)), 2962.1 (m, ν(C-H)), 2932.8 (m, ν(C-H)), 1673.9 (vs, ν(C=O)), 1657.4 (s, ν(C=O)), 1599.4 (m), 1544.4 (s), 1513.9 (w), 1494.6 (w), 1477.9 (m), 1463.6 (m), 1452.6 (m), 1431.4 (m), 1417.4 (m), 1381.8 (w), 1353.1 (m), 1298.5 (m), 1284.8 (m), 1262.9 (m), 1234.3 (s), 1211.9 (vs), 1197.1 (vs), 1185.5 (s), 1175.2 (s),1136.8 (vs), 1126.6 (s), 1110.5 (vs), 1034.0 (s), 974.4 (w), 950.7 (s), 931.0 (w), 870.8 (w), 849.6 (w), 829.7 (s), 812.4 (s), 802.4 (s), 760.1 (m), 745.8 (m),

722.2 (m), 704.7 (vs), 632.3 (m), 612.4 (m), 574.9 (w), 548.1 (m), 524.7 (m), 512.3(s), 474.4 (m), 436.9 (w).

^{1}H-NMR (400 MHz, $CDCl_3$): δ [ppm] = 7.44 (d, J = 2.6 Hz, 5 H, CH_{Ar}^{26-30}), 7.31 (d, J = 9.0 Hz, 2 H, $CH_{Ar}^{16,20}$), 6.79 (d, J = 8.9 Hz, 2 H, $CH_{Ar}^{17,19}$), 5.74 (s, 1 H, CH^{2}), 3.88 – 3.66 (m, 3 H, OCH_3^{22}), 3.58 – 3.25 (m, 2 H, CH_2^{9}), 1.57 (d, J = 58.6 Hz, 2 H, CH_2), 1.19 – 0.91 (m, 4 H, CH_2), 0.75 (t, J = 7.0 Hz, 3 H, CH_3^{25}).

^{13}C-NMR (126 MHz, $CDCl_3$): δ [ppm] = 166.60 (s, $CONR^{4}$), 159.65 (s, C_{Ar}^{18}), 157.11 (s, $CONR^{14}$), 133.39 (s, C_{Ar}^{8}), 130.81 (s, C_{Ar}^{6}), 130.14 (s, CH_{Ar}), 129.93 (s, CH_{Ar}), 129.73 (s, CH_{Ar}), 122.32 (s, $CH_{Ar}^{16,20}$), 114.51 (s, $CH_{Ar}^{17,19}$), 66.56 (s, CH^{2}), 55.89 (s, OCH_3^{22}), 48.23 (s, CH_2^{9}), 29.92 (s, CH_2), 29.12 (s, CH_2), 22.33 (s, CH_2), 14.22 (s, CH_3^{25}).

^{19}F-NMR (376 MHz, $CDCl_3$): δ [ppm] = -85.38 (t, J = 9.9 Hz, 3 F, CF_3^{10}), AB-signal (δ_A = -113.13, δ_B = -114.21, J_{AB} = 301.20 Hz, A and B are split into t, J = 12.3 Hz, CF_2^{13a}), AB-signal (δ_A = -115.78, δ_B = -116.72, J_{AB} = 291.8 Hz, A and B are split into t, J = 12.4 Hz, CF_2^{13a}), -125.48 (s, CF_2), -128.89 (s, CF_2^{11}). Total integral of CF_2 region normalized with respect to the CF_3^{10} group = 6.

ESI-MS [m/z]: $[M + Na]^+$ calculated for $^{12}C_{25}{}^{1}H_{25}{}^{16}O_3{}^{14}N_2{}^{19}F_9{}^{23}Na_1$, 595.1614; found, 595.1615, Δ = 0.13 mmu.

ESI-MS [m/z]: $[2M + Na]^+$ calculated for $^{12}C_{50}{}^{1}H_{50}{}^{16}O_6{}^{14}N_4{}^{19}F_{18}{}^{23}Na_1$, 1167.3335; found, 1167.3348, Δ = 1.32 mmu.

6.2.1.1.7 *Ugi reaction of perfluorononanoic acid, p-anisaldehyde, cyclohexylisocyanide and propargylamine 25*

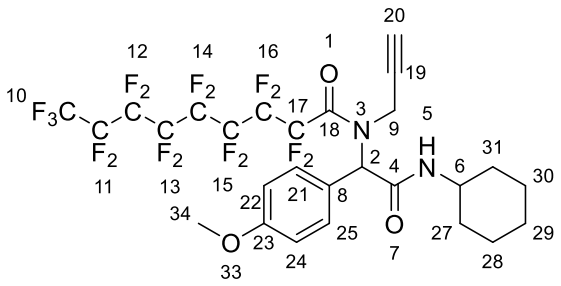

In a 25 mL round bottom flask *p*-anisaldehyde (77.9 µL, 87.3 mg, 641 µmol, 1.70 eq.) isobutyraldehyde and propargylamine (41.4 µL, 35.3 mg, 641 µmol, 1.70 eq.) were

added. The resulting mixture was stirred for 60 min over sodium sulfate. Perfluorononanoic acid (175 mg, 377 µmol, 1.00 eq.) dissolved in 0.5 mL methanol was added to the imine at room temperature and the resulting mixture was stirred for 2 min. Subsequently, cyclohexylisocyanide (79.7 µL, 70.0 mg, 641 µmol, 1.70 eq.) was added to the stirring mixture. The reaction was stirred for 3 d at room temperature. The crude reaction mixture was dried under reduced pressure and purified *via* column chromatography employing Fluoro*Flash*® silica gel. The fluorous fraction was tested for purity *via* TLC and concentrated under reduced pressure. The remaining perfluorononanoic acid was removed with a short silica gel filter column, eluting with *c*-hexane/ethyl acetate (3:1) to yield the Ugi product **25** as a yellow oil (158 mg, 212 µmol, 56.3%).

R_f = 0.36 in *c*-hexane/ethyl acetate (6:1). Visualized *via* fluorescent quench and Seebach staining solution.

IR (ATR): ν [cm^{-1}] = 3314.9 (m, ν(N-H)), 2937.2 (m, ν(C-H)), 2862.0 (w), 1687.5 (vs, ν(C=O)), 1655.8 (vs), 1612.7 (m), 1550.2 (s), 1518.1 (s), 1440.1 (s), 1405.5 (m), 1368.2 (m), 1326.9 (m), 1307.5 (m), 1286.6 (s), 1243.1 (s), 1021.5 (s), 1150.3 (s), 1119.4 (vs), 1079.4 (vs), 1034.4 (vs), 1011.4 (vs), 986.9 (s), 939.2 (m), 894.0 (m), 874.4 (m), 838.6 (m), 776.3 (m), 755.3 (m), 736.6 (m), 707.6 (m), 653.7 (vs), 642.8 (s), 629.0 (vs), 618.8 (vs), 560.0 (s), 527.0 (vs), 441.5 (w), 424.2 (m).

^{1}H-NMR (500 MHz, CD_3OD): δ [ppm] = 7.41 – 7.19 (m, 2 H, CH_{Ar}[21,25]), 7.03 – 6.81 (m, 2 H, CH_{Ar}[22,24]), 5.91 (s, 1 H, CH[2]), 4.40 – 4.18 (m, 2 H, CH_2[9]), 3.80 (s, 3 H, CH_3[34]), 3.69 (s, 1 H, CH[6]), 3.34 – 3.25 (m, 1 H, CH[20]), 1.94 – 1.10 (m, 10 H, CH_2).

^{13}C-NMR (126 MHz, CD_3OD): δ [ppm] = 172.97 (s, CONR[4]), 169.96 (s, CONR[18]), 161.98 (s, C_{Ar}[23]), 133.13 (s, CH_{Ar}[21,25]), 132.10 (s, C_{Ar}[8]), 115.32 (s, CH_{Ar}[22,24]), 61.53 (s, CH[2]), 55.81 (s, CH_3[34]), 50.00 (s, CH[6] or CH[20]), 50.03 (s, CH[6] or CH[20]), 36.89 (s, CH_2[9]), 33.51 (s, CH_2), 33.46 (s, CH_2), 26.99 (s, CH_2), 26.58 (s, CH_2), 26.00 (s, CH_2).

^{19}F-NMR (376 MHz, CD_3OD): δ [ppm] = -88.24 (t, J = 10.3 Hz, 3 F, CF_3[10]), AB-signal (δ_A = -116.45, δ_B = -117.92, J_{AB} = 301.2 Hz, A and B are split into t, additional coupling not resolved, signals broadened, CF_2[17a]), AB-signal (δ_A = -117.79, δ_B = -119.06, J_{AB} = 293.6 Hz, A and B are split into t, additional coupling not resolved, signals broadened, CF_2[17b]), -126.39 – -127.61 (m, CF_2), -128.66 (s, CF_2), -129.62 (s, CF_2), -133.16 (s, CF_2[11]). Total integral of CF_2 region normalized with respect to the CF_3[10] group = 14.

FAB – MS [*m/z*] (relative intensity): 747.2 (25%) $[M - H]^+$, 621.0 (30%) [Fragment A + H]$^+$, 620.0 (45%) [Fragment A]$^+$, 582.0 (34%) [Fragment A + H – C_3H_3]$^+$, 247.1 (33%) [Fragment B + H]$^+$.

HRMS – FAB [*m/z*]: $[M + H]^+$ calculated for $^{12}C_{27}{}^{1}H_{24}{}^{16}O_3{}^{14}N_2{}^{19}F_{17}$, 747.1510; found, 747.1509; Δ = 0.06 mmu.

Fragment A
Chemical Formula: $C_{20}H_{11}F_{17}NO_2^{\bullet}$
Exact Mass: 620,05183

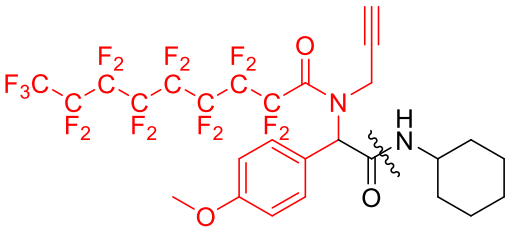

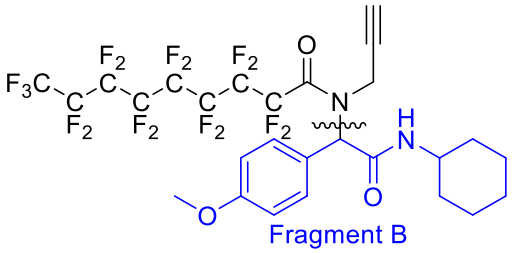

Fragment B
Chemical Formula: $C_{15}H_{20}NO_2^{\bullet}$
Exact Mass: 246,14940

6.2.1.1.8 *Ugi reaction of perfluorononanoic acid, p-anisaldehyde, 4-methoxyphenyl-isocyanide and propargylamine 26*

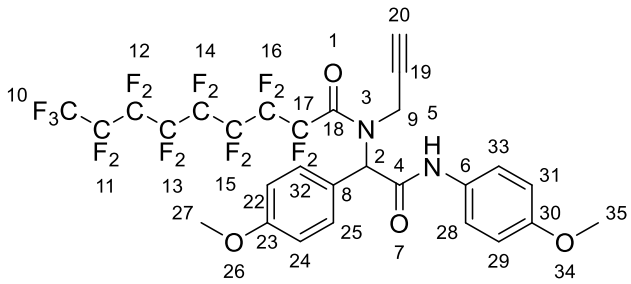

In a 25 mL round bottom flask *p*-anisaldehyde (77.9 µL, 87.3 mg, 641 µmol, 1.70 eq.) and propargylamine (41.1 µL, 35.3 mg, 641 µmol, 1.70 eq.) were added. The resulting mixture was stirred for 60 min over sodium sulfate. Perfluorononanoic acid (175 mg, 377 µmol, 1.00 eq.) dissolved in 0.5 mL methanol was added to the solution at room temperature and the resulting mixture was stirred for 2 min. Subsequently, *4*-methoxyphenyl-isocyanide (85.4 mg, 641 µmol, 1.70 eq.) was added to the stirring mixture. The reaction was stirred for 3 d at room temperature. The crude reaction mixture was dried under reduced pressure and purified *via* column chromatography employing Fluoro*Flash*® silica gel. The fluorous fraction was tested for purity *via* TLC and concentrated under reduced pressure. The remaining perfluorononanoic acid was

removed with a short silica gel filter column, eluting with *c*-hexane/ethyl acetate (3:1) to yield the Ugi product **26** as a yellow oil (190 mg, 247 µmol, 65.4%).

R_f = 0.30 in *c*-hexane/ethyl acetate (4:1). Visualized *via* fluorescent quench and Seebach staining solution.

IR (ATR): ν [cm^{-1}] = 3299.7 (br, ν(N-H)), 1680.0 (s, ν(C=O)), 1656.2 (s), 1606.8 (m), 1549.2 (m), 1510.5 (vs), 1462.2 (m), 1418.1 (m), 1300.9 (m), 1202.6 (vs), 1143.7 (vs), 1034.2 (s), 1004.1 (m), 945.7 (m), 828.0 (s), 781.1 (m), 719.5 (m), 657.6 (s), 632.1 (s), 526.1 (s), 441.3 (w).

^{1}H-NMR (400 MHz, $CDCl_3$): δ [ppm] = 7.59 – 7.29 (m, 4 H, CH_{Ar}[25,32,28,33]), 6.93 (d, J = 8.7 Hz, 2 H, CH_{Ar}[22,24 or 29,31]), 6.81 (d, J = 8.4 Hz, 2 H, CH_{Ar}[22,24 or 29,31]), 6.00 (s, 1 H, CH[2]), 4.45-4.32 (m, 2 H, CH_2[9]), 3.89 (s, 1 H, CH[20]), 3.83 (s, 3 H, CH_3[27 or 35]), 3.77 (s, 3 H, CH_3[27 or 3]).

^{13}C-NMR (101 MHz, $CDCl_3$): δ [ppm] = 171.35 (s, CONR[4]), 166.24 (s, CONR[18]), 160.77 (s, C_{Ar}[23 or 30]),156.94 (s, C_{Ar}[23 or 30]), 131.97 (s, CH_{Ar}[25,32 or 28,33]), 130.26 (s, C_{Ar}[8]), 123.88 (s, C_{Ar}[6]), 122.04 (s, CH_{Ar}[25,32 or 28,33]), 114.76 (s, CH_{Ar}[22,24 or 29,31]), 114.29 CH_{Ar}[22,24 or 29,31]), 64.04 (s, CH[2]), 55.59 (s, CH_3[27 or 3]), 55.49 (s, CH_3[27 or 3]), 36.02 (s, CH_2[9]).

^{19}F-NMR (376 MHz, $CDCl_3$): δ [ppm] = -85.13 (t, J = 9.9 Hz, 3 F, CF_3[10]), AB-signal (δ_A = -113.30, δ_B = -114.73, J_{AB} = 299.3 Hz, additional coupling not resolved, signals broadened, CF_2[17a]), AB-signal (δ_A = -115.21, δ_B = -116.14, J_{AB} = 293.6 Hz, additional coupling not resolved, signals broadened, CF_2[17b]), -124.78 (s, CF_2), -126.13 (s, CF_2), -127.07 (s, CF_2), -130.46 (s, CF_2[11]). Total integral of CF_2 region normalized with respect to the CF_3[10] group = 14.

FAB – MS [*m/z*] (relative intensity): 771.2 (33%) $[M + H]^+$, 770.1 (65%) $[M]^+$, 620.1 (65%) [Fragment A]$^+$, 271.1 (33%) [Fragment B + H]$^+$.

HRMS – FAB [*m/z*]: $[M]^+$ calculated for $^{12}C_{28}{}^1H_{19}{}^{16}O_4{}^{14}N_2{}^{19}F_{17}$, 770.1068; found, 770.1070; Δ = 0.22 mmu.

Chemical Formula: $C_{20}H_{11}F_{17}NO_2^{\bullet}$
Exact Mass: 620,05183
Fragment A

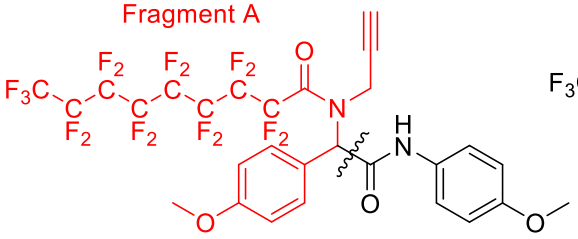

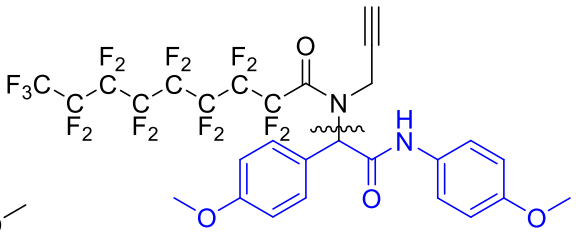

Chemical Formula: $C_{16}H_{16}NO_3^{\bullet}$
Exact Mass: 270,11302
Fragment B

6.2.1.1.9 *Ugi reaction of perfluorononanoic acid, p-anisaldehyde, 2,6-dimethylphenyl-isocyanide and propargylamine 27*

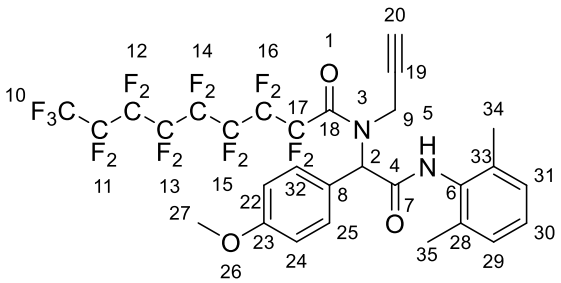

In a 25 mL round bottom flask *p*-anisaldehyde (77.9 µL, 87.3 mg, 641 µmol, 1.70 eq.) and propargylamine (41.1 µL, 35.3 mg, 641 µmol, 1.70 eq.) were added. The resulting mixture was stirred for 60 min over sodium sulfate. Perfluorononanoic acid (175 mg, 377 µmol, 1.00 eq.) dissolved in 0.5 mL methanol was added to the solution at room temperature and the resulting mixture was stirred for 2 min. Subsequently, 2,6-dimethylphenyl-isocyanide (84.1 mg, 641 µmol, 1.70 eq.) was added to the stirring mixture. The reaction was stirred for 3 d at room temperature. The crude reaction mixture was dried under reduced pressure and purified *via* column chromatography employing Fluoro*Flash*® silica gel. The fluorous fraction was tested for purity *via* TLC and concentrated under reduced pressure. The remaining perfluorononanoic acid was removed with a short silica gel filter column, eluting with *c*-hexane/ethyl acetate (3:1) to yield the Ugi product **27** as a yellow oil (114 mg, 149 µmol, 39.5%).

R_f = 0.30 in *c*-hexane/ethyl acetate (4:1). Visualized *via* fluorescent quench and Seebach staining solution.

IR (ATR): ν [cm^{-1}] = 3330.2 (m, ν(N-H)), 1694.4 (m), 1665.2 (s), 1609.3 (w), 1534.7 (m), 1513.8 (m), 1426.0 (w), 1362.7 (w), 1205.8 (w), 1178.3 (vs), 1144.8 (vs), 1109.7 (vs), 1072.8 (s), 1027.5 (m), 1003.6 (s), 937.2 (s), 920.3 (m), 831.6 (m), 802.9 (m), 771.0 (m), 765.8 (m), 703.0 (s), 663.7 (vs), 633.2 (s), 587.1 (m), 559.7 (m), 559.7 (s), 525.1 (s), 444.7 (w).

^{1}H-NMR (400 MHz, $CDCl_3$): δ [ppm] = 7.51 (d, J = 9.5 Hz, 2 H, CH_{Ar}[25,32]), 7.11 – 7.01 (m, 3 H, CH_{Ar}[29,30,31]), 6.97 (d, J = 8.7 Hz, 2 H, CH_{Ar}[22,24]), 5.99 (s, 1 H, CH[2]), 4.32 (s, 2 H, CH_2[9]), 3.85 (s, 3 H, CH_3[37]), 2.16 (s, 6 H, CH_3[34,35]).

^{13}C-NMR (101 MHz, $CDCl_3$): δ [ppm] = 166.72 (s, CONR[4]), 160.85 (s, C_{Ar}[23]), 135.64 (s, C_{Ar}[8 or 6]), 132.17 (s, CH_{Ar}[25,32]), 128.40 (s, C_{Ar}[8 or 6]), 127.76 (s, CH_{Ar}[29,30,31]), 114.70 (s, CH_{Ar}[22,24]), 55.52 (CH_3[27]), 35.96 (s, CH_2[9]), 18.55 (CH_3[34,35]).

^{19}F-NMR (376 MHz, $CDCl_3$): δ [ppm] = -85.10 (t, J = 9.9 Hz, 3 F, CF_3[10]), AB-signal (δ_A = -112.63, δ_B = -114.35, J_{AB} = 297.4 Hz, additional coupling not resolved, signals broadened, CF_2[17a]), AB-signal (δ_A = -115.23, δ_B = -116.38, J_{AB} = 293.6 Hz, additional coupling not resolved, signals broadened, CF_2[17b]), -124.82 (s, CF_2), -126.13 (s, CF_2), -127.06 (s, CF_2), -130.44 (s, CF_2[11]). Total integral of CF_2 region normalized with respect to the CF_3[10] group = 14.

FAB – MS [m/z] (relative intensity): 769.1 (60%) $[M + H]^+$, 620.1 (85%) [Fragment A]$^+$.

HRMS – FAB [m/z]: $[M]^+$ calculated for $^{12}C_{29}{}^{1}H_{22}{}^{16}O_3{}^{14}N_2{}^{19}F_{17}$, 769.1353; found, 769.1355; Δ = 0.18 mmu.

Chemical Formula: $C_{20}H_{11}F_{17}NO_2^{\bullet}$
Exact Mass: 620,05183
Fragment A

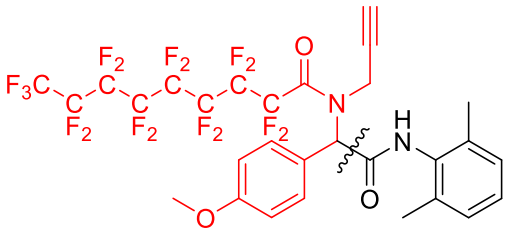

6.2.1.1.10 *Ugi reaction of perfluorononanoic acid, p-anisaldehyde, ethyl-2-isocyanoacetate and propargylamine 28*

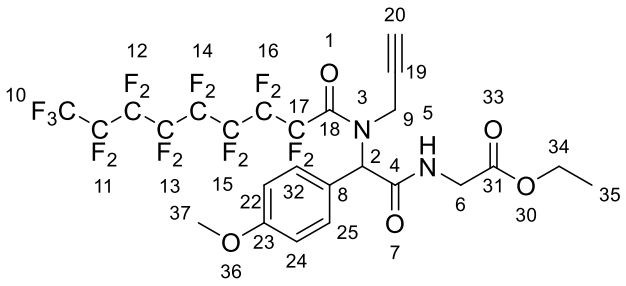

In a 25 mL round bottom flask *p*-anisaldehyde (77.9 µL, 87.3 mg, 641 µmol, 1.70 eq.) and propargylamine (41.1 µL, 35.3 mg, 641 µmol, 1.70 eq.) were added. The resulting mixture was stirred for 60 min over sodium sulfate. Perfluorononanoic acid (175 mg, 377 µmol, 1.00 eq.) dissolved in 0.5 mL methanol was added to the solution at room temperature and the resulting mixture was stirred for 2 min. Subsequently, ethyl-2-isocyanoacetate (82.6 µL, 72.5 mg, 641 µmol, 1.70 eq.) was added to the stirring mixture. The reaction was stirred for 3 d at room temperature. The crude reaction mixture was dried under reduced pressure and purified *via* column chromatography employing Fluoro*Flash*® silica gel. The fluorous fraction was tested for purity *via* TLC and concentrated under reduced pressure. The remaining perfluorononanoic acid was removed with a short silica gel filter column, eluting with *c*-hexane/ethyl acetate (3:1) to yield the Ugi product **28** as a yellow oil (65.8 mg, 87.8 µmol, 23.3%).

R_f = 0.30 in *c*-hexane/ethyl acetate (4:1). Visualized *via* fluorescent quench and Seebach staining solution.

IR (ATR): ν [cm^{-1}] = 3269.5 (m, ν(N-H)), 2924.6 (w, ν(C-H)), 1746.7 (s, ν(C=O)), 1691.8 (s), 1666.2 (s), 1613.2 (w), 1563.9 (m), 1514.8 (m), 1449.1 (m), 1412.8 (m), 1200.9 (vs), 1145.4 (vs), 1106.1 (s), 1036.6 (m), 1004.3 (m), 950.1 (m), 828.4 (m), 768.2 (m), 702.4 (s), 672.2 (s), 636.9 (s), 558.2 (s), 529.1 (s), 430.2 (w), 390.0 (w).

^{1}H-NMR (400 MHz, $CDCl_3$): δ [ppm] = 7.39 (d, J = 8.2 Hz, 2 H, $CH_{Ar}^{25,32}$), 6.93 (d, J = 8.7 Hz, 2 H, $CH_{Ar}^{22,24}$), 5.92 (s, 1 H, CH^{2}), 4.46 – 3.96 (m, 6 H, $CH_2^{34,6,9}$), 3.89 (s, 1 H, CH^{20}), 3.83 (s, 3 H, CH_3^{37}), 1.42 – 1.09 (m, 3 H, CH_3^{35}).

^{13}C-NMR (101 MHz, $CDCl_3$): δ [ppm] = 169.44 (s, CONR^{4}), 164.76 (s, CONR^{18}), 160.74 (s, C_{Ar}^{23}), 132.14 (s, CH_{Ar}^{25,32}), 129.61 (s, C_{Ar}^{8}), 114.69 (s, C_{Ar}^{22,24}), 61.83 (s, CH^{2}), 55.73 (s, CH^{20}), 55.50 (s, OCH_3^{37}), 41.77 (s, CH_2^{6}), 35.98 (s, CH_2^{9}), 14.23 (CH_3^{35}).

^{19}F-NMR (376 MHz, $CDCl_3$): δ [ppm] = -85.10 (t, J = 9.9 Hz, 3 F, CF_3^{10}), AB-signal (δ_A = -113.26, δ_B = -114.63, J_{AB} = 297.4 Hz, additional coupling not resolved, signals broadened, CF_2^{17a}), AB-signal (δ_A = -115.22, δ_B = -116.19, J_{AB} = 291.8 Hz, additional coupling not resolved, signals broadened, CF_2^{17b}), -124.84 (s, CF_2), -126.12 (s, CF_2), -127.05 (s, CF_2), -130.44 (s, CF_2^{11}). Total integral of CF_2 region normalized with respect to the CF_3^{10} group = 14.

FAB – MS [*m/z*] (relative intensity): 750.1 (90%) $[M]^+$, 620.1 (17%) [Fragment A]$^+$, 250.1 (33%) [Fragment B]$^+$, 120.1 [Fragment C]$^+$.

HRMS – FAB [*m/z*]: $[M]^+$ calculated for $^{12}C_{29}{}^{1}H_{19}{}^{16}O_5{}^{14}N_2{}^{19}F_{17}$, 750.1017; found, 750.1018; Δ = 0.13 mmu.

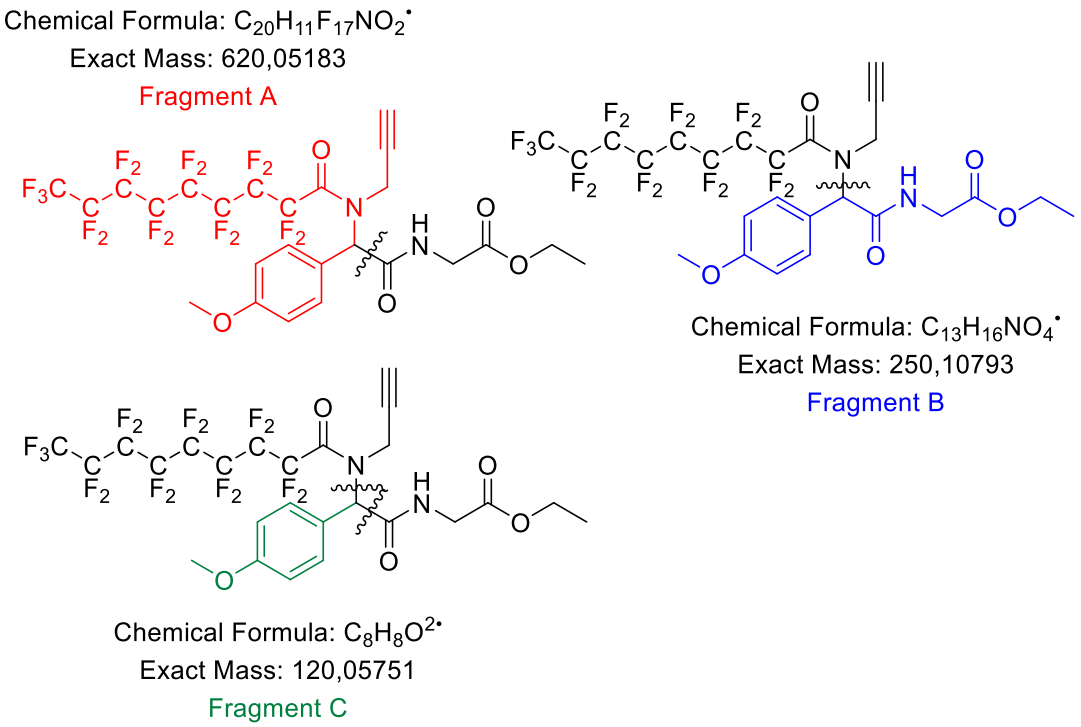

6.2.1.1.11 *Ugi reaction of perfluorononanoic acid, 4-hydroxybenzaldehyde, cyclohexylisocyanide and propargylamine 29*

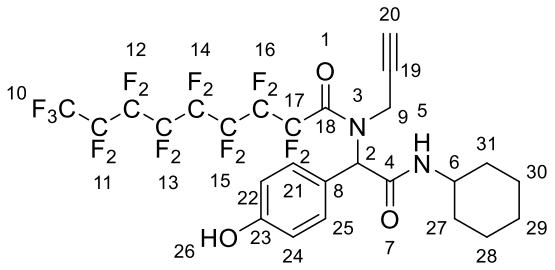

In a 25 mL round bottom flask 4-hydroxybenzaldehyd (59.6 mg, 489 µmol, 1.30 eq.) was dissolved in 1.5 mL methanol, subsequently propargylamine (31.4 µL, 27.0 mg, 490 µmol, 1.30 eq.) was added and the resulting mixture was stirred for 60 min over sodium sulfate. Afterwards, the mixture was filtrated. The solid was washed with 10 mL methanol three times. Subsequently, the filtrate was concentrated under reduced pressure. Perfluorononanoic acid (175 mg, 377 µmol, 1.00 eq.) dissolved in 1 mL methanol was added to the imine at room temperature and the resulting mixture was stirred for 2 min. Subsequently, cyclohexylisocyanide (56.3 µL, 49.4 mg, 453 µmol, 1.20 eq.) was added to the stirring mixture. The reaction was stirred for 1 d at room temperature. The crude reaction mixture was dried under reduced pressure and purified *via* column chromatography employing Fluoro*Flash*® silica gel. The fluorous fraction was tested for purity *via* TLC and concentrated under reduced pressure. The Ugi product **29** was obtained as a yellow oil (93.9 mg, 128 µmol, 34.1%).

R_f = 0.66 in *c*-hexane/ethyl acetate (6:1). Visualized *via* fluorescent quench and Seebach staining solution.

IR (ATR): ν [cm^{-1}] = 3301.6 (br, ν(N-H)), 3103.4 (br, ν(O-H)), 2928.2 (w, ν(C-H)), 2855.1 (w, ν(C-H)), 1650.1 (m, ν(C=O)), 1614.5 (w), 1598.5 (w), 1566.03 (m), 1514.2 (m), 1452.4 (w), 1425.6 (w), 1367.3 (w), 1347.2 (w), 1200.5 (s), 1149.3 (vs), 988.9 (w), 945.4 (m), 891.3 (w), 864.1 (w), 837.2 (w), 821.1 (w), 806.3 (w), 806.3 (w), 769.8 (w), 712.8 (m), 678.2 (m), 638.9 (s), 558.5 (m), 544.7 (m), 515.6 (s), 451.2 (w), 440.3 (w), 415.3 (w).

^{1}H-NMR (400 MHz, CD_3OD): δ [ppm] = 7.20 (dd, J = 25.7, 7.3 Hz, 2 H, CH_{Ar}*^{22,24}*), 6.86 (d, J = 7.3 Hz, 2 H, CH_{Ar}*^{21,25}*), 5.89 (d, J = 17.6 Hz, 1 H, CH*^{2}*), 4.41 – 3.93 (m, 2 H, CH_2*^{9}*), 3.77 – 3.57 (m, 1 H, CH*^{6}*), 1.97 – 1.06 (m, 11 H, CH*^{20}* + CH_2).

^{13}C-NMR (126 MHz, CD_3OD): δ [ppm] = 170.13 (s, CONR^{4}), 159.80 (s, CONR^{18}), 141.03 (s, C$_{Ar}$^{23}), 133.21 (s, CH$_{Ar}$$^{22, 24}$), 125.03 (s, C$_{Ar}$^{8}), 116.69 (s, CH$_{Ar}$$^{21, 25}$), 73.04 (s, C^{19}), 64.48 (s, CH^{2}), 48.79 (s, CH^{6}), 36.94 (s, CH$_2$^{9}), 33.48 (s, CH_2), 26.58 (s, 2 CH_2), 26.01 (s, 2 CH_2), 24.39 (s, CH^{20}).

^{19}F-NMR (376 MHz, CD_3OD): δ [ppm] = -86.69 (t, J = 10.3 Hz, 3 F, CF_3^{10}), AB-signal (δ_A = -114.86, δ_B = -116.45, J_{AB} = 286.1 Hz, A and B are split into t, CF_2^{17a}, additional coupling not resolved, signals broadened), AB-signal (δ_A = -116.24, δ_B = -117.50, J_{AB} = 293.6 Hz, A and B are split into t, CF_2^{17b}, additional coupling not resolved, signals broadened), - 125.00 (s, CF_2), -125.59 (m, CF_2), -127.10 (s, CF_2), -128.07 (s, CF_2), -131.60 (s, CF_2^{11}). Total integral of CF_2 region normalized with respect to the CF_3^{10} group = 14.

FAB – MS [*m/z*] (relative intensity): 733.2 (65%) $[M + H]^+$, 606.0 (75%) [Fragment A]$^+$, 568.0 (22%) [Fragment A + H – C_3H_3]$^+$, 232.1 (83%) [Fragment B]$^+$.

HRMS – FAB [*m/z*]: $[M + H]^+$ calculated for $^{12}C_{26}{}^{1}H_{22}{}^{16}O_3{}^{14}N_2{}^{19}F_{17}$, 733.1353; found, 733.1352; Δ = 0.14 mmu.

Chemical Formula: $C_{19}H_9F_{17}NO_2^{\bullet}$
Exact Mass: 606,03618

Fragment A

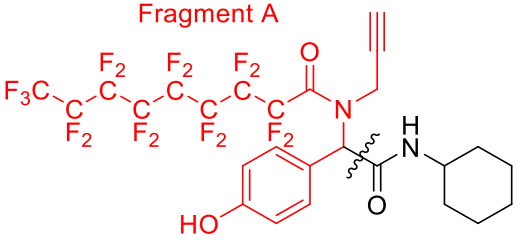

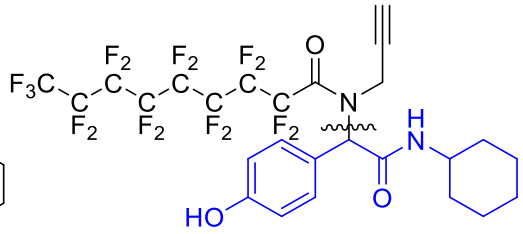

Chemical Formula: $C_{14}H_{18}NO_2^{\bullet}$
Exact Mass: 232,13375

Fragment B

6.2.1.1.12 *Ugi reaction of perfluorononanoic acid, benzaldehyde, cyclohexylisocyanide and propargylamine 30*

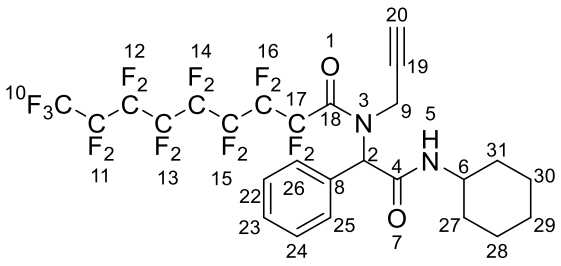

In a 25 mL round bottom flask benzaldehyde (65.4 µL, 68.0 mg, 641 µmol, 1.70 eq.) and propargylamine (41.4 µL, 35.3 mg, 641 µmol, 1.70 eq.) were added. The resulting mixture was stirred for 60 min over sodium sulfate. Perfluorononanoic acid (175 mg, 377 µmol, 1.00 eq.) dissolved in 0.5 mL methanol was added to the solution at room temperature and the resulting mixture was stirred for 2 min. Subsequently, cyclohexylisocyanide (79.7 µL, 70.0 mg, 641 µmol, 1.70 eq.) was added to the stirring mixture. The reaction was stirred for 3 d at room temperature. The crude reaction mixture was dried under reduced pressure and purified *via* column chromatography employing Fluoro*Flash*® silica gel. The fluorous fraction was tested for purity *via* TLC and concentrated under reduced pressure. The remaining perfluorononanoic acid was removed with a short silica gel filter column, eluting with *c*-hexane/ethyl acetate (3:1) to yield the Ugi product **30** as a yellow oil (41.3 mg, 57.8 µmol, 15.3%).

R_f = 0.43 in *c*-hexane/ethyl acetate (6:1). Visualized *via* fluorescent quench and Seebach staining solution.

IR (ATR): ν [cm^{-1}] = 3292.6 (m, ν(N-H)), 2937.3 (m, ν(C-H)), 2857.2 (w, ν(C-H)), 1681.4 (s, ν(C=O)), 1645.5 (m, ν(N-H)), 1549.9 (m), 1494.1 (w), 1456.2 (m), 1421.6 (m), 1365.9 (m), 1329.4 (m), 1202.6 (vs), 1147.9 (vs), 1081.6 (m), 1029.4 (s), 1002.3 (m), 940.7 (m), 926.3 (m), 895.4 (w), 870.3 (w), 805.7 (m), 789.9 (m), 769.1 (s), 744.5 (s), 699.2 (vs), 669.8 (s), 633.2 (s), 559.7 (s), 520.3 (vs), 464.3 (w).

^{1}H-NMR (500 MHz, CD_3OD): δ [ppm] = 7.40 (s, 5 H, CH_{Ar}*22-26*), 5.99 (s, 1 H, CH*2*), 4.52 – 4.20 (m, 2 H, CH_2*9*), 4.09 – 3.85 (m, 1 H, CH*6*), 3.77 – 3.53 (m, 1 H, CH*20*), 1.92 – 1.54 (m, 4 H, CH_2), 1.40 – 1.06 (m, 6 H, CH_2).

^{13}C-NMR (126 MHz, CD_3OD): δ [ppm] = 169.61 (s, CONR*4*), 157.51 (s, CONR*18*), 131.73 (s, C_{Ar}*8*), 130.71 (s, CH_{Ar}), 130.32 (s, CH_{Ar}), 129.96 (s, CH_{Ar}), 64.15 (s, CH*2*),

53.36 (s, CH^{6}), 50.04 (s, CH^{20}), 36.64 (s, CH_2^{9}), 33.51 (s, CH_2), 33.43 (s, CH_2), 26.99 (s, CH_2), 26.57 (s, CH_2), 25.99 (s, CH_2).

^{19}F-NMR (376 MHz, CD_3OD): δ [ppm] = -88.26 (t, J = 10.2 Hz, 3 F, CF_3^{10}), AB-signal (δ_A = -116.51, δ_B = -117.81, J_{AB} = 301.2 Hz, A and B are split into t, CF_2^{17a}, additional coupling not resolved, signals broadened), AB-signal (δ_A = -117.81, δ_B = -119.02, J_{AB} = 295.5 Hz, A and B are split into t, CF_2^{17b}, additional coupling not resolved, signals broadened), -126.28 – -127.72 (m, CF_2), -128.68 (s, CF_2), -129.64 (s, CF_2), -133.18 (s, CF_2^{11}). Total integral of CF_2 region normalized with respect to the CF_3^{10} group = 14.

FAB – MS [*m/z*] (relative intensity): 717.2 (87%) $[M + H]^+$, 591.0 (17%) [Fragment A + H]$^+$, 590.0 (60%) [Fragment A]$^+$, 552.0 (15%) [Fragment A + H – C_3H_3]$^+$, 217.1 (23%) [Fragment B + H]$^+$.

HRMS – FAB [*m/z*]: $[M + H]^+$ calculated for $^{12}C_{26}{}^{1}H_{22}{}^{16}O_2{}^{14}N_2{}^{19}F_{17}$, 717.1403; found, 717.1404; Δ = 0.11 mmu.

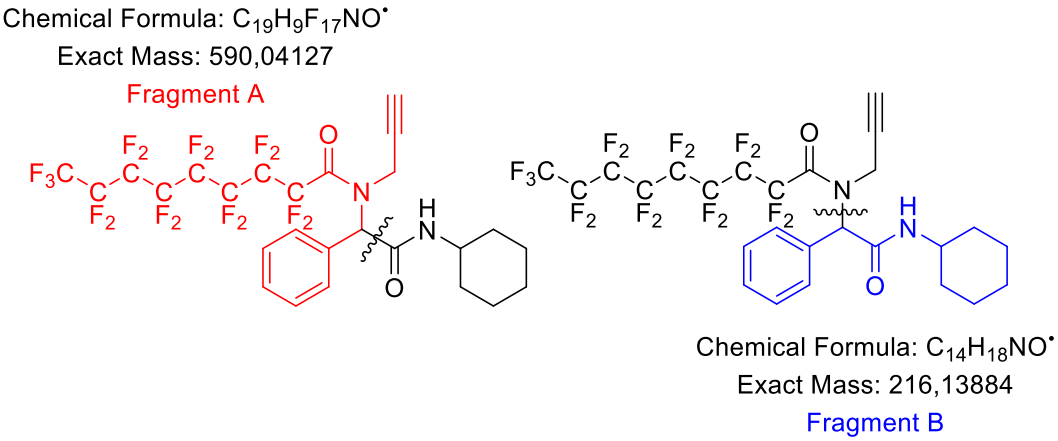

6.2.1.1.13 *Ugi reaction of perfluorononanoic acid, isobutyraldehyde, cyclohexylisocyanide and pentylamine 31*

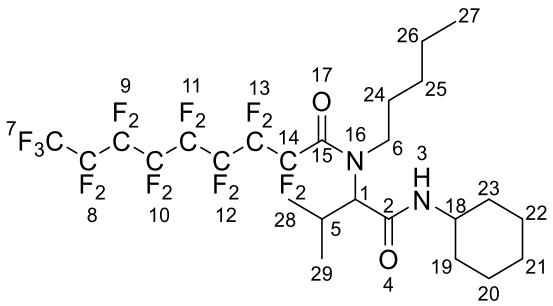

In a 25 mL round bottom flask isobutyraldehyde (83.6 µL, 66.0 mg, 916 µmol, 1.70 eq.) and pentylamine (106 µL, 79.8 mg, 916 µmol, 1.70 eq.) were added and the resulting mixture was stirred for 60 min over sodium sulfate. Perfluorononanoic acid (250 mg, 539 µmol, 1.00 eq.) dissolved in 0.5 mL methanol was added to the imine at room temperature and the resulting mixture was stirred for 2 min. Subsequently, cyclohexylisocyanide (114 µL, 100 mg, 916 µmol, 1.70 eq.) was added to the stirring mixture. The reaction was stirred for 3 d at room temperature. The crude reaction mixture was dried under reduced pressure. The residue was adsorbed onto celite® and purified *via* column chromatography employing silica gel as stationary phase and eluting with a gradual solvent mixture of ethyl acetate and *c*-hexane (1:10 → 1:3) to yield the Ugi product **31** as a yellow oil (95.1 mg, 133 mmol, 24.7%).

R_f = 0.54 in *c*-hexane/ethyl acetate (6:1). Visualized *via* permanganate staining solution.

IR (ATR): ν [cm^{-1}] = 3303.7 (br, ν(N-H)), 2927.3 (s, ν(C-H)), 2855.9 (m), 1764.4 (w), 1707.2 (s, ν(C=O)), 1673.4 (m), 1626.5 (s), 1538.8 (m), 1451.3 (m), 1429.5 (s), 1378.9 (m), 1239.5 (vs), 1211.9 (vs), 1146.6 (s), 1088.2 (m), 891.7 (w), 726.2 (w), 626.7 (m), 557.7 (w), 529.1 (w), 481.3 (w), 402.1 (w).

^{1}H-NMR (400 MHz, CD_3OD): δ [ppm] = 3.71 – 3.30 (m, 2 H, CH^{1} + CH^{18}), 3.27 – 3.21 (m, 2 H, CH_2^{6}), 2.88 – 2.79 (m, 2 H, CH_2), 2.00 – 1.70 (m, 3 H, CH^{5} + CH_2), 1.67 – 1.53 (m, 2 H, CH_2), 1.50 – 1.16 (m, 12 H, CH_2), 1.06 (d, J = 6.8 Hz, 3 H, $CH_3^{28, 29}$), 0.97 – 0.77 (m, 6 H, $CH_3^{28, 29}$ + CH_3^{27}).

^{13}C-NMR (101 MHz, CD_3OD): δ [ppm] = 166.95 (s, $CONR^{2}$), 162.79 (s, $CONR^{15}$), 51.75 (s, CH^{1}), 50.15 (s, CH^{18}), 42.48 (s, CH_2^{6}), 40.70 (s, CH_2), 33.08 (s, CH^{5}), 32.50 (s,

CH_2), 30.86 (s, CH_2), 30.50 (s, CH_2), 30.10 (s, CH_2), 29.57 (s, CH_2), 28.78 (s, CH_2), 25.47 (s, CH_2), 25.42 (s, CH_2), 19.97 (s, CH_3*28, 29*), 19.94 (s, CH_3*28, 29*), 14.28 (s, CH_3*27*).

^{19}F-NMR (376 MHz, CD_3OD): δ [ppm] = -86.72 (t, *J* = 10.3 Hz, 3F, CF_3*7*), -122.25 (t, *J* = 12.5 Hz, CF_2*14*), -126.96 (s, CF_2), -127.28 (s, CF_2), -127.92 (s, CF_2), -128.12 (s, CF_2), -131.66 (s, CF_2*8*). Total integral of CF_2 region normalized with respect to the CF_3*7* group = 14.

ESI-MS [*m/z*]: $[M + Na]^+$ calculated for $^{12}C_{25}{}^{1}H_{31}{}^{16}O_2{}^{14}N_2{}^{19}F_{17}{}^{23}Na_1$, 737.2011; found, 737.2006, Δ = 0.42 mmu.

6.2.1.1.14 *Ugi reaction of perfluorononanoic acid, valeraldehyde, cyclohexylisocyanide and pentylamine 32*

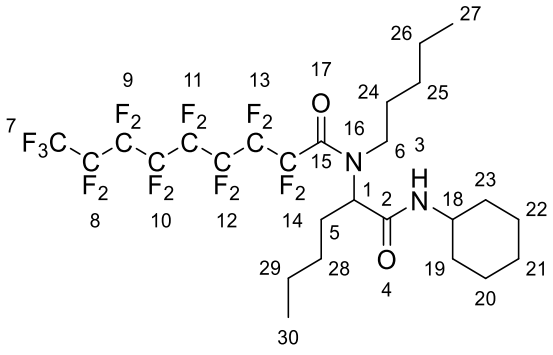

In a 25 mL round bottom flask valeraldehyde (52.1 µL, 42.2 mg, 490 µmol, 1.30 eq.) was dissolved in 1.5 mL methanol, subsequently pentylamine (56.6 µL, 42.7 mg, 490 µmol, 1.30 eq.) was added and the resulting mixture was stirred for 60 min over sodium sulfate. Afterwards, the mixture was filtrated and the solid was washed with 10 mL methanol three times. Subsequently, the filtrate was concentrated under reduced pressure. Perfluorononanoic acid (175 mg, 377 µmol, 1.00 eq.) dissolved in 1 mL methanol was added to the imine at room temperature and the resulting mixture was stirred for 2 min. Subsequently, cyclohexylisocyanide (56.3 µL, 59.4 mg, 453 µmol, 1.20 eq.) was added to the stirring mixture. The reaction was stirred for 4 d at room temperature. The crude reaction mixture was dried under reduced pressure and purified *via* column chromatography employing Fluoro*Flash*® silica gel. The fluorous fraction was tested for purity *via* TLC and concentrated under reduced pressure. The remaining perfluoro acid was removed with a short silica gel filter column, eluting with

c-hexane/ethyl acetate (3:1) to yield the Ugi product **32** as a colorless solid (86.0 mg, 118 µmol, 31.4%).

R_f = 0.40 in *c*-hexane/ethyl acetate (6:1). Visualized *via* Seebach staining solution.

IR (ATR): ν [cm^{-1}] = 3325.5 (br, ν(N-H)), 2933.4 (m, ν(C-H)), 2859.3 (m, ν(C-H)), 1651.9 (s, ν(C=O)), 1534.7 (m), 1452.3 (m), 1367.9 (w), 1237.4 (vs), 1203.2 (vs), 1146.7 (vs), 1054.4 (w), 965.9 (w), 890.9 (w), 777.3 (m), 735.3 (m), 703.5 (m), 656.3 (m), 557.8 (m), 528.9 (m).

^{1}H-NMR (400 MHz, CD_3OD): δ [ppm] = 4.59 (t, J = 7.6 Hz, CH*[1a]*), 4.50 (t, J = 7.2 Hz, total integral of CH*[1]* = 1 H, CH*[1b]*), 3.69 – 3.43 (m, 3 H, CH_2*[6 or 5]* + CH*[18]*), 2.03 – 1.60 (m, 10 H, CH_2), 1.43 – 1.15 (m, 12 H, CH_2), 0.92 (t, J = 7.2 Hz, 6 H, CH_3*[27,30]*).

^{13}C-NMR (101 MHz, CD_3OD): δ [ppm] = 170.35 (s, CONR*[2]*), 159.72 (s, CONR*[15]*), 62.03 (s, CH*[1a]*), 61.39 (s, CH*[1b]*), 50.06 (s, CH*[18]*), 47.19 (s, CH_2*[6 or 5]*), 33.55 (s, CH_2), 33.38 (s, CH_2), 31.97 (s, CH_2), 31.41 (s, CH_2), 30.42 (s, CH_2), 30.01 (s, CH_2), 29.62 (s, CH_2), 29.50 (s, CH_2), 28.38 (s, CH_2), 26.58 (s, CH_2), 26.04 (s, CH_2), 23.46 (s, CH_2), 23.26 (s, CH_2), 14.30 (s, CH_3*[27 or 30]*), 14.23 (s, CH_3*[27 or 30]*).

^{19}F-NMR (376 MHz, CD_3OD): δ [ppm] = -88.27 (t, J = 10.4 Hz, 3 F, CF_3*[7]*), AB-signal (δ_A = -116.17, δ_B = -116.99, J_{AB} = 301.2 Hz, A and B are split into t, J = 12.4 Hz, CF_2*[14a]*), AB-signal (δ_A = -118.12, δ_B = -118.63, J_{AB} = 293.6 Hz, A and B are split into t, J = 12.3 Hz CF_2*[14b]*), -126.20 (s, CF_2), -126.78 (s, CF_2), -127.15 (s, CF_2), -128.74 (s, CF_2), -129.66 (s, CF_2), -133.17 (s, CF_2*[8]*). Total integral of CF_2 region normalized with respect to the CF_3*[7]* group = 14.

FAB – MS [*m/z*] (relative intensity): 729.3 (55%) $[M + H]^+$, 631.2 (10%) [Fragment A]$^+$, 630.2 (28%) [Fragment A – H]$^+$, 281.3 (7%) [Fragment B]$^+$, 197.2 (16%) [Fragment C + H]$^+$.

HRMS – FAB [*m/z*]: $[M + H]^+$ calculated for $^{12}C_{26}{}^{1}H_{34}{}^{16}O_2{}^{14}N_2{}^{19}F_{17}$, 729.2343; found, 729.2342; Δ = 0.16 mmu.

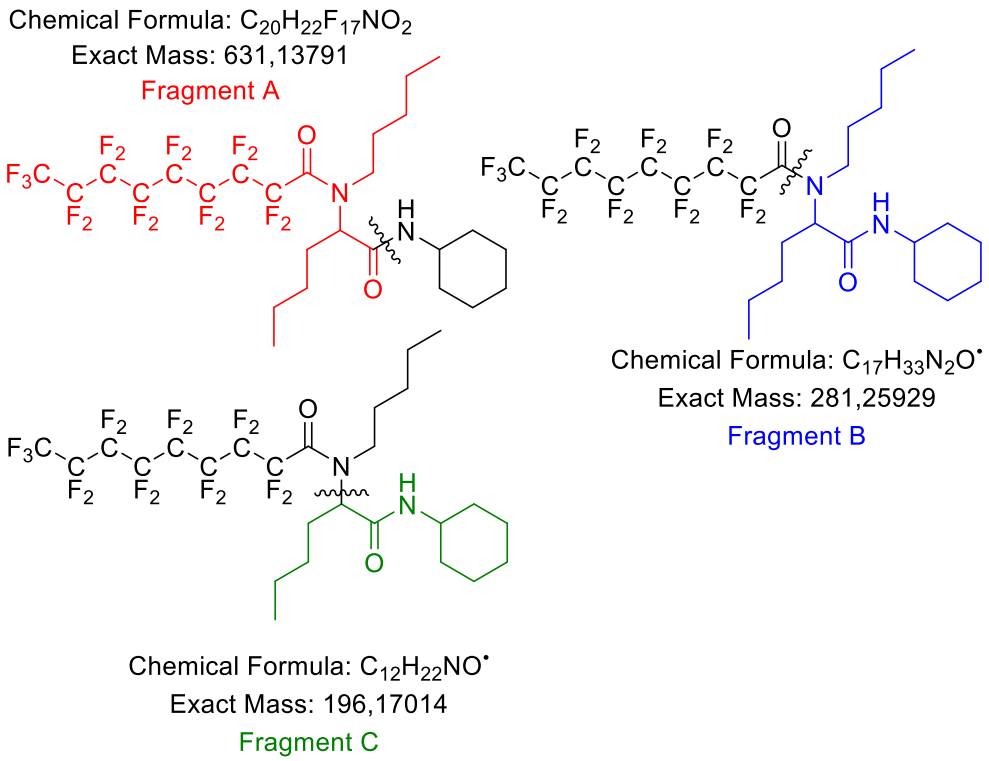

6.2.1.1.15 *Ugi reaction of perfluorononanoic acid, cyclohexancarboxaldehyde, cyclohexylisocyanide and pentylamine 33*

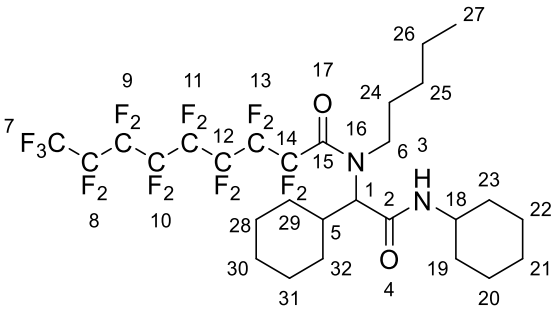

In a 25 mL round bottom flask cyclohexancarboxaldehyde (59.4 µL, 55.0 mg, 490 µmol, 1.30 eq.) was dissolved in 1.5 mL methanol, subsequently pentylamine (56.6 µL, 42.7 mg, 490 µmol, 1.30 eq.) was added and the resulting mixture was stirred for 60 min over sodium sulfate. Afterwards, the mixture was filtrated and the solid was washed with 10 mL methanol three times. Subsequently, the filtrate was concentrated under reduced pressure. Perfluorononanoic acid (175 mg, 377 µmol, 1.00 eq.) dissolved in 1 mL methanol was added to the imine at room temperature and the resulting mixture was stirred for 2 min. Subsequently, cyclohexylisocyanide (56.3 µL, 59.4 mg, 453 µmol, 1.20 eq.) was added to the stirring mixture. The reaction was stirred for 4 d at room temperature. The crude reaction mixture was dried under reduced

pressure and purified *via* column chromatography employing Fluoro*Flash*® silica gel. The fluorous fraction was tested for purity *via* TLC and concentrated under reduced pressure. The remaining perfluoro acid was removed with a short silica gel filter column, eluting with *c*-hexane/ethyl acetate (3:1) to yield the Ugi product **33** as a colorless solid (103 mg, 137 µmol, 36.3%).

R_f = 0.45 in *c*-hexane/ethyl acetate (6:1). Visualized *via* Seebach staining solution and permanganate staining.

IR (ATR): ν [cm^{-1}] = 3317.7 (br, ν(N-H)), 2930.9 (s, ν(C-H)), 2856.6 (m, ν(C-H)), 1653.4 (s, ν(C=O)), 1536.7 (m), 1451.4 (m), 1351.0 (m), 1237.9 (vs), 1203.5 (vs), 1147.1 (vs), 1117.8 (s), 1053.5 (m), 962.2 (m), 891.1 (w), 777.5 (m), 735.4 (m), 703.4 (m), 656.3 (m), 557.6 (m), 528.6 (m).

^{1}H-NMR (400 MHz, CD_3OD): δ [ppm] = 4.47 (d, J = 11.0 Hz, CH*1a*), 4.19 – 3.90 (m, total integral of CH*1* = 1 H, CH*1b*), 3.71 – 3.35 (m, 3 H, CH_2 + CH*18*), 2.24 – 1.95 (m, 1 H, CH*5*), 1.96 – 1.46 (m, 12 H, CH_2), 1.41 – 1.01 (m, 14 H, CH_2), 0.92 (t, J = 7.1 Hz, 3 H, CH_3*27*).

^{13}C-NMR (101 MHz, CD_3OD): δ [ppm] = 169.95 (s, CONR*2*), 160.29 (s, CONR*15*), 66.46 (s, CH*1a*), 65.68 (s, CH*1b*), 49.88 (s, CH*18*), 46.34 (s, CH_2), 39.02 (s, CH*5a*), 37.55 (s, CH*5b*), 33.51 (s, CH_2), 33.31 (s, CH_2), 31.42 (s, CH_2), 31.14 (s, CH_2), 30.75 (s, CH_2), 30.05 (s, CH_2), 27.28 (s, CH_2), 26.58 (s, CH_2), 25.93 (s, CH_2), 23.24 (s, CH_2), 14.22 (s, CH_3*27*).

^{19}F-NMR (376 MHz, CD_3OD): δ [ppm] = -88.27 (t, J = 10.5 Hz, 3 F, CF_3*7*), -115.58 (t, J = 10.8 Hz, CF_2*14a*), AB-signal (δ_A = -117.67, δ_B = -118.82, J_{AB} = 293.6 Hz, A and B are split into t, J = 12.0 Hz, CF_2*14b*), -125.59 (s, CF_2), -126.65 (s, CF_2), -126.92 (s, CF_2), -128.72 (s, CF_2), -129.66 (s, CF_2), -133.20 (s, CF_2*8*). Total integral of CF_2 region normalized with respect to the CF_3*7* group = 14.

FAB – MS [*m/z*] (relative intensity): 755.3 (67%) $[M + H]^+$, 629.2 (27%) [Fragment A + H]$^+$, 307.3 (8%) [Fragment B]$^+$, 223.2 (23%) [Fragment C + H]$^+$.

HRMS – FAB [*m/z*]: $[M + H]^+$ calculated for $^{12}C_{28}{}^{1}H_{36}{}^{16}O_2{}^{14}N_2{}^{19}F_{17}$, 755.2501; found, 755.2500; Δ = 0.14 mmu.

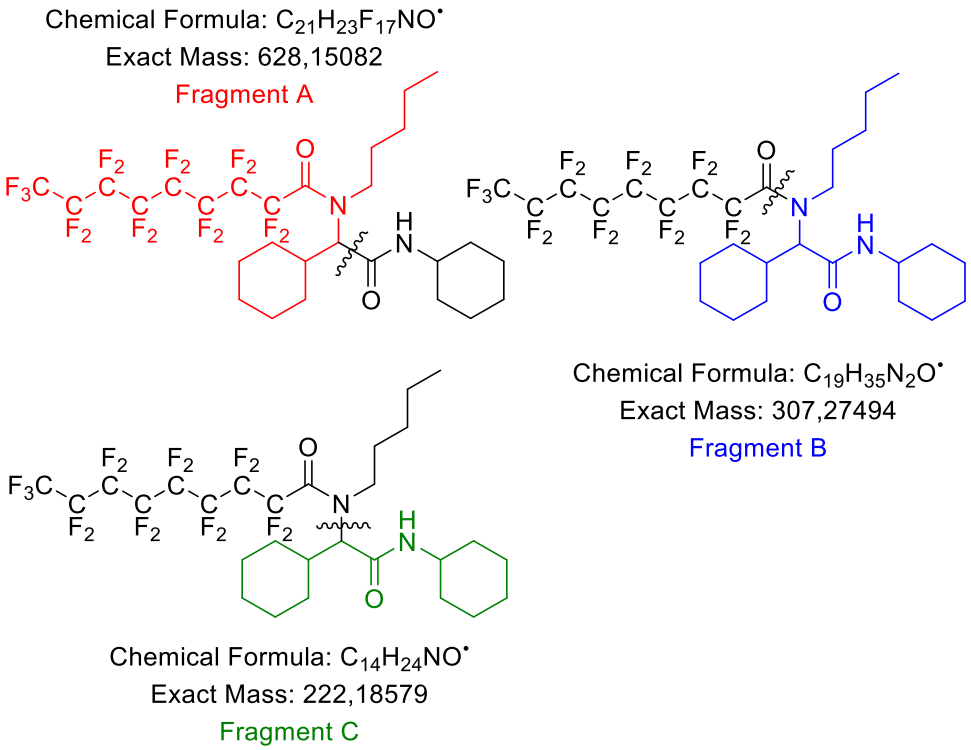

6.2.1.1.16 *Ugi reaction of perfluorononanoic acid, valeraldehyde, tert-butylisocyanide and pentylamine 34*

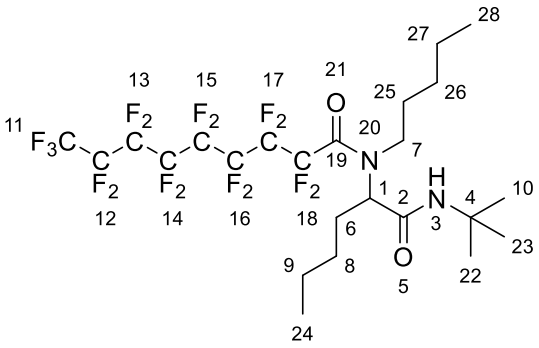

In a 25 mL round bottom flask valeraldehyde (42.2 mg, 490 µmol, 1.30 eq.) was dissolved in 1.5 mL methanol, subsequently pentylamine (56.6 µL, 42.7 mg, 490 µmol, 1.30 eq.) was added and the resulting mixture was stirred for 60 min over sodium sulfate. Afterwards, the mixture was filtrated. The solid was washed with 10 mL methanol three times. Subsequently, the filtrate was concentrated under reduced pressure. Perfluorononanoic acid (175 mg, 377 µmol, 1.00 eq.) dissolved in 1 mL methanol was added to the imine at room temperature and the resulting mixture was stirred for 2 min. Subsequently, *tert*-butylisocyanide (51.2 µL, 37.6 mg, 453 µmol, 1.20 eq.) was added to the stirring mixture. The reaction was stirred for 3 d at room

temperature. The crude reaction mixture was dried under reduced pressure and purified *via* column chromatography employing Fluoro*Flash*® silica gel. The fluorous fraction was concentrated and the residue was adsorbed onto celite® and purified *via* column chromatography employing silica gel as stationary phase and eluting with a gradual solvent mixture of ethyl acetate and *c*-hexane (0:1 → 1:1) to yield the Ugi product **34** as a highly viscous yellow oil (42.7 mg, 60.3 µmol, 16.0%).

R_f = 0.49 in *c*-hexane/ethyl acetate (6:1). Visualized *via* Seebach staining solution and permanganate staining.

IR (ATR): ν [cm^{-1}] = 3367.2 (br, ν(N-H)), 2962.9 (m, ν(C-H)), 2875.3 (w), 1661.9 (s, ν(C=O)), 1532.8 (m), 1456.6 (m), 1366.2 (m), 1204.6 (vs), 1147.5 (vs), 996.7 (w), 778.1 (m), 735.4 (m), 703.2 (m), 656.5 (m), 558.6 (m), 528.9 (m).

^{1}H-NMR (400 MHz, CD_3OD): δ [ppm] = 7.43 (s, 1 H, NH*3*), 4.57 (t, *J* = 7.6 Hz, 1 H, CH*1*), 3.58 – 3.37 (m, 2 H, CH_2*7*), 2.04 – 1.85 (m, 2 H, CH_2*6*), 1.79 – 1.57 (m, 2 H, CH_2*25*), 1.40 – 1.19 (m, 17 H, CH_3*10,22,23* + CH_2), 0.92 (t, *J* = 7.2 Hz, 6 H, CH_3*24,28*).

^{13}C-NMR (101 MHz, CD_3OD): δ [ppm] = 170.58 (s, CONR*2*), 159.73 (s, CONR*19*), 62.36 (s, CH*1*), 52.39 (s, C*4*), 47.12 (s, CH_2*7*), 32.09 (s, CH_2*25*), 31.48 (s, CH_2), 30.42 (s, CH_2), 30.00 (s, CH_2), 29.67 (s, CH_2*6*), 29.44 (s, CH_2), 28.69 (s, CH_3*22,23,10*), 23.24 (s, CH_2), 14.30 (s, CH_3*24 or 28*), 14.23 (s, CH_3*24 or 28*).

^{19}F-NMR (376 MHz, CD_3OD): δ [ppm] = -88.27 (t, *J* = 10.3 Hz, 3 F, CF_3*11*), AB-signal (δ_A = -116.39, δ_B = -117.10, J_{AB} = 288.0 Hz, A and B are split into t, *J* = 11.7 Hz, CF_2*18a*), AB-signal (δ_A = -118.10, δ_B = -118.55, J_{AB} = 291.8 Hz, A and B are split into t, *J* = 12.5 Hz, CF_2*18b*), -126.95 (s, CF_2), -128.68 (s, CF_2), -129.65 (s, CF_2), -133.16 (s, CF_2*12*). Total integral of CF_2 region normalized with respect to the CF_3*11* group = 14.

FAB – MS [*m/z*] (relative intensity): 703.2 (65%) $[M + H]^+$, 630.1 (25%) [Fragment A – H]$^+$, 560.5 (28%) [Fragment A – C_5H_{11}]$^+$.

HRMS – FAB [*m/z*]: $[M + H]^+$ calculated for $^{12}C_{24}{}^{1}H_{31}{}^{16}O_2{}^{14}N_2{}^{19}F_{17}$, 703.2187; found, 703.2188; Δ = 0.13 mmu.

Chemical Formula: $C_{20}H_{22}F_{17}NO_2$
Exact Mass: 631,13791
Fragment A

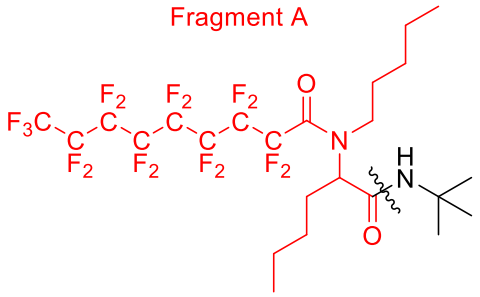

6.2.1.1.17 *Ugi reaction of perfluorononanoic acid, benzaldehyde, cyclohexylisocyanide and pentylamine 35*

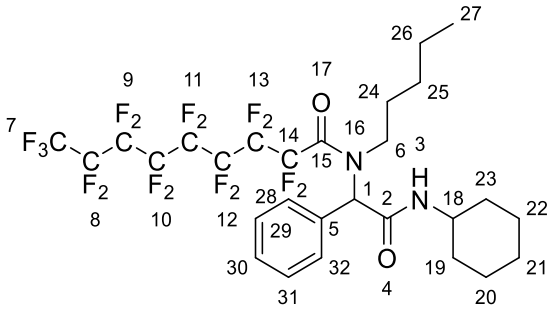

In a 25 mL round bottom flask benzaldehyde (56.3 µL, 49.4 mg, 453 µmol, 1.20 eq.) was dissolved in 1.5 mL methanol, subsequently pentylamine (56.6 µL, 42.7 mg, 490 µmol, 1.30 eq.) was added and the resulting mixture was stirred for 60 min over sodium sulfate. Afterwards, the mixture was filtrated and the solid was washed with 10 mL methanol three times. Subsequently, the filtrate was concentrated under reduced pressure. Perfluorononanoic acid (175 mg, 377 µmol, 1.00 eq.) dissolved in 1 mL methanol was added to the imine at room temperature and the resulting mixture was stirred for 2 min. Subsequently, cyclohexylisocyanide (56.3 µL, 59.4 mg, 453 µmol, 1.20 eq.) was added to the stirring mixture. The reaction was stirred for 4 d at room temperature. The crude reaction mixture was dried under reduced pressure and purified *via* column chromatography employing Fluoro*Flash*® silica gel. The fluorous fraction was tested for purity *via* TLC and concentrated under reduced pressure. The remaining perfluoro acid was removed with a short silica gel filter column, eluting with *c*-hexane/ethyl acetate (3:1) to yield the Ugi product **35** as a colorless solid (106 mg, 140 µmol, 42.3%).

R_f = 0.47 in *c*-hexane/ethyl acetate (6:1). Visualized *via* fluorescent quench and Seebach staining solution.

IR (ATR): ν [cm^{-1}] = 3306.5 (br, ν(N-H)), 2922.9 (m, ν(C-H)), 2851.1 (w), 2186.6 (vw), 2044.9 (vw), 1971.1 (vw), 1672.8 (s, ν(C=O)), 1654.2 (s, ν(C=O)), 1556.4 (m), 1451.0 (w), 1428.8 (m), 1369.9 (m), 1234.2 (s), 1193.9 (s), 1145.5 (s), 1119.6 (s), 1062.2 (m), 975.9 (m), 923.8 (m), 859.2 (w), 762.6 (w), 709.5 (s), 683.4 (m), 666.9 (m), 643.2 (m), 559.2 (m), 516.4 (m), 463.7 (w), 437.2 (w).

^{1}H-NMR (400 MHz, CD_3OD): δ [ppm] = 7.54 – 7.22 (m, 5 H, CH_{Ar}[28-32]), 5.87 (d, J = 29.9 Hz, 1 H, CH[1]), 3.84 – 3.52 (m, 1 H, CH_2[6a]), 3.41 – 3.35 (m, 1 H, CH[18]), 3.24 – 3.13 (m, 1 H, CH_2[6b]), 1.90 – 1.52 (m, 6 H, CH_2), 1.44 – 1.24 (m, 4 H, CH_2), 1.21 – 1.04 (m, 4 H, CH_2), 1.04 – 0.68 (m, 2 H, CH_2[26]), 0.66 – 0.53 (m, 3 H, CH_3[27]).

^{13}C-NMR (101 MHz, CD_3OD): δ [ppm] = 169.93 (s, CONR[2]), 158.75 (s, CONR[15]), 135.72 (s, C_{Ar}[5]), 131.66 (s, CH_{Ar}), 130.87 (s, CH_{Ar}), 130.05 (s, CH_{Ar}), 65.47 (s, CH[1a]), 64.05 (s, CH[1b]), 50.03 (s, CH[18]), 47.29 (s, CH_2[6]), 33.45 (s, CH_2), 30.34 (s, CH_2), 26.58 (s, CH_2), 26.01 (s, CH_2), 20.99 (s, CH_2), 20.74 (s, CH_2[26]), 13.73 (s, CH_3[27]).

^{19}F-NMR (376 MHz, CD_3OD): δ [ppm] = -88.27 (t, J = 9.4 Hz, 3 F, CF_3[7]), AB-signal (δ_A = -116.01, δ_B = -117.30, J_{AB} = 299.3 Hz, A and B are split into t, J = 12.8 Hz, CF_2[14a]), AB-signal (δ_A = -117.97, δ_B = -119.28, J_{AB} = 291.8 Hz, A and B are split into t, J = 11.3 Hz, CF_2[14b]), -126.38 (s, CF_2), -127.08 (s, CF_2), -128.67 (s, CF_2), -129.65 (s, CF_2), -133.20 (s, CF_2[8]). Total integral of CF_2 region normalized with respect to the CF_3[7] group = 14.

FAB – MS [*m/z*] (relative intensity): 749.2 $[M + H]^+$ (80%), 552.0 (92%) [Fragment A + H]$^+$, 217.1 (68%) [Fragment B + H]$^+$.

HRMS – FAB [*m/z*]: $[M + H]^+$ calculated for $^{12}C_{28}{}^{1}H_{29}{}^{16}O_2{}^{14}N_2{}^{19}F_{17}$, 749.2030; found, 749.2032; Δ = 0.17 mmu.

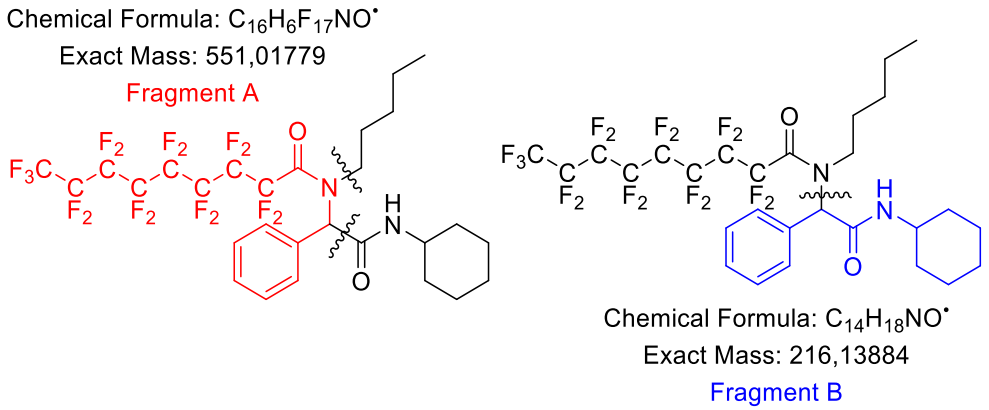

6.2.1.1.18 *Ugi reaction of perfluorononanoic acid, valeraldehyde, tert-butylisocyanide and cyclohexylamine 36*

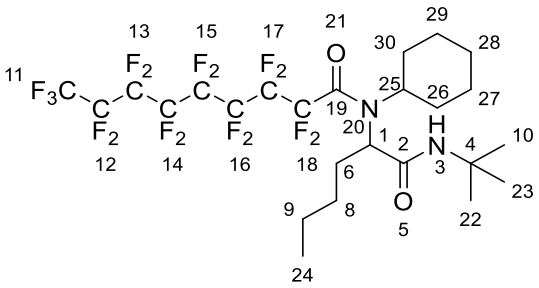

In a 25 mL round bottom flask valeraldehyde (126 mg, 1.46 mmol, 1.70 eq.) was stirred with cyclohexylamine (145 mg, 1.46 mmol, 1.70 eq.) for 60 min over sodium sulfate. Perfluorononanoic acid (400 mg, 862 µmol, 1.00 eq.) dissolved in 1 mL methanol was added to the imine at room temperature and the resulting mixture was stirred for 2 min. Subsequently, *tert*-butylisocyanide (165 µL, 122 mg, 1.46 mmol, 1.70 eq.) was added to the stirring mixture. The reaction was stirred for 4 d at room temperature. The crude reaction mixture was dried under reduced pressure and purified *via* column chromatography employing Fluoro*Flash*® silica gel. The fluorous fraction was concentrated and the residue was adsorbed onto celite® and purified *via* column chromatography employing silica gel as stationary phase and eluting with a gradual solvent mixture of ethyl acetate and *c*-hexane (0:1 → 1:1) to yield the Ugi product **36** as a highly viscous yellow oil (42.2 mg, 61.2 µmol, 7.1%).

R_f = 0.52 in *c*-hexane/ethyl acetate (6:1). Visualized *via* Seebach staining solution and permanganate staining.

IR (ATR): ν [cm^{-1}] = 3337.4 (br, ν(N-H)), 2933.4 (s, ν(C-H)), 2875.3 (m), 1675.6 (s, ν(C=O)), 1534.8 (s), 1453.0 (m), 1238.8 (vs), 1206.8 (vs), 1148.2 (vs), 1109.0 (s), 999.9 (w), 896.1 (w), 785.3 (w), 735.0 (m), 702.4 (m), 668.5 (m), 557.5 (m), 528.0 (m).

^{1}H-NMR (400 MHz, CD_3OD): δ [ppm] = 4.02 – 3.66 (m, 1 H, CH^{1}), 2.80 – 1.69 (m, 7 H, CH_2 + CH^{25}), 1.59 – 1.05 (m, 19 H, $CH_3^{10,22,23}$ + CH_2), 1.00 – 0.83 (m, 3 H, CH_3^{24}).

^{13}C-NMR (101 MHz, CD_3OD): δ [ppm] = 180.17 (s, $CONR^{2}$), 171.76 (s, $CONR^{19}$), 63.54 (s, CH^{1a}), 59.74 (s, CH^{1b}), 32.50 (s, CH_2), 32.20 (s, CH_2), 30.60 (s, CH_2), 30.48 (s, CH_2), 30.35 (s, CH^{25}), 28.70 (s, CH_2), 28.64 (s, $CH_3^{10,22,23}$), 26.79 (s, CH_2), 26.61 (s, CH_2), 25.95 (s, CH_2), 23.61 (s, CH_2), 14.23 (s, CH_3^{24}).

^{19}F-NMR (376 MHz, CD_3OD): δ [ppm] = -86.69 (t, J = 10.6 Hz, 3 F, CF_3^{11}), -114.08 – -114.49 (m, CF_2^{18a}), AB-signal (δ_A = -115.38, δ_B = -116.76, J_{AB} = 293.6 Hz, CF_2^{18b}, additional coupling not resolved, signals broadened), -124.02 – -124.67 (m, CF_2), -124.86 – -125.21 (m, CF_2), -125.30 – -125.50 (m, CF_2), -126.98 (s, CF_2), -127.23 (s, CF_2), -128.08 (s, CF_2), -131.58 (s, CF_2^{12}). Total integral of CF_2 region normalized with respect to the CF_3^{11} group = 14.

ESI-MS [*m/z*]: $[M + Na]^+$ calculated for $^{12}C_{26}{}^{1}H_{31}{}^{16}O_2{}^{14}N_2{}^{19}F_{17}{}^{23}Na_1$, 737.2006; found, 737.2008, Δ = 0.20 mmu.

6.2.1.1.19 ***Ugi reaction of perfluorononanoic acid, isobutyraldehyde, tert-butylisocyanide and cyclohexylamine 37***

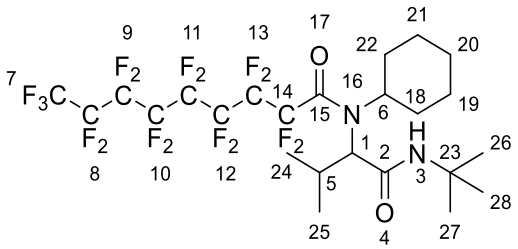

In a 25 mL round bottom flask isobutyraldehyde (83.6 µL, 66.0 mg, 916 µmol, 1.70 eq.) and cyclohexylamine (105 µL, 90.8 mg, 916 µmol, 1.70 eq.) were added and the resulting mixture was stirred for 60 min over sodium sulfate. Perfluorononanoic acid (250 mg, 539 µmol, 1.00 eq.) dissolved in 0.5 mL methanol was added to the solution at room temperature and the resulting mixture was stirred for 2 min. Subsequently, *tert*-butylisocyanide (104 µL, 76.1 mg, 916 µmol, 1.70 eq.) was added to the stirring

mixture. The reaction was stirred for 3 d at room temperature. The crude reaction mixture was dried under reduced pressure. The residue was adsorbed onto celite® and purified *via* column chromatography on silica gel eluting with a gradual solvent mixture of ethyl acetate and *c*-hexane (1:10 → 1:3) to yield the Ugi product **37** as a yellow solid (75.0 mg, 102 µmol, 19.1%).

R_f = 0.54 in *c*-hexane/ethyl acetate (6:1). Visualized *via* permanganate staining solution.

IR (ATR): ν [cm^{-1}] = 2927.2 (vs, ν(C-H)), 2854.9 (s, ν(C-H)), 1673.1 (s, ν(C=O)), 1596.0 (m), 1539.9 (m), 1450.7 (s), 1367.1 (m), 1349.4 (m), 1232.6 (vs), 1148.6 (s), 1130.7 (s), 991.2 (m), 890.6 (w), 802.1 (m), 721.0 (w), 701.0 (m), 660.6 (w), 553.3 (m).

^{1}H-NMR (400 MHz, CD_3OD): δ [ppm] = 3.75 (s, CH^{1a}), 3.66 – 3.50 (m, 1 H, CH^{6}), 3.40 – 3.33 (m, total integral of CH^{1} = 1 H, CH^{1b}), 2.38 – 1.98 (m, 1 H, CH^{5}), 1.95 – 1.49 (m, 8 H, CH_2), 1.47 – 1.11 (m, 11 H, CH_2 +$CH_3^{26,27,28}$), 1.04 – 0.79 (m, 6 H, $CH_3^{24,25}$).

^{13}C-NMR (101 MHz, CD_3OD): δ [ppm] =170.15 (s, CONR^{2}), 164.06 (s, CONR^{15}), 57.53 (s, CH^{1}), 56.28 (s, CH^{6}), 54.77 (s, C^{23}), 34.97 (s, CH^{1}), 34.39 (s, CH_2), 31.65 (s, CH_2), 31.55 (s, CH_2), 30.76 (s, CH_2), 29.23 (s, CH^{5}), 25.51 (s, $CH_3^{26\text{ - }28}$), 25.30 (s, $CH_3^{26\text{ - }28}$), 22.21 (s, CH_2), 18.70 (s, $CH_3^{24,\ 25}$), 18.50 (s, $CH_3^{24,\ 25}$).

^{19}F-NMR (376 MHz, CD_3OD): δ [ppm] = -88.25 (t, J = 10.4 Hz, 3 F, CF_3^{7}), AB-signal (δ_A = -116.39, δ_B = -117.11, J_{AB} = 301.2 Hz, A and B are split into t, J = 11.0 Hz, CF_2^{14a}), AB-signal (δ_A = -118.11, δ_B = -118.55, J_{AB} = 293.6 Hz, A and B are split into t, J = 12.3 Hz, CF_2^{14b}), -126.26 (s, CF_2), -126.73 (s, CF_2), -127.10 (s, CF_2), -128.75 (s, CF_2), -129.64 (s, CF_2), -133.22 (s, CF_2^{8}). Total integral of CF_2 region normalized with respect to the CF_3^{7} group = 14.

ESI-MS [*m/z*]: $[M + Na]^+$ calculated for $^{12}C_{24}{}^{1}H_{29}{}^{16}O_2{}^{14}N_2{}^{19}F_{17}{}^{23}Na_1$, 723.18498; found, 723.18591, Δ = 1.02 mmu.

6.2.1.1.20 *Ugi reaction of perfluorononanoic acid, isobutyraldehyde, pentylisocyanide and cyclohexylamine 38*

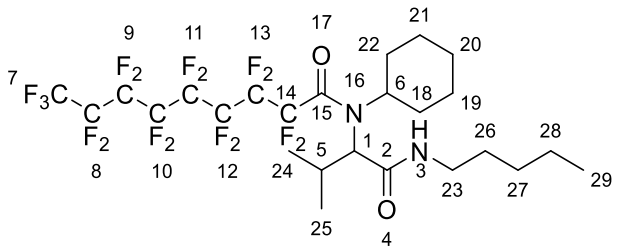

In a 25 mL round bottom flask isobutyraldehyde (46.2 mg, 641 µmol, 1.70 eq.) was dissolved in 1.5 mL methanol, subsequently cyclohexylamine (674 µL, 63.6 mg, 641 µmol, 1.70 eq.) was added and the resulting mixture was stirred for 60 min over sodium sulfate. Afterwards, the mixture was filtrated and the solid was washed with 10 mL methanol three times. Subsequently, the filtrate was concentrated under reduced pressure. Perfluorononanoic acid (175 mg, 377 µmol, 1.00 eq.) dissolved in 0.5 mL methanol was added to the imine at room temperature and the resulting mixture was stirred for 2 min. Subsequently, pentylisocyanide (80.6 µL, 62.2 mg, 641 µmol, 1.70 eq.) was added to the stirring mixture. The reaction was stirred for 6 d at room temperature. The crude reaction mixture was dried under reduced pressure and purified *via* column chromatography employing Fluoro*Flash*® silica gel. The fluorous fraction was tested for purity *via* TLC and concentrated under reduced pressure. The remaining perfluoro acid was removed with a short silica gel filter column, eluting with *c*-hexane/ethyl acetate (3:1) to yield the Ugi product **38** as a highly viscous yellow oil (9.1 mg, 12.6 µmol, 3.34%).

R_f = 0.54 in *c*-hexane/ethyl acetate (6:1). Visualized *via* permanganate staining solution.

IR (ATR): ν [cm^{-1}] = 3338.2 (br, ν(N-H)), 2930.9 (s, ν(C-H)), 2859.9 (s, ν(C-H)), 1659.8 (s, ν(C=O)), 1540.8 (m), 1457.7 (m), 1369.4 (m), 1238.5 (vs), 1206.8 (vs), 1148.7 (vs), 998.0 (m), 777.8 (w), 735.1 (m), 703.1 (m), 656.7 (m), 558.1 (m), 528.8 (w).

^{1}H-NMR (400 MHz, CD_3OD): δ [ppm] = 4.42 (d, J = 11.0 Hz, CH^{1a}), 4.10 (d, J = 7.1 Hz, total integral of CH^{1} = 1 H, CH^{1b}), 3.73 – 3.36 (m, 1 H, CH_2^{23a}), 3.22 – 3.04 (m, 1 H, CH_2^{23b}), 2.51 – 2.12 (m, 1 H, CH^{6}), 1.93 – 1.49 (m, 6 H, CH_2), 1.46 (s, 1 H, CH^{5}), 1.38 – 1.14 (m, 10 H, CH_2), 1.05 – 0.84 (m, 9 H, $CH_3^{24,25}$+ CH_3^{29}).

^{13}C-NMR (101 MHz, CD_3OD): δ [ppm] = 170.91 (s, CONR^{2}), 67.35 (s, CH^{1}), 46.09 (s, CH$_2^{23a}$), 40.40 (s, CH$_2^{23b}$), 31.41 (s, CH$_2$), 30.90 (s, CH$_2$), 30.16 (s, CH$_2$), 30.08 (s, CH^{5}), 29.48 (s, CH$_2$), 28.21 (s, CH$_2$), 23.23 (s, CH$_2$), 20.85 (s, CH^{6}), 19.96 (s, CH$_3^{24, 25}$), 18.73 (s, CH$_3^{24, 25}$), 14.25 (s, CH$_3^{29}$).

^{19}F-NMR (376 MHz, CD_3OD): δ [ppm] = -83.25 (s, CF_3), -88.25 (t, J = 10.3 Hz, 3 F, CF_3^{7}), AB-signal (δ_A = -114.98, δ_B = -115.37, J_{AB} = 207.1 Hz, A and B are split into A and B are split into t, J = 12.0 Hz, CF_2^{14a}), AB-signal (δ_A = -117,60, δ_B = -119,02, J_{AB} = 293.6 Hz, A and B are split into t, J = 12.6 Hz, CF_2^{14b}), -125.47 (s, CF_2), -126.86 (s, CF_2), -128.72 (s, CF_2), -129.63(s, CF_2), -133.14(s, CF_2^{8}). Total integral of CF_2 region normalized with respect to the CF_3^{7} group = 14.

ESI-MS [*m/z*]: $[M + Na]^+$ calculated for $^{12}C_{25}{}^{1}H_{31}{}^{16}O_2{}^{14}N_2{}^{19}F_9{}^{23}Na_1$, 737.2006; found, 737.2013, Δ = 0.66 mmu.

6.2.1.1.21 *Ugi reaction of perfluorononanoic acid, isobutyraldehyde, cyclohexylisocyanide and cyclohexylamine 39*

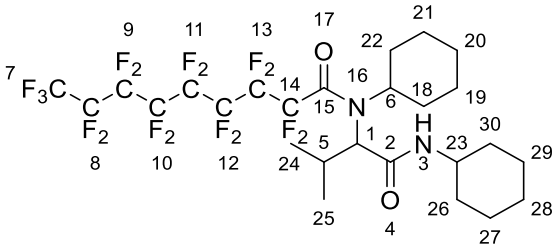

In a 25 mL round bottom flask isobutyraldehyde (46.2 mg, 641 µmol, 1.70 eq.) was dissolved in 1.5 mL methanol, subsequently cyclohexylamine (73.5 µL, 63.6 mg, 641 µmol, 1.70 eq.) was added and the resulting mixture was stirred for 60 min over sodium sulfate. Afterwards, the mixture was filtrated and the solid was washed with 10 mL methanol three times. Subsequently, the filtrate was concentrated under reduced pressure. Perfluorononanoic acid (175 mg, 377 µmol, 1.00 eq.) dissolved in 0.5 mL methanol was added to the imine at room temperature and the resulting mixture was stirred for 2 min. Subsequently, cyclohexylisocyanide (79.9 µL, 70.0 mg, 641 µmol, 1.70 eq.) was added to the stirring mixture. The reaction was stirred for 6 d at room temperature. The crude reaction mixture was dried under reduced pressure and purified *via* column chromatography employing Fluoro*Flash*® silica gel. The fluorous fraction was tested for purity *via* TLC and concentrated under reduced pressure. The

remaining perfluoro acid was removed with a short silica gel filter column, eluting with *c*-hexane/ethyl acetate (3:1) to yield the Ugi product **39** as a highly viscous yellow oil (31.2 mg, 42.9 µmol, 11.4%).

R_f = 0.64 in *c*-hexane/ethyl acetate (6:1). Visualized *via* permanganate staining solution.

IR (ATR): ν [cm^{-1}] = 3343.1 (br, ν(N-H)), 2933.8 (m, ν(C-H)), 2856.3 (m, ν(C-H)), 1675.5 (s, ν(C=O)), 1535.2 (m), 1453.3 (m), 1325.8 (w), 1238.3 (s), 1205.6 (vs), 1148.5 (vs), 1109.9 (m), 1000.4 (w), 896.2 (w), 785.3 (w), 735.4 (m), 702.4 (m), 668.3 (m), 556.8 (w), 529.4 (w), 409.9 (w).

^{1}H-NMR (400 MHz, CD_3OD): δ [ppm] = 3.98 – 3.73 (m, 1 H, CH*1*), 3.72 – 3.59 (m, 1 H, CH*23*), 3.44 (d, *J* = 11.1 Hz, 1 H, CH*6*), 3.02 – 2.80 (m, 1 H, CH*5*), 1.99 – 1.51 (m, 10 H, CH_2), 1.45 – 1.16 (m, 10 H, CH_2), 1.04 – 0.76 (m, 6 H, CH_3*24,25*).

^{13}C-NMR (101 MHz, CD_3OD): δ [ppm] = 172.62 (s, CONR*2*), 160.62 (s, CONR*15*), 71.64 (s, CH*6*), 61.52 (s, CH*1*), 49.86 (s, CH*23*), 33.10 (s, CH_2), 32.65 (s, CH_2), 32.32 (s, CH_2), 27.79 (s, CH*5*), 26.92 (s, CH_2), 26.56 (s, CH_2), 25.89 (s, CH_2), 25.15 (s, CH_2), 20.28 (s, CH_3*24, 25*), 20.00 (s, CH_3*24, 25*).

^{19}F-NMR (376 MHz, CD_3OD): δ [ppm] = -88.29 (t, *J* = 9.9 Hz, 3 F, CF_3*7*), -114.97 (s, CF_2*14a*), AB-signal (δ_A = -116.37, δ_B = -118.34, J_{AB} = 293.6 Hz, A and B are split into t, *J* = 11.3 Hz CF_2*14b*), -125.13 (s, CF_2), -126.01 (s, CF_2), -126.68 (d, *J* = 73.4 Hz, CF_2), -128.66 (d, *J* = 77.4 Hz, CF_2), -129.66 (s, CF_2), -133.16 (s, CF_2*8*). Total integral of CF_2 region normalized with respect to the CF_3*7* group = 14.

FAB – MS [*m/z*] (relative intensity): 755.3 (67%) $[M + H]^+$, 600.1 (31%) [Fragment A]$^+$, 518.0 (100%) [Fragment A – C_6H_{10}]$^+$, 98.1 (15%) [Fragment B – CHO]$^+$.

HRMS – FAB [*m/z*]: $[M + H]^+$ calculated for $^{12}C_{26}{}^{1}H_{32}{}^{16}O_2{}^{14}N_2{}^{19}F_{17}$, 727.2187; found, 727.2185; Δ = 0.22 mmu.

Chemical Formula: $C_{19}H_{19}F_{17}NO^{\bullet}$
Exact Mass: 600,11952
Fragment A

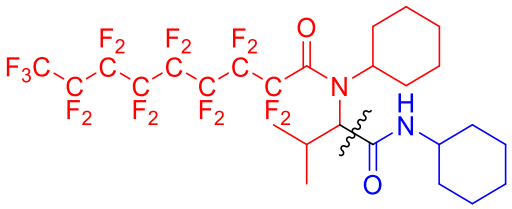

Chemical Formula: $C_7H_{12}NO^{\bullet}$
Exact Mass: 126,09189
Fragment B

6.2.1.1.22 *Ugi reaction of perfluorononanoic acid, undec-10-enal, cyclohexylamine and benzylisocyanide 40*

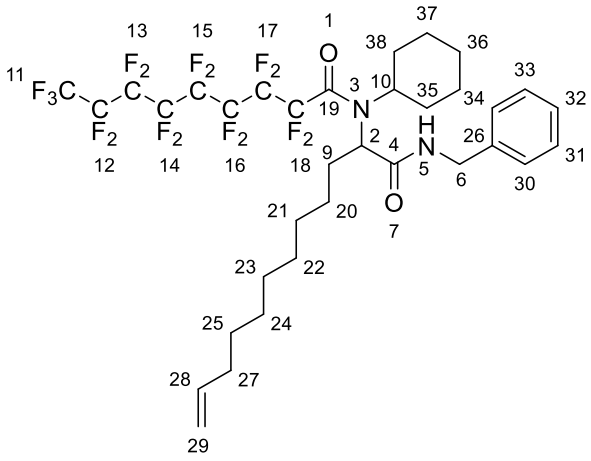

In a 25 mL round bottom flask undec-10-enal (97.6 µL, 84.5 mg, 490 µmol, 1.30 eq.) was dissolved in 1.5 mL methanol, subsequently cyclohexylamine (56.5 µL, 48.9 mg, 490 µmol, 1.30 eq.) was added and the resulting mixture was stirred for 60 min over sodium sulfate. Afterwards the mixture was filtrated and the solid was washed with 10 mL methanol three times. Subsequently, the filtrate was concentrated under reduced pressure. Perfluorononanoic acid (175 mg, 377 µmol, 1.00 eq.) was added at room temperature and the resulting mixture stirred for 2 min. Subsequently, benzylisocyanide (53.9 µL, 53.0 mg, 453 µmol, 1.20 eq.) was added to the stirring mixture. The reaction was stirred for 5 d at room temperature. The crude reaction mixture was dried under reduced pressure and purified *via* column chromatography employing silica gel and eluted with a gradual solvent mixture of ethyl acetate and *c*-hexane (0:1 → 1:3) to remove the remaining perfluoro acid. The product containing

fractions were collected and further purified *via* column chromatography employing Fluoro*Flash*® silica gel to yield the Ugi product **40** as a highly viscous yellow oil (59.4 mg, 71.5 µmol, 19.0%).

R_f = 0.50 in *c*-hexane/ethyl acetate (6:1). Visualized *via* fluorescent quench and Seebach staining solution.

IR (ATR): ν [cm^{-1}] = 3324.4 (br, ν(N-H)), 2926.4 (s, ν(C-H)), 2855.8 (m, ν(C-H)), 1663.4 (s, ν(C=O)), 1528.8 (w, ν(C=C)), 1455.2 (w), 1364.2 (w), 1238.6 (vs), 1208.1 (vs), 1147.9 (s), 1029.0 (w), 992.2 (w), 909.4 (m), 723.2 (s), 698.2 (s), 655.9 (m), 559.2 (m), 528.9 (m).

^{1}H-NMR (400 MHz, $CDCl_3$): δ [ppm] = 7.65 – 6.99 (m, 5 H, CH_{Ar}[30-34]), 6.70 (t, J = 5.7 Hz, 1 H, NH[5]), 5.95 – 5.64 (m, 2 H, CH_2[29]), 5.11 – 4.83 (m, 1 H, CH[28]), 4.58 (s, 1 H, CH[2]), 4.50 – 4.26 (m, 3 H, CH_2[6] + CH[10]), 3.61 – 3.16 (m, 2 H, CH_2[9]) 2.17 – 1.94 (m, 4 H, CH_2), 1.88 – 1.42 (m, 4 H, CH_2), 1.41 – 1.03 (m, 16 H, CH_2).

^{13}C-NMR (101 MHz, $CDCl_3$): δ [ppm] = 170.40 (s, CONR[4]), 160.51 (s, CONR[19]), 140.4 (s, CH_2[29]), 138.63 (s, C_{Ar}[26]), 129.55 (s, CH_{Ar}), 128.49 (s, CH_{Ar}), 128.41 (s, CH_{Ar}), 115.04 (s, CH[28]), 62.83 (s, CH[2 or 10]), 61.85 (s, CH[2 or 10]), 47.52 (s, CH_2), 44.48 (s, CH_2[6]), 34.67 (s, CH_2), 32.08 (s, CH_2), 30.94 (s, CH_2), 30.60 (s, CH_2), 30.29 (s, CH_2), 30.18(s, CH_2), 29.93 (s, CH_2), 29.54 (s, CH_2), 28.70 (s, CH_2), 27.71 (s, CH_2), 27.36 (s, CH_2), 26.92 (s, CH_2).

^{19}F-NMR (376 MHz, $CDCl_3$): δ [ppm] = -85.11 (t, J = 10.3 Hz, 3 F, CF_3[11]), AB-signal (δ_A = -112.77, δ_B = -113.30, J_{AB} = 299.3 Hz, A and B are split into t, J = 12.7 Hz, CF_2[18a]), AB-signal (δ_A = -115.50, δ_B = -115.86, J_{AB} = 289.9 Hz, A and B are split into t, J = 13.2 Hz, CF_2[18b]), -124.62 (s, CF_2), -126.11 (s, CF_2), -127.05 (s, CF_2), -130.44 (s, CF_2[12]). Total integral of CF_2 region normalized with respect to the CF_3[11] group = 14.

FAB – MS [*m/z*] (relative intensity): 831.4 (45%) $[M + H]^+$, 726.3 (73%) [Fragment A + H]$^+$, 106.0 (17%) [Fragment B]$^+$.

HRMS – FAB [*m/z*]: $[M + H]^+$ calculated for $^{12}C_{34}{}^{1}H_{40}{}^{16}O_2{}^{14}N_2{}^{19}F_{17}$, 831.2813; found, 821.2814; Δ = 0.13 mmu.

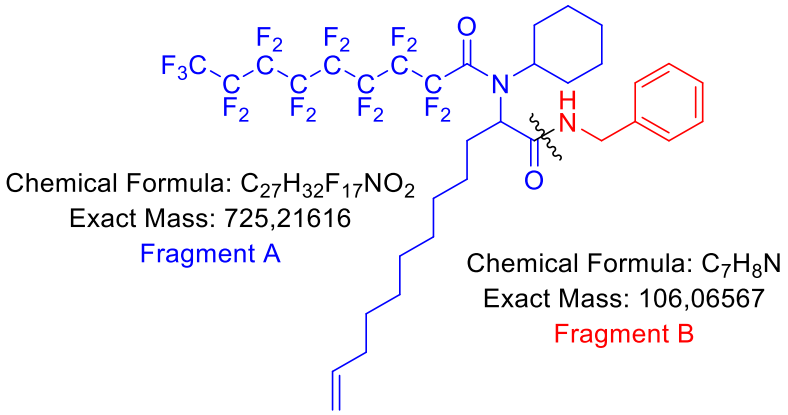

6.2.1.1.23 *Ugi reaction of perfluorononanoic acid, p-anisaldehyde, cyclohexylisocyanide and allylamine 41*

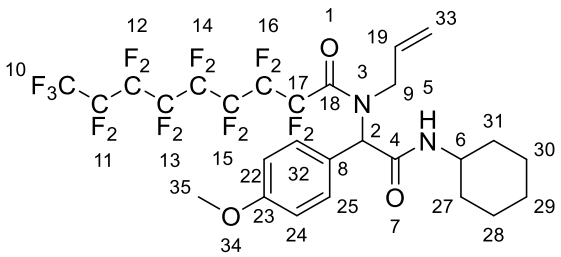

In a 25 mL round bottom flask *p*-anisaldehyde (77.9 µL, 87.3 mg, 641 µmol, 1.70 eq.) and allylamine (48.1 µL, 36.6 mg, 641 µmol, 1.70 eq.) were added. The resulting mixture was stirred for 60 min over sodium sulfate. Perfluorononanoic acid (175 mg, 377 µmol, 1.00 eq.) dissolved in 0.5 mL methanol was added to the solution at room temperature and the resulting mixture was stirred for 2 min. Subsequently, cyclohexylisocyanide (79.7 µL, 70.0 mg, 641 µmol, 1.70 eq.) was added to the stirring mixture. The reaction was stirred for 3 d at room temperature. The crude reaction mixture was dried under reduced pressure and purified *via* column chromatography employing Fluoro*Flash*® silica gel. The fluorous fraction was tested for purity *via* TLC and concentrated under reduced pressure. The remaining perfluorononanoic acid was removed with a short silica gel filter column, eluting with *c*-hexane/ethyl acetate (3:1) to yield the Ugi product **41** as a yellow oil (193 mg, 259 µmol, 68.9%).

R_f = 0.43 in *c*-hexane/ethyl acetate (6:1). Visualized *via* fluorescent quench and Seebach staining solution.

IR (ATR): ν [cm^{-1}] = 3286.2 (br, ν(N-H)), 3083.6 (w), 2926.3 (m, ν(C-H)), 2849.5 (m), 1675.0 (s, ν(C=O)), 1655.9 (s), 1616.8 (m), 1555.6 (s), 1515.9 (s), 1417.2 (m), 1369.6

(m), 1330.1 (w), 1308.9 (w), 1248.4 (w), 1195.6 (s), 1143.4 (vs), 1116.4 (vs), 1042.2 (s), 989.9 (m), 943.3 (m), 927.1 (m), 889.1 (m), 863.4 (m), 840.1 (m), 805.7 (m), 760.8 (m), 716.6 (m), 681.4 (m), 649.5 (m), 633.9 (m), 615.3 (m), 564.7 (m), 549.9 (s), 519.5 (s), 481.4 (s), 450.5 (w).

^{1}H-NMR (400 MHz, CD_3OD): δ [ppm] = 7.30 – 7.22 (m, 2 H, $CH_{Ar}^{25,32}$), 6.97 – 6.89 (m, 2 H, $CH_{Ar}^{22,24}$), 5.90 (s, 1 H, CH^{2}), 5.85 – 5.75 (m, 2 H, CH_2^{33}), 5.45 – 5.04 (m, 1 H, CH^{19}), 4.81 – 4.58 (m, 2 H, CH_2^{9}), 3.79 (s, 3 H, CH_3^{35}), 3.77 – 3.60 (m, 1 H, CH^{6}), 1.95 – 1.01 (m, 10 H, CH_2).

^{13}C-NMR (126 MHz, CD_3OD): δ [ppm] = 172.96 (s, $CONR^{4}$), 170.19(s, C_{Ar}^{23}), 161.96 (s, $CONR^{18}$), 135.22 (s C_{Ar}^{8}), 133.20 (s, CH^{19}), 132.29 (s, $CH_{Ar}^{25,32}$), 116.58 (s, CH_2^{9}), 115.16 (s, $C_{Ar}^{22,24}$), 64.94 (s, CH^{2}), 61.53 (s, CH_2^{33}), 55.81 (s, CH_3^{35}), 50.05 (s, CH^{6}), 33.56 (s, CH_2), 33.45 (s, CH_2), 26.60 (s, CH_2), 26.02 (s, CH_2), 20.86 (s, CH_2).

^{19}F-NMR (376 MHz, CD_3OD): δ [ppm] = -88.26 (t, J = 10.5 Hz, 3 F, CF_3^{10}), AB-signal (δ_A = -116.14, δ_B = -117.58, J_{AB} =299.3 Hz, J_{AB} = 297.4 Hz, A and B are split into t, J = 12.3 Hz, CF_2^{17a}), AB-signal (δ_A = 117.23, δ_B = -118.91, J_{AB} = 295.5 Hz, A and B are split into t, J = 12.6 Hz, CF_2^{17b}), -126.44 (s, CF_2), -126.96 – -127.37 (m, CF_2), -128.69 (s, CF_2), -129.65 (s, CF_2), -133.16(s, CF_2^{11}). Total integral of CF_2 region normalized with respect to the CF_3^{10} group = 14.

FAB – MS [m/z] (relative intensity): 749.1 (25%) $[M + H]^+$, 622.0 (68%) [Fragment A]$^+$, 582.0 (52%) $[Fragment A + H – C_3H_5]^+$, 247.1 (28%) [Fragment B + H]$^+$.

HRMS – FAB [m/z]: $[M + H]^+$ calculated for $^{12}C_{27}{}^{1}H_{26}{}^{16}O_3{}^{14}N_2{}^{19}F_{17}$, 749.1665; found, 749.1666; Δ = 0.18 mmu.

Chemical Formula: $C_{20}H_{13}F_{17}NO_2^{\bullet}$
Exact Mass: 622,06748
Fragment A

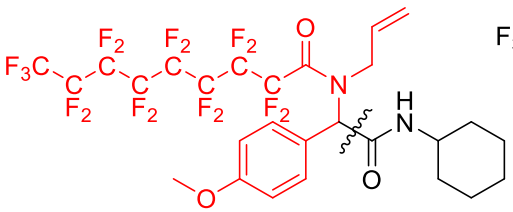

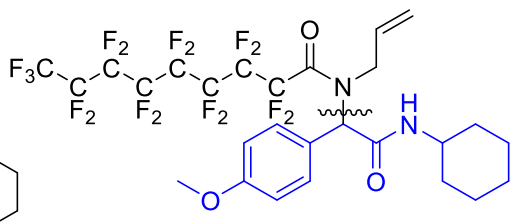

Chemical Formula: $C_{15}H_{20}NO_2^{\bullet}$
Exact Mass: 246,14940
Fragment B

6.2.1.1.24 *Ugi reaction of perfluorononanoic acid, benzaldehyde, cyclohexylisocyanide and octylamine 42*

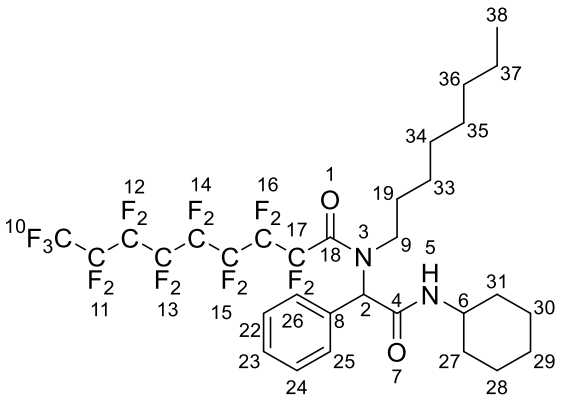

In a 25 mL round bottom flask benzaldehyde (65.4 µL, 68.0 mg, 641 µmol, 1.70 eq.) and octylamine (106 µL, 82.9 mg, 641 µmol, 1.70 eq.) were added. The resulting mixture was stirred for 60 min over sodium sulfate. Pefluornonanoic acid (175 mg, 377 µmol, 1.00 eq.) dissolved in 0.5 mL methanol was added to the solution at room temperature and the resulting mixture was stirred for 2 min. Subsequently, cyclohexylisocyanide (79.7 µL, 70.0 mg, 641 µmol, 1.70 eq.) was added to the stirring mixture. The reaction was stirred for 3 d at room temperature. The crude reaction mixture was dried under reduced pressure and purified *via* column chromatography employing Fluoro*Flash*® silica gel. The fluorous fraction was tested for purity *via* TLC and concentrated under reduced pressure. The remaining perfluorononanoic acid was removed with a short silica gel filter column, eluting with *c*-hexane/ethyl acetate (3:1) to yield the Ugi product **42** as a yellow oil (41.8 mg, 52.8 µmol, 14.0%).

R_f = 0.36 in *c*-hexane/ethyl acetate (6:1). Visualized *via* fluorescent quench and Seebach staining solution.

IR (ATR): ν [cm^{-1}] = 2924.8 (s, ν(C-H)), 2853.3 (s, ν(C-H)), 1768.8 (w, ν(C=O)), 1712.5 (s, ν(C=O)), 1646.9 (s, ν(C=O)), 1450.9 (m), 1375.6 (m), 1240.5 (s), 1214.7 (s), 1150.2 (m), 753.2 (s), 693.2 (s), 496.5 (w).

^{1}H-NMR (500 MHz, $CDCl_3$): δ [ppm] = 6.99 – 6.90 (m, 5 H, CH_{Ar}*25-26*), 4.30 (s, 1 H, CH*2*), 3.26 – 3.08 (m, 3 H, CH*6* + CH_2*9*), 1.28 – 1.16 (m, 4 H, CH_2), 0.96 – 0.68 (m, 16 H, CH_2), 0.49 – 0.28 (m, 3 H, CH_3*38*).

^{13}C-NMR (126 MHz, CD_3OD): δ [ppm] = 171.58 (s, CONR*4*), 160.84 (s, CONR*18*), 136.48 (s, C_{Ar}*8*), 128.67 (s, CH_{Ar}), 128.13 (s, CH_{Ar}), 127.44 (s, CH_{Ar}), 65.49 (s, CH*2*),

63.40 (s, CH_2), 61.96 (s, CH^6), 31.99 (s, CH_2), 31.06 (s, CH_2), 29.84 (s, CH_2), 29.56 (s, CH_2), 29.40 (s, CH_2), 27.50 (s, CH_2), 26.78(s, CH_2), 25.16 (s, CH_2), 22.80 (s, CH_2), 14.23 (s, CH_3^8).

^{19}F-NMR (376 MHz, $CDCl_3$): δ [ppm] = -85.11 (t, J = 9.0 Hz, 3 F, CF_3^{10}), AB-signal (δ_A = -112.92, δ_B = -114.05, J_{AB} =295.5 Hz, A and B are split into t, CF_2^{17a}, additional coupling not resolved, signals broadened), AB-signal (δ_A = -115.47, δ_B = -116.59, J_{AB} = 291.8 Hz, A and B are split into t, CF_2^{17b}, additional coupling not resolved, signals broadened), -123.73 – -124.95 (m, CF_2), -126.12 (s, CF_2), -127.05 (s, CF_2), -130.46 (s, CF_2^{11}). Total integral of CF_2 region normalized with respect to the CF_3^{10} group = 14.

FAB – MS [*m/z*] (relative intensity): 791.3 (40%) $[M + H]^+$, 552.0 (22%) [Fragment A + H]$^+$, 118.0 (23%) [Fragment B – H]$^+$, 98.0 (31%) [Fragment C]$^+$.

HRMS – FAB [*m/z*]: $[M + H]^+$ calculated for $^{12}C_{31}{}^{1}H_{36}{}^{16}O_2{}^{14}N_2{}^{19}F_{17}$, 797.2500; found, 791.2501; Δ = 0.14 mmu.

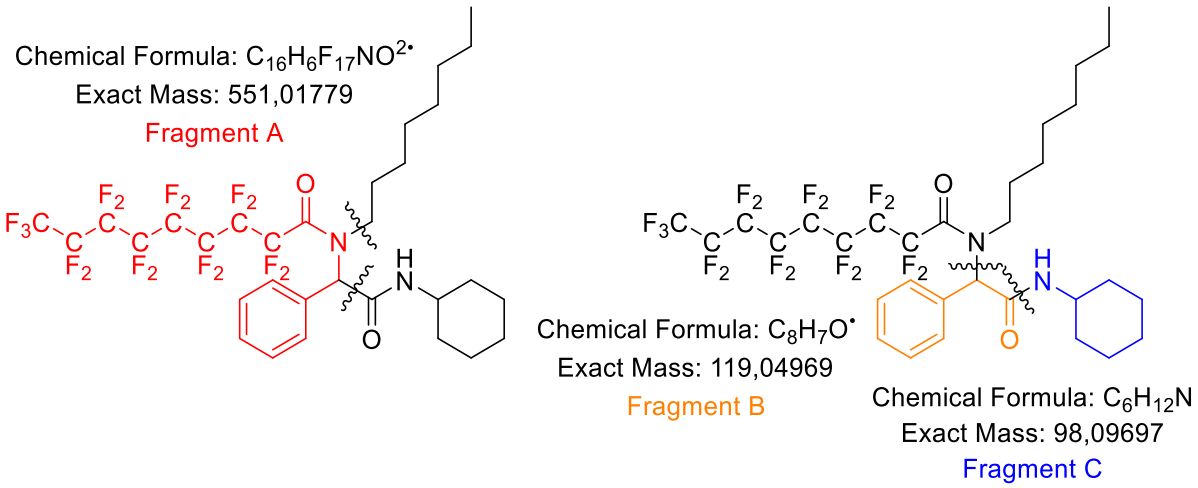

6.2.1.1.25 *Ugi reaction of perfluorononanoic acid, p-anisaldehyde, cyclohexylisocyanide and heptylamine 43*

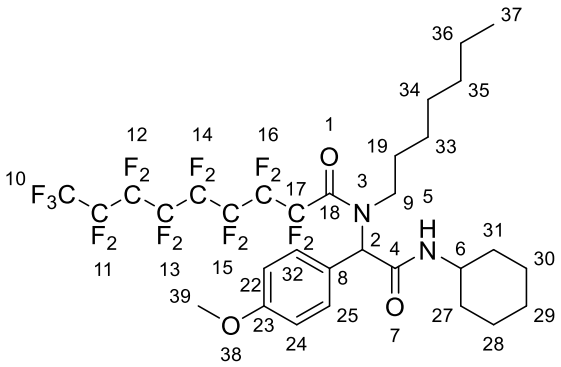

In a 25 mL round bottom flask *p*-anisaldehyde (77.9 µL, 87.3 mg, 641 µmol, 1.70 eq.) and heptylamine (95.0 µL, 73.8 mg, 641 µmol, 1.70 eq.) were mixed. The resulting mixture was stirred for 60 min over sodium sulfate. Perfluorononanoic acid (175 mg, 377 µmol, 1.00 eq.) dissolved in 0.5 mL methanol was added to the solution at room temperature and the resulting mixture was stirred for 2 min. Subsequently, cyclohexylisocyanide (79.9 µL, 70.0 mg, 641 µmol, 1.70 eq.) was added to the stirring mixture. The reaction was stirred for 3 d at room temperature. The crude reaction mixture was dried under reduced pressure and purified *via* column chromatography employing Fluoro*Flash*® silica gel. The fluorous fraction was tested for purity *via* TLC and concentrated under reduced pressure. The remaining perfluorononanoic acid was removed with a short silica gel filter column, eluting with *c*-hexane/ethyl acetate (3:1) to yield the Ugi product **43** as a yellow oil (76.9 mg, 95.4 µmol, 25.3%).

R_f = 0.36 in *c*-hexane/ethyl acetate (4:1). Visualized *via* fluorescent quench and Seebach staining solution.

IR (ATR): ν [cm^{-1}] = 3295.4 (br, ν(N-H)), 2927.7 (m, ν(C-H)), 2853.7 (w, ν(C-H)), 1675.3 (s, ν(C=O)), 1645.9 (vs, ν(C=O)), 1612.2 (w), 1555.6 (m), 1513.0 (m), 1437.6 (w), 1200.7 (vs), 1144.6 (vs), 1028.7 (m), 977.1 (m), 918.3 (w), 822.1 (m), 773.1 (m), 703.4 (m), 662.7 (m), 561.6 (m), 527.0 (s), 443.0 (w).

^{1}H-NMR (400 MHz, $CDCl_3$): δ [ppm] = 7.33 (d, J = 8.7 Hz, 2 H, CH_{Ar}*[25,32]*), 6.91 (d, J = 8.8 Hz, 2 H, CH_{Ar}*[22,24]*), 5.54 (s, 1 H, CH*[2]*), 3.83 (s, 3 H, OCH_3*[39]*), 3.81 – 3.75 (m, 1 H, CH*[6]*), 3.38 (s, 2 H, CH_2*[9]*), 1.94 – 1.84 (m, 2 H, CH_2), 1.69 – 1.55 (m, 4 H, CH_2), 1.38 – 0.94 (m, 16 H, CH_2), 0.83 (t, J = 7.2 Hz, 3 H, CH_3*[37]*).

^{13}C-NMR (101 MHz, $CDCl_3$): δ [ppm] = 167.36 (s, CONR^{4}), 160.34 (s, C_{Ar}^{23}), 159.02 (s, CONR^{10}), 131.34 (s, CH_{Ar}^{25,32}), 125.47 (s, C_{Ar}^{8}), 114.56 (s, C_{Ar}^{22,24}), 64.82 (s, CH^{2}), 55.47 (s, OCH_3^{39}), 48.90 (s, CH^{6}), 47.49 (s, CH_2^{9}), 32.83(s, CH_2), 31.65(s, CH_2), 29.98 (s, CH_2), 28.60 (s, CH_2), 27.06 (s, CH_2), 26.66 (s, CH_2), 25.59 (s, CH_2), 24.88 (s, CH_2), 22.59 (s, CH_2), 14.10 (s, CH_3^{37}).

^{19}F-NMR (376 MHz, $CDCl_3$): δ [ppm] = -85.11 (t, J = 9.9 Hz, 3 F, CF_3^{10}), AB-signal (δ_A = -112.88, δ_B = -114.15, J_{AB} = 295.5 Hz, A and B are split into t, J = 13.3 Hz, CF_2^{17a}), AB-signal (δ_A = -115.47, δ_B = -116.63, J_{AB} = 291.8 Hz, A and B are split into t, J = 13.7 Hz, CF_2^{17b}), -123.87 – 125.00 (m, CF_2), -126.13 (s, CF_2), -127.06 (s, CF_2), -130.45 (s, CF_2^{11}). Total integral of CF_2 region normalized with respect to the CF_3^{10} group = 14.

FAB – MS [*m/z*] (relative intensity): 807.3 (25%) $[M + H]^+$, 708.1 (23%) [Fragment A +H]$^+$, 681.2 [Fragment B +H]$^+$.

HRMS – FAB [*m/z*]: $[M + H]^+$ calculated for $^{12}C_{31}{}^{1}H_{36}{}^{16}O_3{}^{14}N_2{}^{19}F_{17}$, 807.2449; found, 807.2449; Δ = 0.03 mmu.

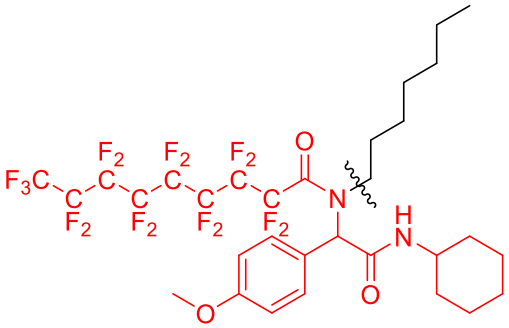

Chemical Formula: $C_{24}H_{20}F_{17}N_2O_3^{\bullet}$
Exact Mass: 707,12025
Fragment A

Chemical Formula: $C_{24}H_{23}F_{17}NO_2^{\bullet}$
Exact Mass: 680,14573
Fragment B

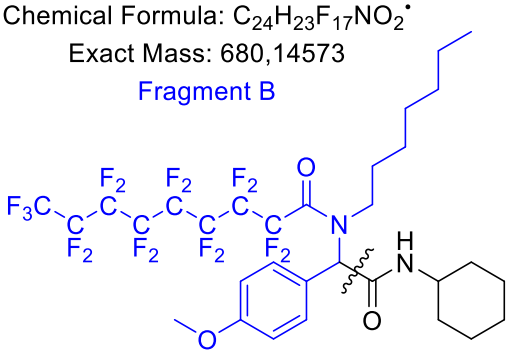

6.2.1.1.26 *Ugi reaction of perfluorononanoic acid, valeraldehyde, tert-butylisocyanide and tert-butylamine 44*

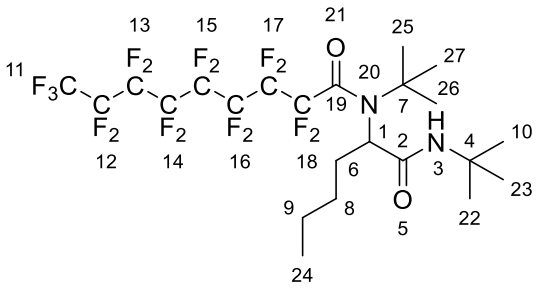

In a 25 mL round bottom flask valeraldehyde (126 mg, 1.46 mmol, 1.70 eq.) and *tert*-butylamine (107 mg, 1.46 mmol, 1.70 eq.) were stirred for 60 min over sodium sulfate. Perfluorononanoic acid (400 mg, 826 µmol, 1.00 eq.) dissolved in 1 mL methanol was added to the imine at room temperature and the resulting mixture was stirred for 2 min. Subsequently, *tert*-butylisocyanide (165 µL, 122 mg, 1.46 mmol, 1.70 eq.) was added to the stirring mixture. The reaction was stirred for 5 d at room temperature. The crude reaction mixture was dried under reduced pressure and purified *via* column chromatography employing Fluoro*Flash*® silica gel. The fluorous fraction was concentrated and the residue was adsorbed onto celite® and purified *via* column chromatography employing silica gel as stationary phase and eluting with a gradual solvent mixture of ethyl acetate and *c*-hexane (0:1 → 1:1) to yield the Ugi product **44** as a highly viscous yellow oil (109 mg, 141 µmol, 17.3%).

R_f = 0.58 in *c*-hexane/ethyl acetate (6:1). Visualized *via* Seebach staining solution and permanganate staining.

IR (ATR): ν [cm^{-1}] = 2965.2 (m, ν(C-H)), 1683.9 (s, ν(C=O)), 1509.6 (m), 1456.9 (m), 1394.9 (m), 1366.9 (m), 1205.7 (s), 1146.3 (s), 1040.6 (w), 985.7 (w), 879.4 (w), 821.3 (w), 783.1 (w), 735.7 (m), 710.2 (m), 669.4 (m), 635.8 (m), 559.7 (m), 530.2 (m), 473.4 (w).

^{1}H-NMR (400 MHz, CD_3OD): δ [ppm] = 4.34 (t, J = 6.8 Hz, 1 H, CH^{1}), 2.40 – 2.14 (m, 1 H, CH_2^{6a}), 1.86 – 1.66 (m, 1 H, CH_2^{6b}), 1.55 – 1.05 (m, 22 H, $CH_2^{8,9}$ + $CH_3^{10,22,23,25\text{-}27}$), 0.95 (t, J = 7.1 Hz, 3 H, CH_3^{24}).

^{13}C-NMR (101 MHz, CD_3OD): δ [ppm] = 169.54 (s, $CONR^{2}$), 160.81 (s, $CONR^{19}$), 62.13 (s, $C^{4\ or\ 7}$), 61.30 (s, CH^{6}), 51.25 (s, $C^{4\ or\ 7}$), 32.17 (s, CH_2), 30.03 (s, CH_2), 28.25 (s, $CH_3^{10,22,23\ or\ 25\text{-}27}$), 27.24 (s, $CH_3^{10,22,23\ or\ 25\text{-}27}$), 22.34 (s, CH_2), 12.78 (s, CH_3^{24}).

^{19}F-NMR (376 MHz, CD_3OD): δ [ppm] = -88.25 (t, J = 10.2 Hz, 3 F, CF_3*11*), -113.23 – -116.89 (m, CF_2*18*), -125.75 (s, CF_2), -128.64 (d, J = 64.9 Hz, CF_2), -129.65 (s, CF_2), -133.15 (s, CF_2*12*). Total integral of CF_2 region normalized with respect to the CF_3*11* group = 14.

ESI-MS [*m/z*]: $[M + Na]^+$ calculated for $^{12}C_{23}{}^{1}H_{29}{}^{16}O_2{}^{14}N_2{}^{19}F_{17}{}^{23}Na_1$, 711.1850 found, 711.18064, Δ = 1.35 mmu.

6.2.1.1.27 *Ugi reaction of perfluorononanoic acid, dodecanal, pentylisocyanide and benzylamine 45*

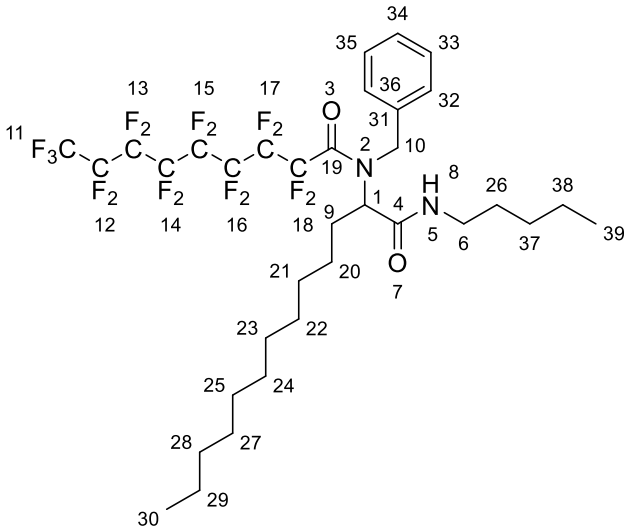

In a 25 mL round bottom flask dodecyl aldehyde (90.4 mg, 490 µmol, 1.30 eq.) was dissolved in 1.5 mL methanol, subsequently benzylamine (56.0 µL, 52.5 mg, 490 µmol, 1.30 eq.) was added and the resulting mixture was stirred for 60 min over sodium sulfate. Afterwards, the mixture was filtrated and the solid was washed with 10 mL methanol three times. Subsequently, the filtrate was concentrated under reduced pressure. Perfluorononanoic acid (175 mg, 377 µmol, 1.00 eq.) dissolved in 1 mL methanol was added to the imine at room temperature and the resulting mixture was stirred for 2 min. Subsequently, pentylisocyanide (56.9 µL, 43.9 mg, 453 µmol, 1.20 eq.) was added to the stirring mixture. The reaction was stirred for 3 d at room temperature. The crude reaction mixture was dried under reduced pressure and purified *via* column chromatography employing Fluoro*Flash*® silica gel. The fluorous fraction was tested for purity *via* TLC and concentrated under reduced pressure. The remaining perfluoro acid was removed with a short silica gel filter column, eluting with

c-hexane/ethyl acetate (3:1) to yield the Ugi product **45** as a highly viscous yellow oil (57.1 mg, 68.4 µmol, 18.1%).

R_f = 0.69 in *c*-hexane/ethyl acetate (6:1). Visualized *via* fluorescent quench and Seebach staining solution.

IR (ATR): ν [cm^{-1}] = 3327.8 (br, ν(N-H)), 2924.6 (m, ν(C-H)), 2854.8 (w, ν(C-H)), 1659.9 (m, ν(C=O)), 1539.8 (w, ν(N-H)), 1455.2 (w), 1364.5 (s), 1239.1 (s), 1209.2 (vs), 1148.2 (s), 956.2 (w), 722.9 (m), 699.5 (m), 657.1 (m), 559.4 (w), 529.2 (w), 463.1 (w).

^{1}H-NMR (400 MHz, $CDCl_3$): δ [ppm] = 7.38 – 7.13 (m, 5 H, CH_{Ar}[32-36]), 6.17 (t, J = 5.5 Hz, 1 H, NH[8]), 5.04 – 4.55 (m, 2 H, CH_2[10]), 4.43 (t, J = 14.8, 1 H, CH[1]), 3.34 – 2.92 (m, 2 H, CH_2[6]), 1.96 – 1.67 (m, 2 H, CH_2[9]), 1.66 – 1.37 (m, 2 H, CH_2[38 or 29]), 1.36 – 1.06 (m, 22 H, CH_2), 0.87 (s, 6 H, CH_3[30 + 39]).

^{13}C-NMR (126 MHz, $CDCl_3$): δ [ppm] = 168.30 (s, CONR[4]), 159.01 (s, CONR[19]), 135.90 (s, C_{Ar}[31]), 127.98 (s, CH_{Ar}), 127.27 (s, CH_{Ar}), 126.51 (s, CH_{Ar}), 60.71 (s, CH[1]), 40.30 (s, CH_2[6]), 31.55 (s, CH_2[26]), 28.41 (s, CH_2), 28.25 (s, CH_2), 22.33 (s, CH_2), 21.94 (s, CH_2), 13.80 (s, CH_3[30 or 39]), 13.59 (s, CH_3[30 or 39]).

^{19}F-NMR (376 MHz, $CDCl_3$) δ [ppm] = -85.10 (t, J = 9.9 Hz, 3 F, CF_3[11]), -112.37 – -114.22 (m, CF_2[18a]), AB-signal (δ_A = -114.15, δ_B = -115.22, J_{AB} = 291.8 Hz, A and B are split into t, J = 13.1 Hz, CF_2[18b]), 124.25 (s, CF_2), -126.13 (s, CF_2), -127.05 (s, CF_2), -130.44 (s, CF_2[12]). Total integral of CF_2 region normalized with respect to the CF_3[11] group = 14.

FAB – MS [*m/z*] (relative intensity): 835.4 (65%) $[M + H]^+$, 387.3 (10%) [Fragment A]$^+$, 283.2 (32%) [Fragment B + H]$^+$.

HRMS – FAB [*m/z*]: $[M + H]^+$ calculated for $^{12}C_{34}{}^{1}H_{44}{}^{16}O_2{}^{14}N_2{}^{19}F_{17}$, 835.3126; found, 835.3125; Δ = 0.06 mmu.

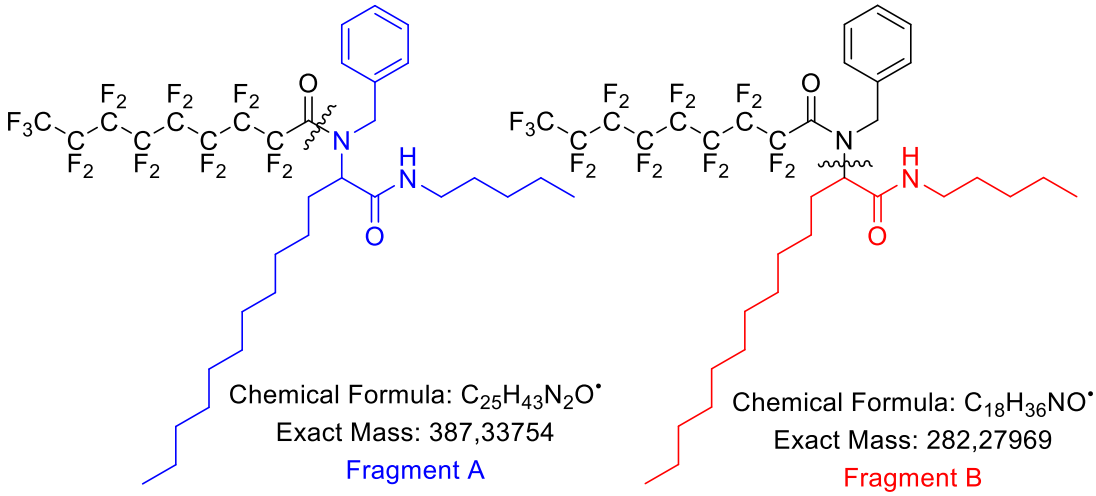

6.2.1.1.28 *Ugi reaction of perfluorononanoic acid, cyclamen aldehyde, tert-butylisocyanide and 2-pentylamine 46*

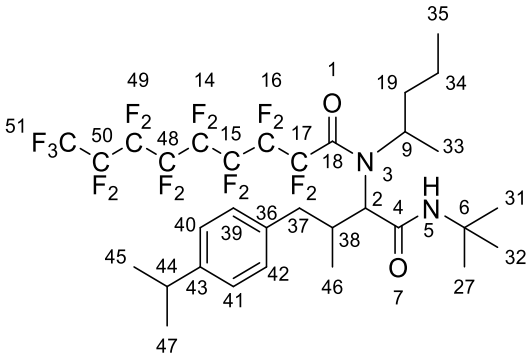

In a 25 mL round bottom flask cyclamen aldehyde (906 µL, 861 mg, 4.53 mmol, 3.00 eq.) and 2-pentylamine (493 µL, 394 mg, 4.53 mmol, 3.00 eq.) were stirred for 60 min over sodium sulfate. The mixture was diluted with 0.5 mL methanol and perfluorononanoic acid (700 mg, 1.51 mmol, 1.00 eq.) was added at room temperature. Subsequently, *tert*-butylisocyanide (512 µL, 376 mg, 4.53 mmol, 3.00 eq.) was added to the stirring mixture. The reaction was stirred for 4 d at room temperature. The crude reaction mixture was dried under reduced pressure and purified *via* column chromatography employing Fluoro*Flash*® silica gel and eluting with 8 mL methanol/water (8:2) to elute the organic fraction, subsequently the fluorous fraction was eluted with pure methanol. The remaining perfluoro acid was removed with a short silica gel filter column, eluting with *c*-hexane/ethyl acetate (3:1). After drying under reduced pressure, the fluoro-tagged product **46** (diastereomer mixture) was obtained as a yellow oil (209 mg, 251 µmol, 16.7%).

R_f = 0.75 in *c*-hexane/ethyl acetate (3:1). Visualized *via* fluorescent quench and Seebach staining solution.

IR (ATR): ν [cm^{-1}] = 3305.2 (br, ν(N-H)), 2959.7 (vs, ν(C-H)), 2929.3 (s, ν(C-H)), 2870.8 (m, ν(C-H)), 2711.1 (m), 1725.1 (vs, ν(C=O)), 1674.4 (s, ν(C=O)), 1512.6 (m), 1457.4 (m), 1419.9 (w), 1382.2 (w), 1363.0 (w), 1282.5 (w), 1217.7 (m), 1114.2 (s), 1050.7 (m), 1019.5 (w), 923.8 (w), 879.9 (m), 837.5 (w), 704.4 (w), 548.6 (m).

^{1}H-NMR (500 MHz, CD_3OD): δ [ppm] = 7.20 – 6.95 (m, 4 H, CH_{Ar}[39-42]), 4.87 (s, 1 H), 4.30 (dd, *J* = 5.0, 2.3 Hz, 1 H, CH[2]), 3.04 – 2.50 (m, 5 H, CH_2[19+37] + CH[9]), 2.31 (ddd, *J* = 13.4, 9.4, 2.6 Hz, 2 H, CH_2[34]), 1.94 – 1.80 (m, 2 H, CH[38] + CH[44]), 1.42 – 1.12 (m, 18 H, CH_3[45,47] + CH_3[27,31,32] + CH_3[33]), 1.03 – 0.82 (m, 6 H, CH_3[35+46]).

^{13}C-NMR (126 MHz, CD_3OD): δ [ppm] = 147.26 (s, CONR[4]), 139.32 (s, CONR[18]), 139.21 (s, C_{Ar}), 130.21 (s, C_{Ar}), 127.38 (s, CH_{Ar}), 127.09 (s, CH_{Ar}), 102.07 (s, CH[2]), 42.71 (s, CH[38 or 44]), 42.39 (s, CH[38 or 44]), 38.91 (s, CH_2), 38.72 (s, CH_2), 35.50 (s, CH_2), 34.89 (s, CH[9]), 24.59 (s, CH_3), 24.52 (s, CH_3), 14.19 (s, CH_3[35or46]), 14.11 (s, CH_3[35or46]).

^{19}F-NMR (376 MHz, CD_3OD): δ [ppm] = -86.41 (t, *J* = 10.4 Hz, 3 F, CF[51]), -113.47 – -116.61 (m, CF_2[17]), -124.05 – -125.24 (m, CF_2), -126.48 (s, CF_2), -126.67 – -127.14 (m, CF_2), -127.72 (d, *J* = 17.1 Hz, CF_2), -127.84 (s, CF_2), -130.95 – -131.61 (m, CF_2[50]). Total integral of CF_2 region normalized with respect to the CF_3[51] group = 14.

ESI – MS [*m/z*]: $[M + Na]^+$ calculated for $^{12}C_{32}{}^{1}H_{39}{}^{16}O_2{}^{14}N_2{}^{19}F_{17}Na_1$, 829.2638; found, 829.2636; Δ = 0.19 mmu.

6.2.2 Synthetic procedures for chapter 4.2

Additional data such as displayed NMR spectra can be found in the supplementary information of the previous publication and are included in the electronic version of this thesis on the CD.[23]

6.2.2.1 Biginelli reactions

6.2.2.1.1 *Biginelli compound 47 derived from benzaldehyde, benzyl acetoacetate and urea*

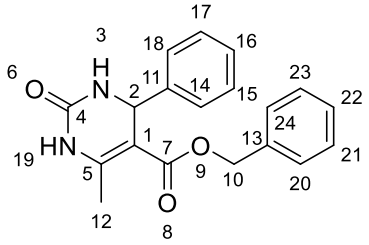

In a tube vial, finely powdered urea (1.50 g, 24.9 mmol, 1.50 eq.) and benzaldehyde (1.76 g, 16.6 mmol, 1.70 mL, 1.00 eq.) were suspended in 3.33 mL dimethyl sulfoxide (5.00 M for 1.00 eq.). Subsequently, benzyl acetoacetate (3.84 g, 20.0 mmol, 3.45 mL) and 4-methylbenzenesulfonic acid (99.9 mg, 833 µmol, 0.05 eq.) were added. The resulting mixture was stirred at 110 °C for 24 h. TLC indicated complete conversion of benzaldehyde. Subsequently, the crude reaction mixture was added dropwise into 100 mL water while stirring. The suspension was stirred for 3 h until a precipitate was formed. The precipitate was filtered off, crushed, washed with water (3 × 30 mL) and dried. Then, the precipitate was washed with and *n*-hexane (2 × 30 mL) and dried under reduced pressure to yield the Biginelli product **47** as a pale yellow solid (4.86 g, 15.1 mmol, 90.5%).

IR (ATR): ν [cm^{-1}] = 3352.9 (w, ν(N-H)), 3108.6 (br,ν(N-H)), 2975.5 (br, ν(C-H), 1701.2 (s, ν(C=O)), 1684.5 (s, ν(C=O)), 1634.3 (s), 1493.8 (w), 1453.9 (m), 1421.1 (m), 1376.4 (m), 1320.2 (m), 1292.4 (m), 1221.1 (vs), 1137.0 (w), 1082.1 (vs), 1025.1 (m), 963.5 (w), 791.7 (w), 750.7 (w), 720.1 (m), 699.0 (s), 660.3 (m), 612.5 (w), 523.0 (w), 488.3 (m), 385.9 (w).

^{1}H-NMR (300 MHz, DMSO-d_6): δ [ppm] = 9.28 (s, 1 H, NH^{19}), 7.77 (s, 1 H, NH^{3}), 7.36 – 7.11 (m, 10 H, CH$_{Ar}$), 5.18 (d, J = 2.7 Hz, 1 H, CH^{2}), AB-signal (δ A = 5.05, δ B = 5.00, J_{AB} = 13.5 Hz, CH$_2^{10}$), 2.28 (s, 3 H, CH$_3^{12}$).

^{13}C-NMR (101 MHz, DMSO-d_6): δ [ppm] = 165.10 (s, CO$_2$R^{7}), 152.03 (s, CO^{4}), 149.31 (s, C^{5}), 144.68 (s, C$_{Ar}^{11}$), 136.54 (s, C$_{Ar}^{13}$), 128.46 (s, CH$_{Ar}$), 128.30 (s, CH$_{Ar}$), 127.74 (s, CH$_{Ar}$), 127.57 (s, CH$_{Ar}$), 127.35 (s, CH$_{Ar}$), 126.33 (s, CH$_{Ar}$), 98.76 (s, C^{1}), 64.84 (s, CH$_2^{10}$), 53.96 (s, CH^{2}), 17.89 (s, CH$_3^{12}$).

FAB – MS [m/z] (relative intensity): 323.3 (100%) $[M + H]^+$, 245.1 (30%) $[M – C_7H_7O]^+$, 231.0 (35%) $[M – C_7H_7]^+$, 215.0 (20%) $[M – C_7H_7]^+$.

HRMS – FAB [m/z]: $[M + H]^+$ calculated for $^{12}C_{19}{}^{1}H_{19}{}^{16}O_3{}^{14}N_2$, 321.1390; found, 323.1388; Δ = 0.19 mmu.
Spectral data is in accordance to earlier reported.[340]

6.2.2.1.2 *Biginelli acid 48 derived from Biginelli benzyl ester 47*

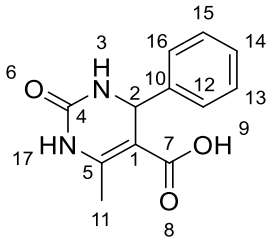

In a tube vial equipped with a magnetic stir bar, the Biginelli benzyl ester **47** (800 mg, 2.48 mmol, 1.00 eq.) was dissolved in 8.00 mL acetic acid/ethanol (1:3). Subsequently, palladium on activated charcoal (10 wt.% Pd, 80.0 mg) was added to the solution and the vial was placed inside an autoclave. Hydrogen gas (20 bar) was applied and the reaction was stirred for 15 h at 50 °C. The crude reaction mixture was concentrated under reduced pressure and stirred with 10 mL 1M sodium hydroxide solution for 20 min. The suspension was filtered, and the yellow filtrate was acidified with hydrochloric acid (pH = 1). The white precipitate was filtered off, washed with water (2 × 30 mL), diethyl ether (3 × 50 mL) and was subsequently dried under reduced pressure: The Biginelli-acid **48** was obtained as a colorless solid (533 mg, 2.29 mmol, 92.5%).

IR (ATR): ν [cm^{-1}] = 3214,7 (br, ν(N-H)), 3087.0 (br, ν(N-H)), 2975.3 (w, ν(C-H), 1700.7 (s, ν(C=O)), 1643.2 (s, ν(C=O)), 1477.9 (m), 1421.7 (m), 1381.7 (w), 1325.1 (m),

1294.5 (w), 1266.7 (w), 1227.9 (vs), 1217.9 (vs), 1106.6 (w), 889.1 (w), 834.0 (w),753.3 (m), 692.1 (m), 651.8 (s), 613.9 (s), 565.5 (m), 522.6 (w), 483.3 (m), 393.4 (w).

^{1}H-NMR (300 MHz, DMSO-d_6): δ [ppm] = 11.80 (br s, 1 H, CO_2H^{9}), 9.09 (s, 1 H, NH^{17}), 7.68 (s, 1 H, NH^{3}), 7.53 – 7.00 (m, 5 H, CH_{Ar}^{12-16}), 5.12 (d, J = 3.0 Hz, 2 H, CH^{2}), 2.24 (s, 3 H, CH_3^{11}).

^{13}C-NMR (101 MHz, DMSO-d_6): δ [ppm] = 167.20 (s, CO_2H^{7}), 152.46 (s, CO^{4}), 147.78 (s, C^{5}), 144.85 (s, C_{Ar}^{10}), 128.40 (s, $CH_{Ar}^{12,16}$), 127.20 (s, CH_{Ar}^{14}), 126.28 (s, $CH_{Ar}^{13,15}$), 99.85 (s, C^{1}), 54.00 (s, CH^{2}), 17.79 (s, CH_3^{11}).

FAB – MS [m/z] (relative intensity): 233.0 (40%) $[M + H]^+$, 155.0 (100%) $[M – C_6H_5]^+$.

HRMS – FAB [m/z]: $[M + H]^+$ calculated for $^{12}C_{12}{}^{1}H_{13}{}^{16}O_3{}^{14}N_2$, 233.0921; found, 233.0922; Δ = 0.17 mmu.
^{1}H-NMR data is in accordance to earlier reported.[26]

6.2.2.1.3 ***Biginelli acid 49 derived from hydantoic acid, benzaldehyde and ethyl acetoacetate***

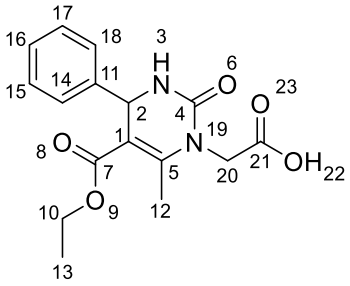

In a 50 mL round bottom flask, finely powdered *N*-carbomoylglycine (1.00 g, 8.46 mmol, 1.20 eq.) and benzaldehyde (748 mg, 7.06 mmol, 1.00 eq.) were suspended in 2.50 mL acetic acid/ethanol (3:1) (2.80 M for 1.00 eq.). Subsequently, ethyl acetoacetate (1.10 g, 8.46 mmol, 1.08 mL, 1.20 eq.) and 4-methylbenzenesulfonic acid (84.7 mg, 706 µmol, 0.10 eq.) were added. The resulting suspension was stirred at 40 °C for 1 h and then slowly heated to 80 °C and stirred for 4 h to obtain a yellow solution. TLC indicated complete conversion of benzaldehyde. The crude reaction mixture was added dropwise into 100 mL of water while stirring; the slurry was stirred for 1 h until a precipitate was formed, which was filtered off, crushed, washed with water (3 × 20 mL), dried and washed with *n*-hexane (3 × 20 mL).

The crude product was dried under reduced pressure yielding Biginelli acid **49** as a colorless solid (1.42 g, 5.33 mmol, 63.1%).

Spectral data is in accordance to earlier reported.[341]

IR (ATR): ν [cm^{-1}] = 3290.5 (br, ν(N-H)), 2979.6 (w, ν(C-H), 1725.4 (s, ν(C=O)), 1701.0 (s, ν(C=O)), 1631.2 (s, ν(C=O)), 1453.2 (m), 1402.1 (m), 1364.6 (w), 1311.5 (w), 1279.6 (w), 1233.7 (m), 1213.9 (m), 1181.0 (s), 1120.9 (m), 1058.7 (m), 945.1 (m), 830.0 (m), 783.9 (m), 747.3 (m), 701.6 (s), 679.9 (m), 623.3 (s), 522.3 (m), 483.3 (m), 419.1 (w).

^{1}H-NMR (300 MHz, DMSO-d_6): δ [ppm] = 12.90 (s, 1 H, CO_2H^{22}), 8.06 (d, J = 3.4 Hz, 1 H, NH^{3}), 7.40 – 7.17 (m, 5 H, CH_{Ar}^{14-18}), 5.19 (d, J = 3.1 Hz, 1 H, CH^{2}), AB-signal (δ A = 4.49, δ B = 4.35, J_{AB} = 18.0 Hz, CH_2^{20}), 4.03 (q, J = 7.1 Hz, 2 H, CH_2^{10}), 2.40 (s, 3 H, CH_3^{12}), 1.10 (t, J = 7.1 Hz, 3 H, CH_3^{13}).

^{13}C-NMR (100 MHz, DMSO-d_6): δ [ppm] = 171.06 (s, CO_2H^{21}), 165.57 (s, CO_2R^{7}), 152.33 (s, CO^{4}), 149.00 (s, C^{5}), 144.18 (s, C_{Ar}^{11}), 128.39 (s, $CH_{Ar}^{14,18}$), 127.43 (s, CH_{Ar}^{16}), 126.54 (s, $CH_{Ar}^{15,17}$), 102.92 (s, C^{1}), 59.66 (s, CH_2^{10}), 53.13 (s, CH^{2}), 43.95 (s, CH_2^{20}), 15.64 (s, CH_3^{12}), 14.01 (s, CH_3^{13}).

FAB – MS [*m/z*] (relative intensity): 319.1 (100%) $[M + H]^+$, 241.0 (25%) $[M - C_6H_5]^+$.

HRMS – FAB [*m/z*]: $[M + H]^+$ calculated for $^{12}C_{16}{}^{1}H_{19}{}^{16}O_5{}^{14}N_2$, 319.1288; found, 319.1290; Δ = 0.15 mmu.

6.2.2.1.4 ***Biginelli acid 50 derived from hydantoic acid, benzaldehyde and benzyl acetoacetate***

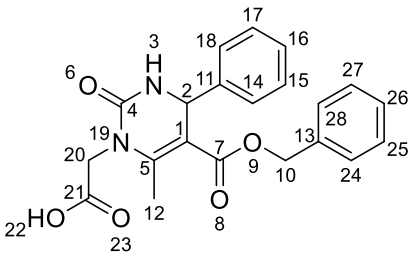

In a 25 mL round bottom flask finely powdered *N*-carbomoylglycine (4.00 g, 33.8 mmol, 1.20 eq.) and benzaldehyde (2.99 g, 28.2 mmol, 2.88 mL, 1.00 eq.) were suspended in 6 mL dimethyl sulfoxide (4.7 M for 1.00 eq.). Subsequently, benzyl acetoacetate

(4.40 g, 33.8 mmol, 4.32 mL) and 4-methylbenzenesulfonic acid (169 mg, 1.42 mmol, 0.05 eq.) were added. The resulting mixture was stirred at 110 °C for 48 h. Subsequently, the crude reaction mixture was added dropwise into 300 mL water while stirring. The suspension was stirred for 4 h until a precipitate was formed. The precipitate was filtered off, crushed and washed with water (4 × 50 mL), dried and washed again with *n*-hexane/ethyl acetate (4:1) (3 × 100 mL) and dried under reduced pressure in a desiccator over calcium chloride to yield the Biginelli acid **50** as a colorless solid (8.35 g, 21.9 mmol, 77.7%).

IR (ATR): ν [cm^{-1}] = 3258.6 (br, $\nu(CO_2H)$), 3077.5 (br, ν(N-H)), 2938.8 (w, ν(C-H), 1709.2 (s, ν(C=O)), 1649.3 (s, ν(C=O)), 1430.7 (m), 1403.4 (m), 1386.8 (m), 1356.9 (w), 1315.2 (w), 1277.7 (m), 1239.1 (m), 1222.4 (m), 1205.4 (s), 1181.7 (vs), 1114.2 (s), 1055.9 (m), 977.8 (w), 830.5 (w), 782.8 (m), 733.0 (w), 694.9 (s), 641.8 (m), 592.4 (w), 502.6 (w), 461.1 (w).

^{1}H-NMR (300 MHz, DMSO-d_6): δ [ppm] = 12.95 (br s, 1 H, OH^{22}), 8.08 (d, J = 3.5 Hz, 1 H, NH^{3}), 7.76 – 6.88 (m, 10 H, CH_{Ar}), 5.21 (d, J = 3.5 Hz, 1 H, CH^{2}), 5.06 (s, 2 H, CH_2^{10}), AB-signal (δ A = 4.50, δ B = 4.34, J_{AB} = 18.1 Hz, CH_2^{20}), 2.43 (s, 3 H, CH_3^{12}).

^{13}C-NMR (100 MHz, DMSO-d_6): δ [ppm] = 171.00 (s, CO_2H^{21}), 165.31 (s, CO_2R^{7}), 152.23 (s, CO^{4}), 149.97 (s, C^{5}), 143.95 (s, C_{Ar}^{11}), 136.29 (s, C_{Ar}^{13}), 128.40 (s, CH_{Ar}), 128.32 (s, CH_{Ar}), 127.83 (s, CH_{Ar}), 127.70 (s, CH_{Ar}), 127.45 (s, CH_{Ar}), 126.57 (s, CH_{Ar}), 102.38 (s, C^{1}), 65.27 (s, CH_2^{10}), 53.04 (s, CH^{2}), 43.99 (s, CH_2^{20}), 15.70 (s, CH_3^{12}).

FAB – MS [*m/z*] (relative intensity): 381.2 (35%) $[M + H]^+$, 321.2 (10%) $[M – C_2H_3O_2]^+$, 289.1 (25%) $[M – C_7H_7]^+$.

HRMS – FAB [*m/z*]: $[M + H]^+$ calculated for $^{12}C_{21}{}^{1}H_{21}{}^{16}O_5{}^{14}N_2$, 381.1445; found, 381.1146; Δ = 0.15 mmu.

6.2.2.1.5 *Biginelli acid 51 derived from 4-formylbenzoic acid, urea and ethyl acetoacetate*

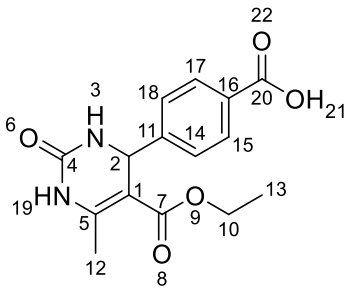

In a 25 mL round bottom flask, finely powdered urea (1.50 g, 24.9 mmol, 1.50 eq.) and 4-formylbenzoic acid (2.50 g, 16.6 mmol, 1.00 eq.) were suspended in 4 mL DMSO. Subsequently, ethyl acetoacetate (3.25 g, 24.9 mmol, 1.50 eq.) and 4-methylbenzenesulfonic acid (p-TSA) (200 mg, 1.65 mmol, 0.10 eq.) were added. The resulting mixture was stirred at 110 °C for 48 h and subsequently at 40 °C for 24 h. Subsequently, the crude reaction mixture was diluted with ethanol and added dropwise into 300 mL water. The suspension was stirred for 1 h until a precipitate was formed. The precipitate was filtered off, crushed, washed with water (3 × 20 mL) and dried. Afterwards, the precipitate was washed with *n*-hexane (3 × 20 mL). After drying under reduced pressure in a desiccator over calcium chloride, the Biginelli acid **51** was obtained as a colorless solid (4.57 g, 15.1 mmol, 90.1%).

IR (ATR): ν [cm^{-1}] = 3309.4 (br, ν(O-H)), 3206.7 (br, ν(N-H)), 3084.8 (br, ν(N-H)), 2971.9 (br, ν(C-H), 1723.3 (s, ν(C=O)), 1702.5 (s, ν(C=O)), 1649.1 (s, ν(C=O)), 1608.9 (m), 1474.3 (m), 1419.7 (w), 1379.8 (w), 1317.7 (w), 1288.1 (w), 1225.0 (vs), 1170.0 (m), 1087.6 (s), 1018.3 (m), 875.7 (w), 843.2 (w), 792.4 (m), 754.5 (s), 700.5 (m), 667.9 (w), 638.1 (s), 568.9 (w), 527.2 (w), 501.4 (w), 466.9 (w), 408.5 (w).

^{1}H-NMR (300 MHz, DMSO-*d*$_6$): δ [ppm] = 12.90 (s, 1 H, CO_2H^{21}), 9.27 (s, 1 H, NH^{19}), 7.91 (d, *J* = 7.8 Hz, 2 H, $CH_{Ar}^{15,17}$), 7.81 (s, 1 H, NH^{3}), 7.35 (d, *J* = 7.9 Hz, 2 H, $CH_{Ar}^{14,18}$), 5.21 (d, *J* = 2.8 Hz, 1 H, CH^{2}), 3.97 (q, *J* = 6.9 Hz, 2 H, CH_2^{10}), 2.25 (s, 3 H, CH_3^{12}), 1.08 (t, *J* = 7.1 Hz, 3 H, CH_3^{13}).

^{13}C-NMR (75 MHz, DMSO-*d*$_6$): δ [ppm] = 167.13 (s, CO_2H^{20}), 165.24 (s, CO_2R^{7}), 152.00 (s, CO^{4}), 149.57 (s, C^{5}), 148.91 (s, C_{Ar}^{11}), 129.84 (s, C_{Ar}^{16}), 129.66 (s, $CH_{Ar}^{15,17}$), 126.56 (s, $CH_{Ar}^{14,18}$), 98.71 (s, C^{1}), 59.32 (s, CH_2^{10}), 53.93 (s, CH^{2}), 17.88 (s, CH_3^{12}), 14.10 (s, CH_3^{13}).

FAB – MS [*m/z*] (relative intensity): 305.1 (100%) $[M + H]^+$.

HRMS – FAB [*m/z*]: $[M + H]^+$ calculated for $^{12}C_{15}{}^{1}H_{17}{}^{16}O_5{}^{14}N_2$, 305.1132; found, 305.1131; Δ = 0.12 mmu.
NMR spectral data is in accordance to earlier reported.[342]

6.2.2.1.6 *Biginelli acid 52 derived from 4-formylbenzoic acid, urea and benzyl acetoacetate*

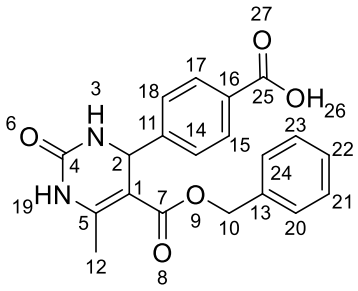

In a 25 mL round bottom flask finely powdered urea (1.50 g, 24.9 mmol, 1.50 eq.) and 4-formylbenzoic acid (2.50 g, 16.6 mmol, 1.00 eq.) were suspended in 4 mL dimethyl sulfoxide. Subsequently, benzyl acetoacetate (3.84 g, 20.0 mmol, 1.20 eq.) and 4-methylbenzenesulfonic acid (200 mg, 1.65 mmol, 0.10 eq.) were added. The resulting mixture was stirred at 110 °C for 48 h and subsequently at 40 °C for 24 h. Subsequently, the crude reaction mixture was diluted with ethanol and added dropwise into 300 mL water. The suspension was stirred for 1 h until a precipitate was formed. The precipitate was separated, washed with water (3 × 20 mL) and dried. Afterwards the precipitate was washed with *n*-hexane (3 × 20 mL). After drying in a desiccator over calcium chloride the Biginelli acid **52** was obtained as a colorless solid (5.55 g, 15.2 mmol, 91.0%).

IR (ATR): ν [cm^{-1}] = 3273.7 (br, ν(O-H)), 3068.9 (br, ν(N-H)), 2931.0 (w, ν(C-H), 1678.3 (s, ν(C=O)), 1642.6 (s, ν(C=O)), 1608.6 (m), 1466.5 (m), 1381.5 (m), 1325.2 (m), 1275.3 (m), 1228.5 (s), 1090.8 (s), 1017.7 (w), 953.9 (w), 909.7 (w), 860.3 (w), 773.3 (m), 738.2 (m), 694.8 (m), 665.2 (m), 642.2 (w), 577.3 (w), 518.3 (m), 504.9 (m), 452.8 (w), 394.7 (w).

^{1}H-NMR (400 MHz, DMSO-d_6): δ [ppm] = 12.92 (s, 1 H, CO_2H^{26}), 9.35 (d, J = 1.4 Hz, 1 H, NH^{19}), 7.88 (d, J = 8.3 Hz, 3 H, CH_{Ar}), 7.85 – 7.83 (m, 1 H, NH^{3}), 7.32 (d, J = 8.3

Hz, 2 H, $CH_{Ar}^{14,18}$), 7.30 – 7.25 (m, 3 H, CH_{Ar}), 7.19 – 7.08 (m, 2 H, CH_{Ar}), 5.24 (d, *J* = 3.2 Hz, 1 H, CH^{2}), 5.15 – 4.90 (m, 2 H, CH_2^{10}), 2.28 (s, 3 H, CH_3^{12}).

^{13}C-NMR (101 MHz, DMSO-d_6): δ [ppm] = 167.10 (s, CO_2H^{25}), 164.96 (s, CO_2R^{7}), 151.83 (s, CO^{4}), 149.76 (s, C^{5}), 149.33 (s, C_{Ar}^{16}), 136.46 (s, C_{Ar}^{11}), 129.86 (s, C_{Ar}^{13}), 129.66 (s, CH_{Ar}), 128.28 (s, CH_{Ar}), 127.79 (s, CH_{Ar}), 127.66 (s, CH_{Ar}), 126.57 (s, CH_{Ar}), 98.20 (s, C^{1}), 64.91 (s, CH_2^{10}), 53.87 (s, CH^{2}), 17.95 (s, CH_3^{12}).

FAB – MS [*m/z*] (relative intensity): 367.1 (100%) $[M + H]^+$.

HRMS – FAB [*m/z*]: $[M + H]^+$ calculated for $^{12}C_{20}{}^{1}H_{19}{}^{16}O_5{}^{14}N_2$, 367.1288; found, 367.1289; Δ = 0.05 mmu.

6.2.2.2 Passerini reactions of Biginelli acids

6.2.2.2.1 *Passerini product 53 derived from Biginelli acid 51, tert-butyl isocyanide and heptanal*

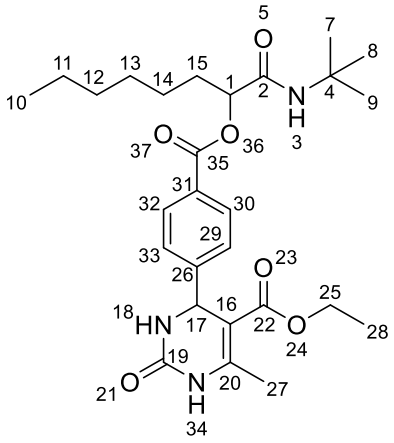

In a tube vial, finely powdered Biginelli-acid **51** (300 mg, 986 µmol, 1.00 eq.) was dissolved in 0.5 mL dimethyl sulfoxide and diluted with 0.9 mL dichloromethane. Subsequently, heptanal (169 mg, 1.48 mmol, 205 µL, 1.50 eq.) and *tert*-butylisocyanide (123 mg, 1.48 mmol, 142 µL, 1.50 eq.) were added. The mixture was and stirred at room temperature for 2 d. Subsequently, the crude reaction mixture was added dropwise into a stirred mixture of 10 mL water and 10 mL dichloromethane. The aqueous phase was extracted with 10 mL dichloromethane three times. The combined organic phases were concentrated under reduced pressure. The concentrate was added dropwise into 30 mL of *n*-hexane/ethyl acetate (4:1) while

stirring. After stirring for 1 h, a precipitate was formed, which was separated, washed with 30 mL *n*-hexane three times and dried under reduced pressure. The Passerini product **53** was obtained as a colorless solid (332 mg, 661 µmol, 67.1%).

IR (ATR): ν [cm^{-1}] = 3292.8 (br, ν(N-H)), 3086.2 (br, ν(N-H)), 2926.6 (m, ν(C-H), 1704.6 (vs, ν(C=O)), 1645.3 (s, ν(C=O)), 1607.6 (w), 1554.3 (w), 1453.5 (m), 1426.2 (m), 1407.4 (w), 1364.5 (w), 1312.9 (m), 1262.7 (m), 1219.1 (vs), 1179.6 (w), 1099.6 (s), 1017.2 (w), 949.2 (w), 868.2 (w), 825.6 (w), 763.5 (m), 706.7 (m), 654.5 (m), 605.5 (w), 522.6 (w), 456.2 (w).

^{1}H-NMR (300 MHz, DMSO-d_6): δ [ppm] = 9.29 (s, 1 H, NH^{34}), 7.94 (d, J = 7.8 Hz, 2 H, CH$_{Ar}^{32,30}$), 7.84 (s, 1 H, NH^{18}), 7.63 (s, 1 H, NH^{3}), 7.39 (d, J = 7.8 Hz, 2 H, CH$_{Ar}^{29,33}$), 5.22 (s, 1 H, CH^{17}), 4.98 (s, 1 H, CH^{1}), 3.98 (q, J = 6.9 Hz, 2 H, CH^{25}), 2.26 (s, 3 H, CH$_3^{27}$), 1.86 – 1.60 (m, 2 H, CH$_2^{15}$), 1.43 – 1.16 (m, 19 H, CH$_2$+CH$_3^{7-9}$), 1.09 (t, J = 6.9 Hz, 4 H, CH$_3^{28}$), 0.93 – 0.74 (m, 3 H, CH$_3^{10}$).

^{13}C-NMR (75 MHz, DMSO-d_6): δ [ppm] = 168.51 (s, CONR^{2}), 165.16 (s, CO$_2$R^{22}), 164.92 (s, CO$_2$R^{35}), 151.92 (s, CO^{19}), 150.10 (s, C^{20}), 148.97 (s, C$_{Ar}^{26}$), 129.62 (s, CH$_{Ar}^{30,32}$), 128.67 (s, C$_{Ar}^{31}$), 126.66 (s, CH$_{Ar}^{29,33}$), 98.57 (s, C^{16}), 74.04 (s, CH^{1}), 59.29 (s, CH$_2^{25}$), 53.90 (s, CH^{17}), 50.22 (s, C^{4}), 31.65 (s, CH$_2$), 31.12 (s, CH$_2$), 28.45 (s, CH$_3^{7-9}$), 28.36 (s, CH$_2$), 24.63 (s, CH$_2$), 22.00 (s, CH$_2$), 17.82 (s, CH$_3^{27}$), 14.08 (s, CH$_3^{28}$), 13.91 (s, CH$_3^{10}$).

FAB – MS [*m/z*] (relative intensity): 502.3 (30%) [M + H]$^+$, 456.3 (10%) [M – C$_2$H$_5$O]$^+$, 287.1 (100%) [Fragment A]$^+$.

HRMS – FAB [*m/z*]: [M + H]$^+$ calculated for ^{12}C$_{27}$^{1}H$_{40}$^{16}O$_6$^{14}N$_3$, 502.2912; found, 502.2911; Δ = 0.08 mmu.

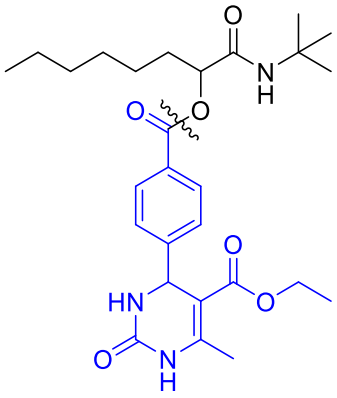

Fragment A
Chemical Formula: $C_{15}H_{15}N_2O_4^{\bullet}$
Exact Mass: 287,10318

6.2.2.2.2 *Passerini product 54 derived from Biginelli acid 52, tert-butyl isocyanide and heptanal*

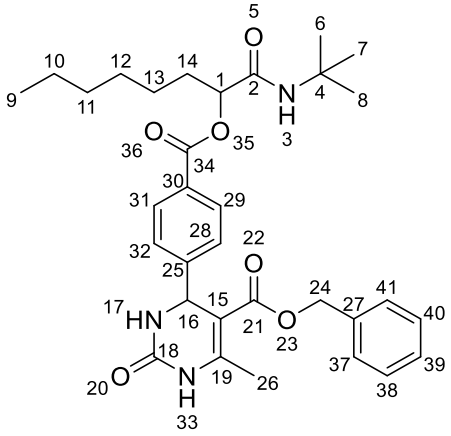

In a tube vial, finely powdered Biginelli-acid **52** (300 mg, 819 µmol, 1.00 eq.) was dissolved in 1.5 mL dimethyl sulfoxide and diluted with 1.5 mL dichloromethane. Subsequently, heptanal (140 mg, 1.23 mmol, 171 µL, 1.50 eq.) and *tert*-butylisocyanide (102 mg, 1.23 mmol, 118 µL, 1.50 eq.) were added. The mixture was stirred at room temperature for 4 d. Subsequently, the crude reaction mixture was added dropwise into a stirred mixture of 10 mL water and 10 mL ethyl acetate. The aqueous phase was extracted with 10 mL ethyl acetate three times. The combined organic phases were concentrated under reduced pressure. The concentrate was purified *via* column chromatography employing silica gel and eluting with a gradual solvent mixture of ethyl acetate/*c*-hexane (1:3 → 1:0). The Passerini product **54** was obtained as a colorless solid (103 mg, 182 µmol, 22.3%).

IR (ATR): ν [cm^{-1}] = 3233.8 (br, ν(N-H)), 3089.1 (br, ν(N-H)), 2926.9 (m, ν(C-H), 2858.2 (w, ν(C-H), 1697.2 (s, ν(C=O)), 1639.5 (s, ν(C=O)), 1523.2 (w), 1453.7 (m), 1380.0 (w), 1314.7 (w), 1261.5 (s), 1219.1 (vs), 1074.3 (s), 1017.6 (w), 859.8 (w), 825.0 (w), 794.6 (w), 753.0 (w), 696.2 (m), 651.6 (w), 586.2 (w), 524.7 (w), 491.7 (w), 438.9 (w).

^{1}H-NMR (300 MHz, DMSO-d_6): δ [ppm] = 9.35 (s, 1 H, NH^{33}), 7.90 (d, J = 7.4 Hz, 2 H, CH$_{Ar}$^{29,31}), 7.85 (s, 1 H, NH^{17}), 7.64 (s, 1 H, NH^{3}), 7.34 (d, J = 8.0 Hz, 2 H, CH$_{Ar}$^{28,32}), 7.26 (d, J = 4.4 Hz, 3 H, CH$_{Ar}$), 7.17 – 7.08 (m, 2 H, CH$_{Ar}$), 5.25 (d, J = 2.8 Hz, 1 H, CH^{16}), 5.07 – 4.94 (m, 3 H, CH^{1} + CH$_2$^{24}), 2.28 (s, 3 H, CH$_3$^{26}), 1.91 – 1.66 (m, 2 H, CH$_2$^{14}), 1.45 – 1.13 (m, 19 H, CH$_3$$^{6-8}$ + CH$_2$), 0.84 (d, J = 6.4 Hz, 3 H, CH$_3$^{9}).

^{13}C-NMR (75 MHz, DMSO-d_6): δ [ppm] = 168.50 (s, CONR^{2}), 164.91 (s, CO$_2$R^{34}), 151.71 (s, CO^{18}), 149.85 (s, C$_{Ar}$^{25}), 149.80 (s, CO$_2$R^{21}), 136.45 (s, C$_{Ar}$^{27}), 129.65 (s, CH$_{Ar}$^{29,31}), 128.69 (s, C$_{Ar}$^{30}), 128.26 (s, CH$_{Ar}$), 127.70 (s, CH$_{Ar}$), 127.63 (s, CH$_{Ar}$), 126.70 (s, CH$_{Ar}$^{28,32}), 98.05 (s, C^{15}), 74.02 (s, CH^{1}), 64.84 (s, CH$_2$^{24}), 53.89 (s, CH^{16}), 50.22 (s, C^{4}), 31.65 (s, CH$_2$), 31.13 (s, CH$_2$), 28.45 (s, CH$_3$$^{6-8}$), 28.34 (s, CH$_2$), 24.64 (s, CH$_2$), 21.99 (s, CH$_2$), 17.90 (s, CH$_3$^{26}), 13.92 (s, CH$_3$^{9}).

FAB – MS [m/z] (relative intensity): 564.3 (20%) [M + H]$^+$, 456.3 (15%) [M – C$_7$H$_7$O]$^+$, 349.1 (80%) [Fragment A]$^+$, 214.0 (10%) [Fragment B]$^+$.

HRMS – FAB [m/z]: [M + H]$^+$ calculated for ^{12}C$_{32}$^{1}H$_{42}$^{16}O$_6$^{14}N$_3$, 564.3068; found, 564.3069; Δ = 0.09 mmu.

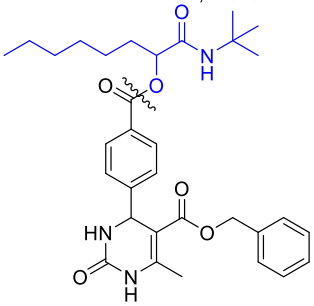

6.2.2.2.3 *Passerini product 55 derived from Biginelli acid 51, cyclohexyl isocyanide and 2-phenylpropanal*

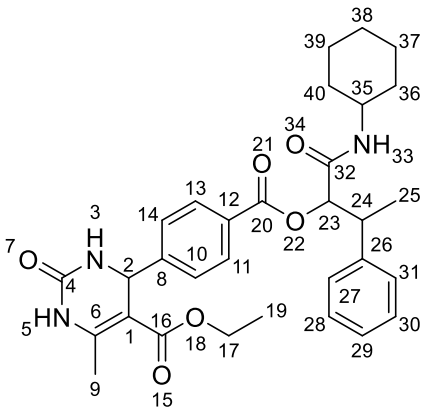

In a tube vial, finely powdered Biginelli-acid **51** (300 mg, 986 µmol, 1.00 eq.) was dissolved in 0.3 mL dimethyl sulfoxide with 2.00 mL dichloromethane. Subsequently, 2-phenylpropanal (172 mg, 1.28 mmol, 1.30 eq.) and then cyclohexyl isocyanide (139 mg, 1.28 mmol, 1.30 eq.) were added. The mixture was stirred at room temperature for 3 d. Subsequently, the crude reaction mixture was concentrated under reduced pressure and purified *via* column chromatography employing silica gel and eluting with a gradual solvent mixture of ethyl acetate/*c*-hexane (1:2 → 1:0). The Passerini product **55** was obtained as a colorless solid (536 mg, 969 µmol, 98.3%).

R_f = 0.37 in ethyl acetate

IR (ATR): ν [cm^{-1}] = 3270.2 (br, ν(N-H)), 2929.4 (w, ν(C-H)), 2853.0 (w, ν(C-H)), 1701.9 (vs, ν(C=O)), 1642.7 (vs, ν(C=O)), 1536.9 (w), 1449.3 (w), 1367.3 (w), 1266.6 (m), 1220.8 (vs, ν(COOR)), 1085.3 (vs, ν(COOR)), 1017.3 (m), 761.3 (m), 699.4 (s), 652.2 (w), 526.0 (w), 459.2 (w).

^{1}H-NMR (600 MHz, DMSO-d_6): δ [ppm] = 9.26 (d, J = 14.0 Hz, 1 H, NH^{5}), 8.03 (t, J = 7.1 Hz, 0.5 H, NH^{33a}), 7.95 (dd, J = 8.3, 1.8 Hz, 1 H, CH$_{Ar}$^{13,11a}), 7.89 (d, J = 7.9 Hz, 0.5 H, NH^{33b}), 7.83 – 7.77 (m, 2 H, CH$_{Ar}$^{13,11b} + NH^{3}), 7.38 (dd, J = 16.3, 7.9 Hz, 2 H, CH$_{Ar}$), 7.33 (d, J = 8.2 Hz, 2 H, CH$_{Ar}$), 7.31 – 7.25 (m, 2 H, CH$_{Ar}$), 7.20 – 7.16 (m, 1 H, CH$_{Ar}$), 5.24 – 5.17 (m, 1 H, CH^{2}), 5.14 (dd, J = 11.0, 3.6 Hz, 1 H, CH^{23}), 3.98 (dq, J = 14.0, 7.1 Hz, 2 H, CH$_2$^{17}), 3.58 – 3.45 (m, 1 H, CH^{35}), 3.43 – 3.28 (m, 1 H, CH^{24}), 2.28 – 2.21 (m, 3 H, CH$_3$^{9}), 1.63 (m, 5 H, CH$_2$$^{c\text{-}hex}$), 1.31 (dd, J = 46.8, 6.5 Hz, 3 H, CH$_3$^{25}), 1.20 (dt, J = 14.2, 7.7 Hz, 5 H, CH$_2$$^{c\text{-}hex}$), 1.13 – 1.04 (m, 3 H, CH$_3$^{19}).

^{13}C-NMR (75 MHz, DMSO-d_6): δ [ppm] = 166.91 (s, CONR^{32}), 166.72 (s, CONR^{32}), 165.15 (s, CO_2R^{20}), 164.76 (s, CO_2R^{20}), 164.68 (s, CO_2R^{16}), 151.88 (s, CO^{4}), 151.83 (s, CO^{4}), 150.14 (s, C_{Ar}^{12}), 148.93 (s, C^{6}), 142.60 (s, C_{Ar}^{26}), 142.27 (s, C_{Ar}^{26}), 129.69 (s, CH_{Ar}), 129.52 (s, CH_{Ar}), 128.44 (s, CH_{Ar}), 128.30 (s, CH_{Ar}), 128.13 (s, CH_{Ar}), 128.10 (s, CH_{Ar}), 127.78 (s, CH_{Ar}), 126.64 (s, CH_{Ar}), 126.56 (s, CH_{Ar}), 98.57 (s, C^{1}), 98.51 (s, C^{1}), 78.18 (s, CH^{23}), 77.65 (s, CH^{23}), 59.26 (s, CH_2^{17}), 53.87 (s, CH^{2}), 47.46 (s, CH^{35}), 41.15 (s, CH^{24}), 40.98 (s, CH^{24}), 32.25 (s, $CH_2^{c\text{-}hex}$), 32.13 (s, $CH_2^{c\text{-}hex}$), 25.14 (s, $CH_2^{c\text{-}hex}$), 24.56 (s, $CH_2^{c\text{-}hex}$), 24.47 (s, $CH_2^{c\text{-}hex}$), 17.79 (s, CH_3^{9}), 17.70 (s, CH_3^{25}), 17.66 (s, CH_3^{25}), 14.87 (s, CH_3^{25}), 14.80 (s, CH_3^{25}), 14.06 (s, CH_3^{19}), 14.04 (s, CH_3^{19}).

FAB – MS [*m/z*] (relative intensity): 548.3 (40%) $[M + H]^+$, 502.2 (5%) $[M - C_2H_5O]^+$, 303.1 (5%) [Fragment C]$^+$, 287.1 (100%) [Fragment A – H]$^+$, 244.1 (20%) [Fragment B]$^+$, 183.1 (20%) [Fragment D]$^+$.

HRMS – FAB [*m/z*]: $[M + H]^+$ calculated for $^{12}C_{31}{}^{1}H_{38}{}^{16}O_6{}^{14}N_3$, 548.2755; found, 548.2755; Δ = 0.05 mmu.

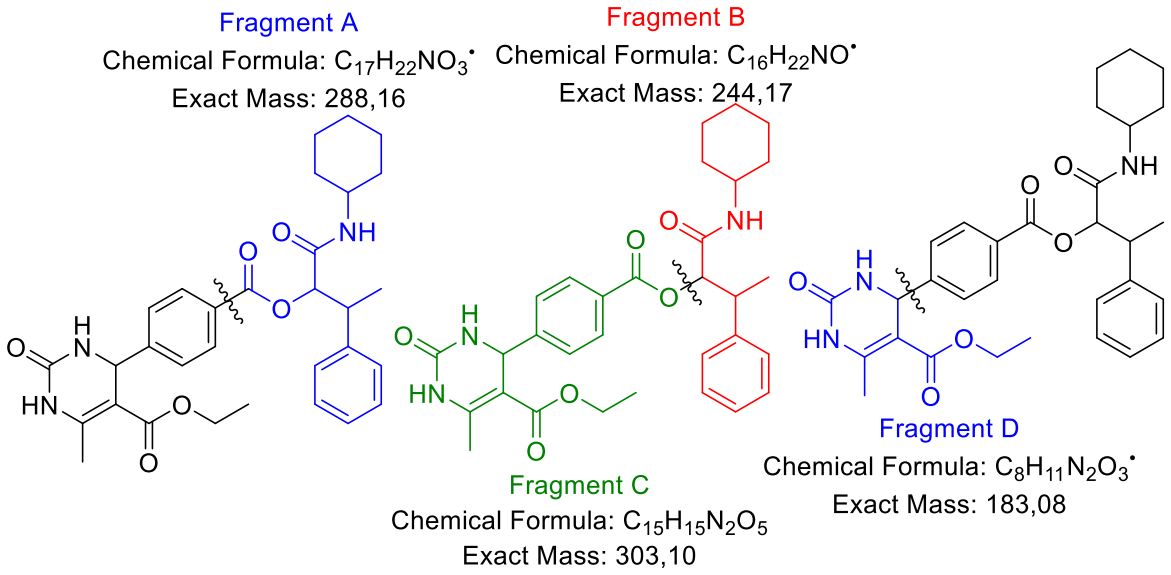

6.2.2.2.4 *Passerini product 56 derived from Biginelli-acid 49, iso-butyl aldehyde and tert-butyl isocyanide*

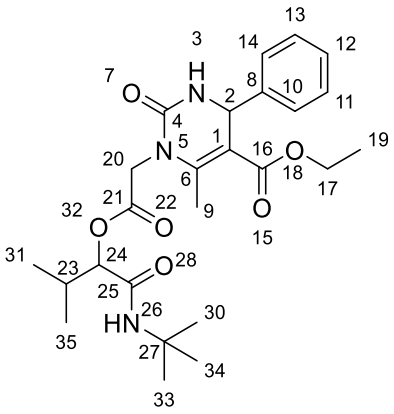

In a 5 mL round bottom flask, finely powdered Biginelli-acid **49** (500 mg, 1.57 mmol, 1.20 eq.) was dissolved in a minimal amount of dimethyl sulfoxide (0.5 mL). Subsequently, *iso*-butyraldehyde (123 mg, 1.73 mmol, 157 µL, 1.10 eq.) and *tert*-butyl isocyanide (131 mg, 1.57 mmol, 150 µL) were added. The mixture was diluted with dichloromethane (0.5 mL) and stirred at room temperature for 6 h. Subsequently, a second portion of aldehyde (56.6 mg, 0.50 eq.) and isocyanide (65.3 mg, 0.50 eq.) were added. The resulting mixture was stirred for 3 d at room temperature. The crude reaction mixture was added dropwise into a stirred mixture of 50 mL water and 50 mL dichloromethane. The organic phase was separated, dried over sodium sulfate and concentrated under reduced pressure. The solid residue was purified *via* column chromatography on silica gel eluting with a gradual solvent mixture of *c*-hexane and diethyl ether (1:0 → 0:1). The Passerini product **56** was obtained as a colorless solid (563 mg, 1.18 µmol, 75.6%).

IR (ATR): ν [cm^{-1}] = 3316.3 (br, ν(O-H)), 2964.6 (m, ν(C-H)), 2161.3 (w), 1751.9 (w, ν(C=O)), 1681.3 (vs, ν(C=O)), 1528.6 (s), 1454.1 (s), 1386.6 (m), 1309.8 (w), 1178.0 (vs), 1104.3 (s), 1056.6 (m), 1015.2 (m), 940.6 (w), 760.3 (w), 698.2 (m).

^{1}H-NMR (400 MHz, DMSO-d_6): δ [ppm] = 8.18 (dd, J = 15.1, 3.7 Hz, 1 H, NH^{3}), 7.42 (d, J = 32.9 Hz, 1 H, NH^{26}), 7.34 – 7.22 (m, 5 H, CH$_{Ar}^{10-14}$), 5.20 (t, J = 3.8 Hz, 1 H, CH^{2}), 4.71 – 4.40 (m, 3 H, CH^{24} + CH$_2^{20}$), 4.02 (q, J = 7.0, 2 H, CH$_2^{17}$), 2.41 (s, 3 H, CH$_3^{9}$), 2.15 – 1.90 (m, 1 H, CH^{23}), 1.28 – 1.24 (m. 10 H, CH$_3^{30,33,34}$), 1.10 (t, J = 7.1 Hz, 3 H, CH$_3^{19}$), 0.91 – 0.82 (m, 6 H, CH$_3^{31,35}$), 0.74 (d, J = 6.8 Hz, 1 H).

^{13}C-NMR (75 MHz, DMSO-d_6): δ [ppm] = 172.59 (s), 169.00 (s, CO_2R^{21}), 168.98 (s, CO_2R^{21}), 167.45 (s, $CONR^{25}$), 165.50 (s, CO_2R^{16}), 165.44 (s, CO_2R^{16}), 152.60 (s, CO^{4}), 152.43 (s, CO^{4}), 149.06 (s, C^{6}), 148.80 (s, C^{6}), 143.98 (s, C_{Ar}^{8}), 143.83 (s, C_{Ar}^{8}), 128.41 (s, $CH_{Ar}^{10,14}$), 128.40 (s, $CH_{Ar}^{10,14}$), 127.46 (s, CH_{Ar}^{12}), 127.44 (s, CH_{Ar}^{12}), 126.43 (s, $CH_{Ar}^{11,13}$), 126.38 (s, $CH_{Ar}^{11,13}$), 103.25 (s, C^{1}), 103.12 (s, C^{1}), 78.52 (s, CH^{24}), 78.17 (s, CH^{24}), 59.72 (s, CH_2^{17}), 59.68 (s, CH_2^{17}), 53.02 (s, CH^{2}), 52.93 (s, CH^{2}), 50.39 (s, C^{27}), 50.30 (s, C^{27}), 49.74 (s, C), 44.18 (s, CH_2^{20}), 31.24 (s), 30.04 (s, CH^{23}), 29.88 (s, CH^{23}), 28.46 (s, $CH_3^{30,33,34}$), 28.37 (s, $CH_3^{30,33,34}$), 28.35 (s, $CH_3^{30,33,34}$), 19.21 (s, $CH_3^{31,35}$), 18.59 (s, $CH_3^{31,35}$), 18.55 (s, $CH_3^{31,35}$), 16.95 (s, $CH_3^{31,35}$), 16.78 (s, $CH_3^{31,35}$), 15.54 (s, CH_3^{9}), 15.50 (s, CH_3^{9}), 13.95 (s, CH_3^{19}).

FAB – MS [*m/z*] (relative intensity): 474.3 (100%) $[M + H]^+$, 428.2 (30%) $[M – C_2H_5O]^+$. HRMS – FAB [*m/z*]: $[M + H]^+$ calculated for $^{12}C_{25}{}^{1}H_{36}{}^{16}O_6{}^{14}N_3$, 474.2599; found, 474.2600; Δ = 0.11 mmu.

6.2.2.2.5 ***Passerini product 57 derived from Biginelli-acid 49, undec-10-enal and tert-butyl isocyanide***

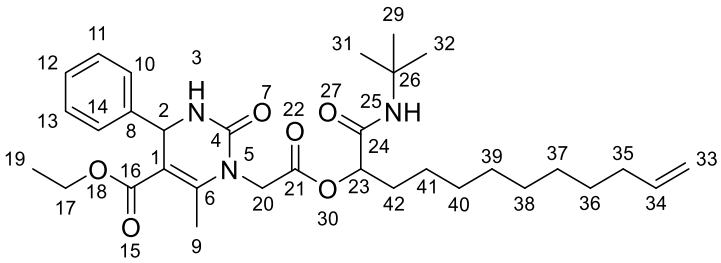

In a 5 mL round bottom flask, finely powdered Biginelli-acid **49** (500 mg, 1.57 mmol, 1.20 eq.) was dissolved in 1 mL dimethyl sulfoxide/dichloromethane (1:1). Subsequently, undec-10-enal (344 mg, 2.04 mmol, 409 µL, 1.30 eq.) and *tert*-butylisocyanide (170 mg, 2.04 mmol, 196 µL) were added. The mixture was diluted with dichloromethane (0.5 mL) and stirred at room temperature for 8 h. Subsequently, a second portion of aldehyde (79.3 mg, 0.30 eq.) and isocyanide (39.2 mg, 0.30 eq.) were added to the mixture and stirred at room temperature for 3 d. The crude reaction mixture was added dropwise into a stirred emulsion of 50 mL water and 50 mL dichloromethane. The organic phase was separated, dried over sodium sulfate and dried under reduced pressure. The oily residue was purified *via* column chromatography on silica gel eluting with a gradual solvent mixture of *c*-hexane and

diethyl ether (0:1 → 1:0). The Passerini product **57** was obtained as a colorless oil (893 mg, 1.56 mmol, 99.7%).

IR (ATR): ν [cm^{-1}] = 3323.2 (br, ν(N-H)), 2924.7 (m, ν(C-H)), 2853.1 (w, ν(C-H)), 1752.5 (w, ν(C=O)), 1681.5 (vs, ν(C=O)), 1529.2 (m), 1453.7 (m), 1385.8 (m), 1364.8 (m), 1309.4 (w), 1278.1 (w), 1257.7 (w), 1176.3 (vs), 1103.6 (s), 1056.2 (m), 941.7 (w), 909.0 (w), 861.3 (w), 828.5 (w), 759.6 (m), 697.5 (s), 651.6 (w).

^{1}H-NMR (400 MHz, DMSO-d_6): δ [ppm] = 8.16 (dd, J = 16.9, 3.6 Hz, 1 H, NH^{3}), 7.43 (d, J = 11.2 Hz, 1 H, NH^{25}), 7.34 – 7.21 (m, 5 H, CH_{Ar}^{10-14}), 5.84 – 5.73 (m, 1 H, CH^{34}), 5.19 (t, J = 3.5 Hz, 1 H, CH^{2}), 5.02 – 4.91 (m, 2 H, CH_2^{33}), 4.84 (t, J = 6.3 Hz, 1 H, CH^{23}), 4.74 – 4.40 (m, 2 H, CH_2^{20}), 4.06 – 3.96 (m, 2 H, CH_2^{17}), 2.43 (d, J = 17.4 Hz, 3 H, CH_3^{9}), 2.00 (q, J = 6.9 Hz, 2 H, CH_2^{35}), 1.69 – 1.61 (m, 2 H, CH_2^{42}), 1.27 – 1.21 (m, 21 H, $CH_3^{29,31,32}$ + CH_2^{36-41}), 1.14 – 1.07 (t, J = 7.1 Hz, 3 H, CH_3^{19}).

^{13}C-NMR (100 MHz, DMSO-d_6): δ [ppm] = 168.95 (s, CO_2R^{21}),), 168.88 (s, CO_2R^{21}),), 168.14 (s, $CONR^{24}$), 165.43 (s, CO_2R^{16}), 165.41 (s, CO_2R^{16}), 152.49 (s, CO^{4}), 152.27 (s, CO^{4}), 148.84 (s, C^{6}), 148.76 (s, C^{6}), 144.05 (s, C_{Ar}^{8}), 143.87 (s, C_{Ar}^{8}), 138.79 (s, CH^{34}), 128.38 (s, $CH_{Ar}^{10,14}$), 128.34 (s, $CH_{Ar}^{10,14}$), 127.41 (s, CH_{Ar}^{12}), 126.49 (s, $CH_{Ar}^{11,13}$), 126.38 (s, $CH_{Ar}^{11,13}$), 114.60 (s, CH_2^{33}), 103.21 (s, C^{1}), 103.19 (s, C^{1}), 74.31 (s, CH^{23}), 74.16 (s, CH^{23}), 59.65 (s, CH_2^{17}), 53.15 (s, CH^{2}), 52.95 (s, CH^{2}), 50.30 (s, C^{26}), 50.26 (s, C^{26}), 44.03 (s, CH_2^{20}), 33.17 (s, CH_2^{35}), 31.37 (s, CH_2^{42}), 31.28 (s, CH_2^{42}), 28.79 (s, CH_2), 28.75 (s, CH_2), 28.65 (s, CH_2), 28.54 (s, CH_2), 28.51 (s, CH_2), 28.45 (s), 28.34 (s, $CH_3^{29,31,32}$), 28.24 (s, CH_2^{41}), 26.32 (s, CH_2^{41}), 24.31 (s,CH_2), 24.27 (s, CH_2^{41}), 15.53 (s, CH_3^{9}), 15.48 (s, CH_3^{9}), 13.93 (s, CH_3^{19}).

FAB – MS [*m/z*] (relative intensity): 570.4 (55%) $[M + H]^+$, 524.3 (35%) $[M - C_2H_5O]^+$, 492.3 (10%) $[M - C_6H_5]^+$, 317.1 (65%) [Fragment A]$^+$, 273.1 (35%) [Fragment B]$^+$.

HRMS – FAB [*m/z*]: $[M + H]^+$ calculated for $^{12}C_{32}{}^{1}H_{48}{}^{16}O_6{}^{14}N_3$, 570.3538; found, 570.3538; Δ = 0.04 mmu.

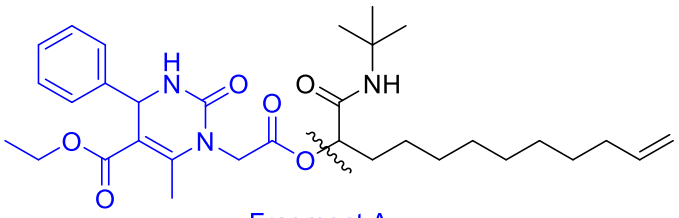

Fragment A
Chemical Formula: $C_{16}H_{17}N_2O_5$•
Exact Mass: 317,11375

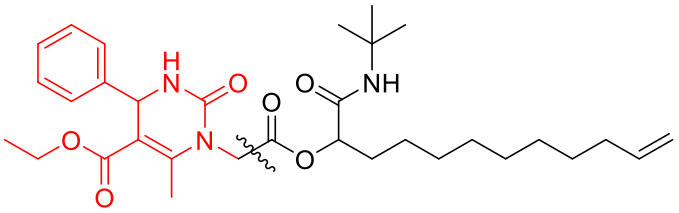

Fragment B
Chemical Formula: $C_{15}H_{17}N_2O_3$•
Exact Mass: 273,12392

6.2.2.2.6 *Passerini compound 58 derived from Biginelli acid 49, octanal and benzyl isocyanide.*

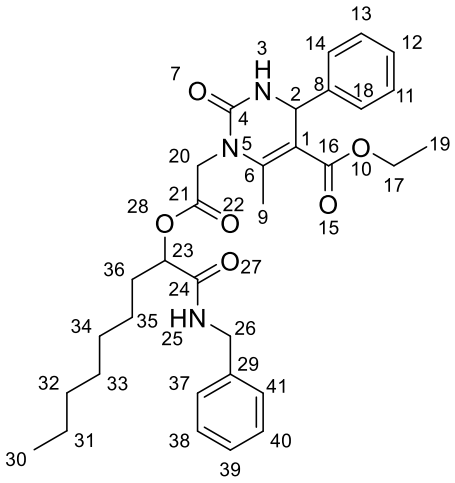

In a tube vial, finely powdered Biginelli-acid **49** (302 mg, 949 µmol, 1.00 eq.) was dissolved in 0.3 mL dimethyl sulfoxide and diluted with 1.0 mL dichloromethane. Subsequently, octanal (178 mg, 1.38 mmol, 217 µL, 1.40 eq.) and benzyl isocyanide (150 mg, 1.28 mmol, 156 µL, 1.30 eq.) were added. The mixture was stirred at room temperature for 3 d. The crude product was purified *via* column chromatography employing silica gel and eluting with a gradual solvent mixture of ethyl acetate and *c*-hexane (1:9 → 1:0). The Passerini product **58** was obtained as a white solid (405 mg, 715 µmol, 76.2%).

IR (ATR): ν [cm^{-1}] = 3279.1 (br, ν(N-H)), 2922.5 (w, ν(C-H)), 2852.7 (w, ν(C-H)), 1737.0 (w, ν(C=O)), 1709.5 (m, ν(C=O), 1681.3 (vs, ν(C=O)), 1662.1 (vs, ν(C=O)), 1613.8 (s,

ν(C=O)), 1541.4 (m), 1495.5 (w), 1453.4 (m), 1405.5 (m), 1373.3 (m), 1306.1 (m), 1278.8 (w), 1253.4 (w), 1189.9 (vs, ν(COOR), 1103.6 (m), 1080.3 (m), 1053.5 (s), 936.8 (m), 859.4 (w), 821.1 (m), 763.8 (m), 695.3 (s), 607.3 (w), 482.9 (w), 407.5 (w).

^{1}H-NMR (500 MHz, DMSO-d_6): δ [ppm] = 8.55 (t, J = 5.9 Hz, 1 H, NH^{25}), 8.17 (d, J = 3.2 Hz, 1 H, NH^{3}), 7.33 – 7.28 (m, 6 H, CH$_{Ar}$), 7.27 – 7.22 (m, 4 H, CH$_{Ar}$), 5.21 (d, J = 3.2 Hz, 1 H, CH^{2}), 5.04 – 4.97 (m, 1 H, CH^{23}), AB-signal (δ A = 4.73, δ B = 4.51, J_{AB} = 17.5 Hz, 2 H, CH$_2^{20}$), 2 H, CH$_2^{20}$), 4.31 (d, J = 5.9 Hz, 2 H, CH$_2^{26}$), 4.02 (q, J = 7.0 Hz, 2 H, CH$_2^{17}$), 2.39 (s, 3 H, CH$_3^{9}$), 1.79 – 1.70 (m, 2 H, CH$_2^{36}$), 1.34 – 1.20 (m, 13 H, CH$_2$), 1.11 (t, J = 7.1 Hz, 3 H, CH$_3^{19}$), 0.85 (t, J = 6.8 Hz, 3 H, CH$_3^{30}$).

^{13}C-NMR (126 MHz, DMSO-d_6): δ [ppm] = 169.24 (s, CO$_2$R^{21}), 169.01 (s, CONR^{24}), 165.43 (s, CO$_2$R^{16}), 152.44 (s, CO^{4}), 148.75 (s, C^{1}), 143.91 (s, C$_{Ar}^{8}$), 139.79 (s, C$_{Ar}^{29}$), 139.11 (s), 128.39 (s, CH$_{Ar}$), 128.21 (s, CH$_{Ar}$), 128.12 (s, CH$_{Ar}$), 127.42 (s, CH$_{Ar}$), 127.14 (s, CH$_{Ar}$), 126.98 (s, CH$_{Ar}$), 126.76 (s, CH$_{Ar}$), 126.60 (s, CH$_{Ar}$), 126.42 (s, CH$_{Ar}$), 103.26 (s, C^{1}), 74.13 (s, CH^{23}), 71.00 (s, CH), 59.69 (s, CH$_2^{17}$), 53.01 (s, CH^{2}), 44.05 (s, CH$_2^{20}$), 41.83 (s, CH$_2^{26}$), 31.31 (s, CH$_2$), 31.19 (s, CH$_2$), 31.08 (s, CH$_2$), 28.85 (s, CH$_2$), 28.66 (s, CH$_2$), 28.49 (s, CH$_2$), 24.58 (s, CH$_2$), 24.37 (s, CH$_2$), 22.07 (s, CH$_2$), 22.04 (s, CH$_2$), 15.57 (s, CH$_3^{9}$), 13.95 (s, CH$_3^{30\ or\ 19}$), 13.90 (s, CH$_3^{30\ or\ 19}$).

FAB – MS [*m/z*] (relative intensity): 564.3 (90%) [M + H]$^+$, 518.3 (35%) [M – C$_2$H$_5$O]$^+$, 317.1 (50%) [Fragment A]$^+$, 301.1 (35%) [Fragment A – O]$^+$, 273.1 (15%) [Fragment C]$^+$, 259.1 (50%) [Fragment C – CH$_2$]$^+$, 246.2 (15%) [Fragment B]$^+$

HRMS – FAB [*m/z*]: [M + H]$^+$ calculated for ^{12}C$_{23}$^{1}H$_{25}$^{16}O$_6$^{14}N$_2$, 425.1707; found, 425-1705; Δ = 0.05 mmu.

Fragment A
Chemical Formula: $C_{16}H_{17}N_2O_5$
Exact Mass: 317,11

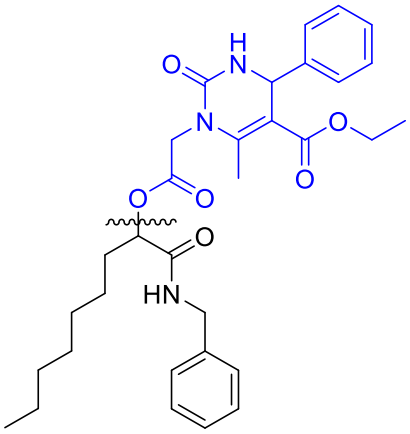

Fragment C
Chemical Formula: $C_{15}H_{17}N_2O_3^{\bullet}$
Exact Mass: 273,12

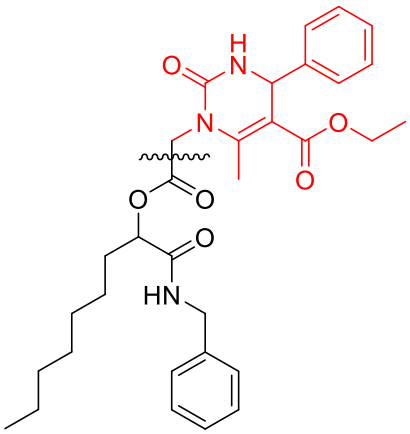

Fragment B
Chemical Formula: $C_{16}H_{24}NO^{\bullet}$
Exact Mass: 246,19

6.2.2.2.7 ***Passerini compound 59 derived from Biginelli acid 49, octanal and 2-morpholinoethyl isocyanide.***

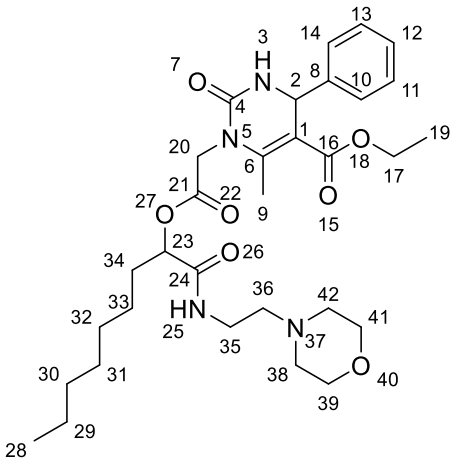

In a tube vial, finely powdered Biginelli-acid **49** (302 mg, 949 µmol, 1.00 eq.) was dissolved in 0.3 mL dimethyl sulfoxide and diluted with 1.5 mL dichloromethane. Subsequently, octanal (158 mg, 1.23 mmol, 193 µL, 1.30 eq.) and 2-morpholinoethyl isocyanide (186 mg, 1.32 mmol, 182 µL, 1.40 eq.) were added. The mixture was stirred at room temperature for 3 d. The reaction mixture was evaporated under reduced pressure. The crude product was purified *via* column chromatography employing silica gel and eluting with a gradual solvent mixture of ethyl acetate and *c*-hexane (0:1 → 1:1) and finally with a solvent mixture of dichloromethane, methanol and triethylamine (90:5:5). The product containing fractions were dried under reduced pressure to yield

a viscous oil. The oil was suspended in 50 mL water, sonicated for 1 h and washed with 30 mL water (this washing was repeated three times). After drying under reduced pressure, the Passerini product **59** was obtained as a yellow solid (222 mg, 372 µmol, 39.2%).

IR (ATR): ν [cm^{-1}] = 3304.4 (br, ν(N-H)), 2925.8 (w, ν(C-H)), 2854.4 (w, ν(C-H)), 1751.8 (w, ν(C=O)), 1675.6 (vs, ν(C=O)), 1541.3 (w), 1493.8 (m), 1453.9 (s), 1384.2 (m), 1307.5 (w), 1277.7 (w), 1258.5 (w), 1174.9 (vs), 1109.9 (s), 1055.6 (s), 939.9 (w), 862.8 (w), 829.0 (m), 758.1 (s), 697.8 (w), 650.1 (w), 624.4 (w), 511.8 (w), 458.7 (w).

^{1}H-NMR (400 MHz, DMSO-d_6): δ [ppm] = 8.16 (dd, J = 21.1, 3.6 Hz, 1 H, NH^{3}), 7.92 (dt, J = 15.2, 5.7 Hz, 1 H, NH^{25}), 7.40 – 7.11 (m, 5 H, CH$_{Ar}$), 5.19 (t, J = 3.5 Hz, 1 H, CH^{2}), 4.93 (dt, J = 10.0, 5.0 Hz, 1 H, CH^{23}), 4.79 – 4.44 (m, 2 H, CH$_2^{20}$), 4.06 – 3.96 (m, 2 H, CH$_2^{17}$), 3.58 – 3.45 (m, 6 H, CH$_2^{36+38,42}$), 3.26 – 3.12 (m, 2 H, CH$_2^{35}$), 2.41 (d, J = 10.5 Hz, 3 H, CH$_3^{9}$), 2.39 – 2.30 (m, 2 H, CH$_2^{39,41}$), 1.76 – 1.63 (m, 2 H, CH$_2^{34}$), 1.34 – 1.15 (m, 12 H, CH$_2$), 1.13 – 1.06 (m, 3 H, CH$_3^{19}$), 0.85 (t, J = 6.8 Hz, 3 H, CH$_3^{28}$).

^{13}C-NMR (101 MHz, DMSO-d_6): δ [ppm] = 169.13 (s, CO$_2$R^{20}), 169.04 (s, CO$_2$R^{20}), 168.78 (s, CONR^{24}), 168.77 (s, CONR^{24}), 165.44 (s, CO$_2$R^{16}), 165.42 (s, CO$_2$R^{16}), 152.48 (s, CO^{4}), 152.24 (s, CO^{4}), 148.73 (s, C^{6}), 148.59 (s, C^{6}), 144.05 (s, C$_{Ar}^{8}$), 143.89 (s, C$_{Ar}^{8}$), 128.40 (s, CH$_{Ar}$), 128.32 (s, CH$_{Ar}$), 127.42 (s, CH$_{Ar}$), 126.65 (s, CH$_{Ar}$), 126.51 (s, CH$_{Ar}$), 126.43 (s, CH$_{Ar}$), 103.34 (s, C^{1}), 103.27 (s, C^{1}), 74.07 (s, CH^{23}), 74.03 (s, CH^{23}), 66.16 (s, CH$_2^{36+38,42}$), 59.70 (s, CH$_2^{17}$), 57.12 (s, CH$_2^{39,41}$), 53.19 (s, CH^{2}), 44.09 (s, CH$_2^{20}$), 43.88 (s, CH$_2^{20}$), 35.73 (s, CH$_2^{35}$), 31.37 (s, CH$_2$), 31.30 (s, CH$_2$), 31.12 (s, CH$_2$), 28.56 (s, CH$_2$), 28.50 (s, CH$_2$), 28.48 (s, CH$_2$), 24.29 (s, CH$_2$), 24.27 (s, CH$_2$), 22.05 (s, CH$_2$), 15.60 (s, CH$_3^{9}$), 15.59 (s, CH$_3^{9}$), 13.94 (s, CH$_3^{28}$), 13.90 (s, CH$_3^{28}$).

FAB – MS [*m/z*] (relative intensity): 587.3 (100%) [M + H]$^+$, 541.3 (15%) [M – C$_2$H$_5$O]$^+$.

HRMS – FAB [*m/z*]: [M + H]$^+$ calculated for ^{12}C$_{31}$^{1}H$_{47}$^{16}O$_7$^{14}N$_4$, 587.3439; found, 587.3441; Δ = 0.16 mmu.

6.2.2.2.8 *Passerini compound 60 derived from Biginelli acid 49, 2-ethylbutanal and 1-pentyl isocyanide*

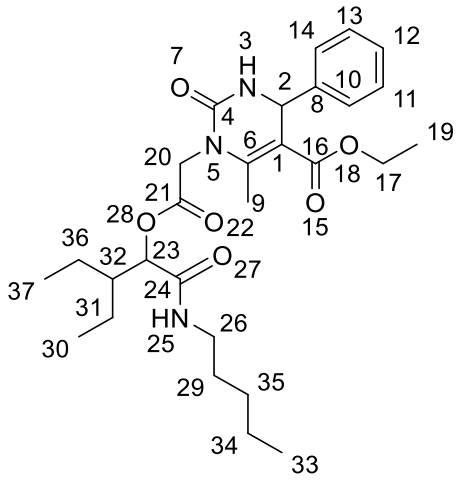

In a tube vial, finely powdered Biginelli-acid **49** (300 mg, 942 µmol, 1.00 eq.) was dissolved in 0.3 mL dimethyl sulfoxide and diluted with 1.0 mL dichloromethane. Subsequently, 2-ethylbutanal (200 mg, 2.00 mmol, 246 µL, 2.10 eq.) and 1-pentyl isocyanide (120 mg, 1.23 mmol, 155 µL, 1.30 eq.) were added. The mixture was stirred at room temperature for 3 d. The crude product was purified *via* column chromatography employing silica gel and eluting with a gradual solvent mixture of diethyl ether and *c*-hexane (0:1 → 5:1). The Passerini product **60** was obtained as a colorless solid (381 mg, 739 µmol, 78.5%).

IR (ATR): ν [cm^{-1}] = 3304.9 (br, ν(N-H)), 2958.8 (w, ν(C-H), 2930.1 (w, ν(C-H), 2872.3 (w, ν(C-H), 1752.2 (s, ν(C=O)), 1681.1 (vs, ν(C=O)), 1535.4 (m), 1455.7 (m), 1383.7 (m), 1309.7 (w), 1278.3 (w), 1177.3 (vs), 1104.9 (m), 1055.6 (m), 940.8 (w), 830.3 (w), 760.0 (w), 697.6 (w), 651.4 (w).

^{1}H-NMR (400 MHz, DMSO-d_6): δ [ppm] = 8.19 (dd, J = 32.9, 3.7 Hz, 1 H, NH^{3}), 7.93 (dt, J = 33.8, 5.7 Hz, 1 H, NH^{25}), 7.34 – 7.22 (m, 5 H, CH$_{Ar}$), 5.20 (dd, J = 5.6, 3.8 Hz, 1 H, CH^{2}), 4.99 (dd, J = 17.2, 3.9 Hz, 1 H, CH^{23}), 4.75 – 4.45 (m, 2 H, CH$_2^{20}$), 4.02 (p, J = 7.0 Hz, 2 H, CH$_2^{17}$), 3.14 – 2.99 (m, 2 H, CH$_2^{26}$), 2.43 (d, J = 25.0 Hz. 3 H, CH$_3^{9}$), 1.78 – 1.66 (m, 1 H, CH^{32}), 1.45 – 1.32 (m, 4 H, CH$_2$), 1.33 – 1.15 (m, 6 H, CH$_2$), 1.10 (td, J = 7.1, 4.6 Hz, 3 H, CH$_3^{19}$), 0.89 – 0.79 (m, 9 H, CH$_3^{30,37}$).

^{13}C-NMR (101 MHz, DMSO-d_6): δ [ppm] = 169.24 (s, CO$_2$R^{21}), 169.21 (s, CO$_2$R^{21}), 168.37 (s, CONR^{24}), 165.50 (s, CO$_2$R^{16}), 165.44 (s, CO$_2$R^{16}), 152.78 (s, CO^{4}), 152.37 (s, CO^{4}), 148.78 (s, C^{6}), 148.72 (s, C^{6}), 144.00 (s, C$_{Ar}^{8}$), 143.78 (s, C$_{Ar}^{8}$), 128.45 (s,

CH_{Ar}), 128.39 (s, CH_{Ar}), 127.49 (s, CH_{Ar}), 127.45 (s, CH_{Ar}), 126.51 (s, CH_{Ar}), 126.40 (s, CH_{Ar}), 103.42 (s, C^{1}), 103.21 (s, C^{1}), 75.13 (s, CH^{23}), 75.02 (s, CH^{23}), 59.76 (s, $CH_2{}^{17}$), 59.69 (s, $CH_2{}^{17}$), 53.16 (s, CH^{2}), 52.92 (s, CH^{2}), 44.34 (s, $CH_2{}^{20}$), 44.12 (s, $CH_2{}^{20}$), 42.53 (s, CH^{32}), 42.51 (s, CH^{32}), 38.34 (s, $CH_2{}^{26}$), 28.62 (s, CH_2), 28.57 (s, CH_2), 28.48 (s, CH_2), 28.46 (s, CH_2), 21.80 (s, CH_2), 21.44 (s, CH_2), 21.26 (s, CH_2), 15.65 (s, $CH_3{}^{9}$), 15.62 (s, $CH_3{}^{9}$), 13.97 (s, $CH_3{}^{19}$), 13.91 (s, $CH_3{}^{19}$), 11.38 (s, $CH_3{}^{30,37}$), 11.33 (s, $CH_3{}^{30,37}$), 11.26 (s, $CH_3{}^{30,37}$).

FAB – MS [*m/z*] (relative intensity): 516.3 (100%) $[M + H]^+$, 470.2 (30%), $[M – C_2H_5O]^+$, 317.1 (35%) [Fragment A]$^+$, 301.1 (35%) [Fragment A – O]$^+$, 259.1 (45%) [Fragment C]$^+$, 198.2 (30%) [Fragment B]$^+$.

HRMS – FAB [*m/z*]: $[M + H]^+$ calculated for $^{12}C_{28}{}^{1}H_{42}{}^{16}O_6{}^{14}N_3$, 516.3068; found, 516.3069; Δ = 0.07 mmu.

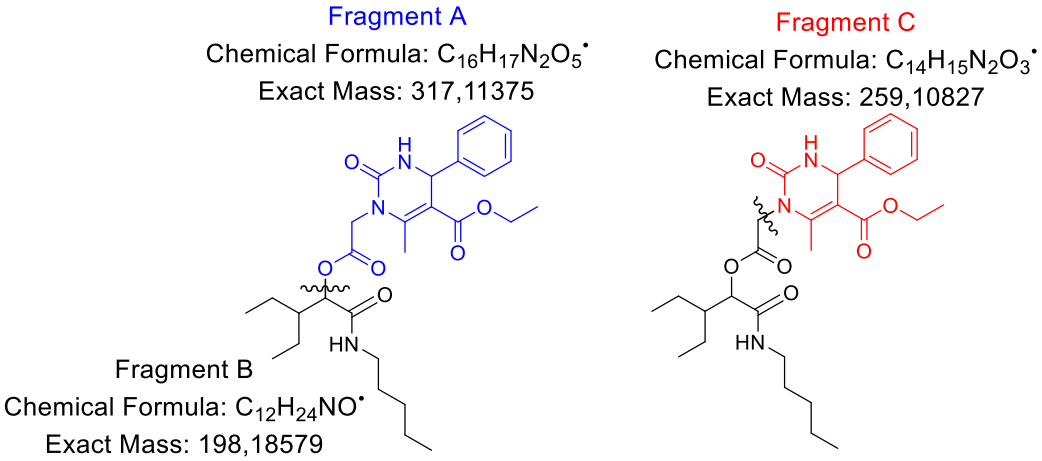

6.2.2.3 Biginelli-Passerini one-pot tandem reaction

6.2.2.3.1 *Biginelli-Passerini product 61 prepared in one-pot procedure from 4-fluorobenzaldehyde, N-carbomoylglycine, ethyl acetoacetate and pentylisocyanide*

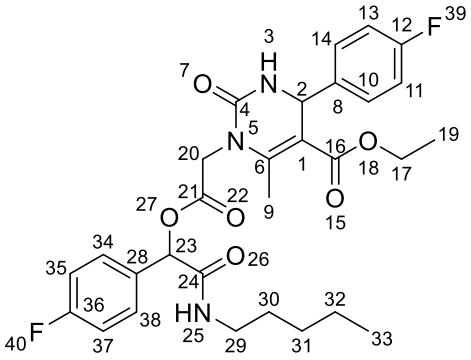

In a tube vial, finely powdered *N*-carbomoylglycine (500 mg, 4.23 mmol, 1.00 eq.), 4-fourobenzaldehyde (1.57 g, 12.7 mmol, 3.00 eq.) and ethyl acetoacetate (551 mg, 4.23 mmol, 1.00 eq.) were stirred at 110 °C for 24 h and subsequently at 80 °C for another 24 h. Subsequently, the crude reaction mixture was cooled to ambient temperature and diluted with 3 mL dichloromethane. Pentylisocyanide (617 mg, 6.35 mmol, 1.50 eq.) was added while stirring. The resulting mixture was stirred for 3 d at room temperature. The reaction mixture was dried under reduced pressure and purified *via* column chromatography employing silica gel and eluting with a gradual solvent mixture of ethyl acetate and *c*-hexane (1:5 → 1:0) to yield the Biginelli-Passerini one-pot product **61** as a colorless solid (972 mg, 1.74 mmol, 41.1%). Note: impure fractions can be purified by precipitation from ethyl acetate in *c*-hexane and crystallization through slow evaporation of the solvents overnight in an open flask.

R_f = 0.51 in ethyl acetate/*c*-hexane (2:1).

IR (ATR): ν [cm^{-1}] = 3287.9 (br, ν(N-H)), 3097.3 (br, ν(N-H)), 2931.7 (w, ν(C-H)), 2860.3 (w, ν(C-H)), 1737.5 (m, ν(C=O)), 1682.1 (vs, ν(C=O)), 1659.4 (vs), 1621.6 (s), 1602.6 (s), 1556.4 (s), 1508.3 (vs), 1449.9 (m), 1411.3 (m), 1369.2 (m), 1308.4 (m), 1277.5 (m), 1256.0 (m), 1188.6 (vs), 1157.4 (s), 1098.5 (m), 1055.2 (m), 1013.6 (w), 940.1 (w), 806.4 (w), 758.7 (w), 648.2 (w), 579.8 (w), 515.6 (w).

^{1}H-NMR (500 MHz, DMSO-d_6): δ [ppm] = 8.27 (q, J = 5.6 Hz, 1 H, NH^{25}), 8.16 (dd, J = 16.4, 3.4 Hz, 1 H, NH^{3}), 7.54 – 7.50 (m, 2 H, CH$_{Ar}$), 7.35 (ddd, J = 31.1, 8.3, 5.6 Hz, 2 H, CH$_{Ar}$), 7.23 (td, J = 8.8, 3.7 Hz, 2 H, CH$_{Ar}$), 7.17 – 7.06 (m, 2 H, CH$_{Ar}$), 5.92 (d, J = 10.2 Hz, 1 H, CH^{23}), 5.20 (t, J = 3.7 Hz, 1 H, CH^{2}), 4.92 – 4.52 (m, 2 H, CH$_2^{20}$), 4.07 – 3.95 (m, 2 H, CH$_2^{17}$), 3.10 – 2.98 (m, 2 H, CH$_2^{29}$), 2.43 (d, J = 10.8 Hz, 3 H, CH$_3^{9}$), 1.43 – 1.33 (m, 2 H, CH$_2$), 1.28 – 1.05 (m, 7 H, CH$_2$ + CH$_3^{19}$), 0.87 – 0.74 (m, 3 H, CH$_3^{33}$).

^{13}C-NMR (126 MHz, DMSO-d_6): δ [ppm] = 169.00 (s, CO$_2$R^{21}), 168.96 (s, CO$_2$R^{21}), 167.29 (s, CONR^{24}), 167.26 (s, CONR^{24}), 165.37 (s, CO$_2$R^{16}), 165.36 (s, CO$_2$R^{16}), 162.25 (d, J = 244.9 Hz, CF$_{Ar}$), 162.23 (d, J = 245.1 Hz, CF$_{Ar}$), 161.45 (d, J = 243.3 Hz, CF$_{Ar}$), 161.42 (d, J = 243.4 Hz, CF$_{Ar}$), 152.16 (s, CO^{4}), 152.01 (s, CO^{4}), 148.92 (s, C^{6}), 148.73 (s, C^{6}), 140.36 (d, J = 2.9 Hz, C$_{Ar}^{8}$), 140.19 (d, J = 3.0 Hz, C$_{Ar}^{8}$), 131.85 (d, J = 2.9 Hz, C$_{Ar}^{28}$), 131.76 (d, J = 2.9 Hz, C$_{Ar}^{28}$), 129.63 (s, CH$_{Ar}$), 129.56 (s, CH$_{Ar}$), 129.48 (s, CH$_{Ar}$), 128.69 (s, CH$_{Ar}$), 128.62 (s, CH$_{Ar}$), 128.54 (s, CH$_{Ar}$), 128.47 (s, CH$_{Ar}$), 128.43 (s, CH$_{Ar}$), 128.37 (s, CH$_{Ar}$), 115.43 (s, CH$_{Ar}$), 115.25 (s, CH$_{Ar}$), 115.18 (s, CH$_{Ar}$), 115.16 (s, CH$_{Ar}$), 115.01 (s, CH$_{Ar}$), 114.99 (s, CH$_{Ar}$), 114.71 (s, CH$_{Ar}$), 114.54 (s, CH$_{Ar}$), 103.28 (s, C^{1}), 103.16 (s, C^{1}), 75.12 (s, CH^{23}), 75.00 (s, CH^{23}), 59.77 (s, CH$_2^{17}$), 52.66 (s, CH^{2}), 52.44 (s, CH^{2}), 43.91 (s, CH$_2^{20}$), 43.74 (s, CH$_2^{20}$), 38.39 (s, CH$_2^{29}$), 38.36 (s, CH$_2^{29}$), 28.79 (s, CH$_2$), 28.56 (s, , CH$_2$), 28.54 (s, CH$_2$), 28.49 (s, CH$_2$), 28.30 (s, CH$_2$), 21.73 (s, CH$_2$), 15.61 (s, CH$_3^{9}$), 13.97 (s, CH$_3^{19}$), 13.95 (s, CH$_3^{19}$), 13.84 (s, CH$_3^{33}$), 13.83 (s, CH$_3^{33}$).

^{19}F-NMR (377 MHz, DMSO-d_6): δ [ppm] = -117.49 (s, CF$_{Ar}$), -117.50 (s, CF$_{Ar}$), -119.43 (s, CF$_{Ar}$), -119.49 (s, CF$_{Ar}$).

FAB – MS [m/z] (relative intensity): 558.3 (80%) [M + H]$^+$, 512.2 (40%) [M – C$_2$H$_5$O]$^+$, 335.1 (100%) [Fragment A]$^+$, 222.1 (30%) [Fragment B]$^+$, 136.0 (70%) [Fragment B – C$_5$H$_{12}$N]$^+$.

HRMS – FAB [m/z]: [M + H]$^+$ calculated for ^{12}C$_{29}$^{1}H$_{34}$^{16}O$_6$^{14}N$_3$^{19}F$_2$, 558.2410; found, 558.2411; Δ = 0.11 mmu.

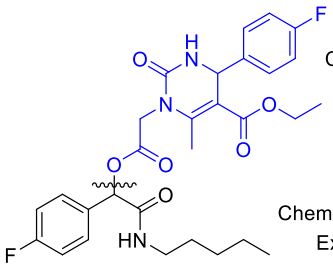

Fragment A
Chemical Formula: $C_{16}H_{16}FN_2O_5^{\bullet}$
Exact Mass: 335,10432

Fragment B
Chemical Formula: $C_{13}H_{17}FNO^{\bullet}$
Exact Mass: 222,12942

6.2.3 Synthetic procedures for chapter 4.3

Additional data such as displayed NMR spectra and tandem-MS mass spectra can be found in the supplementary information of the previous publication and are included in the electronic version of this thesis on the CD.[209]

6.2.3.1 Bifunctional components

6.2.3.1.1 *11-ureidoundecanoic acid*

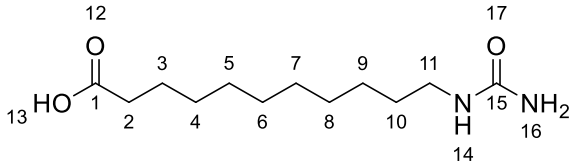

In a 100 mL round bottom flask equipped with a magnetic stir bar urea (4.47 g, 74.5 mmol, 3.00 eq.) and 11-aminoundecanoic acid (5.00 g, 24.8 mmol, 1.00 eq.) were suspended in 15 mL dimethyl sulfoxide. The resulting mixture was stirred at 120 °C for 2 h while adding 0.7 mL concentrated hydrochloric acid (37%) every 30 min. The clear solution was subsequently cooled to room temperature and stirred overnight. The suspension was diluted with 10 mL 1 M hydrochloric acid and the precipitate was filtered off. The solid was washed with water (3 × 20 mL), dried on the filter and subsequently washed with ice cold ethyl acetate/ethanol (1:1) (2 × 30 mL). The residual solvent was removed under reduced pressure. 11-ureidoundecanoic acid was obtained as a colorless solid (4.98 g, 20.6 mmol, 82.8%).

Spectral data is in accordance to earlier reported.[343]

IR (ATR): ν [cm^{-1}] = 3411.6 (m, ν(O-H)), 3346.2 (br, ν(N-H)), 3209.9 (br, ν(N-H)), 2917.3 (w, ν(C-H)), 2848.3 (w, ν(C-H)), 1707.0 (s, ν(C=O)), 1665.8 (s, ν(C=O)), 1553.9 (vs), 1481.9 (m), 1466.3 (m), 1400.3 (m), 1379.6 (m), 1351.8 (m), 1297.4 (m), 1270.1 (m), 1243.5 (m), 1209.0 (s), 1182.1 (s), 1121.1 (m), 974.0 (m), 899.1 (w), 776.0 (w), 721.4 (w), 684.8 (w), 575.8 (s), 468.3 (m), 416.4 (w), 379.1 (w).

^{1}H-NMR (400 MHz, DMSO-d_6): δ [ppm] = 11.94 (s, 1 H, CO_2H^{13}), 5.89 (t, J = 5.7 Hz, 1 H, NH^{14}), 5.35 (s, 2 H, NH^{16}), 2.92 (q, J = 6.5 Hz, 2 H, CH_2^{11}), 2.18 (t, J = 7.3 Hz, 2 H,

CH_2^{2}), 1.47 (t, *J* = 7.1 Hz, 2 H, CH_2^{3}), 1.33 (t, *J* = 6.7 Hz, 2 H, CH_2^{10}), 1.24 (s, 12 H, CH_2^{4-9}).

^{13}C-NMR (101 MHz, DMSO-d_6) δ [ppm] = 174.52 (s, CO_2H^{1}), 158.72 (s, CON_2R^{15}), 38.86 (s, CH_2^{11}), 33.69 (s, CH_2^{2}), 30.01 (s, CH_2^{10}), 29.02 (s, CH_2), 28.89 (s, CH_2), 28.83 (s, CH_2), 28.76 (s, CH_2), 28.56 (s, CH_2), 26.43 (s, CH_2), 24.51 (s, CH_2^{3}).

FAB – MS [*m/z*] (relative intensity): 245.3 (100%) $[M + H]^+$.

HRMS – FAB [*m/z*]: $[M + H]^+$ calculated for $^{12}C_{12}{}^{1}H_{25}{}^{16}O_3{}^{14}N_2$, 245.1860; found, 245.1859; Δ = 0.09 mmu.

6.2.3.1.2 *6-ureidohexanoic acid*

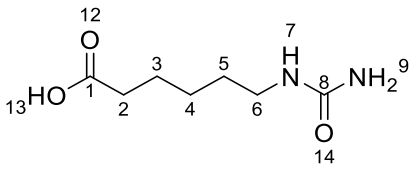

In a 250 mL round bottom flask equipped with a magnetic stir bar urea (13.7 g, 228 mmol, 3.00 eq.) and 6-aminohexanoic acid (10.00 g, 76.2 mmol, 1.00 eq.) were suspended in 40 mL dimethyl sulfoxide. The resulting mixture was stirred at 120 °C for 2 h while adding 2 mL concentrated hydrochloric acid (37%) every 30 min. The clear solution was subsequently stirred at 100 °C for 2 h, then 30 mL 1 M hydrochloric acid were added, and the mixture was left to stand over night at room temperature. The solid was filtrated and recrystallized from ethanol/water (98:2), washed with 20 mL ice cold ethanol three times and dried under reduced pressure. 6-ureidohexanoic acid was obtained as a colorless solid (9.51 g, 54.6 mmol, 71.6%). Note: additional product could be crystalized from the mother liquor upon concentration and cooling.

IR (ATR): ν [cm^{-1}] = 3403.5 (m, ν(O-H)), 3344.9 (br, ν(N-H)), 3204.7 (br, ν(N-H)), 2946.4 (w, ν(C-H)), 2870.8 (w, ν(C-H)), 1896.3 (br), 1705.4 (s, ν(C=O)), 1658.3 (s, ν(C=O)), 1555.2 (vs), 1476.4 (m), 1449.8 (w), 1402.0 (s), 1374.3 (s), 1296.3 (m), 1242.7 (m), 1194.3 (m), 1152.0 (w), 1101.3 (s), 1050.0 (m), 982.6 (s), 898.5 (w), 846.6 (w), 776.7 (w), 728.8 (w), 681.1 (w), 567.3 (m), 531.9 (m), 414.4 (w).

^{1}H-NMR (400 MHz, DMSO-d_6): δ [ppm] = 12.03 (s, 1 H, CO_2H^{13}), 5.91 (t, *J* = 5.8 Hz, 1 H, NH^{7}), 5.37 (s, 2 H, NH^{9}), 3.02 – 2.79 (m, 2 H, CH_2^{6}), 2.18 (t, *J* = 7.4 Hz, 2 H, CH_2^{2}),

1.48 (p, *J* = 7.4 Hz, 2 H, CH_2^3), 1.34 (dq, *J* = 11.0, 6.8, 6.2 Hz, 2 H CH_2^5), 1.24 (qd, *J* = 7.5, 3.2 Hz, 2 H, CH_2^4).

^{13}C-NMR (101 MHz, DMSO-d_6) δ [ppm] = 174.53 (s, CO_2H^1), 158.78 (s, CON_2R^8), 33.71 (s, CH_2^2), 29.80 (s, CH_2^5), 26.02 (s, CH_2^4), 24.34 (s, CH_2^3).

EI – MS [*m/z*] (relative intensity): 174.2 (80%) $[M + H]^+$, 130.1 (100%) $[M - CH_3NO]^+$, 115.1 (90%) $[M - CH_4N_2O]^+$, 101.1 (80%) $[M - C_2H_5N_2O]^+$, 87.1 (100%) [Fragment A or B]$^+$.

HRMS – EI [*m/z*]: $[M + H]^+$ calculated for $^{12}C_7{}^1H_{14}{}^{16}O_3{}^{14}N_2$, 174.1004; found, 174.1005; Δ = 0.04 mmu.

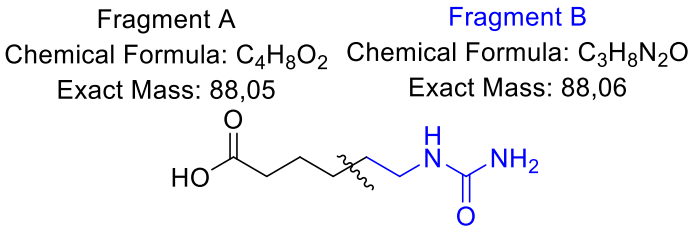

6.2.3.1.3 *Trans-1,4-diformamido cyclohexane obtained from trans-1,4-diamino cyclohexane and ethylformate*

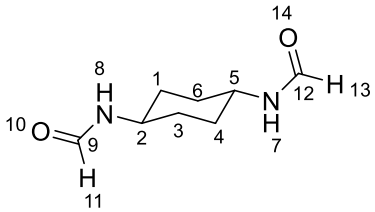

In a 250 mL round-bottom flask equipped with a reflux condenser and a magnetic stir bar *trans*-1,4-diamino cyclohexane (6.00 g, 52.5 mmol, 1.00 eq.) was mixed with ethyl formate (77.8 g, 84.6 mL, 1.05 mol, 20.0 eq.) and heated under reflux overnight (70 °C temperature set) while stirring. The reaction mixture was dried under reduced pressure. The resulting formamide was obtained as a grey solid (8.93 g, 52.5 mmol, 99.8%).

Spectral data is in accordance to earlier reported.[344]

IR (ATR): ν [cm^{-1}] = 3267.1 (br, ν(N-H)), 3066.3 (br, ν(N-H)), 2952.0 (w, ν(C-H)), 2933.3 (w, ν(C-H)), 2882.5 (w, ν(C-H)), 2855.1 (w, ν(C-H)), 1648.4 (vs, ν(C=O)), 1545.5 (s),

1444.6 (m), 1390.5 (s), 1336.9 (m), 1253.1 (m), 1219.6 (m), 1097.0 (w), 1078.9 (m), 967.6 (w), 904.4 (m), 760.0 (s), 719.4 (s), 562.8 (w), 443.3 (w), 411.4 (s).

^{1}H-NMR (300 MHz, DMSO-d_6): δ [ppm] = 8.03 – 7.93 (m, 2 H, NH^{7,8}), 7.91 (s, 2 H, CHO^{11,13}), 3.60 – 3.48 (m, 2 H, CH^{2,5}), 1.83 – 1.71 (m, 4 H, CH$_2^{1,3,4,6\ axial}$), 1.41 – 1.10 (m, 4 H, CH$_2^{1,3,4,6\ equatorial}$).

^{13}C-NMR (75 MHz, DMSO-d_6) δ [ppm] = 159.93 (s, CONR^{12}), 45.49 (s, CH^{2,5}), 32.56 (s, CH$_2$), 30.71 (s, CH$_2$).

FAB – MS [*m/z*] (relative intensity): 341.2 (40%) $[2\ M + H]^+$, 171.0 (100%) $[M + H]^+$, 126.1 (20%) $[M – CH_2NO]^+$.

HRMS – FAB [*m/z*]: $[M + H]^+$ calculated for $^{12}C_8{}^{1}H_{15}{}^{16}O_2{}^{14}N_2$, 171.1128; found, 171.1125; Δ = 0.34 mmu.

6.2.3.1.4 *Trans-1,4-diisocyano cyclohexane obtained from trans-1,4-diformamido cyclohexane*

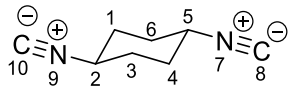

Trans-1,4-diformamido cyclohexane (8.90 g, 52.3 mmol, 1.00 eq.) was suspended in a three necked round-bottom flask equipped with a dropping funnel, a thermometer, a condenser and a magnetic stir bar in 40 mL dichloromethane and diisopropylamine (44.9 g, 62.4 mL, 444 mmol, 8.50 eq.) was added while stirring. The mixture was cooled to 0 °C and phosphoryl chloride (22.5 g, 13.4 mL, 146 mmol, 2.80 eq.) was added dropwise at such a rate that the reaction temperature remained below 0 °C. The mixture was stirred for 2 h at room temperature, then added carefully in portions into 200 mL ice-water containing 50 g potassium carbonate maintaining the temperature below 25 °C. The resulting emulsion was stirred for 30 min at room temperature. The organic layer was separated, the aqueous layer extracted three times with 50 mL dichloromethane and the combined organic layers were dried over potassium carbonate. Purification by column chromatography employing silica gel as stationary phase and eluting with a gradual solvent mixture of *c*-hexane/ethyl acetate (5:1 → 3:1) and concentration *in vacuo* yielded *trans*-1,4-diisocyano cyclohexane as a pale solid (2.99 g, 22.3 mmol, 42.6%).

R_f = 0.51 in *c*-hexane/ethyl acetate (3:1). Visualized *via* Seebach staining solution.

Spectral data is in accordance to earlier reported.[344]

IR (ATR): ν [cm^{-1}] = 2951.8 (m, ν(C-H)), 2867.8 (w, ν(C-H)), 2136.6 (vs, ν(NC)), 1445.0 (s), 1366.6 (m), 1354.5 (m), 1330.7 (s), 1217.5 (s), 1127.3 (m), 1007.2 (m), 970.9 (m), 920.1 (vs), 861.4 (m), 836.1 (m), 672.5 (w), 499.4 (m), 419.5 (w).

^{1}H-NMR (400 MHz, DMSO-d_6): δ [ppm] = 3.94 – 3.74 (m, 2 H, CH^{2,5}), 1.94 (d, J = 9.8 Hz, 4 H, CH$_2^{1,3,4,6\ axial}$), 1.64 (tt, J = 8.8, 4.7 Hz, 4 H, CH$_2^{,1,3,4,6\ equatorial}$).

^{13}C-NMR (101 MHz, DMSO-d_6) δ [ppm] = 155.23 (t, J = 4.8 Hz, NC^{8,10}), 49.30 (t, J = 5.4 Hz, CH^{2,5}), 27.87 (CH$_2^{1,3,4,6}$).

FAB – MS [*m/z*] (relative intensity): 134.1 (30%) [M + H]$^+$.

HRMS – FAB [*m/z*]: [M + H]$^+$ calculated for $^{12}C_8{}^1H_{10}{}^{14}N_2$, 134.0838; found, 134.0840; Δ = 0.10 mmu.

6.2.3.1.5 *p-Xylenediformamide obtained from p-xylenediamine and ethylformate*

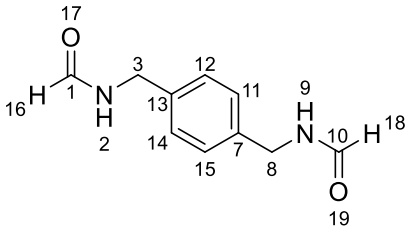

In a 250 mL round-bottom flask equipped with a reflux condenser and a magnetic stir bar *p*-xylenediamine (4.00 g, 29.4 mmol, 1.00 eq.) was mixed with ethyl formate (43.5 g, 47.3 mL, 587 mol, 20.0 eq.) and heated under reflux overnight (85 °C temperature set) while stirring. The reaction mixture was died under reduced pressure. The formamide was obtained as a colorless solid (5.60 g, 99.2%, 29.0 mmol).

Spectral data is in accordance to earlier reported.[344]

IR (ATR): ν [cm^{-1}] = 3271.6 (br, ν(N-H)), 3026.2 (br, ν(N-H)), 2886.0 (w, ν(C-H)), 1643.9 (vs, ν(C=O)), 1525.1 (s), 1459.3 (m), 1425.0 (m), 1374.9 (s), 1347.0 (s), 1212.7 (s), 1109.5 (w), 1029.5 (w), 948.6 (w), 826.9 (w), 827.0 (m), 696.2 (s), 544.9 (s).

^{1}H-NMR (400 MHz, DMSO-d_6): δ [ppm] = 8.50 (br s, 2 H, NH^{2,9}), 8.13 (d, J = 1.5 Hz, 2 H, CH^{16,18}), 7.22 (s, 4 H, CH$_{Ar}^{11,12,14,15}$), 4.28 (d, J = 6.1 Hz, 2 H, CH$_2^{3,8}$).

^{13}C-NMR (101 MHz, DMSO-d_6) δ [ppm] = 161.04 (s, CONR^{1,10}), 137.66 (s, C$_{Ar}^{7,13}$), 127.37 (s, CH$_{Ar}^{11,12,14,15}$), 40.50 (s, CH$_2^{3,8}$).

FAB – MS [*m/z*] (relative intensity): 385.2 (40%) $[2\ M + H]^+$, 193.1 (100%) $[M + H]^+$.

HRMS – FAB [*m/z*]: $[M + H]^+$ calculated for $^{12}C_{10}{}^{1}H_{13}{}^{16}O_2{}^{14}N_2$, 193.0972; found, 193.0973; Δ = 0.14 mmu.

6.2.3.1.6 *p-Xylenediisocyanide obtained from p-xylenediformamide*

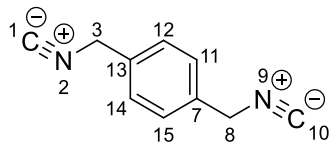

p-Xylenediformamide (5.50 g, 28.6 mmol, 1.00 eq.) was suspended in a three necked round-bottom flask equipped with a dropping funnel, a thermometer, a condenser and a magnetic stir bar in 40 mL dichloromethane and diisopropylamine (24.6 g, 34.2 mL, 243 mmol, 8.50 eq.) was added while stirring. The mixture was cooled to 0 °C and phosphoryl chloride (12.2 g, 7.31 mL, 80.1 mmol, 2.80 eq.). The mixture was stirred for 1 h at room temperature, then added carefully in portions into 200 mL ice-water containing 50 g potassium carbonate maintaining the temperature below 25 °C. The resulting emulsion was stirred for 30 min at room temperature. The organic layer was separated, the aqueous layer extracted three times with 50 mL dichloromethane and the combined organic layers were dried over potassium carbonate. Purification by column chromatography employing silica gel as stationary phase and eluting with a gradual solvent mixture of *c*-hexane/ethyl acetate (5:1 → 3:1) and concentration *in vacuo* yielded *p*-xylenediisocyanide as a yellow solid (2.60 g, 16.7 mmol, 58.1%).

R_f = 0.40 in *c*-hexane/ethyl acetate (3:1). Visualized *via* Seebach staining solution.

Spectral data is in accordance to earlier reported.[344]

IR (ATR): ν [cm^{-1}] = 2964.5 (m, ν(C-H)), 2155.1 (vs, ν(NC)), 1894.9 (w), 1632.0 (w), 1517.9 (m), 1436.7 (s), 1420.6 (s), 1350.0 (m), 1331.8 (w), 1258.4 (m), 1127.3 (w), 1019.5 (m), 971.3 (w), 949.5 (s), 785.9 (vs), 741.8 (s), 554.3 (m), 467.1 (vs).

^{1}H-NMR (400 MHz, DMSO-d_6): δ [ppm] = 7.43 (s, 4 H, $CH_{Ar}^{11,12,14,15}$), 4.89 – 4.88 (m, 2 H, $CH_2^{3,8}$).

^{13}C-NMR (101 MHz, DMSO-d_6) δ [ppm] = 156.81 – 156.65 (t, J = 5.1 Hz, $NC^{1,10}$), 133.30 (s, $C_{Ar}^{7,13}$), 127.34 (s, $CH_{Ar}^{11,12,14,15}$), 44.83 – 44.33 (t, J = 6.5 Hz, $CH_2^{3,8}$).

FAB – MS [*m/z*] (relative intensity): 156.1 (50%) $[M + H]^+$, 130.1 (70%) $[M – CN]^+$, 116.1 (100%) $[M – CH_2CN]^+$.

HRMS – FAB [*m/z*]: $[M + H]^+$ calculated for $^{12}C_{10}{}^{1}H_8{}^{14}N_2$, 156.0682; found, 156.0682; Δ = 0.01 mmu.

6.2.3.1.7 *N,N'-hexane-1,6-diformamide obtained from hexamethylene diamine and ethylformate*

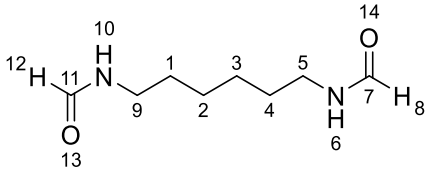

A solution of hexamethylene diamine (10.0 g, 86.1 mmol, 1.00 eq.) in ethyl formate (150 g, 162 mL, 2.02 mol, 23.5 eq.) was heated under reflux overnight (70 °C temperature set). The reaction mixture was concentrated *in vacuo.* The diformamide was obtained as a colorless solid (14.9 g, 86.7 mmol, 98.9%).

R_f = 0.30 in dichloromethane/methanol (9:1). Visualized *via* Seebach staining solution.

Spectral data is in accordance to earlier reported.[66]

IR (ATR) ν [cm^{-1}] = 3271.5 (br, ν(N-H)), 3027.8 (vw, ν(C-H)), 2942.8 (w, ν(C-H)), 2911.2 (w, ν(C-H)), 2852.1 (w, ν(C-H)), 1625.8 (m, ν(C=O)), 1527.0 (m), 1474.7 (w), 1460.3 (w), 1385.3 (m), 1236.2 (m), 1210.6 (w), 1082.6 (vw), 776.5 (w), 704.7 (m), 460.9 (w).

1H-NMR (300 MHz, DMSO-d6): δ [ppm] = 7.97 (s, 4 H, NH6,10, CHO8,12), 3.05 (dd, J = 12.7, 6.4 Hz, 4 H, CH25,9), 1.36 (dd, J = 16.5, 10.3 Hz, 4 H, $CH_2^{1,4}$), 1.27 (d, J = 14.4 Hz, 4 H, $CH_2^{2,3}$).

^{13}C-NMR (126 MHz, $CDCl_3$) δ [ppm] = 160.89 (s, CHO^{7,11}), 37.01 (s, $CH_2^{5,9}$), 28.97 (s, $CH_2^{1,4}$), 26.02 (s, $CH_2^{2,3}$).

FAB-MS *m/z* (relative intensity): 345.3 (25%) $[2\ M + H]^+$, 173.1 (100%) $[M + H]^+$, 100.1 (5%) [Fragment A]$^+$.

HRMS–FAB (*m/z*): $[M + H]^+$ calculated for $^{12}C_8{}^1H_{17}{}^{16}O_2{}^{14}N_2$, 173.1285; found, 173.1287; Δ = 0. 20 mmu.

Fragment A
Chemical Formula: $C_5H_{10}NO^{\bullet}$
Exact Mass: 100,07624

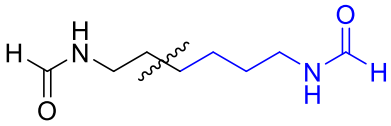

6.2.3.1.8 *1,6-Diisocyanohexane obtained from N,N'-hexane-1,6-diformamide*

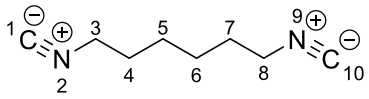

N,N'-hexane-1,6-diformamide (14.0 g, 81.3 mmol, 1.00 eq.) was suspended in 175 mL dichloromethane and diisopropylamine (49.4 g, 68.8 mL, 487 mmol, 6.00 eq.) was added. The mixture was cooled to 0 °C and phosphoryl chloride (34.9 g, 21.3 mL, 228 mmol, 2.80 eq.) was added dropwise at such a rate that the reaction temperature remained below 0 °C. The mixture was stirred for 2 d, then poured into 500 mL ice-water containing 50 g potassium carbonate. The resulting emulsion was stirred for 30 min at room temperature. The organic layer was separated, the aqueous layer extracted three times with 50 mL dichloromethane and the combined organic layers were dried over potassium carbonate and subsequently under reduced pressure. The batch was separated into two equal amounts and each was purified separately by column chromatography employing silica gel as stationary phase (*c*-hexane/ethyl acetate 5:1 → 1:1) yielding 1,6-diisocyanohexane as a yellowish oil (8.64 g, 63.4 mmol, 78.0%).

R_f = 0.52 in *c*-hexane/ethyl acetate (1:1). Visualized *via* Seebach staining solution.

Spectral data is in accordance to earlier reported.[66]

IR (ATR) ν [cm^{-1}] = 2942.2 (m, ν(C-H)), 2862.2 (w, ν(C-H)), 2146.0 (m, ν(NC)), 1452.9 (s), 1350.8 (m), 1175.5 (w), 956.4 (m), 819.6 (s), 727.5 (m), 553.5 (w).

^{1}H-NMR (500 MHz, DMSO-d_6): δ [ppm] = 3.57 – 3.37 (m, 4 H, $CH_2^{3,8}$), 1.60 (d, J = 2.1 Hz, 4 H, $CH_2^{4,7}$), 1.43 – 1.29 (m, 4 H, $CH_2^{5,6}$).

^{13}C-NMR (126 MHz, DMSO-d_6) δ [ppm] = 155.45 (t, J = 5.6 Hz, $C^{1,10}$), 41.03 (t, J = 5.9 Hz, $CH_2^{3,8}$), 28.20 (s, $CH_2^{4,7}$), 24.90 (s, $CH_2^{5,6}$).

EI-MS *m/z* (relative intensity): 137.2 (100%) $[M + H]^+$.

HRMS–EI (*m/z*): $[M]^+$ calculated for $^{12}C_8{}^{1}H_{12}{}^{14}N_2$, 136.0995; found, 136.0994; Δ = 0.10 mmu.

6.2.3.1.9 *Benzyl 6-hydroxyhexanoate 62 and discrete oligomers 63 – 66 obtained from ε-caprolactone and benzyl alcohol*

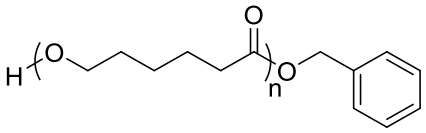

In a 250 mL round bottom flask equipped with dropping funnel, a temperature controller and magnetic stir bar benzyl alcohol (28.4 g, 27.3 mL, 262 mmol, 5.00 eq.) was stirred with DBU (800 mg, 784 µL, 5.25 mmol, 0.10 eq.) at room temperature. Subsequently, ε-caprolactone (6.00 g, 5.56 mL, 52.5 mmol, 1.00 eq.) dissolved in 30 mL dichloromethane was slowly added dropwise to the stirring solution at room temperature. The reaction mixture was stirred for 1 d at 85 °C. TLC indicated complete conversion of ε-caprolactone.

Distillation: Thermal stress will favor oligomer formation

Exceeding benzyl alcohol was removed by distillation (0.01 mbar, 65 °C). The residue was adsorbed onto celite® and purified *via* column chromatography on silica gel eluting with a gradual solvent mixture of *c*-hexane and diethyl ether (6:1 → 0:1). The monomeric benzyl ester **62** was obtained as a clear oil (1.37 g, 6.16 mmol, 11.7%). Furthermore, discrete oligomers (n = 2 – 5) were obtained as clear oils. Dimer (626 mg, 1.86 mol, 3.54%) **63**, timer **64** (468 g, 1.04 mmol, 1.98%), tetramer **65** (267 mg, 472 µmol, 0.9%), pentamer **66** (267 mg, 393 µmol, 0.7%).

Washing procedure: Milder than distillation, provides the monomer in higher yields

The reaction mixture was diluted with 200 mL ethyl acetate. Exceeding benzyl alcohol was removed by extracting six times with 200 mL water (if necessary with addition of brine) and 100 mL brine once. The organic phase was dried under reduced pressure and purified *via* chromatography (adsorbed onto celite®) on silica gel eluting with a gradual solvent mixture of *c*-hexane and diethyl ether (6:1 → 0:1). The monomeric benzyl ester **62** was obtained as a clear oil (3.32 g, 14.5 mmol, 27.6%).

Monomer **62**:

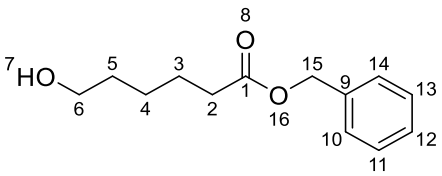

R_f = 0.47 in diethyl ether/*c*-hexane (4:1). Visualized *via* Seebach staining solution.

IR (ATR): ν [cm^{-1}] = 3400.4 (br, ν(O-H)), 3033.8 (w), 2935.6 (m, ν(C-H)), 2864.0 (w, ν(C-H)), 1731.1 (vs, ν(C=O)), 1497.6 (w), 1455.3 (m), 1417.3 (w), 1383.1 (w), 1352.0 (m), 1259.0 (m), 1212.6 (s), 1149.9 (vs), 1073.9 (s), 1052.2 (s), 1026.5 (m), 802.5 (s), 735.9 (vs), 696.3 (m), 578.9 (w), 498.1 (w), 452.8 (w).

^{1}H-NMR (400 MHz, DMSO-d_6): δ [ppm] = 7.49 – 7.24 (m, 5 H, $CH_{Ar}^{10\text{-}14}$), 5.08 (s, 2 H, CH_2^{15}), 4.35 (t, J = 5.2 Hz, 1 H, OH^7), 3.40 – 3.32 (m, 2 H, CH_2^6), 2.35 (t, J = 7.4 Hz, 2 H, CH_2^2), 1.54 (p, J = 7.4 Hz, 2 H, CH_2^3), 1.40 (dq, J = 8.7, 6.1 Hz, 2 H, CH_2^5), 1.33 – 1.22 (m, 2 H, CH_2^4).

^{13}C-NMR (101 MHz, DMSO-d_6): δ [ppm] = 172.77 (s, CO_2R^1), 136.29 (s, C_{Ar}^9), 128.42 (s, CH_{Ar}), 127.96 (s, CH_{Ar}), 127.91 (s, CH_{Ar}), 65.28 (s, CH_2^{15}), 60.51 (s, CH_2^6), 33.52 (s, CH_2^2), 32.14 (s, CH_2^5), 25.03 (s, CH_2^4), 24.39 (s, CH_2^3).

FAB – MS [*m/z*] (relative intensity): 223.0 (100%) $[M + H]^+$, 135.0 (15%) [Fragment A]$^+$. HRMS – FAB [*m/z*]: $[M + H]^+$ calculated for $^{12}C_{13}{}^1H_{19}{}^{16}O_3$, 223.1329; found, 223.1327; Δ = 0.17 mmu.

Fragment A
Chemical Formula: $C_8H_7O_2^{\bullet}$
Exact Mass: 135,04

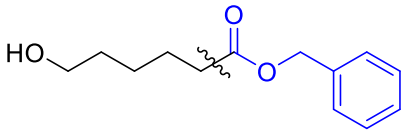

Dimer **63**:

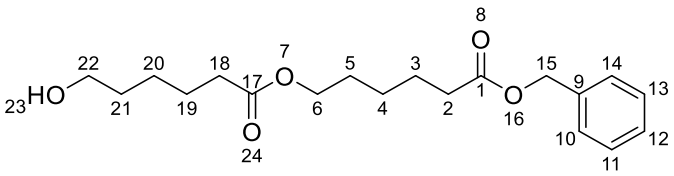

R_f = 0.43 in diethyl ether/*c*-hexane (4:1). Visualized *via* Seebach staining solution.

IR (ATR): ν [cm^{-1}] = 3431.4 (br, ν(O-H)), 2936.2 (m, ν(C-H)), 2863.1 (m, ν(C-H)), 1729.3 (vs, ν(C=O)), 1497.7 (m), 1455.5 (w), 1385.1 (w), 1353.3 (w), 1154.6 (vs), 1080.1 (m), 736.3 (m), 697.5 (s), 579.8 (w), 498.1 (w).

^{1}H-NMR (400 MHz, DMSO-d_6): δ [ppm] = 7.66 – 7.18 (m, 5 H, CH_{Ar}^{10-14}), 5.08 (s, 2 H, CH_2^{15}), 4.35 (t, J = 5.2 Hz, 1 H, OH^{23}), 3.97 (t, J = 6.6 Hz, 2 H, CH_2^{6}), 3.36 (td, J = 6.5, 5.2 Hz, 2 H, CH_2^{22}), 2.36 (t, J = 7.4 Hz, 2 H, CH_2^{2}), 2.26 (t, J = 7.4 Hz, 2 H, CH_2^{18}), 1.62 – 1.46 (m, 6 H, CH_2^{3+5+19}), 1.45 – 1.35 (m, 2 H, CH_2^{21}), 1.35 – 1.21 (m, 4 H, CH_2^{4+20}).

^{13}C-NMR (101 MHz, DMSO-d_6): δ [ppm] = 172.89 (s, $CO_2R^{1\ or\ 17}$), 172.66 (s, $CO_2R^{1\ or\ 17}$), 136.26 (s, C_{Ar}^{9}), 128.40 (s, CH_{Ar}), 127.96 (s, CH_{Ar}), 127.90 (s, CH_{Ar}), 65.30 (s, CH_2^{15}), 63.45 (s, CH_2^{6}), 60.52 (s, CH_2^{22}), 33.57 (s, CH_2^{18}), 33.32 (s, CH_2^{2}), 32.14 (s, CH_2^{21}), 27.78 (s, CH_2), 25.04 (s, CH_2), 24.87 (s, CH_2), 24.41 (s, CH_2), 24.07 (s, CH_2).

FAB – MS [*m/z*] (relative intensity): 337.2 (100%) $[M + H]^+$.

HRMS – FAB [*m/z*]: $[M + H]^+$ calculated for $^{12}C_{19}{}^{1}H_{29}{}^{16}O_5$, 337.2015; found, 337.2014; Δ = 0.08 mmu.

Trimer **64**:

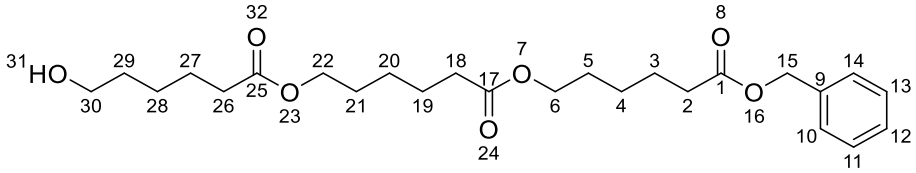

R_f = 0.39 in diethyl ether/*c*-hexane (4:1). Visualized *via* Seebach staining solution.

^{1}H-NMR (300 MHz, DMSO-d_6): δ [ppm] = 7.47 – 7.22 (m, 5 H, CH_{Ar}^{10-14}), 5.08 (s, 2 H, CH_2^{15}), 4.34 (t, J = 5.2 Hz, 1 H, OH^{31}), 3.98 (t, J = 6.5 Hz, 4 H, CH_2), 3.40 – 3.33 (m, 2 H, CH_2^{30}), 2.36 (t, J = 7.3 Hz, 2 H, CH_2^{2}), 2.26 (td, J = 7.3, 3.4 Hz, 4 H, CH_2^{2+26}), 1.69 – 1.46 (m, 10 H, CH_2), 1.47 – 1.36 (m, 2 H, CH_2^{29}), 1.37 – 1.16 (m, 6 H, $CH_2^{4+20+28}$).

^{13}C-NMR (101 MHz, DMSO-d_6): δ [ppm] = 172.92 (s, CO_2R), 172.82 (s, CO_2R), 172.69 (s, CO_2R), 136.28 (s, C_{Ar}^{9}), 128.42 (s, CH_{Ar}), 127.99 (s, CH_{Ar}), 127.92 (s, CH_{Ar}), 65.33 (s, CH_2^{15}), 63.52 (s, $CH_2^{6\ or\ 22}$), 63.48 (s, $CH_2^{6\ or\ 22}$), 60.54 (s, CH_2^{30}), 33.59 (s, $CH_2^{2\ or\ 18\ or\ 26}$), 33.38 (s, $CH_2^{2\ or\ 18\ or\ 26}$), 33.34 (s, $CH_2^{2\ or\ 18\ or\ 26}$), 32.17 (s, CH_2), 27.82 (s, CH_2), 27.80 (s, CH_2), 25.06 (s, CH_2), 24.90 (s, CH_2), 24.44 (s, CH_2), 24.11 (s, CH_2), 24.09 (s, CH_2), 20.77 (s, CH_2).

Tetramer **65**:

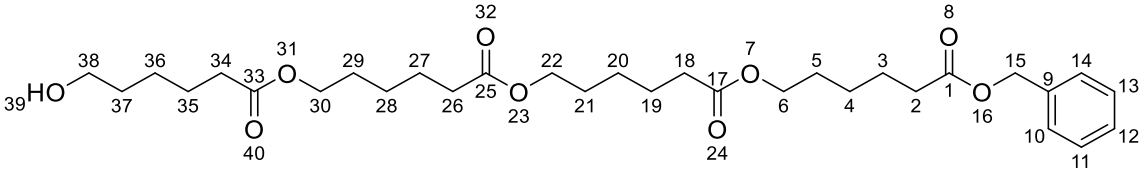

R_f = 0.34 in diethyl ether/*c*-hexane (4:1). Visualized *via* Seebach staining solution.

IR (ATR): ν [cm^{-1}] = 3528.8 (br, ν(O-H)), 2936.8 (m, ν(C-H)), 2863.0 (w, ν(C-H)), 1730.0 (vs, ν(C=O)), 1455.7 (m), 1388.0 (m), 1354.3 (m), 1158.8 (s), 1090.7 (m), 738.0 (w), 698.3 (m), 580.7 (w), 387.8 (w).

^{1}H-NMR (300 MHz, DMSO-d_6): δ [ppm] = 7.77 – 7.00 (m, 5 H, CH_{Ar}^{10-14}), 5.08 (s, 2 H, CH_2^{15}), 4.33 (t, J = 5.1 Hz, 1 H, OH^{39}), 3.98 (t, J = 6.5 Hz, 6 H, $CH_2^{6+22+30}$), 3.40 – 3.33 (m, 2 H, CH_2^{38}), 2.36 (t, J = 7.4 Hz, 2 H, CH_2^{2}), 2.32 – 2.22 (m, 6 H, $CH_2^{18+26+34}$), 1.64 – 1.45 (m, 14 H, CH_2), 1.44 – 1.36 (m, 2 H, CH_2^{37}), 1.36 – 1.21 (m, 8 H, $CH_2^{4+20+28+36}$).

^{13}C-NMR (101 MHz, DMSO-d_6): δ [ppm] = 172.90 (s, CO_2R), 172.80 (s, CO_2R), 172.67 (s, CO_2R),128.41 (s, CH_{Ar}), 127.97 (s, CH_{Ar}), 127.91 (s, CH_{Ar}), 65.31 (s, CH_2^{15}), 63.50 (s, $CH_2^{6\ or\ 22\ or\ 30}$), 63.46 (s, $CH_2^{6\ or\ 22\ or\ 30}$), 60.53 (s, CH_2^{38}), 33.58 (s, $CH_2^{18\ or\ 26\ or\ 34}$), 33.32 (s, CH_2^{2}), 32.16 (s, CH_2), 27.80 (s, CH_2), 25.05 (s, CH_2), 24.89 (s, CH_2), 24.42 (s, CH_2), 24.09 (s, CH_2), 24.07 (s, CH_2).

FAB – MS [*m/z*] (relative intensity): 565.3 (100%) $[M + H]^+$.

HRMS – FAB [*m/z*]: $[M + H]^+$ calculated for $^{12}C_{31}{}^{1}H_{48}{}^{16}O_9$, 565.3337; found, 565.3375; Δ = 0.15 mmu.

Pentamer **66**:

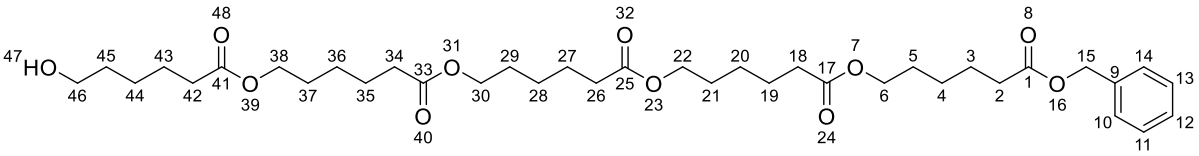

R_f = 0.30 in diethyl ether/*c*-hexane (4:1). Visualized *via* Seebach staining solution.

IR (ATR): ν [cm^{-1}] = 3536.2 (br, ν(O-H)), 2937.5 (m, ν(C-H)), 2863.8 (w, ν(C-H)), 1728.2 (vs, ν(C=O)), 1456.0 (m), 1388.8 (w), 1354.9 (m), 1156.7 (vs), 1090.4 (m), 736.5 (m), 697.9 (m), 579.5 (w), 498.4 (w).

^{1}H-NMR (300 MHz, DMSO-d_6): δ [ppm] = 7.72 – 6.77 (m, 5 H, $CH_{Ar}^{10\text{-}14}$), 5.08 (s, 2 H, CH_2^{15}), 4.33 (t, J = 5.1 Hz, 1 H, OH^{47}), 3.98 (t, J = 6.5 Hz, 8 H, $CH_2^{6+22+30+38}$), 3.42 – 3.33 (m, 2 H, CH_2^{46}), 2.36 (t, J = 7.3 Hz, 2 H, CH_2^{2}), 2.32 – 2.18 (m, 8 H, $CH_2^{18+26+34+42}$), 1.63 – 1.46 (m, 18 H, CH_2), 1.44 – 1.36 (m, 2 H, CH_2^{45}), 1.66 – 1.41 (m, 20 H, CH_2), 1.36 – 1.21 (m, 10 H, $CH_2^{4+20+28+36+44}$).

^{13}C-NMR (101 MHz, DMSO-d_6): δ [ppm] = 172.91 (s, CO_2R), 172.81 (s, CO_2R), 172.68 (s, CO_2R), 136.28 (s, C_{Ar}^{9}), 128.42 (s, CH_{Ar}), 127.98 (s, CH_{Ar}), 127.92 (s, CH_{Ar}), 65.32 (s, CH_2^{15}), 63.52 (s, $CH_2^{6\ or\ 30\ or\ 38}$), 63.48 (s, $CH_2^{6\ or\ 30\ or\ 38}$), 60.54 (s, CH_2^{46}), 33.59 (s, CH_2), 33.38 (s, CH_2), 33.33 (s, CH_2), 32.17 (s, CH_2), 27.81 (s, CH_2), 25.06 (s, CH_2), 24.90 (s, CH_2), 24.44 (s, CH_2), 24.11 (s, CH_2), 24.09 (s, CH_2).

FAB – MS [*m/z*] (relative intensity): 679.4 (100%) $[M + H]^+$.

HRMS – FAB [*m/z*]: $[M + H]^+$ calculated for $^{12}C_{37}{}^{1}H_{59}{}^{16}O_{11}$, 679.4057; found, 679.4056; Δ = 0.17 mmu.

6.2.3.1.10 *C6-Benzylacetoacetate 68 derived from C6-benzylalcohol 62 and diketene acetone adduct 67*

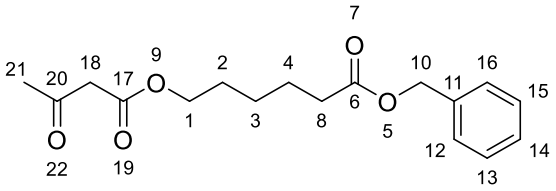

In carousel tube vial equipped with a magnetic stir bar the monomer benzyl alcohol **62** (200 mg, 900 µmol, 1.00 eq.) was dissolved in 2 mL dimethyl sulfoxide. Subsequently, diketene acetone adduct **67** (256 mg, 239 µL, 1.80 mmol, 2.00 eq. 900 µL) was added while stirring at room temperature. The reaction mixture was heated to 110 °C. Reduced pressure was applied to the reaction vial (300 mbar) every 30 min for 3 min until the boiling of acetone stopped. TLC indicated complete conversion of the benzyl alcohol **62**. After completion of the reaction, the mixture was diluted with 30 mL diethyl ether and washed with 30 mL water twice and with 20 mL brine once. The combined organic phases were dried under reduced pressure and purified by flash column chromatography employing silica gel as stationary phase and eluting with ethyl acetate/*c*-hexane (1:2). The acetoacetate product **68** was obtained as a yellow oil (189 mg, 621 µmol, 69.0%).

R_f in ethyl acetate/*c*-hexane (1:1) = 0.45. Visualized *via* Seebach staining solution.

IR (ATR): ν [cm^{-1}] = 2946.1 (m, ν(C-H)), 1730.5 (vs, ν(C=O)), 1647.9 (w), 1497.8 (w), 1455.3 (w), 1413.9 (w), 1383.9 (w), 1358.4 (w), 1314.3 (m), 1234.5 (s), 1149.1 (vs), 1104.9 (w), 1029.9 (w), 963.2 (w), 802.2 (w), 738.0 (s), 697.8 (s), 578.3 (w), 541.9 (w), 497.5 (w).

^{1}H-NMR (400 MHz, DMSO-d_6): δ [ppm] = 7.55 – 7.07 (m, 5 H, $CH_{Ar}{}^{12-16}$), 5.08 (s, 2 H, $CH_2{}^{10}$), 4.02 (t, J = 6.5 Hz, 2 H, $CH_2{}^{1}$), 3.58 (s, 2 H, $CH_2{}^{18}$), 2.35 (t, J = 7.4 Hz, 2 H, $CH_2{}^{8}$), 2.16 (s, 3 H, $CH_3{}^{21}$), 1.61 – 1.50 (m, 4 H, $CH_2{}^{2+4}$), 1.37 – 1.22 (m, 2 H, $CH_2{}^{3}$).

^{13}C-NMR (101 MHz, DMSO-d_6) δ [ppm] = 201.55 (s, CO^{20}), 172.67 (s, CO_2R^{6}), 167.26 (s, CO_2R^{17}), 136.27 (s, $C_{Ar}{}^{11}$), 128.42 (s, CH_{Ar}), 127.97 (s, CH_{Ar}), 127.93 (s, CH_{Ar}),

65.32 (s, CH_2^{10}), 64.24 (s, CH_2^{1}), 49.57 (s, CH_2^{18}), 33.32 (s, CH_2^{8}), 30.05 (s, CH_3^{21}), 27.66 (s, $CH_2^{2\ or\ 8}$), 24.75 (s, CH_2^{3}), 24.03 (s, $CH_2^{2\ or\ 4}$).

ESI – MS [*m/z*]: [M + Na]$^+$ calculated for $^{12}C_{17}{}^{1}H_{22}{}^{16}O_5{}^{14}N_4{}^{23}Na_1$, 329.1359; found, 329.1359; Δ = 0.05 mmu.

6.2.3.1.11 ***Pentamer-benzyl acetoacetate 69 derived from pentamer-benzyl alcohol 66 and diketene acetone adduct 67***

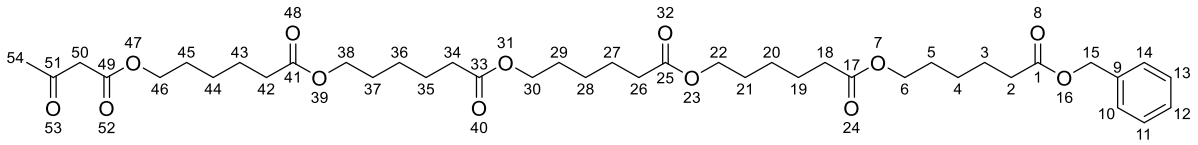

In a carousel tube vial equipped with a magnetic stir bar the benzyl alcohol **66** (197 mg, 290 µmol, 1.00 eq.) was dissolved in 1.5 mL dimethyl sulfoxide. Subsequently, diketene acetone adduct **67** (82.5 mg, 77.1 µL, 580 mmol, 2.00 eq.) was added while stirring at room temperature. The reaction mixture was stirred at 90 °C for 1 h and at 110 °C for three hours. Reduced pressure was applied to the reaction vial (300 mbar) every 30 min for a few seconds until the boiling of acetone stopped. TLC indicated complete conversion of the benzyl alcohol **66**. After completion of the reaction, the mixture was diluted with 30 mL diethyl ether and washed with 30 mL water twice and with 20 mL brine once. The combined organic phases were dried under reduced pressure and purified *via* column chromatography employing silica gel as stationary phase and eluting with diethyl ether /*c*-hexane (2:1 → 3:1). The acetoacetate product **69** was obtained as a yellow highly viscous oil (133 mg, 174 µmol, 60.1%).

R_f = 0.59 in diethyl ether/*c*-hexane (4:1).

IR (ATR): ν [cm^{-1}] = 2938.6 (s, ν(C-H)), 2863.6 (m, ν(C-H)), 1727.6 (vs, ν(C=O)), 1455.8 (w), 1417.6 (m), 1357.6 (m), 1233.5 (s), 1154.9 (vs), 1094.1 (s), 1039.8 (m), 960.8 (m), 736.6 (m), 698.2 (w), 541.1 (w).

^{1}H-NMR (300 MHz, DMSO-d_6): δ [ppm] = 11.63 (s, 0.2 H, $OH^{52\ or\ 53,\ enol}$), 7.35 (s, 5 H, CH_{Ar}^{10-14}), 5.08 (s, 2 H, CH_2^{15}), 4.07 – 3.93 (m, 10 H, $CH_2^{6+22+30+38+46}$), 3.58 (s, 1.8 H, CH_2^{50}), 2.35 (t, *J* = 7.3 Hz, 2 H, CH_2^{2}), 2.27 (t, *J* = 7.3 Hz, 8 H, $CH_2^{18+26+34+42}$), 2.16 (s, 3 H, CH_3^{54}), 1.67 – 1.41 (m, 20 H, CH_2), 1.38 – 1.16 (m, 10 H, $CH_2^{4+20+28+36+44}$).

^{13}C-NMR (101 MHz, DMSO-d_6) δ [ppm] = 201.51 (s, CO^{51}), 172.78 (s, $CO_2R^{1+17+25+33+41}$), 167.26 (s, CO_2R^{49}), 136.27 (s, $C_{Ar}{}^{9}$), 128.40 (s, CH_{Ar}), 127.96 (s, CH_{Ar}), 127.90 (s, CH_{Ar}), 65.31 (s, $CH_2{}^{15}$), 64.24 (s, $CH_2{}^{46}$), 63.50 (s, $CH_2{}^{6+22+30+38}$), 49.56 (s, $CH_2{}^{50}$), 33.37 (s, $CH_2{}^{18\ or\ 26\ or\ 35\ or\ 42}$), 33.32 (s, $CH_2{}^{18\ or\ 26\ or\ 35\ or\ 42}$), 30.04 (s, $CH_3{}^{54}$), 27.80 (s, CH_2), 27.69 (s, CH_2), 24.89 (s, CH_2), 24.78 (s, CH_2), 24.09 (s, CH_2), 24.07 (s, CH_2), 24.05 (s, CH_2).

ESI – MS [*m/z*]: $[M + Na]^+$ calculated for $^{12}C_{41}{}^{1}H_{62}{}^{16}O_{13}{}^{23}Na_1$, 785.4088; found, 785.4079; Δ = 0.88 mmu.

6.2.3.2 Biginelli acids

6.2.3.2.1 *Biginelli acid 70 derived from 11-ureidoundecanoic acid, benzaldehyde and benzyl acetoacetate*

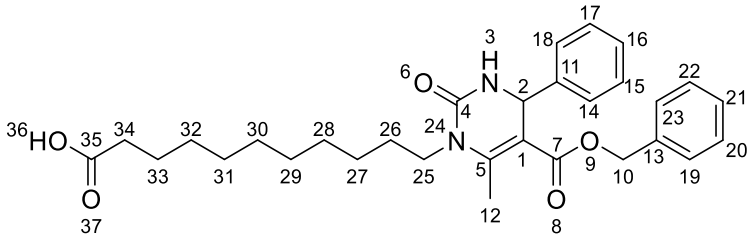

In a 25 mL round bottom flask finely powdered 11-ureidoundecanoic acid (1.00 g, 4.09 mmol, 1.00 eq.) and benzaldehyde (654 mg, 6.14 mmol, 626 µL, 1.50 eq.) were suspended in 4 mL dimethyl sulfoxide. Subsequently, benzyl acetoacetate (1.18 g, 6.14 mmol, 1.06 mL, 1.50 eq.) and 4-methylbenzenesulfonic acid (49.1 mg, 409 µmol, 0.10 eq.) were added. The resulting mixture was stirred under argon atmosphere at 110 °C over night and at 80 °C for another 24 h. Subsequently, the crude reaction mixture was added extracted with 200 mL water and 100 mL dichloromethane. The aqueous phase was extracted with 50 mL dichloromethane three times. The combined organic phases were washed with 50 mL water and concentrated under reduced pressure. The resulting concentrate was diluted with 20 mL ethyl acetate/*c*-hexane (4:1) and left to crystallize overnight. The precipitate was filtered and washed three times with 20 mL ice cold ethyl acetate and dried under reduced pressure. The Biginelli acid **70** was obtained as a colorless solid (930 mg, 1.83 mmol, 44.9%).

IR (ATR): ν [cm^{-1}] = 3365.7 (br, ν(N-H)), 2923.6 (w, ν(C-H)), 2847.4 (w, ν(C-H)), 1723.1 (s, ν(C=O)), 1682.5 (s, ν(C=O)), 1656.8 (vs, ν(C=O)), 1616.3 (m), 1418.2 (w), 1384.3 (s), 1315.5 (s), 1289.3 (s), 1265.6 (m), 1243.8 (m), 1222.7 (m), 1196.9 (m), 1158.0 (vs), 1087.6 (s), 1049.1 (m), 1011.0 (w), 827.9 (w), 719.2 (w), 770.0 (w), 752.1 (w), 734.6 (m), 715.2 (m), 699.8 (s), 633.0 (s), 516.9 (w), 496.1 (w), 430.5 (w), 393.0 (w).

^{1}H-NMR (400 MHz, DMSO-d_6): δ [ppm] = 11.96 (s, 1 H, CO_2H^{36}), 7.95 (d, J = 3.9 Hz, 1 H, NH^{3}), 7.32 – 7.13 (m, 10 H, $CH_{Ar}^{14-18\ +\ 19-23}$), 5.17 (d, J = 3.8 Hz, 1 H, CH^{2}), AB-signal (δ_A = 5.09, δ_B = 5.05 J_{AB} = 12.0 Hz, 2 H, CH_2^{10}), 3.91 – 3.41 (m, 2 H, CH_2^{25}), 2.51 (underneath solvent signal, CH_3^{12}), 2.18 (t, J = 7.4 Hz, 2 H, CH_2^{34}), 1.47 (p, J = 7.2 Hz, 2 H, CH_2^{33}), 1.35 (dt, J = 6.7, 6.3 Hz, 2 H, CH_2^{26}), 1.29 – 1.00 (m, 12 H, CH_2^{27-32}).

^{13}C-NMR (101 MHz, DMSO-d_6) δ [ppm] = 174.47 (s, CO_2H^{36}), 165.36 (s, CO_2R^{7}), 152.62 (s, CO^{4}), 150.51 (s, C^{5}), 143.80 (s, C_{Ar}^{11}), 136.35 (s, C_{Ar}^{13}), 128.34 (s, CH_{Ar}), 128.28 (s, CH_{Ar}), 127.78 (s, CH_{Ar}), 127.63 (s, CH_{Ar}), 127.29 (s, CH_{Ar}), 126.05 (s, CH_{Ar}), 102.53 (s, C^{1}), 65.16 (s, CH_2^{10}), 52.24 (s, CH^{2}), 41.58 (s, CH_2^{25}), 33.67 (s, CH_2^{34}), 29.33 (s, CH_2), 28.92 (s, CH_2), 28.83 (s, CH_2), 28.72 (s, CH_2), 28.52 (s, CH_2), 26.16 (s, CH_2), 24.50 (s, CH_2^{33}), 15.71 (s, CH_3^{12}).

FAB – MS [m/z] (relative intensity): 507.3 (100%) $[M + H]^+$, 429.2 (20%) [M – C_6H_5], 415.2 (50%) [M – C_7H_7], 399.2 (50%) [M – C_7H_7O], 371.2 (10%) [M – $C_7H_7O_2$], 312.1 (10%) [Fragment A]$^+$.

HRMS – FAB [m/z]: $[M + H]^+$ calculated for $^{12}C_{30}{}^{1}H_{39}{}^{16}O_5{}^{14}N_2$, 507.2853; found, 507.2853; Δ = 0.07 mmu.

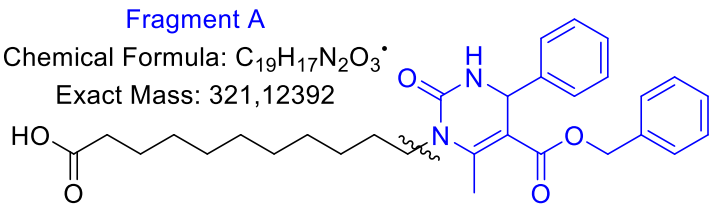

6.2.3.2.2 *Biginelli acid 71 derived from 11-ureidoundecanoic acid, 4-methoxy benzaldehyde and benzyl acetoacetate*

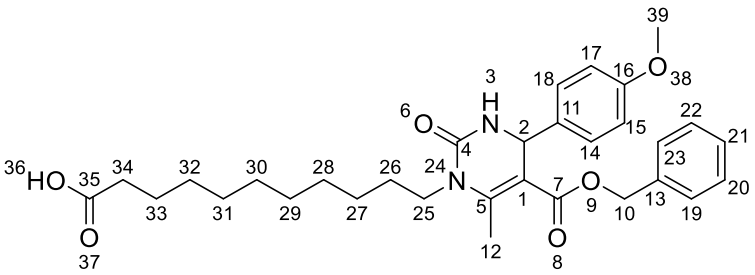

In a 25 mL round bottom flask finely powdered 11-ureidoundecanoic acid (1.00 g, 4.09 mmol, 1.00 eq.) and 4-methoxy benzaldehyde (835 mg, 6.14 mmol, 1.50 eq.) were suspended in 5 mL dimethyl sulfoxide. Subsequently, benzyl acetoacetate (1.17 g, 6.14 mmol, 1.50 eq.) and 4-methylbenzenesulfonic acid (49.1 mg, 409 µmol, 0.10 eq.) were added. The resulting mixture was stirred at 110 °C over night. Subsequently, the crude reaction mixture was added extracted with 50 mL water and 30 mL dichloromethane. The aqueous phase was extracted with 30 mL dichloromethane three times. The combined organic phases were dried under reduced pressure. The resulting oil was diluted with 20 mL ethyl acetate/*c*-hexane (6:1) and left to crystallize overnight at 7 °C. The precipitate was filtered and washed three times with 20 mL ice cold ethyl acetate and dried under reduced pressure. The washing solution was dried under reduced pressure and the crystallization procedure was repeated to recover additional product. The Biginelli acid **71** was obtained as a yellow solid (858 mg, 1.60 mmol, 39.2%).

IR (ATR): ν [cm^{-1}] = 3366.3 (br, ν(N-H)), 2922.8 (w, ν(C-H)), 2848.9 (w, ν(C-H)), 1723.3 (s, ν(C=O)), 1682.5 (vs, ν(C=O)), 1657.7 (s), 1609.3 (m), 1586.8 (m), 1511.4 (s), 1497.1 (m), 1454.0 (m), 1441.8 (s), 1419.7 (m), 1384.0 (w), 1315.8 (m), 1287.3 (w), 1272.0 (s), 1244.6 (w), 1223.2 (w), 1196.5 (m), 1156.5 (m), 1107.4 (s), 1086.2 (m), 1048.7 (m), 1031.8 (s), 1011.0 (w), 1000.0 (w), 967.0 (m), 897.2 (w), 861.1 (w), 831.8 (w), 804.9 (m), 746.8 (w), 719.3 (w), 692.6 (w), 638.6 (w), 623.3 (w), 584.1 (m), 554.5 (w), 530.8 (w), 508.4 (m), 454.2 (w), 427.3 (w).

^{1}H-NMR (300 MHz, DMSO-d_6): δ [ppm] = 11.93 (s, 1 H, CO_2H^{36}), 7.88 (d, J = 3.8 Hz, 1 H, NH^{3}), 7.38 – 7.25 (m, 3 H, CH_{Ar}^{19-23}), 7.25 – 7.13 (m, 2 H, CH_{Ar}^{19-23}), 7.09 (d, J = 8.4 Hz, 2 H, $CH_{Ar}^{15,17}$), 6.83 (d, J = 8.3 Hz, 2 H, $CH_{Ar}^{14,18}$), 5.12 (d, J = 3.9 Hz, 1 H, CH^{2}), 5.10 – 4.99 (m, 2 H, CH_2^{10}), 3.90 – 3.76 (m, 1 H, CH_2^{25a}), 3.72 (s, 3 H, OCH_3^{39}),

3.53 – 3.40 (m, 1 H, CH_2^{25b}), 2.50 (underneath solvent signal, CH_3^{12}), 2.18 (t, *J* = 7.3 Hz, 2 H, CH_2^{34}), 1.48 (t, *J* = 7.1 Hz, 2 H, CH_2), 1.38 – 1.02 (m, 14 H, CH_2).

^{13}C-NMR (75 MHz, DMSO-d_6) δ [ppm] = 174.48 (s, CO_2H^{36}), 165.40 (s, CO_2R^{7}), 158.49 , 156.31 (s, $C_{Ar}^{15,17}$), 152.64 (s, CO^{4}), 150.21 (s, C^{5}), 136.40 (s, C_{Ar}^{13}), 135.92 (s, C_{Ar}^{16}), 128.28 (s, CH_{Ar}), 127.77 (s, CH_{Ar}), 127.60 (s, CH_{Ar}), 127.25 (s, CH_{Ar}), 113.63 (s, $CH_{Ar}^{14,18}$), 102.86 (s, C^{1}), 65.10 (s, CH_2^{10}), 55.04 (s, OCH_3^{39}), 51.64 (s, CH^{2}), 41.55 (s, CH_2^{25}), 33.66 (s, CH_2^{34}), 29.37 (s, CH_2), 28.99 (s, CH_2), 28.87 (s, CH_2), 28.78 (s, CH_2), 28.74 (s, CH_2), 28.54 (s, CH_2), 26.20 (s, CH_2), 24.50 (s, CH_2^{33}), 15.68 (s, CH_3^{12}).

FAB – MS [*m/z*] (relative intensity): 537.3 (100%) $[M + H]^+$, 445.3 (80%) $[M – C_7H_7]$, 429.3 (50%) $[M – C_7H_7O]$, 401.3 (20%) $[M – C_8H_7O_2]$.

HRMS – FAB [*m/z*]: $[M + H]^+$ calculated for $^{12}C_{31}{}^{1}H_{41}{}^{16}O_6{}^{14}N_2$, 537.2965; found, 537.2666; Δ = 0.16 mmu.

6.2.3.2.3 ***Biginelli acid 72 derived from 11-ureidoundecanoic acid, 4-methyl benzaldehyde and benzyl acetoacetate***

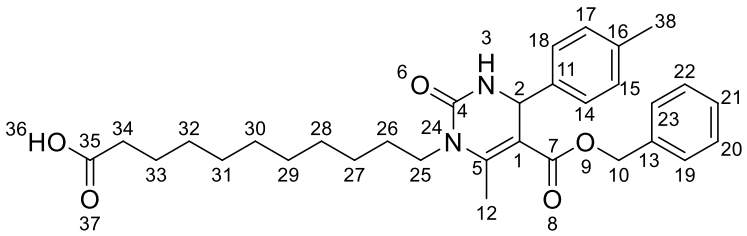

In a 25 mL round bottom flask finely powdered 11-ureidoundecanoic acid (1.00 g, 4.09 mmol, 1.00 eq.) and 4-methyl benzaldehyde (738 mg, 6.14 mmol, 1.50 eq.) were suspended in 5 mL dimethyl sulfoxide. Subsequently, benzyl acetoacetate (1.17 g, 6.14 mmol, 1.50 eq.) and 4-methylbenzenesulfonic acid (49.1 mg, 409 µmol, 0.10 eq.) were added. The resulting mixture was stirred at 110 °C over night. Subsequently, the crude reaction mixture was added extracted with 50 mL water and 30 mL dichloromethane. The aqueous phase was extracted with 30 mL dichloromethane three times. The combined organic phases were dried under reduced pressure. The resulting oil was diluted with 20 mL diethyl ether and left to crystallize overnight at 7 °C. The precipitate was filtered and washed three times with 20 mL ice cold diethyl ether then with 20 mL *c*-hexane and dried under reduced pressure. The washing solution was dried under reduced pressure and the crystallization procedure was repeated to

recover additional product. The Biginelli acid **72** was obtained as a yellow solid (953 mg, 1.83 mmol, 44.7%).

IR (ATR): ν [cm^{-1}] = 3367.0 (br, ν(N-H)), 2922.4 (m, ν(C-H)), 2849.5 (w, ν(C-H)), 1723.8 (m, ν(C=O)), 1681.6 (s), 1660.1 (vs), 1617.4 (s), 1512.5 (w), 1421.2 (w), 1387.3 (m), 1336.5 (m), 1317.4 (w), 1284.2 (m), 1243.3 (m), 1224.0 (w), 1197.0 (m), 1155.2 (s), 1088.3 (m), 1040.6 (vs), 1001.1 (m), 804.0 (w), 776.9 (w), 754.4 (w), 719.6 (w), 697.6 (w), 647.9 (m), 627.1 (w), 589.4 (w), 553.3 (w), 503.3 (m), 429.7 (w).

^{1}H-NMR (300 MHz, DMSO-d_6): δ [ppm] = 11.96 (s, 1 H, CO_2H^{36}), 7.90 (d, J = 3.9 Hz, 1 H, NH^{3}), 7.35 – 7.24 (m, 3 H, CH_{Ar}), 7.24 – 7.15 (m, 2 H, CH_{Ar}), 7.13 – 7.01 (m, 4 H, CH_{Ar}), 5.14 (d, J = 3.7 Hz, 1 H, CH^{2}), 5.11 – 4.97 (m, 2 H, CH_2^{10}), 3.94 – 3.38 (m, 2 H, CH_2^{25}), 2.50 (underneath solvent signal, CH_3^{12}), 2.26 (s, 3 H, CH_3^{38}), 2.19 (t, J = 7.4 Hz, 2 H, CH_2^{34}), 1.60 – 1.37 (m, 4 H, CH_2), 1.34 – 1.01 (m, 12 H, CH_2).

^{13}C-NMR (75 MHz, DMSO-d_6) δ [ppm] = 174.47 (s, CO_2H^{36}), 165.39 (s, CO_2R^{7}), 152.68 (s, CO^{4}), 150.35 (s, C^{5}), 140.86 (s, C_{Ar}^{11}), 136.41 (s, $C_{Ar}^{13\ or\ 16}$), 136.38 (s, $C_{Ar}^{13\ or\ 16}$), 128.84 (s, CH_{Ar}), 128.28 (s, CH_{Ar}), 127.78 (s, CH_{Ar}), 127.64 (s, CH_{Ar}), 125.95 (s, CH_{Ar}), 102.74 (s, C^{1}), 65.13 (s, CH_2^{10}), 51.88 (s, CH^{2}), 41.53 (s, CH_2^{25}), 33.66 (s, CH_2^{34}), 29.38 (s, CH_2), 28.97 (s, CH_2), 28.88 (s, CH_2), 28.78 (s, CH_2), 28.55 (s, CH_2), 26.18 (s, CH_2), 24.51 (s, CH_2), 20.61 (s, CH_3^{38}), 15.69 (s, CH_3^{12}).

ESI–MS [m/z]: $[M + Na]^+$ calculated for $^{12}C_{31}{}^{1}H_{40}{}^{16}O_5{}^{14}N_2{}^{23}Na_1$, 543.2829; found, 543.2829; Δ = 0.02 mmu.

6.2.3.2.4 *Biginelli acid 73 derived from 11-ureidoundecanoic acid, benzaldehyde and C6-benzyl acetoacetate 68*

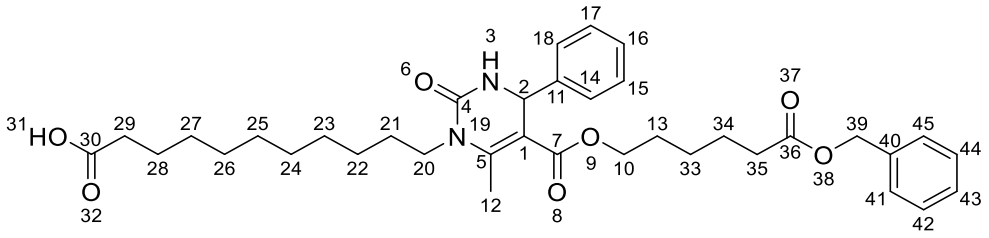

In a 25 mL round bottom flask finely powdered 11-ureidoundecanoic acid (215 mg, 881 µmol, 1.50 eq.) and benzaldehyde (93.5 mg, 881 µmol, 1.50 eq.) were dissolved in 2.5 mL dimethyl sulfoxide. Subsequently, C6-benzyl acetoacetate **68** (180 mg,

587 µmol, 1.00 eq.) and 4-methylbenzenesulfonic acid (49.1 mg, 409 µmol, 0.10 eq.) were added. The resulting mixture was stirred at 110 °C over night. TLC indicated complete conversion of the C6-benzyl acetoacetate **68**. Subsequently, the crude reaction mixture was extracted with 50 mL water and 30 mL dichloromethane. The aqueous phase was extracted with 30 mL dichloromethane three times. The combined organic phases were dried under reduced pressure. The residue was adsorbed onto celite® and purified *via* column chromatography on silica gel eluting with a gradual solvent mixture of ethyl acetate and *c*-hexane (1:4 → 1:0). The Biginelli acid **73** was obtained as an orange oil (243 mg, 66.8%, 391 µmol).

R_f in ethyl acetate/*c*-hexane (1:1) = 0.18. Visualized *via* fluorescence quench and Seebach staining solution.

IR (ATR): ν [cm^{-1}] = 3363.8 (br, ν(CO_2H, NH)), 2920.5 (vs, ν(C-H)), 2851.0 (s, ν(C-H)), 1738.0 (s, ν(C=O)), 1706.6 (vs, ν(C=O)), 1455.1 (m), 1388.2 (m), 1230.2 (m), 1158.5 (vs), 1090.3 (m), 966.5 (w), 860.3 (w), 799.7 (w), 751.7 (w), 696.6 (w), 463.1 (w).

^{1}H-NMR (500 MHz, DMSO-d_6): δ [ppm] = 12.00 (br s, 1 H, CO_2H^{31}), 8.06 (d, J = 4.0 Hz, 0.2 H, $NH^{3\ minor}$), 7.93 (d, J = 3.8 Hz, 0.8 H, $NH^{3\ major}$), 7.43 – 7.16 (m, 10 H, $CH_{Ar}^{14-18\ +\ 41-45}$), 5.16 (d, J = 3.9 Hz, 0.2 H, $CH^{2\ minor}$), 5.13 (d, J = 3.7 Hz, 0.8 H, $CH^{2\ major}$), 5.07 (s, 1.5 H, $CH_2^{39\ major}$), 5.06 (s, 0.5 H, $CH_2^{39\ minor}$), 3.99 – 3.89 (m, 2 H, CH_2^{10}), 3.88 – 3.76 (m, 1 H, CH_2^{20a}), 3.53 – 3.41 (m, 1 H, CH_2^{20b}), 2.49 (s, 3 H, CH_3^{12}), 2.25 (t, J = 7.4 Hz, 2 H, CH_2^{29}), 2.20 – 2.15 (m, 2 H, CH_2^{35}), 1.55 – 1.41 (m, 6 H, CH_2), 1.38 –1.01 (m, 18 H, CH_2).

^{13}C-NMR (126 MHz, DMSO-d_6) δ [ppm] = 174.53 (s, CO_2H^{30}), 172.65 (s, CO_2R^{36}), 172.58 (s, CO_2R^{36}), 165.78 (s, CO_2R^{7}), 165.65 (s, CO_2R^{7}), 153.31 (s, CO^{4}), 152.64 (s, CO^{4}), 149.94 (s, C^{5}), 148.75 (s, C^{5}), 143.95 (s, C_{Ar}^{11}), 143.53 (s, C_{Ar}^{11}), 136.29 (s, C_{Ar}^{40}), 135.69 (s, C_{Ar}^{40}), 128.67 (s, CH_{Ar}), 128.60 (s, CH_{Ar}), 128.44 (s, CH_{Ar}), 128.35 (s, CH_{Ar}), 128.12 (s, CH_{Ar}), 128.00 (s, CH_{Ar}), 127.95 (s, CH_{Ar}), 127.34 (s, CH_{Ar}), 127.29 (s, CH_{Ar}), 126.90 (s, CH_{Ar}), 126.07 (s, CH_{Ar}), 126.05 (s, CH_{Ar}), 104.54 (s, C^{1}), 102.80 (s, C^{1}), 65.33 (s, CH_2^{39}), 65.30 (s, CH_2^{39}), 63.73 (s, CH_2^{10}), 63.31 (s, CH_2^{10}), 52.40 (s, CH^{2}), 52.25 (s, CH^{2}), 41.54 (s, CH_2^{20}), 33.69 (s, CH_2^{29}), 33.31 (s, CH_2^{35}), 33.22 (s, CH_2^{35}), 29.39 (s, CH_2), 28.98 (s, CH_2), 28.93 (s, CH_2), 28.88 (s, CH_2), 28.82 (s, CH_2), 28.80 (s, CH_2), 28.77 (s, CH_2), 28.69 (s, CH_2), 28.67 (s, CH_2), 28.56 (s, CH_2), 28.52 (s, CH_2), 27.82 (s, CH_2), 27.77 (s, CH_2), 26.21 (s, CH_2), 25.88 (s, CH_2), 25.05 (s, CH_2),

24.89 (s, CH_2), 24.53 (s, CH_2), 24.51 (s, CH_2), 24.00 (s, CH_2), 20.79 (s, CH_2), 15.63 (s, CH_3[12]).

ESI–MS [*m/z*]: $[M + Na]^+$ calculated for $^{12}C_{36}{}^{1}H_{48}{}^{16}O_7{}^{14}N_2{}^{23}Na_1$, 643.3354; found, 643.3354; Δ = 0.02 mmu.

6.2.3.2.5 *Biginelli acid 74 derived from 6-ureidohexanoic acid, benzaldehyde and benzyl acetoacetate*

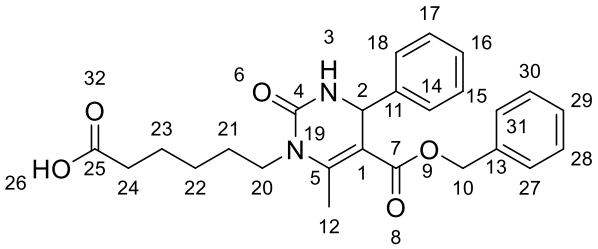

In a 10 mL round bottom flask finely powdered 6-ureidohexanoic acid (2.39 g, 13.7 mmol, 1.00 eq.) and benzaldehyde (1.89 g, 17.8 mmol, 1.30 eq.) were suspended in 5 mL dimethyl sulfoxide. Subsequently, benzyl acetoacetate (3.43 g, 17.9 mmol, 1.30 eq.) and 4-methylbenzenesulfonic acid (*p*-TSA) (236 mg, 1.37 mmol, 0.10 eq.) were added. The resulting mixture was stirred at 110 °C over night. Subsequently, the crude reaction mixture was diluted with 10 mL ethanol and precipitated in water. The water was decanted, and the sticky precipitate was dissolved in 50 mL ethyl acetate and extracted with 50 mL water. The combined aqueous phases were reextracted with 50 mL ethyl acetate three times. The combined organic phases were washed with 30 mL brine and dried under reduced pressure. The residue was recrystallized from ethanol. The Biginelli-acid **74** was obtained as a yellow solid (3.29 g, 7.54 mmol, 54.9%). Note: additional product could be crystalized from the mother liquor upon concentration and cooling.

IR (ATR): ν [cm^{-1}] = 3214.9 (m, ν(O-H)), 3064.5 (br, ν(N-H)), 2941.9 (w, ν(C-H)), 1888.4 (br), 1707.5 (vs, ν(C=O)), 1651.2 (s, ν(C=O)), 1620.2 (s), 1495.8 (w), 1454.6 (m), 1419.7 (m), 1389.9 (m), 1358.9 (s), 1317.9 (m), 1292.3 (s), 1277.0 (s), 1246.5 (s), 1221.1 (m), 1201.1 (s), 1189.4 (m), 1159.5 (s), 1115.7 (vs), 1091.1 (s), 1076.8 (s), 1054.4 (m), 1027.8 (m), 975.8 (m), 925.4 (w), 879.2 (w), 851.6 (w), 832.2 (w), 757.8 (w), 734.8 (w), 717.5 (m), 694.2 (w), 668.7 (w), 638.2 (w), 624.7 (w), 578.0 (w), 547.7 (w), 501.8 (m), 482.4 (w), 460.9 (w), 434.2 (w), 409.0 (w).

^{1}H-NMR (400 MHz, DMSO-d_6): δ [ppm] = 12.00 (s, 1 H, CO_2H^{26}), 7.96 (d, J = 3.8 Hz, 1 H, NH^{3}), 7.37 – 7.12 (m, 10 H, $CH_{Ar}^{14-18\,+\,27-31}$), 5.18 (d, J = 3.8 Hz, 1 H, CH^{2}), 5.13 – 5.01 (m, 2 H, CH_2^{10}), 3.91 – 3.42 (m, 2 H, CH_2^{20}), 2.51 (s, 3 H, CH_3^{12}), 2.13 (t, J = 7.4 Hz, 2 H, CH_2^{24}), 1.58 – 1.22 (m, 4 H, CH_2^{21+23}), 1.22 – 1.05 (m, 2 H, CH_2^{22}).

^{13}C-NMR (101 MHz, DMSO-d_6) δ [ppm] = 174.33 (s, CO_2H^{25}), 165.32 (s, CO_2R^{7}), 152.56 (s, CO^{19}), 150.47 (s, C^{5}), 143.78 (s, C_{Ar}^{11}), 136.32 (s, C_{Ar}^{13}), 128.35 (s, CH_{Ar}), 128.26 (s, CH_{Ar}), 127.76 (s, CH_{Ar}), 127.61 (s, CH_{Ar}), 127.30 (s, CH_{Ar}), 126.05 (s, CH_{Ar}), 102.47 (s, C^{1}), 65.13 (s, CH_2^{10}), 52.25 (s, CH^{2}), 41.47 (s, CH_2^{20}), 33.50 (s, CH_2^{24}), 28.98 (s, CH_2), 25.66 (s, CH_2^{22}), 24.11 (s, CH_2), 15.64 (s, CH_3^{12}).

FAB – MS [*m/z*] (relative intensity): 473.2 (100%) $[M + H]^+$, 359.2 (30%) $[M - C_6H_5]^+$, 345.2 (70%) $[M - C_7H_7]^+$.

HRMS – FAB [*m/z*]: $[M + H]^+$ calculated for $^{12}C_{25}{}^{1}H_{29}{}^{16}O_5{}^{14}N_2$, 437.2076; found, 437.2077; Δ = 0.04 mmu.

6.2.3.2.6 ***Biginelli acid 75 derived from hydantoic acid, benzyl acetoacetate and 4-bromobenzaldehyde***

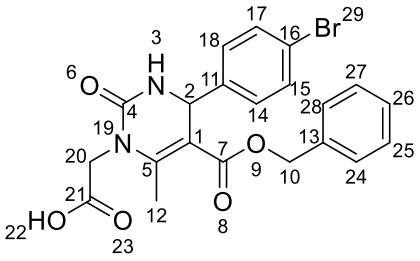

Finely powdered *N*-carbomoylglycine (2.50 g, 21.2 mmol, 1.20 eq.) and 4-bromobenzaldehyde (3.27 g, 17.6 mmol, 1.00 eq.) were suspended in 6 mL dimethyl sulfoxide and 0.5 mL water in a 50 mL round bottom flask. Subsequently, benzyl acetoacetate (3.73 g, 19.4 mmol, 3.35 mL, 1.10 eq.) and *p*-toluene sulfonic acid (212 mg, 1.76 mmol, 0.10 eq.) were added. The resulting mixture was stirred at 110 °C for 18 h. Subsequently, the crude reaction mixture was diluted with 10 mL ethanol and added dropwise into 300 mL water while stirring. The sticky precipitate was collected and dissolved in 40 mL ethyl acetate. The aqueous phase was extracted with ethyl acetate (3 × 30 mL). The combined organic phases were washed with brine (3 × 30 mL) and dried over sodium sulfate. The solvent was evaporated under reduced pressure

and the precipitate was washed with *c*-hexane/ethyl acetate (2:1) (3 × 100 mL). The solid was dried *in vacuo* to yield the Biginelli acid **75** as a yellowish solid (5.04 g, 1.09 mmol, 62.1%).

R_f = 0.34 in ethanol. Visualized *via* fluorescence quench and Seebach staining solution.

IR (ATR): ν [cm^{-1}] = 3215.5 (br, ν(O-H)), 3092.0 (br, ν(N-H)), 2922.4 (w, ν(C-H), 1689.9 (vs, ν(C=O)), 1617.2 (m), 1487.1 (w), 1427.3 (m), 1396.4 (m), 1379.4 (m), 1309.6 (m), 1272.0 (w), 1247.2 (w), 1208.3 (m), 1191.8 (s), 1174.6 (s), 1105.4 (m), 1072.7 (w), 1042.3 (m), 1009.9 (m), 960.7 (w), 821.2 (w), 756.6 (m), 741.0 (m), 696.2 (m), 638.8 (w), 575.9 (w), 503.3 (m), 461.9 (w).

^{1}H-NMR (500 MHz, DMSO-d_6) δ [ppm] = 12.94 (s, 1 H, CO_2H^{22}), 8.10 (d, J = 3.6 Hz, 1 H, NH^{3}), 7.46 (d, J = 8.4 Hz, 2 H, $CH_{Ar}^{15,17}$), 7.33 – 7.19 (m, 5 H, $CH_{Ar}^{24\text{-}28}$), 7.18 – 7.12 (m, 2 H, $CH_{Ar}^{14,18}$), 5.18 (d, J = 3.4 Hz, 1 H, CH^{2}), 5.10 – 5.02 (AB-Signal, δA = 5.08, δB = 5.04, J_{AB} = 15.0 Hz, 2 H, CH_2^{10}), 4.51 – 4.31 (AB-Signal, δA = 4.49, δB = 4.33, J = 20.0 Hz, 2 H, CH_2^{20}), 2.42 (s, 3 H, CH_3^{12}).

^{13}C-NMR (126 MHz, DMSO-d_6) δ [ppm] = 170.95 (s, CO_2H^{22}), 165.14 (s, CO_2R^{7}), 152.03 (s, CO^{4}), 150.39 (s, C^{5}), 143.28 (s, C_{Ar}^{11}), 136.24 (s, C_{Ar}^{13}), 131.30 (s, $CH_{Ar}^{15,17}$), 128.86 (s, CH_{Ar}), 128.32 (s, CH_{Ar}), 127.88 (s, CH_{Ar}), 127.74 (s, CH_{Ar}), 120.58 (s, C_{Ar}^{16}), 101.87 (s, C^{1}), 65.29 (s, CH_2^{10}), 52.51 (s, CH^{2}), 43.98 (s, CH_2^{20}), 15.73 (s, CH_3^{12}).

FAB – MS [*m/z*] (relative intensity): 461.0 (95%) $[M + H]^+$, 459.0 (100%) $[M + H]^+$, 369.0 $[M – C_7H_8]^+$, 367.0 $[M – C_7H_8]^+$.

HRMS – FAB [*m/z*]: $[M + H]^+$ calculated for $^{12}C_{21}{}^{1}H_{20}{}^{16}O_5{}^{14}N_2{}^{79}Br_1$, 459.0550; found, 459.0548; Δ = 0.21 mmu.

6.2.3.2.7 *Biginelli acid 76 derived from hydantoic acid, 4-flourobenzaldehyde and benzyl acetoacetate*

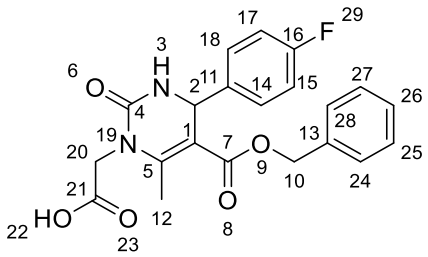

In a 50 mL round bottom flask finely powdered *N*-carbomoylglycine (2.50 g, 21.2 mmol, 1.20 eq.) and 4-fourobenzaldehyde (2.19 g, 17.6 mmol, 1.00 eq.) were suspended in 6 mL dimethyl sulfoxide (3.00 M for 1.00 eq.). Subsequently, benzyl acetoacetate (3.73 g, 19.4 mmol, 3.35 mL, 1.10 eq.) and 4-methylbenzenesulfonic acid (212 mg, 1.76 mmol, 0.10 eq.) were added. The resulting mixture was stirred at 110 °C for 6 h and subsequently at 80 °C for 48 h. The crude reaction mixture was diluted with 30 mL ethyl acetate and added dropwise into 100 mL water. The organic phase was washed with brine (3 × 50 mL). The combined aqueous phases were extracted with ethyl acetate (3 × 50 mL). The combined organic extracts were dried over sodium sulfate and concentrated under reduced pressure. The oily residue was added dropwise into 200 mL of *c*-hexane and stirred for 2 h until a precipitate was formed. The precipitate was filtered off, crushed and washed with *c*-hexane (3 × 80 mL) and with *c*-hexane/ethyl acetate (9:1) (3 × 50 mL). The precipitate was dried under reduced pressure in a desiccator over calcium chloride yielding the Biginelli acid **76** as a colorless solid (4.26 g, 10.2 mmol, 60.7%).

IR (ATR): ν [cm^{-1}] = 3204.7 (br, ν(CO_2-H)), 3056.6 (br, (ν(N-H)), 1708.5 (vs, ν(C=O)), 1642.7 (s, ν(C=O)), 1602.6 (w, ν(C=O)), 1508.0 (s), 1431.8 (m), 1402.2 (m), 1315.0 (m), 1284.2 (w), 1232.5 (m), 1216.3 (s), 1180.6 (vs), 1117.3 (s), 1041.4 (m), 961.8 (m), 839.0 (w), 774.5 (w), 748.0 (s), 699.5 (s), 678.2 (m), 646.5 (m), 599.1 (w), 581.2 (w), 543.5 (w), 514.7 (w), 499,9 (w), 469.9 (w), 390.2 (w).

^{1}H-NMR (400 MHz, DMSO-d_6): δ [ppm] = 12.95 (s, 1 H, CO_2H^{22}), 8.09 (d, J = 3.5 Hz, 1 H, NH^3), 7.37 – 7.24 (m, 5 H, CH_{Ar}), 7.21 – 7.13 (m, 2 H, CH_{Ar}), 7.09 (t, J = 8.8 Hz, 2 H, CH_{Ar}), 5.22 (d, J = 3.3 Hz, 1 H, CH^2), 5.06 (d, J = 4.1 Hz, 1 H, CH_2^{10}), 4.44 (dd, J = 53.0, 18.2 Hz, 2 H, CH_2^{20}), 2.44 (s, 3 H, CH_3^{12}).

^{13}C-NMR (101 MHz, DMSO-d_6): δ [ppm] = 171.04 (s, CO_2H^{21}), 165.24 (s, CO_2Bn^{7}), 161.51 (d, J = 243.4 Hz, CF_{Ar}^{16}), 152.11 (s, CO^{6}), 150.15 (s, C^{5}), 140.25 (s, C_{Ar}), 136.29 (s, C_{Ar}), 128.72 (s, CH_{Ar}), 128.61 (s, CH_{Ar}), 128.34 (s, CH_{Ar}), 127.89 (s, CH_{Ar}), 127.74 (s, CH_{Ar}), 115.26 (s, CH_{Ar}), 114.98 (s, CH_{Ar}), 102.32 (s, C^{1}), 65.32 (s, CH_2^{10}), 52.46 (s, CH^{2}), 43.99 (s, CH_2^{20}), 15.75 (s, CH_3^{12}).

^{19}F-NMR (377 MHz, DMSO-d_6): δ [ppm] = -119.43 (s, CF_{Ar}^{29}).

FAB – MS [*m/z*] (relative intensity): 399.2 $[M + H]^+$ (100%), 307.1 $[M – C_7H_7]^+$ (35%), 263.1 $[M – C_8H_7O_2]^+$ (15%).

HRMS – FAB [*m/z*]: $[M + H]^+$ calculated for $^{12}C_{21}{}^{1}H_{20}{}^{16}O_5{}^{14}N_2{}^{19}F_1$, 399.1351; found, 399.1350; Δ = 0.08 mmu.

6.2.3.2.8 ***Biginelli acid 77 derived from hydantoic acid, benzyl acetoacetate and 4-methoxy benzaldehyde***

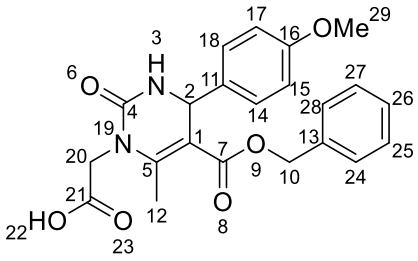

Finely powdered *N*-carbomoylglycine (2.50 g, 21.2 mmol, 1.20 eq.) and 4-methoxybenzaldehyde (2.40 g, 17.6 mmol, 1.00 eq.) were suspended in 6 mL dimethyl sulfoxide in a 50 mL round bottom flask. Subsequently, benzyl acetoacetate (3.73 g, 19.4 mmol, 3.35 mL, 1.10 eq.) and *p*-toluene sulfonic acid (212 mg, 1.76 mmol, 0.10 eq.) were added. The resulting mixture was stirred at 110 °C for 22 h. TLC indicated full conversion of the aldehyde. Subsequently, the crude reaction mixture was diluted with 10 mL ethanol and added dropwise into 400 mL water while stirring. The sticky precipitate was collected and dissolved in 40 mL ethyl acetate. The aqueous phase was extracted with ethyl acetate (3 × 30 mL). The combined organic phases were washed with 50 mL brine and dried over sodium sulfate. The solvent was evaporated under reduced pressure and the precipitate was washed with *c*-hexane/ethyl acetate (2:1) (5 × 30 mL). The solid was dried *in vacuo* to yield the Biginelli acid **77** as a yellowish solid. (3.29 g, 8.02 mmol, 45.4%).

R_f = 0.31 in ethanol. Visualized *via* fluorescence quench and Seebach staining solution.

IR (ATR) ν [cm^{-1}] = 3284.7 (br, ν(CO_2H)), 3235.3 (br, ν(N-H)), 3072.8 (w), 3009.1 (w), 2937.1 (w, ν(C-H)), 2840.4 (w), 2731.4 (w), 2513.4 (w), 2433.2 (w), 1705.1 (vs, ν(C=O)), 1647.5 (s, ν(C=O)), 1606.3 (m, ν(C=O)), 1511.7 (m, ν(C=C)), 1454.1 (m), 1413.0 (m), 1384.2 (m), 1316.3 (w), 1287.5 (m), 1248.4 (s), 1229.9 (m), 1213.5 (vs), 1174.4 (vs), 1114.8 (m), 1059.2 (m), 1028.4 (m), 942.0 (m), 898.8 (w), 851.5 (w), 835.0 (w), 800.1 (w), 785.7 (m), 771.3 (w), 750.7 (w), 730.2 (m), 695.2 (w), 680.8 (w), 654.0 (w), 582.0 (w), 503.9 (m), 438.1 (w).

^{1}H-NMR (500 MHz, DMSO-d_6) δ [ppm] = 12.91 (s, 1 H, CO_2H^{22}), 8.01 (d, J = 3.5 Hz, 1 H, NH^{3}), 7.35 – 7.25 (m, 3 H, CH_{Ar}^{25-27}), 7.21 (s, 1 H, CH_{Ar}), 7.19 (s, 1 H, CH_{Ar}), 7.19 – 7.15 (m, 2 H, $CH_{Ar}^{24,28}$), 6.83 (d, J = 8.7 Hz, 2 H, $CH_{Ar}^{15,17}$), 5.17 (d, J = 3.3 Hz, 1 H, CH^{2}), 5.11 – 4.96 (m, 2 H, CH_2^{10}), 4.52 – 4.32 (AB-Signal, δA = 4.50, δB = 4.43, J_{AB} = 20.0 Hz, 2H, CH_2^{20}), 3.72 (s, 3 H, OCH_3^{29}), 2.42 (s, 3 H, CH_3^{12}).

^{13}C-NMR (126 MHz, DMSO-d_6) δ [ppm] = 171.06 (s, CO_2H^{22}), 165.39 (s, CO_2R^{7}), 158.64 (s, C_{Ar}^{16}),152.26 (s, CO^{4}), 149.63 (s, C^{5}), 136.35 (s, C_{Ar}^{13}), 136.16 (s, C_{Ar}^{11}), 128.34 (s, CH_{Ar}), 127.86 (s, CH_{Ar}), 127.81 (s, CH_{Ar}), 127.70 (s, $CH_{Ar}^{24,28}$), 113.72 (s, $CH_{Ar}^{15,17}$), 102.73 (s, C^{1}), 65.24 (s, CH_2^{10}), 55.10 (s, OCH_3^{29}), 52.46 (s, CH^{2}), 43.98 (s, CH_2^{20}), 15.71 (s, CH_3^{12}).

FAB-MS *m/z* (relative intensity): 411.2 (90%) $[M + H]^+$, 319.1 (54%) $[M – C_7H_7]^+$, 303.1 (47%) $[M – C_7H_7O]^+$, 275.1 (20%) [Fragment A]$^+$, 213.0 (10%) [Fragment C + H]$^+$, 136.0 (28%) [Fragment B + H]$^+$, 107.0 (10%) $[C_7H_7O]^+$, 91.0 (100%) $[C_7H_7]^+$.

HRMS–FAB (*m/z*): $[M + H]^+$ calculated for $^{12}C_{22}{}^{1}H_{23}{}^{16}O_6{}^{14}N_2$, 411.1551; found, 411.1550; Δ = 0.06 mmu.

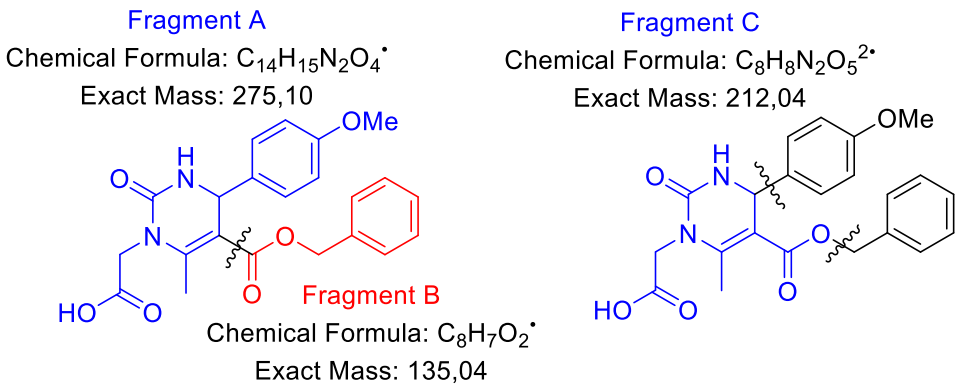

6.2.3.2.9 *Biginelli acid 78 derived from hydantoic acid, benzyl acetoacetate and 4-methylbenzaldehyde*

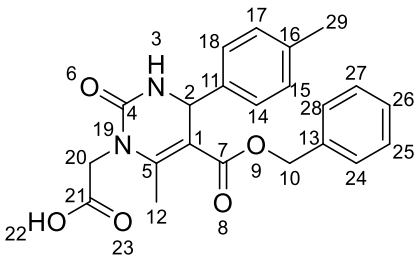

Finely powdered *N*-carbomoylglycine (2.50 g, 21.2 mmol, 1.20 eq.) and 4-methylbenzaldehyde (2.12 g, 17.6 mmol, 1.00 eq.) were suspended in 6 mL dimethyl sulfoxide in a 25 mL round bottom flask. Subsequently, benzyl acetoacetate (3.73 g, 19.4 mmol, 3.35 mL, 1.10 eq.) and *p*-toluene sulfonic acid (212 mg, 1.76 mmol, 0.10 eq.) were added. The resulting mixture was stirred at 110 °C for 4 d. TLC indicated full conversion of the aldehyde. Subsequently, the crude reaction mixture was diluted with 10 mL ethanol and added dropwise into 400 mL water while stirring. The sticky precipitate was collected and dissolved in 40 mL ethyl acetate. The aqueous phase was extracted with ethyl acetate (3 × 30 mL). The combined organic phases were washed with 50 mL brine and dried over sodium sulfate. The solvent was evaporated under reduced pressure and the precipitate was washed with *c*-hexane/ethyl acetate (2:1) (4 × 30 mL). The solid was dried *in vacuo* to yield the Biginelli acid **78** as a brownish solid (4.44 g, 11.3 mmol, 63.8%).

R_f = 0.35 in ethanol. Visualized *via* fluorescence quench and Seebach staining solution.

IR (ATR) ν [cm^{-1}] = 3290.9 (br, ν(N-H)), 3239.4 (vw, ν(N-H)), 3064.6 (vw), 3007.0 (vw), 2984.4 (vw, ν(C-H)), 2957.7 (vw, ν(C-H)), 2922.7 (vw, ν(C-H)), 2869.2 (vw, ν(C-H)), 1721.5 (s, ν(C=O)), 1707.1 (vs, ν(C=O)), 1645.4 (s, ν(C=O)), 1633.1 (s, ν(C=O)), 1583.7 (w), 1511.7 (w), 1497.3 (w), 1454.1 (m), 1415.0 (m), 1382.1 (w), 1363.6 (w), 1316.3 (w), 1285.5 (m), 1269.0 (w), 1227.9 (m), 1213.5 (vs), 1201.1 (vs), 1182.6 (vs), 1174.4 (vs), 1116.8 (s), 1077.7 (w), 1059.2 (s), 1040.7 (w), 1028.4 (w), 1018.1 (m), 979.0 (w), 944.0 (m), 898.8 (w), 874.1 (w), 853.5 (w), 826.8 (w), 783.6 (m), 771.3 (w), 748.6 (m), 732.2 (m), 693.1 (w), 680.8 (m), 652.0 (m), 619.1 (w), 582.0 (w), 565.6 (w), 545.1 (vw), 526.5 (w), 501.8 (w), 495.6 (m), 456.6 (w), 436.0 (w).

^{1}H-NMR (500 MHz, DMSO-d_6) δ [ppm] = 12.91 (s, 1 H, CO_2H^{22}), 8.05 (dd, J = 22.6, 3.5 Hz, 1 H, NH^{3}), 7.35 – 7.26 (m, 3 H, CH_{Ar}^{25-27}), 7.16 (m, 4 H, CH_{Ar}), 7.07 (d, J = 7.9 Hz, 2 H, CH_{Ar}), 5.17 (t, J = 3.4 Hz, 1 H, CH^{2}), 5.05 (s, 2 H, CH_2^{10}), 4.50 – 4.31 (AB-Signal, δA = 4.48, δB = 4.33, J_{AB} = 20.0 Hz, 2 H, CH_2^{20}), 2.41 (s, 3 H, CH_3^{12}), 2.26 (s, 3 H, CH_3^{29}).

^{13}C-NMR (126 MHz, DMSO-d_6) δ [ppm] = 170.99 (s, CO_2H^{22}), 165.36 (s, CO_2R^{7}), 152.27 (s, CO^{4}), 149.80 (s, C^{5}), 141.02 (s, C_{Ar}^{13}), 136.62 (s, C_{Ar}^{16}), 136.32 (s, C_{Ar}^{11}), 128.92 (s, CH_{Ar}), 128.32 (s, CH_{Ar}), 127.84 (s, CH_{Ar}), 127.71 (s, CH_{Ar}), 126.47 (s, CH_{Ar}), 102.51 (s, C^{1}), 65.24 (s, CH_2^{10}), 52.66 (s, CH^{2}), 44.00 (s, CH_2^{20}), 20.69 (s, CH_3^{29}), 15.69 (s, CH_3^{12}).

FAB-MS *m/z* (relative intensity): 395.2 (46%) $[M + H]^+$, 349.2 (6%) $[M – CH_2O]^+$, 303.1 (36%) $[M – C_7H_7]^+$, 287.1 (8%) $[M – C_7H_7O]^+$. 259.1 (12%) [Fragment A]$^+$, 136.0 (19%) [Fragment B]$^+$, 91.0 (100%) $[C_7H_7]^+$.

HRMS–FAB (*m/z*): $[M + H]^+$ calculated for $^{12}C_{22}{}^{1}H_{23}{}^{16}O_5{}^{14}N_2$, 395.1601; found, 395.1598; Δ = 0.32 mmu.

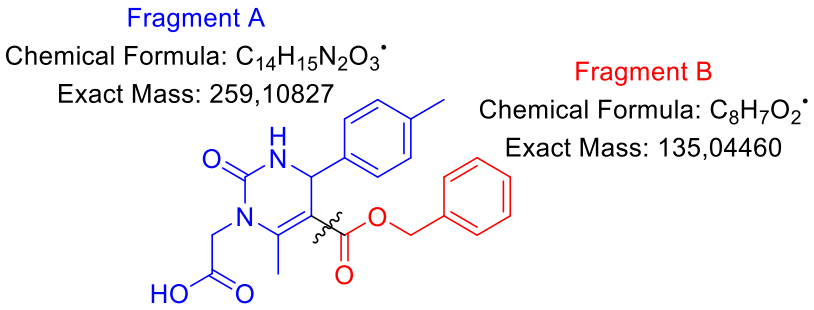

6.2.3.2.10 *Biginelli acid 79 derived from hydantoic acid, 4-(trifluoromethoxy) benzaldehyde and benzyl acetoacetate*

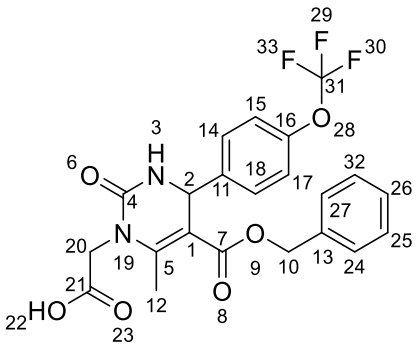

In a 25 mL round bottom flask finely powdered N-carbomoylglycine (1.73 g, 14.7 mmol, 1.20 eq.) and 4-(trifluoromethoxy)benzaldehyde (2.32 g, 12.2 mmol, 1.74 mL, 1.00 eq.) were suspended in 3 mL dimethyl sulfoxide (4.7 M for 1.00 eq.). Subsequently, benzyl acetoacetate (2.81 g, 14.5 mmol, 2.53 mL) and 4-methylbenzenesulfonic acid (73.2 mg, 610 µmol, 0.05 eq.) were added. The resulting mixture was stirred at 110 °C for 4 h and subsequently at 80 °C over night. TLC indicated full conversion of the aldehyde. Subsequently, the crude reaction mixture was added dropwise into 250 mL water. The sticky precipitate was collected and dissolved in ethyl acetate. The aqueous phase was extracted with ethyl acetate (3 × 50 mL). The organic phases and the dissolved precipitate were combined and washed with water (2 × 30 mL) and 30 mL brine. After concentration under reduced pressure the yellow oil was stirred in 50 mL *c*-hexane/ethyl acetate (2:1) for 3 h until a precipitate was formed. The precipitate was filtered off and washed with *c*-hexane (3 × 30 mL) and dried under reduced pressure in a desiccator over calcium chloride to yield the Biginelli acid **79** as a colorless solid (3.86 g, 19.2 mmol, 68.1%).

IR (ATR): ν [cm^{-1}] = 3091.2 (br, ν(N-H)), 2948.3 (w, ν(C-H), 2170.4 (vw), 1699.5 (vs, ν(C=O)), 1632.2 (s, ν(C=O)), 1508.8 (m), 1429.6 (m), 1399.4 (m), 1386.4 (m), 1362.8 (w), 1312.6 (w), 1265.2 (m), 1212.2 (m), 1199.6 (m), 1177.7 (vs), 1155.1 (vs), 1114.6 (s), 1042.4 (m), 1017.9 (m), 962.3 (w), 927.1 (w), 890.0 (w), 862.2 (w), 844.1 (w), 793.5 (w), 744.3 (m), 694.8 (w), 650.4 (s), 635.5 (m), 593.9 (w), 548.2 (w), 514.8 (w), 493.8 (w), 460.2 (w), 413.8 (w).

^{1}H-NMR (500 MHz, DMSO-d_6): δ [ppm] = 12.96 (s, 1 H, CO_2H^{22}), 8.13 (d, J = 3.7 Hz, 1 H, NH^{3}), 7.49 – 7.37 (m, 2 H, CH_{Ar}), 7.35 – 7.23 (m, 5 H, CH_{Ar}), 7.13 (dd, J = 6.6, 3.0

Hz, 2 H, CH_{Ar}), 5.25 (d, *J* = 3.6 Hz, 1 H, CH^{2}), 5.14 – 4.99 (m, 2 H, CH_2^{10}), 4.57 – 4.29 (m, 2 H, CH_2^{20}), 2.44 (s, 3 H, CH_3^{12}).

^{13}C-NMR (126 MHz, DMSO-d_6): δ [ppm] = 170.98 (s, CO_2H^{21}), 165.12 (s, CO_2R^{7}), 152.02 (s, CO^{4}), 150.50 (s, C_q^{5}), 147.57 (s, C_{Ar}^{16}), 143.37 (s, C_{Ar}^{11}), 136.26 (s, C_{Ar}^{13}), 128.57 (s, CH_{Ar}), 128.26 (s, CH_{Ar}), 127.86 (s, CH_{Ar}), 127.69 (s, CH_{Ar}), 121.05 (s, $CH_{Ar}^{15,17}$), 120.09 (q, *J* = 256.1 Hz, CF_3^{31}), 101.92 (s, C_q^{1}), 65.31 (CH_2^{10}), 52.48 (s, CH^{2}), 43.99 (s, CH_2^{20}), 15.74 (s, CH_3^{12}).

^{19}F-NMR (471 MHz, DMSO-d_6) δ [ppm] = -56.83 (s, CF_3).

ESI–MS [*m/z*]: $[M + Na]^+$ calculated for $^{12}C_{22}{}^{1}H_{29}{}^{16}O_6{}^{14}N_2{}^{19}F_1{}^{23}Na_1$, 487.1087; found, 487.1088; Δ = 0.09 mmu.

6.2.3.2.11 ***Biginelli acid 80 derived from hydantoic acid, 4-ethoxy benzaldehyde and benzyl acetoacetate***

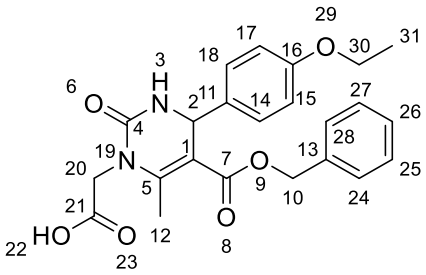

In a 50 mL round bottom flask finely powdered *N*-carbomoylglycine (2.50 g, 21.2 mmol, 1.20 eq.) and 4-ethoxy benzaldehyde (2.64 g, 17.6 mmol, 1.00 eq.) were suspended in 6 mL dimethyl sulfoxide (3.00 M for 1.00 eq.). Subsequently, benzyl acetoacetate (3.73 g, 19.4 mmol, 3.35 mL, 1.10 eq.) and 4-methylbenzenesulfonic acid (212 mg, 1.76 mmol, 0.10 eq.) were added. The resulting mixture was stirred at 110 °C for 8 h and afterwards at 40 °C for 2 d. Subsequently, the crude reaction mixture was diluted with 10 mL ethanol and added dropwise into 100 mL water while stirring. The mixture was stirred for 30 min and extracted with ethyl acetate (4 × 50 mL). The combined organic phases were concentrated under reduced pressure and the residue was stirred in 100 mL diethyl ether for 30 min. The orange oil was separated, washed with diethyl ether (2 × 30 mL) and dried under reduced pressure to yield the Biginelli acid **80** as an orange solid (4.32 g, 10.2 mmol, 57.7%).

IR (ATR): ν [cm^{-1}] = 3241.4 (br, ν(N-H)), 2980.0 (w, ν(C-H), 1710.2 (s, ν(C=O)), 1608.0 (s, ν(C=O)), 1509.0 (s), 1382.0 (m), 1306.7 (m), 1285.9 (m), 1238.1 (w), 1209.5 (w), 1171.7 (s), 1111.4 (s), 1042.7 (m), 952.9 (w), 923.1 (w), 821.7 (w), 772.2 (w), 749.9 (w), 735.6 (w), 695.8 (w), 640.8 (w), 615.6 (w), 591.9 (w), 497.9 (w), 466.0 (w), 417.0 (w).

^{1}H-NMR (400 MHz, DMSO-d_6): δ [ppm] = 12.90 (s, 1 H, CO_2H^{22}), 8.00 (d, J = 3.6 Hz, 1 H, NH^{3}), 7.33 – 7.26 (m, 3 H, CH_{Ar}), 7.22 – 7.14 (m, 4 H, CH_{Ar}), 6.84 – 6.74 (m, 2 H, $CH_{Ar}^{15,17}$), 5.15 (d, J = 3.5 Hz, 1 H, CH^{2}), 5.05 (s, 2 H, CH_2^{10}), 4.43 – 4.40 (m, 2 H, CH_2^{20}), 4.02 – 3.90 (m, 2 H, CH_2^{30}), 2.42 (d, J = 8.8 Hz, 3 H, CH_3^{12}), 1.34 – 1.27 (m, 3 H, CH_3^{31}).

^{13}C-NMR (101 MHz, DMSO-d_6): δ [ppm] = 171.00 (s, CO_2H^{21}), 165.35 (s, CO_2R^{7}), 157.86 (s, C_{Ar}^{16}), 152.21 (s, CO^{4}), 149.55 (s, C^{5}), 136.32 (s, C_{Ar}^{13}), 135.99 (s, C_{Ar}^{11}), 128.30 (s, CH_{Ar}), 127.81 (s, CH_{Ar}), 127.76 (s, CH_{Ar}), 127.66 (s, CH_{Ar}), 114.15 (s, $CH_{Ar}^{15,17}$), 102.69 (s, C^{1}), 65.20 (s, CH_2^{10}), 62.97 (s, CH_2^{30}), 52.42 (s, CH^{2}), 43.94 (s, CH_2^{20}), 15.67 (s, CH_3^{12}), 14.65 (s, CH_3^{31}).

FAB – MS [*m/z*] (relative intensity): 425.2 (95%) $[M + H]^+$, 379.2 (15%) $[M – C_2H_5O]^+$, 333.1 (100%) $[M – C_7H_7]^+$, 303.1 (60%) $[M – C_8H_9O]^+$, 289.1 (50%) $[M – C_8H_7O_2]^+$.

HRMS – FAB [*m/z*]: $[M + H]^+$ calculated for $^{12}C_{23}{}^{1}H_{25}{}^{16}O_6{}^{14}N_2$, 425.1707; found, 425.1705; Δ = 0.05 mmu.

6.2.3.2.12 ***Biginelli acid 81 derived from hydantoic acid, 3,4-dimethoxybenzaldehyde and benzyl acetoacetate***

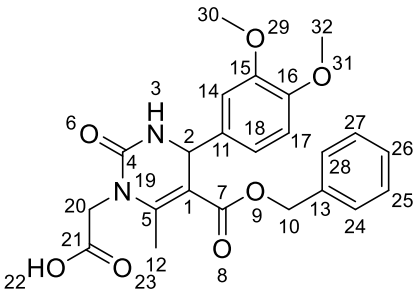

In a 25 mL round bottom flask finely powdered *N*-carbomoylglycine (4.00 g, 33.8 mmol, 1.20 eq.) and 3,4-dimethoxy benzaldehyde (4.69 g, 28.2 mmol, 4.21 mL, 1.00 eq.) were suspended in 6 mL dimethyl sulfoxide. Subsequently, benzyl acetoacetate

(6.51 g, 33.8 mmol, 5.85 mL, 1.20 eq.) and 4-methylbenzenesulfonic acid (169 mg, 1.42 mmol, 0.05 eq.) were added. The resulting mixture was stirred at 110 °C for 8 h and at 80 °C over night. Subsequently, the crude reaction mixture was added dropwise into 400 mL water while stirring. The suspension was stirred for 1 h until a sticky precipitate was formed. The precipitate was collected and dissolved in ethyl acetate. The aqueous phase was extracted with ethyl acetate (3 × 50 mL). The organic phases and the dissolved precipitate were combined and washed with water (2 × 30 mL) and 30 mL brine. After concentration under reduced pressure the red oil was stirred in 50 mL *c*-hexane/ethyl acetate (2:1) for 1 h until a precipitate was formed. The precipitate was filtered off and washed with *c*-hexane/ethyl acetate (2:1) (3 × 30 mL), *c*-hexane (2 × 30 mL) and dried under reduced pressure in a desiccator over calcium chloride to yield the Biginelli acid **81** as a colorless solid (7.73 g, 17.6 mmol, 62.3%).

IR (ATR): ν [cm^{-1}] = 3239.6 (br, ν(CO_2H)), 2932.7 (w, ν(C-H), 2161.3 (vw), 1959.1 (vw), 1712.5 (s, ν(C=O)), 1689.8 (s, ν(C=O)), 1616.5 (m), 1512.8 (w), 1453.7 (w), 1419.7 (m), 1381.8 (m), 1342.3 (w), 1305.9 (w), 1253.1 (m), 1236.3 (m), 1211.3 (m), 1187.3 (s), 1140.0 (vs), 1105.3 (s), 1039.2 (m), 1024.3 (s), 955.3 (w), 918.9 (m), 871.5 (m), 848.9 (w), 813.4 (w), 787.3 (m), 751.3 (s), 697.8 (s), 671.2 (m), 637.5 (w), 600.1 (w), 570.1 (w), 525.2 (w), 503.2 (w), 457.8 (w), 425.8 (w), 407.7 (w).

^{1}H-NMR (300 MHz, DMSO-*d*$_6$): δ [ppm] = 12.93 (s, 1 H, CO_2H^{22}), 8.00 (d, *J* = 3.6 Hz, 1 H, NH^{3}), 7.37 – 7.25 (m, 4 H, CH_{Ar}), 7.26 – 7.14 (m, 2 H, CH_{Ar}), 6.93 – 6.74 (m, 3 H, CH_{Ar}), 5.18 (d, *J* = 3.5 Hz, 1 H, CH^{2}), 5.06 (s, 2 H, CH_2^{10}), 4.66 – 4.23 (m, 2 H, CH_2^{20}), 3.72 (s, 3 H, OCH_3), 3.63 (s, 3 H, OCH_3), 2.43 (s, 3 H, CH_3^{12}).

^{13}C-NMR (75 MHz, DMSO-*d*$_6$): δ [ppm] = 171.10 (s, CO_2H^{21}), 165.41 (s, CO_2R^{7}), 152.17 (CO^{4}), 149.59 (s, C_q^{5}), 148.71 (s, C_{Ar}^{16}), 148.22 (s, C_{Ar}^{15}), 136.55 (s, C_{Ar}^{13}), 136.36 (s, CAr^{11}), 128.32 (s, CH_{Ar}), 127.83 (s, CH_{Ar}), 127.64 (s, CH_{Ar}), 118.58 (s, CH_{Ar}), 111.56 (s, CH_{Ar}), 110.42 (s, CH_{Ar}), 102.56 (s, C_q^{1}), 65.25 (s, CH_2^{10}), 55.56 (s, $OCH_3^{30\ or\ 32}$), 55.34 (s, $OCH_3^{30\ or\ 32}$), 52.88 (s, CH^{2}), 43.84 (CH_2^{20}), 15.72 (s, CH_3^{12}).

ESI–MS [*m/z*] (relative intensity): 463.14746 (100%) $[M + Na]^+$ calculated for $^{12}C_{23}{}^{1}H_{24}{}^{16}O_7{}^{14}N_2{}^{23}Na_1$, 463.1475; found, 463.1475; Δ = 0.08 mmu.

6.2.3.2.13 *Biginelli acid 82 derived from 11-urediundecanoic acid, p-tolualdehyde and pentamer-AA 69*

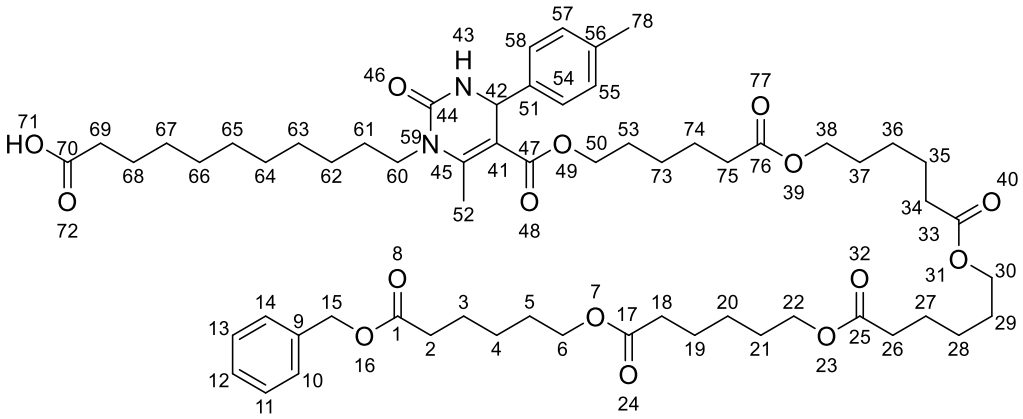

In a 10 mL round bottom flask finely powdered 11-ureidoundecanoic acid (52.8 mg, 216 µmol, 1.50 eq.) and *p*-tolualdehyde (26.0 mg, 216 µmol, 1.50 eq.) were suspended in 1 mL dimethyl sulfoxide. Subsequently, pentamer-benzyl acetoacetate **69** (110 mg, 144 µmol, 1.00 eq.) and 4-methylbenzenesulfonic acid (*p*-TSA) (2.48 mg, 14.4 µmol, 0.10 eq.) were added. The resulting mixture was stirred at 80 °C for 3 h and at 100 °C over night. TLC indicated complete conversion of the pentamer-benzyl acetoacetate **69**. Subsequently, the crude reaction mixture was extracted with 50 mL water and 30 mL dichloromethane. The residue was adsorbed onto celite® and purified *via* column chromatography on silica gel eluting with ethyl acetate/*c*-hexane (1:1) in order to remove impurities and unreacted starting materials and subsequently eluting with dichloromethane/methanol/triethylamine (97:3:1) in order to elute the desired product. The relevant fractions were concentrated under reduced pressure down to a volume of approximately 30 mL, washed with 20 mL water three times, dried over sodium sulfate and dried under reduced pressure to yield the Biginelli acid **82** as a yellow oil (94.3 mg, 86.5 µmol, 60.0%).

IR (ATR): ν [cm^{-1}] = 3452.6 (m, ν(O-H)), 2925.3 (s, ν(C-H)), 2854.7 (m, ν(C-H)), 1729.8 (vs, ν(C=O)), 1704.1 (s, ν(C=O)), 1496.2 (m), 1455.9 (w), 1388.4 (s), 1356.3 (w), 1157.4 (vs), 1090.5 (s), 784.6 (w), 736.6 (w), 698.1 (w), 605.5 (w), 510.6 (w).

^{1}H-NMR (400 MHz, DMSO-d_6): δ [ppm] = 12.02 (s, 1 H, CO_2H^{71}), 8.28 – 7.78 (m, 1 H, NH^{43}), 7.59 – 6.97 (m, 9 H, $CH_{Ar}^{10\text{-}14\ +\ 54,55,57,58}$), 5.07 (s, 3 H, CH^{42} + CH_2^{15}), 3.97 (td, J = 6.5, 1.9 Hz, 10 H, $CH_2^{6,22,30,38,50}$), 3.89 – 3.40 (m, 2 H, CH_2^{60}), 2.48 (s, 3 H, CH_3^{52}),

2.40 – 2.31 (m, 3 H, CH_2), 2.32 – 2.22 (m, 9 H, CH_3*78* + CH_2), 2.17 (dt, *J* = 9.0, 7.3 Hz, 4 H, CH_2), 1.63 – 1.35 (dt, *J* = 17.2, 7.6 Hz, 24 H, CH_2), 1.35 – 1.04 (m, 16 H, CH_2).

^{13}C-NMR (101 MHz, DMSO-*d*$_6$) *δ* [ppm] = 174.44 (s, CO_2H*1*), 172.73 (s, CO_2R), 172.61 (s, CO_2R), 165.58 (s, CO_2R*1*), 152.62 (s, CO*44*), 149.71 (s, C*45*), 140.95 (s, C_{Ar}), 137.29 (s, C_{Ar}), 136.32 (s, C_{Ar}), 129.28 (s, CH_{Ar}), 129.08 (s, CH_{Ar}), 128.78 (s, CH_{Ar}), 128.36 (s, CH_{Ar}), 127.92 (s, CH_{Ar}), 127.85 (s, CH_{Ar}), 125.92 (s, CH_{Ar}), 102.90 (s, C*41*), 65.26 (s, CH_2*15*), 63.45 (s, CH_2), 63.18 (s, CH_2), 51.99 (s, CH*42*), 41.42 (s, CH_2*60*), 33.61 (s, CH_2), 33.32 (s, CH_2), 33.27 (s, CH_2), 29.36 (s, CH_2), 28.94 (s, CH_2), 28.84 (s, CH_2), 28.80 (s, CH_2), 28.78 (s, CH_2), 28.76 (s, CH_2), 28.73 (s, CH_2), 28.68 (s, CH_2), 28.51 (s, CH_2), 27.75 (s, CH_2), 26.15 (s, CH_2), 24.84 (s, CH_2), 24.46 (s, CH_2), 24.04 (s, CH_2), 20.54 (s, CH_3*78*), 15.53 (s, CH_3*52*).

ESI – MS [*m/z*]: $[M + Na]^+$ calculated for $^{12}C_{61}{}^{1}H_{90}{}^{16}O_{15}{}^{14}N_2{}^{23}Na_1$, 1113.6239; found, 1113.6240; Δ = 0.68 mmu.

6.2.3.3 Monomers-NC

6.2.3.3.1 *Monomer-NC 83 obtained from Biginelli acid 50, trans-1,4-diisocyanocyclohexane and octanal*

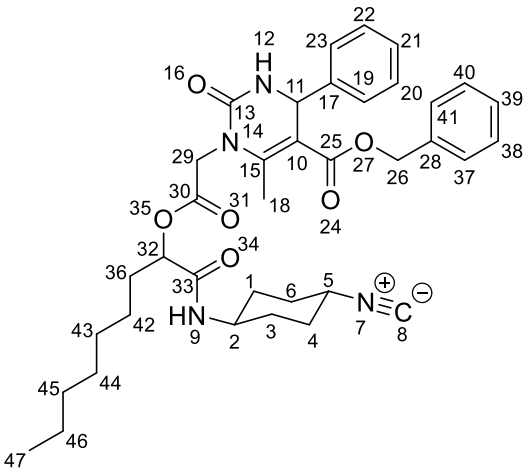

In a 50 mL round bottom flask *trans*-1,4-diisocyanocyclohexane (1.76 g, 13.1 mmol, 5.00 eq.) was stirred in 8 mL dichloromethane under argon atmosphere, subsequently octanal (674 mg, 5.25 mmol, 2.00 eq.) was added. Finely powdered Biginelli acid **50** (1.00 g, 2.62 mmol, 1.00 eq.) was suspended in 5 mL dichloromethane and dimethyl

sulfoxide was added dropwise until a solution was obtained. The dissolved Biginelli acid was added dropwise to the stirring diisocyanide/aldehyde mixture under argon atmosphere. The resulting reaction mixture was stirred at room temperature for 2 d. The crude mixture was dried under reduced pressure. The residue was adsorbed onto celite® and purified *via* column chromatography on silica gel eluting with a gradual solvent mixture of ethyl acetate and *c*-hexane (1:5 → 2:1). The monomer-NC **83** was obtained as a colorless solid (987 mg, 1.55 mmol, 58.7%). The exceeding diisocyanide could be recovered (1.19 g, 8.90 mmol, 84.4%).

R_f in ethyl acetate/*c*-hexane (1:1) = 0.38. Visualized *via* fluorescence quench and Seebach staining solution.

IR (ATR): ν [cm^{-1}] = 3306.3 (br, ν(N-H)), 2925.8 (w, ν(C-H)), 2855.9 (w, ν(C-H)), 2138.8 (m, ν(NC)), 1750.9 (s, ν(C=O)), 1677.5 (vs, ν(C=O)), 1533.9 (s), 1453.3 (s), 1383.8 (s), 1309.3 (m), 1276.1 (w), 1255.8 (m), 1171.3 (vs), 1104.0 (s), 1042.8 (m), 831.1 (w), 755.1 (m), 696.0 (s), 653.7 (w), 583.2 (w), 493.6 (w).

^{1}H-NMR (500 MHz, DMSO-d_6): δ [ppm] = 8.18 (dd, J = 26.3, 3.6 Hz, 1 H, NH^{12}), 7.79 (dd, J = 23.0, 7.7 Hz, 1 H, NH^{9}), 7.33 – 7.24 (m, 8 H, CH$_{Ar}$), 7.20 – 7.14 (m, 2 H, CH$_{Ar}$), 5.23 (dd, J = 5.3, 4.1 Hz, 1 H, CH^{11}), 5.12 – 5.02 (m, 2 H, CH$_2^{26}$), 4.87 (dd, J = 10.7, 5.9 Hz, 1 H, CH^{32}), 4.77 – 4.43 (m, 2 H, CH$_2^{29}$), 3.70 – 3.69 (m, 1 H, CH^{5}), 3.61 – 3.53 (m, 1 H, CH^{2}), 2.45 (d, J = 17.6 Hz, 3 H, CH$_3^{18}$), 2.07 – 1.98 (m, 2 H, CH$_2^{4,6\ axial}$), 1.77 – 1.65 (m, 4 H, CH$_2$), 1.63 – 1.53 (m, 2 H, CH$_2^{4,6\ equatorial}$), 1.35 – 1.16 (m, 12 H, CH$_2$), 0.85 (t, J = 6.8 Hz, 3 H, CH$_3^{47}$).

^{13}C-NMR (126 MHz, DMSO-d_6) δ [ppm] = 169.14 (s, CO$_2$R^{30}), 168.96 (s, CO$_2$R^{30}), 168.14 (s, CONR^{33}), 168.12 (s, CONR^{33}), 165.22 (s, CO$_2$R^{25}), 165.19 (s, CO$_2$R^{25}), 154.46 (s, NC^{8}), 152.47 (s, CO^{13}), 152.19 (s, CO^{13}), 149.68 (s, C^{15}), 149.56 (s, C^{15}), 143.82 (s, C$_{Ar}^{17}$), 143.62 (s, C$_{Ar}^{17}$), 136.19 (s, C$_{Ar}^{28}$), 128.45 (s, CH$_{Ar}$), 128.41 (s, CH$_{Ar}$), 128.30 (s, CH$_{Ar}$), 127.85 (s, CH$_{Ar}$), 127.68 (s, CH$_{Ar}$), 127.51 (s, CH$_{Ar}$), 126.56 (s, CH$_{Ar}$), 126.45 (s, CH$_{Ar}$), 102.79 (s, C^{10}), 102.77 (s, C^{10}), 74.10 (s, CH^{32}), 74.02 (s, CH^{32}), 65.34 (s, CH$_2^{26}$), 59.77 (s), 53.14 (s, CH^{11}), 52.92 (s, CH^{11}), 50.49 (s, CH^{5}), 45.85 (s, CH^{2}), 44.19 (s, CH$_2^{29}$), 43.99 (s, CH$_2^{29}$), 31.28 (s, CH$_2$), 31.21 (s, CH$_2$), 31.12 (s, CH$_2$), 31.10 (s, CH$_2$), 30.89 (s, CH$_2$), 29.00 (s, CH$_2$), 28.51 (s, CH$_2$), 28.48 (s, CH$_2$), 24.36 (s, CH$_2$), 24.33 (s, CH$_2$), 22.06 (s, CH$_2$), 15.66 (s, CH$_3^{18}$), 15.65 (s, CH$_3^{18}$), 13.95 (s, CH$_3^{47}$).

FAB – MS [*m/z*] (relative intensity): 643.4 (80%) $[M + H]^+$, 616.3 (80%) $[M – NC]^+$, 535.3 (70%) $[M – C_7H_7O]^+$.

HRMS – FAB [*m/z*]: $[M + H]^+$ calculated for $^{12}C_{37}{}^{1}H_{47}{}^{16}O_6{}^{14}N_4$, 643.3490; found, 643.3492; Δ = 0.15 mmu.

6.2.3.3.2 ***Monomer-NC 84 obtained from Biginelli acid 50, p-xylenediisocyanide and octanal***

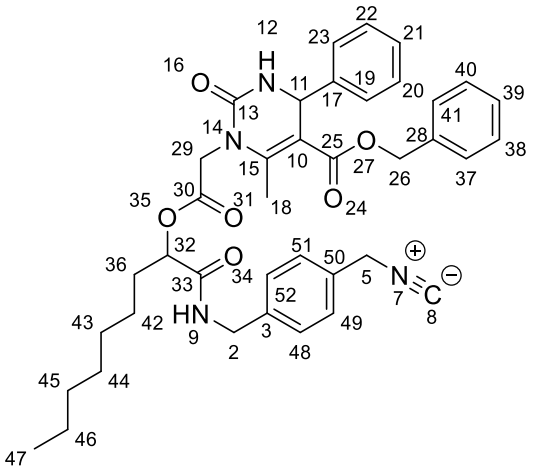

In a 25 mL round bottom flask *p*-xylenediisocyanide (1.03 g, 6.57 mmol, 5.00 eq.) was stirred in 5 mL dichloromethane under argon atmosphere, subsequently octanal (337 mg, 2.63 mmol, 2.00 eq.) was added. Finely powdered Biginelli acid **50** (500 mg, 1.31 mmol, 1.00 eq.) was suspended in 2 mL dichloromethane and dimethyl sulfoxide was added dropwise until a solution was obtained. The dissolved Biginelli acid was added dropwise to the stirring diisocyanide/aldehyde mixture under argon atmosphere. The resulting reaction mixture was stirred at room temperature for 2 d. The crude mixture was dried under reduced pressure. The residue was adsorbed onto celite® and purified *via* column chromatography on silica gel eluting with a gradual solvent mixture of ethyl acetate and *c*-hexane (0:1 → 1:1). The monomer-NC **84** was obtained as a colorless solid (659 mg, 1.10 mmol, 75.6%). The exceeding diisocyanide could be recovered (643 mg, 4.14 mmol, 78.4%).

R_f in ethyl acetate/*c*-hexane (1:1) = 0.30. Visualized *via* fluorescence quench and Seebach staining solution.

IR (ATR): ν [cm^{-1}] = 3297.3 (br, ν(N-H)), 2925.5 (w, ν(C-H)), 2854.9 (w, ν(C-H)), 2148.4 (w, ν(NC)), 1739.5 (m, ν(C=O)), 1707.0 (s, ν(C=O)), 1680.9 (vs, ν(C=O)), 1663.0 (vs, ν(C=O)), 1616.8 (s), 1535.5 (m), 1496.3 (w), 1455.2 (w), 1406.6 (m), 1373.9 (w), 1306.8 (w), 1278.5 (w), 1254.1 (w), 1190.5 (m), 1170.4 (vs), 1105.3 (s), 1081.2 (s), 1042.8 (m), 953.2 (s), 830.3 (m), 750.9 (s), 697.5 (m), 589.3 (s), 558.8 (m), 512.4 (m), 431.1 (m).

^{1}H-NMR (500 MHz, DMSO-d_6): δ [ppm] = 8.65 – 8.52 (m, 1 H, NH^{9}), 8.18 (dd, J = 21.8, 3.6 Hz, 1 H, NH^{12}), 7.40 – 7.21 (m, 12 H, CH$_{Ar}$), 7.21 – 7.12 (m, 2 H, CH$_{Ar}$), 5.23 (t, J = 4.3 Hz, 1 H, CH^{11}), 5.12 – 5.02 (m, 2 H, CH$_2^{26}$), 4.99 (dt, J = 9.7, 4.9 Hz, 1 H, CH^{32}), 4.84 – 4.78 (m, 2 H, CH$_2^{5}$), 4.78 – 4.48 (m, 2 H, CH$_2^{29}$), 4.31 (d, J = 6.0 Hz, 2 H, CH$_2^{2}$), 2.43 (d, J = 16.4 Hz, 3 H, CH$_3^{18}$), 1.81 – 1.67 (m, 2 H, CH$_2^{36}$), 1.37 – 1.19 (m, 10 H, CH$_2^{42\text{-}46}$), 0.85 (t, J = 6.4 Hz, 3 H, CH$_3^{47}$).

^{13}C-NMR (126 MHz, DMSO-d_6) δ [ppm] = 169.24 (s, CO$_2$R^{30}), 169.07 (s, CONR^{33}), 165.23 (s, CO$_2$R^{25}), 165.21 (s, CO$_2$R^{25}), 156.50 (s, NC^{8}), 152.36 (s, CO^{13}), 152.17 (s, CO^{13}), 149.74 (s, C^{15}), 149.61 (s, C^{15}), 143.86 (s, C$_{Ar}^{17}$), 143.71 (s, C$_{Ar}^{17}$), 139.18 (s, C$_{Ar}^{3}$), 136.22 (s, C$_{Ar}^{28}$), 131.91 (s, C$_{Ar}^{50}$), 128.45 (s, CH$_{Ar}$), 128.41 (s, CH$_{Ar}$), 128.31 (s, CH$_{Ar}$), 127.85 (s, CH$_{Ar}$), 127.69 (s, CH$_{Ar}$), 127.51 (s, CH$_{Ar}$), 127.48 (s, CH$_{Ar}$), 126.87 (s, CH$_{Ar}$), 126.60 (s, CH$_{Ar}$), 126.50 (s, CH$_{Ar}$), 102.83 (s, C^{10}), 102.75 (s, C^{10}), 74.17 (s, CH^{32}), 74.08 (s, CH^{32}), 65.33 (s, CH$_2^{26}$), 53.17 (s, CH^{11}), 52.96 (s, CH^{11}), 44.65 (s, CH$_2^{5}$), 44.61 (s, CH$_2^{5}$), 44.58 (s, CH$_2^{5}$), 44.11 (s, CH$_2^{29}$), 43.92 (s, CH$_2^{29}$), 41.56 (s, CH$_2^{2}$), 41.54 (s, CH$_2^{2}$), 31.33 (s, CH$_2^{36}$), 31.31 (s, CH$_2^{36}$), 31.11 (s, CH$_2$), 28.53 (s, CH$_2$), 28.51 (s, CH$_2$), 28.50 (s, CH$_2$), 24.41 (s, CH$_2$), 24.38 (s, CH$_2$), 22.07 (s, CH$_2$), 15.67 (s, CH$_3^{18}$), 15.65 (s, CH$_3^{18}$), 13.95 (s, CH$_3^{47}$).

FAB – MS [*m/z*] (relative intensity): 665.4 (20%) [M + H]$^+$, 638.3 (100%) [M – NC]$^+$, 557.3 (25%) [M – C$_7$H$_7$O]$^+$,

HRMS – FAB [*m/z*]: [M + H]$^+$ calculated for ^{12}C$_{39}$^{1}H$_{45}$^{16}O$_6$^{14}N$_4$, 665.3334; found, 665.3335; Δ = 0.12 mmu.

6.2.3.3.3 *Monomer-NC 85 obtained from Biginelli acid 70, 1,6-diisocyanohexane and octanal*

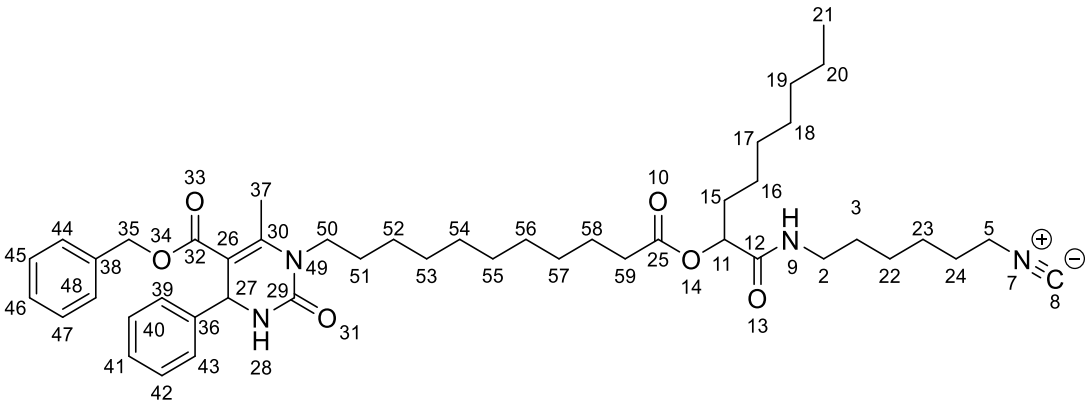

In a 50 mL round bottom flask 1,6-diisocyanohexane (807 g, 5.91 mmol, 5.00 eq.) was stirred in 3 mL dichloromethane under argon atmosphere, subsequently octanal (303 mg, 2.37 mmol, 2.00 eq.) was added. Finely powdered Biginelli acid **70** (600 mg, 1.18 mmol, 1.00 eq.) was suspended in 3 mL dichloromethane and added to the stirring diisocyanide aldehyde mixture. The resulting reaction mixture was stirred at room temperature for 2 d under argon atmosphere. The crude mixture was dried under reduced pressure. The residue was adsorbed onto celite® and purified *via* column chromatography on silica gel eluting with a gradual solvent mixture of ethyl acetate and *c*-hexane (1:3 → 1:1). The monomer-NC **85** was obtained as a yellow oil which crystalized to a colorless solid after several days (882 mg, 1.14 mmol, 96.6%). The exceeding diisocyanide could be recovered (617 mg, 4.54 mmol, 95.7%).

R_f in ethyl acetate/*c*-hexane (1:1) = 0.28. Visualized *via* fluorescence quench and Seebach staining solution.

IR (ATR): ν [cm^{-1}] = 3223.3 (br, ν(N-H)), 3095.6 (br, ν(N-H)), 2924.6 (m, ν(C-H)), 2852.8 (m, ν(C-H)), 2146.7 (w, ν(NC)), 1738.9 (m, ν(C=O)), 1707.4 (vs, ν(C=O)), 1682.1 (vs), 1616.2 (s), 1550.2 (m), 1454.4 (m), 1415.7 (w), 1394.6 (m), 1372.7, 1346.3 (m), 1323.1 (m), 1236.4 (s), 1195.1 (m), 1151.5 (s), 1097.9 (s), 1078.6 (m), 1040.5 (m), 999.8 (w), 913.9 (w), 828.1 (s), 753.6 (m), 722.8 (m), 697.5 (vs), 652.5 (s), 589.7 (m), 570.4 (w), 530.1 (m), 510.2 (m), 446.5 (w).

^{1}H-NMR (400 MHz, DMSO-d_6): δ [ppm] = 7.94 (d, J = 3.8 Hz, 1 H, NH^{28}), 7.91 (t, J = 5.9 Hz, 1 H, NH^{9}), 7.33 – 7.20 (m, 6 H, CH$_{Ar}^{39-48}$), 7.19 – 7.14 (m, 4 H, CH$_{Ar}^{39-48}$), 5.17 (d, J = 3.8 Hz, 1 H, CH^{27}), 5.13 – 5.01 (m, 2 H, CH$_2^{35}$), 4.81 (t, J = 6.3 Hz, 1 H, CH^{11}),

3.90 – 3.41 (m, 4 H, CH_2^{50} + CH_2^{5}), 3.11 – 2.97 (m, 2 H, CH_2^{15}), 2.50 (underneath DMSO signal, CH_3^{37}), 2.34 (t, *J* = 7.3 Hz, 2 H, CH_2^{59}), 1.69 – 1.61 (m, 2 H, CH_2^{2}), 1.60 – 1.41 (m, 6 H, CH_2), 1.41 – 1.30 (m, 6 H), 1.30 – 1.01 (m, 22 H), 0.90 – 0.78 (m, 3 H, CH_3^{21}).

^{13}C-NMR (101 MHz, DMSO-d_6) δ [ppm] = 172.40 (s, CO_2R^{25}), 169.14 (s, $CONR^{12}$), 165.34 (s, CO_2R^{32}), 155.61 – 155.28 (m, NC^{8}), 152.59 (s, CO^{29}), 150.47 (s, C^{30}), 143.81 (s, C_{Ar}^{36}), 136.34 (s, C_{Ar}^{38}), 128.30 (s, CH_{Ar}), 128.26 (s, CH_{Ar}), 127.76 (s, CH_{Ar}), 127.61 (s, CH_{Ar}), 127.26 (s, CH_{Ar}), 126.04 (s, CH_{Ar}), 102.53 (s, C^{26}), 73.09 (s, CH^{11}), 65.14 (s, CH_2^{35}), 52.24 (s, CH^{27}), 41.57 (s, CH_2^{50}), 41.33 – 40.90 (m, CH_2^{5}), 38.08 (s, CH_2^{15}), 33.42 (s, CH_2^{59}), 31.41 (s, CH_2^{2}), 31.12 (s, CH_2), 29.33 (s, CH_2), 28.92 (s, CH_2), 28.83 (s, CH_2), 28.76 (s, CH_2), 28.73 (s, CH_2), 28.68 (s, CH_2), 28.52 (s, CH_2), 28.51 (s, CH_2), 28.39 (s, CH_2), 26.16 (s, CH_2), 25.41 (s, CH_2), 25.31 (s, CH_2), 24.52 (s, CH_2), 24.40 (s, CH_2), 22.04 (s, CH_2), 15.68 (s, CH_3^{37}), 13.90 (s, CH_3^{21}).

FAB – MS [*m/z*] (relative intensity): 771.5 (100%) $[M + H]^+$, 663.5 (50%) $[M – C_7H_7O]^+$, 489.3 (70%) [Fragment A]$^+$, 321.1 (55%) [Fragment B]$^+$, 231.1 (30%) [Fragment B – C_7H_6]$^+$.

HRMS – FAB [*m/z*]: $[M + H]^+$ calculated for $^{12}C_{46}{}^{1}H_{67}{}^{16}O_6{}^{14}N_4$, 771.5055; found, 771.5056; Δ = 0.05 mmu.

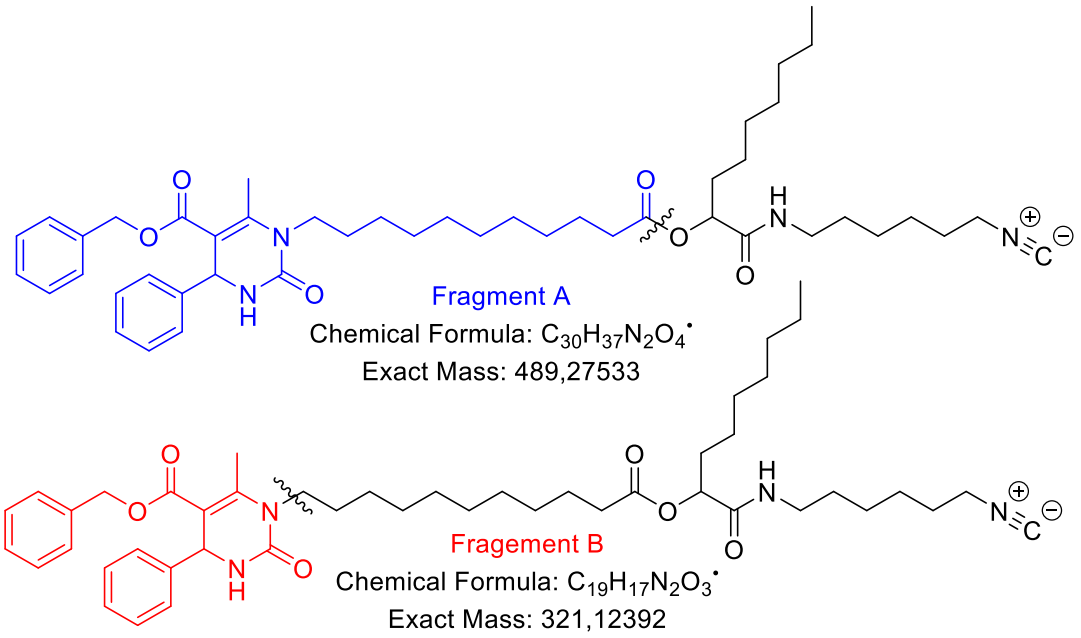

6.2.3.3.4 *Monomer-NC 86 obtained from Biginelli acid 71, 1,6-diisocyanohexane and 2-ethylbutanal*

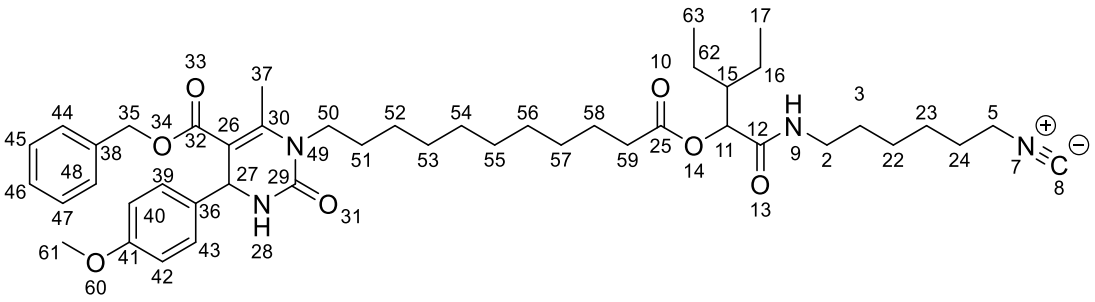

In a 50 mL round bottom flask 1,6-diisocyanohexane (1.01 g, 7.45 mmol, 5.00 eq.) was stirred in 4 mL dichloromethane, subsequently 2-ethylbutanal (300 mg, 2.98 mmol, 2.00 eq.) was added. Finely powdered Biginelli acid **71** (800 mg, 1.49 mmol, 1.00 eq.) was suspended in 3 mL dichloromethane/dimethyl sulfoxide (4:1) and added to the stirring diisocyanide aldehyde mixture. The resulting reaction mixture was stirred at room temperature for 2 d under argon atmosphere. The crude mixture was dried under reduced pressure. The residue was adsorbed onto celite® and purified *via* column chromatography on silica gel eluting with a gradual solvent mixture of ethyl acetate and *c*-hexane (1:5 → 2:1). The monomer-NC **86** was obtained as a yellow solid (702 mg, 907 µmol, 60.9%). The exceeding diisocyanide could be recovered (673 mg, 4.94 mmol, 83.3%).

R_f in ethyl acetate/*c*-hexane (2:1) = 0.51. Visualized *via* fluorescence quench and Seebach staining solution.

IR (ATR): ν [cm^{-1}] = 3323.6 (br, ν(N-H)), 3089.2 (br, ν(N-H)), 2928.1 (s, ν(C-H)), 2854.3 (m, ν(C-H)), 2145.7 (w, ν(NC)), 1736.4 (m, ν(C=O)), 1708.5 (m, ν(C=O)), 1682.4 (s), 1610.5 (vs), 1535.9 (s), 1509.7 (m), 1463.4 (s), 1428.2 (m), 1392.9 (w), 1305.2 (w), 1285.5 (m), 1240.8 (w), 1199.8 (m), 1175.3 (w), 1154.2 (s), 1096.3 (m), 1039.0 (m), 998.4 (s), 960.6 (m), 914.9 (w), 846.1 (m), 795.7 (m), 777.4 (w), 755.6 (m), 724.5 (m), 697.6 (s), 650.3 (m), 588.1 (w), 563.6 (w), 533.2 (m), 510.2 (w), 424.9 (w).

^{1}H-NMR (500 MHz, DMSO-d_6): δ [ppm] = 7.89 (t, J = 5.9 Hz, 1 H, NH^{9}), 7.86 (d, J = 3.9 Hz, 1 H, NH^{28}), 7.32 – 7.30 (m, 3 H, CH$_{Ar}$), 7.20 – 7.16 (m, 2 H, CH$_{Ar}$), 7.09 (d, J = 8.4 Hz, 2 H, CH$_{Ar}^{39,43}$), 6.83 (d, J = 8.5 Hz, 2 H, CH$_{Ar}^{40,42}$), 5.13 (d, J = 3.8 Hz, 1 H, CH^{27}), 5.11 – 5.02 (m, 2 H, CH$_2^{35}$), 4.91 (d, J = 4.3 Hz, 1 H, CH^{11}), 3.85 (ddd, J = 14.7, 8.5, 6.3 Hz, 1 H, CH$_2^{50a}$), 3.72 (s, 3 H, OCH$_3^{61}$), 3.52 – 3.41 (m, 3 H, CH$_2^{50b}$+CH$_2^{5}$),

3.11 – 3.00 (m, 2 H, CH_2^{2}), 2.50 (underneath DMSO signal, CH_3^{37}), 2.38 (t, *J* = 7.3 Hz, 2 H, CH_2^{59}), 1.68 (tt, *J* = 8.0, 3.9 Hz, 1 H, CH^{15}), 1.59 – 1.30 (m, 8 H, CH_2), 1.30 – 1.23 (m, 4 H, CH_2), 1.23 – 1.14 (m, 4 H, CH_2), 1.10 (t, *J* = 7.2 Hz, 2 H, CH_2), 0.84 (q, *J* = 7.8 Hz, 6 H, $CH_3^{17,63}$).

^{13}C-NMR (126 MHz, DMSO-d_6) δ [ppm] = 172.51 (s, CO_2R^{25}), 168.83 (s, $CONR^{12}$), 165.38 (s, CO_2R^{32}), 158.48 (s, C_{Ar}^{41}), 155.45 (t, *J* = 5.5 Hz, NC^{8}), 152.61 (s, CO^{29}), 150.17 (s, C^{30}), 136.38 (s, C_{Ar}^{38}), 135.92 (s, C_{Ar}^{36}), 128.27 (s, CH_{Ar}), 127.75 (s, CH_{Ar}), 127.58 (s, CH_{Ar}), 127.23 (s, CH_{Ar}), 113.61 (s, $CH_{Ar}^{40,42}$), 102.85 (s, C^{26}), 74.08 (s, CH^{11}), 65.08 (s, CH_2^{35}), 55.02 (s, OCH_3^{61}), 51.64 (s, CH^{27}), 42.54 (s, CH^{11}), 41.55 (s, CH_2^{50}), 41.02 (t, *J* = 5.6 Hz, CH_2^{5}), 38.14 (s, CH_2^{2}), 33.48 (s, CH_2^{59}), 29.36 (s, CH_2), 28.94 (s, CH_2), 28.85 (s, CH_2), 28.76 (s, CH_2), 28.74 (s, CH_2), 28.66 (s, CH_2), 28.39 (s, CH_2), 26.18 (s, CH_2), 25.40 (s, CH_2), 25.34 (s, CH_2), 24.41 (s, CH_2), 21.75 (s, CH_2), 21.36 (s, CH_2), 15.66 (s, CH_3^{37}), 11.27 (s, $CH_3^{17\ or\ 63}$), 11.22 (s, $CH_3^{17\ or\ 63}$).

FAB – MS [*m/z*] (relative intensity): 773.5 (80%) $[M + H]^+$, 665.4 (70%) $[M – C_7H_7O]^+$, 535.3 (50%) [Fragment A]$^+$, 519.3 (55%) [Fragment A – O]$^+$, 351.1 (55%) [Fragment B]$^+$.

HRMS – FAB [*m/z*]: $[M + H]^+$ calculated for $^{12}C_{45}{}^{1}H_{65}{}^{16}O_7{}^{14}N_4$, 773.4853; found, 773.4853; Δ = 0.03 mmu.

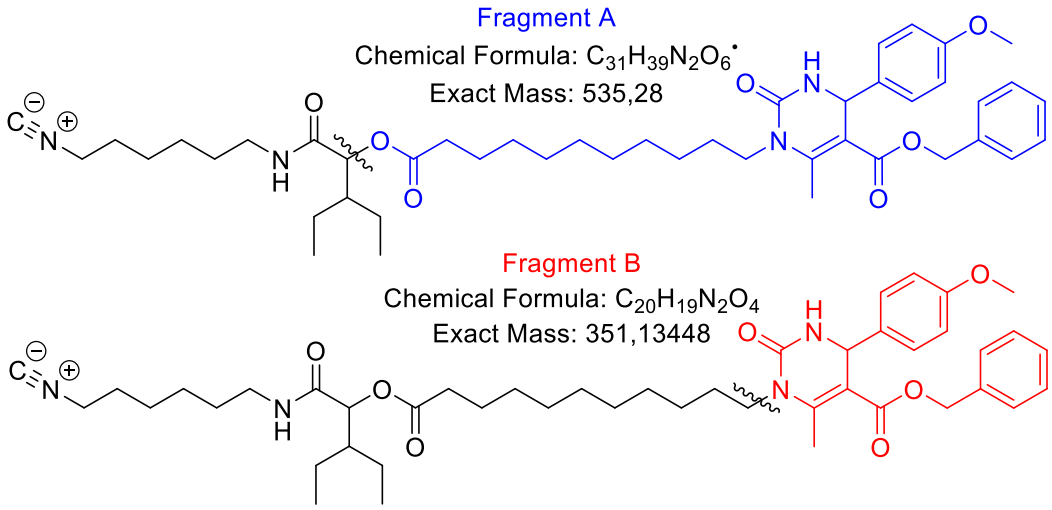

6.2.3.3.5 *Monomer-NC 87 obtained from Biginelli acid 72, 1,6-diisocyanohexane and cyclohexane carbaldehyde*

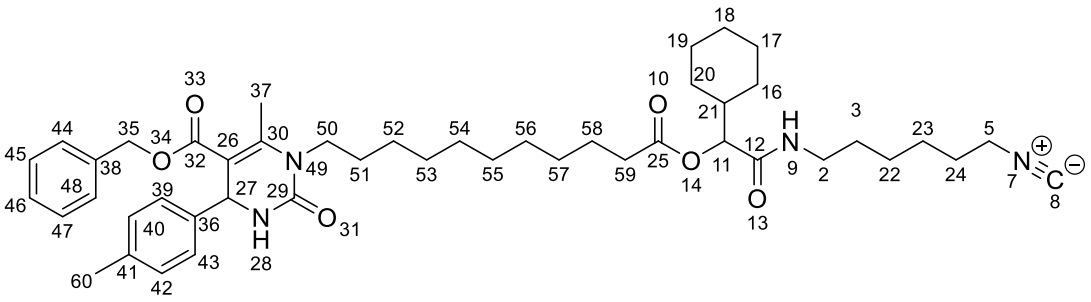

In a 50 mL round bottom flask 1,6-diisocyanohexane (1.04 g, 7.68 mmol, 5.00 eq.) was stirred in 3 mL dichloromethane under argon atmosphere, subsequently cyclohexancarboxaldehyde (345 mg, 30.7 mmol, 2.00 eq.) was added. Finely powdered Biginelli acid **72** (800 mg, 1.54 mmol, 1.00 eq.) was suspended in 3 mL dichloromethane/dimethyl sulfoxide (4:1) and added dropwise to the stirring diisocyanide/aldehyde mixture. The resulting reaction mixture was stirred at room temperature for 2 d under argon atmosphere. The crude mixture was dried under reduced pressure. The residue was adsorbed onto celite® and purified *via* column chromatography on silica gel eluting with a gradual solvent mixture of ethyl acetate and *c*-hexane (1:5 → 1:2). The monomer-NC **87** was obtained as a yellow solid (773 mg, 1.53 µmol, 65.5%). The exceeding diisocyanide could be recovered (514 mg, 3.77 mmol, 61.4%).

R_f in ethyl acetate/*c*-hexane (2:1) = 0.50. Visualized *via* fluorescence quench and Seebach staining solution.

IR (ATR): ν [cm^{-1}] = 3296.4 (br, ν(N-H)), 3090.2 (br, ν(N-H)), 2924.1 (s, ν(C-H)), 2852.0 (m, ν(C-H)), 2146.4 (m, ν(NC)), 1736.7 (m, ν(C=O)), 1708.1 (vs, ν(C=O)), 1681.4 (s), 1615.5 (m), 1541.0 (w), 1452.9 (w), 1422.0 (w), 1391.9 (w), 1363.4 (m), 1336.3 (m), 1322.0 (w), 1302.8 (m), 1274.5 (m), 1233.9 (m), 1194.6 (m), 1146.0 (s), 1095.9 (vs), 1039.6 (s), 985.7 (m), 913.6 (w), 843.8 (w), 776.9 (w), 755.4 (m), 721.4 (m), 696.6 (s), 650.8 (m), 590.0 (m), 554.2 (w), 521.5 (s), 507.4 (s), 429.0 (w).

^{1}H-NMR (500 MHz, DMSO-d_6): δ [ppm] = 7.89 – 7.85 (m, 2 H, NH^{9+28}), 7.36 – 7.26 (m, 3 H, CH$_{Ar}$), 7.23 – 7.13 (m, 2 H, CH$_{Ar}$), 7.11 – 7.01 (m, 4 H, CH$_{Ar}$), 5.14 (d, J = 3.8 Hz, 1 H, CH^{27}), 5.10 – 5.03 (m, 2 H, CH$_2^{35}$), 4.66 (d, J = 5.4 Hz, 1 H, CH^{11}), 3.89 – 3.80 (m, 1 H, CH$_2^{50a}$), 3.53 – 3.39 (m, 3 H, CH$_2^{50b}$+CH$_2^{5}$), 3.11 – 2.96 (m, 2 H, CH$_2^{2}$), 2.49

(s, 3 H, CH_3^{37}), 2.36 (td, *J* = 7.4, 2.4 Hz, 2 H, CH_2^{59}), 2.26 (s, 3 H, CH_3^{60}), 1.82 – 1.64 (m, 4 H, CH_2), 1.64 – 1.49 (m, 4 H, CH_2), 1.48 – 0.99 (m, 22 H, CH_2).

^{13}C-NMR (126 MHz, DMSO-d_6) δ [ppm] = 172.46 (s, CO_2R^{25}), 168.26 (s, $CONR^{12}$), 165.37 (s, CO_2R^{32}), 155.60 – 155.21 (m, NC^{8}), 152.66 (s, CO^{29}), 150.30 (s, C^{30}), 140.86 (s, C_{Ar}^{36}), 136.38 (s, $C_{Ar}^{38\ or\ 41}$), 136.36 (s, $C_{Ar}^{36\ or\ 41}$), 128.81 (s, CH_{Ar}), 128.26 (s, CH_{Ar}), 127.76 (s, CH_{Ar}), 127.61 (s, CH_{Ar}), 125.94 (s, CH_{Ar}), 102.74 (s, C^{26}), 77.03 (s, CH^{11}), 65.11 (s, CH_2^{35}), 51.87 (s, CH^{27}), 41.52 (s, CH_2^{50}), 41.18 – 40.65 (m, CH_2^{5}), 38.05 (s, CH_2^{2}), 33.39 (s, CH_2^{59}), 29.36 (s, CH_2), 28.93 (s, CH_2), 28.86 (s, CH_2), 28.77 (s, CH_2), 28.75 (s, CH_2), 28.68 (s, CH_2), 28.59 (s, CH_2), 28.39 (s, CH_2), 27.33 (s, CH_2), 26.16 (s, CH_2), 25.70 (s, CH_2), 25.50 (s, CH_2), 25.37 (s, CH_2), 25.31 (s, CH_2), 24.40 (s, CH_2), 20.59 (s, CH_3^{60}), 15.67 (s, CH_3^{37}).

ESI–MS [*m/z*]: $[M + Na]^+$ calculated for $^{12}C_{46}{}^{1}H_{64}{}^{16}O_6{}^{14}N_4{}^{23}Na_1$, 791.4718; found, 791.4717; Δ = 0.07 mmu.

6.2.3.3.6 *Monomer-NC 88 obtained from Biginelli acid 73, 1,6-diisocyanohexane and heptanal*

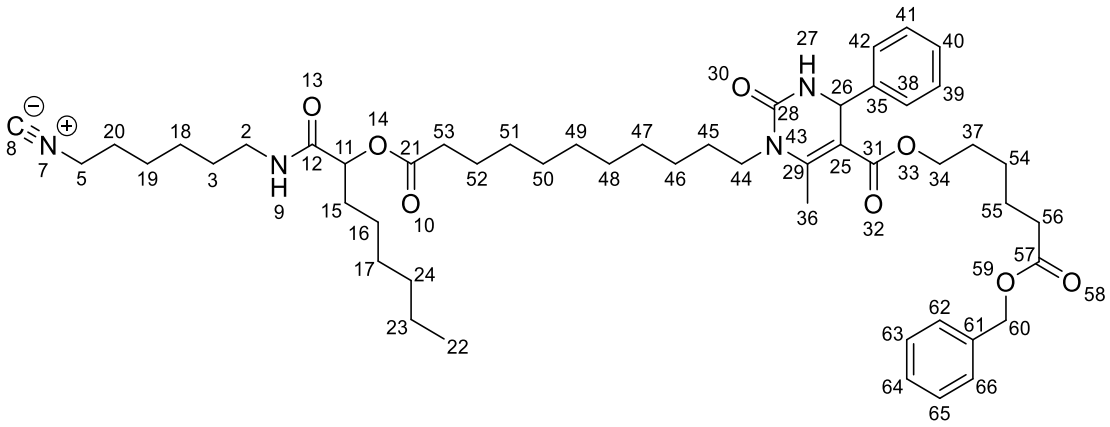

In a 25 mL round bottom flask 1,6-diisocyanohexane (164 mg, 1.21 mmol, 5.00 eq.) was stirred in 1 mL dichloromethane, subsequently heptanal (55.2 mg, 483 µmol, 2.00 eq.) was added. Biginelli acid **73** (150 mg, 242 µmol, 1.00 eq.) was suspended in 1 mL dichloromethane and added dropwise to the stirring diisocyanide aldehyde mixture. The resulting reaction mixture was stirred at room temperature for 3 d under argon atmosphere. The crude mixture was dried under reduced pressure. The residue was adsorbed onto celite® and purified *via* column chromatography on silica gel eluting with a gradual solvent mixture of ethyl acetate and *c*-hexane (1:2 → 1:0). The

monomer-NC **88** was obtained as a yellow oil (171 mg, 196 µmol, 81.3%). The exceeding diisocyanide could be recovered (13.7 mg, 119 µmol, 10.7%).

R_f in ethyl acetate/*c*-hexane (2:1) = 0.60. Visualized *via* fluorescence quench and Seebach staining solution.

IR (ATR): ν [cm^{-1}] = 3310.8 (br, ν(N-H)), 2926.4 (s, ν(C-H)), 2855.4 (s, ν(C-H)), 2146.4 (w, ν(NC)), 1735.3 (s, ν(C=O)), 1674.3 (vs, ν(C=O)), 1619.6 (m), 1536.8 (m), 1495.3 (m), 1454.7 (m), 1386.4 (m), 1234.0 (s), 1155.8 (s), 1088.0 (m), 829.7 (w), 733.6 (m), 696.8 (w), 498.1 (w).

^{1}H-NMR (400 MHz, DMSO-d_6): δ [ppm] = 8.08 – 7.88 (m, 2 H, NH^{9+27}), 7.66 – 7.18 (m, 10 H, CH$_{Ar}^{38-42+62-66}$), 5.16 (d, *J* = 3.9 Hz, 0.3 H, CH$^{26\ minor}$), 5.13 (d, *J* = 3.7 Hz, 0.7 H, CH$^{26\ major}$), 5.07 (s, 1.5 H, CH$_2^{60\ major}$), 5.06 (s, 0.5 H, CH$_2^{60\ minor}$), 4.81 (t, *J* = 6.3 Hz, 1 H, CH^{11}), 4.00 – 3.77 (m, 3 H, CH$_2^{34+44a}$), 3.53 – 3.40 (m, 3 H, CH$_2^{5+44b}$), 3.11 – 2.96 (m, 2 H, CH$_2^{2}$), 2.49 (s, 3 H, CH$_3^{36}$), 2.34 (t, *J* = 7.5 Hz, 2 H, CH$_2^{53}$), 2.25 (t, *J* = 7.4 Hz, 2 H, CH$_2^{56}$), 1.67 – 1.63 (m, 2 H, CH$_2^{15}$), 1.56 – 1.51 (m, 4 H, CH$_2$), 1.42 – 0.99 (m, 34 H, CH$_2$), 0.84 (t, *J* = 7.1, 3 H, CH$_3^{22}$).

^{13}C-NMR (101 MHz, DMSO-d_6) δ [ppm] = 172.61 (s, CO$_2$R$^{21\ or\ 57}$), 172.44 (s, CO$_2$R$^{21\ or\ 57}$), 169.18 (s, CONR^{12}), 165.75 (s, CO$_2$R^{31}), 165.62 (s, CO$_2$R^{31}), 155.52 – 155.37 (t, *J* = 5.5 Hz, NC^{8}), 153.28 (s, CO^{28}), 152.62 (s, CO^{28}), 149.88 (s, C^{29}), 148.70 (s, C^{29}), 143.94 (s, C$_{Ar}^{35}$), 143.53 (s, C$_{Ar}^{35}$), 136.28 (s, C$_{Ar}^{61}$), 135.68 (s, C$_{Ar}^{61}$), 128.65 (s, CH$_{Ar}$), 128.41 (s, CH$_{Ar}$), 128.31 (s, CH$_{Ar}$), 127.97 (s, CH$_{Ar}$), 127.95 (s, CH$_{Ar}$), 127.91 (s, CH$_{Ar}$), 127.25 (s, CH$_{Ar}$), 126.86 (s, CH$_{Ar}$), 126.04 (s, CH$_{Ar}$), 104.56 (s, C^{25}), 102.81 (s, C^{25}), 73.12 (s, CH^{11}), 65.30 (s, CH$_2^{60}$), 65.27 (s, CH$_2^{60}$), 63.70 (s, CH$_2^{34}$), 63.29 (s, CH$_2^{34}$), 52.39 (s, CH^{26}), 52.25 (s, CH^{26}), 41.53 (s, CH$_2^{44}$), 41.04 (t, *J* = 5.85 Hz, CH$_2^{5}$), 38.10 (s, CH$_2^{2}$), 33.43 (s, CH$_2^{53}$), 33.30 (s, CH$_2^{56}$), 33.21 (s, CH$_2$), 31.44 (s, CH$_2^{15}$), 31.12 (s, CH$_2$), 29.37 (s, CH$_2$), 28.95 (s, CH$_2$), 28.86 (s, CH$_2$), 28.78 (s, CH$_2$), 28.76 (s, CH$_2$), 28.70 (s, CH$_2$), 28.63 (s, CH$_2$), 28.51 (s, CH$_2$), 28.40 (s, CH$_2$), 28.24 (s, CH$_2$), 27.75 (s, CH$_2$), 26.19 (s, CH$_2$), 25.88 (s, CH$_2$), 25.43 (s, CH$_2$), 25.32 (s, CH$_2$), 25.03 (s, CH$_2$), 24.88 (s, CH$_2$), 24.51 (s, CH$_2$), 24.42 (s, CH$_2$), 23.98 (s, CH$_2$), 21.97 (s, CH$_2$), 20.77 (s, CH$_2$), 15.61 (s, CH$_3^{36}$), 13.89 (s, CH$_3^{22}$).

ESI–MS [*m/z*]: [M + Na]$^+$ calculated for ^{12}C$_{51}$^{1}H$_{74}$^{16}O$_8$^{14}N$_4$^{23}Na$_1$, 893.5400; found, 893.5405; Δ = 0.54 mmu.

6.2.3.3.7 *Monomer-NC 89 obtained from Biginelli acid 74, 1,6-diisocyanohexane and valeraldehyde*

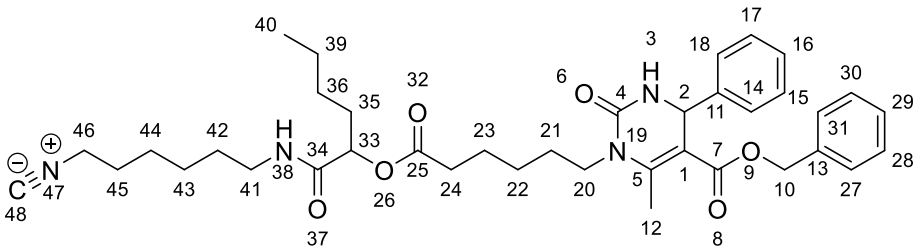

In a 50 mL round bottom flask 1,6-diisocyanohexane (2.50 g, 18.3 mmol, 4.00 eq.) was stirred in 10 mL dichloromethane, subsequently pentanal (974 µL, 789 mg, 9.61 mmol, 2.00 eq.) was added. Biginelli acid **74** (2.00 g, 4.58 mmol, 1.00 eq.) was suspended in 3 mL dichloromethane and dimethyl sulfoxide was added dropwise until the Biginelli acid was fully dissolved, this solution was added dropwise to the stirring diisocyanide/aldehyde mixture. The resulting reaction mixture was degassed with argon and stirred at room temperature for 3 d under argon atmosphere. The crude mixture was dried under reduced pressure, the residue was adsorbed onto celite® and purified *via* column chromatography on silica gel eluting with a gradual solvent mixture of ethyl acetate and *c*-hexane (1:5 → 1:0). The monomer-NC **89** was obtained as a colorless, soft amorphous solid (2.54 g, 4.58 mmol, 84.1%).

R_f in ethyl acetate/*c*-hexane (2:1) = 0.57. Visualized *via* fluorescence quench and Seebach staining solution.

IR (ATR): ν [cm^{-1}] = 3320.6 (br, ν(N-H)), 2934.9 (m, ν(C-H)), 2862.0 (w, ν(C-H)), 2147.4 (w, ν(NC)), 1736.0 (s, ν(C=O)), 1681.0 (vs, ν(C=O)), 1617.2 (s), 1534.4 (m), 1495.7 (m), 1455.0 (s), 1372.4 (s), 1236.7 (vs), 1153.0 (s), 1111.4 (s), 1073.5 (s), 1044.0 (vs), 1002.2 (m), 938.9 (w), 915.8 (w), 831.0 (w), 756.3 (w), 697.6 (s), 633.2 (w), 607.5 (w), 516.9 (w).

^{1}H-NMR (400 MHz, DMSO-d_6): δ [ppm] = 7.96 (d, J = 3.8 Hz, 1 H, NH^{3}), 7.93 (t, J = 5.8 Hz, 1 H, NH^{38}), 7.36 – 7.07 (m, 10 H, CH$_{Ar}^{14\text{-}18\ +\ 27\text{-}31}$), 5.18 (d, J = 3.7 Hz, 1 H, CH^{2}), 5.14 – 4.97 (m, 2 H, CH$_2^{10}$), 4.80 (dd, J = 7.2, 5.5 Hz, 1 H, CH^{33}), 3.89 – 3.74 (m, 1 H, CH$_2^{20a}$), 3.57 – 3.40 (m, 3 H, CH$_2^{46}$ + CH$_2^{20b}$), 3.12 – 2.94 (m, 2 H, CH$_2^{41}$), 2.51 (s, 3 H, CH$_3^{12}$), 2.31 – 2.25 (m, 2 H, CH$_2^{24}$), 1.71 – 1.62 (m, 2 H, CH$_2^{35}$), 1.62 – 1.43 (m, 4 H, CH$_2^{21+23}$), 1.44 – 1.20 (m, 10 H, CH$_2$), 0.89 – 0.78 (m, 3 H, CH$_3^{40}$).

^{13}C-NMR (101 MHz, DMSO-d_6) δ [ppm] = 172.34 (s, CO_2R^{25}), 169.17 (s, $CONR^{34}$), 165.36 (s, CO_2R^{7}), 155.48 – 155.34 (m, NC^{7}), 152.60 (s, CO^{19}), 150.50 (s, C^{5}), 143.85 (s, $C_{Ar}{}^{11}$), 136.36 (s, $C_{Ar}{}^{13}$), 128.38 (s, CH_{Ar}), 128.30 (s, CH_{Ar}), 127.79 (s, CH_{Ar}), 127.65 (s, CH_{Ar}), 127.32 (s, CH_{Ar}), 126.10 (s, CH_{Ar}), 102.55 (s, C^{1}), 102.54 (s, C^{1}), 73.18 (s, CH^{33}), 65.17 (s, $CH_2{}^{10}$), 52.30 (s, CH^{2}), 41.51 (s, $CH_2{}^{20}$), 41.15 – 40.90 (m, $CH_2{}^{46}$), 38.10 (s, $CH_2{}^{41}$), 33.26 (s, $CH_2{}^{24}$), 31.17 (s, $CH_2{}^{35}$), 28.96 (s, CH_2), 28.79 (s, CH_2), 28.39 (s, CH_2), 26.79 (s, CH_2), 25.55 (s, CH_2), 25.42 (s, CH_2), 25.32 (s, CH_2), 24.03 (s, CH_2), 20.76 (s, CH_2), 15.68 (s, $CH_3{}^{12}$), 13.82 (s, $CH_3{}^{40}$).

ESI – MS [*m/z*]: $[M + Na]^+$ calculated for $^{12}C_{38}{}^{1}H_{50}{}^{16}O_6{}^{14}N_4{}^{23}Na_1$, 681.3623; found, 681.3624; Δ = 0.17 mmu.

ESI – MS [*m/z*]: $[2 M + Na]^+$ calculated for $^{12}C_{76}{}^{1}H_{100}{}^{16}O_{12}{}^{14}N_8{}^{23}Na_1$, 1339.7353; found, 1339.7371; Δ = 1.77 mmu.

6.2.3.3.8 *Monomer-NC 90 obtained from Biginelli acid 50, 1,6-diisocyanohexane and acetaldehyde*

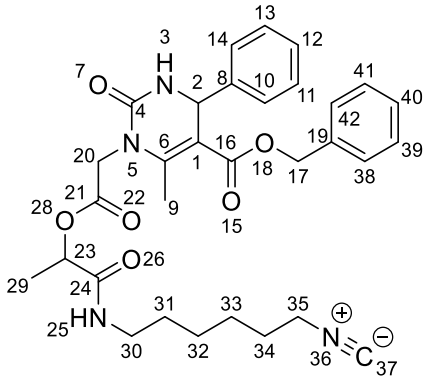

In a 250 mL round bottom flask 1,6-diisocyanohexane (5.45 g, 40.0 mmol, 4.35 eq.) was stirred in 50 mL dichloromethane (0.17 M for 1.00 eq.), subsequently acetaldehyde (1,62 g, 3.68 mmol, 2.06 mL, 4.00 eq.) was added at 0 °C. Finely powdered Biginelli acid **50** (3.50 g, 9.20 mmol, 1.00 eq.) was dissolved in 6 mL dimethyl sulfoxide/dichloromethane (1:2) and added dropwise to the stirring mixture at room temperature. The resulting reaction mixture was stirred at room temperature for 5 d. The crude mixture concentrated under reduced pressure. The residue was purified *via* column chromatography on silica gel eluting with a gradual solvent mixture of ethyl acetate and *c*-hexane (0:1 → 1:0). The monomer-NC **90** was obtained as an

amorphous solid (3.01 g, 5.38 mmol, 58.5%). The exceeding diisocyanide could be recovered (1.25 g, 12.2 mmol, 30.5%).

R_f = 0.38 in ethyl acetate. Visualized *via* fluorescence quench and Seebach staining solution.

IR (ATR): ν [cm^{-1}] = 3306.4 (br, ν(N-H)), 2934.7 (m, ν(C-H)), 2147.9 (br, ν(N-C)), 1752.1 (m, ν(C=O)), 1675.8 (vs, ν(C=O)), 1539.6 (m), 1495.5 (w), 1453.7 (s), 1383.8 (m), 1308.0 (s), 1277.5 (m), 1257.3 (m), 1171.8 (vs), 1104.8 (s), 1041.5 (m), 938.5 (w), 831.1 (w), 754.5 (m), 696.7 (s), 593.1 (w), 497.4 (w), 399.8 (w).

^{1}H-NMR (400 MHz, DMSO-d_6): δ [ppm] = 8.22 – 8.10 (m, 1 H, NH^{3}), 7.95 (dt, J = 8.8, 5.7 Hz, 1 H, NH^{25}), 7.37 – 7.22 (m, 8 H, CH$_{Ar}$), 7.20 – 7.12 (m, 2 H, CH$_{Ar}$), 5.21 (t, J = 3.4 Hz, 1 H, CH^{2}), 5.06 (t, J = 3.0 Hz, 2 H, CH$_2^{17}$), 5.03 – 4.94 (m, 1 H, CH^{23}), 4.79 – 4.44 (m, 2 H, CH$_2^{17}$), 3.48 – 3.39 (m, 2 H, CH$_2^{35}$), 3.13 – 3.00 (m, 2 H, CH$_2^{30}$), 2.43 (d, J = 5.1 Hz, 3 H, CH$_3^{9}$), 1.61 – 1.46 (m, 2 H, CH$_2^{34}$), 1.44 – 1.14 (m, 10 H, CH$_2$+CH$_3^{29}$).

^{13}C-NMR (101 MHz, DMSO-d_6): δ [ppm] = 169.41 (s, CONR^{24}), 169.37 (s, CONR^{24}), 169.05 (s, CO$_2$R^{21}), 168.97 (s, CO$_2$R^{21}), 165.24 (s, CO$_2$R^{16}), 155.47 (t, J = 5.9 Hz, NC^{37}), 155.43 (s, NC^{37}), 155.40 (s, NC^{37}), 152.30 (s, CO^{4}), 152.14 (s, CO^{4}), 149.77 (s, C^{6}), 149.46 (s, C^{6}), 143.87 (s, C$_{Ar}^{8}$), 143.75 (s, C$_{Ar}^{8}$), 136.23 (s, C$_{Ar}^{19}$), 136.21 (s, C$_{Ar}^{19}$), 128.45 (s, CH$_{Ar}$), 128.41 (s, CH$_{Ar}$), 128.33 (s, CH$_{Ar}$), 127.85 (s, CH$_{Ar}$), 127.80 – 127.66 (m, CH$_{Ar}$), 127.55 (s, CH$_{Ar}$), 126.62 (s, CH$_{Ar}$), 126.49 (s, CH$_{Ar}$), 102.87 (s, C^{1}), 102.70 (s, C^{1}), 70.67 (s, CH^{23}), 65.34 (s, CH$_2^{17}$), 53.23 (s, CH^{2}), 52.99 (s, CH^{2}), 44.08 (s, CH$_2^{20}$), 43.87 (s, CH$_2^{20}$), 41.03 (dt, J = 5.9 Hz, 2.1 Hz, CH$_2^{35}$), 38.22 (s, CH$_2^{30}$), 28.75 (s, CH$_2^{31}$), 28.35 (s, CH$_2^{34}$), 25.42 (s, CH$_2^{33}$), 25.29 (s, CH$_2^{32}$), 17.64 (s, CH$_3^{29}$), 17.60 (s, CH$_3^{29}$), 15.71 (s, CH$_3^{9}$), 15.65 (s, CH$_3^{9}$).

FAB – MS [*m/z*] (relative intensity): 561.3 (70%) [M + H]$^+$, 435.2 (25%) [M – C$_7$H$_7$O]$^+$,

HRMS – FAB [*m/z*]: [M + H]$^+$ calculated for ^{12}C$_{31}$^{1}H$_{37}$^{16}O$_6$^{14}N$_4$, 561.2708; found, 561.2709; Δ = 0.18 mmu.

6.2.3.3.9 *Monomer-NC 91 obtained from Biginelli acid 75, 1,6-diisocyanohexane and lauric aldehyde*

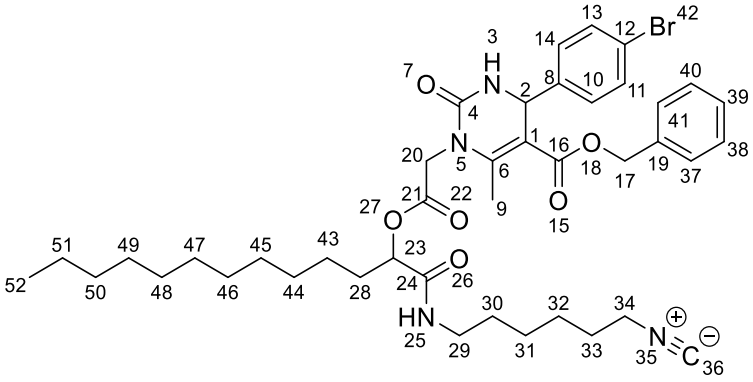

In a 250 mL round bottom flask 1,6-diisocyanohexane (4.52 g, 3.32 mmol, 4.35 eq.) was stirred in 30 mL dichloromethane, subsequently lauric aldehyde (5.63 g, 3.06 mmol, 4.00 eq.) was added. Finely powdered Biginelli acid **75** (3.50 g, 7.64 mmol, 1.00 eq.) was dissolved in 10 mL dimethyl sulfoxide/dichloromethane (1:2) and added dropwise to the stirring mixture. The resulting reaction mixture was stirred at room temperature for 3 d. The crude mixture was dried under reduced pressure. The residue was purified *via* column chromatography on silica gel eluting with a gradual solvent mixture of ethyl acetate and *c*-hexane (0:1 → 1:1). The oily residue was dissolved in 20 mL dichloromethane and dried under reduced pressure to yield the monomer-NC **91** as a colorless, soft amorphous solid (2.99 g, 3.82 mmol, 50.0%).

R_f = 0.29 in ethyl acetate/*c*-hexane (1:1). Visualized *via* fluorescence quench and Seebach staining solution.

IR (ATR): ν [cm^{-1}] = 3281.1 (br, ν(N-H)), 2922.4 (w, ν(C-H)), 2852.9 (w, ν(C-H)), 2147.1 (w, ν(N-C)), 1733.8 (s, ν(C=O)), 1685.3 (vs, ν(C=O)), 1658.0 (s, ν(C=O)), 1623.7 (m), 1541.2 (m), 1486.9 (m), 1455.5 (w), 1410.8 (m), 1373.6 (w), 1307.8 (w), 1254.1 (w), 1206.7 (vs), 1187.3 (s), 1168.4 (s), 1105.3 (s), 1071.0 (m), 1042.7 (m), 1009.1 (m), 956.5 (m), 859.7 (w), 811.3 (w), 763.5 (m), 719.4 (w), 697.5 (w), 644.6 (w), 581.1 (w), 502.8 (m), 435.3 (w).

^{1}H-NMR (400 MHz, DMSO-d_6): δ [ppm] = 8.22 (dd, J = 17.5, 3.7 Hz, 1 H, NH^{3}), 8.00 – 7.90 (m, 1 H, NH^{25}), 7.49 – 7.43 (m, 2 H, CH$_{Ar}$), 7.33 – 7.27 (m, 3 H, CH$_{Ar}$), 7.21 (t, J = 7.9 Hz, 2 H, CH$_{Ar}$), 7.18 – 7.12 (m, 2 H, CH$_{Ar}$), 5.20 (t, J = 3.8 Hz, 1 H, CH^{2}), 5.06 (qd, J = 12.6, 1.8 Hz, 2 H, CH$_2^{17}$), 4.92 – 4.87 (m, 1 H, CH^{23}), 4.78 – 4.45 (m, 2 H, CH$_2^{20}$), 3.49 – 3.40 (m, 2 H, CH$_2^{34}$), 3.12 – 2.98 (m, 2 H, CH$_2^{29}$), 2.45 (s) and 2.43 (s,

3 H, CH_3^{9}), 1.76 – 1.62 (m, 2 H, CH_2^{28}), 1.60 – 1.47 (m, 2 H, CH_2^{33}), 1.43 – 1.12 (m, 28 H, CH_2), 0.89 – 0.81 (m, 3 H, CH_3^{52}).

^{13}C-NMR (101 MHz, DMSO-d_6): δ [ppm] = 169.06 (s, $CONR^{24}$), 168.98 (s, CO_2R^{20}), 168.63 (s, CO_2R^{20}), 165.03 (s, CO_2Bn^{16}), 165.01 (s, CO_2Bn^{16}), 155.51 (s, NC^{36}), 155.46 (s, NC^{36}), 155.40 (s, NC^{36}), 152.18 (s, CO^{4}), 151.98 (s, CO^{4}), 150.14 (s, C^{6}), 149.96 (s, C^{6}), 143.14 (s, C_{Ar}^{8}), 142.99 (s, C_{Ar}^{8}), 136.14 (s, C_{Ar}^{19}), 136.13 (s, C_{Ar}^{19}), 131.32 (s, CH_{Ar}), 131.27 (s, CH_{Ar}), 128.82 (s, CH_{Ar}), 128.75 (s, CH_{Ar}), 128.28 (s, CH_{Ar}), 127.86 (s, CH_{Ar}), 127.70 (s, CH_{Ar}), 127.68 (s, CH_{Ar}), 120.60 (s, C_{Ar}^{12}), 102.33 (s, C^{1}), 102.20 (s, C^{1}), 74.18 (s, CH^{23}), 74.12 (s, CH^{23}), 65.34 (s, CH_2^{17}), 52.59 (s, CH^{2}), 52.41 (s, CH^{2}), 44.12 (s, CH_2^{20}), 43.92 (s, CH_2^{20}), 41.09 (s, CH_2^{34}), 41.03 (s, CH_2^{34}), 40.97 (s, CH_2^{34}), 38.16 (s, CH_2^{29}), 31.29 (s, CH_2^{28}), 29.01 (s, CH_2), 29.00 (s, CH_2), 28.89 (s, CH_2), 28.85 (s, CH_2), 28.82 (s, CH_2), 28.72 (s, CH_2), 28.56 (s, CH_2), 28.38 (s, CH_2^{33}), 25.41 (s, CH_2), 25.31 (s, CH_2), 24.33 (s, CH_2), 22.10 (s, CH_2), 15.69 (s, CH_3^{9}), 15.66 (s, CH_3^{9}), 13.95 (s, CH_3^{52}).

FAB – MS [*m/z*] (relative intensity): 779.4 (45%) $[M(^{81}Br) + H]^+$, 781.4 $[M(^{79}Br) + H]^+$ (40%), 673.3 (25%) $[M(^{81}Br) – C_7H_7O]^+$, 671.3 (30%) $[M(^{79}Br) – C_7H_7O]^+$, 457.0 [Fragment $A(^{81}Br)]^+$ (45%), 457.0 [Fragment $A(^{79}Br)]^+$ (40%), 443.1 [Fragment $A(^{81}Br) – O]^+$ (35%), 441.1 [Fragment $A(^{79}Br) – O]^+$ (40%), 415.1 [Fragment $A(^{81}Br) – CO_2]^+$ (10%), 413.1 [Fragment $A(^{79}Br) – CO_2]^+$ (12%), 401.0 [Fragment $B(^{81}Br)]^+$ (13%), 399.01 [Fragment $B(^{79}Br)]^+$ (12%).

HRMS – FAB [*m/z*]: $[M + H]^+$ calculated for $^{12}C_{41}{}^{1}H_{56}{}^{16}O_6{}^{14}N_4{}^{79}Br_1$, 779.3378; found, 779.3377; Δ = 0.10 mmu.

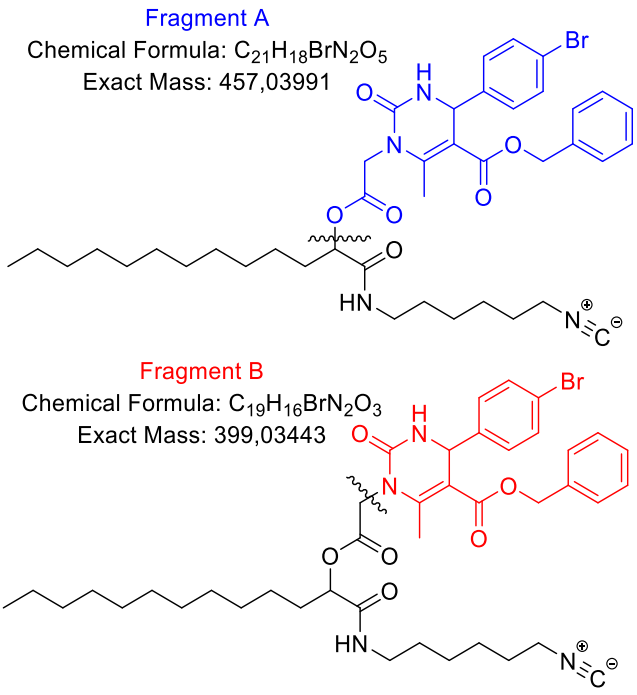

6.2.3.3.10 *Monomer-NC 92 obtained from Biginelli acid 76, 1,6-diisocyanohexane and cyclamen aldehyde*

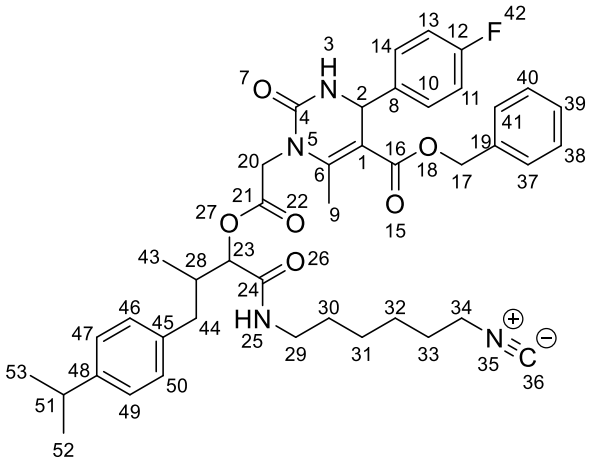

In a 250 mL round bottom flask 1,6-diisocyanohexane (4.10 g, 30.1 mmol, 4.00 eq.) was stirred in 35 mL dichloromethane, subsequently cyclamen aldehyde (4.30 g, 22.6 mmol, 3.00 eq.) was added. Finely powdered Biginelli acid **76** (3.00 g, 7.53 mmol, 1.00 eq.) was dissolved in 6 mL dimethyl sulfoxide/dichloromethane (1:2) and added dropwise to the stirring mixture. The resulting reaction mixture was stirred at room temperature for 5 d. The crude mixture was dried under reduced pressure. The residue was purified *via* column chromatography on silica gel eluting with a gradual solvent

mixture of ethyl acetate and *c*-hexane (1:1 → 1:0), dry load adsorbed on celite®. The monomer-NC **92** was obtained as a yellow oil (2.75 g, 3.80 mmol, 50.5%).

R_f = 0.32 in ethyl acetate/*c*-hexane (1:1). Visualized *via* fluorescence quench and Seebach staining solution.

IR (ATR): ν [cm^{-1}] = 3305.5 (br, ν(N-H)), 2933.8 (w, ν(C-H)), 2862.1 (w, ν(C-H)), 2146.9 (m, ν(N-C)), 1750.6 (s, ν(C=O)), 1681.8 (vs, ν(C=O)), 1539.2 (m), 1507.4 (w), 1453.8 (m), 1382.8 (w), 1309.2 (w), 1212.7 (s), 1172.1 (vs), 1097.5 (m), 1049.1 (m), 848.0 (m), 753.1 (m), 697.2 (w), 597.0 (w), 503.8 (w).

^{1}H-NMR (600 MHz, DMSO-d_6): δ [ppm] = 8.27 (ddd, J = 25.4, 24.2, 3.5 Hz, 1 H, NH^{3}), 7.96 (ddt, J = 50.1, 21.5, 5.7 Hz, 1 H, NH^{25}), 7.36 – 7.25 (m, 5 H, CH$_{Ar}$), 7.22 – 7.06 (m, 7 H, CH$_{Ar}$), 7.06 – 6.99 (m, 1 H, CH$_{Ar}$), 5.27 (d, J = 2.6 Hz, 1 H, CH^{2}), 5.14 – 5.03 (m, 2 H, CH$_2^{17}$), 4.89 – 4.79 (m, 1 H, CH^{23}), 4.78 – 4.51 (m, 2 H, CH$_2^{20}$), 3.52 – 3.48 (m, 2 H, CH$_2^{34}$), 3.47 – 3.42 (m, 2 H, CH$_2^{44}$), 3.10 (tdd, J = 16.1, 11.5, 6.2 Hz, 2 H, CH$_2^{29}$), 2.87 – 2.70 (m, 2 H, CH^{51}), 2.56 (d, J = 10.2 Hz, 2 H, CH$_3^{9a}$), 2.48 – 2.43 (m, 1 H, CH$_3^{9b}$), 2.35 – 2.18 (m, 1 H, CH^{28}), 1.66 – 1.50 (m, 4 H, CH$_2$), 1.48 – 1.21 (m, 11 H, CH$_2$), 1.24 – 1.09 (m, 10 H, CH$_2$ + CH$_3^{52,53}$), 0.81 – 0.76 (m, 3 H, CH$_3^{43}$).

^{13}C-NMR (151 MHz, DMSO-d_6): δ [ppm] = 169.06 (s, CO$_2$R^{21}), 169.04 (s, CO$_2$R^{21}), 168.99 (s, C$_q$), 168.10 (s, C$_q$), 168.02 (s, C$_q$), 167.82 (s, C$_q$), 167.79 (s, C$_q$), 165.16 (s, CO$_2$R^{16}), 165.12 (s, CO$_2$R^{16}), 161.49 (d, J = 243.3 Hz, CF$_{Ar}^{42}$), 155.52 (s, NC^{36}), 155.45 (s, NC^{36}), 152.61 (s, CO^{4}), 152.44 (s, CO^{4}), 152.20 (s, CO^{4}), 150.04 (s, CO^{4}), 149.80 (s, C^{6}), 145.90 (s, C$_{Ar}^{48}$), 140.02 (s, C$_{Ar}^{8}$), 139.84 (s, C$_{Ar}^{8}$), 137.09 (s, C$_{Ar}$), 136.93 (s, C$_{Ar}^{19}$), 136.17 (s, C$_{Ar}^{19}$), 129.14 (s, CH$_{Ar}$), 128.76 (s, CH$_{Ar}$), 128.55 (s, CH$_{Ar}$), 128.27 (s, CH$_{Ar}$), 127.82 (s, CH$_{Ar}$), 127.63 (s, CH$_{Ar}$), 126.13 (s, CH$_{Ar}$), 115.22 (s, CH$_{Ar}$), 115.18 (s, CH$_{Ar}$), 114.98 (s, CH$_{Ar}$), 102.72 (s, C^{1}), 102.61 (s, C^{1}), 77.57 (s, CH^{23}), 75.64 (s, CH^{23}), 65.33 (s, CH$_2^{17}$), 52.41 (s, CH^{2}), 52.28 (s, CH^{2}), 52.20 (s, CH^{2}), 44.51 (s, CH$_2^{20}$), 44.31 (s, CH$_2^{20}$), 44.21 (s, CH$_2^{20}$), 41.06 (s, CH$_2^{34}$), 41.02 (s, CH$_2^{34}$), 40.98 (s, CH$_2^{34}$), 38.31 (s, CH$_2^{39}$), 38.22 (s, CH$_2^{39}$), 36.93 (s, CH^{28}), 36.69 (s, CH^{28}), 32.98 (s, CH^{51}), 28.76 (s, CH$_2$), 28.71 (s, CH$_2$), 28.38 (s, CH$_2$), 28.34 (s, CH$_2$), 28.19 (s, CH$_2$), 25.40 (s, CH$_2$), 24.89 (s, CH$_2$), 23.88 (s, CH$_2$), 20.73 (s, CH$_2$), 15.89 (s, CH$_3^{9}$), 15.78 (s, CH$_3^{9}$), 15.72 (s, CH$_3^{9}$), 15.22 (s, CH$_3^{43}$), 15.11 (s, CH$_3^{43}$), 14.06 (s, CH$_3^{52,53}$), 13.99 (s, CH$_3^{43}$), 13.89 (s, CH$_3^{43}$).

FAB – MS [*m/z*] (relative intensity): 725.3 (80%) $[M + H]^+$, 629.3 (10%) $[M – C_6H_4F]^+$, 617.3 (70%) $[M – C_7H_7O]^+$, 397.1 (90%) [Fragment A]$^+$, 381.1 (100%) [Fragment A – O]$^+$, 381.1 (90%) [Fragment A – $C_2H_2O]^+$.

^{19}F-NMR (377 MHz, DMSO-d_6): δ [ppm] = -119.35 (s, CF_{Ar}[42]), -119.35 (s, CF_{Ar}[42]), -119.37 (s, CF_{Ar}[42]), -119.41 (s, CF_{Ar}[42]).

HRMS – FAB [*m/z*]: $[M + H]^+$ calculated for $^{12}C_{42}{}^{1}H_{50}{}^{16}O_6{}^{14}N_4{}^{19}F_1$, 725.3709; found, 725.3708; Δ = 0.12 mmu.

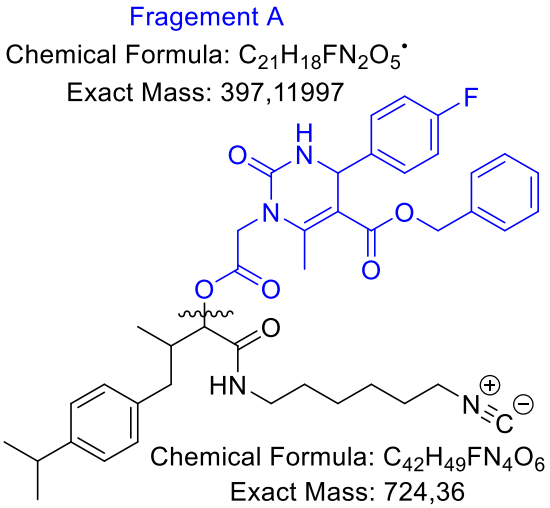

6.2.3.3.11 *Monomer-NC 93 obtained from Biginelli acid 77, 1,6-diisocyanohexane and 2-ethylbutanal*

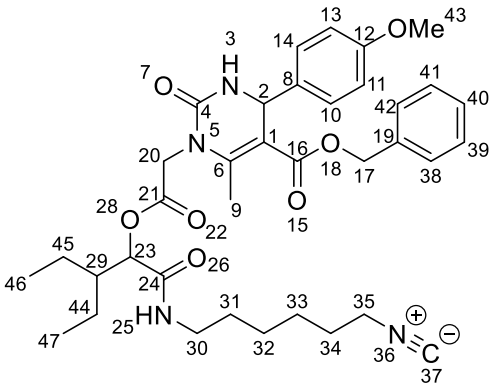

1,6-diisocyanohexane (1.99 g, 14.6 mmol, 4.00 eq.) was stirred in 10 mL dichloromethane in a 100 mL round bottom flask, subsequently 2-ethylbutanal (1.46 g, 14.6 mmol, 4.00 eq.) was added. Finely powdered Biginelli acid **77** (1.50 g, 3.65 mmol, 1.00 eq.) was dissolved in 5 mL dimethyl sulfoxide/dichloromethane (1:4) and added

dropwise to the stirring mixture. The resulting reaction mixture was degassed with argon and stirred at room temperature for 36 h. The crude mixture was dried under reduced pressure. The residue was purified *via* column chromatography on silica gel eluting with a gradual solvent mixture of ethyl acetate and *c*-hexane (0:1 → 1:0). The oily residue dried *in vacuo* to yield the monomer-NC **93** as a colorless, soft amorphous solid (1.00 g, 1.55 mmol, 42.4%).

R_f = 0.33 in *c*-hexane/ethyl acetate (1:1). Visualized *via* fluorescence quench and Seebach staining solution.

IR (ATR) ν [cm^{-1}] = 3313.54 (br, ν(N-H)), 2961.8 (w, ν(C-H)), 2935.0 (w, ν(C-H)), 2875.4 (w, ν(C-H)), 2149.3 (w, ν(NC)), 1752.4 (m, ν(C=O)), 1678.3 (s, ν(C=O)), 1536.4 (w), 1511.7 (m), 1454.1 (m), 1384.2 (m), 1306.0 (w), 1281.4 (w), 1242.3 (s), 1172.3 (vs), 1104.5 (s), 1028.4 (s), 1003.7 (w), 964.6 (w), 835.0 (w), 752.8 (m), 697.2 (m), 654.0 (w), 584.1 (w), 508.0 (w).

^{1}H-NMR (500 MHz, DMSO-d_6) δ [ppm] = 8.15 (dd, J = 42.9, 3.6 Hz, 1 H, NH^{3}), 7.92 (dt, J = 45.3, 5.6 Hz, 1 H, NH^{25}), 7.35 – 7.25 (m, 3 H, CH$_{Ar}$), 7.22 – 7.11 (m, 4 H, CH$_{Ar}$), 6.86 – 6.79 (m, 2 H, CH$_{Ar}$), 5.17 (dd, J = 6.8, 3.6 Hz, 1 H, CH^{2}), 5.11 – 5.03 (m, 2 H, CH$_2^{17}$), 4.99 (dd, J = 24.2, 3.9 Hz, 1 H, CH^{23}), 4.75 – 4.46 (m, 2 H CH$_2^{20}$), 3.72 (s, 3 H, OCH$_3^{43}$), 3.48 – 3.39 (m, 2 H, CH$_2^{35}$), 3.08 (m, 2 H, CH$_2^{30}$), 2.45 (d, J = 31.6 Hz, 3 H, CH$_3^{9}$), 1.82 – 1.63 (m, 1 H, CH^{29}), 1.54 (d, J = 2.2 Hz, 2 H, CH$_2^{34}$), 1.45 – 1.30 (m, 6 H, CH$_2$), 1.29 – 1.15 (m, 4 H, CH$_2$), 0.94 – 0.69 (m, 6 H, CH$_3^{46,47}$).

^{13}C-NMR (126 MHz, DMSO-d_6) δ [ppm] = 169.25 (s, CO$_2$R^{21}), 169.21 (s, CO$_2$R^{21}), 168.42 (s, CONR^{24}), 165.32 (s, CO$_2$Bn^{16}), 165.25 (s, CO$_2$Bn^{16}), 158.66 (s, COMe^{12}), 158.63 (s, COMe^{12}), 155.86 (t, J = 5.5 Hz, NC^{37}), 152.71 (s, C^{4}), 152.30 (s, C^{4}), 149.36 (s, C^{6}), 149.26 (s, C^{6}), 136.28 (s, C$_{Ar}^{19}$), 135.91 (s, C^{8}), 135.71 (s, C^{8}), 128.31 (s, CH$_{Ar}$), 127.86 (s, CH$_{Ar}$), 127.84 (s, CH$_{Ar}$), 127.75 (s, CH$_{Ar}$), 127.67 (s, CH$_{Ar}$), 127.65 (s, CH$_{Ar}$), 127.64 (s, CH$_{Ar}$), 113.77 (s, CH$_{Ar}$), 113.72 (s, CH$_{Ar}$), 103.22 (s, C^{1}), 103.02 (s, C^{1}), 75.14 (s, CH^{23}), 75.05 (s, CH^{23}), 65.30 (s, CH$_2^{17}$), 65.25 (s, CH$_2^{17}$), 55.10 (s, OCH$_3^{43}$), 52.46 (s, CH^{2}), 52.25 (s, CH^{2}), 44.37 (s, CH$_2^{20}$), 44.17 (s, CH$_2^{20}$), 42.51 (s, CH^{29}), 42.48 (s, CH^{29}), 41.50 (t, J = 5.8 Hz, CH$_2^{35}$), 38.26 (s, CH$_2^{30}$), 28.74 (s, CH$_2$), 28.69 (s, CH$_2$), 28.39 (s, CH$_2^{34}$), 25.43 (s, CH$_2$), 25.37 (s, CH$_2$), 21.82 (s, CH$_2$), 21.76 (s, CH$_2$), 21.45 (s, CH$_2$), 21.26 (s, CH$_2$), 15.72 (s, CH$_3^{9}$), 15.68 (s, CH$_3^{9}$), 11.39 (s, CH$_3^{46,47}$), 11.34 (s, CH$_3^{46,47}$), 11.27 (s, CH$_3^{46,47}$).

FAB-MS *m/z* (relative intensity): 647.3 (13%) $[M + H]^+$, 555.3 (3%) $[M – C_7H_7]^+$, 539.3 (15%) $[M – C_7H_7O]^+$, 409.2 (20%) [Fragment A]$^+$, 393.2 (26%) [Fragment A – O]$^+$, 351.1 (15%) [Fragment A – $C_2H_2O_2$]$^+$, 90.9 (100%) $[C_7H_7]^+$.

HRMS–FAB (*m/z*): $[M + H]^+$ calculated for $^{12}C_{36}{}^{1}H_{47}{}^{16}O_7{}^{14}N_4$, 647.3439; found, 647.3441; Δ = 0.18 mmu.

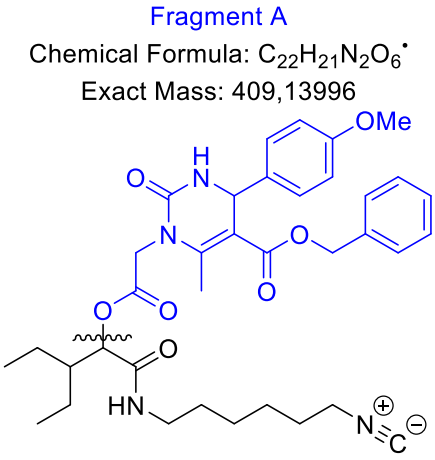

6.2.3.3.12 ***Monomer-NC 94 obtained from Biginelli acid 78, 1,6-diisocyanohexane and octanal***

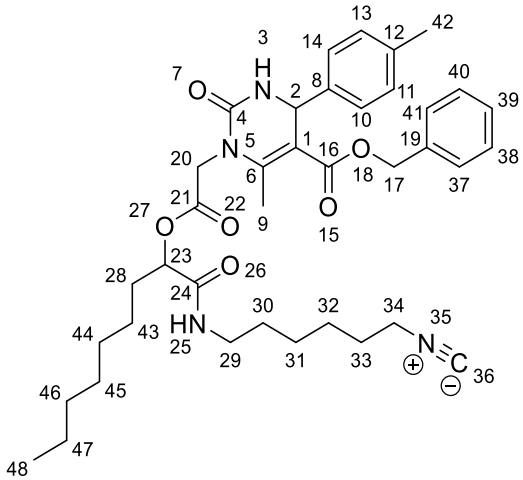

1,6-diisocyanohexane (2.07 g, 15.2 mmol, 4.00 eq.) was stirred in 10 mL dichloromethane in a 100 mL round bottom flask, subsequently octanal (1.95 g, 15.2 mmol, 4.00 eq.) was added. Finely powdered Biginelli acid **78** (1.50 g, 3.80 mmol, 1.00 eq.) was dissolved in 6 mL dimethyl sulfoxide/dichloromethane (1:2) and added dropwise to the stirring mixture. The resulting reaction mixture was degassed with argon and stirred at room temperature for 2 d. The crude mixture was dried under

reduced pressure. The residue was purified *via* column chromatography on silica gel eluting with a gradual solvent mixture of ethyl acetate and *c*-hexane (0:1 → 2:1). The oily residue dried *in vacuo* to yield the monomer-NC **94** as a yellow, viscous liquid (1.72 g, 2.61 mmol, 68.9%).

R_f = 0.36 in *c*-hexane/ethyl acetate (1:1). Visualized *via* fluorescence quench and Seebach staining solution.

IR (ATR) ν [cm^{-1}] = 3379.3 (vw), 3290.9 (br, ν(N-H)), 3093.4 (vw), 3066.7 (vw), 3029.7 (vw), 2951.5 (w, ν(C-H)), 2926.8 (m, ν(C-H)), 2856.9 (w, ν(C-H)), 2147.3 (w, ν(NC)), 1744.1 (m, ν(C=O)), 1709.2 (m, ν(C=O)), 1682.4 (vs, ν(C=O)), 1657.8 (vs, ν(C=O)), 1624.8 (m, ν(C=O)), 1544.6 (w), 1513.8 (w), 1497.3 (vw), 1454.1 (m), 1443.8 (m), 1413.0 (m), 1382.1 (m), 1306.0 (m), 1275. 2 (m), 1252.6 (m), 1205.3 (m), 1186.7 (vs), 1170.3 (vs), 1145.6 (m), 1104.5 (s), 1044.8 (m), 985.2 (w), 966.7 (w), 935.8 (w), 884.4 (vw), 855.6 (vw), 834.3 (vw), 822.7 (vw), 781.5 (w), 761.0 (m), 750.7 (m), 730.1 (m), 697.2 (m), 654.0 (w), 598.5 (vw), 582.0 (w), 561.5 (vw), 534.7 (vw), 497.7 (w), 452.5 (vw), 433.9 (vw).

^{1}H-NMR (500 MHz, DMSO-d_6) δ [ppm] = 8.13 (dd, J = 27.9, 3.6Hz, 1 H, NH^{3}), 7.93 (dt, J = 18.7, 5.7 Hz, 1 H, NH^{25}), 7.30 (dd, J = 9.4, 5.6 Hz, 3 H, CH$_{Ar}$), 7.20 – 7.03 (m, 6 H, CH$_{Ar}$), 5.18 (dd, J = 6.1, 3.8 Hz, 1 H, CH^{2}), 5.09 – 5.01 (m, 2 H, CH$_2^{17}$), 4.90 (dd, J = 10.4, 5.1 Hz, 1 H, CH^{23}), 4.81 – 4.42 (m, 2 H, CH$_2^{20}$), 3.50 – 3.38 (m, 2 H, CH$_2^{34}$), 3.12 – 2.94 (m, 2 H, CH$_2^{29}$), 2.43 (d, J = 13.4, 3 H, CH$_3^{9}$), 2.26 (s, 3 H, CH$_3^{42}$), 1.78 – 1.63 (m, 2 H, CH$_2$), 1.58 – 1.48 (d, J = 2.2 Hz, 2 H, CH$_2$), 1.47 – 1.19 (m, 16 H, CH$_2$), 0.84 (t, J = 6.8 Hz 3H, CH$_3^{48}$).

^{13}C-NMR (126 MHz, DMSO-d_6) δ [ppm] = 169.24 (s, CO$_2$R^{21}), 169.15 (s, CO$_2$R^{21}), 168.78 (s, CONR^{24}), 165.35 (s, CO$_2$Bn^{16}), 165.32 (s, CO$_2$Bn^{16}), 155.52 (t, J = 5.2 Hz, NC^{36}), 152.57 (s, C^{4}), 152.31 (s, C^{4}), 149.61 (s, C^{6}), 149.43 (s, C^{6}), 141.00 (s, C$_{Ar}^{12}$), 140.82 (s, C$_{Ar}^{12}$), 136.74 (s, C$_{Ar}^{19}$), 136.31 (C^{8}), 129.03 (s, CH$_{Ar}$), 128.98 (s, CH$_{Ar}$), 128.38 (s, CH$_{Ar}$), 127.92 (s, CH$_{Ar}$), 127.78 (s, CH$_{Ar}$), 127.76 (s, CH$_{Ar}$), 127.57 (s, CH$_{Ar}$), 126.46 (s, CH$_{Ar}$), 103.07 (s, C^{1}), 103.01 (s, C^{1}), 74.25 (s, CH^{23}), 74.18 (s, CH^{23}), 65.38 (s, CH$_2^{17}$), 52.89 (s, CH^{2}), 52.66 (s, CH^{2}), 44.24 (s, CH$_2^{20}$), 44.02 (s, CH$_2^{20}$), 41.12 (dt, J = 5.8, 2.0 Hz, CH$_2^{34}$), 38.26 (s, CH$_2^{29}$), 31.43 (s, CH$_2$), 31.37 (s, CH$_2$), 31.21 (s, CH$_2$), 28.83 (s, CH$_2$), 28.61 (s, CH$_2$), 28.46 (s, CH$_2$), 25.51 (s, CH$_2$), 25.40 (s, CH$_2$), 24.46 (s,

CH_2), 22.15 (s, CH_2), 20.85 (s, CH_3[42]), 15.74 (s, CH_3[9]), 15.61 (s, CH_3[9]), 14.02 (s, CH_3[48]).

FAB-MS *m/z* (relative intensity): 659.4 (7%) $[M + H]^+$, 393.2 (19%) [Fragment A]$^+$, 377.2 (10%) [Fragment A – O]$^+$, 335.1 (16%) [Fragment A – $C_2H_2O_2$]$^+$, 303.1 (5%) [Fragment A – C_7H_7]$^+$, 214.1 (4%) [Fragment A – 2 C_7H_7]$^+$, 91.0 (100%) $[C_7H_7]^+$.

HRMS–FAB (*m/z*): $[M + H]^+$ calculated for $^{12}C_{38}{}^{1}H_{51}{}^{16}O_6{}^{14}N_4$, 659.3803; found, 659.3805; Δ = 0.17 mmu.

Fragment A
Chemical Formula: $C_{22}H_{22}N_2O_5$
Exact Mass: 394,15

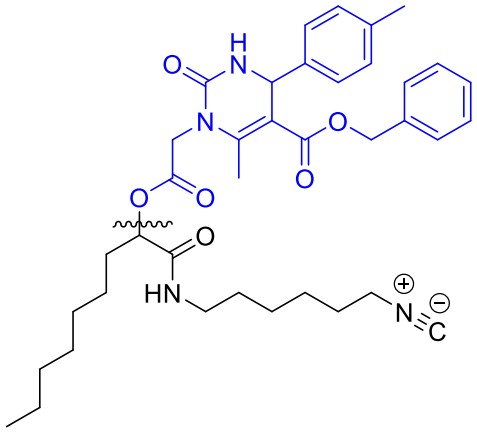

6.2.3.3.13 *Monomer-NC 95 obtained from Biginelli acid 79, 1,6-diisocyanohexane and 4-methoxy benzaldehyde*

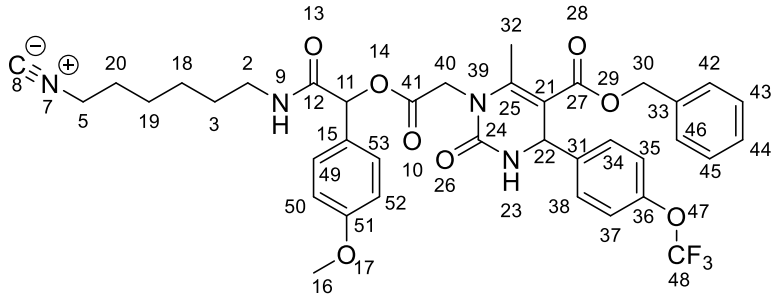

In a 50 mL round bottom flask 1,6-diisocyanohexane (1.47 g, 10.8 mmol, 5.00 eq.) was stirred in 3 mL dichloromethane, subsequently 4-methoxy benzaldehyde (586 mg, 4.31 mmol, 2.00 eq.) was added. Biginelli-acid **79** (1.00 g, 2.15 mmol, 1.00 eq.) was suspended in 2 mL dichloromethane/dimethyl sulfoxide (3:1) and added dropwise to the stirring diisocyanide aldehyde mixture. The resulting reaction mixture was stirred

at room temperature for 7 d under argon atmosphere. The crude mixture was dried under reduced pressure. The residue was adsorbed onto celite® and purified *via* column chromatography on silica gel eluting with a gradual solvent mixture of ethyl acetate and *c*-hexane (1:4 → 1:0). The Passerini product **95** was obtained as a yellow solid (685 mg, 930 µmol, 43.2%).

R_f in ethyl acetate = 0.51. Visualized *via* fluorescence quench and Seebach staining solution.

IR (ATR): ν [cm^{-1}] = 3303.8 (br, ν(N-H)), 2937.2 (w, ν(C-H)), 2148.2 (m, ν(NC)), 1736.0 (s, ν(C=O)), 1682.4 (vs, ν(C=O)), 1626.2 (s), 1540.0 (s), 1512.7 (m), 1454.5 (m), 1374.0 (w), 1305.9 (vs), 1249.6 (vs), 1210.2 (vs), 1166.3 (vs), 1105.4 (s), 1042.1 (m), 834.1 (m), 753.2 (w), 697.7 (w), 633.5 (w), 527.3 (w).

^{1}H-NMR (400 MHz, DMSO-d_6): δ [ppm] = 8.24 – 8.16 (m, 2 H, NH^{9+23}), 7.45 – 7.08 (m, 11 H, CH$_{Ar}$), 6.98 – 6.89 (m, 2 H, CH$_{Ar}$), 5.83 (d, J = 8.9 Hz, 1 H, CH^{11}), 5.25 (t, J = 3.5 Hz, 1 H, CH^{21}), 5.15 – 4.98 (m, 2 H, CH$_2^{30}$), 4.86 – 4.49 (m, 2 H, CH$_2^{40}$), 3.75 (s, 3 H, OCH$_3^{16}$), 3.39 (tt, J = 13.9, 7.4 Hz, 2 H, CH$_2^5$), 3.13 – 2.97 (m, 2 H, CH$_2^9$), 2.46 (d, J = 4.4 Hz, 3 H, CH$_3^{32}$), 1.53 – 1.42 (m, 2 H, CH$_2^{20}$), 1.41 – 1.32 (m, 2 H, CH$_2^3$), 1.32 – 1.21 (m, 2 H, CH$_2^{19}$), 1.21 – 1.10 (m, 2 H, CH$_2^{18}$).

^{13}C-NMR (101 MHz, DMSO-d_6) δ [ppm] = 169.01 (s, CO$_2$R^{41}), 168.94 (s, CO$_2$R^{41}), 167.66 (s, CONR^{12}), 167.61 (s, CONR^{12}), 165.03 (s, CO$_2$R^{30}), 159.61 (s, C$_{Ar}^{51}$), 159.56 (s, CO$_2$R^{41}), 155.46 – 155.33 (m, CN^8), 151.93 (s, CO^{26}), 151.82 (s, C^{25}), 150.00 (s, C^{25}), 147.54 (s, CF$_3^{48}$), 143.26 (s, C$_{Ar}^{31}$), 143.09 (s, C$_{Ar}^{31}$), 136.18 (s, C$_{Ar}^{33}$), 136.16 (s, C$_{Ar}^{33}$), 128.98 (s, CH$_{Ar}$), 128.87 (s, CH$_{Ar}$), 128.57 (s, CH$_{Ar}$), 128.47 (s, CH$_{Ar}$), 128.24 (s, CH$_{Ar}$), 127.87 (s, CH$_{Ar}$), 127.85 (s, CH$_{Ar}$), 127.69 (s, CH$_{Ar}$), 127.65 (s, CH$_{Ar}$), 127.43 (s, CH$_{Ar}$), 127.31 (s, CH$_{Ar}$), 121.32 (s, CH$_{Ar}$), 121.02 (s, CH$_{Ar}$), 113.81 (s, CH$_{Ar}$), 102.37 (s, C^{21}), 102.20 (s, C^{21}), 75.67 (s, CH^{11}), 75.54 (s, CH^{11}), 65.35 (s, CH$_2^{30}$), 55.16 (s, CH$_3^{16}$), 55.14 (s, CH$_3^{16}$), 52.63 (s, CH^{21}), 52.46 (s, CH^{21}), 43.97 (s, CH$_2^{40}$), 43.82 (s, CH$_2^{40}$), 41.08 – 40.85 (m, CH$_2^5$), 38.21 (s, CH$_2^2$), 28.67 (s, CH$_2^3$), 28.35 (s, CH$_2^3$), 28.32 (s, CH$_2^{20}$), 25.32 (s, CH$_2^{19}$), 25.14 (s, CH$_2^{18}$), 15.70 (s, CH$_3^{32}$), 15.67 (s, CH$_3^{32}$).

^{19}F-NMR (376 MHz, DMSO-d_6) δ [ppm] = -61.17 (s, CF$_3^{48a}$), -61.19 (s, CF$_3^{48b}$).

ESI – MS [*m/z*]: [M + Na]$^+$ calculated for ^{12}C$_{38}$^{1}H$_{39}$^{16}O$_8$^{14}N$_4$^{19}F$_3$^{23}Na$_1$, 759.2618; found, 759.2607; Δ = 0.11 mmu.

ESI – MS [*m/z*]: [2 M + Na]$^+$ calculated for $^{12}C_{76}{}^{1}H_{78}{}^{16}O_{16}{}^{14}N_8{}^{19}F_6{}^{23}Na_1$, 1495.5343; found, 1495.5348; Δ = 0.52 mmu.

6.2.3.3.14 ***Monomer-NC 96 obtained from Biginelli acid 80, 1,6-diisocyanohexane and octanal***

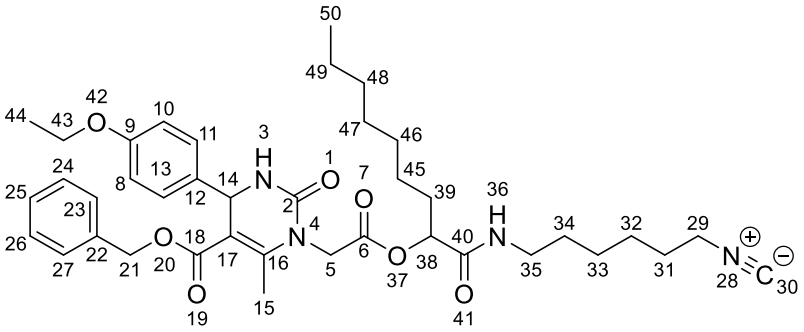

In a 250 mL round bottom flask 1,6-diisocyanohexane (2.88 g, 21.2 mmol, 3.00 eq.) was stirred in 35 mL dichloromethane, subsequently octanal (3.62 g, 28.27 mmol, 4.00 eq.) was added. Finely powdered Biginelli acid **80** (3.00 g, 7.07 mmol, 1.00 eq.) was dissolved in 8 mL dimethyl sulfoxide/dichloromethane (1:2) and added dropwise to the stirring mixture. The resulting reaction mixture was stirred at room temperature for 5 d under argon atmosphere. The crude mixture was dried under reduced pressure. The residue was adsorbed onto celite® and purified *via* column chromatography on silica gel eluting with a gradual solvent mixture of ethyl acetate/*c*-hexane (1:9 → 1:1). The monomer-NC **96** was obtained as a yellow oil (2.96 g, 4.31 mmol, 61.0%). The exceeding 1,6-diisocyanohexane could be recovered (1.04 g, 7.61 mmol, 54.0%).

R_f = 0.61 in ethyl acetate/*c*-hexane (7:3). Visualized *via* fluorescence quench and Seebach staining solution.

IR (ATR): ν [cm^{-1}] = 3306.4 (br, ν(N-H)), 2925.5 (m, ν(C-H)), 2855.4 (w, ν(C-H)), 2145.9 (w, ν(NC)), 1751.0 (w, ν(C=O)), 1677.5 (vs, ν(C=O)), 1608.9 (w), 1535.1 (w), 1508.9 (m), 1453.6 (m), 1384.0 (m), 1305.3 (w), 1240.7 (w), 1172.5 (vs), 1106.1 (s), 1045.1 (s), 923.0 (w), 862.9 (w), 751.5 (m), 696.7 (w), 652.7 (w), 583.3 (w), 509.3 (w), 449.3 (w).

^{1}H-NMR (400 MHz, DMSO-d_6): δ [ppm] = 8.11 (dd, J = 22.3, 3.4 Hz, 1 H, NH^{3}), 7.99 – 7.88 (m, 1 H, NH^{36}), 7.34 – 7.26 (m, 3 H, CH$_{Ar}$), 7.20 – 7.14 (m, 4 H, CH$_{Ar}$), 6.83 – 6.76 (m, 2 H, CH$_{Ar}$), 5.16 (t, J = 4.1 Hz, 1 H, CH^{14}), 5.10 – 5.00 (m, 2 H, CH$_2{}^{21}$), 4.90 (dd, J

= 9.8, 6.1 Hz, 1 H, CH[38]), 4.78 – 4.43 (m, 2 H, CH_2[5]), 4.01 – 3.92 (m, 2 H, CH_2[43]), 3.52 – 3.38 (m, 2 H, CH_2[29]), 3.05 (dt, *J* = 19.2, 6.6 Hz, 2 H, CH_2[35]), 2.43 (d, *J* = 10.3 Hz, 3 H, CH_3[15]), 1.78 – 1.62 (m, 2 H, CH_2[39]), 1.62 – 1.46 (m, 3 H, CH_2[31]), 1.46 – 1.09 (m, 18 H, CH_2), 0.96 – 0.77 (m, 6 H, CH_3[44+50]).

^{13}C-NMR (101 MHz, DMSO-d_6): δ [ppm] = 169.18 (s, CO_2R[6]), 169.15 (s, CO_2R[6]), 169.07 (s, C_q), 168.68 (s, CONR[40]), 168.63 (s, CONR[40]), 165.28 (s, CO_2R[21]), 165.24 (s, CO_2R[21]), 157.90 (s, C_{Ar}[9]), 155.51 (s, NC[30]), 155.47 (s, NC[30]), 155.40 (s, NC[30]), 152.43 (s, CO[2]), 152.17 (s, CO[2]), 149.32 (s, C[16]), 149.13 (s, C[16]), 136.23 (s, C_{Ar}), 135.90 (s, C_{Ar}), 135.71 (s, C_{Ar}), 128.28 (s, CH_{Ar}), 127.82 (s, CH_{Ar}), 127.70 (s, CH_{Ar}), 127.67 (s, CH_{Ar}), 127.65 (s, CH_{Ar}), 114.18 (s, CH_{Ar}[8,10]), 114.13 (s, CH_{Ar}[8,10]), 103.15 (s, C[17]), 103.08 (s, C[17]), 74.15 (s, CH[38]), 74.10 (s, CH[38]), 65.27 (s, CH_2[21]), 62.97 (s, CH[43]), 52.58 (s, CH[14]), 52.36 (s, CH[14]), 44.15 (s, CH_2[5]), 43.93 (s, CH_2[5]), 41.09 (s, CH_2[29]), 41.04 (s, CH_2[29]), 40.98 (s, CH_2[29]), 38.18 (s, CH_2[35]), 31.43 (s, CH_2), 31.35 (s, CH_2), 31.28 (s, CH_2), 31.24 (s, CH_2), 31.12 (s, CH_2), 28.90 (s, CH_2), 28.74 (s, CH_2), 28.69 (s, CH_2), 28.53 (s, CH_2), 28.38 (s, CH_2), 25.76 (s, CH_2), 25.42 (s, CH_2), 25.32 (s, CH_2), 24.54 (s, CH_2), 24.38 (s, CH_2), 22.06 (s, CH_2), 20.75 (s, CH_2), 15.66 (s, CH_3[15]), 15.63 (s, CH_3[15]), 14.64 (s, CH_3[44]), 13.92 (s, CH_3[50]).

FAB – MS [*m/z*] (relative intensity): 689.5 (45%) $[M + H]^+$, 687.5 (30%) $[M – H]^+$, 581.3 (50%) $[M – C_7H_7O]^+$.

HRMS – FAB [*m/z*]: $[M – H]^+$ calculated for $^{12}C_{39}{}^{1}H_{51}{}^{16}O_7{}^{14}N_4$, 687.3752; found, 687.3751; Δ = 0.17 mmu.

6.2.3.3.15 *Monomer-NC 97 obtained from Biginelli acid 52, 1,6-diisocyanohexane and octanal*

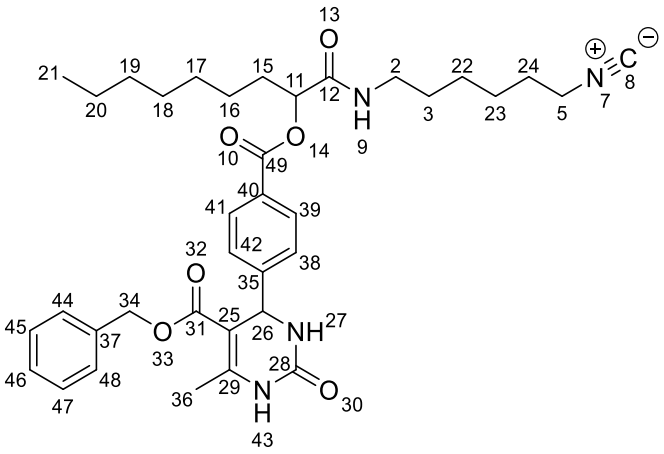

In a 50 mL round bottom flask 1,6-diisocyanohexane (1.86 g, 13.6 mmol, 5.00 eq.) was stirred in 6 mL dichloromethane under argon atmosphere, subsequently octanal (699 mg, 5.45 mmol, 2.00 eq.) was added. Finely powdered Biginelli acid **52** (1.00 g, 2.72 mmol, 1.00 eq.) was suspended in 5 mL dimethyl sulfoxide, diluted with 2 mL dichloromethane. The resulting reaction mixture was stirred at room temperature for 4 d under argon atmosphere. The crude mixture was dried under reduced pressure. The residue was adsorbed onto celite® and purified *via* column chromatography on silica gel eluting with a gradual solvent mixture of ethyl acetate and *c*-hexane (1:3 → 1:0). The monomer-NC **97** was obtained as a yellow solid (1.46 g, 2.31 mmol, 85.2%). The exceeding diisocyanide could be recovered (1.13 g, 8.30 mmol, 76.1%).

R_f in ethyl acetate/ethanol (98:2) = 0.40. Visualized *via* fluorescence quench and Seebach staining solution.

IR (ATR): ν [cm^{-1}] =3235.5 (br, ν(N-H)), 3107.1 (br, ν(N-H)), 2927.0 (w, ν(C-H)), 2857.2 (w, ν(C-H)), 2147.1 (w, ν(NC)), 1700.0 (vs, ν(C=O)), 1639.3(vs, ν(C=O)), 1609.0 (m), 1537.1 (m), 1497.4 (m), 1454.4 (m), 1379.1 (w), 1314.9 (m), 1264.9 (m), 1220.6 (m), 1178.5 (vs), 1085.0 (vs), 1017.8 (m), 949.9 (w), 912.6 (w), 860.5 (w), 824.8 (m), 754.2 (w), 697.4 (w), 655.1 (s), 583.4 (w), 526.3 (w), 496.9 (w), 444.8 (w).

^{1}H-NMR (400 MHz, DMSO-d_6): δ [ppm] = 9.36 (d, J = 2.0 Hz, 1 H, NH^{43}), 8.05 (t, J = 5.7 Hz, 1 H, NH^{9}), 7.93 (dd, J = 8.5, 2.1 Hz, 2 H, CH$_{Ar}$^{39,41}), 7.85 (t, J = 2.7 Hz, 1 H, NH^{27}), 7.36 (dd, J = 8.5, 2.3 Hz, 2 H, CH$_{Ar}$^{38,42}), 7.32 – 7.22 (m, 3 H, CH$_{Ar}$$^{44-48}$), 7.18 – 7.11 (m, 2 H, CH$_{Ar}$$^{44-48}$), 5.26 (d, J = 3.4 Hz, 1 H, CH^{26}), 5.09 – 4.96 (m, 3 H, CH$_2$^{34} +

CH[11]), 3.46 (ddt, *J* = 6.6, 3.9, 1.9 Hz, 2 H, CH_2[5]), 3.11 – 3.03 (m, 2 H, CH_2[2]), 2.28 (s, 3 H, CH_3[36]), 1.86 – 1.77 (m, 2 H, CH_2[15]), 1.63 – 1.49 (m, 2 H, CH2[24]), 1.45 – 1.20 (m, 16 H, CH_2[22-24 + 16-20]), 0.91 – 0.80 (m, 3 H, CH_3[21]).

^{13}C-NMR (101 MHz, DMSO-d_6) δ [ppm] = 169.01 (s, CO_2R^{12}), 164.92 (s, CO_2R^{31} or $CONR^{12}$), 164.88 (s, CO_2R^{31} or $CONR^{12}$), 155.50 – 155.36 (m, NC[8]), 151.76 (s, CO[28]), 149.94 (s, C[29]), 149.91 (s, C[29]), 149.84 (s, C_{Ar}[40]), 149.82 (s, C_{Ar}[40]), 136.45 (s, C_{Ar}[37]), 136.44 (s, C_{Ar}[37]), 129.78 (s, CH_{Ar}), 128.56 (s, CH_{Ar}), 128.54 (s, CH_{Ar}), 128.27 (s, CH_{Ar}), 128.25 (s, CH_{Ar}), 127.71 (s, CH_{Ar}), 127.65 (s, CH_{Ar}), 127.61 (s, CH_{Ar}), 126.63 , 98.08 (s, C[25]), 98.07 (s, C[25]), 74.02 (s, CH[11]), 64.88 (s, CH_2[34]), 53.84 (s, CH[26]), 41.15 – 40.96 (m, CH_2[5]), 38.20 (s, CH_2[15]), 31.55 (s, CH_2), 31.17 (s, CH_2), 28.79 (s, CH_2), 28.60 (s, CH_2), 28.54 (s, CH_2), 28.39 (s, CH_2), 25.43 (s, CH_2), 25.35 (s, CH_2), 24.59 (s, CH_2), 22.07 (s, CH_2), 17.91 (s, CH_2), 14.09 (s, CH_3[36]), 13.94 (s, CH_3[21]).

FAB – MS [*m/z*] (relative intensity): 631.3 (50%) $[M + H]^+$, 523.3 (30%) $[M – C_7H_7O]^+$, 349.1 (100%) [Fragment A]$^+$.

HRMS – FAB [*m/z*]: $[M + H]^+$ calculated for $^{12}C_{36}{}^{1}H_{47}{}^{16}O_6{}^{14}N_4$, 631.3490; found, 631.3493; Δ = 0.30 mmu.

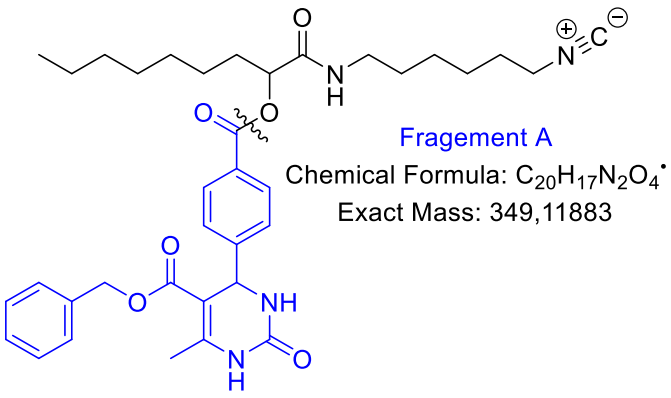

6.2.3.4 Model compounds and macromolecules

6.2.3.4.1 *Passerini compound 98 obtained from Biginelli acid 49, 1,6-diisocyanohexane and acetaldehyde*

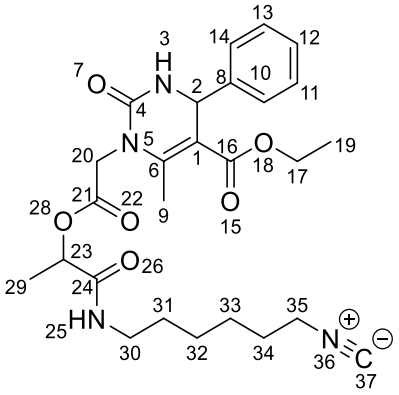

In a 100 mL round bottom flask 1,6-diisocyanohexane (2.57 g, 18.8 mmol, 3.00 eq.) was dissolved in 40 mL dichloromethane. Subsequently, acetaldehyde (1.38 g, 31.4 mmol, 5.00 eq.) was added at 0 °C. The Biginelli acid **49** (2.00 g, 6.28 mmol, 1.00 eq.) was dissolved in 10 mL dimethyl sulfoxide/dichloromethane (1:2) and added to the stirring solution dropwise at room temperature. After the complete addition, the reaction mixture was stirred for 4 days at room temperature. Subsequently the crude reaction mixture was concentrated under reduced pressure and added dropwise into a stirring emulsion of 70 mL water and 70 mL dichloromethane while stirring. The organic phase was separated, the aqueous phase was extracted with 20 mL ethyl acetate three times and the combined organic phases were dried over sodium sulfate and concentrated under reduced pressure. The oily residue was purified *via* column chromatography employing silica gel and eluting with a gradual solvent mixture of ethyl acetate and *c*-hexane (0:1 → 1:0). The Passerini product **98** was obtained as a yellow oil (1.56 g, 2.73 mmol, 43.5%).

R_f = 0.48 in ethyl acetate. Visualized *via* fluorescence quench and Seebach staining solution.

IR (ATR): ν [cm^{-1}] = 3293.0 (br, ν(N-H)), 2936.0 (br, ν(C-H)), 2860.6 (br, ν(C-H)), 2147.2 (m, ν(N-C)), 1752.6 (m, ν(C=O)), 1675.9 (vs, ν(C=O)), 1539.8 (m), 1452.6 (m), 1372.2 (s), 1308.7 (m), 1176.1 (vs), 1095.3 (s), 1056.3 (m), 938.3 (w), 830.3 (w), 761.2 (w), 698.7 (m).

^{1}H-NMR (400 MHz, DMSO-d_6): δ [ppm] = 8.14 (dd, J = 9.2, 3.4 Hz, 1 H, NH^{3}), 7.96 (dd, J = 10.1, 4.8 Hz, 1 H, NH^{27}), 7.38 – 7.18 (m, 5 H, CH$_{Ar}^{10-14}$), 5.19 (s, 1 H, CH^{2}), 5.03 – 4.93 (m, 1 H, CH^{23}), 4.72 – 4.49 (m, 2 H, CH$_2^{20}$), 4.11 – 3.94 (m, 2 H, CH$_2^{17}$), 3.51 – 3.38 (m, 2 H, CH$_2^{35}$), 3.12 – 3.00 (m, 2 H, CH$_2^{30}$), 2.41 (d, J = 3.6 Hz, 3 H, CH$_3^{9}$), 1.62 – 1.45 (m, 2 H, CH$_2^{34}$), 1.47 – 1.13 (m, 12 H, CH$_3^{29}$ + CH$_2$), 1.14 – 1.07 (m, 3 H, CH$_3^{19}$).

^{13}C-NMR (101 MHz, DMSO-d_6): δ [ppm] = 169.38 (s, CONR^{24}), 169.35 (s, CONR^{24}), 169.08 (s, CO$_2$R^{16}), 168.98 (s, CO$_2$R^{16}), 165.45 (s, CO$_2$R^{21}), 155.47 (s, NC^{37}), 155.42 (s, NC^{37}), 155.36 (s, NC^{37}), 152.37 (s, CO^{4}), 152.21 (s, CO^{4}), 148.80 (s, C^{6}), 148.48 (s, C^{6}), 144.08 (s, C$_{Ar}^{8}$), 143.95 (s, C$_{Ar}^{8}$), 128.40 (s, CH$_{Ar}^{10,14}$), 128.36 (s, CH$_{Ar}^{10,14}$), 127.45 (s, CH$_{Ar}^{12}$), 126.58 (s, CH$_{Ar}^{13,11}$), 126.44 (s, CH$_{Ar}^{13,11}$), 103.36 (s, C^{1}), 103.19 (s, C^{1}), 70.63 (s, CH^{23}), 70.61 (s, CH^{23}), 59.71 (s, CH$_2^{17}$), 53.31 (s, CH^{2}), 53.04 (s, CH^{2}), 44.04 (s, CH$_2^{20}$), 43.82 (s, CH$_2^{20}$), 41.10 (s, CH$_2^{35}$), 41.08 (s, CH$_2^{35}$), 41.05 (s, CH$_2^{35}$), 41.03 (s, CH$_2^{35}$), 40.99 (s, CH$_2^{35}$), 40.97 (s, CH$_2^{35}$), 38.22 (s, CH$_2^{30}$), 38.20 (s, CH$_2^{30}$), 28.74 (s, CH$_2$), 28.35 (s, CH$_2$), 25.42 (s, CH$_2$), 25.29 (s, CH$_2$), 20.75 (s, CH$_2$), 17.62 (s, CH$_3^{29}$), 17.59 (s, CH$_3^{29}$), 15.62 (s, CH$_3^{9}$), 15.56 (s, CH$_3^{9}$), 13.96 (s, CH$_3^{19}$), 13.94 (s, CH$_3^{19}$).

FAB – MS [m/z] (relative intensity): 499.1 (50%) [M + H]$^{+}$.

HRMS – FAB [m/z]: [M + H]$^{+}$ calculated for $^{12}C_{26}{}^{1}H_{35}{}^{16}O_{6}{}^{14}N_{4}$, 499.2551; found, 499.2552; Δ = 0.09 mmu.

6.2.3.4.2 *Compound 99 derived from Biginelli acid 50, Passerini compound 98 and heptanal*

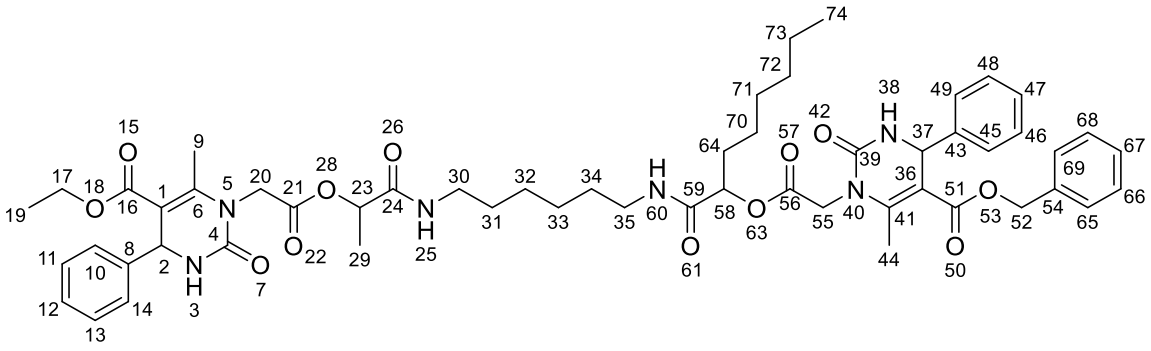

In a tube vial the Passerini compound **98** (200 mg, 401 µmol, 1.00 eq.) was suspended in 2 mL dichloromethane. Subsequently, heptanal (91.6 mg, 802 µmol, 2.00 eq.) and

the Biginelli acid **50** (229 mg, 602 µmol, 1.50 eq.) were added. Afterwards, 0.5 mL dimethyl sulfoxide were added dropwise while stirring until an orange solution was obtained. The reaction mixture was stirred at room temperature for 1 d. Subsequently, the crude reaction mixture was concentrated under reduced pressure and stirred with 30 mL water and 30 mL dichloromethane. The organic phase was separated, dried over sodium sulfate and concentrated under reduced pressure. The oily residue was purified *via* column chromatography employing silica gel and eluting with a gradual solvent mixture of ethyl acetate and *c*-hexane. The desired Passerini product **99** was obtained as a colorless solid (293 mg, 294 µmol, 73.5%).

R_f = 0.41 in ethyl acetate. Visualized *via* fluorescence quench and Seebach staining solution.

IR (ATR): ν [cm^{-1}] = 3306.5 (br, ν(N-H)), 2928.4 (br, ν(C-H)), 2857.6 (br, ν(C-H)), 1751.5 (m, ν(C=O)), 1676.8 (vs, ν(C=O)), 1537.9 (m), 1453.3 (m), 1383.6 (m), 1308.7 (w), 1172.3 (vs), 1102.9 (s), 1054.4 (m), 830.7 (w), 757.0 (w), 696.5 (s), 495.3 (w).

^{1}H-NMR (400 MHz, DMSO-d_6): δ [ppm] = 8.22 – 8.11 (m, 2 H, NH), 7.98 – 7.89 (m, 2 H, NH), 7.36 – 7.21 (m, 13 H, CH_{Ar}), 7.18 – 7.13 (m, 2 H, CH_{Ar}), 5.24 – 5.17 (m, 2 H, CH), 5.10 – 5.02 (m, 2 H, CH), 5.03 – 4.95 (m, 1 H, CH), 4.93 – 4.85 (m, 1 H, CH), 4.78 – 4.65 (m, 2 H, CH_2), 4.54 – 4.43 (m, 2 H, CH_2), 4.08 – 3.95 (m, 2 H, CH_2), 3.12 – 2.96 (m, 2 H, CH_2), 2.44 (d, *J* = 12.7 Hz, 3 H, CH_3), 2.40 (d, *J* = 5.8 Hz, 3 H, CH_3), 1.74 – 1.63 (m, 2 H, CH_2), 1.35 (m, 7 H, CH_2), 1.22 (dq, *J* = 14.3, 7.0 Hz, 14 H), 1.10 (td, *J* = 7.1, 2.2 Hz, 3 H, CH_3), 0.83 (t, *J* = 6.7 Hz, 3 H, CH_3).

^{13}C-NMR (101 MHz, DMSO-d_6): δ [ppm] = 169.32 (s, CONR^{24}), 169.28 (s, CONR^{24}), 169.10 (s, CONR^{59}), 169.03 (s, CO_2R^{16}), 168.96 (s, CO_2R^{16}), 168.62 (s, CO_2R^{55}), 165.44 (s, CO_2R^{51}), 165.22 (s, CO_2R^{21}), 165.19 (s, CO_2R^{21}), 152.42 (s, CO$^{4\ or\ 39}$), 152.37 (s, CO$^{4\ or\ 39}$), 152.20 (s, CO$^{4\ or\ 39}$), 152.17 (s, CO$^{4\ or\ 39}$), 149.69 (s, C$^{6\ or\ 41}$), 149.56 (s, C$^{6\ or\ 41}$), 148.80 (s, C$^{6\ or\ 41}$), 148.50 (s, C$^{6\ or\ 41}$), 144.06 (s, C$^{8\ or\ 43}$), 143.95 (s, C$^{8\ or\ 43}$), 143.82 (s, C$^{8\ or\ 43}$), 143.65 (s, C$^{8\ or\ 43}$), 136.18 (s, C$_{Ar}$^{54}), 128.43 (s, CH_{Ar}), 128.40 (s, CH_{Ar}), 128.38 (s, CH_{Ar}), 128.35 (s, CH_{Ar}), 128.29 (s, CH_{Ar}), 128.29 (s, CH_{Ar}), 127.83 (s, CH_{Ar}), 127.68 (s, CH_{Ar}), 127.44 (s, CH_{Ar}), 126.56 (s, CH_{Ar}), 126.44 (s, CH_{Ar}), 103.34 (s, C$^{1\ or\ 36}$), 103.19 (s, C$^{1\ or\ 36}$), 102.80 (s, C$^{1\ or\ 36}$), 102.76 (s, C$^{1\ or\ 36}$), 74.12 (s, CH^{56}), 74.04 (s, CH^{56}), 70.59 (s, CH^{23}), 65.32 (s, CH_2^{52}), 59.72 (s, CH_2^{17}), 53.29 (s, CH$^{2\ or\ 37}$), 53.13 (s, CH$^{2\ or\ 37}$), 53.04 (s, CH$^{2\ or\ 37}$), 52.91 (s, CH$^{2\ or\ 37}$), 44.15 (s, $CH_2$$^{20\ or}$

^{53}), 44.03 (s, $CH_2^{20\ or\ 53}$), 43.95 (s, $CH_2^{20\ or\ 53}$), 43.82 (s, $CH_2^{20\ or\ 53}$), 38.25 (s, $CH_2^{30,\ 35}$), 31.32 (s, CH_2^{62}), 31.30 (s, CH_2^{62}), 31.04 (s, CH_2), 28.89 (s, CH_2), 28.17 (s, CH_2), 25.87 (s, CH_2), 24.28 (s, CH_2), 21.90 (s, CH_2), 20.75 (s, CH_2), 17.64 (s, CH_3^{29}), 17.61 (s, CH_3^{29}), 15.66 (s, $CH_3^{9\ or\ 44}$), 15.63 (s, $CH_3^{9\ or\ 44}$), 15.57 (s, $CH_3^{9\ or\ 44}$), 14.08 (s, $CH_3^{19\ or\ 67}$), 13.96 (s, $CH_3^{19\ or\ 67}$), 13.94 (s, $CH_3^{19\ or\ 67}$), 13.88 (s, $CH_3^{19\ or\ 67}$).

FAB – MS [*m/z*] (relative intensity): 993.4 (100%) $[M + H]^+$.

HRMS – FAB [*m/z*]: $[M + H]^+$ calculated for $^{12}C_{54}{}^{1}H_{69}{}^{16}O_{12}{}^{14}N_6$, 993.4968; found, 993.4968; Δ = 0.01 mmu.

6.2.3.4.3 *Carboxylic acid 100 via hydrogenolytic deprotection of compound 99*

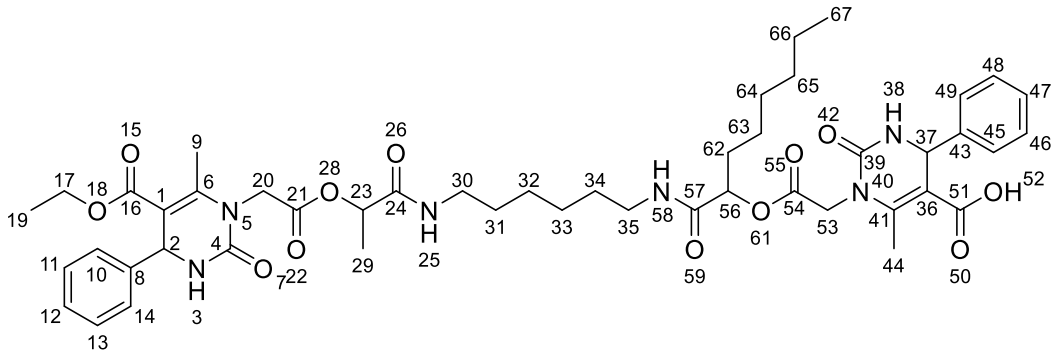

In a 25 mL round bottom flask equipped with a magnetic stir bar the benzyl ester **99** (115 mg, 116µmol, 1.00 eq.) was dissolved in 5.00 mL ethyl acetate. Subsequently, palladium on activated charcoal (10% Pd, 11.5 mg) was added to the solution. The resulting mixture was purged with argon and subsequently with hydrogen gas. The reaction was stirred for 3 d at room temperature under hydrogen atmosphere (balloon). The crude reaction mixture was filtered over celite® and flushed with 15 mL ethyl acetate/dichloromethane (1:1) three times. After evaporation of the solvents and drying under reduced pressure the acid **100** was obtained as a colorless solid (102 mg, 112 µmol, 97.0%).

IR (ATR): ν [cm^{-1}] = 3283.2 (br, ν(N-H)), 2925.5 (w, ν(C-H), 2856.2 (w, ν(C-H), 1751.9 (m, ν(C=O)), 1671.0 (vs, ν(C=O)), 1541.3 (m), 1453.5 (m), 1383.9 (s), 1308.5 (w), 1177.1 (vs), 1096.4 (m), 1056.7 (w), 939.9 (w), 832.2 (w), 759.9 (w), 697.3 (s), 622.3 (w), 464.4 (w), 386.4 (w).

^{1}H-NMR (300 MHz, DMSO-d_6): δ [ppm] = 12.25 (br s, 1 H, CO_2H^{52}), 8.18 – 8.04 (m, 2 H, $NH^{2,38}$), 7.99 – 7.86 (m, 2 H, $NH^{25, 58}$), 7.36 – 7.27 (m, 8 H, CH_{Ar}), 7.27 – 7.20 (m, 3 H, CH_{Ar}), 5.18 (dd, J = 9.1, 4.2 Hz, 2 H, $CH^{2,37}$), 4.98 (p, J = 6.7 Hz, 1 H, CH^{23}), 4.90 (dd, J = 11.8, 5.6 Hz, 1 H, CH^{56}), 4.78 – 4.40 (m, 4 H, $CH_2^{20,53}$), 4.06 – 3.96 (m, 2 H, CH_2^{17}), 3.04 (tt, J = 12.6, 6.3 Hz, 4 H, $CH_2^{30, 35}$), 2.45 – 2.38 (m, 6 H, $CH_3^{9, 44}$), 1.69 (d, J = 5.8 Hz, 3 H, CH_2^{62}), 1.35 (t, J = 8.2 Hz, 8 H, CH_2+CH_3^{29}), 1.31 – 1.14 (m, 17 H, CH_2), 1.10 (td, J = 7.1, 2.2 Hz, 3 H, CH_3^{19}), 0.89 – 0.79 (m, 3 H, CH_3^{67}).

^{13}C-NMR (101 MHz, DMSO-d_6): δ [ppm] = 169.31 (s, C_q), 169.28 (s, C_q), 169.21 (s, C_q), 169.10 (s, C_q), 169.03 (s, C_q), 168.95 (s, C_q), 168.64 (s, C_q), 167.23 (s, CO_2H^{21}), 165.44 (s, CO_2R^{16}), 152.84 (s, $CO^{4 \text{ or } 39}$), 152.54 (s, $CO^{4 \text{ or } 39}$), 152.36 (s, $CO^{4 \text{ or } 39}$), 152.20 (s, $CO^{4 \text{ or } 39}$), 148.79 (s, $C^{6 \text{ or } 41}$), 148.49 (s, $C^{6 \text{ or } 41}$), 144.03 (s, $C^{8 \text{ or } 43}$), 143.94 (s, $C^{8 \text{ or } 43}$), 143.84 (s, $C^{8 \text{ or } 43}$), 128.40 (s, CH_{Ar}), 128.38 (s, CH_{Ar}), 128.35 (s, CH_{Ar}), 128.32 (s, CH_{Ar}), 128.26 (s, CH_{Ar}), 127.44 (s, CH_{Ar}), 127.32 (s, CH_{Ar}), 127.30 (s, CH_{Ar}), 126.57 (s, CH_{Ar}), 126.54 (s, CH_{Ar}), 126.42 (s, CH_{Ar}), 126.41 (s, CH_{Ar}), 103.95 (s, $C^{1 \text{ or } 36}$), 103.34 (s, $C^{1 \text{ or } 36}$), 103.18 (s, $C^{1 \text{ or } 36}$), 74.05 (s, CH^{56}), 70.59 (s, CH^{23}), 70.55 (s, CH^{23}), 59.70 (s, CH_2^{17}), 53.29 (s, $CH^{2 \text{ or } 37}$), 53.03 (s, $CH^{2 \text{ or } 37}$), 44.13 (s, $CH_2^{20 \text{ or } 53}$), 44.04 (s, $CH_2^{20 \text{ or } 53}$), 43.91 (s, $CH_2^{20 \text{ or } 53}$), 43.82 (s, $CH_2^{20 \text{ or } 53}$), 38.27 (s, $CH_2^{30, 35}$), 31.36 (s, CH_2^{62}), 31.28 (s, CH_2^{62}), 31.05 (s, CH_2), 31.03 (s, CH_2), 28.89 (s, CH_2), 28.17 (s, CH_2), 25.88 (s, CH_2), 24.28 (s, CH_2), 21.90 (s, CH_2), 17.65 (s, CH_3^{29}), 17.61 (s, CH_3^{29}), 15.62 (s, $CH_3^{9 \text{ or } 44}$), 15.57 (s, $CH_3^{9 \text{ or } 44}$), 15.52 (s, $CH_3^{9 \text{ or } 44}$), 15.49 (s, $CH_3^{9 \text{ or } 44}$), 13.96 (s, $CH_3^{19 \text{ or } 67}$), 13.95 (s, $CH_3^{19 \text{ or } 67}$), 13.90 (s, $CH_3^{19 \text{ or } 67}$).

FAB – MS [m/z] (relative intensity): 903.4 (100%) $[M + H]^+$.

HRMS – FAB [m/z]: $[M + H]^+$ calculated for $^{12}C_{47}{}^{1}H_{63}{}^{16}O_{12}{}^{14}N_6$, 903.4498; found, 903.4501; Δ = 0.21 mmu.

6.2.3.4.4 *Symmetric dimer-CO_2Bn 101, obtained from sebacic acid, monomer-NC 90 and heptanal*

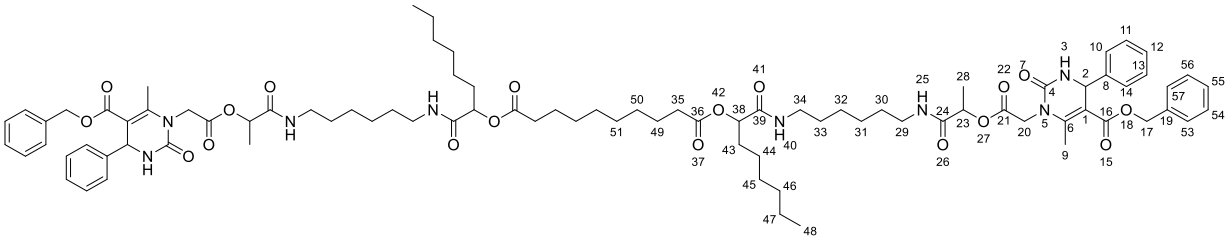

In a tube vial sebacic acid (265 mg, 1.31 mmol, 1.00 eq.) was dissolved in 4 mL dichloromethane/dimethyl sulfoxide (6:1). Subsequently, heptanal (522 mg, 4.58 mmol, 3.50 eq.) and the monomer-NC **90** (2.20 g, 3.92 mmol, 3.00 eq.) were added. The reaction mixture was stirred at room temperature for 4 d and monitored *via* GPC. Subsequently, the crude reaction mixture was concentrated under reduced pressure. The oily residue was purified *via* column chromatography employing silica gel and eluting with a gradual solvent mixture of ethyl acetate and *c*-hexane (0:1 → 1:0). The symmetric dimer **101** was obtained as a colorless solid (1.78 g, 1.15 mmol, 88.0%).

R_f = 0.50 in ethyl acetate. Visualized *via* fluorescence quench and Seebach staining solution.

IR (ATR): ν [cm^{-1}] = 3291.1 (br, ν(N-H)), 2926.4 (m, ν(C-H), 2954.6 (w, ν(C-H), 1740.4 (m, ν(C=O)), 1654.9 (vs, ν(C=O)), 1535.5 (s), 1496.0 (w), 1453.7 (m), 1382.4 (w), 1307.8 (w), 1277.0 (w), 1256.4 (w), 1171.1 (vs), 1103.7 (s), 1042.1 (m), 963.3 (w), 831.1 (w), 753.9 (w), 696.2 (s), 593.7 (w), 516.4 (w), 495.6 (w).

^{1}H-NMR (600 MHz, DMSO-d_6): δ [ppm] = 8.15 (dd, J = 18.8, 3.6 Hz, 2 H, NH^{3}), 7.93 (ddd, J = 15.8, 11.0, 5.4 Hz, 4 H, NH^{25,40}), 7.49 – 7.19 (m, 17 H, CH_{Ar}), 7.16 (dd, J = 6.4, 2.7 Hz, 4 H, CH_{Ar}), 5.22 (t, J = 4.4 Hz, 2 H, CH^{2}), 5.11 – 5.03 (m, 4 H, CH_2^{17}), 4.99 (dq, J = 13.9, 6.8 Hz, 2 H, CH^{23}), 4.82 (t, J = 5.6 Hz, 2 H, CH^{38}), 4.78 – 4.44 (m, 4 H, CH_2^{20}), 3.12 – 2.96 (m, 8 H, $CH_2^{29,34}$), 2.44 (d, J = 8.9 Hz, 6 H, CCH_3^{9}), 2.35 (t, J = 7.3 Hz, 4 H, CH_2^{35}), 1.66 (s, 4 H, CH_2^{43}), 1.51 (dd, J = 23.0, 16.1 Hz, 4 H, CH_2^{49}), 1.44 – 1.31 (m, 16 H, CH_2+CH_3^{28}), 1.32 – 1.13 (m, 38 H, CH_2), 0.85 (t, J = 6.9 Hz, 6 H, CH_3^{48}).

^{13}C-NMR (151 MHz, DMSO-d_6): δ [ppm] = 172.40 (s, CO_2R^{36}), 169.30 (s, $CONR^{24}$), 169.26 (s, $CONR^{24}$), 169.14 (s, $CONR^{39}$), 168.97 (s, CO_2R^{21}), 168.90 (s, CO_2R^{21}), 165.20 (s, CO_2R^{16}), 152.26 (s, CO^{4}), 152.11 (s, CO^{4}), 149.74 (s, C^{6}), 149.45 (s, C^{6}),

143.83 (s, C_{Ar}^{8}), 143.72 (s, C_{Ar}^{8}), 136.20 (s, C_{Ar}^{19}), 136.18 (s, C_{Ar}^{19}), 128.41 (s, CH_{Ar}), 128.37 (s, CH_{Ar}), 128.29 (s, CH_{Ar}), 127.82 (s, CH_{Ar}), 127.70 (s, CH_{Ar}), 127.68 (s, CH_{Ar}), 127.47 (s, CH_{Ar}), 126.59 (s, CH_{Ar}), 126.48 (s, CH_{Ar}), 102.83 (s, C^{1}), 102.67 (s, C^{1}), 73.07 (s. CH^{38}), 70.60 (s, CH^{23}), 70.56 (s, CH^{23}), 65.31 (s, CH_2^{17}), 53.18 (s, CH^{2}), 52.95 (s, CH^{2}), 44.06 (s, CH_2^{20}), 43.86 (s, CH_2^{20}), 38.27 (s, $CH_2^{29\ or\ 39}$), 38.25 (s, $CH_2^{29\ or\ 39}$), 38.14 (s, $CH_2^{29\ or\ 39}$), 33.42 (s, CH_2^{35}), 31.44 (s, CH_2^{43}), 31.09 (s, CH_2), 28.93 (s, CH_2), 28.58 (s, CH_2), 28.36 (s, CH_2), 28.20 (s, CH_2), 25.86 (s, CH_2), 24.48 (s, CH_2), 24.39 (s, CH_2^{49}), 21.94 (s, CH_2), 17.63 (s, CH_3^{28}), 17.60 (s, CH_3^{28}), 15.68 (s, CH_3^{9}), 15.62 (s, CH_3^{9}), 13.87 (s, CH_3^{48}).

FAB – MS [*m/z*] (relative intensity): 1551.4 (100%) $[M]^+$, 1443.5 (35%) $[M - C_7H_7O]^+$.

SEC–ESI–MS [*m/z*]: $[M + Na]^+$ calculated for $^{12}C_{86}{}^{1}H_{118}{}^{16}O_{18}{}^{14}N_8{}^{23}Na_1$, 1573.8456; found, 1573.8450; Δ = 0.60 mmu.

6.2.3.4.5 *Symmetric dimer-CO_2H 102, via hydrogenolytic deprotection of dimer-CO_2Bn 101*

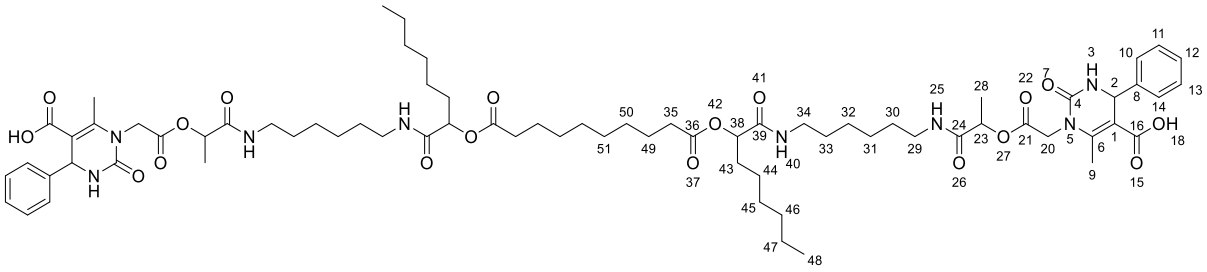

In a 25 mL round bottom flask equipped with a magnetic stir bar the symmetric dimer-CO_2Bn **101** (960 mg, 619 µmol, 1.00 eq.) was dissolved in 10.0 mL ethyl acetate. Subsequently, palladium on activated charcoal (20% Pd, 192 mg) was added to the solution. The solution was purged with argon and subsequently with hydrogen gas. The reaction was stirred at 40 °C for 5 h under hydrogen atmosphere (balloon) cooled to room temperature and 3 mL dichloromethane were added. The resulting solution was stirred for 3 d at room temperature under hydrogen atmosphere (balloon). TLC indicated complete conversion of the dimer-CO_2Bn **101**. The crude reaction mixture was filtered over celite®, and flushed with 50 mL ethyl acetate and 50 mL dichloromethane. After concentration under reduced pressure and drying in high vacuum the symmetric dimer-CO_2H **102** was obtained as a colorless solid (834 mg, 608 µmol, 98.3%).

IR (ATR): ν [cm^{-1}] = 3296.3 (br, ν(N-H)), 2927.2 (m, ν(C-H), 2854.2 (w, ν(C-H), 1741.9 (m, ν(C=O)), 1659.2 (vs, ν(C=O)), 1538.6 (s), 1454.2 (w), 1383.1 (w), 1177.4 (vs), 1095.8 (m), 1029.2 (m), 937.9 (w), 848.5 (w), 760.5 (w), 697.4 (s), 621.2 (w), 494.8 (w), 395.4 (w).

^{1}H-NMR (600 MHz, DMSO-d_6): δ [ppm] = 12.21 (s, 2 H, CO_2H^{18}), 8.02 (dd, J = 20.3, 3.5 Hz, 2 H, NH^{3}), 7.91 – 7.84 (m, 4 H, $NH^{25,40}$), 7.31 (dq, J = 9.7, 7.5 Hz, 8 H, CH_{Ar}), 7.27 – 7.21 (m, 2 H, CH_{Ar}), 5.18 (s, 2 H. CH^{2}), 4.99 (p, J = 6.9 Hz, 2 H, CH^{23}), 4.84 – 4.80 (m, 2 H, CH^{38}), 4.72 – 4.39 (m, 4 H, CH^{20}), 3.11 – 2.97 (m, 8 H, $CH_2^{29,34}$), 2.41 (d, J = 9.2 Hz, 6 H, CH^{9}), 2.34 (t, J = 7.3 Hz, 4 H, CH_2^{35}), 1.65 (t, J = 15.8 Hz, 4 H, CH_2^{43}), 1.52 (dd, J = 13.9, 6.8 Hz, 4 H, CH_2^{49}), 1.41 – 1.30 (m, 15 H, CH_2+CH_3^{28}), 1.32 – 1.20 (m, 36 H, CH_2), 0.85 (t, J = 6.9 Hz, 6 H, CH_3^{48}).

^{13}C-NMR (151 MHz, DMSO-d_6): δ [ppm] = 172.31 (s, CO_2R^{36}), 169.25 (s, $CONR^{24}$), 169.20 (s, $CONR^{24}$), 169.07 (s, $CONR^{39}$), 168.97 (s, CO_2R^{21}), 168.89 (s, CO_2R^{21}), 167.18 (s, CO_2H^{18}), 152.65 (s, CO^{4}), 152.49 (s, CO^{4}), 147.93 (s, C^{6}), 147.63 (s, C^{6}), 143.98 (s, C_{Ar}^{8}), 143.88 (s, C_{Ar}^{8}), 128.27 (s, $CH_{Ar}^{10,14}$), 128.23 (s, $CH_{Ar}^{10,14}$), 127.21 (s, CH_{Ar}^{12}), 126.50 (s, $CH_{Ar}^{11,13}$), 126.39 (s, $CH_{Ar}^{11,13}$), 104.10 (s, C^{1}), 103.98 (s, C^{1}), 73.03 (s, CH^{38}), 70.46 (s, CH^{23}), 70.42 (s, CH^{23}), 53.24 (s, CH^{2}), 53.01 (s, CH^{2}), 44.00 (s, CH_2^{20}), 43.83 (s, CH_2^{20}), 38.25 (s, $NHCH_2^{29\ or\ 34}$), 38.22 (s, $NHCH_2^{29\ or\ 34}$), 38.11 (s, $NHCH_2^{29\ or\ 34}$), 33.38 (s, CH_2^{35}), 31.38 (s, CH_2^{43}), 31.01 (s, CH_2), 28.86 (s, CH_2), 28.83 (s, CH_2), 28.49 (s, CH_2), 28.30 (s, CH_2), 28.12 (s, CH_2), 25.81 (s, CH_2), 24.40 (s, CH_2), 24.32 (s, CH_2), 21.85 (s, CH_2), 17.55 (s, CH_3^{2}), 17.52 (s, CH_3^{28}), 15.50 (s, CH_3^{9}), 15.42 (s, CH_3^{9}), 13.78 (s, CH_3^{48}).

FAB – MS [m/z] (relative intensity): 1393.4 (100%) [M – H + Na]$^+$, 1370.8 (35%) [M]$^+$, 1353.4 (20%) [M – OH]$^+$, 1285.0 (25%) [M – C_6H_{14}]$^+$, 1027.4 (25%) [A + H]$^+$, 245.1 (100%) [B]$^+$.

SEC–ESI–MS [m/z]: [M + Na]$^+$ calculated for $^{12}C_{72}{}^{1}H_{106}{}^{16}O_{18}{}^{14}N_8{}^{23}Na_1$, 1393.7517; found, 1393.7507; Δ = 0.99 mmu.

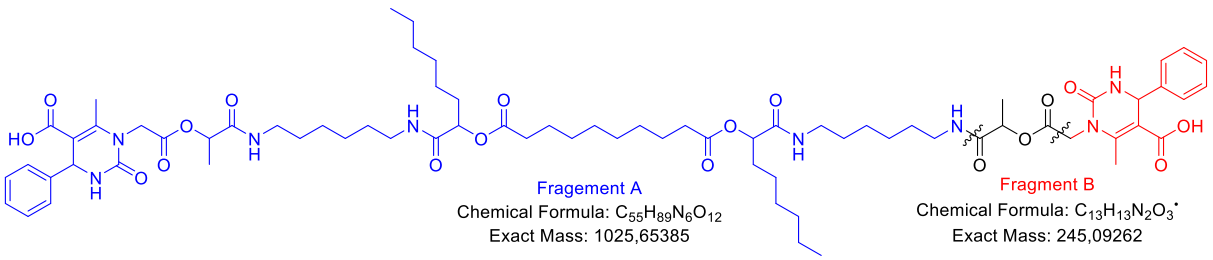

6.2.3.4.6 *Symmetric dimer-CO_2Bn 103, obtained from monomer-NC 85, sebacic acid and acetaldehyde*

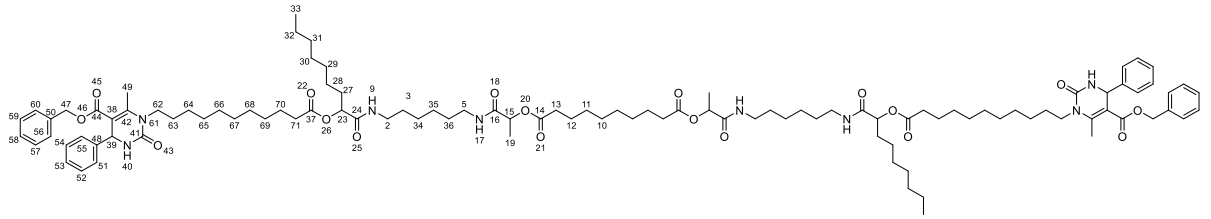

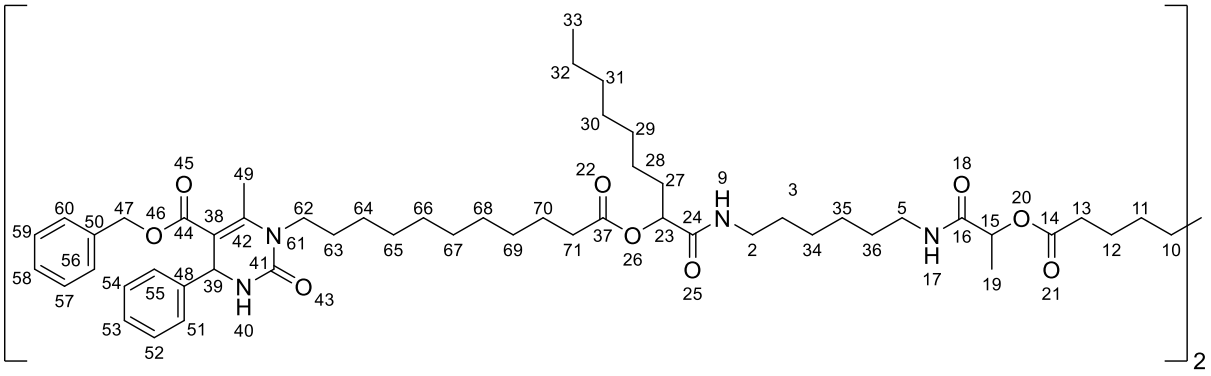

In a 50 mL round bottom flask the monomer-NC **85** (727 mg, 943 µmol, 3.00 eq.) was stirred in 4 mL dichloromethane/dimethyl sulfoxide (3:1) subsequently and degassed with argon. Subsequently, acetaldehyde (55.4 mg, 1.25 mmol, 4.00 eq.) was added at 0 °C. Finely powdered sebacic acid (63.6 mg, 1.18 mmol, 1.00 eq.) was added to the stirring isocyanide aldehyde mixture. The resulting reaction mixture was stirred at room temperature for 2 d under argon atmosphere. Additional acetaldehyde was added after 12 h (55.4 mg, 1.25 mmol, 4.00 eq.). The crude mixture was dried under reduced pressure. The residue was adsorbed onto celite® and purified *via* column chromatography on silica gel eluting with a gradual solvent mixture of ethyl acetate and *c*-hexane (0:1 → 1:1). The dimer-CO_2Bn **103** was obtained as a colorless solid (369 mg, 201 µmol, 64.1%). The exceeding monomer-NC could be recovered (242 mg, 193 µmol, 61.5%).

R_f in ethyl acetate = 0.51. Visualized *via* fluorescence quench and Seebach staining solution.

IR (ATR): ν [cm^{-1}] = 3305.4 (br, ν(N-H)), 2925.7 (m, ν(C-H)), 2854.5 (w, ν(C-H)), 1738.8 (m, ν(C=O)), 1664.4 (vs), 1618.4 (m), 1536.9 (m), 1495.9 (m), 1454.9 (m), 1387.0 (m), 1235.7 (s), 1152.3 (s), 1089.6 (s), 1045.4 (m), 831.4 (m), 755.9 (m), 696.5 (s), 513.4 (m).

^{1}H-NMR (400 MHz, DMSO-d_6): δ [ppm] = 7.94 (d, J = 3.9 Hz, 2 H, NH^{40}), 7.90 (td, J = 5.8, 3.0 Hz, 4 H, NH^{9,17}), 7.32 – 7.10 (m, 20 H, CH$_{Ar}^{51-60}$), 5.17 (d, J = 3.8 Hz, 2 H, CH^{38}), 5.12 – 5.00 (m, 4 H, CH$_2^{47}$), 4.88 (q, J = 6.8 Hz, 2 H, CH^{15}), 4.81 (t, J = 6.3 Hz, 2 H, CH^{23}), 3.92 – 3.39 (m, 4 H, CH$_2^{71}$), 3.10 - 2.81 (m, 8 H, CH$_2^{2,5}$), 2.50 (underneath DMSO signal, CH$_3^{49}$), 2.38 – 2.27 (m, 8 H, CH$_2^{13,71}$), 1.65 (d, J = 6.9 Hz, 4 H, CH$_2^{27}$), 1.58 – 1.43 (m, 10 H, CH$_2$), 1.35 (q, J = 6.8 Hz, 4 H, CH$_2$), 1.28 (d, J = 6.9 Hz, 6 H, CH$_3^{19}$), 1.26 – 1.15 (m, 70 H, CH$_2$), 0.87 – 0.80 (m, 6 H, CH$_3^{33}$).

^{13}C-NMR (101 MHz, DMSO-d_6) δ [ppm] = 172.40 (s, CO$_2$R$^{14\ or\ 37}$), 172.21 (s, CO$_2$R$^{14\ or\ 37}$), 169.74 (s, CONR^{16}), 169.12 (s, CONR^{24}), 165.34 (s, CO$_2$R^{44}), 152.60 (s, CO^{41}), 150.50 (s, C^{42}), 143.81 (s, C$_{Ar}^{48}$), 136.35 (s, C$_{Ar}^{50}$), 128.32 (s, CH$_{Ar}$), 128.28 (s, CH$_{Ar}$), 127.77 (s, CH$_{Ar}$), 127.63 (s, CH$_{Ar}$), 127.28 (s, CH$_{Ar}$), 126.05 (s, CH$_{Ar}$), 102.53 (s, C^{38}), 73.07 (s, CH^{23}), 69.52 (s, CH^{15}), 65.15 (s, CH$_2^{47}$), 52.24 (s, CH^{39}), 41.58 (s, CH$_2^{62}$), 38.13 (s, CH$_2^{2\ or\ 5}$), 38.14 (s, CH$_2^{2\ or\ 5}$), 33.43 (s, CH$_2^{13\ or\ 71}$), 33.32 (s, CH$_2^{13\ or\ 71}$), 31.44 (s, CH$_2^{27}$), 31.13 (s, CH$_2$), 29.34 (s, CH$_2$), 28.96 (s, CH$_2$), 28.85 (s, CH$_2$), 28.75 (s, CH$_2$), 28.70 (s, CH$_2$), 28.56 (s, CH$_2$), 28.54 (s, CH$_2$), 28.52 (s, CH$_2$), 28.40 (s, CH$_2$), 28.35 (s, CH$_2$), 26.18 (s, CH$_2$), 25.83 (s, CH$_2$), 24.53 (s, CH$_2$), 24.42 (s, CH$_2$), 24.28 (s, CH$_2$), 22.05 (s, CH$_2$), 17.70 (s, CH$_3^{19}$), 15.69 (s, CH$_3^{49}$), 13.91 (s, CH$_3^{33}$).

ESI–MS [m/z]: [M + Na]$^+$ calculated for ^{12}C$_{106}$^{1}H$_{158}$^{16}O$_{18}$^{14}N$_8$^{23}Na$_1$, 1854.1586; found, 1854.1629; Δ = 4.33 mmu.

6.2.3.4.7 *Symmetric dimer-CO_2H 104 via hydrogenolytic deprotection of dimer-CO_2Bn 103*

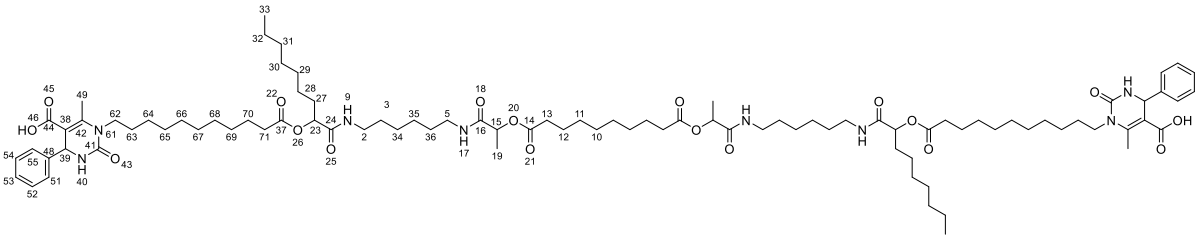

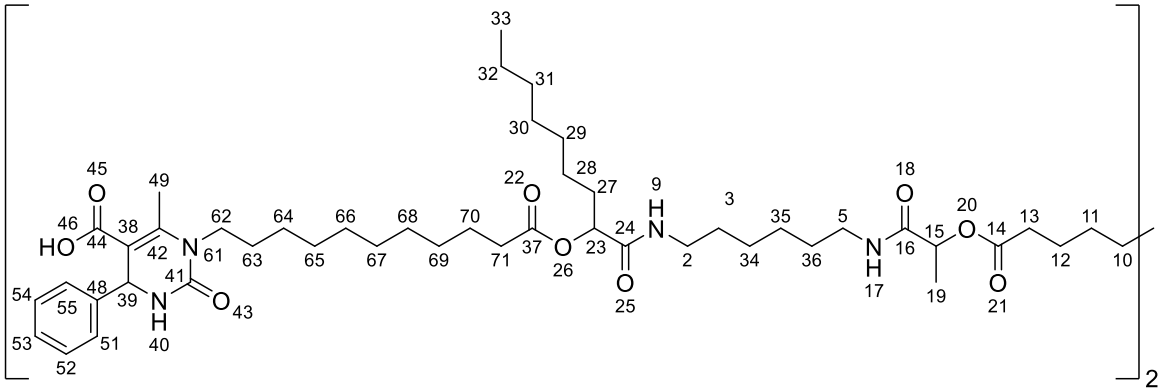

In a 5 mL round bottom flask equipped with a magnetic stir bar the benzyl ester **103** (230 mg, 123 µmol, 1.00 eq.) was dissolved in 4.00 mL tetrahydrofuran. Subsequently, palladium on activated charcoal (20% Pd, 23.0 mg) was added to the solution. The solution was purged with hydrogen gas every 30 minutes for 4 h and stirred for 3 d at 45 °C under hydrogen atmosphere (balloon). The crude reaction mixture was filtered over celite® and flushed with 20 mL tetrahydrofuran three times and with 20 mL dichloromethane twice. After concentration under reduced pressure the residue was washed with 10 mL cold diethyl ether/ethyl acetate (4:1) three times. The solid was dried in high vacuum, yielding the carboxylic acid **104** as a colorless solid (204 mg, 123 µmol, 98.5%).

IR (ATR): ν [cm^{-1}] = 3293.7 (br, ν(N-H)), 2925.6 (s, ν(C-H)), 2854.1 (m, ν(C-H)), 1738.8 (m, ν(C=O)), 1660.2 (vs, ν(C=O)), 1538.4 (s), 1455.0 (m), 1385.9 (m), 1165.2 (m), 1091.8 (s), 759.8 (m), 697.0 (w), 613.3 (w), 500.3 (w).

^{1}H-NMR (400 MHz, DMSO-d_6): δ [ppm] = 12.11 (s, 2 H, CO_2H^{46}), 7.94 – 7.80 (m, 6 H, 7.89 (td, J = 5.8, 3.0 Hz, 4 H, $NH^{9,17}$), 7.84 (d, J = 3.8 Hz, 2 H, NH^{40}), 7.36 – 7.26 (m, 5 H, CH_{Ar}^{51-55}), 7.26 – 7.15 (m, 5 H, CH_{Ar}^{51-55}), 5.13 (d, J = 3.8 Hz, 2 H, CH^{39}), 4.88 (q, J = 6.8 Hz, 2 H, CH^{15}), 4.81 (t, J = 6.3 Hz, 2 H, CH^{23}), 3.84 (ddd, J = 14.6, 8.6, 6.3 Hz, 2H), 3.92 – 3.35 (m, 4 H, CH_2^{62}), 3.13 – 2.91 (m, 8 H, CH_2^{2+5}), 2.47 (s, 6 H, CH_3^{49}),

2.39 – 2.28 (m, 8 H, CH_2^{13+71}), 1.65 (d, *J* = 7.3 Hz, 4 H, CH_2^{27}), 1.51 (q, *J* = 6.7 Hz, 8 H, CH_2^{12+70}), 1.36 (t, *J* = 6.9 Hz, 8 H, $CH_2^{3,36}$), 1.28 (d, *J* = 6.9 Hz, 6 H, CH_3^{19}), 1.27 – 1.03 (m, 56 H, CH_2), 0.90 – 0.76 (m, 6 H, CH_3^{33}).

^{13}C-NMR (101 MHz, DMSO-d_6) δ [ppm] = 172.40 (s, $CO_2R^{14\ or\ 37}$), 172.21 (s, $CO_2R^{14\ or\ 37}$), 169.74 (s, $CONR^{24}$), 169.13 (s, $CONR^{16}$), 167.89 (s, CO_2H^{44}), 153.01 (s, CO^{41}), 144.01 (s, C_{Ar}^{48}), 128.24 (s, CH_{Ar}), 127.11 (s, CH_{Ar}), 126.02 (s, CH_{Ar}), 103.80 (s, C^{38}), 73.07 (s, CH^{23}), 69.52 (s, CH^{15}), 52.33 (s, CH^{39}), 41.40 (s, CH_2^{62}), 38.12 (s, $CH_2^{2\ or\ 5}$), 38.11 (s, $CH_2^{2\ or\ 5}$), 33.43 (s, $CH_2^{13\ or\ 71}$), 33.32 (s, $CH_2^{13\ or\ 71}$), 31.44 (s, CH_2^{27}), 31.13 (s, CH_2), 29.44 (s, CH_2), 28.96 (s, CH_2), 28.86 (s, CH_2), 28.78 (s, CH_2), 28.71 (s, CH_2), 28.55 (s, CH_2), 28.54 (s, CH_2), 28.51 (s, CH_2), 28.40 (s, CH_2), 28.35 (s, CH_2), 26.19 (s, CH_2), 25.83 (s, CH_2), 24.52 (s, CH_2), 24.42 (s, CH_2), 24.28 (s, CH_2), 22.05 (s, CH_2), 17.70 (s, CH_3^{19}), 15.55 (s, CH_3^{49}), 13.92 (s, CH_3^{33}).

ESI–MS [*m/z*]: $[M + Na]^+$ calculated for $^{12}C_{92}{}^{1}H_{146}{}^{16}O_{18}{}^{14}N_8{}^{23}Na_1$, 1674.0647; found, 1674.0686; Δ = 3.87 mmu.

6.2.3.4.8 ***Symmetric tetramer-CO_2Bn 105, obtained from dimer-CO_2H 102, monomer-NC 93 and lauric aldehyde***

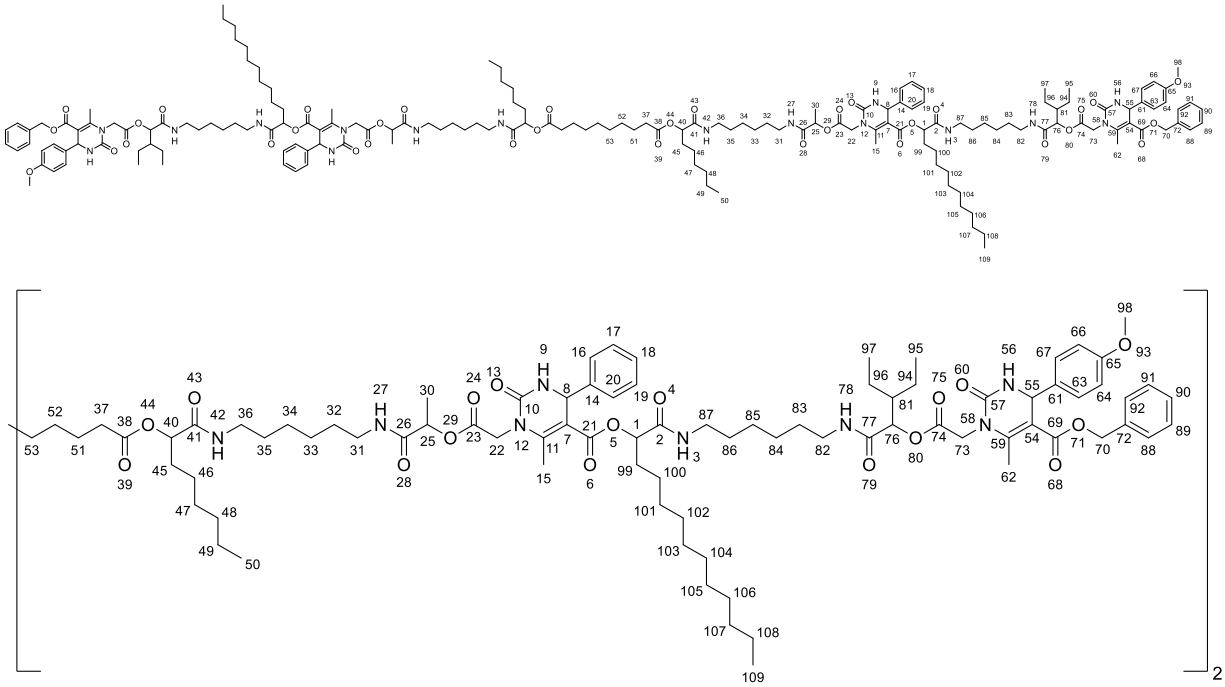

In a tube vial the symmetric dimer-CO_2H **102** (200 mg, 146 µmol, 1.00 eq.) was dissolved in 5 mL dichloromethane. Subsequently, the aldehyde (49.1 mg, 437 µmol,

3.00 eq.) and the monomer-NC **93** (283 mg, 437 µmol, 3.00 eq.) dissolved in 5 mL dichloromethane were added. The mixture was concentrated under reduced pressure down to a volume of 2 mL. The reaction mixture was stirred at room temperature for 3 d. Subsequently, the crude reaction mixture was concentrated under reduced pressure. The oily residue was purified *via* column chromatography (dry loading, adsorbed onto celite®) employing silica gel as stationary phase and eluting with a gradual solvent mixture of ethyl acetate and *c*-hexane (1:2 → 1:0) for the elution of the monomer-NC **93**. The exceeding monomer-NC **93** was almost fully recovered (92.3 mg, 501 µmol, 97.5%). The desired tetramer-CO_2Bn **105** was eluted with ethyl acetate/ethanol (9:1). After concentration under reduced pressure and drying in high vacuum the symmetric tetramer-CO_2Bn **105** was obtained as a colorless solid (397 mg, 131 µmol, 89.7%).

R_f in ethyl acetate/ethanol (9:1) = 0.77. Visualized *via* fluorescence quench and Seebach staining solution.

IR (ATR): ν [cm^{-1}] = 3303.5 (br, ν(N-H)), 2926.0 (m, ν(C-H), 2855.2 (w, ν(C-H), 1748.0 (m, ν(C=O)), 1659.5 (vs, ν(C=O)), 1536.5 (s), 1511.5 (m), 1454.8 (w), 1384.5 (w), 1306.2 (m), 1244.4 (m), 1172.1 (vs), 1103.8 (s), 1039.0 (s), 939.4 (w), 830.5 (w), 754.9 (w), 697.6 (m), 656.6 (w), 584.5 (w), 505.3 (w).

^{1}H-NMR (400 MHz, DMSO-d_6): δ [ppm] = 8.23 – 8.08 (m, 4 H, NH[9,56]), 7.99 – 7.84 (m, 8 H, NH[3,27,42,78]), 7.40 – 7.11 (m, 24 H, CH_{Ar}), 6.82 (dd, J = 8.7, 3.8 Hz, 4 H. CH_{Ar}[64,66]), 5.34 – 5.21 (m, 2 H, CH[8]), 5.19 – 5.14 (m, 2 H, CH[55]), 5.11 – 5.03 (m, 2 H, CH_2[70]), 5.03 – 4.95 (m, 4 H, CH[25,76]), 4.88 – 4.78 (m, 4 H, CH[1,40]), 4.78 – 4.41 (m, 8 H, CH_2[22,73]), 3.72 (s, 6 H, OCH_3[98]), 3.15 – 2.82 (m, 16 H, CH_2[31,36,82,87]), 2.49 – 2.41 (m, 12 H, CH_3[15,63]), 2.34 (t, J = 7.2 Hz, 4 H, CH_2[37]), 1.76 – 1.61 (m, 10 H, CH_2[45,99]+CH[81]), 1.56 – 1.44 (m, 4 H, CH_2[51]), 1.41 – 1.31 (m, 29 H, CH_2+CH_3[30]), 1.29 – 1.13 (m, 82 H, CH_2), 1.03 – 0.94 (m, 6 H, CH_2), 0.93 – 0.68 (m, 24 H, CH_3[50,95,97,109]).

^{13}C-NMR (101 MHz, DMSO-d_6): δ [ppm] = 172.36 (s, CO_2R[36]), 169.30 (s, C_q), 169.26 (s, C_q), 169.17 (s, C_q), 169.13 (s, C_q), 169.01 (s, C_q), 168.94 (s, C_q), 168.90 (s, C_q), 168.33 (s, CONR[77]),165.28 (s, CO_2Bn[69]), 165.21 (s, CO_2Bn[69]), 164.87 (s, CO_2R[21]), 164.85 (s, CO_2R[21]), 164.75 (s, CO_2R[21]), 158.64 (s, C_{Ar}[65]), 158.61 (s, C_{Ar}[65]), 152.68 (s, CO[10or57]), 152.43 (s, CO[10or57]), 152.27 (s, CO[10or57]), 152.11 (s, CO[10or57]), 151.97 (s, CO[10or57]), 150.55 (s, C_q), 150.30 (s, C_q), 149.34 (s, C[59]), 149.23 (s, C[59]), 144.08 (s,

C_{Ar}^{14}), 143.96 (s, C_{Ar}^{14}), 143.73 (s, C_{Ar}), 143.64 (s, C_{Ar}), 136.26 (s, C_{Ar}^{72}), 136.24 (s, C_{Ar}^{72}), 135.93 (s, C_{Ar}^{61}), 135.68 (s, C_{Ar}^{61}), 128.46 (s, CH_{Ar}), 128.42 (s CH_{Ar}), 128.26 (s, $CH_{Ar}^{16,20}$), 127.80 (s, CH_{Ar}), 127.78 (s, CH_{Ar}), 127.71 (s, CH_{Ar}), 127.64 (s, CH_{Ar}), 127.61 (s, CH_{Ar}), 127.60 (s, CH_{Ar}), 126.73 (s, CH_{Ar}), 126.63 (s, CH_{Ar}), 126.51 (s, $CH_{Ar}^{17,19}$), 126.40 (s, $CH_{Ar}^{17,19}$), 113.73 (s, $CH_{Ar}^{64,66}$), 113.68 (s, $CH_{Ar}^{64,66}$), 103.21 (s, C^{54}), 103.00 (s, C^{54}), 102.35 (s, C^{7}), 102.20 (s, C^{7}), 75.10 (s, CH^{76}), 74.99 (s, CH^{76}), 73.29 (s, CH^{1+40}), 73.06 (s, CH^{1+40}), 70.57 (s, CH^{25}), 65.26 (s, CH_2^{70}), 65.20 (s, CH_2^{70}), 55.06 (s, OCH_3^{98}), 53.08 (s, CH_8), 52.89 (s, CH_8), 52.45 (s, CH^{55}), 52.25 (s, CH^{55}), 44.33 (s, CH_2^{22or73}), 44.16 (s, CH_2^{22or73}), 44.01 (s, CH_2^{22or73}), 42.54 (s, CH^{81}), 38.31 (s, $CH_2^{31,36,82,87}$), 38.28 (s, $CH_2^{31,36,82,87}$), 38.18 (s, $CH_2^{31,36,82,87}$), 38.15 (s, $CH_2^{31,36,82,87}$), 33.42 (s, CH_2^{37}), 31.57 (s, CH_2), 31.45 (s, CH_2), 31.31 (s, CH_2), 31.10 (s, CH_2), 29.01 (s, CH_2), 28.98 (s, CH_2), 28.94 (s, CH_2), 28.89 (s, CH_2), 28.85 (s, CH_2), 28.72 (s, CH_2), 28.60 (s, CH_2), 28.38 (s, CH_2), 28.22 (s, CH_2), 25.87 (s, CH_2), 24.49 (s, CH_2), 24.39 (s, CH_2), 22.10 (s, CH_2), 21.95 (s, CH_2), 21.81 (s, CH_2), 21.77 (s, CH_2), 21.44 (s, CH_2), 21.26 (s, CH_2), 17.63 (s, CH_3^{30}), 17.60 (s, CH_3^{30}), 15.90 (s, CH_3^{15or62}), 15.80 (s, CH_3^{15or62}), 15.69 (s, CH_3^{62}), 15.65 (s, CH_3^{62}), 15.47 (s, CH_3^{15}), 15.42 (s, CH_3^{15}), 13.93 (s, $CH_3^{50,109}$), 13.86 (s, $CH_3^{50,109}$), 11.36 (s, $CH_3^{95,97}$), 11.31 (s, $CH_3^{95,97}$), 11.25 (s, $CH_3^{95,97}$).

SEC–ESI–MS [*m/z*]: $[M + Na]^+$ calculated for $^{12}C_{168}{}^{1}H_{246}{}^{16}O_{34}{}^{14}N_{16}{}^{23}Na_1$, 3054.7905; found, 3054.8069; Δ = 16.4 mmu.

6.2.3.4.9 *Symmetric tetramer-CO_2H 106, via hydrogenolytic deprotection of tetramer-CO_2Bn 105*

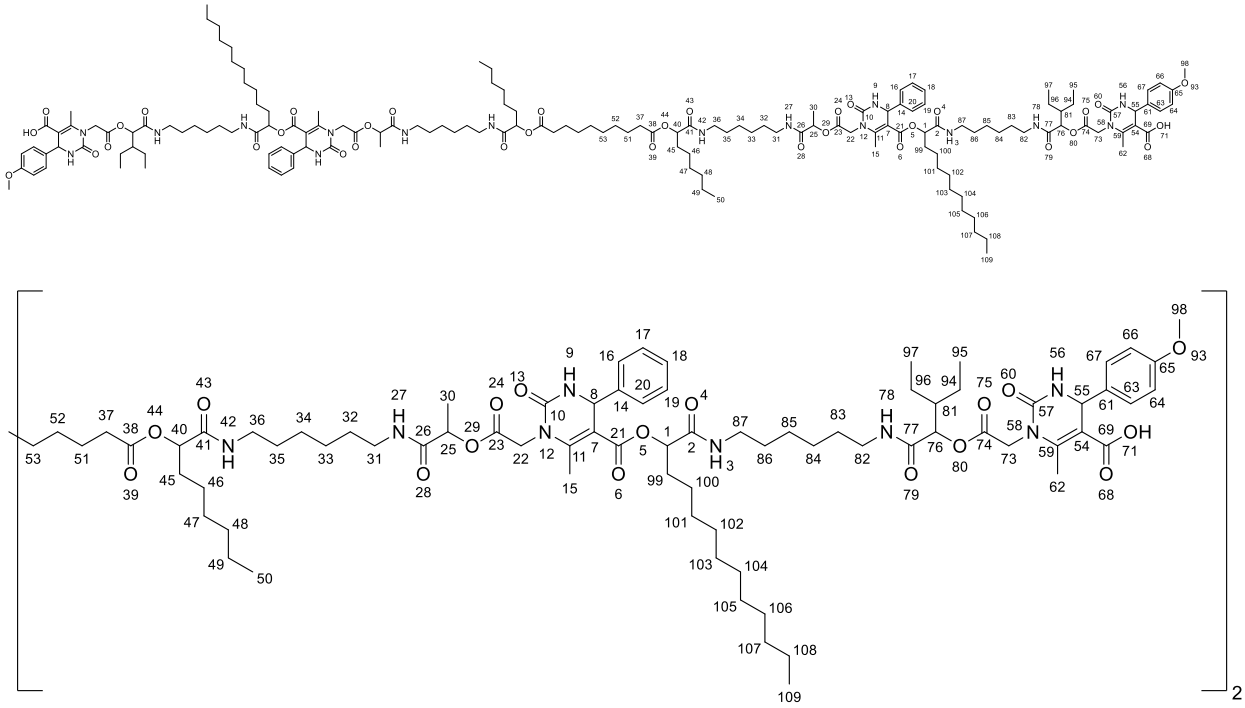

In a 5 mL round bottom flask equipped with a magnetic stir bar the symmetric tetramer-benzyl ester **105** (150 mg, 4.94 µmol, 1.00 eq.) was dissolved in 3.00 mL ethyl acetate/dichloromethane (1:1). Subsequently, palladium on activated charcoal (20 wt.%, 20.0 mg) was added to the solution. The solution was purged with argon for 3 minutes and subsequently with hydrogen gas for 10 minutes. The reaction was stirred for 4 d at room temperature under hydrogen atmosphere (balloon). TLC indicated complete conversion of the tetramer-CO_2Bn **105** (R_f in ethyl acetate/ethanol (9:1) = 0.77). The crude reaction mixture was filtered over celite® and flushed with 50 mL dichloromethane three times and subsequently with 20 mL ethyl acetate. After concentration under reduced pressure and drying in high vacuum the symmetric tetramer-CO_2H **106** was obtained as a colorless solid (131 mg, 46.0 µmol, 93.4%).

IR (ATR): ν [cm^{-1}] = 3306.1 (br, ν(N-H)), 2925.8 (m, ν(C-H), 2854.2 (w, ν(C-H), 1745.1 (m, ν(C=O)), 1652.0 (vs, ν(C=O)), 1538.2 (s), 1511.7 (m), 1455.0 (w), 1377.8 (w), 1246.9 (m), 1172.9 (vs), 1104.7 (s), 1031.7 (s), 831.5 (w), 758.6 (w), 698.7 (m), 632.2 (w), 427.3 (w).

^{1}H-NMR (500 MHz, DMSO-d_6): δ [ppm] = 12.21 (br s, 1 H, CO_2H^{71}), 8.23 – 8.08 (m, 4 H, $NH^{9,56}$), 8.01 – 7.84 (m, 8 H, $NH^{3,27,42,78}$), 7.41 – 7.15 (m, 14 H, CH_{Ar}), 6.85 (dd, J =

8.5, 4.9 Hz, 4 H, CH_{Ar}[64,66]), 5.36 – 5.21 (m, 2 H, CH[8]), 5.13 (dd, *J* = 8.3, 3.4 Hz, 2 H, CH[55]), 5.03 – 4.94 (m, 4 H, CH[25,76]), 4.87 – 4.79 (m, 4 H, CH[1,40]), 4.77 – 4.38 (m, 8 H, CH_2[22,73]), 3.71 (s, 6 H, OCH_3[98]), 3.09 – 2.86 (m, 16 H, CH[31,36,82,87]), 2.47 – 2.38 (m, 12 H, CH_3[15,63]), 2.34 (t, *J* = 7.3 Hz, 4 H, CH_2[37]), 1.80 – 1.62 (m, 10 H, CH_2[45,99]+CH[81]), 1.56 – 1.46 (m, 4 H, CH_2[51]), 1.40 – 1.32 (m, 29 H, CH_2+CH_3[30]), 1.30 – 1.09 (m, 82 H, CH_2), 1.07 – 0.94 (m, 6 H, CH_2), 0.89 – 0.68 (m, 24 H, CH_3[50,95,97,109]).

^{13}C-NMR (101 MHz, DMSO-*d*$_6$): *δ* [ppm] = 172.36 (s, CO_2R[38]), 169.30 (s, C_q), 169.26 (s, C_q), 169.17 (s, C_q), 169.13 (s, C_q), 169.01 (s, C_q), 168.94 (s, C_q), 168.90 (s, C_q), 168.33 (s, CONR[77]),165.28 (s, CO_2Bn[69]), 165.21 (s, CO_2Bn[69]), 164.87 (s, CO_2R[21]), 164.85 (s, CO_2R[21]), 164.75 (s, CO_2R[21]), 158.64 (s, $C_{Ar}OMe$[65]), 158.61 (s, $C_{Ar}OMe$[65]), 152.68 (s, CO[10or57]), 152.43 (s, CO[10or57]), 152.27 (s, CO[10or57]), 152.11 (s, CO[10or57]), 151.97 (s, CO[10or57]), 150.55 (s, C[11]), 150.30 (s, C[11]), 149.34 (s, C[59]), 149.23 (s, C[59]), 144.08 (s, C_{Ar}[14]), 143.96 (s, C_{Ar}[14]), 143.73 (s, C_{Ar}), 143.64 (s, C_{Ar}), 136.26 (s, C_{Ar}[72]), 136.24 (s, C_{Ar}[72]), 135.93 (s, C_{Ar}[61]), 135.68 (s, C_{Ar}[61]), 128.46 (s, CH_{Ar}), 128.42 (s CH_{Ar}), 128.26 (s, CH_{Ar}[16,20]), 127.80 (s, CH_{Ar}), 127.78 (s, CH_{Ar}), 127.71 (s, CH_{Ar}), 127.64 (s, CH_{Ar}), 127.61 (s, CH_{Ar}), 127.60 (s, CH_{Ar}), 126.73 (s, CH_{Ar}), 126.63 (s, CH_{Ar}), 126.51 (s, CH_{Ar}[17,19]), 126.40 (s, CH_{Ar}[17,19]), 113.73 (s, CH_{Ar}[64,66]), 113.68 (s, CH_{Ar}[64,66]), 103.21 (s, C[54]), 103.00 (s, C[54]), 102.35 (s, C[7]), 102.20 (s, C[7]), 75.10 (s, CH[76]), 74.99 (s, CH[76]), 73.29 (s, CH[1+40]), 73.06 (s, CH[1+40]), 70.57 (s, CH[25]), 65.26 (s, CH_2[70]), 65.20 (s, CH_2[70]), 55.06 (s, OCH_3[98]), 53.08 (s, CH[8]), 52.89 (s, CH[8]), 52.45 (s, CH[55]), 52.25 (s, CH[55]), 44.33 (s, CH_2[22or73]), 44.16 (s, CH_2[22or73]), 44.01 (s, CH_2[22or73]), 42.54 (s, CH[81]), 38.31 (s, CH_2[31,36,82,87]), 38.28 (s, CH_2[31,36,82,87]), 38.18 (s, CH_2[31,36,82,87]), 38.15 (s, CH_2[31,36,82,87]), 33.42 (s, CH_2[37]), 31.57 (s, CH_2), 31.45 (s, CH_2), 31.31 (s, CH_2), 31.10 (s, CH_2), 29.01 (s, CH_2), 28.98 (s, CH_2), 28.94 (s, CH_2), 28.89 (s, CH_2), 28.85 (s, CH_2), 28.72 (s, CH_2), 28.60 (s, CH_2), 28.38 (s, CH_2), 28.22 (s, CH_2), 25.87 (s, CH_2), 24.49 (s, CH_2), 24.39 (s, CH_2), 22.10 (s, CH_2), 21.95 (s, CH_2), 21.81 (s, CH_2), 21.77 (s, CH_2), 21.44 (s, CH_2), 21.26 (s, CH_2), 17.63 (s, CH_3[30]), 17.60 (s, CH_3[30]), 15.90 (s, CH_3[15or62]), 15.80 (s, CH_3[15or62]), 15.69 (s, CH_3[62]), 15.65 (s, CH_3[62]), 15.47 (s, CH_3[15]), 15.42 (s, CH_3[15]), 13.93 (s, CH_3[50,109]), 13.86 (s, CH_3[50,109]), 11.36 (s, CH_3[95,97]), 11.31 (s, CH_3[95,97]), 11.25 (s, CH_3[95,97]).

ESI–MS [*m/z*]: $[M + 2 Na]^{2+}$ calculated for $^{12}C_{154}{}^{1}H_{234}{}^{16}O_{34}{}^{14}N_{16}{}^{23}Na_2$, 1448.8429; found, 1448.8455.; Δ = 2.60 mmu.

6.2.3.4.10 *Symmetric tetramer-CO_2Bn 107, obtained from the symmetric dimer-CO_2H 102, monomer-NC 91 and cyclohexane carbaldehyde*

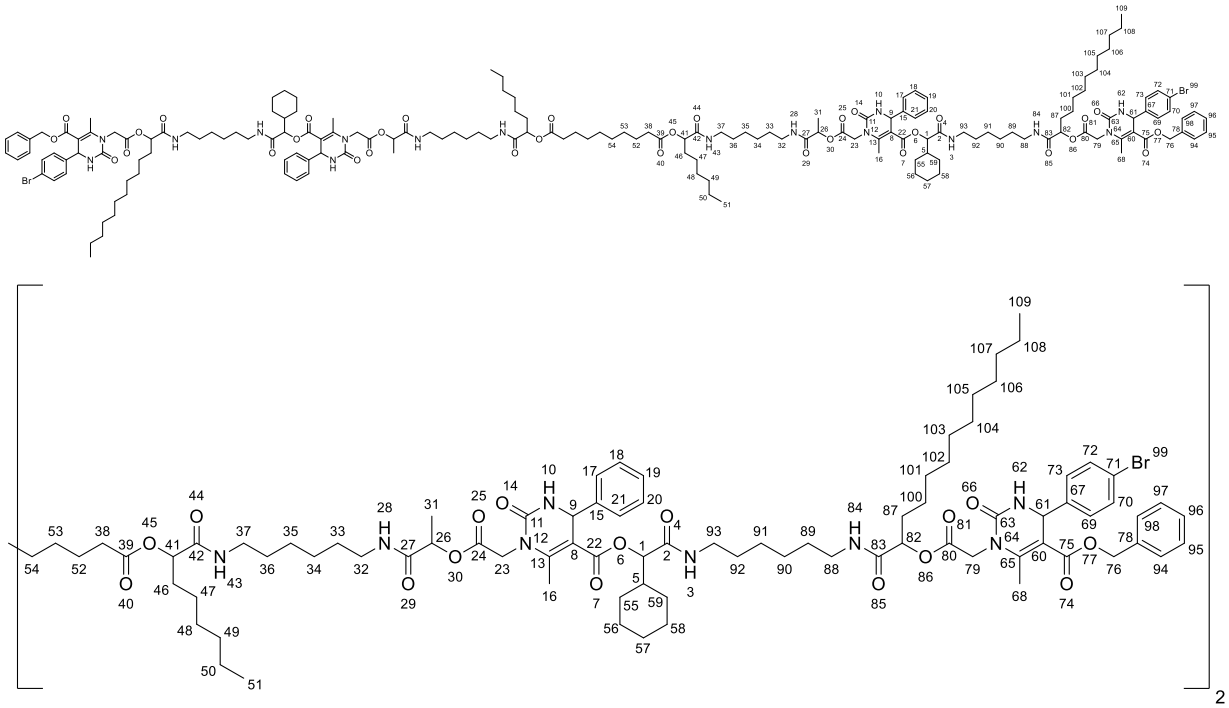

In a tube vial the symmetric dimer-CO_2H **102** (160 mg, 119 µmol, 1.00 eq.) was dissolved in 5 mL dichloromethane. Subsequently, the aldehyde (46.7 mg, 419 µmol, 3.50 eq.) and the monomer-NC **91** (278 mg, 356 µmol, 3.00 eq.) dissolved in 5 mL dichloromethane were added. The mixture was concentrated under reduced pressure down to a volume of 2 mL. The reaction mixture was stirred at room temperature for 4 d. Subsequently, the crude reaction mixture was concentrated under reduced pressure. The oily residue was purified *via* column chromatography (dry loading, adsorbed onto celite®) employing silica gel as stationary phase and eluting with a gradual solvent mixture of ethyl acetate and *c*-hexane (1:3 → 1:0). The symmetric tetramer-CO_2Bn **107** was obtained as a colorless solid (312 mg, 99.1 µmol, 83.3%). The exceeding monomer-NC **91** was recovered as a yellow oil (139 mg, 171 µmol, 96.1%).

R_f = 0.40 in ethyl acetate. Visualized *via* fluorescence quench and Seebach staining solution.

IR (ATR): ν [cm^{-1}] = 3304.6 (br, ν(N-H)), 2923.3 (s, ν(C-H), 2852.6 (m, ν(C-H), 1747.8 (w, ν(C=O)), 1655.2 (vs, ν(C=O)), 1533.6 (s), 1451.1 (w), 1383.7 (m), 1307.9 (w),

1253.8 (w), 1169.2 (vs), 1098.9 (s), 1039.8 (w), 1009.4 (w), 830.7 (w), 756.6 (w), 697.6 (m), 499.2 (w), 399.7 (w).

^{1}H-NMR (600 MHz, DMSO-d_6): δ [ppm] = 8.22 – 8.12 (m, 4 H, NH[10,62]), 7.96 – 7.86 (m, 7 H, NH[3,28,43,84]), 7.45 (t, J = 7.9 Hz, 1 H, CH_{Ar}), 7.41 – 7.24 (m, 16 H, CH_{Ar}), 7.24 – 7.19 (m, 4 H, CH_{Ar}), 7.17 – 7.11 (m, 4 H, CH_{Ar}), 6.94 (s, 1 H, NH), 5.42 – 5.18 (m, 4 H, CH[9,61]), 5.15 – 4.95 (m, 6 H, CH_2[76]+CH[29]), 4.90 (dd, J = 10.5, 5.2 Hz, 2 H, CH[82]), 4.84 – 4.80 (m, 2 H. CH[42]), 4.80 – 4.42 (m, 10 H, CH_2[23,79] + CH[1]), 3.14 – 2.80 (m, 16 H, CH_2[32,37,88,93]), 2.50 – 2.40 (m, 12 H, CH_3[16,68]), 2.34 (t, J = 7.3 Hz, 4 H, CH_2[38]), 1.77 – 1.58 (m, 12 H, CH_2), 1.58 – 1.47 (m, 10 H, CH_2), 1.35 (dd, J = 14.2, 6.0 Hz, 25 H, CH_2 + CH_3[31]), 1.31 – 1.06 (m, 92 H, CH_2), 1.10 – 0.90 (m, 8 H, CH_2^{cyhex}), 0.84 (t, J = 6.6 Hz, 12 H, CH_3[51,109]).

^{13}C-NMR (151 MHz, DMSO-d_6): δ [ppm] = 172.36 (s, CO_2R[39]), 169.29 (s, CONR[27]), 169.13 (s, CONR[42]), 169.01 (s, CO_2R[24]), 168.93 (s, CO_2R[24]), 168.56 (s, CO_2R[22]), 168.36 (s, CONR[3]), 165.01 (s, CO_2R[24]), 164.99 (s, CO_2R[24]), 164.89 (s, CO_2R[80]), 164.78 (s, CO_2R[80]), 152.35 (s, CO[11 or 63]), 152.18 (s, CO[11 or 63]), 151.97 (s, CO[11 or 63]), 150.12 (s, C[65 or 13]), 149.95 (s, C[65 or 13]), 143.13 (s, C_{Ar}[15 or 67]), 142.98 (s, C_{Ar}[15 or 67]), 136.12 (s, C_{Ar}[78]), 136.10 (s, C_{Ar}[78]), 131.29 (s, C_{Ar}[71]), 131.24 (s, C_{Ar}[71]), 128.81 (s, CH_{Ar}[69,73]), 128.74 (s, CH_{Ar}[69,73]), 128.52 (s, CH_{Ar}), 128.49 (s, CH_{Ar}), 128.37 (s, CH_{Ar}), 128.34 (s, CH_{Ar}), 128.25 (s, CH_{Ar}), 127.83 (s, CH_{Ar}), 127.68 (s, CH_{Ar}), 127.66 (s, CH_{Ar}), 126.46 (s, CH_{Ar}), 126.37 (s, CH_{Ar}), 120.57 (s, CH_{Ar}), 120.56 (s, CH_{Ar}), 102.73 (s, C[8]), 102.58 (s, C[8]), 102.33 (s, C[60]), 102.22 (s, C[60]), 77.08 (s), 74.15 (s, CH[82]), 74.08 (s, CH[82]), 73.06 (s, CH[41]), 70.59 (s, CH[26]), 70.57 (s, CH[26]), 70.54 (s, CH[26]), 65.32 (s, CH_2[76]), 52.99 (s, CH[9]), 52.76 (s, CH[9]), 52.59 (s, CH[61]), 52.41 (s, CH[61]), 44.13 (s, CH_2[23 or 79]), 43.93 (s, CH_2[23 or 79]), 38.25 (s, CH_2[32,37,88,93]), 38.15 (s, CH_2[32,37,88,93]), 33.42 (s, CH_2[38]), 31.44 (s, CH_2[45]), 31.28 (s, CH_2[87]), 31.08 (s, CH_2[49,107]), 28.99 (s, CH_2), 28.92 (s, CH_2), 28.88 (s, CH_2), 28.83 (s, CH_2), 28.80 (s, CH_2), 28.70 (s, CH_2), 28.58 (s, CH_2), 28.55 (s, CH_2), 28.54 (s, CH_2), 28.37 (s, CH_2), 28.20 (s, CH_2), 25.86 (s, CH_2[47]), 25.68 (s, CH_2), 25.51 (s, CH_2), 25.43 (s, CH_2), 24.47 (s, CH_2), 24.38 (s, CH_2), 24.31 (s, CH_2), 22.08 (s, CH_2[108]), 21.93 (s, CH_2[50]), 17.61 (s, CH_3[31]), 17.58 (s, CH_3[31]), 15.91 (s, CH_3[16 or 68]), 15.82 (s, CH_3[16 or 68]), 15.68 (s, CH_3[16 or 68]), 15.65 (s, CH_3[16 or 68]), 15.41 (s, CH_3[16 or 68]), 15.35 (s, CH_3[16 or 68]), 13.91 (s, CH_3[109]), 13.84 (s, CH_3[51]).

FAB – MS [*m/z*] (relative intensity): 3153.9 (95%) $[M + H]^+$, $[M – C_2H_5O]^+$, 2695.5 (10%) [Fragment A]$^+$, 2500.9 (15%) [Fragment B]$^+$, 1917.1 (25%) [Fragment C]$^+$, 303.1 (60%) $[M – C_8H_9O]^+$, 1351.3 (35%) [Fragment D]$^+$.

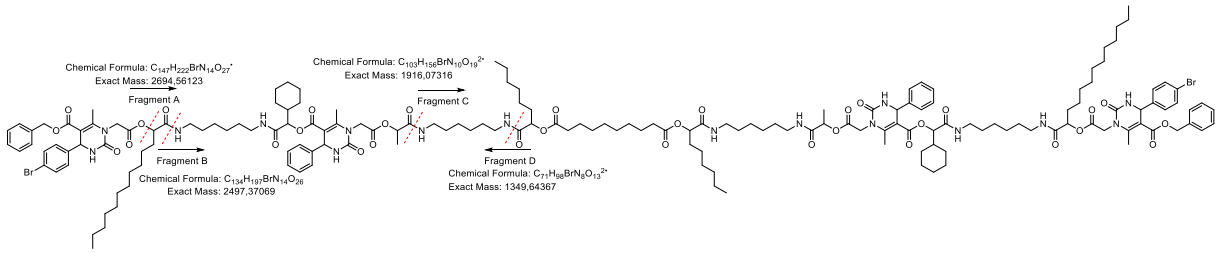

SEC–ESI–MS [*m/z*]: $[M + 2\ Na]^{2+}$ calculated for $^{12}C_{72}{}^{1}H_{106}{}^{16}O_{18}{}^{14}N_8{}^{23}Na_2$, 1598.7898; found, 1598.7910; Δ = 1.23 mmu.

6.2.3.5 Benzyl esters

6.2.3.5.1 *Benzyl ester 108 derived from monomer-NC 85, stearic acid and octanal*

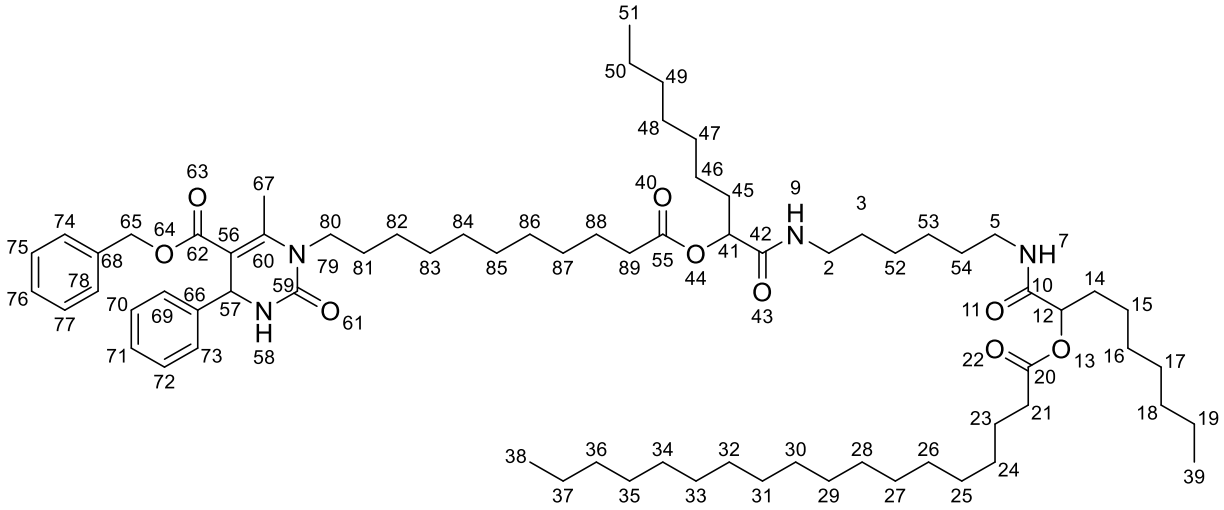

In a 10 mL round bottom flask the monomer-NC **85** (120 mg, 156 µmol, 1.00 eq.) was stirred in 1 mL dichloromethane, subsequently octanal (39.9 mg, 311 µmol, 2.00 eq.) and stearic acid (88.5 mg, 311 µmol, 2.00 eq.) were added. The resulting reaction mixture was degassed with argon and stirred at room temperature for 4 d. The crude mixture was dried under reduced pressure. The residue was adsorbed onto celite® and purified *via* column chromatography on silica gel eluting with a gradual solvent mixture

of ethyl acetate and *c*-hexane (1:4 → 1:1). The benzyl ester **108** was obtained as a colorless solid (142 mg, 120 µmol, 77.2%).

R_f in ethyl acetate/*c*-hexane (1:1) = 0.44. Visualized *via* fluorescence quench and Seebach staining solution.

IR (ATR): ν [cm^{-1}] = 3291.7 (br, ν(N-H)), 3093.8 (m), 2921.2 (vs, ν(C-H)), 2851.8 (s, ν(C-H)), 1739.7 (m, ν(C=O)), 1707.1 (s, ν(C=O)), 1684.4 (vs, ν(C=O)), 1657.2 (s), 1619.3 (m), 1538.5 (m), 1455.1 (m), 1416.1 (m), 1395.7 (m), 1376.2 (w), 1346.5 (w), 1322.4 (m), 1271.9 (m), 1215.5 (m), 1194.5 (m), 1153.1 (vs), 1098.5 (s), 1079.0 (m), 1040.7 (m), 915.3 (w), 828.8 (w), 757.0 (m), 720.9 (m), 699.5 (vs), 652.5 (m), 589.5 (w), 529.1 (m), 510.8 (m), 458.4 (w).

^{1}H-NMR (500 MHz, DMSO-d_6): δ [ppm] = 7.94 (d, J = 3.9 Hz, 1 H, NH^{58}), 7.92 – 7.85 (m, 2 H, NH$^{7\,+\,9}$), 7.33 – 7.13 (m, 10 H, CH$_{Ar}^{69\text{-}78}$), 5.17 (d, J = 3.8 Hz, 1 H, CH^{57}), 5.14 – 5.00 (m, 2 H, CH$_2^{65}$), 4.81 (t, J = 6.3 Hz, 2 H, CH$^{12\,+\,41}$), 3.91 – 3.41 (m, 2 H, CH$_2^{80}$), 3.09 – 2.93 (m, 4 H, CH$_2^{14\,+\,45}$), 2.50 (underneath DMSO signal, CH$_3^{67}$), 2.33 (td, J = 7.3, 2.3 Hz, 4 H, CH$_2^{21\,+\,89}$), 1.76 – 1.61 (m, 4 H, CH$_2^{2\,+\,5}$), 1.61 – 1.43 (m, 4 H, CH$_2$), 1.43 – 1.32 (m, 4 H, CH$_2$), 1.31 – 0.99 (m, 72 H, CH$_2$), 0.90 – 0.78 (m, 9 H, CH$_3^{38\,+\,39\,+\,51}$).

^{13}C-NMR (126 MHz, DMSO-d_6) δ [ppm] = 172.37 (s, CO$_2$R^{55}), 170.33 (s, CO$_2$R^{20}), 169.12 (s, CONR$^{42\,+\,10}$), 165.34 (s, CO$_2$R^{62}), 152.60 (s, CO^{59}), 150.50 (s, C^{60}), 143.83 (s, C$_{Ar}^{66}$), 136.35 (s, C$_{Ar}^{68}$), 128.32 (s, CH$_{Ar}$), 128.28 (s, CH$_{Ar}$), 127.78 (s, CH$_{Ar}$), 127.63 (s, CH$_{Ar}$), 127.27 (s, CH$_{Ar}$), 126.07 (s, CH$_{Ar}$), 102.52 (s, C^{56}), 73.07 (s, CH$^{12\,+\,41}$), 65.16 65.14 (s, CH$_2^{65}$), 52.25 (s, CH^{57}), 41.58 (s, CH$_2^{80}$), 38.02 (s, CH$_2^{14\,+\,45}$), 33.45 (s, CH$_2^{21\,+\,89}$), 31.45 (s, CH$_2^{2\,+\,5}$), 31.33 (s, CH$_2$), 31.18 (s, CH$_2$), 29.37 (s, CH$_2$), 29.06 (s, CH$_2$), 28.98 (s, CH$_2$), 28.93 (s, CH$_2$), 28.89 (s, CH$_2$), 28.79 (s, CH$_2$), 28.73 (s, CH$_2$), 28.58 (s, CH$_2$), 28.43 (s, CH$_2$), 28.40 (s, CH$_2$), 26.21 (s, CH$_2$), 25.76 (s, CH$_2$), 24.56 (s, CH$_2$), 24.43 (s, CH$_2$), 22.12 (s, CH$_2$), 22.09 (s, CH$_2$), 20.78 (s, CH$_2$), 15.68 (s, CH$_3^{67}$), 14.10 (s, CH$_3^{38\,+\,39\,+\,51}$), 13.94 (s, CH$_3^{38\,+\,39\,+\,51}$), 13.92 (s, CH$_3^{38\,+\,39\,+\,51}$).

ESI–MS [*m/z*]: [M + Na]$^+$ calculated for ^{12}C$_{72}$^{1}H$_{118}$^{16}O$_9$^{14}N$_4$^{23}Na$_1$, 1205.8791; found, 1205.8796; Δ = 0.54 mmu.

6.2.3.5.2 ***Benzyl ester 109 derived from monomer-NC 86, stearic acid and octanal***

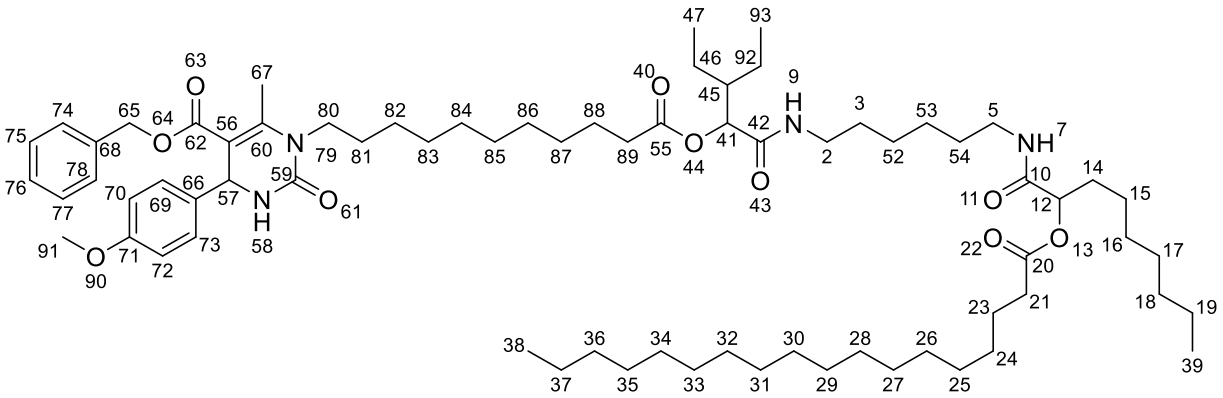

In a 10 mL round bottom flask the isocyanide monomer **86** (100 mg, 129 µmol, 1.00 eq.) was stirred in 2 mL dichloromethane, subsequently (33.2 mg, 258 µmol, 2.00 eq.) and stearic acid (73.6 mg, 258 µmol, 2.00 eq.) were added. The resulting reaction mixture was degassed with argon and stirred at room temperature for 4 d. The crude mixture was dried under reduced pressure. The residue was adsorbed onto celite® and purified *via* column chromatography on silica gel eluting with a gradual solvent mixture of ethyl acetate and *c*-hexane (1:4 → 2:1). The benzyl ester **109** was obtained as a colorless solid (148 mg, 124 µmol, 96.2%).

R_f in ethyl acetate/*c*-hexane (2:1) = 0.42. Visualized *via* fluorescence quench and Seebach staining solution.

IR (ATR): ν [cm^{-1}] = 3282.9 (br, ν(N-H)), 3091.4 (br, ν(N-H)), 2919.9 (vs, ν(C-H)), 2850.9 (s, ν(C-H)), 1742.7 (m, ν(C=O)), 1709.6 (s, ν(C=O)), 1682.6 (vs, ν(C=O)), 1656.4 (s), 1615.2 (m), 1539.1 (m), 1510.2 (w), 1464.7 (m), 1429.2 (m), 1392.2 (w), 1285.2 (w), 1243.2 (s), 1197.6 (vs), 1154.6 (vs), 1097.0 (s), 1040.4 (m), 913.6 (w), 846.2 (w), 777.9 (w), 754.2 (w), 722.3 (w), 696.8 (m), 650.9 (w), 589.6 (w), 534.1 (w), 510.7 (w), 443.9 (w).

^{1}H-NMR (400 MHz, DMSO-d_6): δ [ppm] = 7.96 – 7.81 (m, 3 H, NH^{7+9+58}), 7.29 (dd, J = 5.1, 1.9 Hz, 3 H, CH$_{Ar}$), 7.21 – 7.13 (m, 2 H, CH$_{Ar}$), 7.12 – 7.04 (m, 2 H, CH$_{Ar}$), 6.86 – 6.79 (m, 2 H, CH$_{Ar}$), 5.12 (d, J = 3.8 Hz, 1 H, CH^{57}), 5.10 – 5.01 (m, 2 H, CH$_2^{65}$), 4.91 (d, J = 4.2 Hz, 1 H, CH^{41}), 4.80 (t, J = 6.3 Hz, 1 H, CH^{12}), 3.96 – 3.76 (m, 1 H, CH$_2^{80a}$), 3.71 (s, 3 H, OCH$_3^{91}$), 3.58 – 3.38 (m, 1 H, CH$_2^{80b}$), 3.14 – 2.93 (m, 4 H, CH$_2^{2+5}$), 2.49 (underneath DMSO signal, CH$_3^{67}$), 2.35 (dt, J = 13.4, 7.2 Hz, 4 H, CH$_2^{21+89}$), 1.71 –

1.59 (m, 3 H, CH_2^{14} + CH^{45}), 1.59 – 1.45 (m, 4 H, CH_2^{23+88}), 1.42 – 1.31 (m, 6 H, $CH_2^{3+54+81}$), 1.28 – 1.13 (m, 54 H, CH_2), 0.93 – 0.76 (m, 12 H, $CH_3^{38+39+47,93}$).

^{13}C-NMR (101 MHz, DMSO-d_6) δ [ppm] = 172.46 (s, $CO_2R^{55\ or\ 10}$), 172.36 (s, $CO_2R^{55\ or\ 10}$), 169.10 (s, $CONR^{42\ or\ 10}$), 168.79 (s, $CONR^{42\ or\ 10}$), 165.37 (s, CO_2R^{62}), 158.48 (s, C_{Ar}^{71}), 152.60 (s, CO^{59}), 150.16 (s, C^{60}), 136.38 (s, C_{Ar}^{68}), 135.93 (s, C_{Ar}^{66}), 128.27 (s, CH_{Ar}), 127.75 (s, CH_{Ar}), 127.58 (s, CH_{Ar}), 127.24 (s, CH_{Ar}), 113.60 (s, CH_{Ar}), 102.84 (s, C^{56}), 74.03 (s, CH^{41}), 73.07 (s, CH^{12}), 65.09 (s, CH_2^{65}), 55.01 (s, OCH_3^{90}), 51.64 (s, CH^{57}), 42.58 (s, CH^{45}), 41.56 (s, CH_2^{80}), 38.09 (s, $CH_2^{2\ or\ 5}$), 38.05 (s, $CH_2^{2\ or\ 5}$), 33.50 (s, $CH_2^{21\ or\ 89}$), 33.44 (s, $CH_2^{21\ or\ 89}$), 31.43 (s, CH_2), 31.30 (s, CH_2), 31.16 (s, CH_2), 29.38 (s, CH_2), 29.03 (s, CH_2), 29.00 (s, CH_2), 28.96 (s, CH_2), 28.90 (s, CH_2), 28.80 (s, CH_2), 28.71 (s, CH_2), 28.68 (s, CH_2), 28.56 (s, CH_2), 28.54 (s, CH_2), 28.42 (s, CH_2), 28.37 (s, CH_2), 26.21 (s, CH_2), 25.85 (s, CH_2), 25.81 (s, CH_2), 25.77 (s, CH_2), 24.54 (s, CH_2), 24.43 (s, CH_2), 24.41 (s, CH_2), 22.10 (s, CH_2), 22.07 (s, CH_2), 21.77 (s, CH_2), 21.38 (s, CH_2), 15.66 (s, CH_3^{67}), 13.92 (s, $CH_3^{47\ or\ 93}$), 13.90 (s, $CH_3^{47\ or\ 93}$), 11.28 (s, $CH_3^{38\ or\ 39}$), 11.24 (s, $CH_3^{38\ or\ 39}$).

ESI–MS [*m/z*]: $[M + Na]^+$ calculated for $^{12}C_{71}{}^{1}H_{116}{}^{16}O_{10}{}^{14}N_4{}^{23}Na_1$, 1207.8584; found, 1207.8584; Δ = 0.03 mmu.

6.2.3.5.3 ***Benzyl ester 110 derived from monomer-NC 87, stearic acid and octanal***

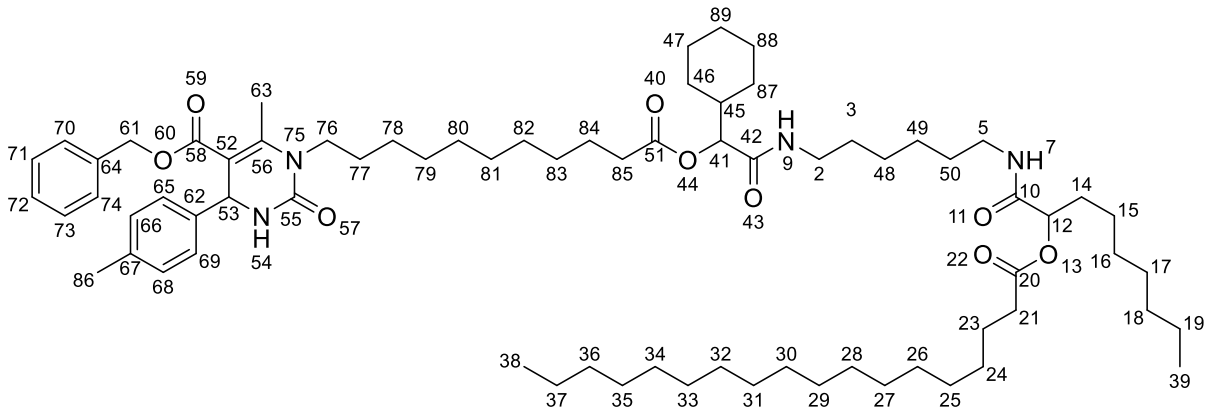

In a 10 mL round bottom flask the isocyanide monomer **87** (100 mg, 130 µmol, 1.00 eq.) was stirred in 2 mL dichloromethane, subsequently octanal (33.3 mg, 260 µmol, 2.00 eq.) and stearic acid (74.0 mg, 260 µmol, 2.00 eq.) were added. The resulting reaction mixture was degassed with argon and stirred at room temperature

for 4 d. The crude mixture was dried under reduced pressure. The residue was adsorbed onto celite® and purified *via* column chromatography on silica gel eluting with a gradual solvent mixture of ethyl acetate and *c*-hexane (1:4 → 1:1). The benzyl ester **110** was obtained as a colorless solid (143 mg, 121 µmol, 93.5%).

R_f in ethyl acetate/*c*-hexane (2:1) = 0.70. Visualized *via* fluorescence quench and Seebach staining solution.

IR (ATR): ν [cm^{-1}] = 3293.9 (br, ν(N-H)), 3088.1 (br, ν(N-H)), 2921.7 (vs, ν(C-H)), 2851.8 (s, ν(C-H)), 1740.1 (m, ν(C=O)), 1708.6 (s, ν(C=O)), 1681.7 (vs), 1657.4 (m), 1617.1 (w), 1540.8 (m), 1465.6 (w), 1422.2 (w), 1391.5 (w), 1374.7 (w), 1336.5 (m), 1321.6 (w), 1274.6 (m), 1234.5 (m), 1194.7 (m), 1151.8 (s), 1096.4 (m), 1040.7 (w), 986.0 (w), 913.8 (w), 843.7 (w), 777.0 (w), 755.2 (w), 721.4 (w), 696.9 (m), 651.2 (w), 590.3 (w), 554.4 (w), 521.6 (m), 447.4 (w).

^{1}H-NMR (400 MHz, DMSO-d_6): δ [ppm] = 7.93 – 7.76 (m, 3 H, NH^{7+9+54}), 7.28 (dd, J = 5.0, 1.9 Hz, 3 H, CH$_{Ar}$), 7.17 (dd, J = 6.7, 2.9 Hz, 2 H, CH$_{Ar}$), 7.10 – 6.98 (m, 5 H, CH$_{Ar}^{70-74}$), 5.13 (d, J = 3.8 Hz, 1 H, CH^{53}), 5.11 – 4.98 (m, 2 H, CH$_2^{61}$), 4.81 (t, J = 7.1 Hz, 1 H, CH^{12}), 4.67 (d, J = 5.3 Hz, 1 H, CH^{41}), 3.92 – 3.74 (m, 1 H, CH$_2^{76a}$), 3.52 – 3.39 (m, 1 H, CH$_2^{76b}$), 3.12 – 2.89 (m, 4 H, CH$_2^{2+5}$), 2.49 (s, 3 H, CH$_3^{63}$), 2.34 (dt, J = 7.7 Hz, J = 7.3 Hz, 4 H, CH$_2^{21+85}$), 2.25 (s, 3 H, CH$_3^{86}$), 1.78 – 1.58 (m, 4 H, CH$_2$), 1.60 – 0.95 (m, 75 H, CH$_2$), 0.84 (t, J = 6.7 Hz, 6 H, CH$_3^{38+39}$).

^{13}C-NMR (101 MHz, DMSO-d_6) δ [ppm] = 172.38 (s, CO$_2$R$^{20 \text{ or } 51}$), 172.30 (s, CO$_2$R$^{20 \text{ or } 51}$), 169.08 (s, CONR^{10}), 168.21 (s, CONR^{42}), 165.34 (s, CO$_2$R^{58}), 152.64 (s, CO^{55}), 150.25 (s, C^{56}), 140.87 (s, C$_{Ar}^{62}$), 136.34 (s, C$_{Ar}^{64}$), 128.77 (s, CH$_{Ar}$), 128.23 (s, CH$_{Ar}$), 127.73 (s, CH$_{Ar}$), 127.59 (s, CH$_{Ar}$), 125.94 (s, CH$_{Ar}$), 102.75 (s, C^{52}), 76.97 (s, CH^{41}), 73.05 (s, CH^{12}), 65.09 (s, CH$_2^{61}$), 51.88 (s, CH^{53}), 41.52 (s, CH$_2^{76}$), 38.03 (s, CH$_2^{2 \text{ or } 5}$), 38.00 (s, CH$_2^{2 \text{ or } 5}$), 33.44 (s, CH$_2^{21 \text{ or } 85}$), 33.41 (s, CH$_2^{21 \text{ or } 85}$), 31.42 (s, CH$_2$), 31.29 (s, CH$_2$), 31.15 (s, CH$_2$), 29.38 (s, CH$_2$), 29.02 (s, CH$_2$), 28.96 (s, CH$_2$), 28.89 (s, CH$_2$), 28.80 (s, CH$_2$), 28.70 (s, CH$_2$), 28.68 (s, CH$_2$), 28.61 (s, CH$_2$), 28.54 (s, CH$_2$), 28.43 (s, CH$_2$), 28.38 (s, CH$_2$), 27.28 (s, CH$_2$), 26.18 (s, CH$_2$), 25.75 (s, CH$_2$), 25.53 (s, CH$_2$), 25.41 (s, CH$_2$), 24.53 (s, CH$_2$), 24.40 (s, CH$_2$), 22.08 (s, CH$_2$), 22.05 (s, CH$_2$), 20.57 (s, CH$_3^{86}$), 15.65 (s, CH$_3^{63}$), 13.88 (s, CH$_3^{38 \text{ or } 39}$), 13.86 (s, CH$_3^{38 \text{ or } 39}$).

ESI–MS [*m/z*]: [M + Na]$^+$ calculated for $^{12}C_{72}{}^{1}H_{116}{}^{16}O_9{}^{14}N_4{}^{23}Na_1$, 1203.8635; found, 1203.8637; Δ = 0.20 mmu.

6.2.3.5.4 ***Benzyl ester 111 derived from monomer-NC 88, stearic acid and octanal***

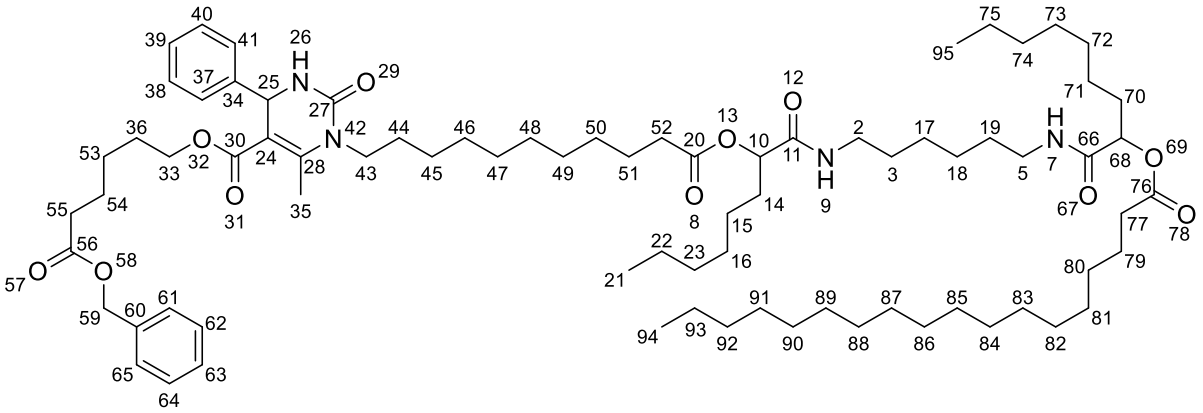

In a 10 mL round bottom flask the isocyanide monomer **88** (130 mg, 149 µmol, 1.00 eq.) was stirred in 2 mL dichloromethane, subsequently octanal (38.3 mg, 298 µmol, 2.00 eq.) and stearic acid (84.9 mg, 298 µmol, 2.00 eq.) were added. The resulting reaction mixture stirred at room temperature for 3 d under argon atmosphere. The crude mixture was dried under reduced pressure. The residue was adsorbed onto celite® and purified *via* column chromatography on silica gel eluting with a gradual solvent mixture of ethyl acetate and *c*-hexane (1:3 → 2:1). The benzyl ester **111** was obtained as a colorless oil (149 mg, 115 µmol, 77.6%).

R_f in ethyl acetate/*c*-hexane (2:1) = 0.67. Visualized *via* fluorescence quench and Seebach staining solution.

IR (ATR): ν [cm^{-1}] = 3270.6 (br, ν(N-H)), 3092.7 (br, ν(N-H)), 2918.9 (vs, ν(C-H)), 2850.3 (s, ν(C-H)), 1741.7 (s, ν(C=O)), 1680.1 (s, ν(C=O)), 1656.1 (vs, ν(C=O)), 1564.0 (m), 1463.5 (m), 1383.0 (m), 1253.6 (m), 1233.4 (m), 1213.8 (m), 1191.2 (m), 1161.0 (vs), 1088.3 (s), 805.8 (m), 722.5 (m), 696.7 (m), 503.9 (w).

^{1}H-NMR (400 MHz, DMSO-d_6): δ [ppm] = 7.93 (d, J = 3.8 Hz, 1 H, NH^{26}), 7.89 (t, J = 5.3 Hz, 2 H, NH^{7+9}), 7.40 – 7.17 (m, 10 H, CH$_{Ar}$$^{37-41+61-65}$), 5.15 (d, J = 3.9 Hz, 0.3 H, CH$^{25\ minor}$), 5.13 (d, J = 3.7 Hz, 0.7 H, CH$^{25\ major}$), 5.07 (s, 1.5 H, CH$_2$$^{59\ major}$), 5.06 (s, 0.5 H, CH$_2$$^{59\ minor}$), 4.81 (t, J = 6.3 Hz, 2 H, CH^{10+68}), 3.98 – 3.88 (m, 2 H, CH$_2$^{34}), 3.88 – 3.72 (m, 1 H, CH$_2$^{43a}), 3.53 – 3.38 (m, 1 H, CH$_2$^{43b}), 3.09 – 2.95 (m, 4 H, CH$_2$$^{2+5}$), 2.48 (s, 3 H, CH$_3$^{35}), 2.33 (td, J = 7.3, 2.1 Hz, 4 H, CH$_2$$^{52\ or\ 55\ or\ 77}$), 2.25 (t, J = 7.4 Hz, 2 H, CH$_2$$^{52\ or\ 55\ or\ 77}$), 1.72 – 1.58 (m, 4 H, CH$_2$$^{14+70}$), 1.57 – 1.41 (m, 10 H, CH$_2$), 1.41 – 0.98 (m, 90 H, CH$_2$), 0.86 – 0.79 (m, 9 H, CH$_3$$^{21+94+95}$).

^{13}C-NMR (101 MHz, DMSO-d_6) δ [ppm] = 172.56 (s, $CO_2R^{20\ or\ 56\ or\ 76}$), 172.54 (s, $CO_2R^{20\ or\ 56\ or\ 76}$), 172.35 (s, $CO_2R^{20\ or\ 56\ or\ 76}$), 169.10 (s, $CONR^{11+66}$), 165.71 (s, CO_2R^{30}), 165.58 (s, CO_2R^{30}), 153.27 (s, CO^{27}), 152.58 (s, CO^{27}), 149.83 (s, C^{28}), 143.94 (s, $C_{Ar}{}^{34}$), 143.53 (s, $C_{Ar}{}^{34}$), 136.26 (s, $C_{Ar}{}^{60}$), 128.38 (s, CH_{Ar}), 128.27 (s, CH_{Ar}), 127.94 (s, CH_{Ar}), 127.92 (s, CH_{Ar}), 127.89 (s, CH_{Ar}), 126.03 (s, CH_{Ar}), 102.80 (s, C^{24}), 73.06 (s, CH^{10+68}), 65.29 (s, $CH_2{}^{59}$), 65.25 (s, $CH_2{}^{59}$), 63.26 (s, $CH_2{}^{33}$), 52.38 (s, CH^{25}), 41.51 (s, $CH_2{}^{43}$), 38.02 (s, $CH_2{}^{2\ or\ 5}$), 33.43 (s, $CH_2{}^{52\ or\ 55\ or\ 77}$), 33.29 (s, $CH_2{}^{52\ or\ 55\ or\ 77}$), 33.19 (s, $CH_2{}^{52\ or\ 55\ or\ 77}$), 31.44 (s, CH_2), 31.30 (s, CH_2), 31.16 (s, CH_2), 31.11 (s, CH_2), 29.38 (s, CH_2), 29.03 (s, CH_2), 28.97 (s, CH_2), 28.90 (s, CH_2), 28.87 (s, CH_2), 28.78 (s, CH_2), 28.71 (s, CH_2), 28.69 (s, CH_2), 28.55 (s, CH_2), 28.41 (s, CH_2), 28.38 (s, CH_2), 28.25 (s, CH_2), 27.75 (s, CH_2), 26.20 (s, CH_2), 25.76 (s, CH_2), 25.02 (s, CH_2), 24.87 (s, CH_2), 24.54 (s, CH_2), 24.50 (s, CH_2), 24.41 (s, CH_2), 23.97 (s, CH_2), 22.10 (s, CH_2), 22.07 (s, CH_2), 21.97 (s, CH_2), 20.75 (s, CH_2), 15.57 (s, $CH_3{}^{35}$), 13.92 (s, $CH_3{}^{21\ or\ 94\ or\ 95}$), 13.90 (s, $CH_3{}^{21\ or\ 94\ or\ 95}$), 13.86 (s, $CH_3{}^{21\ or\ 94\ or\ 95}$).

ESI–MS [*m/z*]: $[M + Na]^+$ calculated for $^{12}C_{77}{}^{1}H_{126}{}^{16}O_{11}{}^{14}N_4{}^{23}Na_1$, 1305.9315; found, 1305.9331; Δ = 1.58 mmu.

6.2.3.5.5 *Benzyl ester 112 derived from monomer-NC 89, stearic acid and octanal*

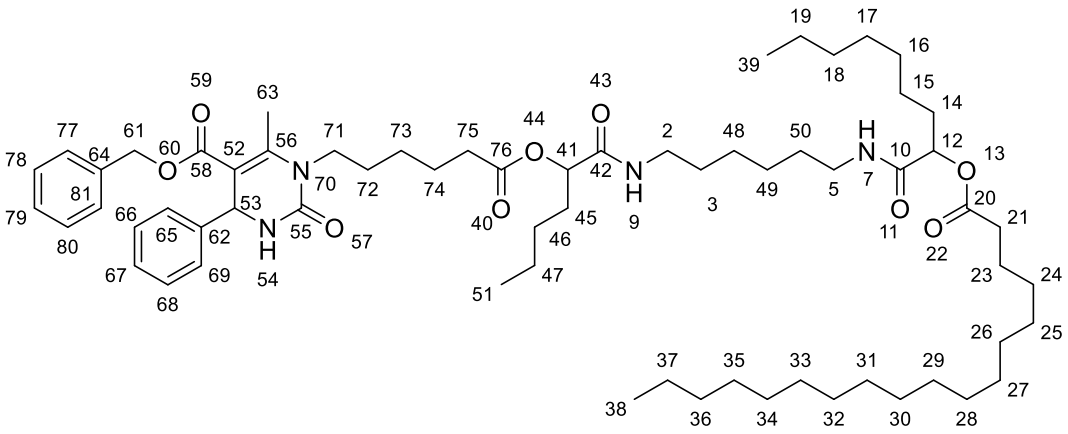

In a 10 mL round bottom flask the monomer-NC **89** (300 mg, 455 µmol, 1.00 eq.) was stirred in 3 mL dichloromethane, subsequently octanal (116 mg, 910 µmol, 2.00 eq.), stearic acid (194 mg, 683 µmol, 1.50 eq.) and a few droplets of dimethyl sulfoxide were added. The resulting reaction mixture was degassed with argon and stirred at room temperature for 3 d under argon atmosphere. The crude mixture was dried under

reduced pressure. The residue was adsorbed onto celite® and purified *via* column chromatography on silica gel eluting with a gradual solvent mixture of ethyl acetate and *c*-hexane (1:2 → 2:1) and dried under reduced pressure to yield the benzyl ester **112** as a colorless solid (396 mg, 369 µmol, 81.2%).

R_f in ethyl acetate/*c*-hexane (2:1) = 0.74.

IR (ATR): ν [cm^{-1}] = 3269.5 (br, ν(N-H)), 3093.2 (br, ν(N-H)), 2919.3 (w, ν(C-H)), 2850.2 (w, ν(C-H)), 1741.0 (s, ν(C=O)), 1681.9 (s, ν(C=O)), 1656.7 (vs), 1617.3 (m), 1539.7 (m), 1495.9 (m), 1456.0 (w), 1372.4 (m), 1235.6 (s), 1191.7 (m), 1161.1 (vs), 1112.7 (m), 1086.9 (w), 1045.4 (s), 938.4 (w), 830.1 (w), 755.9 (m), 723.8 (m), 697.0 (s), 633.7 (w), 514.3 (w).

^{1}H-NMR (400 MHz, DMSO-d_6): δ [ppm] = 7.96 (d, J = 3.9 Hz, 1 H, NH^{54}), 7.90 (q, J = 5.4 Hz, 2 H, NH^{7+9}), 7.32 – 7.12 (m, 10 H, CHAr$^{65\text{-}69\ +\ 77\text{-}81}$), 5.18 (d, J = 3.8 Hz, 1 H, CH^{53}), 5.11 – 5.02 (m, 2 H, CH$_2^{61}$), 4.84 – 4.78 (m, 2 H, CH^{12+41}), 3.87 – 3.43 (m, 2 H, CH$_2^{71}$), 3.03 (tq, J = 13.3, 6.6 Hz, 4 H, CH$_2^{2+5}$), 2.51 (s, 3 H, CH$_3^{63}$), 2.33 (t, J = 7.3 Hz, 2 H, CH$_2^{21\ or\ 75}$), 2.28 (td, J = 7.4, 3.4 Hz, 2 H, CH$_2^{21\ or\ 75}$), 1.73 – 1.59 (m, 4 H, CH$_2^{14+45}$), 1.57 – 1.44 (m, 4 H, CH$_2^{23+74}$), 1.42 – 1.31 (m, 6 H, CH$_2^{72+3+50}$), 1.32 – 1.11 (m, 56 H, CH$_2$), 0.84 (t, J = 6.7 Hz, 9 H, CH$_3^{38+39+51}$).

^{13}C-NMR (101 MHz, DMSO-d_6) δ [ppm] = 172.33 (s, CO$_2$R$^{20\ or\ 76}$), 172.27 (s, CO$_2$R$^{20\ or\ 76}$), 169.10 (s, CONR$^{10\ +\ 42}$), 165.33 (s, CO$_2$R^{58}), 152.58 (s, CO^{55}), 150.47 (s, C^{56}), 143.86 (s, C$_{Ar}^{62}$), 136.34 (s, C$_{Ar}^{64}$), 128.34 (s, CH$_{Ar}$), 128.27 (s, CH$_{Ar}$), 127.76 (s, CH$_{Ar}$), 127.62 (s, CH$_{Ar}$), 127.28 (s, CH$_{Ar}$), 126.11 (s, CH$_{Ar}$), 102.55 (s, C^{52}), 102.53 (s, C^{52}), 73.13 (s, CH$^{12\ or\ 41}$), 73.05 (s, CH$^{12\ or\ 41}$), 65.15 (s, CH$_2^{61}$), 52.30 (s, CH^{53}), 41.50 (s, CH$_2^{71}$), 38.09 (s, CH$_2^{2\ +\ 50}$), 33.47 (s, CH$_2^{21\ or\ 75}$), 33.26 (s, CH$_2^{21\ or\ 75}$), 31.46 (s, CH$_2$), 31.34 (s, CH$_2$), 31.20 (s, CH$_2$), 29.08(s, CH$_2$) , 29.06 (s, CH$_2$), 29.02 (s, CH$_2$), 29.00 (s, CH$_2$), 28.98 (s, CH$_2$), 28.95 (s, CH$_2$), 28.76 (s, CH$_2$), 28.74 (s, CH$_2$), 28.61 (s, CH$_2$), 28.58 (s, CH$_2$), 28.43 (s, CH$_2$), 26.78 (s, CH$_2$), 25.84 (s, CH$_2$), 25.56 (s, CH$_2$), 24.58 (s, CH$_2$), 24.44 (s, CH$_2$), 24.02 (s, CH$_2$), 22.14 (s, CH$_2$), 22.10 (s, CH$_2$), 21.80 (s, CH$_2$), 15.66 (s, CH$_3^{63}$), 13.92 (s, CH$_3^{38\ or\ 39\ or\ 51}$), 13.90 (s, CH$_3^{38\ or\ 39\ or\ 51}$), 13.79 (s, CH$_3^{38\ or\ 39\ or\ 51}$).

ESI – MS [*m/z*]: [M + Na]$^+$ calculated for $^{12}C_{64}{}^{1}H_{102}{}^{16}O_9{}^{14}N_4{}^{23}Na_1$, 1093.7539; found, 1093.7550; Δ = 1.10 mmu.

6.2.3.5.6 *Benzyl ester 113 derived from monomer-NC 90, stearic acid and octanal*

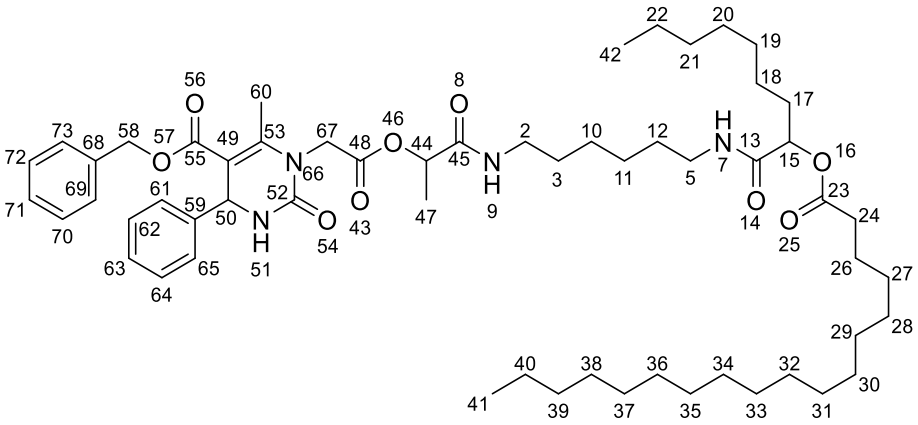

In a 10 mL round bottom flask the monomer-NC **90** (120 mg, 214 µmol, 1.00 eq.) was stirred in 2 mL dichloromethane, subsequently octanal (54.9 mg, 428 µmol, 2.00 eq.) and stearic acid (91.3 mg, 311 µmol, 1.50 eq.) and one droplet of dimethyl sulfoxide were added. The resulting reaction mixture was degassed with Argon and stirred at room temperature for 5 d. The crude mixture was dried under reduced pressure. The residue was adsorbed onto celite® and purified *via* column chromatography on silica gel eluting with a gradual solvent mixture of ethyl acetate and *c*-hexane (1:1 → 1:0). The benzyl ester **113** was obtained as a colorless solid (166 mg, 171 µmol, 80.1%).

R_f in ethyl acetate/*c*-hexane (5:1) = 0.47.

IR (ATR): ν [cm^{-1}] = 3288.9 (br, ν(N-H)), 2922.3 (vs, ν(C-H)), 2852.7 (s, ν(C-H)), 1736.3 (s, ν(C=O)), 1683.8 (vs, ν(C=O)), 1661.0 (vs, ν(C=O)), 1619.3 (m), 1543.3 (m), 1496.5 (m), 1455.4 (w), 1408.1 (w), 1372.7 (m), 1307.4 (w), 1278.5 (w), 1254.5 (s), 1204.3 (s), 1171.4 (vs), 1107.3 (m), 1044.2 (m), 963.0 (w), 883.5 (w), 831.7 (w), 762.0 (w), 697.1 (s), 591.0 (w), 497.7 (w).

^{1}H-NMR (500 MHz, DMSO-d_6): δ [ppm] = 8.17 (dd, J = 16.2, 3.7 Hz, 1 H, NH^{51}), 8.00 – 7.86 (m, 2 H, NH$^{7\,+\,9}$), 7.40 – 7.10 (m, 10 H, CH$_{Ar}$$^{61\text{-}65\,+\,69\text{-}73}$), 5.21 (t, J = 4.3 Hz, 1 H, CH), 5.17 – 5.00 (m, 2 H, CH$_2$^{58}), 5.01 – 4.95 (m, 1 H, CH^{44}), 4.80 (t, J = 6.2 Hz, 1 H, CH^{15}), 4.78 – 4.42 (m, 2 H, CH$_2$^{67}), 3.02 (qq, J = 13.8, 6.7 Hz, 4 H, CH$_2$$^{2+5}$), 2.43 (d, J = 7.6 Hz, 3 H, CH$_3$^{60}), 2.38 – 2.28 (m, 2 H, CH$_2$^{24}), 1.74 – 1.58 (m, 2 H, CH$_2$), 1.58 – 1.44 (m, 2 H, CH$_2$^{17}), 1.44 – 1.35 (m, 4 H, CH$_2$), 1.33 (dd, J = 6.9, 1.7 Hz, 3 H, CH$_3$^{47}), 1.22 (s, 46 H, CH$_2$), 0.84 (td, J = 6.9, 2.2 Hz, 6 H, CH$_3$$^{41+42}$).

^{13}C-NMR (101 MHz, DMSO-d_6) δ [ppm] = 172.46 (s, CO_2R^{23}), 169.35 (s, CO_2R^{48}), 169.30 (s, CO_2R^{48}), 169.17 (s, $CONR^{13\ or\ 45}$), 169.04 (s, $CONR^{13\ or\ 45}$), 168.97 (s, $CONR^{13\ or\ 45}$), 165.23 (s, CO_2R^{55}), 152.29 (s, CO_2R^{52}), 152.13 (s, CO_2R^{52}), 149.85 (s, C^{53}), 149.54 (s, C^{53}), 143.88 (s, C_{Ar}^{59}), 143.76 (s, C_{Ar}^{59}), 136.24 (s, C_{Ar}^{19}), 136.21 (s, C_{Ar}^{19}), 128.47 (s, CH_{Ar}), 128.43 (s, CH_{Ar}), 128.33 (s, CH_{Ar}), 127.98 (s, CH_{Ar}), 127.93 (s, CH_{Ar}), 127.87 (s, CH_{Ar}), 127.75 (s, CH_{Ar}), 127.73 (s, CH_{Ar}), 127.53 (s, CH_{Ar}), 126.65 (s, CH_{Ar}), 126.53 (s, CH_{Ar}), 126.23 (s, CH_{Ar}), 102.82 (s, C^{49}), 102.64 (s, C^{49}), 73.09 (s, CH^{15}), 70.64 (s, CH^{44}), 65.36 (s, CH_2^{58}), 53.23 (s, CH^{50}), 52.98 (s, CH^{50}), 44.09 (s, CH_2^{67}), 43.87 (s, CH_2^{67}), 38.30 (s, $CH_2^{2\ or\ 5}$), 38.27 (s, $CH_2^{2\ or\ 5}$), 38.17 (s, $CH_2^{2\ or\ 5}$), 33.48 (s, CH_2^{24}), 31.48 (s, CH_2), 31.36 (s, CH_2), 31.22 (s, CH_2), 29.11 (s, CH_2), 29.09 (s, CH_2), 29.07 (s, CH_2), 29.03 (s, CH_2), 29.00 (s, CH_2), 28.97 (s, CH_2), 28.78 (s, CH_2), 28.75 (s, CH_2), 28.63 (s, CH_2), 28.58 (s, CH_2), 28.43 (s, CH_2), 25.91 (s, CH_2), 24.62 (s, CH_2), 24.48 (s, CH_2), 22.17 (s, CH_2), 22.14 (s, CH_2), 17.70 (s, CH_3^{47}), 17.67 (s, CH_3^{47}), 15.72 (s, CH_3^{60}), 15.65 (s, CH_3^{60}), 14.02 (s, $CH_3^{41\ or\ 42}$), 13.99 (s, $CH_3^{41\ or\ 42}$).

ESI – MS [*m/z*]: $[M + Na]^+$ calculated for $^{12}C_{57}{}^{1}H_{88}{}^{16}O_9{}^{14}N_4{}^{23}Na_1$, 995.6449; found, 995.6447; Δ = 0.20 mmu.

6.2.3.5.7 ***Benzyl ester 114 derived from monomer-NC 91, stearic acid and octanal***

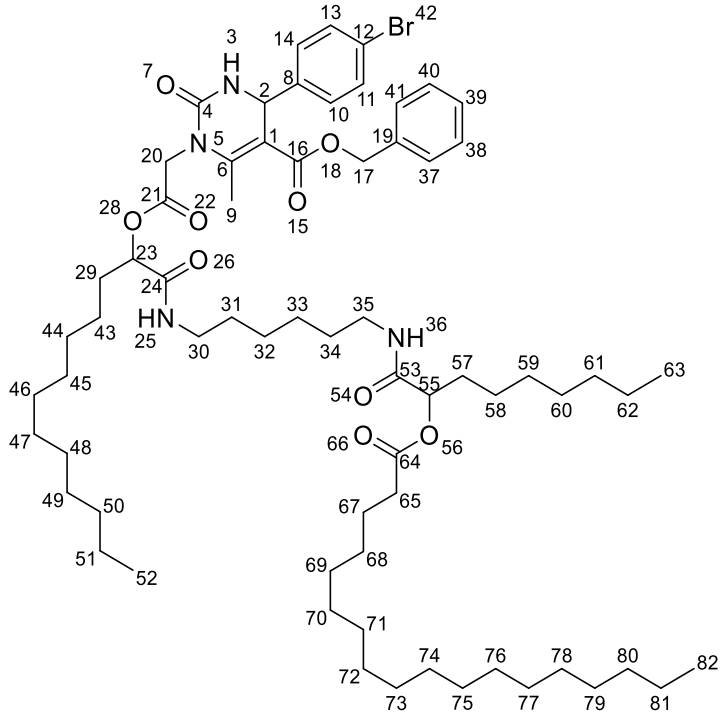

The monomer-NC **91** (200 mg, 256 µmol, 1.00 eq.) was stirred in 2 mL dichloromethane in a tube l, subsequently octanal (6.50 mg, 513 µmol, 2.00 eq.) and stearic acid (110 mg, 385 µmol, 1.50 eq.) were added. The resulting reaction mixture was stirred at room temperature for 3 d. The crude mixture was dried under reduced pressure. The residue was purified *via* column chromatography on silica gel eluting with a gradual solvent mixture of ethyl acetate and *c*-hexane (0:1 → 1:1) and dried *in vacuo* to yield the benzyl ester **114** (229 mg, 192 µmol, 75.0%).

R_f = 0.27 in *c*-hexane/ethyl acetate (2:1). Visualized *via* fluorescence quench and Seebach staining solution.

IR (ATR) ν [cm^{-1}] = 3286.8 (br, ν(N-H)), 3095.5 (br, ν(N-H)), 2922.7 (vs, ν(C-H)), 2852.8 (s, ν(C-H)), 1735.9 (s, ν(C=O)), 1709.2 (m, ν(C=O)), 1686.5 (vs, ν(C=O)), 1657.8 (vs, ν(C=O)), 1624.8 (m, ν(C=O)), 1546.7 (m), 1485.0 (w), 1456.2 (m), 1408.9 (m), 1373.9 (m), 1308.1 (w), 1252.6 (m), 1207.3 (s), 1186.7 (s), 1166.2 (s), 1106.0 (m), 1042.0 (m), 1026.3 (m), 1007.8 (m), 958.4 (w), 861.8 (w), 806.2 (w), 763.0 (m), 719.8 (w), 697.2 (m), 647.9 (w), 582.0 (w), 501.8 (w), 429.8 (w).

^{1}H-NMR (500 MHz, DMSO-d_6) δ [ppm] = 8. 20 (dd, J = 22.0, 3.6 Hz, 1 H, NH[3]), 7.96 – 7.85 (m, 2 H, NH[25,36]), 7.48 – 7.42 (m, 2 H, CH_{Ar}), 7.31 – 7.26 (m, 3 H, CH_{Ar}), 7.21 (t, J = 8.7 Hz, 2 H, CH_{Ar}), 7.14 (d, J = 3.3 Hz, 2 H, CH_{Ar}), 5.22 – 5.18 (m, 1 H, CH[2]), 5.11 – 4.99 (AB-Signal, δA = 5.08, δB = 5.03, J_{AB} = 15.0 Hz, 2 H, CH_2[17]), 4.90 (dt, J = 9.1, 4.6 Hz, 1 H, CH[23]), 4.83 – 4.79 (m, 1 H, CH[55]), 4.77 – 4.43 (m, 2 H, CH_2[20]), 3.12 – 2.94 (m, 4 H, CH_2[30,35]), 2.44 (d, J = 11.6 Hz, 3 H, CH_3[9]), 2.34 (dt, J = 11.4, 6.3 Hz, 2 H, CH_2[57]), 1.70 (m, 5 H, CH_2),1.49 (dt, J = 13.8, 6.7 Hz, 3 H, CH_2), 1.36 (d, J = 5.7 Hz, 5 H, CH_2), 1.22 (s, 57 H, CH_2,), 0.86 – 0.81 (m, 12 H, CH_3).

^{13}C-NMR (126 MHz, DMSO-d_6) δ [ppm] = 174.50 (s, CO_2R[64]), 174.48 (s, CO_2R[64]), 172.39 (s, CONR[53]), 172.34 (s, CONR[53]), 169.13 (s, CO_2R[21]), 169.05 (s, CO_2R[21]), 168.96 (s, CONR[24]), 168.56 (s, CONR[24]), 165.00 (s, CO_2Bn[16]), 152.19 (s, C[4]), 151.98 (s, C[4]), 150.17 (s, C[6]), 150.00 (s, C[6]), 143.15 (s, C_{Ar}[8]), 143.00(s, C_{Ar}[8]), 136.14 (s, C_{Ar}[19]), 131.30 (s, CH_{Ar}), 131.25 (s, CH_{Ar}), 128.84 (s, CH_{Ar}), 128.76 (s, CH_{Ar}), 128.26 (s, CH_{Ar}), 127.84 (s, CH_{Ar})127.70 (s, CH_{Ar}), 127.68 (s, CH_{Ar}), 102.32 (s, C[1]), 102.21 (s, C[1]), 74.15 (s, CH[23]), 74.09 (s, CH[23]), 73.06 (s, CH[46]), 65. 33 (s, CH_2[17]), 52.60 (s, CH[2]), 52. 42 (s, CH[2]), 44.13 (s, CH_2[20]), 44.03 (s, CH_2[20]), 38.16 (s, CH_2), 38.07 (s, CH_2), 33.67 (s, CH_2), 33.46 (s, CH_2), 31.45 (s, CH_2), 31.35 (s, CH_2), 31.33 (s, CH_2), 31.19 (s, CH_2), 29.06 (s, CH_2), 29.01 (s, CH_2), 28.94 (s, CH_2), 28.90 (s, CH_2), 28.78 (s, CH_2), 28.75 (s, CH_2), 28.63 (s, CH_2), 28.60 (s, CH_2), 28.57 (s, CH_2), 28.41 (s, CH_2), 25.82 (s, CH_2), 25.79 (s, CH_2), 24.57 (s, CH_2), 24.51 (s, CH_2), 24.43 (s, CH_2), 24.35 (s, CH_2), 22.13 (s, CH_2), 22.09 (s, CH_2), 22.07 (s, CH_2), 15.69 (s, CH_3[9]), 15.66 (s, CH_3[9]), 13.95 (s, CH_3), 13.92 (s, CH_3), 13.90 (s, CH_3).

ESI–MS (m/z): $[M + Na]^+$ calculated for $^{12}C_{67}{}^{1}H_{107}{}^{79}Br_{1}{}^{16}O_{9}{}^{14}N_{4}{}^{23}Na_{1}$, 1213.7119; found, 1213.7199; Δ = 8.00 mmu.

6.2.3.5.8 ***Benzyl ester 115 derived from monomer-NC 92, stearic acid and octanal***

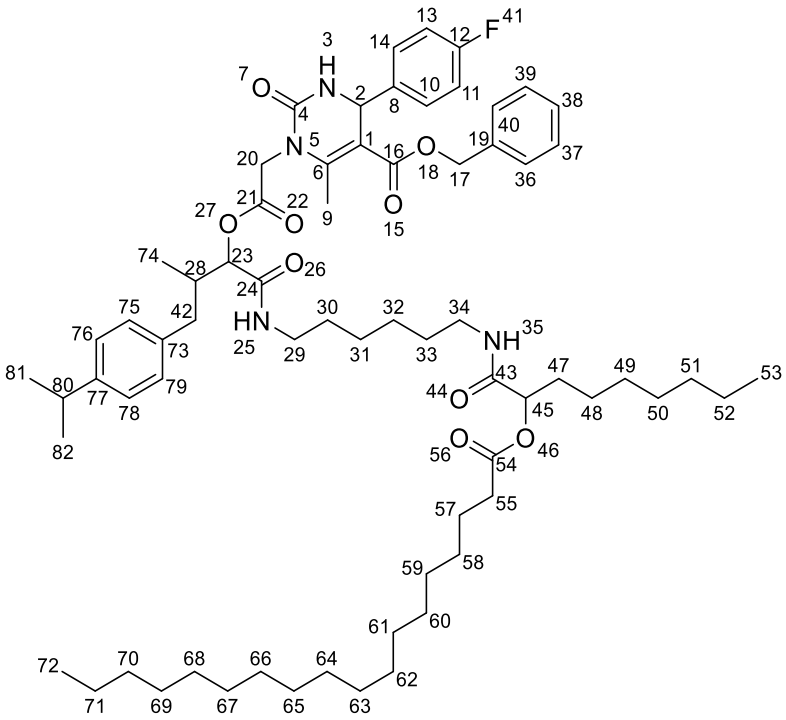

The monomer-NC **92** (100 mg, 138 µmol, 1.00 eq.) was stirred in 1 mL dichloromethane in a 10 mL round bottom flask, subsequently octanal (35.4 mg, 276 µmol, 2.00 eq.) and stearic acid (58.9 mg, 207 µmol, 1.50 eq.) were added. The resulting reaction mixture was degassed with argon and stirred at room temperature for 2 d. After 2 d reaction time the conversion was incomplete and additional monomer-NC **92** (50.4 mg, 69,5 µmol, 0.50 eq.), octanal (24.6 mg, 191 µmol, 1.38 eq.) and stearic acid (42.3 mg, 148 µmol, 1.07 eq.) were added to the mixture and stirred at room temperature for 2 d. The crude mixture was dried under reduced pressure. The residue was purified *via* column chromatography on silica gel eluting with a gradual solvent mixture of ethyl acetate and *c*-hexane (0:1 → 1:1) and dried *in vacuo* to yield the benzyl ester **115** as a colorless oil (99.0 mg, 87.0 µmol, 41.9%).

R_f = 0.67 in *c*-hexane/ethyl acetate (2:3). Visualized *via* fluorescence quench and Seebach staining solution.

IR (ATR) ν [cm^{-1}] = 3286.8 (br, ν(N-H)), 2920.6 (vs, ν(C-H)), 2852.8 (s, ν(C-H)), 1738.0 (m, ν(C=O)), 1709.2 (m, ν(C=O)), 1686.5 (vs, ν(C=O)), 1657.7 (vs, ν(C=O)), 1624.8 (w, ν(C=O)), 1612.5 (w, ν(C=O)), 1583.7 (vw), 1540.5 (w), 1509.7 (m), 1456.2 (m), 1413.0 (w), 1376.0 (m), 1306.0 (w), 1281.4 (w), 1242.3 (s), 1205.3 (s), 1172.3 (vs),

1104.5 (s), 1044.8 (m), 964.6 (vw), 925.5 (vw), 886.4 (vw), 857.6 (vw), 847.4 (vw), 824.7 (vw), 802.1 (vw), 785.7 (vw), 761.0 (w), 721.9 (w), 697.2 (m), 652.0 (w), 614.9 (vw), 592.3 (vw), 559.4 (vw), 534.7 (vw), 508.0 (vw), 444.2 (vw), 425.7 (vw).

^{1}H-NMR (500 MHz, DMSO-d_6) δ [ppm] = 8.35 – 8.19 (m 1 H, NH[3]), 8.18 – 7.81 (m, 2 H, NH[25,35]), 7.35 – 7.24 (m, 5 H, CH_{Ar}), 7.20 – 7.04 (m, 7 H, CH_{Ar}), 7.04 – 6.96 (m, 1 H, CH_{Ar}), 5.24 (t, J = 8.0 Hz, 1 H, CH[2]), 5.13 – 5.01 (m, 2 H, CH_2[17]), 4.91 – 4.78 (m, 2 H, CH[23,45]), 4.77 – 4.49 (m, 2 H, CH_2[20]), 3.16 – 2.96 (m, 4 H, CH_2[29,34]), 2.83 (dq, J = 6.6, 4.3 Hz, 1 H, CH[80]), 2.69 (t, J = 22.1 Hz, 2 H, CH_2[42]), 2.54 – 2.39 (m, 2 H, CH_3[9]), 2.37 – 2.30 (m, 2 H, CH_2[55]), 2.29 – 2.21 (m, 1 H, CH[28]), 1.64 (d, J = 4.5 Hz, 2 H, CH_2), 1.55 – 1.46 (m, 2 H, CH_2), 1.44 – 1.31 (m, 6 H, CH_2), 1.22 (s, 32 H, CH_2,), 1.18 – 1.16 (m, 6 H, CH_3[81,82]), 0.92 – 0.73 (m, 9 H, CH_3[53,72,74]).

^{13}C-NMR (126 MHz, DMSO-d_6) δ [ppm] = 172.39 (s, CO_2R[54]), 169.15 (s, CO_2R[21]), 169.05 (s, CO_2R[21]), 168.05 (s, CONR[24] or CONR[43]), 167.97 (s, s, CONR[24] or CONR[43]), 167.78 (s, CONR[24] or CONR[43]), 167.74 (s, CONR[24] or CONR[43]), 165.16 (s, CO_2Bn[16]), 165.11 (s, CO_2Bn[16]), 162.46 (s, C_{Ar}[12]), 160.53 (s, C_{Ar}[12]), 152.62 (s, C[4]), 152.44 (s, C[4]), 152.30 (s, C[4]), 152.22 (s, C[4]), 150.14 (s, C[6]), 149.95 (s, C[6]), 149.88 (s, C[6]), 146.00 (s, C_{Ar}[77]), 145.89 (s, C_{Ar}[77]), 140.04 (s, C_{Ar}[73]), 139.86 (s, C_{Ar}[73]), 137.13 (s, C_{Ar}[8]), 136.98 (s, C_{Ar}[8]), 136.91 (s, C_{Ar}[8]), 136.18 (s, C_{Ar}[19]), 128.92 (dd, J = 10.7, 5.4 Hz, CH_{Ar}[10,14]), 128.52 (dd, J = 11.5, 6.2 Hz, CH_{Ar}[10,14]), 128.29 (s, CH_{Ar}), 127.86 (s, CH_{Ar}), 127.83 (s, CH_{Ar}), 127.73 (s, CH_{Ar}), 127.69 (s, CH_{Ar}), 127.68 (s, CH_{Ar}), 127.62 (s, CH_{Ar}), 126.17 (s, CH_{Ar}[76,78]), 126.13 (s, CH_{Ar}[76,78]), 115.23 (d, J = 3.9 Hz, CH_{Ar}[11,13]), 115.06 (d, J = 3.9 Hz, CH_{Ar}[11,13]), 102.71 (s, C[1]), 102.59 (s, C[1]), 77.58 (s, CH[23]), 77.52 (s, CH[23]), 75.69 (s, CH[23]), 75.52 (s, CH[23]), 73.06 (s, CH[45]), 65.36 (s, CH_2[17]), 65.32 (s, CH_2[17]), 52.41 (s, CH[2]), 52.28 (s, CH[2]), 52.20 (s, CH[2]), 44.51 (s, CH_2[20]), 44.31 (s, CH_2[20]), 44.21 (s, CH_2[20]), 38.26 (s, CH_2[29,34]), 38.12 (s, CH_2[29,34]), 36.94 (s, CH[28]), 36.77 (s, CH_2[42]), 36.70 (s, CH_2[42]), 36.59 (m, CH_2[42]), 33.46 (s, CH_2[55]), 33.02 (s, CH[80]), 31.44 (s, CH_2), 31.31 (s, CH_2), 31.16 (s, CH_2), 29.04 (s, CH_2), 28.98 (s, CH_2), 28.92 (s, CH_2), 28.73 (s, CH_2), 28.70 (s, CH_2), 28.57 (s, CH_2), 28.54 (s, CH_2), 28.39 (s, CH_2), 26.36 (s, CH_2), 25.90 (s, CH_2), 24.56 (s, CH_2), 24.43 (s, CH_2), 23.93 (s, CH_3[81,82]), 23.89 (s, CH_3[81,82]), 22.12 (s, CH_2), 22.07 (s, CH_2), 15.89 (s, CH_3[9]), 15.78 (s, CH_3[9]), 15.71 (s, CH_3[9]), 15.19 (s, CH_3[74]), 15.08 (s, CH_3[74]), 14.09 (s, CH_3[53 or 72]), 13.94 (s, CH_3[53 or 72]), 13.91 (s, CH_3[53 or 72]).

^{19}F-NMR (400 MHz, DMSO-d_6) δ [ppm] = -119.39 (s, F[41]), -119.40 (s, F[41]), -119.41 (s, F[41]), -119.45 (s, F[41]).

ESI–MS (*m/z*): $[M + Na]^+$ calculated for $^{12}C_{68}{}^{1}H_{101}{}^{16}O_{9}{}^{14}N_{4}{}^{19}F_{1}{}^{23}Na_{1}$, 1159.7445; found, 1159.7449; Δ = 0.40 mmu.

6.2.3.5.9 ***Benzyl ester 116 derived from monomer-NC 83, stearic acid and octanal***

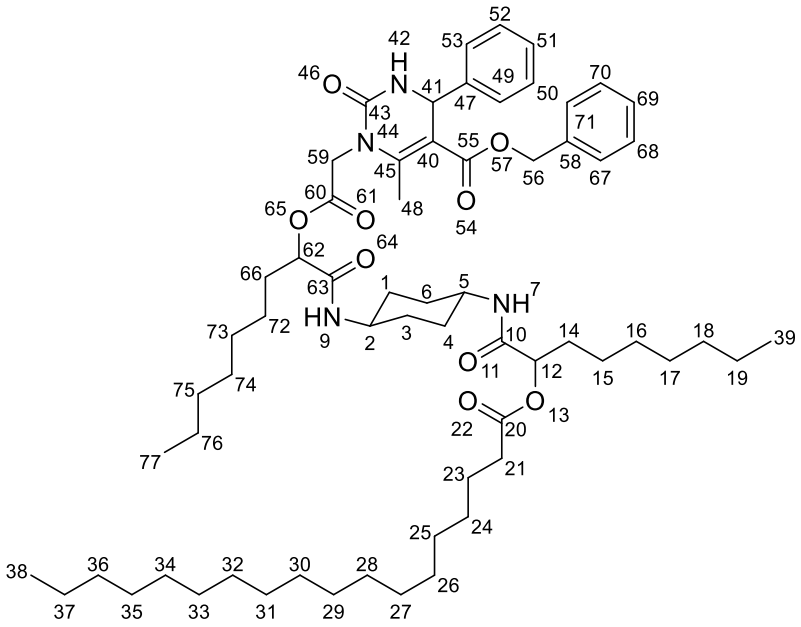

In a 5 mL round bottom flask the monomer-NC **83** (100 mg, 156 µmol, 1.00 eq.) was stirred in 2 mL dichloromethane, subsequently octanal (39.9 mg, 311 µmol, 2.00 eq.) and stearic acid (88.6 mg, 311 µmol, 2.00 eq.) were added. The resulting reaction mixture was degassed with argon and stirred at room temperature for 4 d. The crude mixture was dried under reduced pressure. The residue was adsorbed onto celite® and purified *via* column chromatography on silica gel eluting with a gradual solvent mixture of ethyl acetate and *c*-hexane (1:3 → 1:1) and dried under reduced pressure to yield the benzyl ester **116** as a colorless solid (128 mg, 121 µmol, 78.0%).

R_f in ethyl acetate/*c*-hexane (1:1) = 0.32. Visualized *via* fluorescence quench and Seebach staining solution.

IR (ATR): ν [cm^{-1}] = 3277.9 (br, ν(N-H)), 2915.6 (vs, ν(C-H)), 2848.4 (vs, ν(C-H)), 1737.3 (m, ν(C=O)), 1688.2 (vs, ν(C=O)), 1655.6 (s), 1624.9 (m), 1552.3 (m), 1462.5 (m), 1409.6 (m), 1376.1 (m), 1298.1 (m), 1279.3 (w), 1259.7 (w), 1240.5 (w), 1205.1 (s), 1187.2 (m), 1171.0 (m), 1108.3 (w), 1043.6 (m), 943.6 (m), 763.0 (m), 727.9 (m), 696.3 (m), 592.4 (w), 549.7 (w), 505.2 (w), 449.7 (w).

^{1}H-NMR (500 MHz, DMSO-d_6): δ [ppm] = 8.21 (dd, J = 32.7, 3.7 Hz, 1 H, NH^{42}), 7.85 – 7.68 (m, 2 H, NH^{7+9}), 7.27 (m, 8 H, CH$_{Ar}$$^{49-53}$), 7.19 – 7.12 (m, 2 H, CH$_{Ar}$$^{49-53}$), 5.22 (dd, J = 6.7, 3.7 Hz, 1 H, CH^{41}), 5.12 – 5.00 (m, 2 H, CH$_2$^{56}), 4.91 – 4.83 (m, 1 H, CH^{62}), 4.76 (t, J = 6.7 Hz, 1 H, CH^{12}), 4.74 – 4.39 (m, 2 H, CH$_2$^{59}), 3.56 – 3.43 (m, 2 H, CH^{2+5}), 2.44 (d, J = 16.9 Hz, 3 H, CH$_3$^{48}), 2.32 (t, J = 7.2 Hz, 2 H, CH$_2$^{21}), 1.75 – 1.60 (m, 9 H, CH$_2$), 1.55 – 1.42 (m, 4 H, CH$_2$), 1.31 – 1.15 (m, 88 H, CH$_2$), 0.90 – 0.80 (m, 9 H, CH$_3$$^{38 + 39 + 77}$).

^{13}C-NMR (126 MHz, DMSO-d_6) δ [ppm] = 172.38 (s, CO$_2$R^{20}), 169.09 (s, CO$_2$R^{60}), 168.88 (s, CO$_2$R^{60}), 168.49 (s, CONR^{10}), 167.95 (s, CONR^{63}), 167.92 (s, CONR^{63}), 165.21 (s, CO$_2$R^{55}), 165.18 (s, CO$_2$R^{55}), 152.54 (s, CO^{43}), 152.21 (s, CO^{43}), 149.68 (s, C^{45}), 149.55 (s, C^{45}), 143.81 (s, C$_{Ar}$^{47}), 143.60 (s, C$_{Ar}$^{47}), 136.17 (s, C$_{Ar}$^{58}), 128.43 (s, CH$_{Ar}$), 128.38 (s, CH$_{Ar}$), 128.29 (s, CH$_{Ar}$), 127.83 (s, CH$_{Ar}$), 127.69 (s, CH$_{Ar}$), 127.48 (s, CH$_{Ar}$), 126.55 (s, CH$_{Ar}$), 126.44 (s, CH$_{Ar}$), 102.80 (s, C^{40}), 74.07 (s, CH^{62}), 74.02 (s, CH^{62}), 73.08 (s, CH^{12}), 65.35 (s, CH$_2$^{56}), 65.33 (s, CH$_2$^{56}), 53.12 (s, CH^{41}), 52.89 (s, CH^{41}), 47.02 (s, CH$^{2 or 5}$), 46.97 (s, CH$^{2 or 5}$), 46.87 (s, CH$^{2 or 5}$), 44.23 (s, CH$_2$^{59}), 44.01 (s, CH$_2$^{59}), 33.66 (s, CH$_2$^{21}), 31.42 (s, CH$_2$), 31.32 (s, CH$_2$), 31.17 (s, CH$_2$), 31.12 (s, CH$_2$), 31.10 (s, CH$_2$), 30.83 (s, CH$_2$), 30.80 (s, CH$_2$), 29.37 (s, CH$_2$), 29.05 (s, CH$_2$), 28.98 (s, CH$_2$), 28.94 (s, CH$_2$), 28.91 (s, CH$_2$), 28.77 (s, CH$_2$), 28.73 (s, CH$_2$), 28.70 (s, CH$_2$), 28.57 (s, CH$_2$), 28.54 (s, CH$_2$), 28.52 (s, CH$_2$), 28.48 (s, CH$_2$), 28.36 (s, CH$_2$), 24.56 (s, CH$_2$), 24.51 (s, CH$_2$), 24.47 (s, CH$_2$), 24.34 (s, CH$_2$), 24.31 (s, CH$_2$), 22.12 (s, CH$_2$), 22.08 (s, CH$_2$), 22.06 (s, CH$_2$), 15.68 (s, CH$_3$^{48}), 15.67 (s, CH$_3$^{48}), 13.96 (s, CH$_3$$^{38 or 39 or 77}$), 13.95 (s, CH$_3$$^{38 or 39 or 77}$), 13.93 (s, CH$_3$$^{38 or 39 or 77}$).

ESI–MS [m/z]: [M + Na]$^+$ calculated for ^{12}C$_{63}$^{1}H$_{98}$^{16}O$_9$^{14}N$_4$^{23}Na$_1$, 1077.7226; found, 1077.7230; Δ = 0.42 mmu.

6.2.3.5.10 ***Benzyl ester 117 derived from monomer-NC 84, stearic acid and octanal***

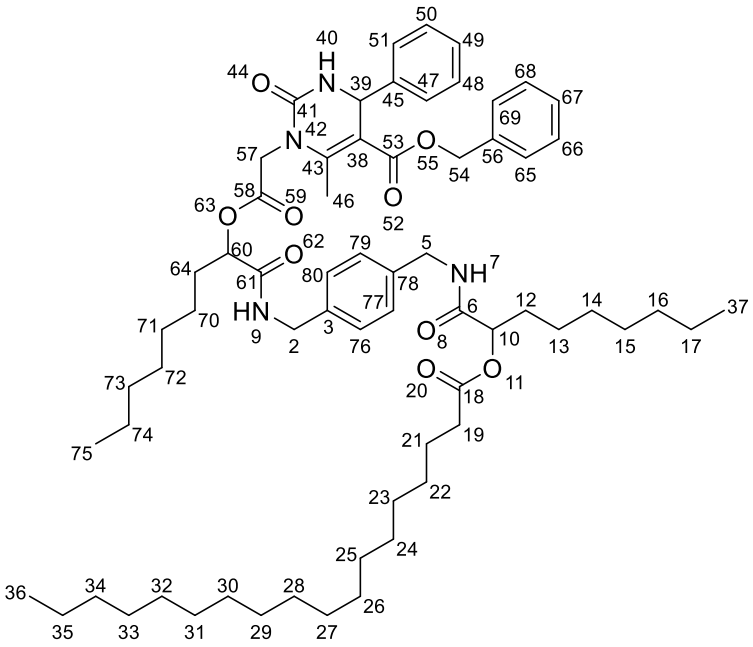

In a 5 mL round bottom flask the isocyanide monomer **84** (100 mg, 155 µmol, 1.00 eq.) was stirred in 2 mL dichloromethane, subsequently octanal (39.8 mg, 310 µmol, 2.00 eq.) and stearic acid (88.2 mg, 310 µmol, 2.00 eq.) were added. The resulting reaction mixture was degassed with argon and stirred at room temperature for 4 d. The crude mixture was dried under reduced pressure. The residue was adsorbed onto celite® and purified *via* column chromatography on silica gel eluting with a gradual solvent mixture of ethyl acetate and *c*-hexane (1:4 → 1:1). The benzyl ester **117** was obtained as a colorless solid (164 mg, 152 µmol, 98.2%).

R_f in ethyl acetate/*c*-hexane (1:1) = 0.41. Visualized *via* fluorescence quench and Seebach staining solution.

IR (ATR): ν [cm^{-1}] = 3281.8 (br, ν(N-H)), 2917.1 (vs, ν(C-H)), 2849.4 (s, ν(C-H)), 1736.7 (m, ν(C=O)), 1686.1(vs, ν(C=O)), 1660.5 (s), 1614.6 (m), 1538.9 (m), 1455.6 (m), 1375.7 (m), 1307.7 (m), 1279.1 (m), 1256.3 (m), 1203.9 (s), 1169.3 (s), 1105.9 (m), 1043.1 (m), 1027.1 (m), 962.0 (m), 833.0 (w), 763.5 (m), 720.5 (m), 696.7 (s), 590.2 (w), 497.7 (w), 438.0 (w).

^{1}H-NMR (500 MHz, DMSO-d_6): δ [ppm] = 8.54 (dt, J = 11.5, 6.0 Hz, 1 H, NH^{9}), 8.47 (td, J = 6.1, 2.4 Hz, 1 H, NH^{7}), 8.16 (dd, J = 21.3, 3.7 Hz, 1 H, NH^{40}), 7.34 – 7.23 (m, 8 H, CH$_{Ar}$), 7.20 – 7.08 (m, 6 H, CH$_{Ar}$), 5.22 (t, J = 4.5 Hz, 1 H, CH^{39}), 5.12 – 5.01 (m,

2 H, CH_2^{54}), 4.98 (dt, *J* = 7.5, 4.7 Hz, 1 H, CH^{60}), 4.89 (dd, *J* = 7.3, 5.3 Hz, 1 H, CH^{10}), 4.83 – 4.45 (m, 2 H, CH_2^{57}), 4.30 – 4.20 (m, 4 H, CH_2^{2+5}), 2.43 (d, *J* = 16.5 Hz, 3 H, CH_3^{46}), 2.35 (td, *J* = 7.3, 2.4 Hz, 2 H, CH_2^{19}), 1.78 – 1.64 (m, 4 H, CH_2^{12+64}), 1.62 – 1.43 (m, 2 H, CH_2^{21}), 1.42 – 1.05 (m, 50 H, CH_2), 0.93 – 0.72 (m, 9 H, $CH_3^{36+37+75}$).

^{13}C-NMR (126 MHz, DMSO-d_6) δ [ppm] = 172.50 (s, CO_2R^{18}), 169.46 ($CONR^{6}$), 169.18 (s, $CONR^{61}$), 168.95 (s, CO_2R^{57}), 168.92 (s, CO_2R^{57}), 165.22 (s, CO_2R^{53}), 165.19 (s, CO_2R^{53}), 152.34 (s, CO^{41}), 152.16 (s, CO^{41}), 149.75 (s, C^{43}), 149.62 (s, C^{43}), 143.85 (s, C_{Ar}^{45}), 143.70 (s, C_{Ar}^{45}), 137.88 , 137.64 , 136.20 (s, C_{Ar}^{56}), 136.19 (s, C_{Ar}^{56}), 128.44 (s, CH_{Ar}), 128.39 (s, CH_{Ar}), 128.30 (s, CH_{Ar}), 127.83 (s, CH_{Ar}), 127.68 (s, CH_{Ar}), 127.48 (s, CH_{Ar}), 126.95 (s, CH_{Ar}), 126.58 (s, CH_{Ar}), 126.49 (s, CH_{Ar}), 102.81 (s, C^{38}), 102.73 (s, C^{38}), 74.12 (s, CH^{60}), 74.02 (s, CH^{60}), 73.05 (s, CH^{10}), 65.32 (s, CH_2^{54}), 53.16 (s, CH^{39}), 52.96 (s, CH^{39}), 44.11 (s, CH_2^{57}), 43.94 (s, CH_2^{57}), 41.62 (s, $CH_2^{2 \text{ or } 5}$), 41.52 (s, $CH_2^{2 \text{ or } 5}$), 33.68 (s, CH_2^{19}), 33.48 (s, CH_2^{19}), 31.45 (s, CH_2), 31.33 (s, $CH_2^{12 \text{ or } 64}$), 31.18 (s, $CH_2^{12 \text{ or } 64}$), 31.14 (s, CH_2), 29.05 (s, CH_2), 29.03 (s, CH_2), 28.93 (s, CH_2), 28.78 (s, CH_2), 28.74 (s, CH_2), 28.59 (s, CH_2), 28.53 (s, CH_2), 28.41 (s, CH_2), 24.62 (s, CH_2), 24.52 (s, CH_2), 24.45 (s, CH_2), 24.40 (s, CH_2), 22.13 (s, CH_2), 22.10 (s, CH_2), 22.09 (s, CH_2), 15.68 (s, CH_3^{46}), 15.65 (s, CH_3^{46}), 13.97 (s, $CH_3^{36 \text{ or } 37 \text{ or } 75}$), 13.95 (s, $CH_3^{36 \text{ or } 37 \text{ or } 75}$).

ESI–MS [*m/z*]: $[M + Na]^+$ calculated for $^{12}C_{65}{}^{1}H_{96}{}^{16}O_9{}^{14}N_4{}^{23}Na_1$, 1099.7069; found, 1099.7074; Δ = 0.50 mmu.

6.2.3.5.11 ***Benzyl ester 118 derived from monomer-NC 93, stearic acid and octanal***

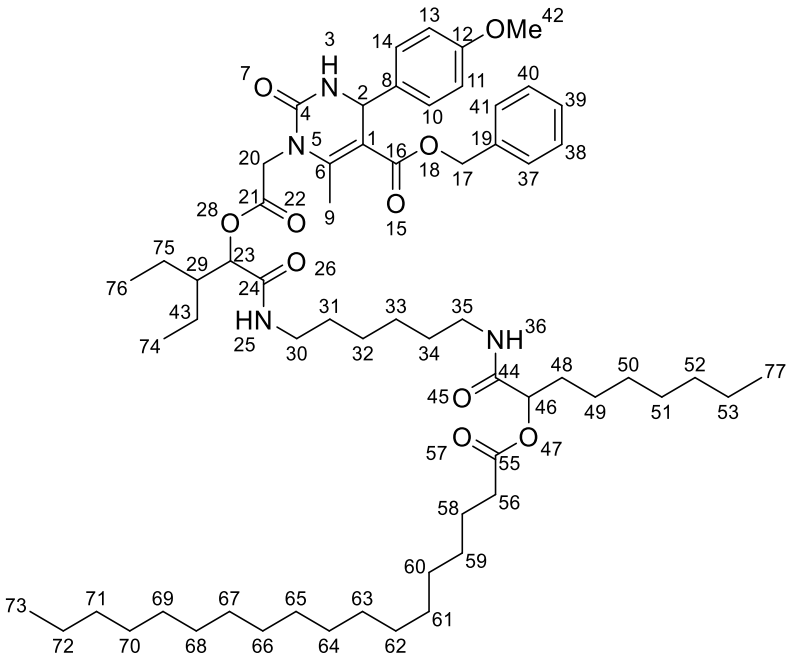

The monomer-NC **93** (150 mg, 232 µmol, 1.00 eq.) was stirred in 2 mL dichloromethane in a 10 mL round bottom flask, subsequently octanal (59.5 mg, 464 µmol, 2.00 eq.) and stearic acid (99.0 mg, 348 µmol, 1.50 eq.) were added. The resulting reaction mixture was concentrated under reduced pressure, degassed with argon and stirred at room temperature for 1 d. The crude mixture was dried under reduced pressure. The residue was purified *via* column chromatography on silica gel eluting with a gradual solvent mixture of ethyl acetate and *c*-hexane (0:1 → 1:1) and dried *in vacuo* to yield the benzyl ester **118** (235 mg, 221 µmol, 95.4%).

R_f = 0.55 in *c*-hexane/ethyl acetate (1:1). Visualized *via* fluorescence quench and Seebach staining solution.

IR (ATR) ν [cm^{-1}] = 3315.5 (br, ν(N-H)), 2924.8 (s, ν(C-H)), 2852.8 (m, ν(C-H)), 1748.3 (m, ν(C=O)), 1682.4 (s, ν(C=O)), 1653.6 (s, ν(C=O)), 1583.7 (vw), 1540.5 (m), 1511.7 (m), 1456.2 (m), 1415.0 (w), 1384.2 (m), 1306.0 (m), 1279.3 (m), 1244.3 (s), 1213.5 (s), 1174.4 (vs), 1104.5 (m), 1040.7 (m), 1003.7 (m), 964.6 (vw), 935.8 (vw), 884.4 (vw), 847.4 (vw), 830.9 (vw), 785.7 (vw), 752.8 (w), 730.1 (w), 697.2 (m), 654.0 (w), 586.1 (vw), 553.2 (vw), 530.6 (vw), 508.0 (vw).

^{1}H-NMR (500 MHz, DMSO-d_6) δ [ppm] = 8.14 (dd, J = 41.3, 3.6 Hz, 1 H, NH^{3}), 7.90 (tt, J = 16.3, 5.6 Hz, 2 H, NH^{25,36}), 7.33 – 7.26 (m, 3 H, CH$_{Ar}$), 7.16 (dt, J = 5.7, 5.1 Hz,

4 H, CH_{Ar}), 6.87 – 6.78 (m, 2 H, CH_{Ar}), 5.17 (dd, *J* = 7.9, 3.6 Hz, 1 H, CH^{2}), 5.11 – 5.03 (m, 2 H, CH_2^{17}), 4.99 (dd, *J* = 24.3, 3.8 Hz, 1 H, CH^{23}), 4.82 – 4.79 (m, 1 H, CH^{46}), 4.75 – 4.44 (m, 2 H CH_2^{20}), 3.72 (s, 3 H, OCH_3^{42}), 3.15 – 2.95 (m, 4 H, $CH_2^{30,35}$), 2.45 (d, *J* = 32.7 Hz, 3 H, CH_3^{9}), 2.37 – 2.30 (m, 2 H, CH_2^{56}), 1.78 – 1.68 (m, 1 H, CH^{29}), 1.65 (d, *J* = 5.6 Hz, 2 H, CH_2),1.53 (dd, *J* = 18.9, 12.2 Hz, 2 H, CH_2), 1.44 – 1.31 (m, 7 H, CH_2), 1.23 (s, 47 H, $CH_{2,}$), 0.91 – 0.76 (m, 12 H, CH_3).

^{13}C-NMR (126 MHz, DMSO-d_6) δ [ppm] = 172.40 (s, CO_2R^{55}), 169.19 (s, $CONR^{24}$ or $CONR^{44}$ or CO_2R^{21}), 169.15 (s, $CONR^{24}$ or $CONR^{44}$ or CO_2R^{21}), 168.34 (s, $CONR^{24}$ or $CONR^{44}$ or CO_2R^{21}), 165.29 (s, CO_2Bn^{16}), 165.22 (s, CO_2Bn^{16}), 158.65 (s, $COMe^{12}$), 158.62 (s, $COMe^{12}$), 152.69 (s, C^{4}), 152.28 (s, C^{4}), 149.38 (s, C^{6}), 149.27 (s, C^{6}), 136.26 (s, C_{Ar}^{19}), 135.94 (s, C_{Ar}^{8}), 135.69 (s, C_{Ar}^{8}), 128.28 (s, CH_{Ar}), 127.82 (s, CH_{Ar}), 127.80 (s, CH_{Ar}), 127.73 (s, CH_{Ar}), 127.65 (s, CH_{Ar}), 127.62 (s, CH_{Ar}), 127.61 (s, CH_{Ar}), 113.73 (s, CH_{Ar}), 113.69 (s, CH_{Ar}), 103.21 (s, C^{1}), 103.00 (s, C^{1}), 75.08 (s, CH^{23}), 74.98 (s, CH^{23}), 73.07 (s, CH^{46}), 65.28 (s, CH_2^{17}), 65.21 (s, CH_2^{17}), 55.06 (s, OCH_3^{43}), 52.45 (s, CH^{2}), 52.24 (s, CH^{2}), 44.36 (s, CH_2^{20}), 44.16 (s, CH_2^{20}), 42.55 (s, CH^{29}), 42.52 (s, CH^{29}), 38.28 (s, CH_2), 38.14 (s, CH_2), 33.45 (s, CH_2^{56}), 31.45 (s, CH_2), 31.32 (s, CH_2), 31.17 (s, CH_2), 29.05 (s, CH_2), 28.99 (s, CH_2), 28.92 (s, CH_2), 28.73 (s, CH_2), 28.71 (s, CH_2), 28.58 (s, CH_2), 28.55 (s, CH_2), 28.39 (s, CH_2), 25.94 (s, CH_2), 25.88 (s, CH_2), 24.56 (s, CH_2), 24.43 (s, CH_2), 22.12 (s, CH_2), 22.08 (s, CH_2), 21.82 (s, CH_2), 21.77 (s, CH_2), 15.70 (s, CH_3^{9}), 15.66 (s, CH_3^{9}), 13.94 (s, CH_3), 13.91 (s, CH_3), 11.37 (s, CH_3), 11.32 (s, CH_3), 11.26 (s, CH_3).

FAB-MS *m/z* (relative intensity): 1059.9 (32%) $[M + H]^+$, 951.8 (10%) $[M – C_7H_7O]^+$, 409.1 (34%) [Fragment A]$^+$, 393.1 (34%) [Fragment A – O]$^+$, 351.1 (50%) [Fragment A – $C_2H_2O_2]^+$, 303.1 (11%) [Fragment A – $C_7H_7O]^+$, 275.1 (17%), 261.0 (8%) [Fragment B – $C_7H_7]^+$, 163.0 (9%), 162.0 (54%), 90.9 (100%) $[C_7H_7]^+$.

HRMS–FAB (*m/z*): $[M + H]^+$ calculated for $^{12}C_{62}{}^{1}H_{99}{}^{16}O_{10}{}^{14}N_4$, 1059.7356; found, 1059.7353; Δ = 0.28 mmu.

Fragment A
Chemical Formula: $C_{22}H_{21}N_2O_6^{\bullet}$
Exact Mass: 409,13996

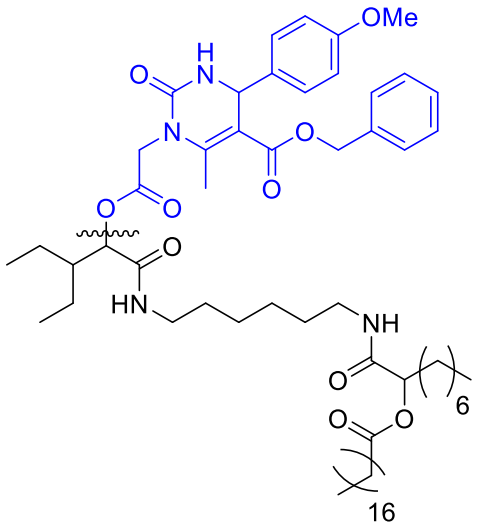

6.2.3.5.12 *Benzyl ester 119 derived from monomer-NC 94, stearic acid and octanal*

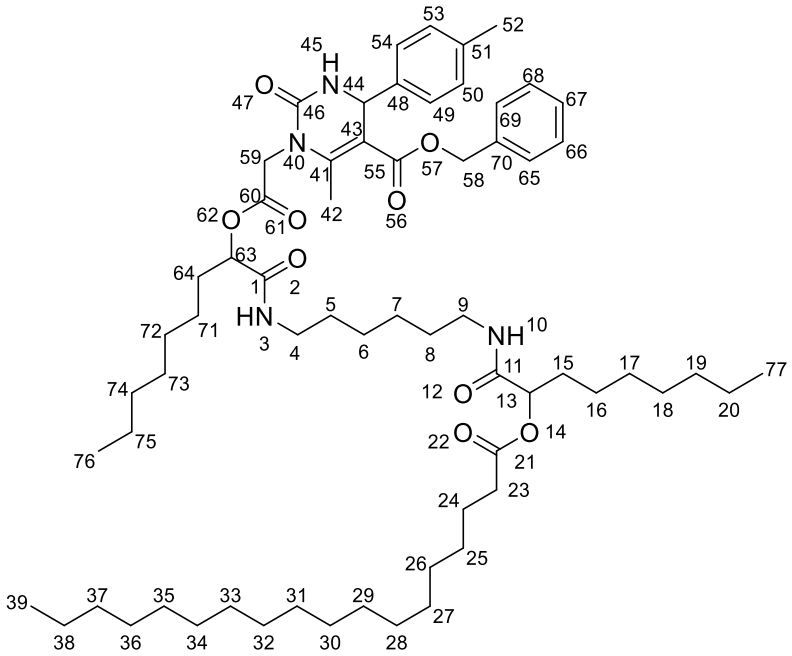

In a 10 mL round bottom flask the monomer-NC **94** (197 mg, 298 µmol, 1.00 eq.) was stirred in 1.2 mL dichloromethane, subsequently octanal (76.2 mg, 594 µmol, 2.00 eq.) and stearic acid (129 mg, 455 µmol, 1.50 eq.) were added. The resulting reaction mixture was stirred at room temperature for 1 d. Subsequently, the crude mixture was dried under reduced pressure. The residue was adsorbed onto celite® and purified *via*

column chromatography on silica gel eluting with a gradual solvent mixture of ethyl acetate and *c*-hexane (0:1 → 1:1) to yield the benzyl ester **119** as a pale highly viscous oil. (243 mg, 230 µmol, 75.4%).

R_f = 0.46 in *c*-hexane/ethyl acetate (1:1). Visualized *via* fluorescence quench and Seebach staining solution.

IR (ATR): ν [cm^{-1}] = 3292.1 (w, ν(N-H)), 2917.8 (s, ν(C-H)), 2849.9 (s, ν(C-H)), 1737.3 (m, ν(C=O)), 1687.5 (s, ν(C=O)), 1660.5 (s), 1547.3 (m), 1455.7 (m), 1411.7 (w), 1376.1 (m), 1307.1 (m), 1277.1 (m), 1258.0 (m), 1205.3 (s), 1170.0 (vs), 1106.7 (s), 1043.5 (m), 963.9 (w), 843.9 (w), 800.8 (m), 765.9 (m), 721.2 (m), 697.0 (m), 588.8 (w), 503.4 (m).

^{1}H-NMR (500 MHz, DMSO-d_6): δ [ppm] = 8.12 (dd, *J* = 27.6, 3.6 Hz, 1 H, NH^{45}), 7.96 – 7.86 (m, 2 H, NH^{3+10}), 7.31 – 7.27 (m, 3 H, CH$_{Ar}$), 7.18 – 7.11 (m, 4 H, CH$_{Ar}$), 7.10 – 7.04 (m, 2 H, CH$_{Ar}^{50,53}$), 5.17 (dd, *J* = 6.6, 3.6 Hz, 1 H, CH^{44}), 5.12 – 5.00 (m, 2 H, CH$_2^{58}$), 4.93 – 4.85 (m, 1 H, CH^{63}), 4.81 (t, *J* = 6.3 Hz, 1 H, CH^{13}), 4.76 – 4.41 (m, 2 H, CH$_2^{59}$), 3.11 – 2.94 (m, 4 H, CH$_2^{4,9}$), 2.43 (d, *J* = 14.5 Hz, 3 H, CH$_3^{42}$), 2.36 – 2.30 (m, 1 H, CH$_2^{23a}$), 2.26 (s, 3 H, CH$_3^{52}$), 2.17 (t, *J* = 7.4 Hz, 1 H, CH$_2^{23b}$), 1.74 – 1.61 (m, 4 H, CH$_2^{15,64}$), 1.55 – 1.44 (m, 4 H, CH$_2^{24}$), 1.35 – 1.33 (m, 6 H, CH$_2^{4,9}$), 1.31 – 1.14 (m, 68 H, CH$_2$), 0.90 – 0.79 (m, 9 H, CH$_3^{39,76,77}$).

^{13}C-NMR (126 MHz, DMSO-d_6): δ [ppm] = 174.50 (s, CO$_2$R^{21}), 172.40 (s, CONR^{11}), 169.13 (s, CO$_2$R^{60}), 169.11 (s, CO$_2$R^{60}), 169.02 (s, CONR^{1}), 168.61 (s, CONR^{1}), 165.24 (s, CO$_2$R^{55}), 165.21 (s, CO$_2$R^{55}), 152.48 (s, CO^{46}), 152.22 (s, CO^{46}), 149.53 (s, C^{41}), 149.37 (s, C^{41}), 140.91 (s, C$_{Ar}^{51}$), 140.73 (s, C$_{Ar}^{51}$), 136.60 (s, C$_{Ar}^{48}$), 136.20 (s, C$_{Ar}^{70}$), 128.93 (s, CH$_{Ar}^{50,53}$), 128.88 (s, CH$_{Ar}^{50,53}$), 128.28 (s, CH$_{Ar}$), 127.82 (s, CH$_{Ar}$), 127.68 (s, CH$_{Ar}$), 127.67 (s, CH$_{Ar}$), 126.47 (s, CH$_{Ar}^{49,54}$), 126.37 (s, CH$_{Ar}^{49,54}$), 102.93 (s, C^{43}), 74.12 (s, CH^{63}), 74.03 (s, CH^{63}), 73.06 (s, CH^{13}), 65.28 (s, CH$_2^{58}$), 52.79 (s, CH^{44}), 52.56 (s, CH^{44}), 44.15 (s, CH$_2^{59}$), 43.94 (s, CH$_2^{59}$), 43.01 (s, CH), 38.19 (s, CH$_2^{4,9}$), 38.10 (s, CH$_2^{4,9}$), 33.67 (s, CH$_2^{23}$), 33.45 (s, CH$_2^{23}$), 31.45 (s, CH$_2^{15,64}$), 31.32 (s, CH$_2$), 31.18 (s, CH$_2$), 31.14 (s, CH$_2$), 29.05 (s, CH$_2$), 28.94 (s, CH$_2$), 28.73 (s, CH$_2$), 28.52 (s, CH$_2$), 28.39 (s, CH$_2$), 25.84 (s, CH$_2$), 24.56 (s, CH$_2$), 24.51 (s, CH$_2$), 24.43 (s, CH$_2$), 24.38 (s, CH$_2$), 22.12 (s, CH$_2$), 22.09 (s, CH$_2^{24}$), 20.66 (s, CH$_3^{52}$), 15.65 (s, CH$_3^{42}$), 15.62 (s, CH$_3^{42}$), 13.95 (s, CH$_3^{39,76,77}$), 13.92 (s, CH$_3^{39,76,77}$).

FAB – MS [*m/z*] (relative intensity): 1071.9 (10%) [M + H]$^+$, 335.1 (20%) [Fragment A]$^+$.

HRMS – FAB [*m/z*]: $[M + H]^+$ calculated for $^{12}C_{64}{}^{1}H_{103}{}^{16}O_{9}{}^{14}N_{4}$, 1071.76468; found, 1071.7720; Δ = 0.28 mmu.

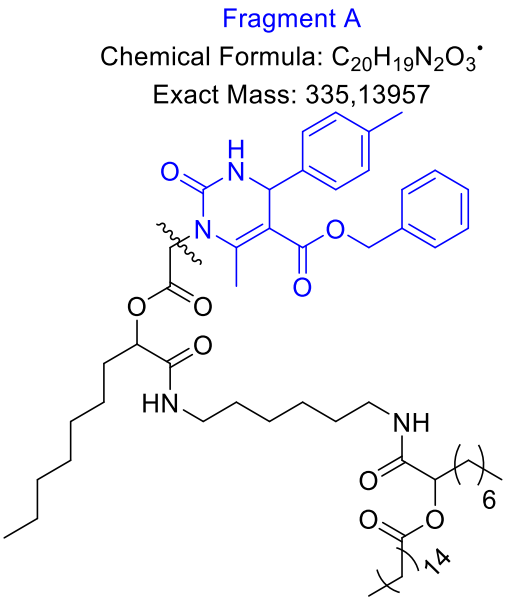

6.2.3.5.13 ***Benzyl ester 120 derived from monomer-NC 95, stearic acid and octanal***

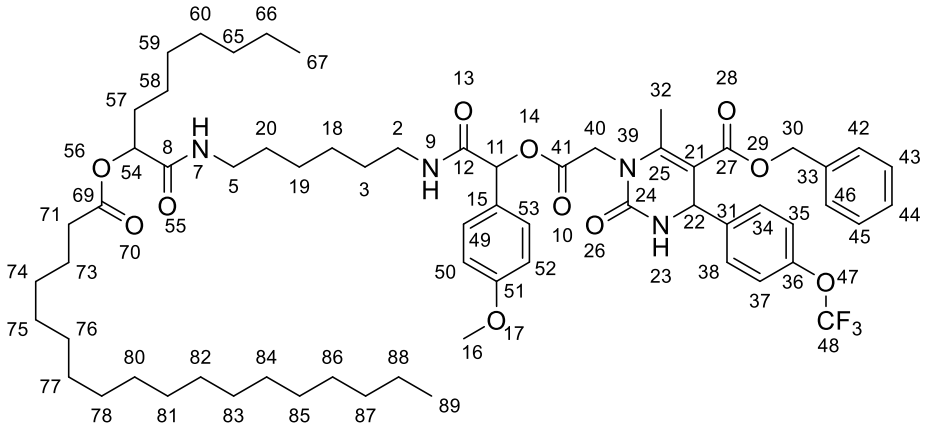

In a 10 mL round bottom flask the monomer-NC **95** (300 mg, 407 µmol, 1.00 eq.) was stirred in 3 mL dichloromethane, subsequently octanal (104 mg, 814 µmol, 2.00 eq.), stearic acid (173 mg, 610 µmol, 1.50 eq.) and one droplet of dimethyl sulfoxide were added. The resulting reaction mixture was degassed with argon and stirred at room temperature for 7 d under argon atmosphere. The crude mixture was dried under reduced pressure. The residue was adsorbed onto celite® and purified *via* column chromatography on silica gel eluting with a gradual solvent mixture of ethyl acetate and

c-hexane (1:3 → 2:1) and dried under reduced pressure to yield the Passerini product **120** as a colorless solid (333 mg, 289 µmol, 71.2%).

R_f in ethyl acetate/*c*-hexane (2:1) = 0.71. Visualized *via* fluorescence quench and Seebach staining solution.

IR (ATR): ν [cm^{-1}] = 3306.9 (br, ν(N-H)), 2924.0 (s, ν(C-H)), 2853.9 (m, ν(C-H)), 1740.1 (s, ν(C=O)), 1684.5 (vs, ν(C=O)), 1540.0 (m), 1513.6 (s), 1456.5 (m), 1374.4 (w), 1306.0 (vs), 1253.8 (vs), 1218.8 (vs), 1166.5 (vs), 1106.5 (s), 1042.7 (s), 833.6 (w), 752.8 (w), 697.2 (w), 634.2 (m), 529.2 (w), 433.9 (w).

^{1}H-NMR (400 MHz, DMSO-d_6): δ [ppm] = 8.21 (d, J = 3.7 Hz, 1 H, NH^{23}), 8.17 (t, J = 3.3 Hz, 1 H, NH^{9}), 7.88 (q, J = 5.6 Hz, 1 H, NH^{7}), 7.46 – 7.07 (m, 11 H, CH$_{Ar}$), 6.92 (d, J = 8.7 Hz, 2 H, CH$_{Ar}$), 5.83 (d, J = 8.9 Hz, 1 H, CH^{11}), 5.24 (t, J = 3.7 Hz, 1 H, CH^{21}), 5.16 – 4.94 (m, 2 H, CH$_2^{30}$), 4.87 – 4.47 (m, 3 H, CH$_2^{40}$ + CH^{54}), 3.74 (s, 3 H, OCH$_3^{16}$), 3.11 – 2.90 (m, 4 H, CH$_2^{2+5}$), 2.46 (d, J = 5.3 Hz, 3 H, CH$_3^{32}$), 2.33 (t, J = 7.2 Hz, 2 H, CH$_2^{71}$), 1.64 (s, 2 H, CH$_2^{57}$), 1.58 – 1.44 (m, 2 H, CH$_2^{73}$), 1.37 – 1.19 (m, 42 H, CH$_2$), 0.86 – 0.76 (m, 6 H, CH$_3^{67+89}$).

^{13}C-NMR (101 MHz, DMSO-d_6) δ [ppm] = 172.40 (s, CO$_2$R^{69}), 169.12 (s, CO$_2$R^{41}), 168.94 (s, CO$_2$R^{41}), 168.88 (s, CONR^{8}), 167.53 (s, CONR^{12}), 165.01 (s, CO$_2$R^{30}), 159.58 (s, C$_{Ar}^{51}$), 159.54 (s, C$_{Ar}^{51}$), 151.92 (s, CO^{26}), 151.82 (s, CO^{26}), 150.21 (s, C^{25}), 150.02 (s, C^{25}), 147.53 (s, OCF$_3^{48}$), 143.23 (s, C$_{Ar}^{31}$), 143.07 (s, C$_{Ar}^{31}$), 136.16 (s, C$_{Ar}^{33}$), 136.14 (s, C$_{Ar}^{33}$), 128.96 (s, CH$_{Ar}$), 128.86 (s, CH$_{Ar}$), 128.57 (s, CH$_{Ar}$), 128.46 (s, CH$_{Ar}$), 128.22 (s, CH$_{Ar}$), 127.83 (s, CH$_{Ar}$), 127.68 (s, CH$_{Ar}$), 127.64 (s, CH$_{Ar}$), 127.46 (s, CH$_{Ar}$), 127.34 (s, CH$_{Ar}$), 120.98 (s, CH$_{Ar}$), 113.78 (s, CH$_{Ar}$), 102.35 (s, C^{21}), 102.20 (s, C^{21}), 75.64 (s, CH^{11}), 75.49 (s, CH^{11}), 73.06 (s, CH^{54}), 65.33 (s, CH$_2^{30}$), 55.13 (s, OCH$_3^{16}$), 55.11 (s, OCH$_3^{16}$), 52.62 (s, CH^{21}), 52.46 (s, CH^{21}), 43.96 (s, CH$_2^{40}$), 43.83 (s, CH$_2^{40}$), 39.20 (s, CH$_2^{2 \text{ or } 5}$), 38.29 (s, CH$_2^{2 \text{ or } 5}$), 38.11 (s, CH$_2^{2 \text{ or } 5}$), 33.45 (s, CH$_2^{71}$), 31.44 (s, CH$_2$), 31.30 (s, CH$_2$), 31.15 (s, CH$_2$), 29.03 (s, CH$_2$), 29.01 (s, CH$_2$), 28.97 (s, CH$_2$), 28.90 (s, CH$_2$), 28.86 (s, CH$_2$), 28.71 (s, CH$_2$), 28.69 (s, CH$_2$), 28.56 (s, CH$_2$), 28.52 (s, CH$_2$), 28.38 (s, CH$_2$), 25.80 (s, CH$_2$), 25.75 (s, CH$_2$), 24.56 (s, CH$_2$), 24.43 (s, CH$_2$), 22.10 (s, CH$_2$), 22.07 (s, CH$_2$), 20.77, 15.69 (s, CH$_3^{32}$), 15.66 (s, CH$_3^{32}$), 13.94 (s, CH$_3^{67 \text{ or } 89}$), 13.91 (s, CH$_3^{67 \text{ or } 89}$).

^{19}F-NMR (376 MHz, DMSO-d_6) δ [ppm] = -61.19 (s, CF$_3^{48a}$), -61.21 (s, CF$_3^{48b}$).

ESI – MS [*m/z*]: $[M + Na]^+$ calculated for $^{12}C_{64}{}^{1}H_{91}{}^{16}O_{11}{}^{14}N_4{}^{19}F_3{}^{23}Na_1$, 1171.6529; found, 1171.6543; Δ = 1.43 mmu.

6.2.3.5.14 ***Benzyl ester 121 derived from monomer-NC 96, stearic acid and octanal***

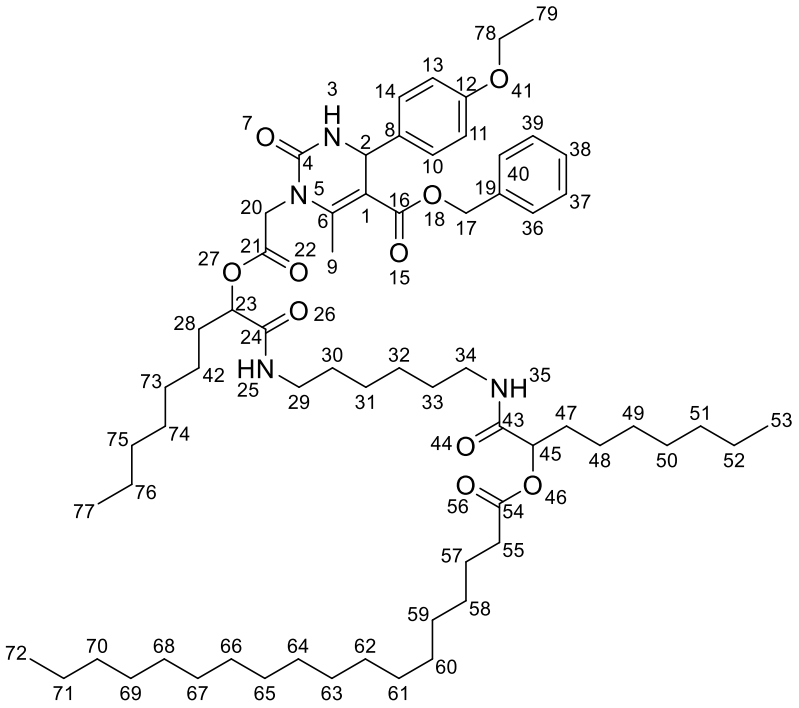

The monomer-NC **96** (100 mg, 145 µmol, 1.00 eq.) was stirred in 0.6 mL dichloromethane in a 10 mL round bottom flask, subsequently octanal (37.2 mg, 290 µmol, 2.00 eq.) and stearic acid (61.9 mg, 218 µmol, 1.50 eq.) were added. The resulting reaction mixture was degassed with argon and stirred at room temperature for 2 d. The crude mixture was dried under reduced pressure. The residue was purified *via* column chromatography on silica gel eluting with a gradual solvent mixture of ethyl acetate and *c*-hexane (0:1 → 1:1) and dried *in vacuo* to yield the benzyl ester **121** as a colorless oil (82.7 mg, 75.1 µmol, 51.7%).

R_f = 0.69 in *c*-hexane/ethyl acetate (2:3). Visualized *via* fluorescence quench and Seebach staining solution.

IR (ATR) ν [cm^{-1}] = 3288.8 (br, ν(N-H)), 3105.8 (br, $\nu(CO_2H)$), 2953.5 (m, ν(C-H)), 2920.6 (vs, ν(C-H)), 2850.7 (s, ν(C-H)), 1738.0 (m, ν(C=O)), 1709.2 (m, ν(C=O)), 1686.5 (vs, ν(C=O)), 1657.8 (vs, ν(C=O)), 1626.9 (m, ν(C=O)), 1610.4 (m, ν(C=O)), 1583.7 (w), 1540.5 (m), 1509.7 (m), 1456.3 (m), 1441.8 (m), 1415.0 (w), 1378.0 (m),

1328.7 (w), 1306.0 (m), 1281.4 (m), 1244.3 (s), 1205.3 (s), 1170.3 (vs), 1147.7 (m), 1106.5 (s), 1044.8 (m), 983.1(w), 962.5 (w), 939.9 (w), 925.5 (w), 886.4 (vw), 857.6 (vw), 847.4 (w), 824.7 (w), 800.1 (vw), 785.7 (w), 758.9 (w), 721.9 (m), 697.2 (m), 678.7 (w), 652.0 (w), 612.9 (vw), 592.3 (w), 580.0 (w), 559.4 (vw), 532.7 (w), 503.9 (w), 442.2 (vw), 425.7 (vw).

^{1}H-NMR (400 MHz, DMSO-d_6) δ [ppm] = 8.10 (dd, J = 22.3, 3.5 Hz, 1 H, NH^{3}), 7.98 – 7.82 (m, 2 H, NH^{25,35}), 7.33 – 7.23 (m, 3 H, CH_{Ar}), 7.22 – 7.06 (m, 4 H, CH_{Ar}), 6.89 – 6.72 (m, 2 H, CH_{Ar}), 5.19 – 5.12 (m, 1 H, CH^{2}), 5.10 – 4.99 (m, 2 H, CH_2^{17}), 4.95 – 4.86 (m, 1 H, CH^{23}), 4.81 (t, J = 6.3 Hz, 1 H, CH^{45}), 4.77 – 4.42 (m, 2 H, CH_2^{20}), 3.98 (q, J = 6.9 Hz, 2 H, CH_2^{78}), 3.14 – 2.88 (m, 4 H, CH_2^{29,34}), 2.43 (d, J = 10.9 Hz, 3 H, CH_3^{9}), 2.33 (t, J = 7.2 Hz, 2 H, CH_2^{55a}), 2.17 (t, J = 7.4 Hz, 2 H, CH_2^{55b}),1.69 (dd, J = 15.4, 7.8 Hz, 4 H, CH_2), 1.48 (dd, J = 15.8, 7.2 Hz, 4 H, CH_2), 1.41 – 1.33 (m, 4 H, CH_2), 1.30 (s, J = 7.1 Hz, 3 H, CH_3^{79}), 1.26 – 1.13 (m, 52 H, CH_2,), 0.87 – 0.78 (m, 9 H, CH_3^{53,72,77}).

^{13}C-NMR (101 MHz, DMSO-d_6) δ [ppm] = 174.45 (s, CO_2R^{54}), 172.34 (s, CO_2R^{21}), 169.12 (s, CONR^{24}), 169.03 (s, CONR^{24}), 168.60 (s, CONR^{43}), 165.26 (s, CO_2Bn^{16}), 165.22 (s, CO_2Bn^{16}), 157.89 (s, COEt^{12}), 152.42 (s, C^{4}), 152.16 (s, C^{4}), 149.32 (s, C^{6}), 149.15 (s, C^{6}), 136.22 (s, C_{Ar}^{19}), 135.89 (C_{Ar}^{8}), 135.70 (C_{Ar}^{8}), 128.26 (s, CH_{Ar}), 127.79 (s, CH_{Ar}), 127.69 (s, CH_{Ar}), 127.65 (s, CH_{Ar}), 127.63 (s, CH_{Ar}), 114.15 (s, CH_{Ar}), 114.10 (s, CH_{Ar}), 103.13 (s, C^{1}), 103.08 (s, C^{1}), 74.11 (s, CH^{23}), 74.04 (s, CH^{23}), 73.05 (s, CH^{45}), 65.25 (s, CH_2^{17}), 62.95 (s, CH_2^{78}), 52.60 (s, CH^{2}), 52.35 (s, CH^{2}), 44.15 (s, CH_2^{20}), 43.90 (s, CH_2^{20}), 38.19 (s, $CH_2$$^{29\ or\ 34}$), 38.10 (s, $CH_2$$^{29\ or\ 34}$), 33.66 (s, CH_2^{55}), 33.46 (s, CH_2^{55}), 31.18 (s, CH_2), 31.14 (s, CH_2), 29.05 (s, CH_2), 28.93 (s, CH_2), 28.78 (s, CH_2), 28.73 (s, CH_2), 28.59 (s, CH_2), 28.55 (s, CH_2), 28.40 (s, CH_2), 25.83 (s, CH_2), 24.56 (s, CH_2), 24.51 (s, CH_2), 24.43 (s, CH_2), 24.37 (s, CH_2), 22.11 (s, CH_2), 22.08 (s, CH_2), 22.05 (s, CH_2), 20.75 (s, CH_2), 15.64 (s, CH_3^{9}), 15.61 (s, CH_3^{9}), 14.62 (s, CH_3^{79}), 14.08 (s, $CH_3$$^{53\ or\ 72\ or\ 77}$), 13.91 (s, $CH_3$$^{53\ or\ 72\ or\ 77}$), 13.89 (s, $CH_3$$^{53\ or\ 72\ or\ 77}$).

ESI–MS (*m/z*): $[M + Na]^+$ calculated for $^{12}C_{65}{}^{1}H_{104}{}^{16}O_{10}{}^{14}N_4{}^{23}Na_1$, 1123.7645; found, 1123.7674; Δ = 2.90 mmu.

6.2.3.5.15 *Benzyl ester 122 derived from monomer-NC 97, stearic acid and octanal*

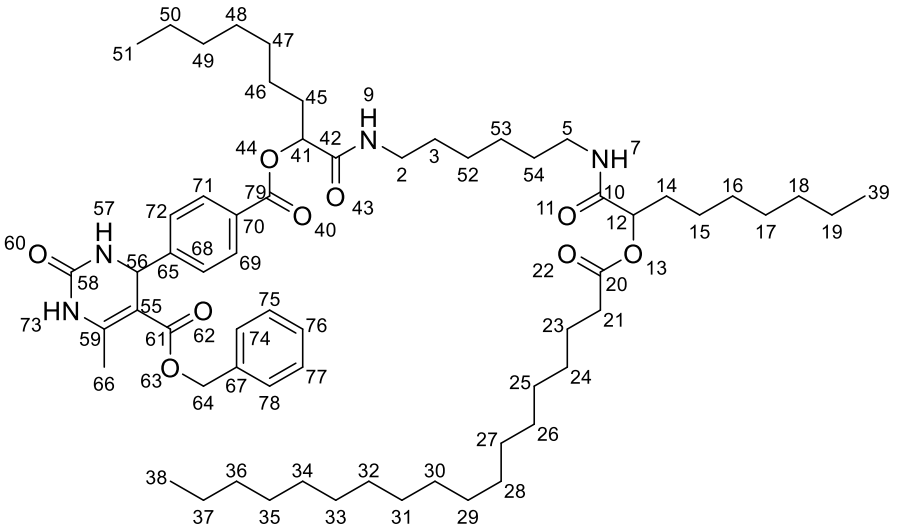

In a 10 mL round bottom flask the monomer-NC **97** (100 mg, 159 µmol, 1.00 eq.) was stirred in 1 mL dichloromethane, subsequently octanal (40.7 mg, 317 µmol, 2.00 eq.) and stearic acid (90.2 mg, 317 µmol, 2.00 eq.) were added. The resulting reaction mixture was degassed with argon and stirred at room temperature for 4 d. The crude mixture was dried under reduced pressure. The residue was adsorbed onto celite® and purified *via* column chromatography on silica gel eluting with a gradual solvent mixture of ethyl acetate and *c*-hexane (1:2 → 1:1). The benzyl ester **122** was obtained as a colorless solid (143 mg, 137 µmol, 78.6%).

R_f in ethyl acetate/*c*-hexane (1:1) = 0.48. Visualized *via* fluorescence quench and Seebach staining solution.

IR (ATR): ν [cm^{-1}] = 3286.5 (br, ν(N-H)), 3097.2 (w, ν(N-H)), 2922.5 (vs, ν(C-H)), 2853.0 (s, ν(C-H)), 1702.1 (vs, ν(C=O)), 1651.3 (vs, ν(C=O)), 1539.1 (m), 1455.8 (m), 1378.0 (m), 1264.3 (s), 1220.0 (vs), 1178.3 (m), 1088.1 (vs), 1018.3 (m), 861.6 (w), 824.1 (m), 753.8 (m), 696.8 (m), 658.4 (m), 527.3 (w), 493.7 (w).

^{1}H-NMR (500 MHz, DMSO-d_6): δ [ppm] = 9.35 (d, J = 1.9 Hz, 1 H, NH^{73}), 8.02 (t, J = 5.8 Hz, 1 H, NH^{9}), 7.95 – 7.88 (m, 3 H, CH$_{Ar}^{69,71}$ + NH^{7}), 7.86 (m, 1 H, NH^{57}), 7.38 – 7.31 (m, 2 H, CH$_{Ar}^{68,72}$), 7.30 – 7.22 (m, 3 H, CH$_{Ar}^{75-78}$), 7.16 – 7.10 (m, 2 H, CH$_{Ar}^{75-78}$), 5.25 (d, J = 3.3 Hz, 1 H, CH^{56}), 5.10 – 4.97 (m, 3 H, CH$_2^{64}$ + CH^{41}), 4.81 (t, J = 6.3 Hz, 1 H, CH^{12}), 3.13 – 2.94 (m, 4 H, CH$_2^{2+5}$), 2.33 (t, J = 7.3 Hz, 2 H, CH$_2^{21}$), 2.28 (s, 3 H, CH$_3^{66}$), 1.85 – 1.78 (m, 2 H, CH$_2^{45}$), 1.69 – 1.62 (m, 2 H, CH$_2^{14}$), 1.56 – 1.48 (m, 2 H,

CH_2^{23}), 1.43 – 1.32 (m, 8 H, $CH_2^{3,52-54}$), 1.32 – 1.14 (m, 58 H, CH_2), 0.87 – 0.81 (m, 9 H, $CH_3^{38\,+\,39\,+\,51}$).

^{13}C-NMR (126 MHz, DMSO-d_6) δ [ppm] = 172.34 (s, CO_2R^{20}), 169.11 (s, $CONR^{10\ or\ 42}$), 168.93 (s, $CONR^{10\ or\ 42}$), 164.87 (s, CO_2R^{61}), 151.76 (s, CO^{58}), 149.93 (s, $C_{Ar}^{65\ or\ 70}$), 149.92 (s, $C_{Ar}^{65\ or\ 70}$), 149.83 (s, $C_{Ar}^{65\ or\ 70}$), 149.81 (s, $C_{Ar}^{65\ or\ 70}$), 136.43 (s, C_{Ar}^{67}), 129.76 (s, $CH_{Ar}^{69,71}$), 128.55 (s, CH_{Ar}), 128.24 (s, CH_{Ar}), 128.22 (s, CH_{Ar}), 127.68 (s, CH_{Ar}), 127.64 (s, CH_{Ar}), 127.60 (s, CH_{Ar}), 126.59 (s, $CH_{Ar}^{68,72}$), 98.06 (s, C^{55}), 73.96 (s, CH^{41}), 73.06 (s, CH^{12}), 64.86 (s, CH_2^{64}), 53.83 (s, CH^{56}), 38.19 (s, CH_2), 38.09 (s, CH_2), 33.46 (s, CH_2), 31.59 (s, CH_2), 31.45 (s, CH_2), 31.33 (s, CH_2), 31.20 (s, CH_2), 31.19 (s, CH_2), 29.06 (s, CH_2), 28.99 (s, CH_2), 28.94 (s, CH_2), 28.74 (s, CH_2), 28.64 (s, CH_2), 28.59 (s, CH_2), 28.57 (s, CH_2), 28.41 (s, CH_2), 25.89 (s, CH_2), 25.86 (s, CH_2), 24.60 (s, CH_2), 24.57 (s, CH_2), 24.44 (s, CH_2), 22.12 (s, CH_2), 22.09 (s, CH_2), 17.89 (s, CH_3^{66}), 13.92 (s, $CH_3^{38\,+\,39\,+\,51}$), 13.91 (s, $CH_3^{38\,+\,39\,+\,51}$).

ESI–MS [*m/z*]: $[M + Na]^+$ calculated for $^{12}C_{62}{}^{1}H_{98}{}^{16}O_9{}^{14}N_4{}^{23}Na_1$, 1065.7226; found, 1065.7230; Δ = 0.42 mmu.

6.2.3.6 Carboxylic acids

6.2.3.6.1 *Carboxylic acid 123 derived from benzyl ester 108 via hydrogenolytic deprotection*

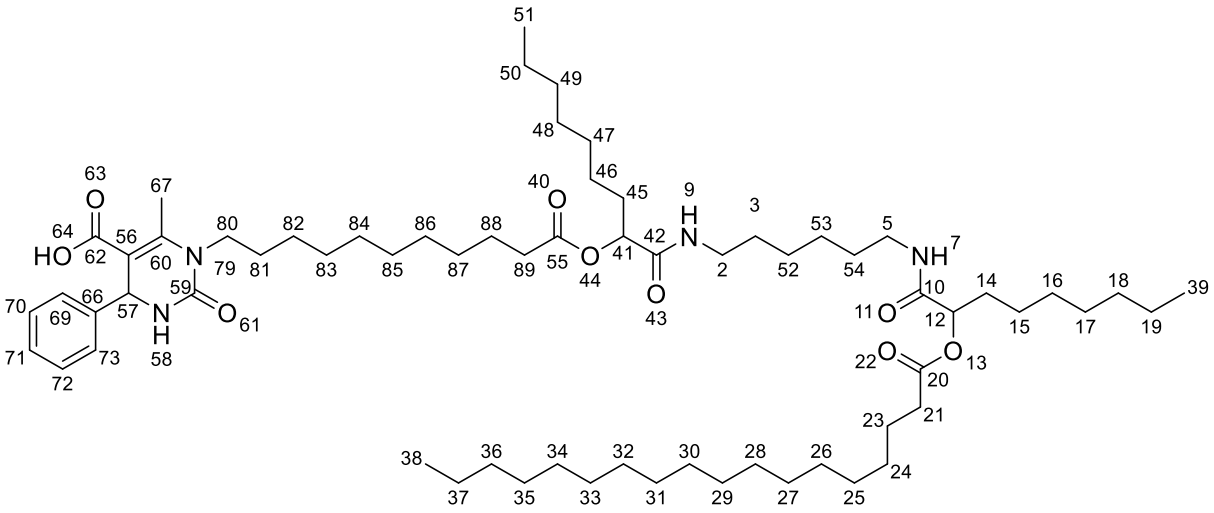

In a 5 mL round bottom flask equipped with a magnetic stir bar the benzyl ester **108** (67.7 mg, 57.2 µmol, 1.00 eq.) was dissolved in 2.00 mL ethyl acetate. Subsequently,

palladium on activated charcoal (20% Pd, 20.0 mg) was added to the solution. The solution was purged with hydrogen gas for 5 minutes and stirred for 1 d at room temperature under hydrogen atmosphere (balloon). TLC indicated complete conversion of the benzyl ester **108**. The crude reaction mixture was filtered over celite® and flushed with 20 mL ethyl acetate three times and with 20 mL dichloromethane twice. After concentration under reduced pressure and drying in high vacuum the carboxylic acid **123** was obtained as a colorless solid (62.0 mg, 56.7 µmol, 99.2%).

IR (ATR): ν [cm^{-1}] = 3267.7 (br, ν(N-H)), 2919.5 (vs, ν(C-H)), 2850.9 (s, ν(C-H)), 1743.9 (m, ν(C=O)), 1656.7 (vs, ν(C=O)), 1541.2 (m), 1464.1 (m), 1385.1 (m), 1193.1 (m), 1163.6 (s), 1091.6 (m), 759.5 (w), 721.6 (m), 696.6 (m), 621.4 (w), 514.2 (w), 458.8 (w).

^{1}H-NMR (500 MHz, DMSO-d_6): δ [ppm] = 12.22 (s, 1 H, CO_2H^{64}), 7.92 – 7.78 (m, 3 H, $NH^{7 + 9 + 58}$), 7.35 – 7.16 (m, 5 H, CH_{Ar}^{70-73}), 5.14 (d, J = 3.7 Hz, 1 H, CH^{57}), 4.82 (t, J = 6.2 Hz, 2 H, $CH^{12 + 41}$), 3.92 – 3.28 (m, 2 H, CH_2^{80}), 3.09 – 2.94 (m, 4 H, $CH_2^{14 + 45}$), 2.47 (s, 3 H, CH_3^{67}), 2.32 (q, J = 6.9 Hz, 4 H, $CH_2^{21 + 89}$), 1.65 (dq, J = 10.3, 6.4 Hz, 4 H, $CH_2^{2 + 5}$), 1.50 (q, J = 7.4 Hz, 4 H, CH_2), 1.35 (t, J = 6.7 Hz, 4 H, CH_2), 1.30 – 1.05 (m, 71 H, CH_2), 0.83 (t, J = 6.7 Hz, 9 H, $CH_3^{38 + 39 + 51}$).

^{13}C-NMR (126 MHz, DMSO-d_6) δ [ppm] = 172.28 (s, $CO_2R^{20 \text{ or } 55}$), 172.18 (s, $CO_2R^{20 \text{ or } 55}$), 169.12 (s, $CONR^{42 \text{ or } 10}$), 169.10 (s, $CONR^{42 \text{ or } 10}$), 167.54 (s, CO_2H^{64}), 153.04 (s, CO^{59}), 148.54 (s, C^{60}), 144.08 (s, C_{Ar}^{66}), 128.18 (s, CH_{Ar}), 127.03 (s, CH_{Ar}), 126.05 (s, CH_{Ar}), 104.18 (s, C^{56}), 73.05 (s, $CH^{12 \text{ or } 41}$), 73.04 (s, $CH^{12 \text{ or } 41}$), 52.35 (s, CH^{57}), 41.39 (s, CH_2^{80}), 38.00 (s, $CH_2^{14 + 45}$), 33.49 (s, $CH_2^{21 \text{ or } 89}$), 33.45 (s, $CH_2^{21 \text{ or } 89}$), 31.49 (s, $CH_2^{2 \text{ or } 5}$), 31.40 (s, $CH_2^{2 \text{ or } 5}$), 31.25 (s, CH_2), 31.23 (s, CH_2), 29.50 (s, CH_2), 29.16 (s, CH_2), 29.14 (s, CH_2), 29.03 (s, CH_2), 28.99 (s, CH_2), 28.95 (s, CH_2), 28.83 (s, CH_2), 28.64 (s, CH_2), 28.50 (s, CH_2), 26.25 (s, CH_2), 25.73 (s, CH_2), 24.61 (s, CH_2), 24.59 (s, CH_2), 24.45 (s, CH_2), 22.17 (s, CH_2), 22.12 (s, CH_2), 15.50 (s, CH_3^{67}), 13.86 (s, $CH_3^{38 + 39 + 51}$), 13.84 (s, $CH_3^{38 + 39 + 51}$).

ESI–MS [*m/z*]: $[M + Na]^+$ calculated for $^{12}C_{65}H_{112}{}^{16}O_9{}^{14}N_4{}^{23}Na_1$, 1115.8322; found, 1115.8328; Δ = 0.61 mmu.

6.2.3.6.2 *Carboxylic acid 124 derived from benzyl ester 109 via hydrogenolytic deprotection*

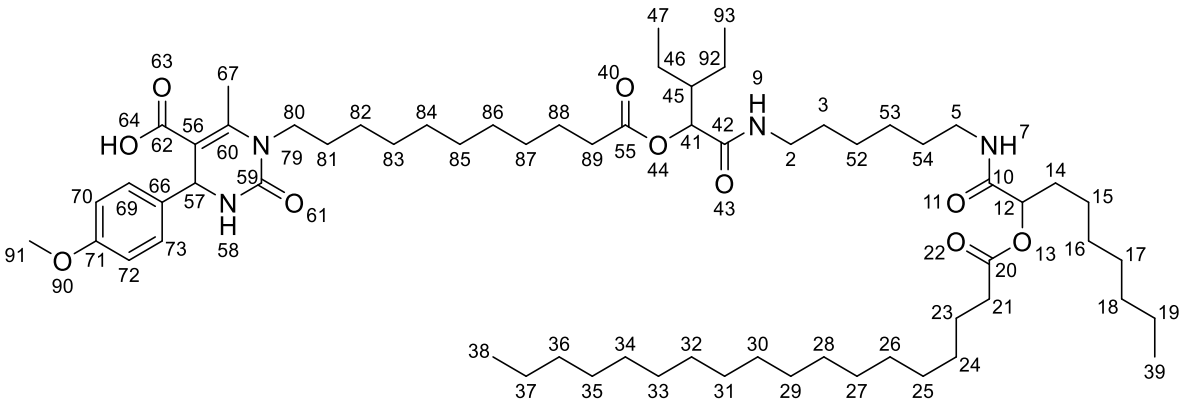

In a 5 mL round bottom flask equipped with a magnetic stir bar the benzyl ester **109** (100 mg, 84.3 µmol, 1.00 eq.) was dissolved in 2.00 mL ethyl acetate. Subsequently, palladium on activated charcoal (20% Pd, 20.0 mg) was added to the solution. The solution was purged with hydrogen gas for 5 minutes and stirred for 1 d at room temperature under hydrogen atmosphere (balloon) while purging the first 4 h every 30 min. TLC indicated complete conversion of the benzyl ester **109**. The crude reaction mixture was filtered over celite® and flushed with 20 mL ethyl acetate three times and with 20 mL dichloromethane twice. After concentration under reduced pressure and drying in high vacuum the carboxylic acid **124** was obtained as a colorless solid (89.0 mg, 83.5 µmol, 98.9%).

IR (ATR): ν [cm^{-1}] = 3272.1 (br, ν(N-H, CO_2H)), 2919.2 (vs, ν(C-H)), 2850.4 (s, ν(C-H)), 1744.2 (s, ν(C=O)), 1657.5 (vs, ν(C=O)), 1537.9 (m), 1510.9 (m), 1463.8 (m), 1382.9 (m), 1248.3 (s), 1164.1 (vs), 1091.3 (m), 1037.0 (w), 937.7 (w), 793.5 (w), 756.5 (w), 721.3 (w), 618.7 (w), 591.3 8 (w), 502.1 (w).

^{1}H-NMR (400 MHz, DMSO-d_6): δ [ppm] = 12.18 (br s, 1 H, CO_2H^{64}), 7.92 – 7.84 (m, 2 H, NH^{7+9}), 7.76 (d, J = 3.8 Hz, 1 H, NH^{58}), 7.12 (d, J = 8.7 Hz, 2 H, $CH_{Ar}^{66,73}$), 6.84 (d, J = 8.7 Hz, 2 H, $CH_{Ar}^{70,72}$), 5.07 (d, J = 3.7 Hz, 1 H, CH^{57}), 4.91 (d, J = 4.2 Hz, 1 H, CH^{41}), 4.81 (dd, J = 7.0, 5.9, 5.5 Hz, 1 H, CH^{12}), 3.90 – 3.76 (m, 1 H, CH_2^{80a}), 3.70 (s, 3 H, OCH_3^{91}), 3.61 – 3.14 (underneath water peak, CH_2^{80b}), 3.11 – 2.93 (m, 4 H, CH_2^{2+5}), 2.46 (s, 3 H, CH_3^{67}), 2.35 (dt, J = 12.8, 7.2 Hz, 4 H, CH_2^{21+89}), 1.75 – 1.59 (m, 3 H, CH_2^{14}+CH^{45}), 1.58 – 1.47 (m, 4 H, CH_2^{23+88}), 1.43 – 1.32 (m, 4 H, CH_2^{3+54}), 1.31 – 1.02 (m, 64 H, CH_2), 0.90 – 0.74 (m, 12 H, $CH_3^{38+39+47,93}$).

^{13}C-NMR (101 MHz, DMSO-d_6) δ [ppm] = 172.43 (s, CO_2R^{55}), 172.33 (s, CO_2R^{20}), 169.09 (s, $CONR^{10}$), 168.77 (s, $CONR^{42}$), 167.53 (s, CO_2H^{64}), 158.34 (s, C_{Ar}^{71}), 153.04 (s, CO^{59}), 148.20 (s, C^{60}), 136.15 (s, C_{Ar}^{66}), 127.18 (s, $CH_{Ar}^{66,73}$), 113.52 (s, $CH_{Ar}^{70,72}$), 104.49 (s, C^{56}), 74.02 z(s, CH^{41}), 73.05 (s, CH^{12}), 54.98 (s, OCH_3^{91}), 51.74 (s, CH^{57}), 42.58 (s, CH^{45}), 41.34 (s, CH_2^{80}), 38.10 (s, $CH_2^{2 \text{ or } 5}$), 38.05 (s, $CH_2^{2 \text{ or } 5}$), 33.49 (s, $CH_2^{21 \text{ or } 89}$), 33.43 (s, $CH_2^{21 \text{ or } 89}$), 31.42 (s, CH_2^{14}), 31.29 (s, CH_2), 31.15 (s, CH_2), 29.47 (s, CH_2), 29.01 (s, CH_2), 28.99 (s, CH_2), 28.95 (s, CH_2), 28.94 (s, CH_2), 28.89 (s, CH_2), 28.83 (s, CH_2), 28.70 (s, CH_2), 28.67 (s, CH_2), 28.54 (s, CH_2), 28.42 (s, CH_2), 28.37 (s, CH_2), 26.21 (s, CH_2), 25.81 (s, CH_2), 25.77 (s, CH_2), 24.52 (s, CH_2), 24.42 (s, CH_2), 24.40 (s, CH_2), 22.08 (s, CH_2), 22.05 (s, CH_2), 21.77 (s, CH_2), 21.37 (s, CH_2), 15.48 (s, CH_3^{67}), 13.90 (s, $CH_3^{38 \text{ or } 39}$), 13.88 (s, $CH_3^{38 \text{ or } 39}$), 11.26 (s, $CH_3^{43 \text{ or } 93}$), 11.22 (s, $CH_3^{43 \text{ or } 93}$).

ESI–MS [*m/z*]: $[M + Na]^+$ calculated for $^{12}C_{64}{}^{1}H_{110}{}^{16}O_{10}{}^{14}N_4{}^{23}Na_1$, 1117.8114; found, 1117.8119; Δ = 0.47 mmu.

6.2.3.6.3 *Carboxylic acid 125 derived from benzyl ester 110 via hydrogenolytic deprotection*

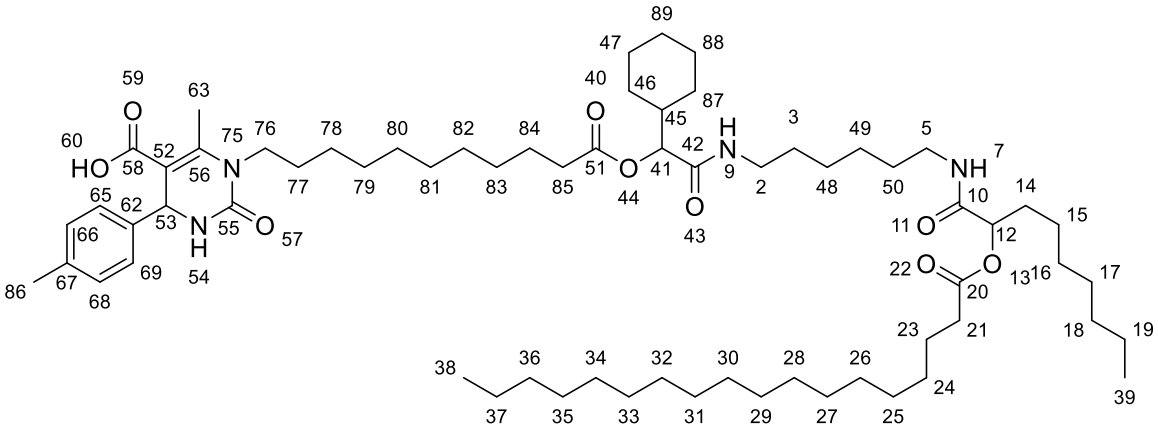

In a 5 mL round bottom flask equipped with a magnetic stir bar the benzyl ester **110** (100 mg, 84.6 µmol, 1.00 eq.) was dissolved in 2.00 mL ethyl acetate. Subsequently, palladium on activated charcoal (20% Pd, 20.0 mg) was added to the solution. The solution was purged with hydrogen gas for 5 minutes and stirred for 1 d at room temperature under hydrogen atmosphere (balloon) while purging every 30 minutes for the first four hours. TLC indicated complete conversion of the benzyl ester **110**. The crude reaction mixture was filtered over celite® and flushed with 20 mL ethyl acetate

three times and with 20 mL dichloromethane twice. After concentration under reduced pressure and drying in high vacuum the carboxylic acid **125** was obtained as a colorless solid (90.8 mg, 83.2 µmol, 98.3%).

IR (ATR): ν [cm^{-1}] = 3305.5 (br, ν(N-H, CO_2H)), 2922.0 (vs, ν(C-H)), 2852.3 (s, ν(C-H)), 1741.0 (s, ν(C=O)), 1660.9 (vs, ν(C=O)), 1537.7 (s), 1453.0 (m), 1385.4 (m), 1166.2 (m), 1092.7 (m), 987.6 (w), 844.3 (w), 762.4 (w), 720.6 (w), 620.3 (w), 585.4 (w), 496.2 (w), 430.2 (w).

^{1}H-NMR (400 MHz, DMSO-d_6): δ [ppm] = 12.13 (s, 1 H, CO_2H^{60}), 7.88 (dt, J = 10.9, 5.8 Hz, 2 H, NH^{7+9}), 7.78 (d, J = 3.9 Hz, 1 H, NH^{54}), 7.16 – 7.01 (m, 4 H, $CH_{Ar}^{65,66,68,69}$), 5.09 (d, J = 3.8 Hz, 1 H, CH^{53}), 4.81 (t, J = 6.3 Hz, 1 H, CH^{12}), 4.66 (d, J = 5.3 Hz, 1 H, CH^{41}), 3.84 (dt, J = 14.7, 7.4 Hz, 1 H, CH_2^{76a}), 3.56 – 3.19 (m, underneath water signal, CH_2^{76b}), 3.12 – 2.92 (m, 4 H, CH_2^{2+5}), 2.46 (s, 3 H, CH_3^{63}), 2.34 (q, J = 7.5 Hz, 4 H, CH_2^{21+85}), 2.24 (s, 3 H, CH_3^{86}), 1.78 – 1.56 (m, 12 H, CH_2), 1.56 – 1.47 (m, 4 H, CH_2), 1.43 – 1.30 (m, 4 H, CH_2), 1.31 – 1.12 (m, 53 H, CH_2), 1.14 – 0.97 (m, 4 H, CH_2), 0.92 – 0.75 (m, 6 H, CH_3^{38+39}).

^{13}C-NMR (101 MHz, DMSO-d_6) δ [ppm] = 172.40 (s, CO_2R^{20}), 172.33 (s, CO_2R^{51}), 169.09 (s, $CONR^{10}$), 168.22 (s, $CONR^{42}$), 167.54 (s, CO_2H^{58}), 153.09 (s, CO^{55}), 148.36 (s, C^{56}), 141.10 (s, C_{Ar}^{62}), 136.10 (s, C_{Ar}^{67}), 128.70 (s, $CH_{Ar}^{65,69}$), 125.92 (s, $CH_{Ar}^{66,68}$), 104.38 (s, C^{52}), 76.98 (s, CH^{41}), 73.05 (s, CH^{12}), 51.98 (s, CH^{53}), 41.32 (s, CH_2^{76}), 38.05 (s, $CH_2^{2 \text{ or } 5}$), 38.02 (s, $CH_2^{2 \text{ or } 5}$), 33.44 (s, $CH_2^{21 \text{ or } 85}$), 33.41 (s, $CH_2^{21 \text{ or } 85}$), 31.29 (s, CH_2), 31.15 (s, CH_2), 29.02 (s, CH_2), 29.00 (s, CH_2), 28.96 (s, CH_2), 28.89 (s, CH_2), 28.70 (s, CH_2), 28.55 (s, CH_2), 27.29 (s, CH_2), 26.20 (s, CH_2), 25.81 (s, CH_2), 25.79 (s, CH_2), 25.78 (s, CH_2), 25.75 (s, CH_2), 25.72 (s, CH_2), 25.53 (s, CH_2), 25.41 (s, CH_2), 24.53 (s, CH_2), 24.41 (s, CH_2), 22.09 (s, CH_2), 20.57 (s, CH_3^{86}), 15.49 15.65 (s, CH_3^{63}), 13.90 (s, $CH_3^{38 \text{ or } 39}$), 13.88 (s, $CH_3^{38 \text{ or } 39}$).

ESI–MS [*m/z*]: $[M + Na]^+$ calculated for $^{12}C_{65}{}^{1}H_{110}{}^{16}O_9{}^{14}N_4{}^{23}Na_1$, 1113.8165; found, 1113.8167; Δ = 0.15 mmu.

6.2.3.6.4 *Carboxylic acid 126 derived from benzyl ester 111 via hydrogenolytic deprotection*

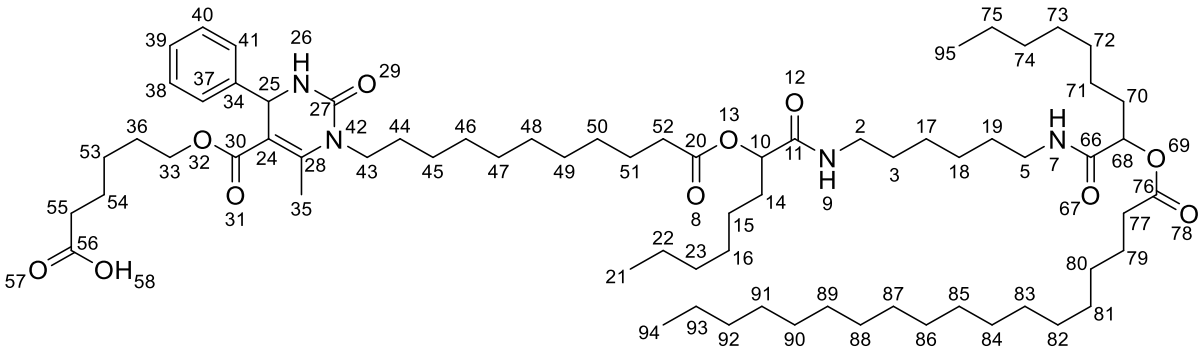

In a 5 mL round bottom flask equipped with a magnetic stir bar the benzyl ester **111** (100 mg, 77.9 µmol, 1.00 eq.) was dissolved in 3.00 mL ethyl acetate. Subsequently, palladium on activated charcoal (20 wt.% Pd, 20.0 mg) was added to the solution. The solution was purged with hydrogen gas for 10 minutes and stirred for 1 d at room temperature under hydrogen atmosphere (balloon). During the first 4 h the mixture was purged for 5 minutes every 30 minutes. TLC indicated complete conversion of the benzyl ester **111**. The crude reaction mixture was filtered over celite® and flushed with 30 mL ethyl acetate three times and with 30 mL dichloromethane three times. After concentration under reduced pressure and drying in high vacuum the carboxylic acid **126** was obtained as a colorless solid (90.3 mg, 75.6 µmol, 97.2%).

IR (ATR): ν [cm^{-1}] = 3272.7 (br, ν(CO_2H, N-H)), 3094.9 (br, ν(N-H)), 2919.0 (vs, ν(C-H)), 2850.2 (s, ν(C-H)), 1741.5 (s, ν(C=O)), 1656.1 (vs, ν(C=O)), 1541.3 (m), 1464.1, 1386.9 (m), 1234.5 (s), 1192.2 (m), 1162.6 (vs), 1090.1 (s), 758.3 (m), 720.9 (m), 698.2 (m).

^{1}H-NMR (500 MHz, DMSO-d_6): δ [ppm] = 8.05 – 7.85 (m, 3 H, NH^{7+9+26}), 7.34 – 7.16 (m, 5 H, CH_{Ar}^{37-41}), 5.13 (d, J = 3.9 Hz, 1 H, CH^{25}), 4.80 (t, J = 6.3 Hz, 2 H, CH^{10+68}), 4.01 – 3.89 (m, 2 H, CH_2^{33}), 4.01 – 3.89 (m, 1 H, CH_2^{43a}), 3.35 (underneath water signal, CH_2^{43b}), 3.13 – 2.95 (m, 4 H, CH_2^{2+5}), 2.49 (s, 3 H, CH_3^{35}), 2.33 (dt, J = 10.6, 5.2 Hz, 4 H, CH_2^{52+77}), 2.09 (t, J = 7.1 Hz, 2 H, CH_2^{55}), 1.71 – 1.57 (m, 4 H, CH_2^{14+70}), 1.56 – 1.29 (m, 16 H, CH_2), 1.31 – 1.06 (m, 70 H, CH_2), 0.83 (t, J = 6.6 Hz, 9 H, $CH_3^{21+94+95}$).

^{13}C-NMR (101 MHz, DMSO-d_6) δ [ppm] = 174.44 (s, CO_2H^{56}), 172.43 (s, $CO_2R^{20\ or\ 76}$), 172.40 (s, $CO_2R^{20\ or\ 76}$), 169.18 (s, $CONR^{11+66}$), 165.64 (s, CO_2R^{30}), 165.13 (s,

CO_2R^{30}), 152.64 (s, CO^{27}), 149.92 (s, C^{28}), 144.00 (s, $C_{Ar}{}^{34}$), 143.81 (s, $C_{Ar}{}^{34}$), 128.36 (s, CH_{Ar}), 127.30 (s, CH_{Ar}), 126.10 (s, CH_{Ar}), 103.16 (s, C^{24}), 102.82 (s, C^{24}), 73.10 (s, CH^{10+68}), 63.55 (s, $CH_2{}^{33}$), 63.39 (s, $CH_2{}^{33}$), 52.44 (s, CH^{25}), 52.12 (s, CH^{25}), 41.57 (s, $CH_2{}^{43}$), 38.05 (s, $CH_2{}^{2+5}$), 33.59 (s, $CH_2{}^{52\text{ or }55\text{ or }77}$), 33.49 (s, $CH_2{}^{52\text{ or }55\text{ or }77}$), 33.47 (s, $CH_2{}^{52\text{ or }55\text{ or }77}$), 31.52 (s, CH_2), 31.50 (s, CH_2), 31.40 (s, CH_2), 31.26 (s, CH_2), 31.21 (s, CH_2), 29.45 (s, CH_2), 29.14 (s, CH_2), 29.08 (s, CH_2), 29.03 (s, CH_2), 29.01 (s, CH_2), 28.97 (s, CH_2), 28.86 (s, CH_2), 28.82 (s, CH_2), 28.80 (s, CH_2), 28.67 (s, CH_2), 28.64 (s, CH_2), 28.50 (s, CH_2), 28.47 (s, CH_2), 28.34 (s, CH_2), 27.92 (s, CH_2), 26.29 (s, CH_2), 25.81 (s, CH_2), 25.78 (s, CH_2), 25.06 (s, CH_2), 24.63 (s, CH_2), 24.58 (s, CH_2), 24.48 (s, CH_2), 24.13 (s, CH_2), 22.20 (s, CH_2), 22.16 (s, CH_2), 22.07 (s, CH_2), 15.61 (s, $CH_3{}^{35}$), 13.99 (s, $CH_3{}^{21\text{ or }94\text{ or }95}$), 13.97 (s, $CH_3{}^{21\text{ or }94\text{ or }95}$), 13.94 (s, $CH_3{}^{21\text{ or }94\text{ or }95}$).

ESI–MS [*m/z*]: $[M + Na]^+$ calculated for $^{12}C_{70}{}^{1}H_{120}{}^{16}O_{11}{}^{14}N_4{}^{23}Na_1$, 1215.8846; found, 1215.8851; Δ = 0.55 mmu.

6.2.3.6.5 *Carboxylic acid 127 derived from benzyl ester 112 via hydrogenolytic deprotection*

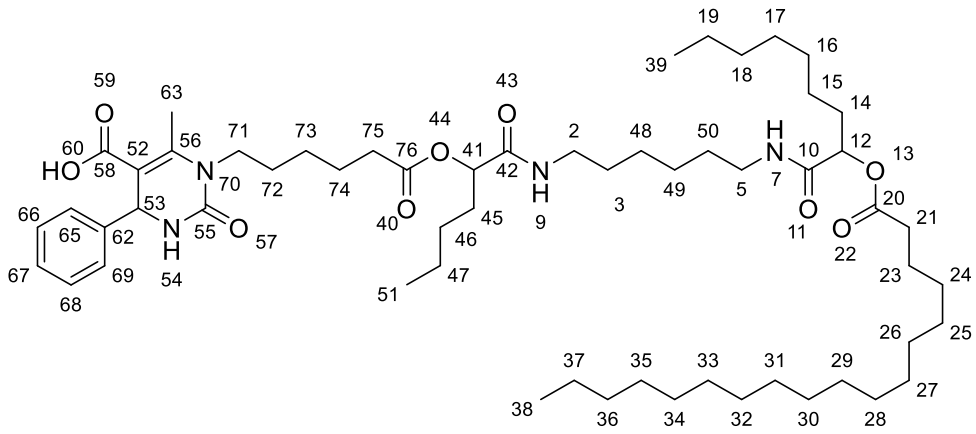

In a 5 mL round bottom flask equipped with a magnetic stir bar the benzyl ester **112** (114 mg, 106 µmol, 1.00 eq.) was dissolved in 2.00 mL ethyl acetate. Subsequently, palladium on activated charcoal (20 wt.% Pd, 22.8 mg) was added to the solution. The solution was purged with hydrogen gas for 10 minutes and stirred for 1 d at room temperature under hydrogen atmosphere (balloon). During the first 4 h the mixture was purged with hydrogen for 5 minutes every 30 minutes. TLC indicated complete conversion of the benzyl ester **112**. The crude reaction mixture was filtered over celite® and flushed with 50 mL ethyl acetate three times and with 50 mL dichloromethane

twice. After concentration under reduced pressure and drying in high vacuum the carboxylic acid **127** was obtained as a colorless solid (103 mg, 104 µmol, 98.7%).

IR (ATR): ν [cm^{-1}] = 3290.3 (br, ν(N-H)), 2922.4 (vs, ν(C-H)), 2853.1 (s, ν(C-H)), 1740.5 (m, ν(C=O)), 1659.8 (vs, ν(C=O)), 1538.4 (m), 1455.9 (m), 1386.3 (m), 1161.8 (vs), 1113.9 (s), 1073.5 (m), 833.0 (w), 759.9 (w), 697.2 (s), 612.6 (w), 515.2 (w).

^{1}H-NMR (400 MHz, DMSO-d_6): δ [ppm] = 12.17 (s, 1 H, CO_2H^{58}), 7.95 – 7.88 (m, 2 H, NH^{7+9}), 7.87 (s, 1 H, NH^{54}), 7.36 – 7.13 (m, 5 H, CH_{Ar}^{65-69}), 5.14 (d, J = 3.8 Hz, 1 H, CH^{53}), 4.87 – 4.77 (m, 2 H, CH^{12+41}), 3.89 – 3.36 (m, 2 H, CH_2^{71}), 3.02 (h, J = 6.7 Hz, 4 H, CH_2^{2+5}), 2.48 (s, 3 H, CH_3^{63}), 2.36 – 2.20 (m, 6 H, $CH_2^{21+72+75}$), 1.76 – 1.59 (m, 4 H, CH_2^{14+45}), 1.58 – 1.41 (m, 4 H, CH_2^{23+74}), 1.42 – 1.32 (m, 4 H, CH_2), 1.22 (s, 56 H, CH_2), 0.89 – 0.75 (m, 9 H, $CH_3^{38+39+51}$).

^{13}C-NMR (101 MHz, DMSO-d_6) δ [ppm] = 172.23 (s, $CO_2R^{20\ or\ 76}$), 172.20 (s, $CO_2R^{20\ or\ 76}$), 169.11 (s, $CONR^{10\ or\ 42}$), 169.08 (s, $CONR^{10\ or\ 42}$), 167.53 (s, CO_2H^{58}), 153.04 (s, CO^{55}), 148.53 (s, C^{56}), 144.10 (s, C_{Ar}^{62}), 128.23 (s, CH_{Ar}), 127.06 (s, CH_{Ar}), 126.08 (s, CH_{Ar}), 104.22 (s, C^{52}), 73.12 (s, $CH^{12\ or\ 41}$), 73.02 (s, $CH^{12\ or\ 41}$), 52.39 (s, CH^{53}), 41.30 (s, CH_2^{71}), 38.11 (s, $CH_2^{2\ +\ 5}$), 33.51 (s, $CH_2^{21\ or\ 75}$), 33.28 (s, $CH_2^{21\ or\ 75}$), 31.49 (s, CH_2), 31.39 (s, CH_2), 31.23 (s, CH_2), 29.15 (s, CH_2), 29.12 (s, CH_2), 29.10 (s, CH_2), 29.02 (s, CH_2), 28.82 (s, CH_2), 28.65 (s, CH_2), 28.62 (s, CH_2), 28.50 (s, CH_2), 26.79 (s, CH_2), 25.86 (s, CH_2), 25.58 (s, CH_2), 24.61 (s, CH_2), 24.47 (s, CH_2), 24.05 (s, CH_2), 22.16 (s, CH_2), 22.12 (s, CH_2), 21.82 (s, CH_2), 15.49 (s, CH_3^{63}), 13.84 (s, $CH_3^{38\ or\ 39\ or\ 51}$), 13.76 (s, $CH_3^{38\ or\ 39\ or\ 51}$).

ESI – MS [*m/z*]: $[M + Na]^+$ calculated for $^{12}C_{57}{}^{1}H_{96}{}^{16}O_9{}^{14}N_4{}^{23}Na_1$, 1003.7070; found, 1003.7072; Δ = 0.26 mmu.

6.2.3.6.6 *Carboxylic acid 128 derived from benzyl ester 113 via hydrogenolytic deprotection*

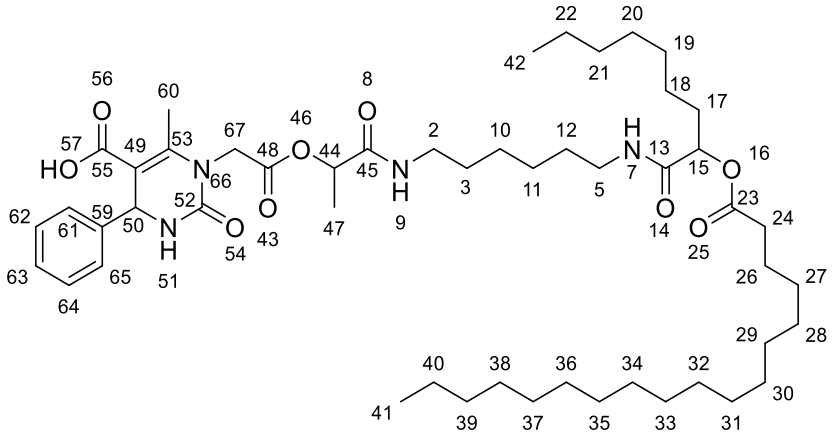

In a 5 mL round bottom flask equipped with a magnetic stir bar the benzyl ester **113** (150 mg, 154 µmol, 1.00 eq.) was dissolved in 2.00 mL ethyl acetate. Subsequently, palladium on activated charcoal (20 wt.% Pd, 30.0 mg) was added to the solution. The solution was purged with hydrogen gas for 10 minutes and stirred for 1 d at room temperature under hydrogen atmosphere (balloon). During the first 4 h the mixture was purged for 5 minutes every 30 minutes. TLC indicated complete conversion of the benzyl ester **113**. The crude reaction mixture was filtered over celite® and flushed with 20 mL ethyl acetate three times and with 20 mL dichloromethane twice. After concentration under reduced pressure and drying in high vacuum the carboxylic acid **128** was obtained as a colorless solid (134 mg, 151 µmol, 98.5%).

IR (ATR): ν [cm^{-1}] = 3296.7 (br, ν(N-H)), 2918.7 (vs, ν(C-H)), 2850.6 (s, ν(C-H)), 1744.9 (s, ν(C=O)), 1660.0 (vs, ν(C=O)), 1542.7 (m), 1455.6 (m), 1384.2 (m), 1301.0 (w), 1181.6 (vs), 1097.2 (m), 1038.5 (w), 940.2 (w), 849.3 (w), 761.5 (w), 720.4 (w), 697.9 (m), 646.2 (w), 621.9 (w), 498.3 (w).

^{1}H-NMR (400 MHz, DMSO-d_6): δ [ppm] = 12.23 (s, 1 H, COH^{57}), 8.08 (dd, J = 14.2, 3.7 Hz, 1 H, NH^{51}), 8.00 – 7.85 (m, 2 H, NH^{7+9}), 7.42 – 7.14 (m, 5 H, CH$_{Ar}$$^{61-65}$), 5.22 – 5.13 (m, 1 H, CH^{50}), 5.04 – 4.93 (m, 1 H, CH^{44}), 4.81 (t, J = 6.3 Hz, 1 H, CH^{15}), 4.76 – 4.39 (m, 2 H, CH$_2$^{67}), 3.15 – 2.88 (m, 4 H, CH$_2$$^{2+5}$), 2.41 (d, J = 6.2 Hz, 3 H, CH$_3$^{60}), 2.34 (t, J = 7.2 Hz, 2 H, CH$_2$^{24}), 1.65 (q, J = 7.3, 6.7 Hz, 2 H, CH$_2$^{17}), 1.51 (q, J = 7.1 Hz, 2 H, CH$_2$^{26}), 1.41 – 1.30 (m, 7 H, CH$_2$ + CH$_3$^{47}), 1.30 – 1.18 (m, 46 H, CH$_2$), 0.85 (t, J = 6.7 Hz, 6 H, CH$_3$$^{41+42}$).

^{13}C-NMR (101 MHz, DMSO-d_6) δ [ppm] = 172.37 (s, CO_2R^{23}), 169.32 (s, CO_2R^{48}), 169.28 (s, $CONR^{13\ or\ 45}$), 169.12 (s, $CONR^{13\ or\ 45}$), 169.06 (s, CO_2R^{23}), 167.25 (s, CO_2H^{55}), 152.67 (CO^{52}), 152.50 (CO^{52}), 148.32 (s, C^{53}), 148.24 (C^{53}), 143.92 (s, C_{Ar}^{59}), 143.77 (s, C_{Ar}^{59}), 128.36 (s, CH_{Ar}), 128.32 (s, CH_{Ar}), 127.31 (s, CH_{Ar}), 126.59 (s, CH_{Ar}), 126.46 (s, CH_{Ar}), 103.98 (s, C^{49}), 103.82 (s, C^{49}), 73.05 (s, CH^{15}), 70.53 (s, CH^{44}), 70.49 (s, CH^{44}), 53.30 (s, CH^{50}), 53.05 (s, CH^{50}), 44.05 (s, CH_2^{67}), 43.85 (s, CH_2^{67}), 38.30 (s, $CH_2^{2\ or\ 5}$), 38.27 (s, $CH_2^{2\ or\ 5}$), 38.17 (s, $CH_2^{2\ or\ 5}$), 33.48 (s, CH_2^{24}), 31.46 (s, CH_2^{17}), 31.33 (s, CH_2), 31.18 (s, CH_2), 29.06 (s, CH_2), 29.04 (s, CH_2), 29.00 (s, CH_2), 28.96 (s, CH_2), 28.93 (s, CH_2), 28.74 (s, CH_2), 28.72 (s, CH_2), 28.59 (s, CH_2), 28.55 (s, CH_2), 28.41 (s, CH_2), 25.90 (s, CH_2), 24.58 (s, CH_2^{26}), 24.45 (s, CH_2), 22.13 (s, CH_2), 22.09 (s, CH_2), 17.65 (s, CH_3^{47}), 17.62 (s, CH_3^{47}), 15.57 (s, CH_3^{60}), 15.50 (s, CH_3^{60}), 13.94 (s, $CH_3^{41\ or\ 42}$), 13.92 (s, $CH_3^{41\ or\ 42}$).

ESI – MS [*m/z*]: $[M + Na]^+$ calculated for $^{12}C_{50}{}^{1}H_{82}{}^{16}O_9{}^{14}N_4{}^{23}Na_1$, 905.5974; found, 905.5972; Δ = 0.23 mmu.

6.2.3.6.7 *Carboxylic acid 129 derived from benzyl ester 115 via hydrogenolytic deprotection*

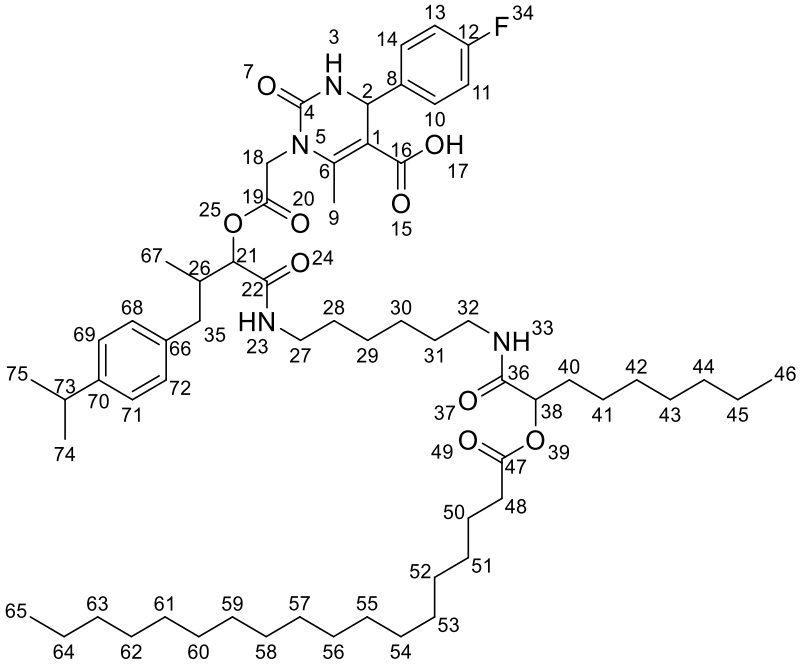

The benzyl ester **115** (66 mg, 58 µmol, 1.00 eq.) was dissolved in 0.9 mL ethyl acetate in a 10 mL round bottom flask. Subsequently, palladium on activated coal (20% Pd, 12 mg) was added to the solution. The resulting mixture was purged with argon and

subsequently with hydrogen gas. The reaction was stirred for 1 d at room temperature under hydrogen atmosphere (balloon). The crude reaction mixture was filtered over celite® and flushed with 15 mL ethyl acetate/dichloromethane (1:1) three times. After evaporation of the solvents under reduced pressure and drying *in vacuo* the acid **129** was obtained as a colorless solid (55.9 mg, 54.1 µmol, 92.1%).

R_f = 0.15 in *c*-hexane/ethyl acetate (2:3). Visualized *via* fluorescence quench and Seebach staining solution.

IR (ATR) ν [cm^{-1}] = 3301.2 (br, ν(NH)), 3089.3 (br, ν(CO_2H)), 2955.6 (m, ν(CH)), 2922.7 (vs, ν(CH)), 2852.7 (s, ν(CH)), 1746.2 (m, ν(CO)), 1657.8 (vs, ν(CO)), 1606.3 (m, ν(CO)), 1540. 5 (m), 1507.6 (m), 1456.2 (m), 1414.0 (w), 1382.1 (m), 1363.6 (w), 1299.9 (w), 1275.2 (w), 1254.6 (w), 1178.5 (vs), 1110.6 (m), 1086.2 (m), 1067.4 (w), 1048.9 (w), 1016.0 (w), 991.3 (w), 939.9 (vw), 859.7 (w), 851.5 (w), 837.1 (w), 802.2 (vw), 763.0 (w), 719.8 (w), 637.6 (w), 580.0 (vw), 551.2 (w), 528.3 (vw), 497.7 (vw).

^{1}H-NMR (500 MHz, DMSO-d_6) δ [ppm] = 8.18 (ddd, J = 22.0, 19.4, 3.5 Hz, 1 H, NH[3]), 8.08 – 7.80 (m, 2 H, NH[23,33]), 7.44 – 7.31 (m, 2 H, CH_{Ar}), 7.17 – 7.09 (m, 4 H, CH_{Ar}), 7.09 – 7.05 (m, 1 H, CH_{Ar}), 7.04 – 6.99 (m, 1 H, CH_{Ar}), 5.26 – 5.20 (m, 1 H, CH[2]), 4.92 – 4.78 (m, 2 H, CH[21,38]), 4.78 – 4.45 (m, 2 H, CH_2[20]), 3.16 – 2.96 (m, 4 H, CH_2[27,32]), 2.83 (dt, J = 13.6, 6.7 Hz, 1 H, CH[73]), 2.72 (dd, J = 9.5, 4.7 Hz, 2 H, CH_2[35]), 2.53 – 2.43 (m, 3 H, CH_3[9]), 2.32 (t, J = 7.1 Hz, 2 H, CH_2[48]), 1.65 (s, 2 H, CH_2), 1.50 (d, J = 6.5 Hz, 2 H, CH_2), 1.45 – 1.31 (m, 5 H, CH_2), 1.22 (s, 45 H, CH_2), 1.17 (d, J = 6.9 Hz, 6 H, CH_3[74,75]), 0.87 – 0.80 (m, 6 H, CH_3[46,65]), 0.80 – 0.73 (m, 3 H, CH_3[67]).

^{13}C-NMR (126 MHz, DMSO-d_6) δ [ppm] = 172.33 (s, CO_2R[47]), 169.15 (s, CONR[36]), 167.83 (s, s, CONR[22]), 167.79 (s, CONR[22]), 167.31 (s, CONR[22]), 167.27 (s, CONR[22]), 165.10 (s, CO_2H[16]), 165.03 (s, CO_2H[16]), 162.40 (s, C_{Ar}[12]), 160.47 (s, C_{Ar}[12]), 153.19 (s, C[4]), 152.98 (s, C[4]), 152.75 (s, C[4]), 152.66 (s, C[4]), 148.36 (s, C[6]), 148.14 (s, C[6]), 148.08 (s, C[6]), 145.99 (s, C_{Ar}[70]), 145.90 (s, C_{Ar}[70]), 145.86 (s, C_{Ar}[70]), 140.28 (s, C_{Ar}[73]), 140.09 (s, C_{Ar}[73]), 140.02 (s, C_{Ar}[73]), 137.18 (s, C_{Ar}[8]), 137.02 (s, C_{Ar}[8]), 136.95 (s, C_{Ar}[8]), 129.01 (s, CH_{Ar}[69,71]), 128.94 (s, CH_{Ar}[69,71]), 128.90 (s, CH_{Ar}[69,71]), 128.57 (s, CH_{Ar}), 128.50 (s, CH_{Ar}), 128.45 (s, CH_{Ar}), 128.44 (s, CH_{Ar}), 128.39 (s, CH_{Ar}), 126.18 (s, CH_{Ar}[68,72]), 126.16 (s, CH_{Ar}[68,72]), 115.17 (d, J = 5.2 Hz, CH_{Ar}[11,13]), 115.00 (d, J = 4.9 Hz, CH_{Ar}[11,13]), 104.20 (s, C[1]), 103.99 (s, C[1]), 77.51 (s, CH[21]), 77.46 (s, CH[21]), 75.63 (s, CH[21]), 75.49 (s, CH[21]), 73.05 (s, CH[38]), 52.53 (s, CH[2]), 52.37 (s, CH[2]), 52.28 (s, CH[2]), 44.53 (s, CH_2[20]), 44.30

(s, CH_2^{20}), 44.18 (s, CH_2^{20}), 38.37 (s, $CH_2^{27\ or\ 32}$), 38.29 (s, $CH_2^{27\ or\ 32}$), 38.16 (s, $CH_2^{27\ or\ 32}$), 36.98 (s, CH_2^{35}), 36.80 (s, CH_2^{35}), 36.70 (s, CH_2^{35}), 36.63 (m, CH_2^{35}), 33.49 (s, CH_2^{48}), 33.05 (s, CH^{73}), 31.47 (s, CH_2), 31.36 (s, CH_2), 31.20 (s, CH_2), 29.10 (s, CH_2), 29.08 (s, CH_2), 29.05 (s, CH_2), 28.78 (s, CH_2), 28.61 (s, CH_2), 28.58 (s, CH_2), 28.45 (s, CH_2), 26.03 (s, CH_2), 25.98 (s, CH_2), 25.92 (s, CH_2), 25.88 (s, CH_2), 24.60 (s, CH_2), 24.46 (s, CH_2), 23.93 (s, $CH_3^{74,75}$), 23.88 (s, $CH_3^{74,75}$), 22.14 (s, CH_2), 22.10 (s, CH_2), 15.73 (s, CH_3^{9}), 15.63 (s, CH_3^{9}), 15.58 (s, CH_3^{9}), 15.25 (s, CH_3^{67}), 15.09 (s, CH_3^{67}), 13.91 (s, $CH_3^{46\ or\ 65}$), 13.89 (s, $CH_3^{46\ or\ 65}$).

^{19}F-NMR (377 MHz, DMSO-d_6) δ [ppm] = -119.70 (s, F^{34}), -119.71 (s, F^{34}), -119.72 (s, F^{34}), -119.75 (s, F^{34}).

FAB-MS *m/z* (relative intensity): 1069.7 (60%) $[M + Na]^+$, 1029.9 (10%) $[M + H - F]^+$, 291.0 (100%), [Fragment A]$^+$.

HRMS–FAB (*m/z*): $[M + Na]^+$ calculated for $^{12}C_{61}{}^{1}H_{95}{}^{16}O_9{}^{14}N_4{}^{19}F_1{}^{23}Na_1$, 1069.6975; found, 1069.6986; Δ = 1.09 mmu.

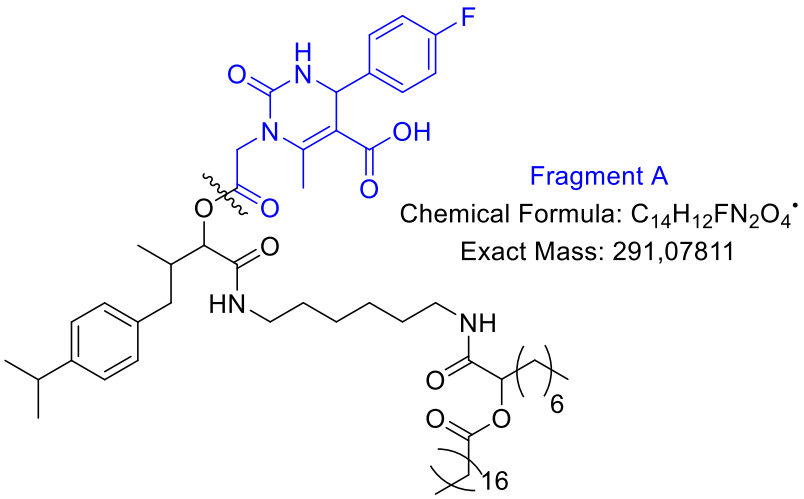

Fragment A
Chemical Formula: $C_{14}H_{12}FN_2O_4^{\bullet}$
Exact Mass: 291,07811

6.2.3.6.8 *Carboxylic acid 130 derived from benzyl ester 116 via hydrogenolytic deprotection*

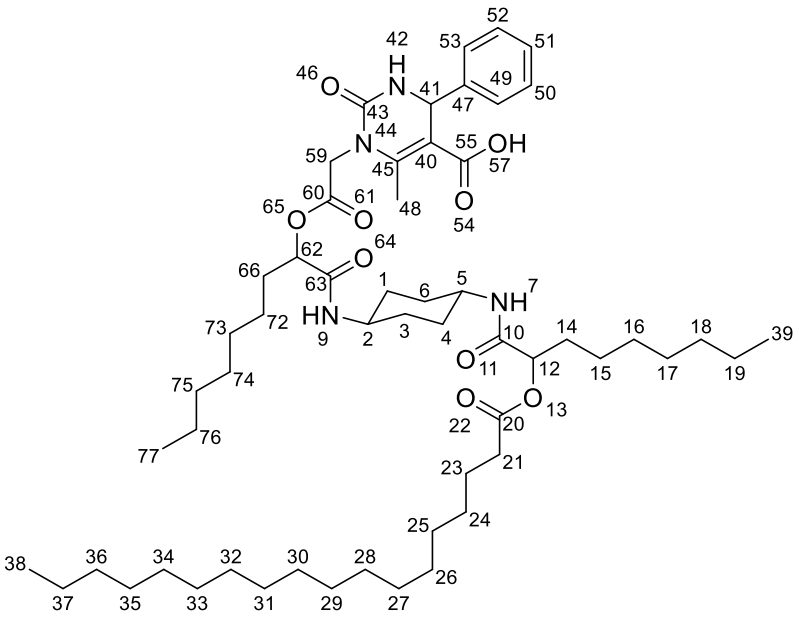

In a 10 mL round bottom flask equipped with a magnetic stir bar the benzyl ester **116** (134 mg, 127 µmol, 1.00 eq.) was dissolved in 5.00 mL ethyl acetate. Subsequently, palladium on activated charcoal (20% Pd, 26.8 mg) was added to the solution. The solution was purged with argon for 5 minutes, subsequently with hydrogen gas for 5 min and stirred for 1 d at room temperature under hydrogen atmosphere (balloon). TLC indicated complete conversion of the benzyl ester **116**. The crude reaction mixture was filtered over celite® and flushed with 40 mL ethyl acetate three times and with 30 mL dichloromethane twice. After concentration under reduced pressure and drying in high vacuum the carboxylic acid **130** was obtained as a colorless solid (119 mg, 120 µmol, 94.4%).

IR (ATR): ν [cm^{-1}] = 3276.3 (br, ν(N-H)), 2916.5 (vs, ν(C-H)), 2849.1 (s, ν(C-H)), 1742.9 (m, ν(C=O)), 1672.9 (s, ν(C=O)), 1655.1 (s), 1546.0 (m), 1454.8 (m), 1409.5 (m), 1379.1 (m), 1298.7 (w), 1279.0 (w), 1259.8 (w), 1199.5 (s), 1109.9 (m), 940.8 (m), 856.4 (w), 766.0 (m), 720.1 (m), 695.8 (m), 622.6 (w), 518.1 (w).

^{1}H-NMR (500 MHz, DMSO-d_6): δ [ppm] = 12.12 (s, 1 H, CO_2H^{57}), 8.13 (dd, J = 37.2, 3.7 Hz, 1 H, NH^{42}), 7.85 – 7.67 (m, 2 H, NH^{7+9}), 7.39 – 7.15 (m, 5 H, CH_{Ar}^{49-53}), 5.18 (t, J = 4.6 Hz, 1 H, CH^{41}), 4.88 (dt, J = 9.4, 6.1 Hz, 1 H, CH^{62}), 4.77 (t, J = 6.4 Hz, 1 H, CH^{12}), 4.73 – 4.38 (m, 2 H, CH_2^{59}), 3.53 – 3.43 (m, 2 H, CH^{2+5}), 2.42 (d, J = 15.9 Hz,

3 H, CH_3^{48}), 2.31 (t, *J* = 7.2 Hz, 2 H, CH_2^{21}), 1.81 – 1.55 (m, 9 H, CH_2), 1.49 (dt, *J* = 20.3, 7.1 Hz, 4 H, CH_2), 1.23 (s, 93 H, CH_2), 0.85 (t, *J* = 6.8 Hz, 9 H, $CH_3^{38\,+\,39\,+\,77}$).

^{13}C-NMR (126 MHz, DMSO-d_6) δ [ppm] = 174.45 (s, CO_2H^{57}), 172.33 (s, CO_2R^{20}), 169.21 (s, CO_2R^{60}), 168.97 s, CO_2R^{60}), 168.48 (s, $CONR^{10}$), 167.98 (s, $CONR^{10}$), 167.93 (s, $CONR^{63}$), 167.28 (s, $CONR^{63}$), 153.00 (s, CO^{43}), 152.62 (s, CO^{43}), 148.05 (s, C^{45}), 147.88 (s, C^{45}), 144.04 (s, C_{Ar}^{47}), 143.81 (s, C_{Ar}^{47}), 128.37 (s, CH_{Ar}), 128.31 (s, CH_{Ar}), 127.31 (s, CH_{Ar}), 104.10 (s, C^{40}), 104.05 (s, C^{40}), 73.97 (s, CH^{62}), 73.93 (s, CH^{62}), 73.06 (s, CH^{12}), 53.23 (s, CH^{41}), 52.97 (s, CH^{41}), 47.03 (s, $CH^{2\ or\ 5}$), 46.98 (s, $CH^{2\ or\ 5}$), 46.88 (s, $CH^{2\ or\ 5}$), 44.23 (s, CH_2^{59}), 43.99 (s, CH_2^{59}), 33.68 (s, CH_2^{21}), 33.45 (s, CH_2^{21}), 31.43 (s, CH_2), 31.34 (s, CH_2), 31.19 (s, CH_2), 31.16 (s, CH_2), 31.12 (s, CH_2), 30.82 (s, CH_2), 29.08 (s, CH_2), 29.02 (s, CH_2), 28.97 (s, CH_2), 28.95 (s, CH_2), 28.81 (s, CH_2), 28.76 (s, CH_2), 28.73 (s, CH_2), 28.61 (s, CH_2), 28.51 (s, CH_2), 28.39 (s, CH_2), 24.58 (s, CH_2), 24.53 (s, CH_2), 24.49 (s, CH_2), 24.36 (s, CH_2), 24.30 (s, CH_2), 22.14 (s, CH_2), 22.09 (s, CH_2), 22.08 (s, CH_2), 15.53 (s, CH_3^{48}), 15.50 (s, CH_3^{48}), 13.94 (s, $CH_3^{38\ or\ 39\ or\ 77}$), 13.93 (s, $CH_3^{38\ or\ 39\ or\ 77}$), 13.92 (s, $CH_3^{38\ or\ 39\ or\ 77}$).

ESI–MS [*m/z*]: $[M + Na]^+$ calculated for $^{12}C_{56}{}^{1}H_{92}{}^{16}O_9{}^{14}N_4{}^{23}Na_1$, 987.6757; found, 987.6756; Δ = 0.05 mmu.

6.2.3.6.9 *Carboxylic acid 131 derived from benzyl ester 117 via hydrogenolytic deprotection*

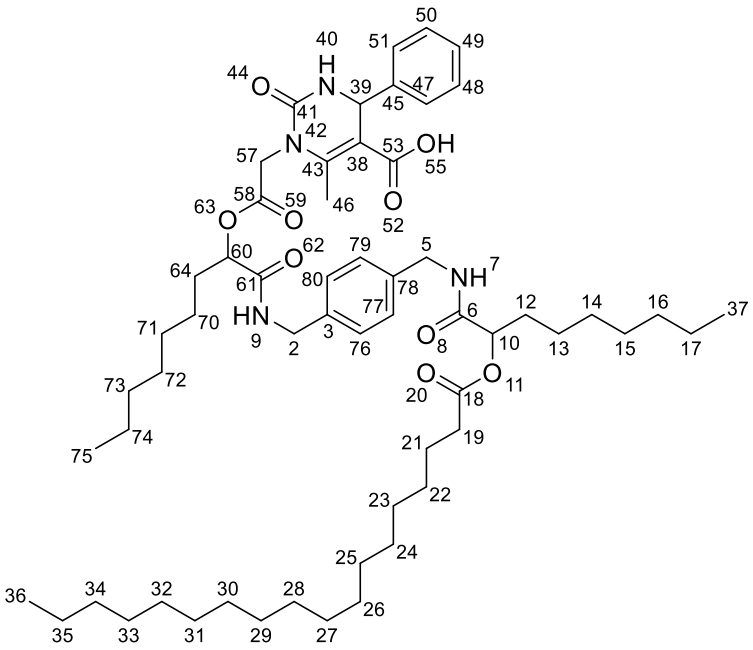

In a 10 mL round bottom flask equipped with a magnetic stir bar the benzyl ester **117** (147 mg, 137 µmol, 1.00 eq.) was dissolved in 5.00 mL ethyl acetate. Subsequently, palladium on activated charcoal (20% Pd, 29.5 mg) was added to the solution. The solution was purged with hydrogen gas for 5 minutes and stirred for 1 d at 40 °C under hydrogen atmosphere (balloon). TLC indicated complete conversion of the benzyl ester **117**. The crude reaction mixture was filtered over celite® and flushed with 20 mL ethyl acetate three times and with 20 mL dichloromethane twice. After concentration under reduced pressure and drying in high vacuum the carboxylic acid **131** was obtained as a colorless solid (130 mg, 131 µmol, 96.3%).

IR (ATR): ν [cm^{-1}] = 3272.8 (br, ν(N-H)), 2919.2 (s, ν(C-H)), 2850.9 (m, ν(C-H)), 1739.2 (m, ν(C=O)), 1710.3 (m), 1656.4 (vs, ν(C=O)), 1620.5 (m), 1551.9 (m), 1495.1 (w), 1455.0 (m), 1377.2 (m), 1302.5 (w), 1199.0 (vs), 1116.3 (m), 1026.1 (w), 938.0 (w), 856.4 (w), 765.6 (m), 695.2 (m), 624.1 (w), 575.3 (w), 521.2 (w), 459.8 (w).

^{1}H-NMR (500 MHz, DMSO-d_6): δ [ppm] = 12.24 (s, 1 H, CO_2H^{55}), 8.53 (dt, J = 11.7, 6.0 Hz, 1 H, NH^{9}), 8.47 (t, J = 6.0 Hz, 1 H, NH^{7}), 8.08 (dd, J = 26.0, 3.6 Hz, 1 H, NH^{40}), 7.38 – 7.09 (m, 9 H, $CH_{Ar}^{47\text{-}51\ +\ 76\text{-}79,80}$), 5.19 (t, J = 4.0 Hz, 1 H, CH^{39}), 4.99 (dd, J = 7.7, 4.6 Hz, 1 H, CH^{60}), 4.89 (dd, J = 7.5, 5.1 Hz, 1 H, CH^{10}), 4.78 – 4.41 (m, 2 H, CH_2^{57}), 4.34 – 4.19 (m, 4 H, CH_2^{2+5}), 2.41 (d, J = 15.9 Hz, 3 H, CH_3^{46}), 2.35 (t, J = 7.2 Hz, 2 H,

CH_2^{19}), 1.80 – 1.61 (m, 4 H, CH_2^{12+64}), 1.59 – 1.43 (m, 2 H, CH_2^{21}), 1.38 – 1.13 (m, 60 H, CH_2), 0.94 – 0.80 (m, 9 H, $CH_3^{36 + 37 + 75}$).

^{13}C-NMR (126 MHz, DMSO-d_6) δ [ppm] = 172.42 (s, CO_2R^{18}), 169.43 (s, $CONR^{6}$), 169.30 (s, $CONR^{61}$), 169.28 (s, $CONR^{61}$), 168.96 (s, CO_2R^{58}), 168.94 (s, CO_2R^{58}), 167.31 (s, CO_2H^{55}), 167.30 (s, CO_2H^{55}), 152.80 (s, CO^{41}), 152.57 (s, CO^{41}), 147.94 (s, C^{43}), 147.80 (s, C^{43}), 144.09 (s, C_{Ar}^{45}), 143.93 (s, C_{Ar}^{45}), 137.88 (s, $C_{Ar}^{3 \text{ or } 78}$), 137.64 (s, $C_{Ar}^{3 \text{ or } 78}$), 128.35 (s, CH_{Ar}), 128.31 (s, CH_{Ar}), 127.28 (s, CH_{Ar}), 126.97 (s, CH_{Ar}), 126.95 (s, CH_{Ar}), 126.58 (s, CH_{Ar}), 126.46 (s, CH_{Ar}), 104.18 (s, C^{38}), 104.13 (s, C^{38}), 74.04 (s, CH^{60}), 73.96 (s, CH^{60}), 73.03 (s, CH^{10}), 53.28 (s, CH^{39}), 53.06 (s, CH^{39}), 44.07 (s, CH_2^{57}), 43.87 (s, CH_2^{57}), 41.64 (s, $CH_2^{2 \text{ or } 5}$), 41.54 (s, $CH_2^{2 \text{ or } 5}$), 33.71 (s, CH_2^{19}), 33.50 (s, CH_2^{19}), 31.46 (s, CH_2), 31.36 (s, CH_2), 31.21 (s, $CH_2^{12 \text{ or } 64}$), 31.17 (s, $CH_2^{12 \text{ or } 64}$), 29.10 (s, CH_2), 29.07 (s, CH_2), 29.05 (s, CH_2), 28.98 (s, CH_2), 28.83 (s, CH_2), 28.78 (s, CH_2), 28.62 (s, CH_2), 28.55 (s, CH_2), 28.46 (s, CH_2), 24.64 (s, CH_2), 24.55 (s, CH_2), 24.46 (s, CH_2), 22.15 (s, CH_2), 22.12 (s, CH_2), 22.11 (s, CH_2), 15.53 (s, CH_3^{46}), 15.49 (s, CH_3^{46}), 13.93 (s, $CH_3^{36 \text{ or } 37 \text{ or } 75}$), 13.93 (s, $CH_3^{36 \text{ or } 37 \text{ or } 75}$), 13.92 (s, $CH_3^{36 \text{ or } 37 \text{ or } 75}$).

ESI–MS [*m/z*]: $[M + Na]^+$ calculated for $^{12}C_{58}{}^{1}H_{90}{}^{16}O_9{}^{14}N_4{}^{23}Na_1$, 1009.6600; found, 1009.6604; Δ = 0.40 mmu.

6.2.3.6.10 *Carboxylic acid 132 derived from benzyl ester 118 via hydrogenolytic deprotection*

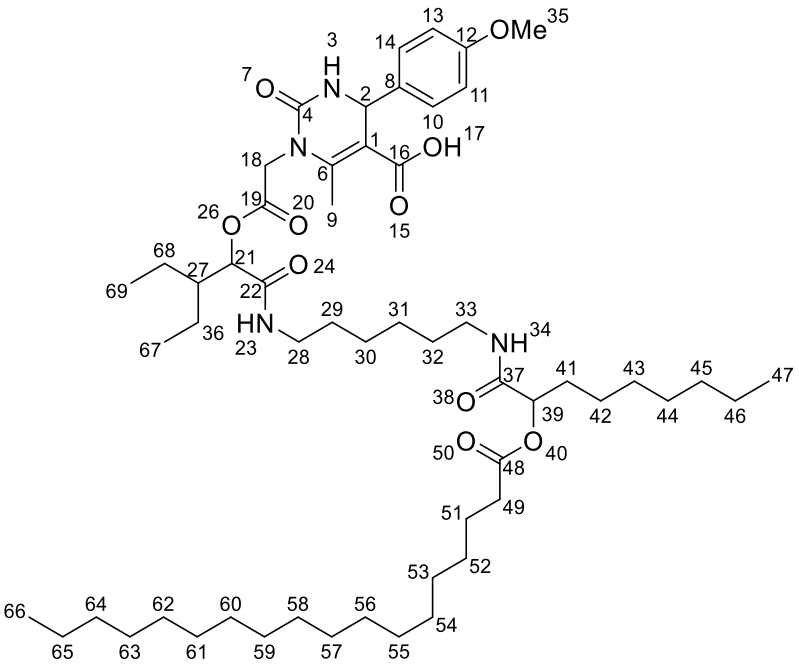

The benzyl ester **118** (130 mg, 124 µmol, 1.00 eq.) was dissolved in 3 mL ethyl acetate in a 25 mL round bottom flask. Subsequently, palladium on activated coal (20 wt.% Pd, 20 mg) was added to the solution. The resulting mixture was purged with argon and subsequently with hydrogen gas. The reaction was stirred for 4 d at room temperature under hydrogen atmosphere (balloon). The crude reaction mixture was filtered over celite®, and flushed with 15 mL ethyl acetate/dichloromethane (1:1) three times. After evaporation of the solvents under reduced pressure and drying *in vacuo* the acid **132** was obtained as a colorless solid (120 mg, 124 µmol, 99.8%).

R_f = 0.21 in *c*-hexane/ethyl acetate (1:1). Visualized *via* fluorescence quench and Seebach staining solution.

IR (ATR) ν [cm^{-1}] = 3303.2 (br, ν(NH)), 3083.1 (br, ν(CO$_2$H)), 2955.6 (m, ν(CH)), 2922.7 (vs, ν(CH)), 2852.8 (m, ν(CH)), 1746.2 (m, ν(C=O)), 1668.0 (vs, ν(C=O)), 1657.7 (vs, ν(C=O)), 1585.8 (w), 1538.5 (m), 1511.7 (m), 1456.2 (m), 1410.9 (w), 1384.2 (m), 1304.0 (w), 1277.7 (m), 1246.4 (s), 1174.4 (vs), 1102.6 (m), 1032.5 (m), 1005.7 (w), 929.9 (vw), 857.6 (w), 830.9 (w), 765.1 (w), 719.8 (w), 699.3 (vw), 633.5 (w), 588.2 (w), 555.3 (vw), 528.6 (vw), 503.3 (vw), 466.9 (vw), 454.5 (vw).

^{1}H-NMR (500 MHz, DMSO-d_6) δ [ppm] = 12.18 (s, 1 H, CO_2H^{17}), 8.05 (d, J = 46.2 Hz, 1 H, NH^{3}), 7.97 – 7.84 (m, 2 H, $NH^{23,34}$), 7.21 (t, J = 7.8 Hz, 2 H, $CH_{Ar}^{11,13}$), 6.85 (dd, J = 8.6, 5.2 Hz, 2 H, $CH_{Ar}^{10,14}$), 5.12 (dd, J = 8.5, 3.4 Hz, 1 H, CH^{2}), 4.99 (dd, J = 26.8, 3.8 Hz, 1 H, CH^{21}), 4.86 – 4.78 (m, 1 H, CH^{39}), 4.55 (ddd, J = 40.8, 24.4, 18.3 Hz, 2 H, CH_2^{18}), 3.71 (s, 3 H, OCH_3^{35}), 3.04 (m, 4 H, $CH_2^{28,33}$), 2.42 (d, J = 30.7 Hz, 3 H, CH_3^{9}), 2.33 (m, 2 H, CH_2^{49}), 1.78 – 1.68 (m, 1 H, CH^{27}), 1.65 (d, J = 5.8 Hz, 2 H, CH_2),1.60 – 1.46 (m, 3 H, CH_2), 1.36 (dd, J = 13.3, 6.7 Hz, 7 H, CH_2), 1.23 (s, 41 H, CH_2,), 0.93 – 0.76 (m, 12 H, CH_3).

^{13}C-NMR (126 MHz, DMSO-d_6) δ [ppm] = 172.44 (s, CO_2R^{48}), 169.33 (s, CO_2R^{19}), 169.25 (s, CO_2H^{16}), 169.15 (s, $CONR^{37}$), 168.38 (s, $CONR^{22}$), 158.50 (s, $COMe^{12}$), 152.70 (s, C^{4}), 150.21 (s, C^{6}), 135.92 (s, C^{8}), 127.69 (s, $CH_{Ar}^{10,14}$), 127.59 (s, $CH_{Ar}^{10,14}$), 113.71 (s, $CH_{Ar}^{11,13}$), 113.66 (s, $CH_{Ar}^{11,13}$), 104.89 (s, C^{1}), 104.54 (s, C^{1}), 75.02 (s, CH^{21}), 74.90 (s, CH^{21}), 73.07 (s, CH^{39}), 55.06 (s, OCH_3^{35}), 52.54 (s, CH^{2}), 44.35 (s, CH_2^{18}), 44.12 (s, CH_2^{18}), 42.55 (s, CH^{27}), 38.29 (s, CH_2), 38.14 (s, CH_2), 33.44 (s, CH_2^{49}), 31.44 (s, CH_2), 31.30 (s, CH_2), 31.16 (s, CH_2), 29.02 (s, CH_2), 28.96 (s, CH_2), 28.90 (s, CH_2), 28.71 (s, CH_2), 28.68 (s, CH_2), 28.56 (s, CH_2), 28.52 (s, CH_2), 28.37 (s, CH_2), 25.95 (s, CH_2), 25.92 (s, CH_2), 25.89 (s, CH_2), 25.86 (s, CH_2), 24.55 (s, CH_2), 24.42 (s, CH_2), 22.11 (s, CH_2), 22.07 (s, CH_2), 21.84 (s, CH_2), 21.75 (s, CH_2), 21.48 (s, CH_2), 20.78 (s, CH_2), 15.48 (s, CH_3^{9}), 14.10 (s, CH_3^{9}), 13.97 (s, CH_3), 13.94 (s, CH_3), 11.40 (s, CH_3), 11.34 (s, CH_3), 11.29 (s, CH_3).

FAB-MS *m/z* (relative intensity): 991.8 (13%) $[M + Na]^+$, 951.8 (16%) $[M – CH_3]^+$, 649.5 (6%) [Fragment B]$^+$, 319.1 (97%) [Fragment A]$^+$, 303.1 (91%) [Fragment A – O]$^+$, 261.0 (100%) [Fragment A – $C_2H_2O_2$]$^+$.

HRMS–FAB (*m/z*): $[M + Na]^+$ calculated for $^{12}C_{55}{}^{1}H_{92}{}^{16}O_{10}{}^{14}N_4{}^{23}Na_1$, 991.6706; found, 991.6704; Δ = 0.17 mmu.

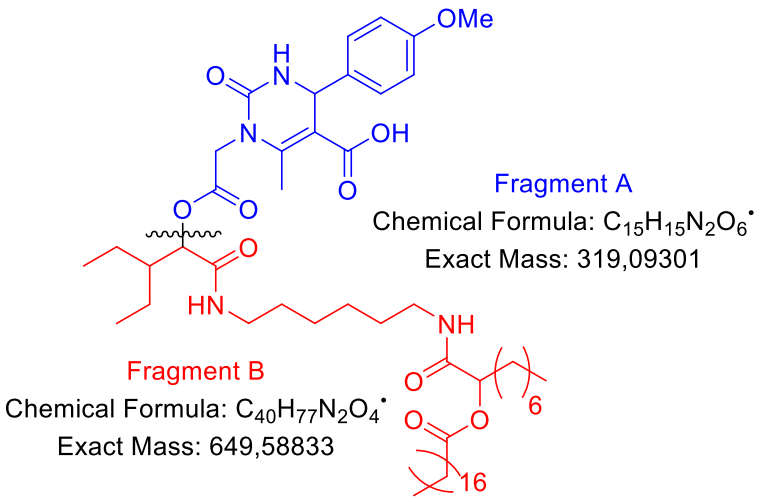

6.2.3.6.11 *Carboxylic acid 133 derived from benzyl ester 119 via hydrogenolytic deprotection*

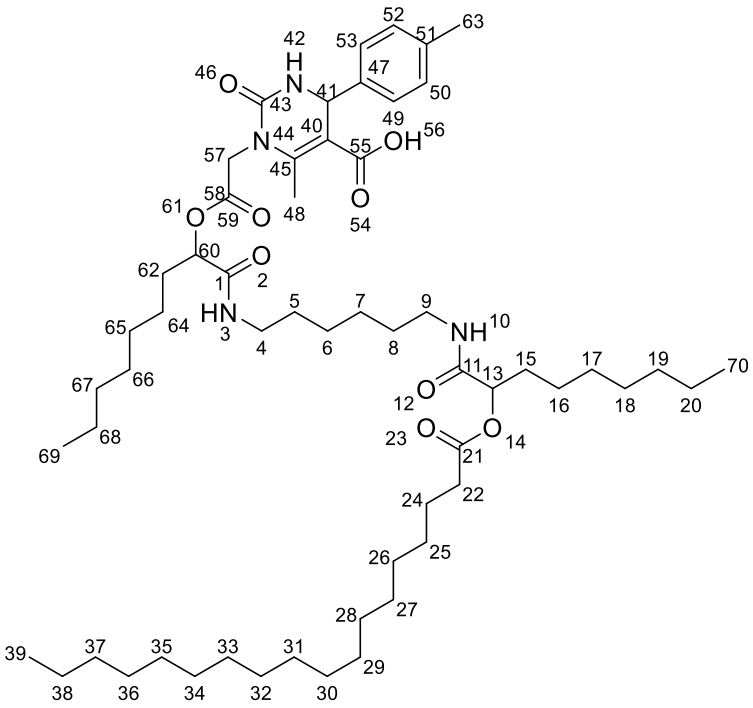

In a 25 mL round bottom flask equipped with a magnetic stir bar the benzyl ester **119** (120 mg, 113 µmol, 1.00 eq.) was dissolved in 3.00 mL ethyl acetate. Subsequently, palladium on activated charcoal (20 wt.% Pd/C, 24 mg) was added to the solution. The resulting mixture was purged with hydrogen gas and stirred for 18 h at room temperature under hydrogen atmosphere (balloon). The crude reaction mixture was filtered over celite® and flushed with 30 mL ethyl acetate/dichloromethane (1:1) three

times. After evaporation of the solvents and drying under reduced pressure the corresponding acid **133** was obtained as a colorless solid. (109 mg, 111 µmol, 99.4%).

R_f = 0.46 in *c*-hexane/ethyl acetate (1:1). Visualized *via* fluorescence quench and Seebach staining solution.

IR (ATR): ν [cm^{-1}] = 3292.1 (w, ν(N-H)), 2917.8 (s, ν(C-H)), 2849.9 (s, ν(C-H)), 1737.3 (m, ν(C=O)), 1687.5 (s, ν(C=O)), 1660.5 (s), 1547.3 (m), 1455.7 (m), 1411.7 (w), 1376.1 (m), 1307.1 (m), 1277.1 (m), 1258.0 (m), 1205.3 (s), 1170.0 (vs), 1106.7 (s), 1043.5 (m), 963.9 (w), 843.9 (w), 800.8 (m), 765.9 (m), 721.2 (m), 697.0 (m), 588.8 (w), 503.4 (m).

^{1}H-NMR (400 MHz, DMSO-d_6): δ [ppm] = 12.20 (br s, 1 H, CO_2H[56]), 8.04 (dd, *J* = 25.7, 3.6 Hz, 1 H, NH[24]), 7.91 (dt, *J* = 10.5, 5.2 Hz, 2 H, NH[3,10]), 7.22 – 7.15 (m, 2 H, CH_{Ar}[52,50]), 7.09 (dd, *J* = 8.0, 3.4 Hz, 2 H, CH_{Ar}[49,53]), 5.14 (t, *J* = 4.1 Hz, 1 H, CH[41]), 4.93 – 4.87 (m, 1 H, CH[60]), 4.81 (t, *J* = 6.3 Hz, 1 H, CH[13]), 4.72 – 4.37 (m, 2 H, CH_2[58]), 3.13 – 2.90 (m, 4 H, CH_2[4,9]), 2.40 (d, *J* = 11.0 Hz, 3 H, CH_3[48]), 2.33 (t, *J* = 7.2 Hz, 1 H, CH_2[22a]), 2.25 (s, 3 H, CH_3[63]), 2.17 (t, *J* = 7.4 Hz, 1 H, CH_2[22b]), 1.77 – 1.57 (m, 4 H, CH_2[15,62]), 1.57 – 1.42 (m, 4 H, CH_2[24]), 1.42 – 1.31 (m, 5 H, CH_2), 1.31 – 1.11 (m, 80 H, CH_2), 0.84 (t, *J* = 6.6 Hz, 12 H, CH_3[39,69,70]).

^{13}C-NMR (101 MHz, DMSO-d_6): δ [ppm] = 174.49 (s, CO_2R[21]), 172.38 (s, CONR[11]), 169.23 (s, CO_2R[58]), 169.14 (s, CO_2R[58]), 168.65 (s, CONR[1]), 167.32 (s, CO_2H[55]), 152.94 (s, CO[43]), 152.64 (s, CO[43]), 147.86 (s, C[45]), 147.63 (s, C[45]), 141.12 (s, C_{Ar}[51]), 140.93 (s, C_{Ar}[51]), 136.39 (s, C_{Ar}[47]), 128.88 (s, CH_{Ar}[52,50]), 128.83 (s, CH_{Ar}[52,50]), 126.46 (s, CH_{Ar}[49,54]), 126.34 (s, CH_{Ar}[49,54]), 104.23 (s, C[40]), 74.05 (s, CH[60]), 73.95 (s, CH[13]), 73.06 (s, CH[13]), 52.90 (s, CH[41]), 52.65 (s, CH[41]), 44.14 (s, CH_2[57]), 43.90 (s, CH_2[57]), 38.21 (s, CH_2[4,9]), 38.12 (s, CH_2[4,9]), 33.69 (s, CH_2[22]), 33.47 (s, CH_2[22]), 31.46 (s, CH_2), 31.33 (s, CH_2), 31.19 (s, CH_2), 29.06 (s, CH_2), 29.00 (s, CH_2), 28.94 (s, CH_2), 28.79 (s, CH_2), 28.75 (s, CH_2), 28.59 (s, CH_2), 28.56 (s, CH_2), 28.41 (s, CH_2), 25.87 (s, CH_2), 24.57 (s, CH_2), 24.52 (s, CH_2), 24.44 (s, CH_2), 24.39 (s, CH_2), 22.13 (s, CH_2), 22.09 (s, CH_2[24]), 20.77 (s, CH_3[63]), 20.65 (s, CH3[63]), 15.51 (s, CH_3[42]), 15.47 (s, CH_3[42]), 13.95 (s, CH_3[39,69,70]), 13.93 (s, CH_3[39,69,70]).

FAB – MS [*m/z*] (relative intensity): 981.9 (100%) $[M + H]^+$, 935.8 (15%) $[M - CO_2H]^+$, 697.4 (10%) [Fragment A]$^+$, 977.6 (16%) [Fragment B]$^+$, 245.0 (25%) [Fragment C – $C_2H_2O_2$]$^+$.

HRMS – FAB [*m/z*]: $[M + H]^+$ calculated for $^{12}C_{57}{}^{1}H_{97}{}^{16}O_9{}^{14}N_4$, 981.7520; found, 981.7249; Δ = 0.08 mmu.

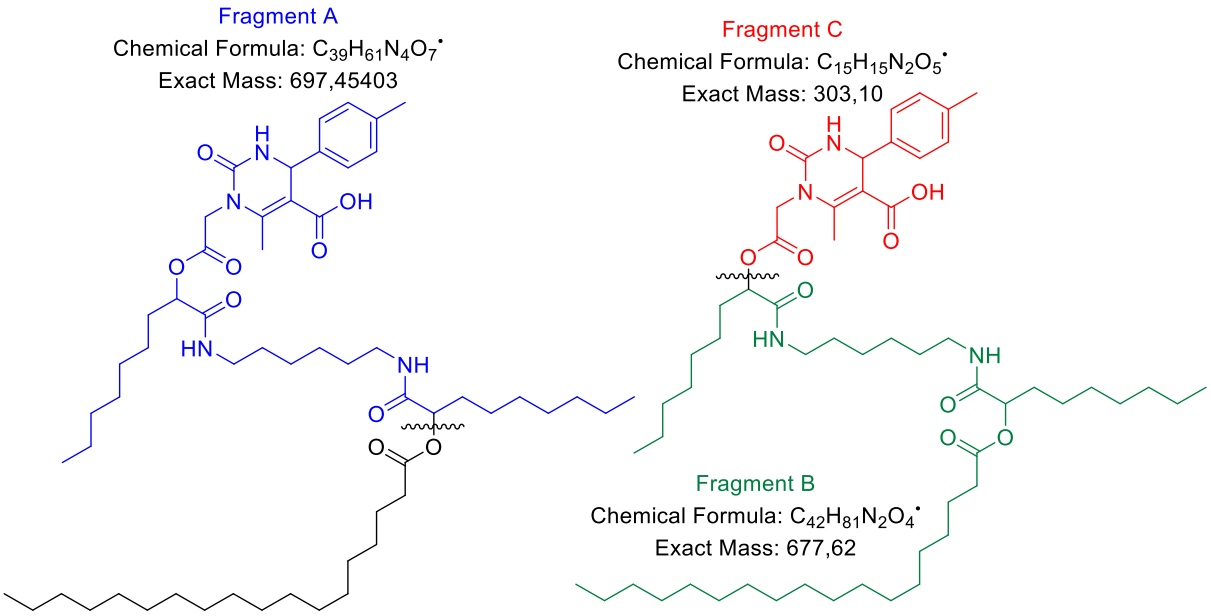

6.2.3.6.12 *Carboxylic acid 134 derived from benzyl ester 120 via hydrogenolytic deprotection*

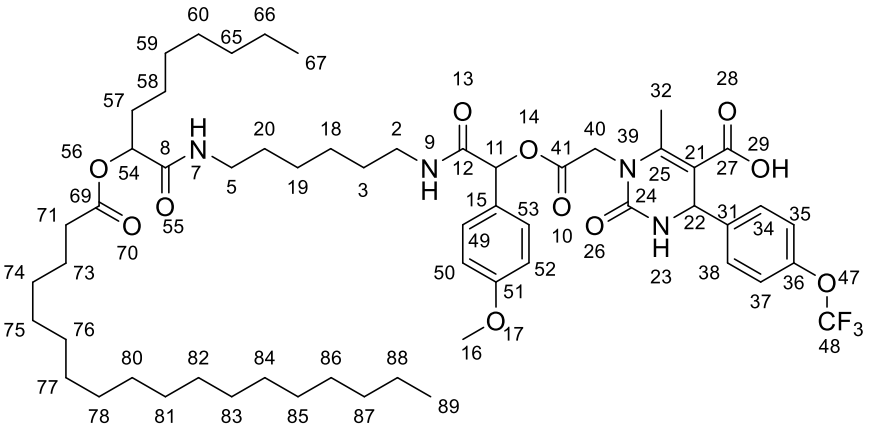

In a 5 mL round bottom flask equipped with a magnetic stir bar the benzyl ester **120** (155 mg, 135 µmol, 1.00 eq.) was dissolved in 4.00 mL ethyl acetate. Subsequently, palladium on activated charcoal (20 wt.% Pd, 31.0 mg) was added to the solution. The solution was purged with hydrogen gas for 10 minutes and stirred for 1 d at room temperature under hydrogen atmosphere (balloon). During the first 2 h the mixture was purged with hydrogen for 5 minutes every 30 minutes. TLC indicated complete conversion of the benzyl ester **120**. The crude reaction mixture was filtered over celite® and flushed with 50 mL ethyl acetate three times and with 50 mL dichloromethane

three times. After concentration under reduced pressure and drying in high vacuum the carboxylic acid **134** was obtained as a colorless solid (141 mg, 133 µmol, 98.5%).

IR (ATR): ν [cm^{-1}] = 3280.3 (br, ν(O-H)), 3087.3 (br, ν(N-H)), 2917.4 (vs, ν(C-H)), 2850.0 (s, ν(C-H)), 1745.1 (s, ν(C=O)), 1713.0 (s, ν(C=O)), 1644.0 (vs), 1612.2 (m), 1553.2 (m), 1513.2 (m), 1464.7 (s), 1434.9 (m), 1403.1 (m), 1385.5 (m), 1246.8 (vs), 1208.4 (s), 1162.0 (vs), 1120.7 (w), 1033.3 (w), 945.6 (w), 871.0 (w), 819.0 (w), 721.6 (w), 681.5 (w), 629.0 (w), 518.2 (w), 433.7 (w).

^{1}H-NMR (400 MHz, DMSO-d_6/$CDCl_3$ 8:2): δ [ppm] = 12.45 (s, 1 H, CO_2H^{29}), 8.00 (d, J = 3.6 Hz, 1 H, NH^{23}), 7.88 – 7.77 (m, 2 H, NH^{7+9}), 7.51 – 7.42 (m, 2 H, CH_{Ar}), 7.22 (d, J = 8.2 Hz, 2 H, CH_{Ar}), 7.18 – 7.11 (m, 2 H, CH_{Ar}), 6.84 – 6.77 (m, 2 H, CH_{Ar}), 5.20 (d, J = 3.6 Hz, 1 H, CH^{22}), 4.81 (t, J = 6.3 Hz, 2 H, CH^{54}), 4.56 – 4.21 (m, 2 H, CH_2^{40}), 3.71 (s, 3 H, OCH_3^{16}), 3.01 (q, J = 6.6 Hz, 4 H, CH_2^{2+5}), 2.41 (s, 3 H, CH_3^{32}), 2.32 (t, J = 7.3 Hz, 2 H, CH_2^{71}), 1.72 – 1.62 (m, 2 H, CH_2^{57}), 1.53 (t, J = 7.2 Hz, 2 H, CH_2^{73}), 1.43 – 1.32 (m, 6 H, CH_2), 1.22 (s, 56 H, CH_2), 0.90 – 0.80 (m, 6 H, CH_3^{67+89}).

^{13}C-NMR (101 MHz, DMSO-d_6/$CDCl_3$ 8:2) δ [ppm] = 172.19 (s, CO_2R^{69}), 170.89 (s, CO_2R^{41}), 170.19 (s, $CONR^{8\ or\ 12}$), 169.17 (s, $CONR^{8\ or\ 12}$), 167.07 (s, CO_2H^{27}), 157.73 (s, C_{Ar}^{51}), 152.33 (s, CO^{24}), 148.62 (s, C^{25}), 147.42 (s, OCF_3^{48}), 143.33 (s, C_{Ar}^{31}), 129.69 (s, CH_{Ar}), 128.35 (s, CH_{Ar}), 128.31 (s, CH_{Ar}), 120.63 (s, CH_{Ar}), 113.36 (s, CH_{Ar}), 103.15 (s, C^{21}), 72.99 (s, CH^{54}), 54.78 (s, OCH_3^{16}), 52.50 (s, CH^{21}), 43.71 (s, CH_2^{40}), 38.40 (s, $CH_2^{2\ or\ 5}$), 38.11 (s, $CH_2^{2\ or\ 5}$), 33.46 (s, CH_2^{71}), 31.44 (s, CH_2), 31.28 (s, CH_2), 31.14 (s, CH_2), 29.02 (s, CH_2), 28.98 (s, CH_2), 28.89 (s, CH_2), 28.69 (s, CH_2), 28.56 (s, CH_2), 28.54 (s, CH_2), 28.42 (s, CH_2), 25.91 (s, CH_2), 25.83 (s, CH_2), 24.52 (s, CH_2), 24.36 (s, CH_2), 22.07 (s, CH_2), 22.04 (s, CH_2), 15.50 (s, CH_3^{32}), 13.84 (s, $CH_3^{67\ or\ 89}$), 13.81 (s, $CH_3^{67\ or\ 89}$).

^{19}F-NMR (376 MHz, DMSO-d_6/$CDCl_3$ 8:2) δ [ppm] = -61.36 (s, CF_3^{48}).

ESI – MS [*m/z*]: $[M + Na]^+$ calculated for $^{12}C_{57}{}^{1}H_{85}{}^{16}O_{11}{}^{14}N_4{}^{19}F_3{}^{23}Na_1$, 1081.6059; found, 1181.6064; Δ = 0.50 mmu.

6.2.3.6.13 *Carboxylic acid 135 derived from benzyl ester 121 via hydrogenolytic deprotection*

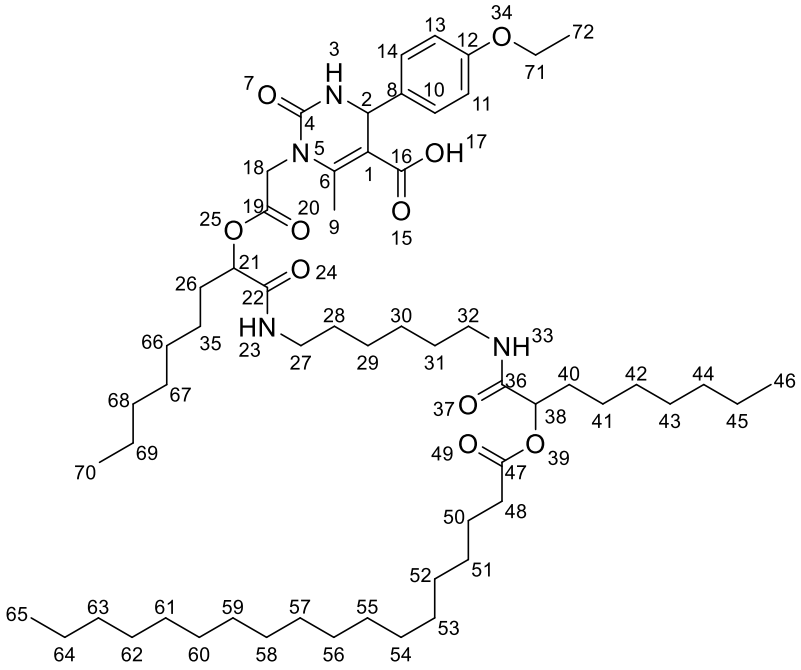

The benzyl ester **121** (49.5 mg, 45.0 µmol, 1.00 eq.) was dissolved in 0.9 mL ethyl acetate in a 10 mL round bottom flask. Subsequently, palladium on activated coal (20% Pd, 12 mg) was added to the solution. The resulting mixture was purged with argon and subsequently with hydrogen gas. The reaction was stirred for 3 d at room temperature under hydrogen atmosphere (balloon). The crude reaction mixture was filtered over celite® and flushed with 15 mL ethyl acetate/dichloromethane (1:1) three times. After evaporation of the solvents under reduced pressure and drying *in vacuo* the acid **135** was obtained as a colorless solid (42.3 mg, 41.9 µmol, 93.0%).

R_f = 0.17 in *c*-hexane/ethyl acetate (2:3). Visualized *via* fluorescence quench and Seebach staining solution.

IR (ATR) ν [cm^{-1}] = 3292.9 (br, ν(N-H, CO_2H)), 2951.5 (m, ν(C-H)), 2916.5 (vs, ν(C-H)), 2884.7 (vs, ν(C-H)), 1744.1 (m, ν(C=O)), 1680.4 (s, ν(C=O)), 1659.8 (s, ν(C=O)), 1612.5 (m, ν(C=O)), 1583.7 (w), 1540.5 (m), 1511.7 (m), 1462.4 (m), 1437.7 (m), 1408.9 (w), 1384.2 (m), 1330.7 (w), 1297.8 (m), 1279.3 (m), 1242.3 (m), 1201.1 (s), 1174.4 (vs), 1114.8 (m), 1102.4 (m), 1048.9 (w), 1014.0 (w), 936.9 (w), 925.5 (w), 890.6 (vw), 859.7 (w), 824.7 (vw), 761.0 (w), 719.8 (w), 689.0 (w), 639.6 (w), 608.8 (w), 559.4 (vw), 534.7 (vw), 503.9 (vw), 452.5 (vw).

^{1}H-NMR (500 MHz, DMSO-d_6) δ [ppm] = 12.14 (s, 1 H, CO_2H^{17}), 8.01 (dd, J = 32.1, 3.5 Hz, 1 H, NH^{3}), 7.95 – 7.85 (m, 2 H, $NH^{23,33}$), 7.21 (dd, J = 13.0, 8.7 Hz, 2 H, $CH_{Ar}^{11,13}$), 6.82 (dd, J = 8.6, 5.1 Hz, 2 H, $CH_{Ar}^{10,14}$), 5.12 (t, J = 4.3 Hz, 1 H, CH^{2}), 4.90 (dt, J = 10.8, 5.3 Hz, 1 H, $CH^{21\ or\ 38}$), 4.85 – 4.78 (m, 1 H, $CH^{21\ or\ 38}$), 4.78 – 4.35 (m, 2 H, CH_2^{18}), 3.97 (q, J = 7.0 Hz, 2 H, CH_2^{71}), 3.04 (ddq, J = 19.4, 12.8, 6.4 Hz, 4 H, $CH_2^{27,32}$), 2.40 (d, J = 13.0 Hz, 3 H, CH_3^{9}), 2.33 (t, J = 7.2 Hz, 2 H, CH_2^{48}), 2.17 (t, J = 7.4 Hz, 1 H, CH_2^{48}), 1.71 – 1.61 (m, 4 H, $CH_2^{26.40}$), 1.55 – 1.44 (m, 2 H, CH_2^{50}), 1.35 (m, 4 H, CH_2), 1.29 (t, J = 7.0 Hz, 3 H, CH_3^{72}), 1.23 (s, 52 H, CH_2), 0.84 (t, J = 6.8 Hz, 9 H, $CH_3^{46,65,78}$).

^{13}C-NMR (126 MHz, DMSO-d_6) δ [ppm] = 174.46 (s, CO_2R^{47}), 172.33 (s, CO_2R^{47}), 169.28 (s, CO_2R^{19}), 169.12 (s, $CONR^{22\ or\ 36}$), 168.63 (s, $CONR^{22\ or\ 36}$), 167.33 (s, CO_2H^{16}), 167.30 (s, CO_2H^{16}), 157.79 (s, $COEt^{12}$), 152.87 (s, CO^{4}), 152.57 (s, CO^{4}), 147.69 (s, C^{6}), 147.51 (s, C^{6}), 136.11 (s, C^{8}), 135.90 (s, C^{8}), 127.76 (s, $CH_{Ar}^{11,13}$), 127.64 (s, $CH_{Ar}^{11,13}$), 114.12 (s, $CH_{Ar}^{10,14}$), 114.07 (s, $CH_{Ar}^{10,14}$), 104.36 (s, C^{1}), 74.04 (s, CH^{21}), 73.97 (s, CH^{21}), 73.04 (s, CH^{38}), 62.93 (s, CH_2^{71}), 52.67 (s, CH^{2}), 52.43 (s, CH^{2}), 44.12 (s, CH_2^{18}), 43.87 (s, CH_2^{18}), 38.20 (s, $CH^{27\ or\ 32}$), 38.12 (s, $CH^{27\ or\ 32}$), 33.69 (s, CH_2^{48}), 33.48 (s, CH_2^{48}), 31.46 (s, $CH_2^{26\ or\ 40}$), 31.35 (s, $CH_2^{26\ or\ 40}$), 31.20 (s, $CH_2^{26\ or\ 40}$), 31.16 (s, $CH_2^{26\ or\ 40}$), 29.09 (s, CH_2), 28.96 (s, CH_2), 28.82 (s, CH_2), 28.77 (s, CH_2), 28.61 (s, CH_2), 28.58 (s, CH_2), 28.43 (s, CH_2), 25.85 (s, CH_2), 24.58 (s, CH_2), 24.53 (s, CH_2), 24.45 (s, CH_2), 24.39 (s, CH_2), 22.14 (s, CH_2), 22.10 (s, CH_2), 15.50 (s, CH_3^{9}), 15.47 (s, CH_3^{9}), 14.64 (s, CH_3^{72}), 13.91 (s, $CH_3^{46\ or\ 65\ or\ 78}$), 13.88 (s, $CH_3^{46\ or\ 65\ or\ 78}$).

FAB-MS *m/z* (relative intensity): 1033.9 (13%) $[M + Na]^+$, 1011.9 (21%) $[M + H]^+$, 333.1 (92%) [Fragment A]$^+$, 317.3 (62%) [Fragment A – O]$^+$, 275.0 (100%) [Fragment A – $C_2H_2O_2$]$^+$.

HRMS–FAB (*m/z*): $[M + H]^+$ calculated for $^{12}C_{58}{}^{1}H_{99}{}^{16}O_{10}{}^{14}N_4$, 1011.7356; found, 1011.7354; Δ = 0.16 mmu.

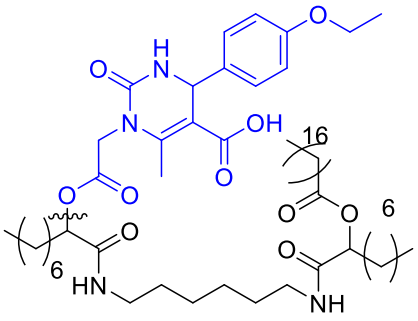

Fragment A´
Chemical Formula: $C_{16}H_{17}N_2O_6^{\bullet}$
Exact Mass: 333,10866

7 Appendix

7.1 Bibliography

[1] R. L. Ackoff, *J. Appl. Syst. Anal.* **1989**, *16*, 3–9.

[2] P. Hall, *Sci. Am.* **1998**, *100*, 106–112.

[3] J. S. C. Kilby, *ChemPhysChem* **2001**, *2*, 482–489.

[4] D. Panda, K. A. Molla, M. J. Baig, A. Swain, D. Behera, M. Dash, *3 Biotech* **2018**, *8*, 239.

[5] V. Zhirnov, R. M. Zadegan, G. S. Sandhu, G. M. Church, W. L. Hughes, *Nat. Mater.* **2016**, *15*, 366–370.

[6] J. R. Powell, *Proc. IEEE* **2008**, *96*, 1247–1248.

[7] R. Chepesiuk, *Environ. Health Perspect.* **1999**, *107*, A452–A457.

[8] E. D. Williams, R. U. Ayres, M. Heller, *Environ. Sci. Technol.* **2002**, *36*, 5504–5510.

[9] A. Extance, *Nature* **2016**, *537*, 22–24.

[10] G. M. Church, Y. Gao, S. Kosuri, *Science* **2012**, *337*, 1628–1628.

[11] T. Lindahl, *Nature* **1993**, *362*, 709–715.

[12] A. Sreedhara, J. A. Cowan, *J. Biol. Inorg. Chem.* **2001**, *6*, 337–347.

[13] Y. Erlich, D. Zielinski, *Science* **2017**, *355*, 950–954.

[14] D. I. Lou, J. A. Hussmann, R. M. McBee, A. Acevedo, R. Andino, W. H. Press, S. L. Sawyer, *Proc. Natl. Acad. Sci.* **2013**, *110*, 19872–19877.

[15] M. A. DePristo, E. Banks, R. Poplin, K. V. Garimella, J. R. Maguire, C. Hartl, A. A. Philippakis, G. del Angel, M. A. Rivas, M. Hanna, et al., *Nat. Genet.* **2011**, *43*, 491–498.

[16] E. T. Kool, J. C. Morales, K. M. Guckian, *Angew. Chem. Int. Ed.* **2000**, *39*, 990–1009.

[17] J. Florián, J. Leszczyński, *J. Am. Chem. Soc.* **1996**, *118*, 3010–3017.

[18] J. Lutz, *Polym. Chem.* **2010**, *1*, 55–62.

[19] S. C. Solleder, R. V. Schneider, K. S. Wetzel, A. C. Boukis, M. A. R. Meier, *Macromol. Rapid Commun.* **2017**, *38*, 1600711.

[20] H. Colquhoun, J.-F. Lutz, *Nat. Chem.* **2014**, *6*, 455–456.

[21] A. C. Boukis, *Neue Monomere Und Polymere Mittels Der Biginelli Reaktion*, Masterthesis, Karlsruher Institut Für Technologie, **2015**.

[22] A. C. Boukis, A. Llevot, M. A. R. Meier, *Macromol. Rapid Commun.* **2016**, *37*, 643–649.

[23] A. C. Boukis, B. Monney, M. A. R. Meier, *Beilstein J. Org. Chem.* **2017**, *13*, 54–62.

[24] A. Llevot, A. C. Boukis, S. Oelmann, K. Wetzel, M. A. R. Meier, *Top. Curr. Chem.* **2017**, *375*, 66.

[25] A. Sehlinger, M. A. R. Meier, *Adv. Polym. Sci.* **2015**, *269*, 61–86.

[26] B. Desai, D. Dallinger, C. O. Kappe, *Tetrahedron* **2006**, *62*, 4651–4664.

[27] A. Stadler, C. O. Kappe, *J. Comb. Chem.* **2001**, *3*, 624–630.

[28] S. Brauch, S. S. van Berkel, B. Westermann, *Chem. Soc. Rev.* **2013**, *42*, 4948.

[29] I. Ugi, A. Dömling, W. Hörl, *Endeavour* **1994**, *18*, 115–122.

[30] Y. Gu, *Green Chem.* **2012**, *14*, 2091–2128.

[31] B. B. Touré, D. G. Hall, *Chem. Rev.* **2009**, *109*, 4439–4486.

[32] J. D. Sunderhaus, S. F. Martin, *Chem. Eur. J.* **2009**, *15*, 1300–1308.

[33] D. M. D'Souza, T. J. J. Müller, *Chem. Soc. Rev.* **2007**, *36*, 1095–1108.

[34] B. Ganem, *Acc. Chem. Res.* **2009**, *42*, 463–472.

[35] B. Trost, *Science* **1991**, *254*, 1471–1477.

[36] L. F. Tietze, *Chem. Rev.* **1996**, *96*, 115–136.

[37] K. C. Nicolaou, D. J. Edmonds, P. G. Bulger, *Angew. Chem. Int. Ed.* **2006**, *45*, 7134–7186.

[38] A. Dömling, I. Ugi, *Angew. Chem.* **2000**, *39*, 3168–3210.

[39] J. Zhu, H. Bienaymé, *Multicomponent Reactions*, John Wiley & Sons, Hoboken, New Jersey, **2006**.

[40] K. P. C. Vollhardt, N. E. Schore, *Organische Chemie*, John Wiley & Sons, Hoboken, New Jersey, **2011**.

[41] R. M. Kellogg, T. J. Van Bergen, H. Van Doren, D. Hedstrand, J. Kooi, W. H. Kruizinga, C. B. Troostwijk, *J. Org. Chem.* **1980**, *45*, 2854–2861.

[42] L. Kurti, B. Czakó, *Strategic Applications of Named Reactions in Organic Synthesis*, Elsevier, Amsterdam, **2005**.

[43] C. O. Kappe, *Tetrahedron* **1993**, *49*, 6937–6963.

[44] M. Pramanik, A. Bhaumik, *ACS Appl. Mater. Interfaces* **2014**, *6*, 933–941.

[45] S. C. Solleder, M. A. R. Meier, *Angew. Chem.* **2014**, *126*, 729–732.

[46] A. Sehlinger, R. Schneider, M. A. R. Meier, *Eur. Polym. J.* **2014**, *50*, 150–157.

[47] A. Sehlinger, O. Kreye, M. A. R. Meier, *Macromolecules* **2013**, *46*, 6031–6037.

[48] O. Kreye, O. Türünç, A. Sehlinger, J. Rackwitz, M. A. R. Meier, *Chem. Eur. J.* **2012**, *18*, 5767–5776.

[49] A. Strecker, *Ann. der Chemie und Pharm.* **1850**, *75*, 27–45.

[50] A. Strecker, *Ann. der Chemie und Pharm.* **1854**, *91*, 349–351.

[51] M. S. Iyer, K. M. Gigstad, N. D. Namdev, M. Lipton, *J. Am. Chem. Soc.* **1996**, *118*, 4910–4911.

[52] J. Wang, X. Liu, X. Feng, *Chem. Rev.* **2011**, *111*, 6947–6983.

[53] K. Harada, *Nature* **1963**, *200*, 1201–1201.

[54] S. J. Zuend, M. P. Coughlin, M. P. Lalonde, E. N. Jacobsen, *Nature* **2009**, *461*, 968–970.

[55] A. Hantzsch, *Ber. Dtsch. Chem. Ges.* **1881**, *14*, 1637–1638.

[56] J. J. Xia, G. W. Wang, *Synthesis* **2005**, 2379–2383.

[57] R. Miri, K. Javidnia, B. Hemmateenejad, M. Tabarzad, M. Jafarpour, *Chem. Biol. Drug Des.* **2009**, *73*, 225–235.

[58] K. S. Atwal, B. N. Swanson, S. E. Unger, D. M. Floyd, S. Moreland, A. Hedberg, B. C. O'Reilly, *J. Med. Chem.* **1991**, *34*, 806–811.

[59] P. Biginelli, *Ber. Dtsch. Chem. Ges.* **1893**, *26*, 447–450.

[60] C. Mannich, W. Krösche, *Arch. Pharm.* **1912**, *250*, 647–667.

[61] S. Mitsumori, H. Zhang, P. Ha-Yeon Cheong, K. N. Houk, F. Tanaka, C. F. Barbas, *J. Am. Chem. Soc.* **2006**, *128*, 1040–1041.

[62] S. Lou, P. Dai, S. E. Schaus, *J. Org. Chem.* **2007**, *72*, 9998–10008.

[63] A. Córdova, S. Watanabe, F. Tanaka, W. Notz, C. F. Barbas, *J. Am. Chem. Soc.* **2002**, *124*, 1866–1867.

[64] L. Banfi, G. Guanti, R. Riva, *Chem. Commun.* **2000**, 985–986.

[65] A. R. Kazemizadeh, A. Ramazani, *Curr. Org. Chem.* **2012**, *16*, 418–450.

[66] A. Sehlinger, P.-K. Dannecker, O. Kreye, M. A. R. Meier, *Macromolecules* **2014**, *47*, 2774–2783.

[67] B. Yang, Y. Zhao, C. Fu, C. Zhu, Y. Zhang, S. Wang, Y. Wei, L. Tao, *Polym. Chem.* **2014**, *5*, 2704–2708.

[68] R. Kakuchi, *Angew. Chem. Int. Ed.* **2014**, *53*, 46–48.

[69] P. Biginelli, *Ber. Dtsch. Chem. Ges.* **1891**, *24*, 1317–1319.

[70] C. O. Kappe, *J. Org. Chem.* **1997**, *62*, 7201–7204.

[71] M. Puripat, R. Ramozzi, M. Hatanaka, W. Parasuk, V. Parasuk, K. Morokuma, *J. Org. Chem.* **2015**, *80*, 6959–6967.

[72] H. G. O. Alvim, E. N. da Silva Júnior, B. A. D. Neto, *RSC Adv.* **2014**, *4*, 54282–54299.

[73] K. Folkers, T. B. Johnson, *J. Am. Chem. Soc.* **1933**, *55*, 3784–3791.

[74] F. Sweet, J. D. Fissekis, *J. Am. Chem. Soc.* **1973**, *95*, 8741–8749.

[75] K. S. Atwal, G. C. Rovnyak, B. C. O'Reilly, J. Schwartz, *J. Org. Chem.* **1989**, *54*, 5898–5907.

[76] C. O. Kappe, *Eur. J. Med. Chem.* **2000**, *35*, 1043–1052.

[77] A. Dondoni, A. Massi, S. Sabbatini, *Tetrahedron Lett.* **2001**, *42*, 4495–4497.

[78] K. S. Atwal, G. C. Rovnyak, S. D. Kimball, D. M. Floyd, S. Moreland, B. N. Swanson, J. Z. Gougoutas, J. Schwartz, K. M. Smillie, M. F. Malley, *J. Med. Chem.* **1990**, *33*, 2629–2635.

[79] G. C. Rovnyak, K. S. Atwal, A. Hedberg, S. D. Kimball, S. Moreland, J. Z. Gougoutas, B. C. O'Reilly, J. Schwartz, M. F. Malley, *J. Med. Chem.* **1992**, *35*, 3254–3263.

[80] C. O. Kappe, W. M. F. Fabian, M. A. Semones, *Tetrahedron* **1997**, *53*, 2803–2816.

[81] F. Bossert, W. Vater, *Med. Res. Rev.* **2000**, *9*, 291–324.

[82] B. Kenny, S. Ballard, J. Blagg, D. Fox, *J. Med. Chem.* **1997**, *40*, 1293–1315.

[83] A. Jordan, J. a. Hadfield, N. J. Lawrence, A. T. McGown, *Med. Res. Rev.* **1998**, *18*, 259–296.

[84] E. W. Hurst, *Ann. N. Y. Acad. Sci.* **1962**, *98*, 275–286.

[85] B. B. Snider, J. Chen, A. D. Patil, A. J. Freyer, *Tetrahedron Lett.* **1996**, *37*, 6977–6980.

[86] L. Heys, C. G. Moore, P. J. Murphy, *Chem. Soc. Rev.* **2000**, *29*, 57–67.

[87] P. Wipf, A. Cunningham, *Tetrahedron Lett.* **1995**, *36*, 7819–7822.

[88] A. Dondoni, A. Massi, *Tetrahedron Lett.* **2001**, *42*, 7975–7978.

[89] C. O. Kappe, *QSAR Comb. Sci.* **2003**, *22*, 630–645.

[90] F. Drouet, G. Masson, J. Zhu, *Org. Lett.* **2013**, *15*, 2854–2857.

[91] N. Hadjichristidis, S. Pispas, G. Floudas, *Block Copolymers*, John Wiley & Sons, Inc., Hoboken, USA, **2002**.

[92] H. Wu, L. Yang, L. Tao, *Polym. Chem.* **2017**, *8*, 5679–5687.

[93] Z. Wang, Y. Yu, Y. Li, L. Yang, Y. Zhao, G. Liu, Y. Wei, X. Wang, L. Tao, *Polym. Chem.* **2017**, *8*, 5490–5495.

[94] L. Tao, C. Zhu, Y. Wei, Y. Zhao, in *Multi-Component Seq. React. Polym. Synth.*, Springer, **2014**, pp. 43–59.

[95] Y. Zhao, Y. Yu, Y. Zhang, X. Wang, B. Yang, Y. Zhang, Q. Zhang, C. Fu, Y. Wei, L. Tao, *Polym. Chem.* **2015**, *6*, 4940–4945.

[96] H. Xue, Y. Zhao, H. Wu, Z. Wang, B. Yang, Y. Wei, Z. Wang, L. Tao, *J. Am. Chem. Soc.* **2016**, *138*, 8690–8693.

[97] Y. Zhao, H. Wu, Y. Zhang, X. Wang, B. Yang, Q. Zhang, X. Ren, C. Fu, Y. Wei, Z. Wang, et al., *ACS Macro Lett.* **2015**, *4*, 843–847.

[98] H. Wu, C. Fu, Y. Zhao, B. Yang, Y. Wei, Z. Wang, L. Tao, *ACS Macro Lett.* **2015**, *4*, 1189–1193.

[99] M. Passerini, L. Simone, *Gazz. Chim. Ital.* **1921**, *51*, 126–129.

[100] I. Ugi, *Angew. Chem. Int. Ed.* **1962**, *1*, 8–21.

[101] R. H. Baker, D. Stanonis, *J. Am. Chem. Soc.* **1951**, *73*, 699–702.

[102] I. Ugi, R. Meyr, *Chem. Ber.* **1961**, *94*, 2229–2233.

[103] I. Hagedorn, U. Eholzer, *Chem. Ber.* **1965**, *98*, 936–940.

[104] M. C. Pirrung, K. Das Sarma, *J. Am. Chem. Soc.* **2004**, *126*, 444–445.

[105] S. Maeda, S. Komagawa, M. Uchiyama, K. Morokuma, *Angew. Chem. Int. Ed.* **2011**, *50*, 644–649.

[106] R. Ramozzi, K. Morokuma, *J. Org. Chem.* **2015**, *80*, 5652–5657.

[107] H. Bock, I. Ugi, *J. für Prakt. Chemie/Chemiker-Zeitung* **1997**, *339*, 385–389.

[108] R. Frey, S. G. Galbraith, S. Guelfi, C. Lamberth, M. Zeller, *Synlett* **2003**, *2003*, 1536–1538.

[109] L. Moni, L. Banfi, A. Basso, E. Martino, R. Riva, *Org. Lett.* **2016**, *18*, 1638–1641.

[110] L. Banfi, G. Guanti, R. Riva, *Chem. Commun.* **2000**, 985–986.

[111] U. Kusebauch, B. Beck, K. Messer, E. Herdtweck, A. Dömling, *Org. Lett.* **2003**, *5*, 4021–4024.

[112] P. R. Andreana, C. C. Liu, S. L. Schreiber, *Org. Lett.* **2004**, *6*, 4231–4233.

[113] A. Dömling, *Chem. Rev.* **2006**, *106*, 17–89.

[114] U. Fetzer, I. Ugi, *Justus Liebigs Ann. Chem.* **1962**, *659*, 184–189.

[115] P. Slobbe, E. Ruijter, R. V. A. Orru, *Med. Chem. Commun.* **2012**, *3*, 1189–1218.

[116] T. Sperka, J. Pitlik, P. Bagossi, J. Tözsér, *Bioorg. Med. Chem. Lett.* **2005**, *15*, 3086–3090.

[117] N. A. M. Yehia, W. Antuch, B. Beck, S. Hess, V. Schauer-Vukašinović, M. Almstetter, P. Furer, E. Herdtweck, A. Dömling, *Bioorg. Med. Chem. Lett.* **2004**, *14*, 3121–3125.

[118] I. Akritopoulou-Zanze, *Curr. Opin. Chem. Biol.* **2008**, *12*, 324–331.

[119] A. Dömling, B. Beck, W. Baumbach, G. Larbig, *Bioorg. Med. Chem. Lett.* **2007**, *17*, 379–384.

[120] P. Weyermann, A. Von Sprecher, M. Hennebohle, H. Herzner, C. Lescop, H. Siendt, *Alpha-Keto Carbonyl Calpain Inhibitors*, **2008**, US Patent Application No. 11/574,035.

[121] L. F. Tietze, A. Modi, *Med. Res. Rev.* **2000**, *20*, 304–322.

[122] A. Dömling, W. Wang, K. Wang, *Chem. Rev.* **2012**, *112*, 3083–3135.

[123] O. Kreye, T. Tóth, M. A. R. Meier, *J. Am. Chem. Soc.* **2011**, *133*, 1790–1792.

[124] A. Lv, X.-X. Deng, L. Li, Z.-L. Li, Y.-Z. Wang, F.-S. Du, Z.-C. Li, *Polym. Chem.* **2013**, *4*, 3659.

[125] O. Kreye, C. Trefzger, A. Sehlinger, M. A. R. Meier, *Macromol. Chem. Phys.* **2014**, *215*, 2207–2220.

[126] M. Rubinshtein, C. R. James, J. L. Young, Y. J. Ma, Y. Kobayashi, N. C. Gianneschi, J. Yang, *Org. Lett.* **2010**, *12*, 3560–3563.

[127] A. Sehlinger, B. Verbraeken, M. A. R. Meier, R. Hoogenboom, *Polym. Chem.* **2015**, *6*, 3828–3836.

[128] S. Oelmann, S. C. Solleder, M. A. R. Meier, *Polym. Chem.* **2016**, *7*, 1857–1860.

[129] J. A. Jee, L. A. Spagnuolo, J. G. Rudick, *Org. Lett.* **2012**, *14*, 3292–3295.

[130] W. Lin, X. Guan, T. Sun, Y. Huang, X. Jing, Z. Xie, *Colloids Surfaces B Biointerfaces* **2015**, *126*, 217–223.

[131] J. Zhang, M. Zhang, F.-S. Du, Z.-C. Li, *Macromolecules* **2016**, *49*, 2592–2600.

[132] M. von Czapiewski, K. Gugau, L. Todorovic, M. A. R. Meier, *Eur. Polym. J.* **2016**, *83*, 359–366.

[133] S. Schmidt, M. Koldevitz, J.-M. Noy, P. J. Roth, *Polym. Chem.* **2015**, *6*, 44–54.

[134] I. Ugi, R. Meyr, U. Fetzer, C. Steinbrückner, *Angew. Chem.* **1959**, *71*, 373–388.

[135] I. Ugi, C. Steinbrückner, *Angew. Chem.* **1960**, *72*, 267–268.

[136] O. Mumm, *Ber. Dtsch. Chem. Ges.* **1910**, *43*, 886–893.

[137] I. Ugi, B. Werner, A. Dömling, *Molecules* **2003**, *8*, 53–66.

[138] T. Godet, Y. Bonvin, G. Vincent, D. Merle, A. Thozet, M. A. Ciufolini, *Org. Lett.* **2004**, *6*, 3281–3284.

[139] C. Iacobucci, S. Reale, J.-F. Gal, F. De Angelis, *Eur. J. Org. Chem.* **2014**, *2014*, 7087–7090.

[140] G. A. Medeiros, W. A. da Silva, G. A. Bataglion, D. A. C. Ferreira, H. C. B. de Oliveira, M. N. Eberlin, B. A. D. Neto, *Chem. Commun.* **2014**, *50*, 338–340.

[141] C. Faggi, M. García-Valverde, S. Marcaccini, G. Menchi, *Org. Lett.* **2010**, *12*, 788–791.

[142] N. Chéron, R. Ramozzi, L. El Kaïm, L. Grimaud, P. Fleurat-Lessard, *J. Org. Chem.* **2012**, *77*, 1361–1366.

[143] H. Kunz, W. Pfrengle, *J. Am. Chem. Soc.* **1988**, *110*, 651–652.

[144] R. Urban, I. Ugi, *Angew. Chem. Int. Ed.* **1975**, *14*, 61–62.

[145] G. Eberle, I. Ugi, *Angew. Chem.* **1976**, *88*, 509–510.

[146] K. Oertel, G. Zech, H. Kunz, *Angew. Chem. Int. Ed.* **2000**, *39*, 1431–1433.

[147] I. Ugi, F. K. Rosendahl, F. Bodesheim, *Justus Liebigs Ann. Chem.* **1963**, *666*, 54–61.

[148] I. Ugi, C. Steinbrückner, *Chem. Ber.* **1961**, *94*, 2802–2814.

[149] T. A. Keating, R. W. Armstrong, *J. Org. Chem.* **1998**, *63*, 867–871.

[150] L. El Kaim, L. Grimaud, *Tetrahedron* **2009**, *65*, 2153–2171.

[151] L. El Kaïm, L. Grimaud, J. Oble, *Angew. Chem. Int. Ed.* **2005**, *44*, 7961–7964.

[152] L. El Kaïm, M. Gizolme, L. Grimaud, J. Obie, *J. Org. Chem.* **2007**, *72*, 4169–4180.

[153] A. A. Levy, H. C. Rains, S. Smiles, *J. Chem. Soc.* **1931**, *02*, 3264–3269.

[154] I. Ugi, C. Steinbrückner, *Chem. Ber.* **1961**, *94*, 734–742.

[155] A. Dömling, S. Achatz, B. Beck, *Bioorg. Med. Chem. Lett.* **2007**, *17*, 5483–5486.

[156] X. Fan, X. Zhang, C. Bories, P. M. Loiseau, P. F. Torrence, *Bioorg. Chem.* **2007**, *35*, 121–136.

[157] C. C. Musonda, D. Taylor, J. Lehman, J. Gut, P. J. Rosenthal, K. Chibale, *Bioorg. Med. Chem. Lett.* **2004**, *14*, 3901–3905.

[158] A. Sehlinger, K. Ochsenreither, N. Bartnick, M. A. R. Meier, *Eur. Polym. J.* **2015**, *65*, 313–324.

[159] N. Gangloff, D. Nahm, L. Döring, D. Kuckling, R. Luxenhofer, *J. Polym. Sci. Part A Polym. Chem.* **2015**, *53*, 1680–1686.

[160] A. Sehlinger, R. Schneider, M. A. R. Meier, *Macromol. Rapid Commun.* **2014**, *35*, 1866−1871.

[161] M. Hartweg, C. R. Becer, *Green Chem.* **2016**, *18*, 3272–3277.

[162] X. Zhang, S. Wang, J. Liu, Z. Xie, S. Luan, C. Xiao, Y. Tao, X. Wang, *ACS Macro Lett.* **2016**, *5*, 1049–1054.

[163] X.-X. Deng, F.-S. Du, Z.-C. Li, *ACS Macro Lett.* **2014**, *3*, 667–670.

[164] L. A. Wessjohann, M. Henze, O. Kreye, D. G. Rivera, *WO Patent 134,607, 2011*, **2013**.

[165] L. F. Tietze, *Chem. Rev.* **1996**, *96*, 115–136.

[166] P. J. Parsons, C. S. Penkett, A. J. Shell, *Chem. Rev.* **1996**, *96*, 195–206.

[167] A. Behr, A. J. Vorholt, K. A. Ostrowski, T. Seidensticker, *Green Chem.* **2014**, *16*, 982–1006.

[168] J. Zhou, *Chem. Asian J.* **2010**, *5*, 422–434.

[169] R. A. Batey, *J. Am. Chem. Soc.* **2007**, *129*, 7476–7476.

[170] R. C. Cioc, E. Ruijter, R. V. a. Orru, *Green Chem.* **2014**, *16*, 2958–2975.

[171] D. E. Portlock, R. Ostaszewski, D. Naskar, L. West, *Tetrahedron Lett.* **2003**, *44*, 603–605.

[172] D. E. Portlock, D. Naskar, L. West, R. Ostaszewski, J. J. Chen, *Tetrahedron Lett.* **2003**, *44*, 5121–5124.

[173] T. H. Al-Tel, R. A. Al-Qawasmeh, W. Voelter, *Eur. J. Org. Chem.* **2010**, *29*, 5586–5593.

[174] N. Elders, D. Van Der Born, L. J. D. Hendrickx, B. J. J. Timmer, A. Krause, E. Janssen, F. J. J. De Kanter, E. Ruijter, R. V. A. Orru, *Angew. Chem. Int. Ed.* **2009**, *48*, 5856–5859.

[175] S. Brauch, L. Gabriel, B. Westermann, *Chem. Commun.* **2010**, *46*, 3387–3389.

[176] S. Werner, D. M. Turner, M. A. Lyon, D. M. Huryn, P. Wipf, *Synlett* **2006**, *14*, 2334–2338.

[177] S. W. Fewell, C. M. Smith, M. A. Lyon, T. P. Dumitrescu, P. Wipf, B. W. Day, J. L. Brodsky, *J. Biol. Chem.* **2004**, *279*, 51131–51140.

[178] N. M. Kovalchuk, A. Trybala, V. Starov, O. Matar, N. Ivanova, *Adv. Colloid Interface Sci.* **2014**, *210*, 65–71.

[179] M. Bonnet, *Kunststoffe in Der Ingenieuranwendung: Verstehen Und Zuverlässig Auswählen (German Edition)*, Vieweg+Teubner Verlag, Wiesbaden, **2009**.

[180] A. Endres, G. Maas, *Chemie unserer Zeit* **2000**, *34*, 382–393.

[181] M. P. Krafft, J. G. Riess, *Chem. Rev.* **2009**, *109*, 1714–1792.

[182] D. P. Curran, S. Hadida, M. He, *J. Org. Chem.* **1997**, *62*, 6714–6715.

[183] L. E. Kiss, I. Kövesdi, J. Rábai, *J. Fluor. Chem.* **2001**, *108*, 95–109.

[184] M. Matsugi, *D. P. Org. Lett.* **2004**, *6*, 2717–2720.

[185] W. Zhang, in *Encycl. Reagents Org. Synth.*, John Wiley & Sons, Ltd, Chichester, UK, **2008**.

[186] W. Zhang, D. P. Curran, *Tetrahedron* **2006**, *62*, 11837–11865.

[187] A. D. Jenkins, P. Kratochvíl, R. F. T. Stepto, U. W. Suter, *Pure Appl. Chem.* **1996**, *68*, 2287–2311.

[188] W. Müller-Esterl, *Biochemie - Eine Einführung Für Mediziner Und Natruwissenschaftler*, Spektrum Akademischer Verlag, Heidelberg, **2011**.

[189] J.-F. Lutz, *Macromol. Rapid Commun.* **2017**, *38*, 1700582.

[190] A. M. Rosales, R. A. Segalman, R. N. Zuckermann, *Soft Matter* **2013**, *9*, 8400–8414.

[191] H. Cui, M. J. Webber, S. I. Stupp, *Biopolymers* **2010**, *94*, 1–18.

[192] J.-F. Lutz, M. Ouchi, D. R. Liu, M. Sawamoto, *Science* **2013**, *341*, 1238149–1238149.

[193] N. D. Knöfel, H. Rothfuss, J. Willenbacher, C. Barner-Kowollik, P. W. Roesky, *Angew. Chem. Int. Ed.* **2017**, *56*, 4950–4954.

[194] H. Echols, M. F. Goodman, *Annu. Rev. Biochem.* **1991**, *60*, 477–511.

[195] D. Boneh, C. Dunworth, R. J. Lipton, J. Sgall, *Discret. Appl. Math.* **1996**, *71*, 79–94.

[196] L. Hartmann, S. Häfele, R. Peschka-Süss, M. Antonietti, *Chem. Eur. J.* **2008**, *14*, 2025–2033.

[197] T. Terashima, T. Mes, T. F. A. De Gress, M. A. J. Gillissen, P. Besenius, A. R. A. Palmans, E. W. Meijer, *J. Am. Chem. Soc.* **2011**, *133*, 4742–4745.

[198] D. M. Rosenbaum, D. R. Liu, *J. Am. Chem. Soc.* **2003**, *125*, 13924–13925.

[199] S. Martens, J. Van den Begin, A. Madder, F. E. Du Prez, P. Espeel, *J. Am. Chem. Soc.* **2016**, *138*, 14182–14185.

[200] N. Zydziak, F. Feist, B. Huber, J. O. Mueller, C. Barner-Kowollik, *Chem. Commun.* **2015**, *51*, 1799–1802.

[201] N. Zydziak, W. Konrad, F. Feist, S. Afonin, S. Weidner, C. Barner-Kowollik, *Nat. Commun.* **2016**, *7*, 13672.

[202] R. L. Kanasty, A. J. Vegas, L. M. Ceo, M. Maier, K. Charisse, J. K. Nair, R. Langer, D. G. Anderson, *Angew. Chem. Int. Ed.* **2016**, *55*, 9529–9533.

[203] S. C. Solleder, K. S. Wetzel, M. A. R. Meier, *Polym. Chem.* **2015**, *6*, 3201–3204.

[204] S. C. Solleder, D. Zengel, K. S. Wetzel, M. A. R. Meier, *Angew.Chem. Int. Ed.* **2016**, *55*, 1204–1207.

[205] S. C. Solleder, S. Martens, P. Espeel, F. Du Prez, M. A. R. Meier, *Chem. Eur. J.* **2017**, *23*, 13906–13909.

[206] Y.-H. Wu, J. Zhang, F.-S. Du, Z.-C. Li, *ACS Macro Lett.* **2017**, *6*, 1398–1403.

[207] M. Hartweg, C. J. C. Edwards-Gayle, E. Radvar, D. Collis, M. Reza, M. Kaupp, J. Steinkoenig, J. Ruokolainen, R. Rambo, C. Barner-Kowollik, et al., *Polym. Chem.* **2018**, *9*, 482–489.

[208] A. C. Boukis, K. Reiter, M. Frölich, D. Hofheinz, M. A. R. Meier, *Nat. Commun.* **2018**, *9*, 1439.

[209] A. C. Boukis, M. A. R. Meier, *Eur. Polym. J.* **2018**, *104*, 32–38.

[210] C. E. Shannon, *Bell Syst. Tech. J.* **1948**, *27*, 379–423.

[211] H. A. Erlich, *J. Clin. Immunol.* **1989**, *9*, 437–447.

[212] L. Garibyan, N. Avashia, *J. Invest. Dermatol.* **2013**, *133*, 1–4.

[213] S. Carson, M. Wanunu, *Nanotechnology* **2015**, *26*, 074004.

[214] J. Shendure, H. Ji, *Nat. Biotechnol.* **2008**, *26*, 1135–1145.

[215] L. T. C. França, E. Carrilho, T. B. L. Kist, *Q. Rev. Biophys.* **2002**, *35*, 169–200.

[216] K. Sadakane, *Theory Comput. Syst.* **2007**, *41*, 589–607.

[217] S. Sato, S. Tabata, H. Hirakawa, E. Asamizu, K. Shirasawa, S. Isobe, T. Kaneko, Y. Nakamura, D. Shibata, K. Aoki, et al., *Nature* **2012**, *485*, 635–641.

[218] A. Al Ouahabi, J.-A. Amalian, L. Charles, J.-F. Lutz, *Nat. Commun.* **2017**, *8*, 967.

[219] G. Cavallo, A. Al Ouahabi, L. Oswald, L. Charles, J.-F. Lutz, *J. Am. Chem. Soc.* **2016**, *138*, 9417–9420.

[220] J. A. Amalian, T. T. Trinh, J. F. Lutz, L. Charles, *Anal. Chem.* **2016**, *88*, 3715–3722.

[221] R. K. Roy, C. Laure, D. Fischer-Krauser, L. Charles, J.-F. Lutz, *Chem. Commun.* **2015**, *51*, 15677–15680.

[222] J.-F. Lutz, *Macromolecules* **2015**, *48*, 4759–4767.

[223] G. Cavallo, S. Poyer, J. Amalian, F. Dufour, A. Burel, C. Carapito, L. Charles, J. Lutz, *Angew. Chem. Int. Ed.* **2018**, *57*, 6266–6269.

[224] T. T. Trinh, L. Oswald, D. Chan-Seng, J.-F. Lutz, *Macromol. Rapid Commun.* **2014**, *35*, 141–145.

[225] T. T. Trinh, L. Oswald, D. Chan-Seng, L. Charles, J.-F. Lutz, *Chem. Eur. J.* **2015**, *21*, 11961–11965.

[226] R. K. Roy, A. Meszynska, C. Laure, L. Charles, C. Verchin, J.-F. Lutz, *Nat. Commun.* **2015**, *6*, 7237.

[227] X. Ji, R.-T. Wu, L. Long, X.-S. Ke, C. Guo, Y.-J. Ghang, V. M. Lynch, F. Huang, J. L. Sessler, *Adv. Mater.* **2018**, *30*, 1705480.

[228] A. N. Shipway, E. Katz, I. Willner, in *Mol. Mach. Mot.*, Springer, Berlin, Heidelberg, **2001**, pp. 237–281.

[229] S. C. Solleder, K. S. Wetzel, M. A. R. Meier, *Polym. Chem.* **2015**, *6*, 3201–3204.

[230] B. B. Zaidan, A. A. Zaidan, A. K. Al-Frajat, H. A. Jalab, *J. Appl. Sci.* **2010**, *10*, 1650–1655.

[231] E. C. Reinke, *Class. J.* **1962**, *53*, 113–121.

[232] A. J. Raphael, V. Sundaram, *Int. J. Comput. Technol. Appl.* **2011**, *2*, 626–630.

[233] R. J. Anderson, F. A. P. Petitcolas, *IEEE J. Sel. Areas Commun.* **1998**, *16*, 474–481.

[234] NIST, *Fed. Inf. Process. Stand. Publ.* **2001**, *197*, 311.

[235] C. E. Shannon, *Bell Syst. Tech. J.* **1949**, *28*, 656–715.

[236] D. Rijmenants, *Cipher Mach. Cryptol.* **2010**, 1–27.

[237] P. C. Kocher, in *Adv. Cryptol. — CRYPTO '96*, Springer, Berlin, Heidelberg, **1996**, pp. 104–113.

[238] T. Sarkar, K. Selvakumar, L. Motiei, D. Margulies, *Nat. Commun.* **2016**, *7*, 11374.

[239] K. Challita, H. Farhat, *Int. J. New Comput. Archit. Their Appl.* **2011**, *1*, 199–208.

[240] J. F. Dooley, *Cryptologia* **2016**, *40*, 107–112.

[241] H. Sun, S. Liu, W. Lin, K. Y. Zhang, W. Lv, X. Huang, F. Huo, H. Yang, G. Jenkins, Q. Zhao, et al., *Nat. Commun.* **2014**, *5*, 3601.

[242] X. Hou, C. Ke, C. J. Bruns, P. R. McGonigal, R. B. Pettman, J. F. Stoddart, *Nat. Commun.* **2015**, *6*, 6884.

[243] T. Mutai, H. Satou, K. Araki, *Nat. Mater.* **2005**, *4*, 685–687.

[244] A. Kishimura, T. Yamashita, K. Yamaguchi, T. Aida, *Nat. Mater.* **2005**, *4*, 546–549.

[245] S.-J. Yoon, J. W. Chung, J. Gierschner, K. S. Kim, M.-G. Choi, D. Kim, S. Y. Park, *J. Am. Chem. Soc.* **2010**, *132*, 13675–13683.

[246] K. Li, Y. Xiang, X. Wang, J. Li, R. Hu, A. Tong, B. Z. Tang, *J. Am. Chem. Soc.* **2014**, *136*, 1643–1649.

[247] Y. Wu, Y. Xie, Q. Zhang, H. Tian, W. Zhu, A. D. Q. Li, *Angew. Chem. Int. Ed.* **2014**, *53*, 2090–2094.

[248] A. Credi, *Angew. Chem. Int. Ed.* **2007**, *46*, 5472–5475.

[249] G. Strack, H. R. Luckarift, G. R. Johnson, E. Katz, in *Biomol. Inf. Process.*, Wiley-VCH Verlag GmbH & Co. KGaA, Weinheim, Germany, **2012**, pp. 103–116.

[250] A. Prasanna de Silva, M. R. James, B. O. F. McKinney, D. A. Pears, S. M. Weir, *Nat. Mater.* **2006**, *5*, 787–789.

[251] R. Sjöback, J. Nygren, M. Kubista, *Spectrochim. Acta Part A Mol. Biomol. Spectrosc.* **1995**, *51*, L7–L21.

[252] C. J. Chang, E. M. Nolan, J. Jaworski, S. C. Burdette, M. Sheng, S. J. Lippard, *Chem. Biol.* **2004**, *11*, 203–210.

[253] J. Jose, K. Burgess, *Tetrahedron* **2006**, *62*, 11021–11037.

[254] X. Wu, Z. Li, X.-X. Chen, J. S. Fossey, T. D. James, Y.-B. Jiang, *Chem. Soc. Rev.* **2013**, *42*, 8032.

[255] L. Götzke, K. Gloe, K. A. Jolliffe, L. F. Lindoy, A. Heine, T. Doert, A. Jäger, K. Gloe, *Polyhedron* **2011**, *30*, 708–714.

[256] T. Sakamoto, A. Ojida, I. Hamachi, *Chem. Commun.* **2009**, 141–152.

[257] P. L. Abhayawardhana, P. A. Marzilli, F. R. Fronczek, L. G. Marzilli, *Inorg. Chem.* **2014**, *53*, 1144–1155.

[258] Z. H. Chohan, M. Z. Hernandes, F. R. Sensato, D. R. M. Moreira, V. R. Alves Pereira, J. K. D. A. L. Neves, A. P. de Oliveira, B. C. de Oliveira, A. C. Lima Leite, *J. Enzyme Inhib. Med. Chem.* **2014**, *29*, 230–236.

[259] M. Vonlanthen, C. M. Connelly, A. Deiters, A. Linden, N. S. Finney, *J. Org. Chem.* **2014**, *79*, 6054–6060.

[260] P. D. Beer, P. A. Gale, *Angew. Chem. Int. Ed.* **2001**, *40*, 486–516.

[261] R. Custelcean, *Chem. Commun.* **2008**, 295–307.

[262] D. A. Adsmond, D. J. W. Grant, *J. Pharm. Sci.* **2001**, *90*, 2058–2077.

[263] C. T. Clelland, V. Risca, C. Bancroft, *Nature* **1999**, *399*, 533–534.

[264] T. Anwar, S. Paul, S. K. Singh, *Int. J. Bio-Science Bio-Technology* **2014**, *6*, 215–222.

[265] J. Yang, J. Ma, S. Liu, C. Zhang, *Chinese Sci. Bull.* **2014**, *59*, 1192–1198.

[266] A. Leier, C. Richter, W. Banzhaf, H. Rauhe, *Biosystems* **2000**, *57*, 13–22.

[267] G. Xiao, M. Lu, L. Qin, X. Lai, *Sci. Bull.* **2006**, *51*, 1413–1420.

[268] J. Ling, G. Naren, J. Kelly, T. S. Moody, A. P. de Silva, *J. Am. Chem. Soc.* **2015**, *137*, 3763–3766.

[269] J. Andréasson, U. Pischel, *Chem. Soc. Rev.* **2015**, *44*, 1053–1069.

[270] K. Szaciłowski, *Infochemistry*, John Wiley & Sons, Ltd, Chichester, UK, **2012**.

[271] J. Ling, B. Daly, V. A. D. Silverson, A. P. de Silva, *Chem. Commun.* **2015**, *51*, 8403–8409.

[272] C. Zhang, J. Yang, J. Xu, *Chinese Sci. Bull.* **2011**, *56*, 3566–3571.

[273] M. Baroncini, M. Semeraro, A. Credi, *Isr. J. Chem.* **2011**, *51*, 23–35.

[274] J. E. Poje, T. Kastratovic, A. R. Macdonald, A. C. Guillermo, S. E. Troetti, O. J. Jabado, M. L. Fanning, D. Stefanovic, J. Macdonald, *Angew. Chem. Int. Ed.* **2014**, *53*, 9222–9225.

[275] S. Shoshani, R. Piran, Y. Arava, E. Keinan, *Angew. Chem. Int. Ed.* **2012**, *51*, 2883–2887.

[276] J. Ling, G. Naren, J. Kelly, D. B. Fox, A. Prasanna de Silva, *Chem. Sci.* **2015**, *6*, 4472–4478.

[277] J. Andréasson, U. Pischel, S. D. Straight, T. A. Moore, A. L. Moore, D. Gust, *J. Am. Chem. Soc.* **2011**, *133*, 11641–11648.

[278] X.-J. Jiang, D. K. P. Ng, *Angew. Chem. Int. Ed.* **2014**, *53*, 10481–10484.

[279] J. Chen, S. Zhou, J. Wen, *Angew. Chem. Int. Ed.* **2014**, *54*, 446–450.

[280] C. P. Carvalho, Z. Domínguez, J. P. Da Silva, U. Pischel, *Chem. Commun.* **2015**, *51*, 2698–2701.

[281] D. Margulies, C. E. Felder, G. Melman, A. Shanzer, *J. Am. Chem. Soc.* **2007**, *129*, 347–354.

[282] G. Strack, M. Ornatska, M. Pita, E. Katz, *J. Am. Chem. Soc.* **2008**, *130*, 4234–4235.

[283] Z. Guo, W. Zhu, L. Shen, H. Tian, *Angew. Chem. Int. Ed.* **2007**, *46*, 5549–5553.

[284] W. Sun, C.-H. Xu, Z. Zhu, C.-J. Fang, C.-H. Yan, *J. Phys. Chem. C* **2008**, *112*, 16973–16983.

[285] Y. Liu, J. Ren, Y. Qin, J. Li, J. Liu, E. Wang, *Chem. Commun.* **2012**, *48*, 802–804.

[286] J. Halámek, T. K. Tam, S. Chinnapareddy, V. Bocharova, E. Katz, *J. Phys. Chem. Lett.* **2010**, *1*, 973–977.

[287] T. Ratner, O. Reany, E. Keinan, *ChemPhysChem* **2009**, *10*, 3303–3309.

[288] M. A. Palacios, E. Benito-Pena, M. Manesse, A. D. Mazzeo, C. N. LaFratta, G. M. Whitesides, D. R. Walt, *Proc. Natl. Acad. Sci.* **2011**, *108*, 16510–16514.

[289] K.-W. Kim, V. Bocharova, J. Halámek, M.-K. Oh, E. Katz, *Biotechnol. Bioeng.* **2011**, *108*, 1100–1107.

[290] I. B. Burgess, L. Mishchenko, B. D. Hatton, M. Kolle, M. Lončar, J. Aizenberg, *J. Am. Chem. Soc.* **2011**, *133*, 12430–12432.

[291] M. H. Ohlmeyer, R. N. Swanson, L. W. Dillard, J. C. Reader, G. Asouline, R. Kobayashi, M. Wigler, W. C. Still, *Proc. Natl. Acad. Sci.* **1993**, *90*, 10922–10926.

[292] J. J. Thomson, *London, Edinburgh, Dublin Philos. Mag. J. Sci.* **1897**, *44*, 293–316.

[293] J. M. Thomas, *Angew. Chem. Int. Ed.* **2006**, *45*, 6797–6800.

[294] J. Griffiths, *Anal. Chem.* **2008**, *80*, 5678–5683.

[295] A. J. Dempster, *Phys. Rev.* **1918**, *11*, 316–325.

[296] W. E. Stephens, *Phys. Rev.* **1946**, *69*, 691.

[297] W. Paul, H. Steinwedel, *Zeitschrift für Naturforsch. A* **1953**, *8*, 448–450.

[298] R. A. Yost, C. G. Enke, *J. Am. Chem. Soc.* **1978**, *100*, 2274–2275.

[299] M. Barber, R. S. Bordoli, R. D. Sedgwick, A. N. Tyler, *J. Chem. Soc. Chem. Commun.* **1981**, 325–327.

[300] M. Barber, R. S. Bordoli, R. D. Sedgwick, A. N. Tyler, *Nature* **1981**, *293*, 270–275.

[301] J. Fenn, M. Mann, C. Meng, S. Wong, C. Whitehouse, *Science* **1989**, *246*, 64–71.

[302] K. Tanaka, H. Waki, Y. Ido, S. Akita, Y. Yoshida, T. Yoshida, T. Matsuo, *Rapid Commun. Mass Spectrom.* **1988**, *2*, 151–153.

[303] J. V. Olsen, B. Macek, O. Lange, A. Makarov, S. Horning, M. Mann, *Nat. Methods* **2007**, *4*, 709–712.

[304] R. A. Zubarev, A. Makarov, *Anal. Chem.* **2013**, *85*, 5288–5296.

[305] R. A. Scheltema, J.-P. Hauschild, O. Lange, D. Hornburg, E. Denisov, E. Damoc, A. Kuehn, A. Makarov, M. Mann, *Mol. Cell. Proteomics* **2014**, *13*, 3698–3708.

[306] L. Konermann, E. Ahadi, A. D. Rodriguez, S. Vahidi, *Anal. Chem.* **2013**, *85*, 2–9.

[307] C. J. Hogan, J. A. Carroll, H. W. Rohrs, P. Biswas, M. L. Gross, *Anal. Chem.* **2009**, *81*, 369–377.

[308] M. S. Wilm, M. Mann, *Int. J. Mass Spectrom. Ion Process.* **1994**, *136*, 167–180.

[309] J. Fernandez de la Mora, *Anal. Chim. Acta* **2000**, *406*, 93–104.

[310] S. Nguyen, J. B. Fenn, *Proc. Natl. Acad. Sci.* **2007**, *104*, 1111–1117.

[311] P. Kebarle, U. H. Verkerk, *Mass Spectrom. Rev.* **2009**, *28*, 898–917.

[312] K.-Y. Li, H. Tu, A. K. Ray, *Langmuir* **2005**, *21*, 3786–3794.

[313] J. Fernández de la Mora, *Annu. Rev. Fluid Mech.* **2007**, *39*, 217–243.

[314] Z. Olumee, J. H. Callahan, A. Vertes, *J. Phys. Chem. A* **1998**, *102*, 9154–9160.

[315] B. P. Pozniak, R. B. Cole, *J. Am. Soc. Mass Spectrom.* **2007**, *18*, 737–748.

[316] A. J. R. Heck, R. H. H. van den Heuvel, *Mass Spectrom. Rev.* **2004**, *23*, 368–389.

[317] I. A. Kaltashov, A. Mohimen, *Anal. Chem.* **2005**, *77*, 5370–5379.

[318] E. Ahadi, L. Konermann, *J. Phys. Chem. B* **2012**, *116*, 104–112.

[319] L. Konermann, A. D. Rodriguez, J. Liu, *Anal. Chem.* **2012**, *84*, 6798–6804.

[320] I. Ugi, M. Goebel, B. Gruber, M. Heilingbrunner, C. Heiß, W. Hörl, O. Kern, M. Starnecker, A. Dömling, *Res. Chem. Intermed.* **1996**, *22*, 625–644.

[321] D. P. Demarque, A. E. M. Crotti, R. Vessecchi, J. L. C. Lopes, N. P. Lopes, *Nat. Prod. Rep.* **2016**, *33*, 432–455.

[322] C. C. Tzschucke, C. Markert, W. Bannwarth, S. Roller, A. Hebel, R. Haag, *Angew. Chem. Int. Ed.* **2002**, *41*, 3964–4000.

[323] A. Basso, L. Banfi, G. Guanti, R. Riva, A. Riu, *Tetrahedron Lett.* **2004**, *45*, 6109–6111.

[324] C. Hebach, U. Kazmaier, *Chem. Commun.* **2003**, 596–597.

[325] G. B. Giovenzana, G. C. Tron, S. Di Paola, I. G. Menegotto, T. Pirali, *Angew. Chem. Int. Ed.* **2006**, *45*, 1099–1102.

[326] Z. Luo, Q. Zhang, Y. Oderaotoshi, D. P. Curran, *Science* **2001**, *291*, 1766–1769.

[327] Y. Lu, S. J. Geib, K. Damodaran, B. Sui, Z. Zhang, D. P. Curran, W. Zhang, *Chem. Commun.* **2010**, *46*, 7578.

[328] K. P. Madhusudanan, *J. Mass Spectrom.* **2006**, *41*, 1096–1104.

[329] E. Drabik, G. Krasiński, M. Cypryk, R. Błaszczyk, T. Gajda, M. Sochacki, *J. Am. Soc. Mass Spectrom.* **2013**, *24*, 388–398.

[330] K. Sung, C.-C. Chen, *Tetrahedron Lett.* **2001**, *42*, 4845–4848.

[331] J. Podlech, *Arbeitsmethoden in Der Organischen Chemie*, Lehmanns Media, **2014**.

[332] M. A. Mironov, *QSAR Comb. Sci.* **2006**, *25*, 423–431.

[333] S. C. Solleder, D. Zengel, K. S. Wetzel, M. A. R. Meier, *Angew. Chem. Int. Ed.* **2016**, *55*, 1204–1207.

[334] W. Konrad, F. R. Bloesser, K. S. Wetzel, A. C. Boukis, M. A. R. Meier, C. Barner-Kowollik, *Chem. Eur. J.* **2018**, *24*, 3413–3419.

[335] J. R. Yates Ill, D. Schieltz, A. Koller, J. Venable, in *Cell Biol.*, Elsevier, **2006**, pp. 383–390.

[336] A. I. Nesvizhskii, R. Aebersold, *Drug Discov. Today* **2004**, *9*, 173–181.

[337] E. Altuntaş, U. S. Schubert, *Anal. Chim. Acta* **2014**, *808*, 56–69.

[338] J.-F. Lutz, J.-M. Lehn, E. W. Meijer, K. Matyjaszewski, *Nat. Rev. Mater.* **2016**, *1*, 16024.

[339] W. C. Still, M. Kahn, A. Mitra, *J. Org. Chem.* **1978**, *43*, 2923–2925.

[340] A. Shaabani, A. Bazgir, S. Arab-Ameri, *Phosphorus. Sulfur. Silicon Relat. Elem.* **2004**, *179*, 2169–2175.

[341] E. N. Ostapchuk, A. S. Plaskon, O. O. Grygorenko, A. A. Tolmachev, S. V. Ryabukhin, *J. Heterocycl. Chem.* **2013**, *50*, 1299–1303.

[342] N. A. Liberto, S. De Paiva Silva, Â. De Fátima, S. A. Fernandes, *Tetrahedron* **2013**, *69*, 8245–8249.

[343] C. C. Zhu, Y. Xu, Y. Q. Liu, D. Ben Zhu, *J. Org. Chem.* **1997**, *62*, 1996–2000.

[344] W. Goldeman, A. Nasulewicz-Goldeman, *Bioorg. Med. Chem. Lett.* **2014**, *24*, 3475–3479.

7.2 Registers

7.2.1 List of abbreviations

Abbreviation	Explanation
1D	One dimensional
2D	Two dimensional
3CR	Three-component reaction
3D	Three dimensional
4CR	Four-component reaction
a priori	Lat.: from the earlier
a. u.	Arbitrary unit
ADMET	Acyclic diene metathesis
AES	Advanced Encryption Standard
AIBN	Azobis(isobutyronitril)
ATR	Attenuated total reflection
ATRP	Atom Transfer Radical Polymerization
BC	Before Christ
BINOL	1,1′-Bi-2-naphthol
Bn	Benzyl (~$CH_2C_6H_5$)
BOC	*tert*-Butyloxycarbonyl
Bp.	Boiling point
BQ	*para*-Benzoquinone

br (IR)	Broad
br s (NMR)	Broad singlet
Cas	Chemical abstracts service
Cat.	Catalyst
CD	Compact disk
$CDCl_3$	Deuterated chloroform
CDI	Carbonyldiimidazole
CEM	Chain ejection model
^{c}Hex	*cyclo*-Hexyl (~C_6H_{11})
CO_2	Carbon dioxide
COS	Carbonyl sulfide
COSY	Correlation spectroscopy
CRM	Charged residue model
CS_2	Carbon disulfide
CTA	Chain transfer agent
CTA	Chain transfer agent
CuMCR	Copper-catalyzed multicomponent reaction
d (NMR)	Doublet
DCC	Dicyclohexylcarbodiimide
DCM	Dichloromethane
DEPT	Distortionless enhancement by polarization transfer.
DFT	Density functional theory
DHMP	3,4-dihydropyrimidin-2(1H)-ones

DHP	1,4-dihydropyridines
DMAP	4-(Dimethylamino)-pyridine
DMPA	2,2-Dimethoxy-2-phenylacetophenone
DMSO	Dimethyl sulfoxide
DNA	Deoxyribonucleic acid
DRI	Differential refractive index
DSC	Differential scanning calorimetry
DTA	Differential thermal analysis
DVD	Digital versatile disc
e^-	Electron
e.g.	*exempli gratia* Lat.: for example
EAA	Ethyl acetoacetate
ee	Enantiomeric excess
E-Factor	Ecological factor
EI	Electron ionization
EPO	Erythropoietin
eq.	Equivalent
ESI	Electrospray ionization
Et	Ethyl (~C_2H_5)
et al.	*et alii*, *et aliae*, *et alia*. Lat.: and others
etc.	*Et cetera* Lat.: and other similar things
EtOAc	Ethyl acetate
EtOH	Ethanol

EWG	Electron withdrawing group
FAB	Fast atom bombardment
FRET	fluorescence resonance energy transfer
F-SPE	Fluorous solid phase extraction
F-tag	Fluorous tagged
FZK	Forschungszentrum Karlsruhe
GC-MS	Gas chromatography - mass spectrometry
GPC	Gel permeation chromatography
H^+	Lewis or Brønsted acid
H-bonded	Hydrogen boned
HCD	Higher-energy collisional dissociation
HESI	Heated electrospray ionization
HFIP	Hexafluoro isopropanol
HG-1	Hoveyda-Grubbs catalyst 1st generation
HG-2	Hoveyda-Grubbs catalyst 2nd generation
HIV	Human immunodeficiency virus
HMBC	Heteronuclear multiple bond correlation
HMQC	Heteronuclear multiple quantum coherence
HOAc	Acetic acid
HPLC	High-performance liquid chromatography
HRMS	High resolution mass spectrometry
HSQC	Heteronuclear single quantum coherence
i.e.	*id est* Lat.: that is

^{i}Bu	*iso*-Butyl (~$CH_2CH(CH_3)_2$)
IC50	Half maximal inhibitory concentration
IEM	Ion evaporation model
in situ	Lat.: on site, locally without isolation
in vivo	Lat.: within the living
IR	Infrared spectroscopy
J (NMR)	Coupling constant
KIT	Karlsruhe Institute of Technology
KOH	Potassium hydroxide
LC	Liquid chromatography
LCST	Lower critical solution temperature
L_n	Ligands
m (IR)	Medium
m (NMR)	Multiplet
MAA	Methyl acetoacetate
MA-AA	2-(Methacryloyloxy)ethyl acetoacetate
MALDI	Matrix-assisted Laser Desorption/Ionization
MCR	Multicomponent reaction
MeOH	Methanol
MIC	Minimum inhibitory activity
Monomer-NC	Isocyanide-benzyl ester monomer
Mp.	Melting point
mPEG	Methoxypoly(ethylene glycol)

mPEG	Poly(ethylene glycol) methyl ether
MS	Mass spectrometry
NaOEt	Sodium ethanolate
NEt_3	Triethylamine
NH_3	Ammonia
NMP	*N*-methyl-2-pyrrolidone
NMR	Nuclear magnetic resonance
NOESY	Nuclear Overhauser enhancement and exchange spectroscopy
OTP	One-time pad
P.T.	Proton transfer reaction
Passerini-3CR	Passerini three-component reaction
Pd/C	Palladium on activated charcoal
Ph	Phenyl (~C_6H_5)
polyDHMP	DHMP polymers
PPh_3	Triphenylphosphine
ppm	Parts per million
prec.	Precipitated
PTFE	Polytetrafluoroethylene
p-TSA	*para*-Toluenesulfonic acid
q (NMR)	Quartet
quint. (NMR)	Quintet
r.t.	Room temperature (approximately 23 °C)
RAFT	Reversible addition–fragmentation chain transfer

R_f	Retention factor
RI	Refractive index
RNA	Ribonucleic acid
RSA	Rivest–Shamir–Adleman public-key cryptosystems
s (IR)	Strong
s (NMR)	Singlet (NMR)
SEC	Size-exclusion chromatography
SMILES	Simplified Molecular Input Line Entry Specification
SPE	Solid phase extraction
t	Time factor
t (NMR)	Triplett (NMR)
TBD	1,5,7-Triazabicyclo[4.4.0]dec-5-ene
^{t}Bu	*tert*-Butyl (~C(CH_3)$_3$)
^{t}BuAA	*tert*-Butyl acetoacetate
^{t}BuOK	Potassium *tert*-butanoate
TFFA	Trifluoroacetic acid
TG	Thermo gravimetry
TGA	Thermo gravimetric analysis
THF	Tetrahydrofuran
TLC	Thin layer chromatography
TMS	Trimethyl silane
ToF	Time-of-flight
Ugi-4CR	Ugi four-component reaction

Ugi-5CR	Ugi five-component reaction
UV	Ultra violet
UV/Vis	Ultraviolet–visible spectroscopy
VCI	Verband der chemischen Industrie
via	Lat.: by way of, by means of, using
vice versa	Lat.: the other way around
vs.	*Versus* Lat.: against
w (IR)	Weak
X	Conversion

7.2.2 List of symbols

Symbol	**Term**	**Dimension**
$\tilde{\nu}$	Wavenumber	1 cm^{-1}
°C	Degree centigrade	273.15 K
Å	Ångström	10^{-10} m
amu	Atomic mass unit	1 $g \cdot mol^{-1}$
Bit	Basic unit of information	1 {1 or 0}
Byte	Unit of information	1 B = 8 bits
cm	Centimeter	10^{-2} m
d	Days	86400 s
Da	Dalton	1 $g \cdot mol^{-1}$
$Đ_M$	Dispersity $Đ_M = M_w/M_n$	1

g	Grams	1 g
GB	Gigabyte	10^9 byte
h	Hours	36000 s
J	Coupling constant	1 Hz = 1 s^{-1}
kDa	Kilo Dalton	10^3 g·mol^{-1}
kWh	Kilowatt hours	$3.6 \cdot 10^6$ J
M	Molar mass	1 g·mol^{-1}
m/z	Mass-to-charge ratio	1
MB	Megabyte	10^6 byte
mg	Milligram	10^{-3} g
min	Minutes	60 s
Mio.	Million	10^3
MJ	Megajoule	10^6 J
mL	Milliliter	10^{-3} L = 10^{-6} m^3
mm	Millimeter	10^{-3} m
mmol	Millimole	10^{-3} mol
mmu	Milli mass units	10^{-3} g·mol^{-1}
M_n	Number averaged molecular weight	1 g·mol^{-1}
mol	Mole	$6.023 \cdot 10^{-23}$ particles
M_w	Mass averaged molecular weight	1 g·mol^{-1}
n	Amount of substance	1 mol
N	Normal	1 mol·l^{-1}
nm	Nanometer	10^{-9} m

s	Second	1 s
t	Tons	10^6 g
TB	Terabyte	10^{12} byte
$T_{d\ 5\%}$	Decomposition temperature	1 ° C
T_g	Glass transition temperature	1 ° C
T_m	Melting temperature	1 ° C
X	Conversion	1
Z	Zetta	10^{21}
δ	Chemical shift	1 ppm, 10^{-6}
µL	Microliter	10^{-6} L = 10^{-9} m^3
µm	Micrometer	10^{-6} m
µmol	Micromole	10^{-6} mol
ρ	Density	1 g·cm^{-1}

7.3 List of publications in peer-reviewed journals

May 18 A. C. Boukis, M. A. R. Meier, *Eur. Polym. J.* **2018**, *104*, 32–38. **doi: 10.1016/j.eurpolymj.2018.04.038.**

Apr 18 A. C. Boukis, K. Reiter, M. Frölich, D. Hofheinz, M. A. R. Meier, *Nature Commun.* **2018**, *9*, 1439. **doi: 10.1038/s41467-018-03784-x.**

Jan 18 W. Konrad, F. R. Bloesser, K. S. Wetzel, A. C. Boukis, M. A. R. Meier, C. Barner-Kowollik, *Chem. Eur. J.* **2018**, *24*, 3413-3419. **doi: 10.1002/chem.201705939.**

Sep 17 T. P. Seifert, A. C. Boukis, T. J. Feuerstein, P. W. Roesky, *J. Organomet. Chem.* **2018**, *867*, 92–97. **doi: 10.1016/j.jorganchem.2017.09.023**.

Jun 17 A. Llevot, A. C. Boukis, S. Oelmann, K. S. Wetzel, M. A. R. Meier, *Top. Curr. Chem.* **2017**, *375*, 66. **doi: 10.1007/s41061-017-0153-4.**

Mar 17 S. C. Solleder, R. V. Schneider, K. S. Wetzel, A. C. Boukis, M. A. R. Meier, *Macromol. Rapid Commun.* **2017**, *38*, 1600711. **doi: 10.1002/marc.201600711.**

Jan 17 A. C. Boukis, B. Monney, M. A. R. Meier, *Beilstein J. Org. Chem.* **2017**, *13*, 54–62. **doi: 10.3762/bjoc.13.7.**

Jan 16 A. C. Boukis, A. Llevot, M. A. R. Meier, *Macromol. Rapid Commun.* **2016**, *37*, 643–649. **doi: 10.1002/marc.201500717.**

7.4 List of conferences

Sep 17 4th SFB1176 Graduate School Workshop | Annweiler am Trifels | oral presentation: Ultracentrifuge

Apr 17 3rd SFB1176 Graduate School Workshop | Annweiler am Trifels | oral presentation: Sequence-defined structures *via* a combination of two multicomponent reactions

Mar 17 9th Workshop on Fats and Oils as Renewable Feedstock for the Chemical Industry | KIT | responsible for technical operations

Sep 16 Jahrestagung der Fachgruppe Nachhaltige Chemie | KIT | poster presentation | responsible for posters and technical operations

Sep 16 2nd SFB1176 Workshop | Bad Herrenalb | oral presentation: Free radical polymerization

Mar 16 1st SFB1176 Graduate School Workshop | Bad Herrenalb | oral presentation: Sequence-defined macromolecules *via* multicomponent reactions

Feb 16 3rd Belgian-German Macromolecular Meeting - MacroBeGe 2016 | Houffalize, Belgium | poster presentation

Oct 15	23rd annual Bio-Environmental Polymer Society meeting - BEPS 2015 | KIT | prize for the best poster presentation
Mar 15	8th Workshop on Fats and Oils as Renewable Feedstock for the Chemical Industry | KIT | responsible for posters